

# SIGMA RECEPTORS

EDITED BY: Stephen T. Safrany, Ruth Dorothy Murrell-Lagnado,  
Tangui Maurice, Enrique José Cobos and Ebru Aydar  
PUBLISHED IN: Frontiers in Pharmacology





# frontiers

## Frontiers eBook Copyright Statement

The copyright in the text of individual articles in this eBook is the property of their respective authors or their respective institutions or funders. The copyright in graphics and images within each article may be subject to copyright of other parties. In both cases this is subject to a license granted to Frontiers.

The compilation of articles constituting this eBook is the property of Frontiers.

Each article within this eBook, and the eBook itself, are published under the most recent version of the Creative Commons CC-BY licence.

The version current at the date of publication of this eBook is CC-BY 4.0. If the CC-BY licence is updated, the licence granted by Frontiers is automatically updated to the new version.

When exercising any right under the CC-BY licence, Frontiers must be attributed as the original publisher of the article or eBook, as applicable.

Authors have the responsibility of ensuring that any graphics or other materials which are the property of others may be included in the CC-BY licence, but this should be checked before relying on the CC-BY licence to reproduce those materials. Any copyright notices relating to those materials must be complied with.

Copyright and source acknowledgement notices may not be removed and must be displayed in any copy, derivative work or partial copy which includes the elements in question.

All copyright, and all rights therein, are protected by national and international copyright laws. The above represents a summary only. For further information please read Frontiers' Conditions for Website Use and Copyright Statement, and the applicable CC-BY licence.

ISSN 1664-8714

ISBN 978-2-88966-102-2

DOI 10.3389/978-2-88966-102-2

## About Frontiers

Frontiers is more than just an open-access publisher of scholarly articles: it is a pioneering approach to the world of academia, radically improving the way scholarly research is managed. The grand vision of Frontiers is a world where all people have an equal opportunity to seek, share and generate knowledge. Frontiers provides immediate and permanent online open access to all its publications, but this alone is not enough to realize our grand goals.

## Frontiers Journal Series

The Frontiers Journal Series is a multi-tier and interdisciplinary set of open-access, online journals, promising a paradigm shift from the current review, selection and dissemination processes in academic publishing. All Frontiers journals are driven by researchers for researchers; therefore, they constitute a service to the scholarly community. At the same time, the Frontiers Journal Series operates on a revolutionary invention, the tiered publishing system, initially addressing specific communities of scholars, and gradually climbing up to broader public understanding, thus serving the interests of the lay society, too.

## Dedication to Quality

Each Frontiers article is a landmark of the highest quality, thanks to genuinely collaborative interactions between authors and review editors, who include some of the world's best academicians. Research must be certified by peers before entering a stream of knowledge that may eventually reach the public - and shape society; therefore, Frontiers only applies the most rigorous and unbiased reviews.

Frontiers revolutionizes research publishing by freely delivering the most outstanding research, evaluated with no bias from both the academic and social point of view. By applying the most advanced information technologies, Frontiers is catapulting scholarly publishing into a new generation.

## What are Frontiers Research Topics?

Frontiers Research Topics are very popular trademarks of the Frontiers Journals Series: they are collections of at least ten articles, all centered on a particular subject. With their unique mix of varied contributions from Original Research to Review Articles, Frontiers Research Topics unify the most influential researchers, the latest key findings and historical advances in a hot research area! Find out more on how to host your own Frontiers Research Topic or contribute to one as an author by contacting the Frontiers Editorial Office: [researchtopics@frontiersin.org](mailto:researchtopics@frontiersin.org)



# SIGMA RECEPTORS

Topic Editors:

**Stephen T. Safrany**, Royal College of Surgeons in Ireland (Bahrain), Bahrain

**Ruth Dorothy Murrell-Lagnado**, University of Cambridge, United Kingdom

**Tangui Maurice**, INSERM U1198 Mécanismes Moléculaires dans les Démences Neurodégénératives, France

**Enrique José Cobos**, University of Granada, Spain

**Ebru Aydar**, University College London, United Kingdom

**Citation:** Safrany, S. T., Murrell-Lagnado, R. D., Maurice, T., Cobos, E. J., Aydar, E., eds. (2020). Sigma Receptors. Lausanne: Frontiers Media SA.  
doi: 10.3389/978-2-88966-102-2

# Table of Contents

- 05 Editorial: Sigma Receptors**  
Ebru Aydar, Enrique J. Cobos, Tangui Maurice, Ruth D. Murell-Lagnado and Stephen T. Safrany
- 08 Modulation by Sigma-1 Receptor of Morphine Analgesia and Tolerance: Nociceptive Pain, Tactile Allodynia and Grip Strength Deficits During Joint Inflammation**  
Ángeles Montilla-García, Miguel Á. Tejada, M. Carmen Ruiz-Cantero, Inmaculada Bravo-Caparrós, Sandra Yeste, Daniel Zamanillo and Enrique J. Cobos
- 24 Allosteric Modulators of Sigma-1 Receptor: A Review**  
Edijs Vavers, Liga Zvejniece, Tangui Maurice and Maija Dambrova
- 41 Molecular Interplay Between the Sigma-1 Receptor, Steroids, and Ion Channels**  
Sara L. Morales-Lázaro, Ricardo González-Ramírez and Tamara Rosenbaum
- 53 Supraspinal and Peripheral, but Not Intrathecal,  $\sigma_1$ R Blockade by S1RA Enhances Morphine Antinociception**  
Alba Vidal-Torres, Begoña Fernández-Pastor, Alicia Carceller, José Miguel Vela, Manuel Merlos and Daniel Zamanillo
- 66 Blockade of the Sigma-1 Receptor Relieves Cognitive and Emotional Impairments Associated to Chronic Osteoarthritis Pain**  
Mireia Carcolé, Daniel Zamanillo, Manuel Merlos, Begoña Fernández-Pastor, David Cabañero and Rafael Maldonado
- 81 Anti-tumor Efficacy Assessment of the Sigma Receptor Pan Modulator RC-106. A Promising Therapeutic Tool for Pancreatic Cancer**  
Anna Tesei, Michela Cortesi, Sara Pignatta, Chiara Arienti, Giulio Massimo Dondio, Chiara Bigogno, Alessio Malacrida, Mariarosaria Miloso, Cristina Meregalli, Alessia Chiorazzi, Valentina Carozzi, Guido Cavaletti, Marta Rui, Annamaria Marra, Daniela Rossi and Simona Collina
- 93 Trends in Sigma-1 Receptor Research: A 25-Year Bibliometric Analysis**  
Luz Romero and Enrique Portillo-Salido
- 110 A New Pharmacophore Model for the Design of Sigma-1 Ligands Validated on a Large Experimental Dataset**  
Rosalia Pascual, Carmen Almansa, Carlos Plata-Salamán and José Miguel Vela
- 126 Ligands Exert Biased Activity to Regulate Sigma 1 Receptor Interactions With Cationic TRPA1, TRPV1, and TRPM8 Channels**  
Elsa Cortés-Montero, Pilar Sánchez-Blázquez, Yara Onetti, Manuel Merlos and Javier Garzón
- 138 Sigma-1 Receptor Inhibition Reduces Neuropathic Pain Induced by Partial Sciatic Nerve Transection in Mice by Opioid-Dependent and -Independent Mechanisms**  
Inmaculada Bravo-Caparrós, Gloria Perazzoli, Sandra Yeste, Domagoj Cikes, José Manuel Baeyens, Enrique José Cobos and Francisco Rafael Nieto

- 154 In vitro and in vivo Human Metabolism of (S)-[<sup>18</sup>F]Fluspidine – A Radioligand for Imaging  $\sigma_1$  Receptors With Positron Emission Tomography (PET)**  
Friedrich-Alexander Ludwig, Steffen Fischer, Richard Houska, Alexander Hoepping, Winnie Deuther-Conrad, Dirk Schepmann, Marianne Patt, Philipp M. Meyer, Swen Hesse, Georg-Alexander Becker, Franziska Ruth Zientek, Jörg Steinbach, Bernhard Wünsch, Osama Sabri and Peter Brust
- 168 Role of Sigma Receptors in Alcohol Addiction**  
Sema G. Quadir, Pietro Cottone and Valentina Sabino
- 175 Characterization of Sigma 1 Receptor Antagonist CM-304 and Its Analog, AZ-66: Novel Therapeutics Against Allodynia and Induced Pain**  
Thomas J. Cirino, Shainnel O. Eans, Jessica M. Medina, Lisa L. Wilson, Marco Mottinelli, Sebastiano Intagliata, Christopher R. McCurdy and Jay P. McLaughlin
- 189 Small-Molecule Modulators of Sigma1 and Sigma2/TMEM97 in the Context of Cancer: Foundational Concepts and Emerging Themes**  
Halley M. Oyer, Christina M. Sanders and Felix J. Kim
- 205 Hazards of Using Masking Protocols When Performing Ligand Binding Assays: Lessons From the Sigma-1 and Sigma-2 Receptors**  
Haider Abbas, Preeti Borde, Gary B. Willars, David R. Ferry and Stephen T. Safrany



# Editorial: Sigma Receptors

Ebru Aydar<sup>1</sup>, Enrique J. Cobos<sup>2</sup>, Tangui Maurice<sup>3</sup>, Ruth D. Murell-Lagnado<sup>4</sup> and Stephen T. Safrany<sup>5\*</sup>

<sup>1</sup> Institute of Ophthalmology, University College London, London, United Kingdom, <sup>2</sup> Instituto de Investigación Biosanitaria ibs.GRANADA and Department of Pharmacology, Faculty of Medicine, University of Granada, Granada, Spain, <sup>3</sup> MMDN, Univ Montpellier, EPHE, INSERM, Montpellier, France, <sup>4</sup> School of Life Sciences, University of Sussex, Brighton, United Kingdom, <sup>5</sup> School of Medicine, RCSI-Bahrain, Adliya, Bahrain

**Keywords:** sigma-1 receptor, sigma-2 receptor, pain, cancer, ion channels, allosteric

## Editorial on the Research Topic

### Sigma Receptors

Sigma receptors were initially described as opioid receptors (Martin et al., 1976). They are now considered neither related to other types of receptor nor to each other. While several ligands used to study these receptors [e.g., di-*O*-tolyl guanidine (DTG) and haloperidol] have similar affinities for the sigma-1 and sigma-2 receptors, these proteins show little homology at the primary amino acid level. The sigma-1 receptor was cloned some time ago (Hanner et al., 1996; Kekuda et al., 1996), and the crystal structure of the trimer solved (Schmidt et al., 2016). The molecular identity of the sigma-2 binding site has only recently been determined as TMEM97, a regulator of the sterol transporter NPC1 (Alon et al., 2017). Both proteins appear to be predominantly in the endoplasmic reticulum and, despite some evidence that progesterone and dimethyltryptamine bind the sigma-1 receptor (Fontanilla et al., 2009), are both considered orphan receptors. The sigma receptors have been implicated in a large number of apparently diverse conditions, including addiction, depression, pain, neurodegenerative conditions, cancer, and amyotrophic lateral sclerosis (among others), suggesting that their pharmacological regulation will yield useful drugs to treat several conditions.

Following the successful “Sigma-1 receptors as therapeutic targets” symposium, held at the Pharmacology 2017 meeting of the British Pharmacological Society, we organized a Research Topic entitled “Sigma Receptors” in *Frontiers in Pharmacology*. A total of 15 articles, consisting of 11 original papers and 4 review papers, has been published. Our Research Topic has been well received by the readership, with over 32,000 views to date. Here, we highlight the key outcomes of these publications.

Using a bibliographical approach to sigma receptor research, Romero and Portillo-Salido show how there has been an increase in publication numbers in this area. Focusing on the period 1992–2017, they identify highlights in sigma receptor research. Key findings include their cloning, the production of sigma-1 receptor knock-out mice and solving the crystal structure of the sigma-1 receptor. Their interesting analysis of the research landscape in this very dynamic field reveals numerous potentialities and collaborative networks. Furthermore, they show that ESTEVE, with interests in pain management and treatment of neurodegenerative disorders, is the industry leader of the field in publication number.

Vidal-Torres et al. show that S1RA (E-52862, MR309) alone is unable to elicit an antinociceptive effect by itself in the tail-flick acute pain assay in mice. However, in combination with opioids, a synergistic antinociceptive effect is observed. The enhanced opioid response is only observed following systemic or supraspinal administration of S1RA, but not following spinal administration. Additionally, loperamide, a peripherally restricted opioid, becomes effective as an antinociceptive agent in combination with S1RA. Therefore, both supraspinal and peripheral actions might account for the enhancement of opioid effects by sigma-1 antagonism.

## OPEN ACCESS

### Edited and reviewed by:

Luc Zimmer,  
Université Claude Bernard  
Lyon 1, France

### \*Correspondence:

Stephen T. Safrany  
ssafrany@rcsi-mub.com

### Specialty section:

This article was submitted to  
Experimental Pharmacology  
and Drug Discovery,  
a section of the journal  
*Frontiers in Pharmacology*

**Received:** 01 August 2020

**Accepted:** 12 August 2020

**Published:** 27 August 2020

### Citation:

Aydar E, Cobos EJ, Maurice T,  
Murell-Lagnado RD and Safrany ST  
(2020) Editorial: Sigma Receptors.  
*Front. Pharmacol.* 11:590519.  
doi: 10.3389/fphar.2020.590519

Using an inflammatory pain model (periarticular inflammation induced by Complete Freund's Adjuvant) in mice, Montilla-Garcia et al. show how the sigma-1 receptor antagonist S1RA acts synergistically with morphine to elicit an antinociceptive effect to reverse tactile allodynia. Importantly, S1RA was able to rescue the effect of morphine in tolerant mice following repeated injections of this opioid drug not only in tactile allodynia but also in pain-induced deficits in physical function (grip strength). These two studies point to that sigma-1 antagonists are promising tools as opioid adjuvants in chronic pain indications.

Cirino et al. and Bravo-Caparrós et al. provide further evidence that sigma receptors act directly as antinociceptive targets: Cirino et al. consider analgesic and anti-allodynic activities of two novel sigma ligands – a selective sigma-1 receptor antagonist, CM-304, and a non-selective sigma receptor ligand, AZ-66. Both are effective in a wide array of animal pain models: chronic nerve constriction injury; cisplatin neuropathy; acetic acid-induced writhing; formalin-induced inflammation; and the thermally-induced tail withdrawal tests. These results show that sigma-1 antagonists can have analgesic activity in the absence of exogenous opioid. Using sigma-1 receptor knock-out mice, Bravo-Caparrós et al. give evidence that this receptor is crucial in pain perception and relief using a spared nerve injury model in mice, where tibial and common peroneal branches of the sciatic nerve are ligated. The administration of S1RA decreases neuropathic cold, heat and tactile hypersensitivity. The effects of sigma-1 antagonism on heat and tactile hypersensitivity during neuropathic pain are indirectly mediated by the activation of the peripheral opioid receptors, which together with similar findings previously described during inflammatory hypersensitivity (Tejada et al., 2017), point to the relevance of sigma-1 receptors as a physiological modulator of the opioid system during pain conditions.

A common source of chronic pain is with the development of osteoarthritis. Using a mouse model, induced by an intrarticular injection of monosodium iodoacetate, Carcolé et al. show that S1RA is able to reverse hyperalgesia. Furthermore, S1RA treatment is able to prevent some of the profound behavioral changes induced by chronic pain, such as cognitive deficits (determined using a V-maze), and depressive-like states (determined using the forced-swim test) associated with osteoarthritis pain in mice.

The sigma-1 receptor is also described as a chaperone (Maurice and Su, 2009), and the knowledge on its interactome is increasingly growing. The review by Morales-Lázaro et al. gives further details about the interactions between the sigma-1 receptor and ion channels, bringing together details of how ligands for the sigma-1 receptor can regulate functional properties and the expression of some sodium, calcium, potassium, and TRP ion channels. The effects of agonists and antagonists at the sigma-1 receptor are discussed. Also focusing on the interactome of sigma-1 receptors, Cortés-Montero et al. show that sigma-1 receptors bind specific regions of TRP ankyrin member 1 (TRPA1), TRP vanilloid member 1 (TRPV1), and TRP melastatin member 8 (TRPM8) in a calcium sensitive manner. Agonists and antagonists are able to regulate interactions of the sigma-1 receptor with TRPA1, TRPM8, and TRPV1 in opposing fashions. This study adds significantly to our understanding about the mechanisms of action of sigma-1 receptors on nociception.

Other potential uses of sigma-1 receptor antagonists are in the treatment of cancers. Sigma-1 receptor antagonists show desirable properties, as they readily kill most tumor cell lines, while having minimal effect on most non-tumor cells (Spruce et al., 2004). A rigorous review by Oyer et al. brings together the information regarding the consequences of targeting sigma-1 and sigma-2 receptors in cancer. The consensus lies with sigma-1 receptor antagonists reducing proliferation. While the distinction between agonists and antagonists at the sigma-2 receptor remains uncertain, it appears that agonists at this receptor also possess antiproliferative properties. The pathways involved in sigma receptor signaling are logically presented and this paper provides an excellent guide to both established and naïve researchers in the sigma receptor field.

Adding new evidence on the potential use of sigma ligands as antineoplastics, Tesei et al. show the mixed sigma-1 receptor antagonist/sigma-2 receptor agonist RC-106 has anti-cancer properties in pancreatic cell lines. Treatment of cells with RC-106 drives apoptosis *via* upregulation of GRP78/BiP, ATF4, and CHOP mRNA expression levels, a common means of monitoring the ER unfolded protein response. With favorable pharmacokinetics and pancreas distribution, Tesei et al. propose RC-106 as a good candidate for further investigation *in vivo*.

In addition to the potential antineoplastic effects of sigma ligands, early data with *in vivo* localization of primary tumors and their metastases (Kawamura et al., 2005) in animal models have highlighted the value of imaging tools targeting the sigma receptors. Ludwig et al. further characterize (S)-[<sup>18</sup>F] fluspidine and identify its biological half-life and route of metabolism. The profile obtained *in vitro* and *in vivo* suggest (S)-[<sup>18</sup>F] fluspidine is suitable for PET imaging in humans.

In a review considering alcohol use disorder, Quadir et al. bring together data on the paucity of current treatments and the potential offered by sigma-1 receptor antagonists: antagonists reduce alcohol consumption, motivation to drink, and alcohol-seeking behavior. The use of knock-out mice verifies that sigma-1 receptors play a critical role in alcohol-mediated stimulant, motivational, and reward properties observed.

With so much interest in sigma receptors, it is key that the assays used to quantify receptor number in cells, and characterize ligand interactions are robust. Following on from a previous paper in which sigma-1 receptor binding to antagonists showed two affinity states in a GTP-dependent manner (Brimson et al., 2011), we now see a cautionary tale of why masking protocols, widely used for studying sigma-2 receptor interactions, should not be used. A common practice is to “mask” sigma-1 receptors with (+) pentazocine (or dextrallorphan) while using the pan-sigma ligand, [<sup>3</sup>H] DTG as radioligand. Abbas et al. demonstrate that saturation binding assays will permit DTG to bind sigma-1 receptors, hence over-estimating the sigma-2 receptor population. Equally, (+) pentazocine and dextrallorphan will bind to sigma-2 receptors and affect the apparent affinity of ligands for that receptor.

Remodeling the pharmacophore for the sigma-1 receptor is also undertaken: using the crystal structure (Schmidt et al., 2016) and binding data from over 25,000 ligands, Pascual et al. refine

interaction predictions which can be used to design novel drugs targeting this receptor.

In their review, Vavers et al. lead us through the first identification of an allosteric regulator of sigma-1 receptors: phenytoin, notorious for its zero-order kinetics and induction of cytochrome P450 enzymes, is also a positive allosteric modulator (PAM) of the sigma-1 receptor. While the antiseizure activity of phenytoin is not reversed by BD-1047, a sigma-1 receptor antagonist, the activity of many other PAMs is reversed. Today, several PAMs have been identified acting at the sigma-1 receptor and are shown to exert potent *in vivo* effects, such as improving memory and bearing antidepressant activity.

With such a variety of very important results, articles presented in this topic very nicely illustrate the dynamism and importance of present research in sigma receptors. With such interesting recent developments in the field, we hope we can bring an update in the near future as the research contained herein is brought to fruition.

## AUTHOR CONTRIBUTIONS

All authors contributed to the article and approved the submitted version.

## REFERENCES

- Alon, A., Schmidt, H. R., Wood, M. D., Sahn, J. J., Martin, S. F., and Kruse, A. C. (2017). Identification of the gene that codes for the sigma2 receptor. *Proc. Natl. Acad. Sci. U. S. A.* 114 (27), 7160–7165. doi: 10.1073/pnas.1705154114
- Brimson, J. M., Brown, C. A., and Safrany, S. T. (2011). Antagonists show GTP-sensitive high-affinity binding to the sigma-1 receptor. *Br. J. Pharmacol.* 164 (2b), 772–780. doi: 10.1111/j.1476-5381.2011.01417.x
- Fontanilla, D., Johannessen, M., Hajipour, A. R., Cozzi, N. V., Jackson, M. B., and Ruoho, A. E. (2009). The hallucinogen N,N-dimethyltryptamine (DMT) is an endogenous sigma-1 receptor regulator. *Science* 323 (5916), 934–937. doi: 10.1126/science.1166127
- Hanner, M., Moebius, F. F., Flandorfer, A., Knaus, H. G., Striessnig, J., Kempner, E., et al. (1996). Purification, molecular cloning, and expression of the mammalian sigma1-binding site. *Proc. Natl. Acad. Sci. U. S. A.* 93 (15), 8072–8077. doi: 10.1073/pnas.93.15.8072
- Kawamura, K., Kubota, K., Kobayashi, T., Elsinga, P. H., Ono, M., Maeda, M., et al. (2005). Evaluation of [<sup>11</sup>C]SA5845 and [<sup>11</sup>C]SA4503 for imaging of sigma receptors in tumors by animal PET. *Ann. Nucl. Med.* 19 (8), 701–709. doi: 10.1007/BF02985120
- Kekuda, R., Prasad, P. D., Fei, Y. J., Leibach, F. H., and Ganapathy, V. (1996). Cloning and functional expression of the human type 1 sigma receptor (hSigmaR1). *Biochem. Biophys. Res. Commun.* 229 (2), 553–558. doi: 10.1006/bbrc.1996.1842
- Martin, W. R., Eades, C. G., Thompson, J. A., Huppler, R. E., and Gilbert, P. E. (1976). Effects of Morphine-Like and Nalorphine-Like Drugs in Nondependent and Morphine-Dependent Chronic Spinal Dog. *J. Pharmacol. Exp. Ther.* 197 (3), 517–532.
- Maurice, T., and Su, T. P. (2009). The pharmacology of sigma-1 receptors. *Pharmacol. Ther.* 124 (2), 195–206. doi: 10.1016/j.pharmthera.2009.07.001
- Schmidt, H. R., Zheng, S., Gurpinar, E., Koehl, A., Manglik, A., and Kruse, A. C. (2016). Crystal structure of the human sigma1 receptor. *Nature* 532 (7600), 527–530. doi: 10.1038/nature17391
- Spruce, B. A., Campbell, L. A., McTavish, N., Cooper, M. A., Appleyard, M. V., O'Neill, M., et al. (2004). Small molecule antagonists of the sigma-1 receptor cause selective release of the death program in tumor and self-reliant cells and inhibit tumor growth in vitro and in vivo. *Cancer Res.* 64 (14), 4875–4886. doi: 10.1158/0008-5472.CAN-03-3180
- Tejada, M. A., Montilla-Garcia, A., Cronin, S. J., Cikes, D., Sanchez-Fernandez, C., Gonzalez-Cano, R., et al. (2017). Sigma-1 receptors control immune-driven peripheral opioid analgesia during inflammation in mice. *Proc. Natl. Acad. Sci. U. S. A.* 114 (31), 8396–8401. doi: 10.1073/pnas.1620068114

**Conflict of Interest:** The authors declare that the research was conducted in the absence of any commercial or financial relationships that could be construed as a potential conflict of interest.

Copyright © 2020 Aydar, Cobos, Maurice, Murell-Lagnado and Safrany. This is an open-access article distributed under the terms of the Creative Commons Attribution License (CC BY). The use, distribution or reproduction in other forums is permitted, provided the original author(s) and the copyright owner(s) are credited and that the original publication in this journal is cited, in accordance with accepted academic practice. No use, distribution or reproduction is permitted which does not comply with these terms.





# Modulation by Sigma-1 Receptor of Morphine Analgesia and Tolerance: Nociceptive Pain, Tactile Allodynia and Grip Strength Deficits During Joint Inflammation

Ángeles Montilla-García<sup>1,2</sup>, Miguel Á. Tejada<sup>1,2</sup>, M. Carmen Ruiz-Cantero<sup>1,2</sup>, Inmaculada Bravo-Caparrós<sup>1,2</sup>, Sandra Yeste<sup>3</sup>, Daniel Zamanillo<sup>3</sup> and Enrique J. Cobos<sup>1,2,4,5\*</sup>

<sup>1</sup> Department of Pharmacology, Faculty of Medicine, University of Granada, Granada, Spain, <sup>2</sup> Institute of Neuroscience, The Biomedical Research Centre, University of Granada, Granada, Spain, <sup>3</sup> Drug Discovery and Preclinical Development, ESTEVE, Barcelona, Spain, <sup>4</sup> Teófilo Hernando Institute for Drug Discovery, Madrid, Spain, <sup>5</sup> Biosanitary Research Institute, University Hospital Complex of Granada, Granada, Spain

## OPEN ACCESS

### Edited by:

Ajay Sharma,  
Chapman University, United States

### Reviewed by:

Carmela Parenti,  
Università degli Studi di Catania, Italy  
Salvatore Salomone,  
Università degli Studi di Catania, Italy

### \*Correspondence:

Enrique J. Cobos  
ejcobos@ugr.es

### Specialty section:

This article was submitted to  
Experimental Pharmacology  
and Drug Discovery,  
a section of the journal  
Frontiers in Pharmacology

**Received:** 18 October 2018

**Accepted:** 06 February 2019

**Published:** 22 February 2019

### Citation:

Montilla-García Á, Tejada MÁ, Ruiz-Cantero MC, Bravo-Caparrós I, Yeste S, Zamanillo D and Cobos EJ (2019) Modulation by Sigma-1 Receptor of Morphine Analgesia and Tolerance: Nociceptive Pain, Tactile Allodynia and Grip Strength Deficits During Joint Inflammation. *Front. Pharmacol.* 10:136. doi: 10.3389/fphar.2019.00136

Sigma-1 receptor antagonism increases the effects of morphine on nociceptive pain, even in morphine-tolerant animals. However, it is unknown whether these receptors are able to modulate morphine antinociception and tolerance during inflammatory pain. Here we used a mouse model to test the modulation of morphine effects by the selective sigma-1 antagonist S1RA (MR309), by determining its effect on inflammatory tactile allodynia (von Frey filaments) and on grip strength deficits induced by joint inflammation (a measure of pain-induced functional disability), and compared the results with those for nociceptive heat pain recorded with the unilateral hot plate (55°C) test. The subcutaneous (s.c.) administration of morphine induced antinociceptive effects to heat stimuli, and restored mechanical threshold and grip strength in mice with periarticular inflammation induced by Complete Freund's Adjuvant. S1RA (80 mg/kg, s.c.) administered alone did not induce any effect on nociceptive heat pain or inflammatory allodynia, but was able to partially reverse grip strength deficits. The association of S1RA with morphine, at doses inducing little or no analgesic-like effects when administered alone, resulted in a marked antinociceptive effect to heat stimuli and complete reversion of inflammatory tactile allodynia. However, S1RA administration did not increase the effect of morphine on grip strength deficits induced by joint inflammation. When S1RA (80 mg/kg, s.c.) was administered to morphine-tolerant animals, it rescued the analgesic-like effects of this opioid in all three pain measures. However, when S1RA was repeatedly given during the induction of morphine tolerance (and not on the day of behavioral evaluation) it failed to affect tolerance to the effects of morphine on nociceptive heat pain or inflammatory allodynia, but completely preserved the effects of this opioid on grip strength deficits. These effects of S1RA on morphine tolerance cannot be explained by pharmacokinetic interactions, given that

the administration of S1RA did not modify concentrations of morphine or morphine-3-glucuronide (a major morphine metabolite) in morphine-tolerant animals in plasma or brain tissue. We conclude that sigma-1 receptors play a pivotal role in the control of morphine analgesia and tolerance in nociceptive and inflammatory pain, although in a manner dependent on the type of painful stimulus explored.

**Keywords:** sigma-1 receptors, morphine, pain, analgesia, tolerance, joint inflammation, grip strength, von Frey threshold

## INTRODUCTION

Inflammatory pain is characterized by a decrease in the cutaneous sensory threshold, and by pain-induced decreases in physical function, which affect the quality of life of patients with inflammatory conditions (Salaffi et al., 2009). Cutaneous mechanical thresholds and physical function can be measured, in both humans and rodents, with von Frey filaments (cutaneous sensitivity) and grip strength testing (physical function) (Chandran et al., 2009; Cobos and Portillo-Salido, 2013; Lee, 2013; Helfert et al., 2015). Alterations in von Frey thresholds and pain-induced grip strength deficits during inflammation result (at least partially) from non-overlapping mechanisms, including the involvement of different subsets of primary afferents (Montilla-García et al., 2017). Despite their differences, both of these outcomes are sensitive to opioid analgesics, which can restore both normal sensory thresholds and physical functioning (Montilla-García et al., 2017).

Sigma-1 receptors are a promising novel pharmacological target for pain treatment (Romero et al., 2016; Sánchez-Fernández et al., 2017). Among the selective sigma-1 antagonists, the best characterized is S1RA, also known as MR309 (Vela et al., 2015). This compound is the only sigma-1 antagonist which has been evaluated in clinical trials with an intended indication for pain relief. S1RA has already been evaluated with positive results in several Phase II clinical trials for neuropathic pain (Bruna et al., 2018). Preclinical studies have shown that sigma-1 inhibition enhances the antinociception induced by opioid drugs, including morphine (reviewed in Zamanillo et al., 2013; Sánchez-Fernández et al., 2017). In addition, sigma-1 antagonism is able to rescue morphine antinociception in mice rendered tolerant to this opioid (Vidal-Torres et al., 2013; Rodríguez-Muñoz et al., 2015). Therefore, sigma-1 antagonists are promising tools as opioid adjuvants (Vela et al., 2015; Sánchez-Fernández et al., 2017), and in fact a further potential indication for S1RA in human patients might be to enhance opioid analgesia (Vela et al., 2015). Preclinical findings on the enhancement of opioid antinociception by sigma-1 inhibition have thus far been reported exclusively in models of nociceptive pain. It is known that opioid receptor functioning can change during inflammation (reviewed in Stein et al., 2009); therefore, the mechanisms involved in the modulation of opioid antinociception by sigma-1 receptor may not be the same during inflammation as in conditions not involving injury.

In light of these antecedents, we aimed to test whether the sigma-1 receptor antagonist S1RA enhanced morphine

antinociception or modulated morphine analgesic tolerance during inflammatory pain. We measured both the antiallodynic effect of morphine as a measure of cutaneous sensory hypersensitivity, and the recovery of grip strength deficits induced by this opioid as a measure of the impact of pain on physical function. As a control for the known effects of sigma-1 antagonism on nociceptive pain, we also investigated heat antinociception in animals without inflammation. This allowed us to compare the effects of morphine, S1RA, and their association on nociceptive heat pain, inflammatory tactile allodynia and functional deficits (grip strength) induced by inflammatory pain.

## MATERIALS AND METHODS

### Experimental Animals

Female CD1 mice (Charles River, Barcelona, Spain) were used in all experiments. We choose female animals because it has been reported that women may be at greater risk for pain-related disability than men (e.g., Unruh, 1996; Stubbs et al., 2010). Animals weighing 25–30 g were tested randomly throughout the estrous cycle. This mouse strain has been previously reported not to show variations in opioid analgesia during the phases of the estrous cycle (Mogil et al., 2000). All mice were housed in colony cages with free access to food and water prior to the experiments, and were kept in temperature- and light-controlled rooms ( $22 \pm 2^\circ\text{C}$ , 12-h light–dark cycle). The experiments were performed during the light phase from 9:00 a.m. to 3:00 p.m. Animal care was provided in accordance with institutional (Research Ethics Committee of the University of Granada, Granada, Spain), regional (Junta de Andalucía, Spain) and international standards (European Communities Council directive 2010/63). All mice were used in only one experimental procedure (heat nociception, von Frey testing or grip strength measurement).

### CFA-Induced Periarticular Inflammation

To induce the inflammation, mice were injected periarticularly with Complete Freund's Adjuvant (CFA) (Sigma-Aldrich, Madrid, Spain) according to a previously described method (Montilla-García et al., 2017). In most experiments, CFA was administered subcutaneously (s.c.) around the tibiotarsal joint in two separate injections to the inner and outer side of the joint, at a volume of 15  $\mu\text{L}$ /injection (30  $\mu\text{L}$ /paw) to



obtain homogeneous inflammation. In some experiments CFA was administered with the same procedure described above but using a lower injection volume (5  $\mu$ L/injection; i.e., 10  $\mu$ L/paw). Control animals received the same volume of sterile physiological saline (0.9% NaCl) with the same procedure. Injections were made with a 1710 TLL Hamilton microsyringe (Teknokroma, Barcelona, Spain) and a 30 $\frac{1}{2}$ -gauge needle under isoflurane anesthesia (IsoVet®, B. Braun, Barcelona, Spain). Behavioral evaluations in mice with induced inflammation were done 2 days after CFA or saline injection, since we previously reported that both tactile allodynia and grip strength deficits peak at this time (Montilla-García et al., 2017). Inflammatory edema was monitored by measuring ankle thickness with an electronic caliper (Montilla-García et al., 2017), also 2 days after CFA administration.

## Drugs and Drug Administration

We used the opioid agonist morphine (supplied by the General Directorate of Pharmacy and Drugs, Spanish Ministry of Health, Spain). S1RA (4-[2-[[5-methyl-1-(2-naphthalenyl)1H-pyrazol-3-yl]oxy]ethyl] morpholine hydrochloride) (DC Chemicals, Shanghai, China) was used as a selective sigma-1 antagonist (Cobos et al., 2008; Romero et al., 2012). The dose of sigma-1 antagonist used in the present study (80 mg/kg) was high enough to induce a maximal effect in several pain models (Nieto et al., 2012; Sánchez-Fernández et al., 2013, 2014; Tejada et al., 2014, 2017). This same dose has been used in the formalin test (Romero et al., 2012), and higher doses of this compound (128 mg/kg) have been used in inflammatory heat hyperalgesia (Tejada et al., 2014, 2017), neuropathic cold allodynia (Nieto et al., 2012), and visceral pain (González-Cano et al., 2013). This last study showed that the s.c. administration of S1RA at 128 mg/kg still had selective analgesic effects (present in wild-type but absent in sigma-1 knockout mice). PRE-084 ([2-(4-morpholinethyl) 1-phenylcyclohexanecarboxylate hydrochloride]) (Tocris Cookson Ltd., Bristol, United Kingdom) was used as a selective sigma-1 agonist (Hayashi and Su, 2004; Cobos et al., 2008). We used half of the dose for PRE-084 than the dose used for S1RA in all experiments (i.e., 40 mg/kg of PRE-084). This dose was selected based in our previous experience in which we usually use this proportion of PRE-084/S1RA to fully reverse the effects of the sigma-1 antagonist (e.g., Sánchez-Fernández et al., 2013, 2014). In addition, in some experiments we used (+)-pentazocine (Sigma-Aldrich S.A.) as an additional selective sigma-1 agonist (Hayashi and Su, 2004; Cobos et al., 2008). All drugs were dissolved in sterile physiological saline (0.9% NaCl); the PRE-084 solution was appropriately alkalized with NaOH. To evaluate the effects of systemic treatments, drugs were injected s.c. into the interscapular zone in a volume of 5 mL/kg. When the effect of the association of two or more drugs was tested, each drug was injected into a different area of the interscapular zone.

In experiments on the acute effects of systemic morphine alone or its association with S1RA, morphine was injected s.c. 30 min before the behavioral evaluation, and S1RA immediately before morphine injection. When PRE-084 or (+)-pentazocine

were used to reverse the effect of S1RA, they were injected s.c. 5 min before S1RA.

Morphine tolerance was induced by a modification of the protocol we used in a previous study (Vidal-Torres et al., 2013). Briefly, morphine tolerance was induced with a 3-day cumulative dosage regimen consisting of twice-daily s.c. injections (b.i.d.) at 9:30 a.m. and 9:30 p.m., starting on day 1 at 9:30 a.m. The individual doses were 30 mg/kg (a.m.) and 45 mg/kg (p.m.) on day 1, 60 mg/kg (a.m.) and 80 mg/kg (p.m.) on day 2, and 100 mg/kg (a.m.) and 120 mg/kg (p.m.) on day 3. To avoid tissue lesions by repeated injections, morphine administration was rotated in each of the four quadrants of the back of the mice.

To study whether S1RA administration was able to rescue morphine antinociception from tolerance once the latter was fully developed, on day 4, after the tolerance protocol was completed, mice were randomized to receive a test dose of morphine s.c. (4 mg/kg in tactile allodynia, and 8 mg/kg in heat nociception and grip strength) alone or associated with S1RA (80 mg/kg, s.c. for both tests), and then the behavioral effects were recorded (Figure 1, Protocol I). As in the protocol used to explore the acute effect of morphine alone and the influence of S1RA on the effects of this opioid, morphine was administered immediately after S1RA, 30 min before the behavioral evaluation. PRE-084 was administered 5 min before S1RA.

To study whether S1RA was able to prevent the development of morphine tolerance, mice were given S1RA (b.i.d. 80 mg/kg, s.c.) immediately after each morphine injection during the induction of analgesic tolerance (Figure 1, Protocol II). For each set of injections, each drug was injected in a different area of the interscapular zone according to the rotation protocol. Behavioral testing was done on day 4 with the same doses of morphine as reported in the preceding paragraph.

Injections of the drug solvent (saline) were used in all cases as a control.

## Measurement of Heat Nociception (Unilateral Hot Plate)

Heat nociception was assessed as previously described (Menéndez et al., 2002; Montilla-García et al., 2018). The plantar side of the stimulated hind paw was placed on the surface of a thermal analgesiometer (Model PE34, Series 8, IITC Life Science Inc., Los Angeles, CA, United States) previously set at  $55 \pm 1^\circ\text{C}$  until the animal showed a paw withdrawal response. The latency in seconds from paw stimulation to the behavioral response was measured with a digital chronometer. Only a clear unilateral withdrawal of the paw was recorded as a nociceptive response. We avoided simultaneous heat stimulation in both hind paws by placing the plantar side of the tested hind paw on the hot plate while the other hind paw was placed on filter paper (off the hot plate) during observations (see Supplementary Video 2 in2 in Montilla-García et al., 2018). Two alternating evaluations were done in each hind paw at intervals of 1 min between each stimulation. A 50-s cut-off was used for each measurement to prevent tissue damage. The mean value of the two averaged

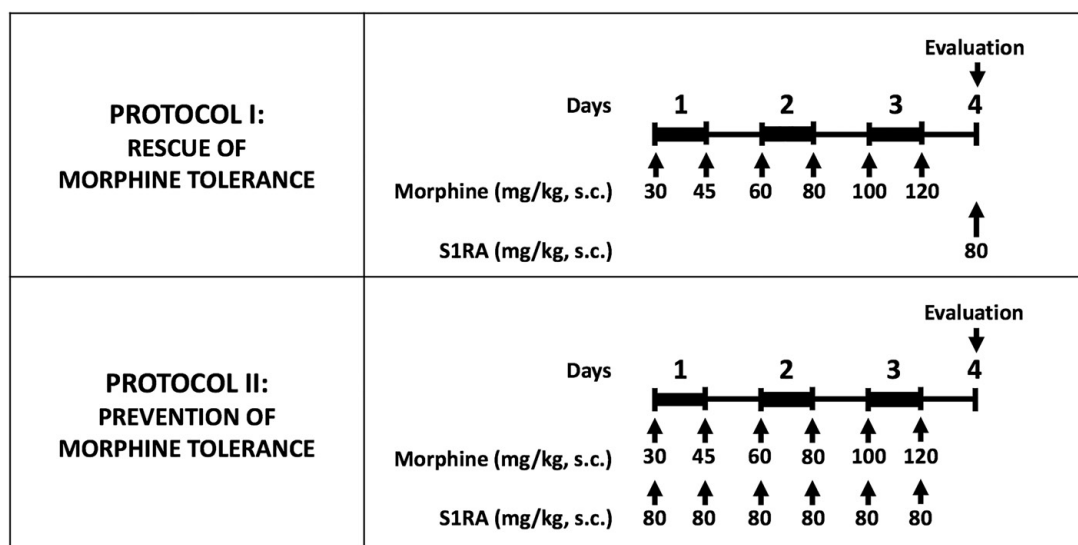


**FIGURE 1 |** Experimental protocols used to investigate the effect of S1RA on morphine tolerance. Morphine tolerance was induced with a 3-day cumulative dosage regimen using the subcutaneous doses of morphine shown in the Figure. The upper panel shows the protocol used to test the effects of S1RA on rescue of the effect of morphine from tolerance once it was fully developed. The lower panel shows the protocol to study the effect of S1RA on prevention of the development of morphine tolerance. Drugs or their solvent (saline) were administered subcutaneously (s.c.). In all cases, “Evaluation” indicates the time when heat nociception, von Frey threshold or grip strength was measured, which was always on day 4 after the first morphine administration. On the evaluation day all animals received a dose of morphine (4 or 8 mg/kg sc. depending on the experiment; see text for details) 30 min before the pain response was evaluated.

measurements for each hind paw was used to analyze the effects of treatments.

### Measurement of von Frey Threshold

Tactile allodynia to a punctate stimulus was studied with the method described in a previous publication (Cobos et al., 2018). Briefly, animals were acclimated for 2 h in methacrylate test compartments (7.5 cm wide × 7.5 cm long × 15 cm high) placed on an elevated mesh-bottomed platform, to provide access to the plantar surface of the hind paws. The von Frey stimulations were applied to the heel, because our CFA injection protocol led to inflammation and tactile allodynia most prominently in this area (Montilla-García et al., 2017). A logarithmic series of calibrated von Frey monofilaments (Stoelting, Wood Dale, IL, United States), with bending forces that ranged from 0.02 to 1.4 g, were applied with the up-down paradigm (Chaplan et al., 1994), starting with the 0.6-g filament. Filaments were applied twice for 2–3 s, with between-application intervals of at least 30 s to avoid sensitization to the mechanical stimuli. The response to the filament was considered positive if immediate licking or biting, flinching or rapid withdrawal of the stimulated paw was observed.

### Measurement of Grip Strength

Grip strength was measured with a computerized grip strength meter (Model 47200, Ugo Basile, Varese, Italy) according to the method reported previously (Montilla-García et al., 2017). To measure grip strength in the hind paws, the experimenter held the mouse gently by the base of the tail, allowing the animal to grasp the metal bar of the grip strength meter

with its hind paws. The metal bar was connected to a force transducer that automatically recorded the peak force of each measurement in grams (g). Hind limb grip strength in each mouse was measured in triplicate. To prevent mice from gripping the metal bar with their forepaws during the recording, the animals were first allowed to grasp a wire mesh cylinder with their forepaws (see Supplementary Video in Montilla-García et al., 2017). Baseline grip strength values were recorded for each animal as the average of two determinations on different days before the administration of CFA or saline. This value was considered 100% of grip strength and used as a reference for subsequent determinations.

### Determination of the Concentration of S1RA, Morphine and Morphine 3-Glucuronide in Plasma and Brain Tissue

To study whether the effects of S1RA on morphine tolerance were due to pharmacokinetic interactions between the sigma-1 antagonist and the opioid drug, we measured the concentration in plasma and brain tissue of S1RA, morphine and morphine-3-glucuronide, the major morphine metabolite in rodents (Pasternak and Pan, 2013). The concentrations of these compounds in plasma and brain tissue were measured according to the time when the behavioral effects of drug treatments were assessed, as described in the Section “Drugs and Drug Administration.” Briefly, a terminal blood sample was drawn from each mouse by cardiac puncture, at the appropriate time after vehicle or compound dosing. Blood

samples were collected in heparinized tubes and centrifuged at 2,000 g for 10 min to obtain plasma. Immediately after blood extraction, whole brains were removed. Plasma samples and brains were stored at  $-80^{\circ}\text{C}$  until analysis. Each brain was weighed and homogenized in 4 mL Dulbecco's phosphate buffered saline immediately before drug concentrations were determined. Protein was precipitated with acetonitrile, and samples were analyzed by high-performance liquid chromatography–triple quadrupole mass spectrometry (HPLC-MS/MS). The concentrations of compounds in plasma and brain were determined by least-squares linear regression with a calibration curve.

## Data Analysis

The data were analyzed with the SigmaPlot 12.0 program (Systat Software Inc., San Jose, CA, United States). One-way, two-way, or two-way repeated-measures analysis of variance (ANOVA) was used depending on the experiment; Student–Newman–Keuls *post hoc* test was done in all cases. The

differences between means were considered significant when the *P*-value was below 0.05.

## RESULTS

### Modulation by S1RA of Morphine-Induced Antinociception to Heat Stimulus

The paw withdrawal latency to a nociceptive heat stimulus in mice without inflammation was short, i.e., less than 5s (**Figure 2A**). Morphine administration (2–8 mg/kg, s.c.) induced dose-dependent robust antinociceptive effects, reaching values of about 30 s at the highest dose tested (**Figure 2A**).

In contrast to morphine, the selective sigma-1 antagonist S1RA (80 mg/kg, s.c.) failed to alter the response latency of mice to a nociceptive heat stimulus (**Figure 2B**). However, when we associated this dose of S1RA with morphine 4 mg/kg (s.c.), the response latency increased markedly (**Figure 2B**).

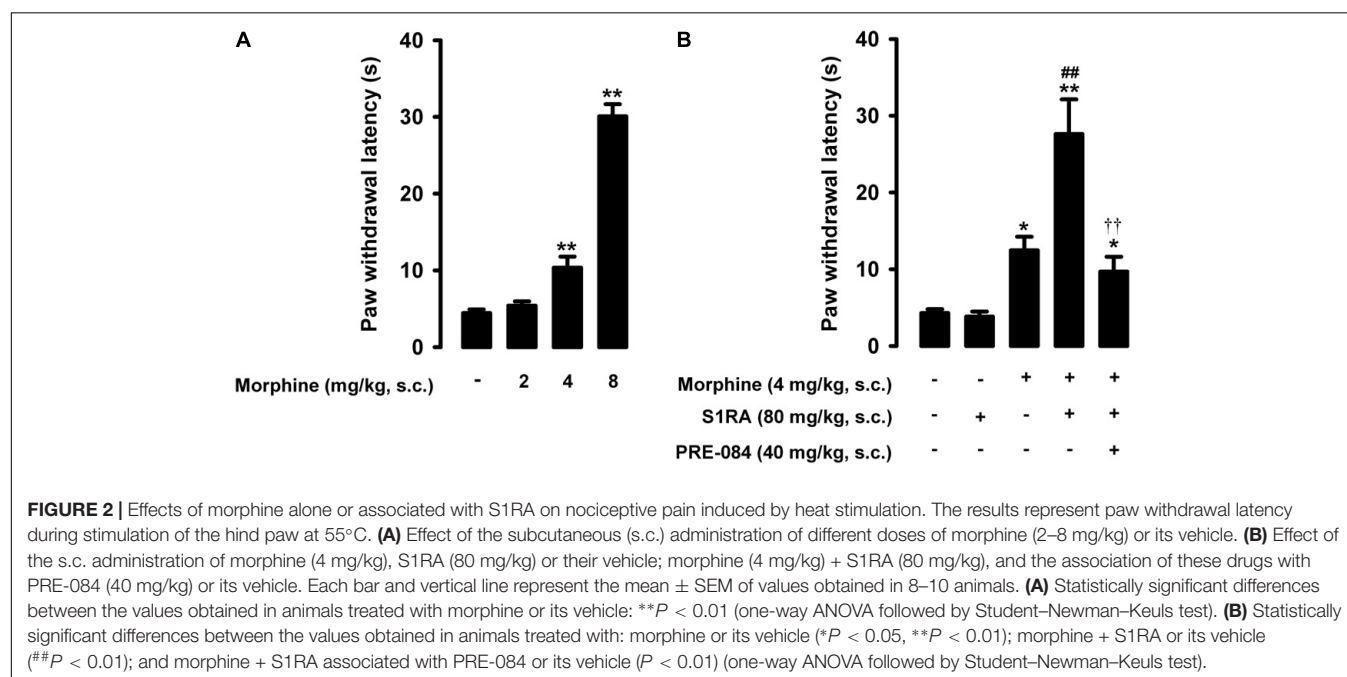


**TABLE 1 |** Summary of the main results for the role of sigma-1 receptors in nociceptive heat pain and inflammation-induced tactile allodynia and grip strength deficits.

Type of pain	Stimulus	Sensitivity to morphine	Sensitivity to S1RA	Potentiation of morphine by S1RA	Effect of S1RA on morphine tolerance	
					Rescue of morphine tolerance	Prevention of morphine tolerance
Nociceptive	Heat	+	–	+	+	–
Inflammatory	von Frey	+++	–	+	+	–
	Grip strength	++	+	–	+	+

S1RA was always administered subcutaneously (s.c.) at 80 mg/kg. The doses of morphine used to test the potentiation of its effect by S1RA varied according to the sensitivity to the opioid in each test (1 mg/kg for von Frey testing in mice with inflammation, and 2–4 mg/kg for nociceptive heat pain and grip strength deficits induced by inflammation), and in the evaluation of analgesic tolerance (4 mg/kg for von Frey testing in mice with inflammation, and 8 mg/kg for nociceptive heat pain and grip strength deficits induced by inflammation).

S1RA also increased the antinociceptive effect induced by morphine 2 mg/kg (s.c.), but to a lesser extent (data not shown). We also evaluated the effects of the sigma-1 agonist PRE-084 (40 mg/kg, s.c.) on heat antinociception induced by the association of S1RA with morphine, and found that treatment with the sigma-1 agonist abolished the S1RA-induced potentiation of morphine antinociception (**Figure 2B**). When PRE-084 was administered alone it failed to induce any effect on nociception (data not shown). These results support the selectivity of the effects induced by S1RA. Therefore, S1RA appeared to enhance the antinociceptive effect of morphine to a heat stimulus through sigma-1 inhibition. These results are summarized in **Table 1**.

### Modulation by S1RA of Tolerance to the Antinociceptive Effect of Morphine in Response to Heat Stimulus

Animals were rendered morphine-tolerant with a 3-day escalating dosage regimen (**Figure 1**). Control non-tolerant mice were treated with the morphine vehicle. On day 4, non-tolerant mice showed a marked increase in the response latency induced by a morphine dose shown in the previous experiments (see section “Modulation by S1RA of Morphine-Induced Antinociception to Heat Stimulus”) to induce evident antinociception (8 mg/kg, s.c.) (**Figure 3A**, black bars). However, the effect induced by this morphine dose was markedly lower in morphine-tolerant mice, with a paw withdrawal latency of  $29.01 \pm 3.67$  s in non-tolerant mice vs.  $9.25 \pm 1.95$  s in tolerant mice in response to morphine (**Figure 3A**). In animals rendered tolerant to morphine, we associated the administration of S1RA (80 mg/kg, s.c.) to morphine (8 mg/kg, s.c.) according to Protocol I in **Figure 1**, and found that the response latency was longer, reaching times similar to those in control non-tolerant mice. This result indicated that S1RA was able to rescue morphine antinociception in tolerant animals (**Figure 3A**). The administration of PRE-084 (40 mg/kg, s.c.) completely abolished the increase in the antinociceptive effect of morphine induced by S1RA in morphine-tolerant mice: the latency values were close to those found in tolerant mice treated with morphine alone on the day of the experiment (**Figure 3A**). When PRE-084 was administered alone it failed to induce any effect on nociception (data not shown).

We also tested whether the repeated administration of S1RA (80 mg/kg, s.c.) before each dose of morphine during the 3-day period of morphine administration had any pre-emptive effect on the appearance of morphine tolerance to its effect on nociceptive heat pain (according to Protocol II in **Figure 1**). When the effect of morphine (8 mg/kg, s.c.) was tested on day 4 without any further administration of S1RA, the effect of morphine was lower (**Figure 3B**). These results indicated that tolerance to the antinociceptive effect of morphine on the response to a heat stimulus was present despite repeated pre-emptive S1RA administration.

Therefore, sigma-1 receptor inhibition by S1RA was able to restore the antinociceptive effect of morphine to heat stimulation in mice tolerant to this opioid, but pre-emptive S1RA

treatment failed to affect the development of tolerance to the effect of morphine on nociceptive heat pain. These results are summarized in **Table 1**.

### Modulation by S1RA of the Antiallodynic Effect of Morphine During Inflammation

In mice with CFA injected around the tibiotarsal joint (30  $\mu$ L/paw), the mechanical pain threshold in the heel was markedly reduced, denoting the presence of tactile allodynia ( $0.73 \pm 0.05$  g and  $0.06 \pm 0.01$  g in mice without and with inflammation, respectively) (**Figure 4A**). Joint inflammation did not induce alterations in the von Frey threshold in the non-inflamed area (pad) of the paw (data not shown), indicating that sensory alterations appeared to be restricted to the inflamed area. Morphine administration (1–4 mg/kg, s.c.) induced a dose-dependent antiallodynic effect in animals with inflammation, and the normal mechanical threshold was fully recovered at the highest dose tested (**Figure 4A**). The effect of morphine was more prominent in tactile allodynia than in nociceptive heat pain: the doses needed to induce significant effects were lower in the former assay (compare **Figures 2A, 4A**).

The administration of S1RA alone (80 mg/kg, s.c.) did not ameliorate inflammatory tactile allodynia (**Figure 4B**). However, the association of this dose of S1RA with a low dose of morphine (1 mg/kg, s.c.), which was also devoid of antiallodynic effect *per se*, resulted in a marked synergistic increase in the mechanical threshold in mice with induced inflammation: the values in these animals were similar to those in mice in which inflammation was not induced (**Figure 4B**). As reported above for heat nociception, the administration of the sigma-1 agonist PRE-084 (40 mg/kg, s.c.) abolished the potentiation induced by S1RA of the antiallodynic effect of morphine (**Figure 4B**); this result supports the notion that the effects induced by S1RA are selective. We thus found that S1RA enhanced the antiallodynic effect of morphine through sigma-1 inhibition. These results are summarized in **Table 1**.

Interestingly, when this dose of S1RA (80 mg/kg, s.c.) was assayed in mice with a lower degree of inflammation (10  $\mu$ L CFA/paw), it was able to fully recover the normal mechanical threshold in mice with inflammation in the absence of morphine administration (**Supplementary Figure S1**), indicating that this compound is able to exert antiallodynic effects, albeit in milder inflammation. The antiallodynic effect induced by S1RA was abolished by PRE-084 (40 mg/kg, s.c.), a result that supports the selectivity of the effects induced by S1RA (**Supplementary Figure S1**).

### Modulation by S1RA of Tolerance to the Antiallodynic Effect of Morphine During Inflammation

As described above for heat nociception, animals were rendered morphine-tolerant with a 3-day escalating dosage regimen (**Figure 1**), whereas control non-tolerant mice received the morphine vehicle. On day 4, non-tolerant mice with inflammation (30  $\mu$ L CFA/paw) showed complete reversion of inflammatory tactile allodynia induced by the acute



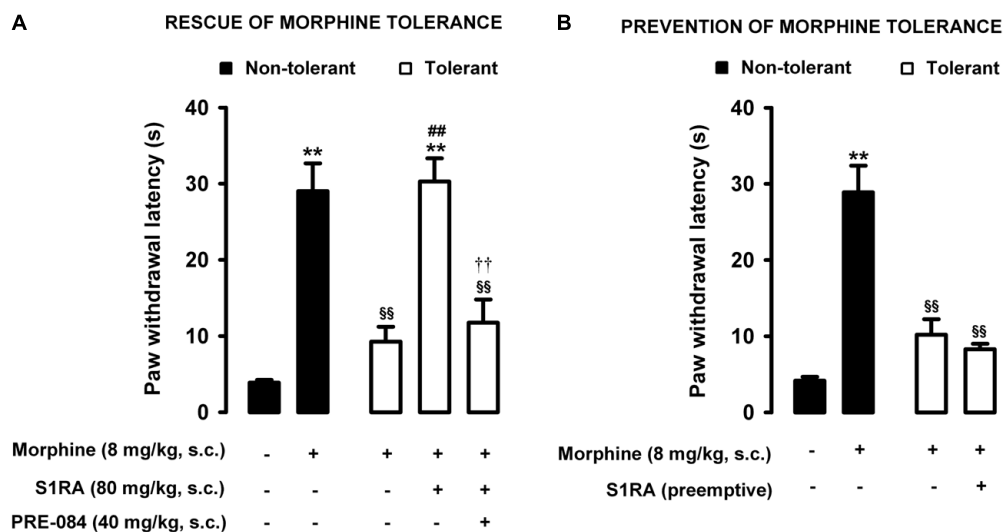


**FIGURE 3 |** Modulation by S1RA of tolerance to the effect of morphine on nociceptive pain caused by heat stimulation. The results represent paw withdrawal latency during stimulation of the hind paw at 55°C. **(A)** Rescue of morphine tolerance by S1RA: animals were repeatedly treated during 3 days with morphine (tolerant, white bars) or its vehicle (non-tolerant, black bars), according to Protocol I in **Figure 1**. On the day of evaluation (day 4) mice were treated subcutaneously (s.c.) with morphine (8 mg/kg) or its vehicle, morphine (8 mg/kg) + S1RA (80 mg/kg) or its vehicle, or the combination of these drugs with PRE-084 (40 mg/kg) or its vehicle. **(B)** Prevention of morphine tolerance by S1RA: animals were treated s.c. with S1RA (80 mg/kg) or its vehicle immediately before each dose of morphine (tolerant, white bars) during the induction of morphine tolerance, according to Protocol II in **Figure 1**. Control mice (non-tolerant, black bars) received the vehicle of morphine and S1RA during 3 days, according to Protocol II in **Figure 1**. On the day of evaluation (day 4) tolerant and non-tolerant mice were treated with morphine only (8 mg/kg, s.c.) or its vehicle. Each bar and vertical line represent the mean  $\pm$  SEM of the values obtained in 8–10 animals. **(A,B)** Statistically significant differences between the values obtained in mice treated with morphine or its vehicle (\*\* $P < 0.01$ ), and between the values obtained in tolerant and non-tolerant animals treated with morphine on the day of the evaluation ( $^{\$}P < 0.01$ ) (one-way ANOVA followed by Student–Newman–Keuls test). **(A)** Statistically significant differences in tolerant mice between the values obtained in mice treated on the day of evaluation with: morphine + S1RA or its vehicle ( $^{\#}P < 0.01$ ); morphine + S1RA associated with PRE-084 or its vehicle ( $P < 0.01$ ) (one-way ANOVA followed by Student–Newman–Keuls test). **(B)** There were no statistically significant differences in the effect of morphine on the day of evaluation between the values in mice treated with S1RA or its vehicle during the induction of morphine tolerance (two-way ANOVA followed by Student–Newman–Keuls test).

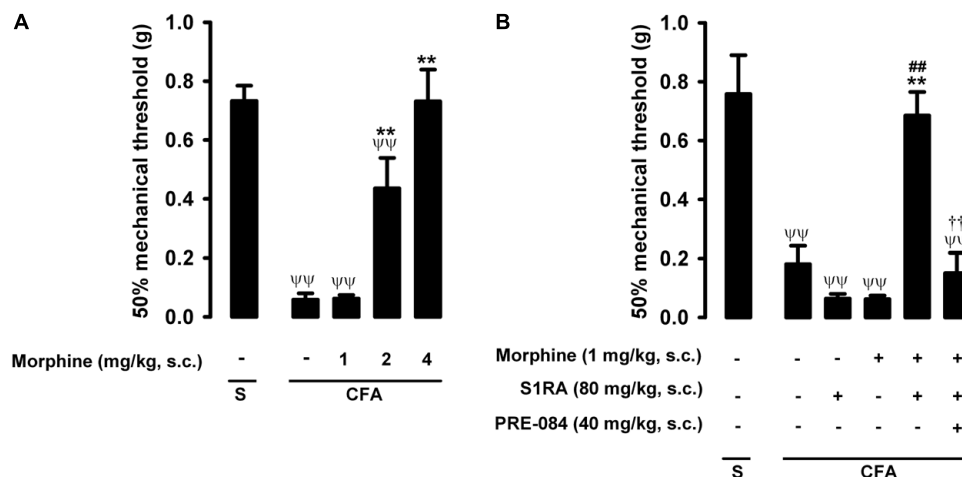
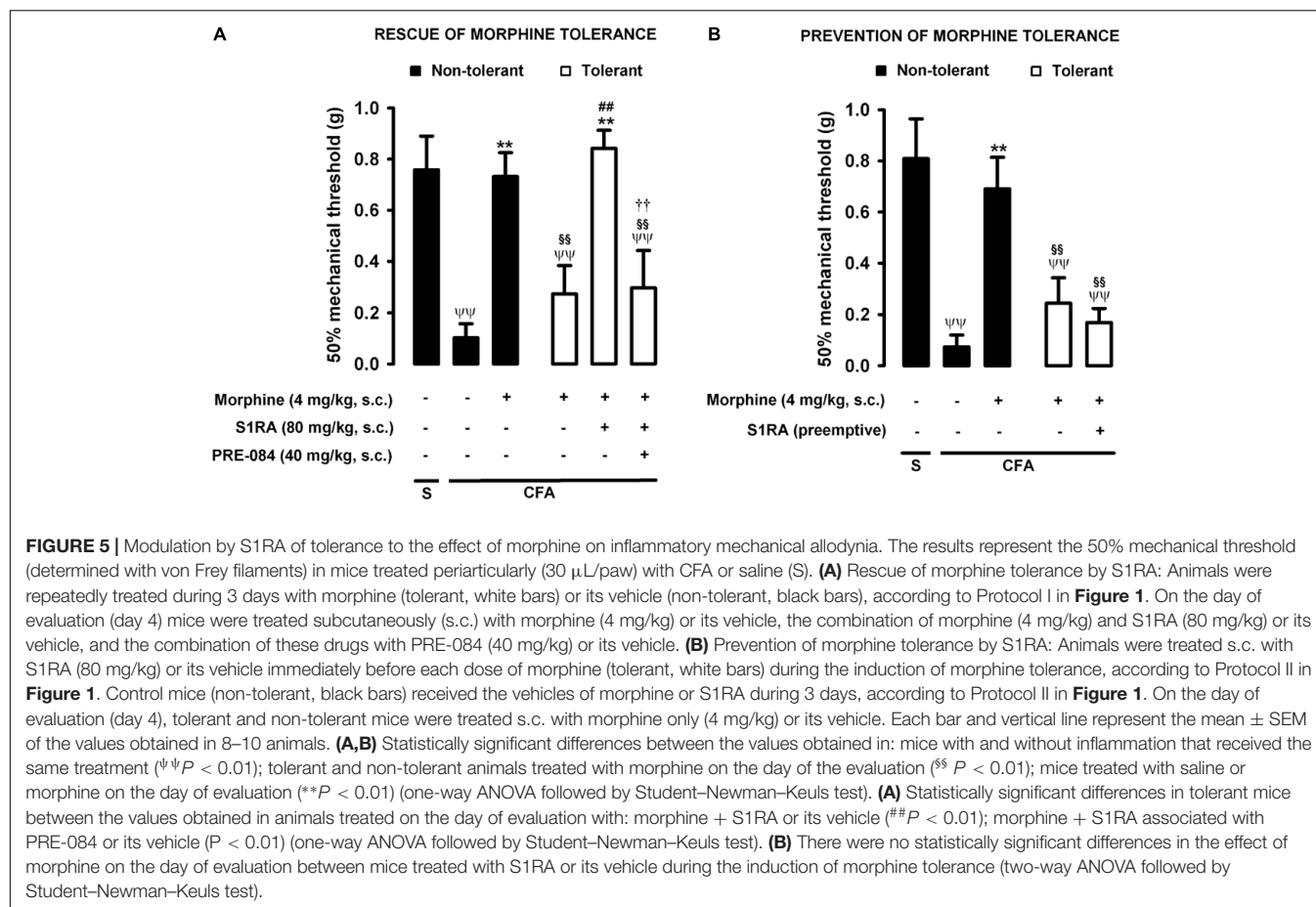


**FIGURE 4 |** Effects of morphine alone or associated with S1RA on inflammatory mechanical allodynia. The results represent the 50% mechanical threshold (determined with von Frey filaments) in mice treated periarticularly (30  $\mu$ L/paw) with CFA or saline (S). **(A)** Effect of the subcutaneous (s.c.) administration of different doses of morphine (1–4 mg/kg) or its vehicle. **(B)** Effect of the s.c. administration of morphine (1 mg/kg), S1RA (80 mg/kg) or its vehicle; morphine (1 mg/kg) + S1RA (80 mg/kg), and the association of these drugs with PRE-084 (40 mg/kg) or its vehicle. Each bar and vertical line represent the mean  $\pm$  SEM of values obtained in 8–10 animals. **(A,B)** Statistically significant differences between the values obtained in: animals with and without inflammation ( $^{\Psi\Psi}P < 0.01$ ); animals treated with morphine or its vehicle (\*\* $P < 0.01$ ) (one-way ANOVA followed by Student–Newman–Keuls test). **(B)** Statistically significant differences between the values obtained in animals with inflammation treated with: morphine + S1RA or its vehicle ( $^{\#}P < 0.01$ ); morphine + S1RA associated with PRE-084 or its vehicle.  $^{\#}P < 0.01$ ) (one-way ANOVA followed by Student–Newman–Keuls test).



administration of morphine 4 mg/kg (s.c.) (**Figure 5A**, black bars). However, in morphine-tolerant mice the antiallodynic effect induced by the same morphine dose was markedly lower, with a mechanical threshold of  $0.73 \pm 0.09$  g in non-tolerant mice vs.  $0.27 \pm 0.11$  g in tolerant mice with inflammation in response to morphine (**Figure 5A**). In animals rendered tolerant to morphine, we associated the administration of S1RA (80 mg/kg, s.c.) to morphine (4 mg/kg, s.c.) according to Protocol I in **Figure 1**, and found that the mechanical threshold was higher and similar to that found in non-tolerant mice with inflammation treated with this opioid drug (**Figure 5A**). These results indicate that S1RA was able to rescue the antiallodynic effect of morphine in tolerant animals. The administration of PRE-084 (40 mg/kg, s.c.) completely abolished the effect of S1RA in morphine-treated tolerant mice, yielding values close to those found in tolerant mice treated with morphine alone on the day of the experiment (**Figure 5A**).

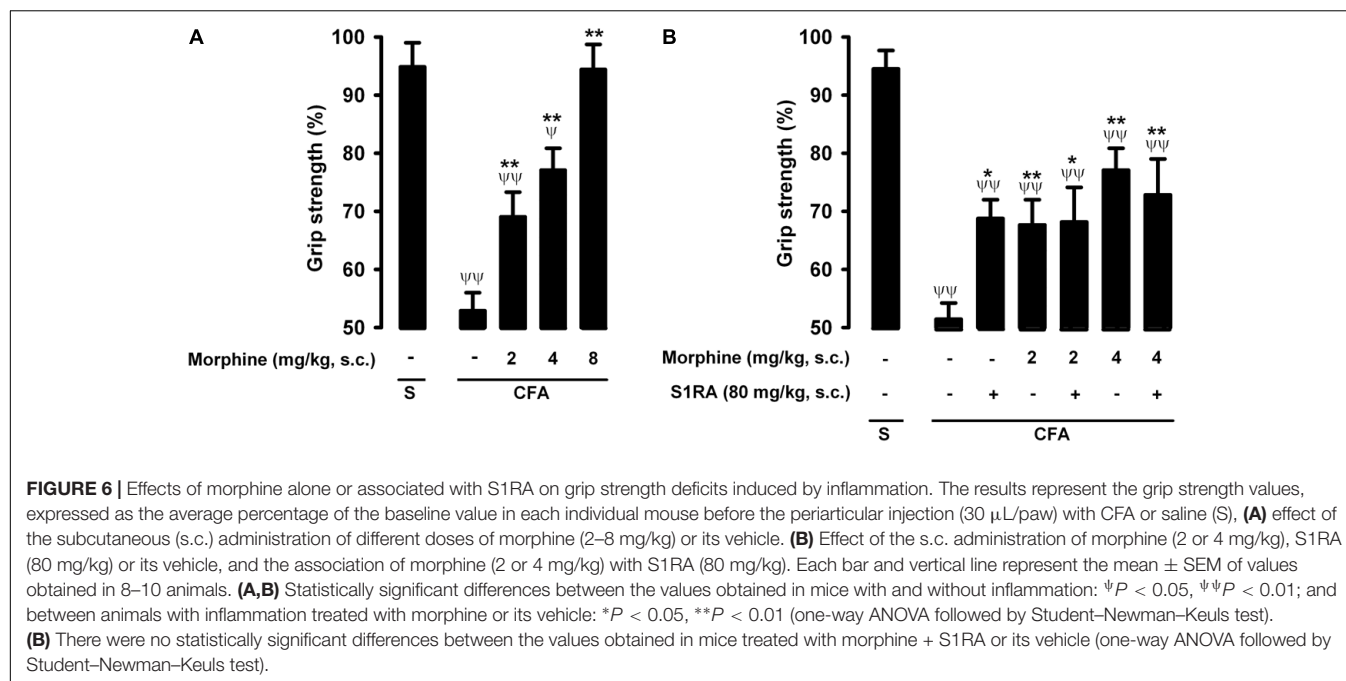
We also tested whether the repeated administration of S1RA (80 mg/kg, s.c.) before each dose of morphine during the 3-day regimen of morphine administration had a pre-emptive effect on the development of morphine tolerance to its antiallodynic effect (according to Protocol II in **Figure 1**). When the effect of morphine (4 mg/kg, s.c.) was tested on day 4 without any further administration of S1RA,

the effect of morphine was reduced (**Figure 5B**). These results indicate that tolerance to the antiallodynic effect of morphine appeared despite the repeated pre-emptive administration of S1RA.

Therefore, as in the results for heat nociception, sigma-1 receptor inhibition by S1RA was able to restore the morphine-induced antiallodynic effects in mice with inflammation tolerant to this opioid, but pre-emptive treatment with S1RA failed to affect the development of tolerance to the antiallodynic effect of morphine. These results are summarized in **Table 1**.

### Absence of Modulation by S1RA of Morphine-Induced Recovery of Grip Strength Deficits During Inflammation

Mice in which saline was injected periarticularly (30  $\mu$ L/paw) showed grip strength values close to 100% of their baseline values, whereas in mice with joint inflammation induced by the injection of the same volume of CFA, grip strength was reduced to about half of its baseline value (**Figure 6A**, first two bars). Morphine administration (2–8 mg/kg, s.c.) induced a dose-dependent recovery of grip strength deficits in animals with inflammation, and the highest dose tested led to full recovery of normal grip strength



values (Figure 6A). Morphine was less potent in reversing grip strength deficits than in inhibiting tactile allodynia during inflammation, and both endpoints were more sensitive to morphine than nociceptive heat pain (compare Figures 2A, 4A, 6A).

The administration of S1RA alone (80 mg/kg, s.c.) induced a slight but significant increase in grip strength values in mice with inflammation (Figure 6B). In contrast to the results for heat nociception and inflammatory tactile allodynia, S1RA administration did not enhance the effect of morphine at either 2 or 4 mg/kg (s.c.) (Figure 6B). To further confirm the lack of effect of S1RA on the effect of morphine on grip strength in mice with inflammation, we performed a time-course study of the drug effects. The association of S1RA with morphine did not alter the effect of this opioid drug administered at 2 mg/kg (s.c.) at any time-point tested between 30 and 180 min after drug administration (Supplementary Figure S2A). Similar results were found when we tested the effects of the association of S1RA with morphine 4 mg/kg (s.c.) (Supplementary Figure S2B).

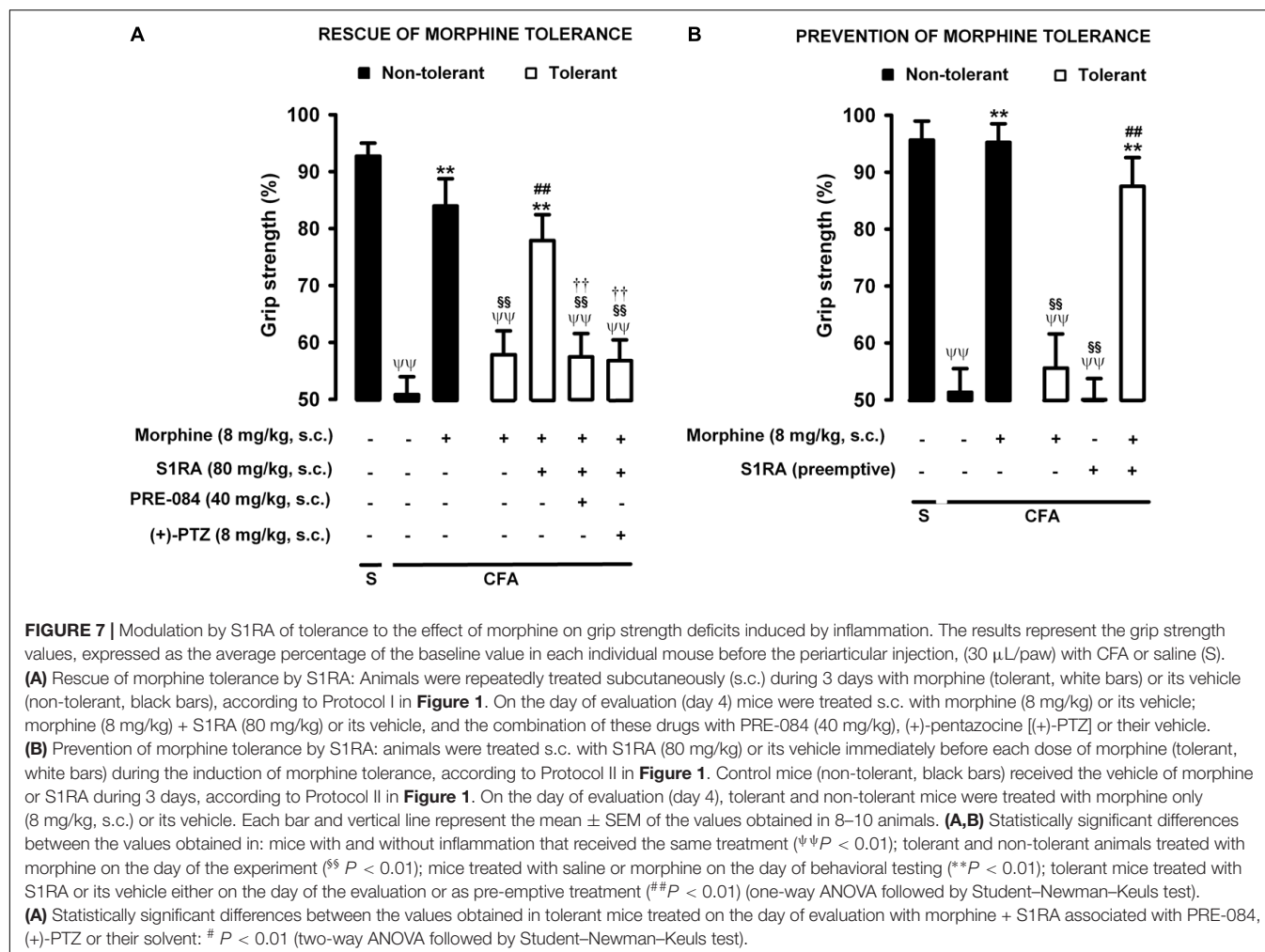
Therefore, in contrast to the potentiation by S1RA of morphine-induced heat antinociception and the antiallodynic effects in mice with inflammation, S1RA was unable to modify the effects of morphine on grip strength deficits induced by joint inflammation. These results are summarized in Table 1.

### Modulation by S1RA of Tolerance to Morphine-Induced Recovery of Grip Strength Deficits During Inflammation

Animals were rendered morphine-tolerant by the same procedure described in previous sections (Figure 1), whereas

control non-tolerant mice received morphine vehicle. In non-tolerant mice with inflammation (30  $\mu$ L CFA/paw), grip strength deficits were markedly reversed in response to the acute administration of morphine 8 mg/kg (s.c.) (Figure 7A, black bars). However, the same morphine dose (8 mg/kg, s.c.) in morphine-tolerant mice had no significant effect on grip strength, which was about half of the baseline value ( $83.95 \pm 4.8\%$  in non-tolerant mice vs.  $57.81 \pm 4.2\%$  in tolerant mice with inflammation in response to morphine) (Figure 7A). In animals rendered tolerant to morphine, we associated the administration of S1RA (80 mg/kg, s.c.) to morphine (8 mg/kg, s.c.) according to Protocol I in Figure 1, and found that grip strength reached values close to 80% of baseline measurements (Figure 7A). The administration of PRE-084 (40 mg/kg, s.c.) or (+)-pentazocine (8 mg/kg, s.c.) completely abolished the effect of the association of S1RA + morphine administered to morphine-treated tolerant mice, with values close to those in tolerant mice treated with morphine alone the day of the experiment (Figure 7A). These results support the selectivity of S1RA-induced effects.

We also tested whether the repeated administration of S1RA (80 mg/kg, s.c.) during the 3-day regimen of morphine administration (according to Protocol II in Figure 1) had a pre-emptive effect on the development of morphine tolerance to its effect on grip strength deficits. The repeated administration of S1RA, when mice were evaluated the day after the last S1RA administration, did not affect grip strength in morphine-tolerant mice with inflammation. However, when morphine (8 mg/kg, s.c.) was administered to these mice on the evaluation day, the effect in response to the opioid was robust (Figure 7B). These results indicate that S1RA was able to prevent morphine tolerance in this particular outcome, in contrast to the results for nociceptive heat



pain and inflammatory tactile allodynia reported in the preceding sections.

Therefore the administration of S1RA, either when morphine tolerance was fully developed or during the induction of tolerance, was able to preserve the effect of morphine on grip strength deficits in mice with joint inflammation. These results are summarized in **Table 1**.

### Morphine, S1RA and PRE-084 do Not Alter Normal Grip Strength or CFA-Induced Inflammatory Edema

We also tested whether the drugs used in the present study altered grip strength in mice without inflammation. The doses of morphine or S1RA (administered acutely or repeatedly) used in this study, as well as the acute administration of PRE-084 (at the dose used in our study), did not alter normal grip strength in animals without inflammation (**Figure 8**). These results suggest that the effects on grip strength in mice with inflammation, reported in the preceding section, were not due to the alteration of normal motor function.

We also tested whether the drugs used in the present study reduced inflammatory edema, by measuring changes in ankle thickness in response to CFA administration. CFA injection produced a marked increase in ankle thickness in comparison to saline-treated mice, and this increase was not significantly altered by either the acute administration of morphine (8 mg/kg, s.c.) or the acute or repeated administration of S1RA (80 mg/kg, s.c.) (**Figure 9**). Therefore, none of these drugs appeared to have an antiedematous effect on CFA-induced inflammation.

### Pharmacokinetic Interaction Between S1RA and Morphine Does Not Affect Their Concentrations in Plasma or Brain Tissue

After a single administration of S1RA (80 mg/kg, s.c.), the concentration of this sigma-1 antagonist was higher in brain tissue than in plasma (compare black bars in the left panels of **Figures 10A,B**). The repeated administration of morphine according to our protocol for the induction of tolerance did not alter the concentration of acutely administered S1RA (80 mg/kg, s.c., according to Protocol I in **Figure 1**) in



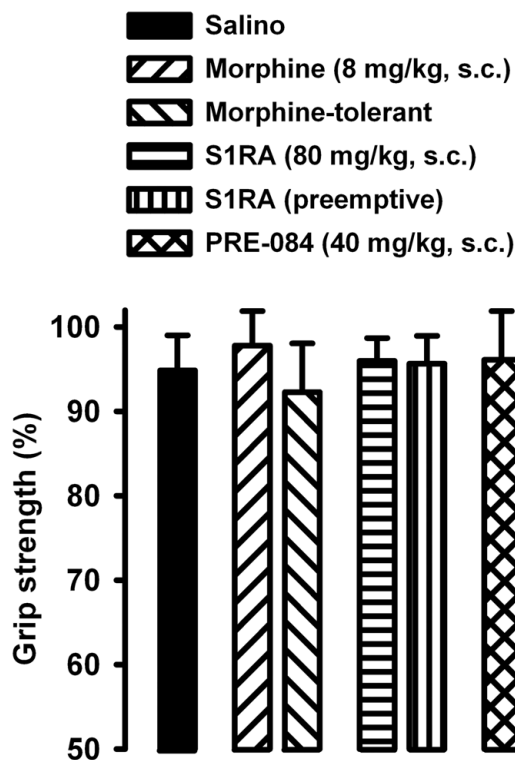


**FIGURE 8 |** Absence of effects of morphine, S1RA and PRE-084 on grip strength in mice without inflammation. The results represent the grip strength values (expressed as the average percentage of the baseline value in each individual mouse before drug administration). Animals were treated subcutaneously (s.c.) with morphine (8 mg/kg), S1RA (80 mg/kg) or PRE-084 (40 mg/kg) on the day of the experiment, or treated twice daily with morphine at escalating doses or with S1RA (80 mg/kg) during the 3 days before the behavioral evaluation (see section “Materials and Methods” for details). Each bar and vertical line represent the mean  $\pm$  SEM of the values obtained in 8 animals. There were no statistically significant differences between values from untreated animals and drug-treated mice (one-way ANOVA).

either plasma or brain tissue (compare black and white bars in the left panels of **Figures 10A,B**). When we measured the concentration of S1RA after its repeated administration (80 mg/kg, s.c.) during the 3-day regimen of morphine administration, without any further S1RA injection on the day of plasma and brain collection (according to Protocol II in **Figure 1**), we observed no appreciable levels of this sigma-1 antagonist in any sample analyzed (see far-right bars in the left panels of **Figures 10A,B** for plasma and brain levels, respectively). Therefore, when S1RA was administered preemptively during the induction of morphine tolerance, there was no remaining S1RA in plasma or brain tissue at the time of the behavioral evaluations.

Morphine levels were higher in plasma than in brain tissue after the acute administration (8 mg/kg, s.c.) of this opioid (compare black bars in the middle panels of **Figures 10A,B**). Repeated morphine administration according to our protocol for the induction of morphine tolerance did not change morphine levels after the administration of this opioid on the day of

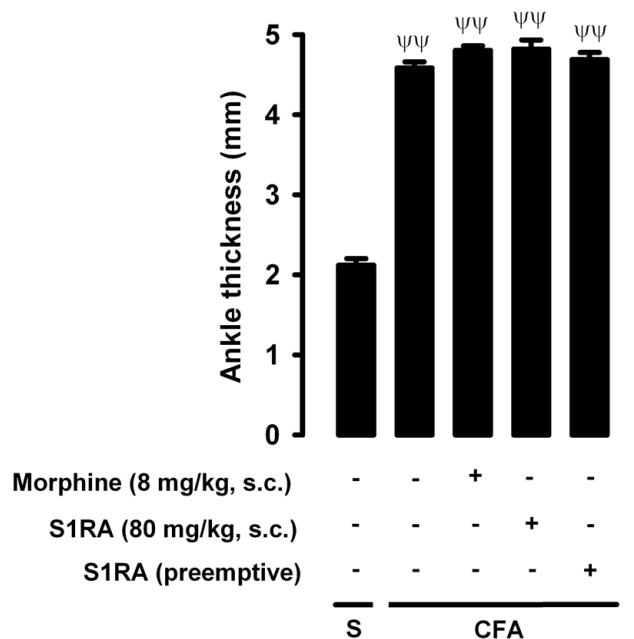
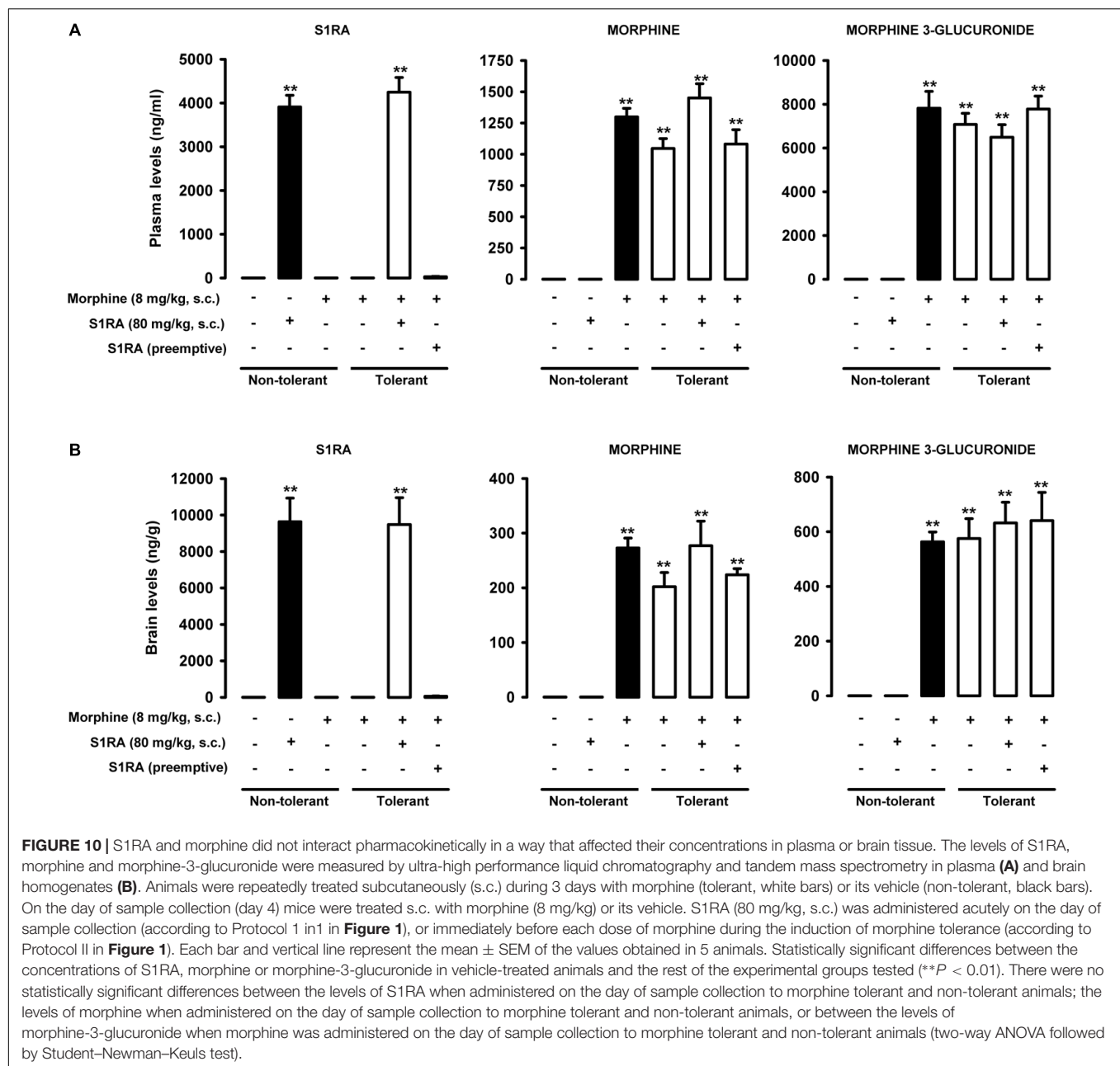


**FIGURE 9 |** Effects of morphine and S1RA on ankle thickness in mice with inflammation. The results represent ankle thickness after the administration of CFA or saline (S). Animals were treated subcutaneously (s.c.) with morphine (8 mg/kg) or S1RA (80 mg/kg) on the day of the experiment, or treated twice daily with S1RA (80 mg/kg) during the 3 days before the evaluation (see section “Materials and Methods” for details). Each bar and vertical line represent the mean  $\pm$  SEM of the values obtained in 8 animals. The differences between the values from mice without or with inflammation were statistically significant ( $^{***}P < 0.01$ ). There were no statistically significant differences between the values from mice with inflammation treated with the drugs and untreated mice with inflammation (one-way ANOVA followed by Student–Newman–Keuls test).

sample collection in either plasma or brain tissue (compare black bar and the first white bar in the middle panels of **Figures 10A,B**). The acute or repeated administration of S1RA (80 mg/kg, s.c. according to Protocol I or II in **Figure 1**) did not alter morphine levels in either plasma or brain tissue in morphine-tolerant animals (see white bars in the middle panels of **Figures 10A,B**).

Like morphine, the concentration of morphine-3-glucuronide was higher in plasma than in brain tissue (compare black bars in the right panels of **Figures 10A,B**). This morphine metabolite was more abundant than the parent compound in both plasma and brain tissue after acute morphine administration (compare black bars in the middle and right panels of **Figures 10A,B** for plasma and brain tissue determinations, respectively). Repeated morphine administration according to our protocol to induce tolerance did not alter morphine-3-glucuronide levels in either plasma or brain samples after the administration of morphine on the day of the behavioral evaluation (compare black bar and the first white bar in the right panels of **Figures 10A,B**). The acute or repeated administration of S1RA (80 mg/kg, s.c.) did not alter morphine-3-glucuronide levels in morphine-tolerant animals in either



plasma or brain tissue (white bars in the right panels of Figures 10A,B).

## DISCUSSION

We compared the effects of morphine, S1RA and their association on three different pain measures: nociceptive heat pain, inflammatory tactile allodynia, and grip strength deficits induced by inflammation. In addition, we studied the effects of S1RA on morphine tolerance in these three different measures.

Our findings show that morphine was able to induce analgesic-like effects on nociceptive heat pain, inflammatory tactile

allodynia and grip strength deficits induced by inflammation. However, the sensitivity to this opioid drug varied depending on the endpoint examined. Inflammatory allodynia and grip strength deficits induced by inflammation were more sensitive to the effects of morphine than nociceptive heat pain. These results are consistent with the widely reported increase in the effects of opioids on cutaneous sensory hypersensitivity during inflammation (reviewed in Stein et al., 2009), and indicate that the enhancement of opioid effects during inflammation, as observed in von Frey filament thresholds, is also evident in the functional deficit associated with this pathological condition. In previous work we compared the pharmacological characteristics of grip strength deficits and tactile allodynia during inflammation

using several drugs from different pharmacological groups, including opioids (oxycodone and tramadol), non-steroidal anti-inflammatory drugs (ibuprofen and celecoxib), and acetaminophen (Montilla-García et al., 2017). Interestingly, with the exception of oxycodone, which showed a similar potency in reversing tactile allodynia and grip strength deficits, the dose of all other known analgesic drugs was lower for functional deficits than for cutaneous hypersensitivity (Montilla-García et al., 2017). Here we show that morphine was less potent in reversing grip strength deficits than tactile allodynia, which supports the notion that the pharmacological sensitivity of these two outcomes during inflammation is not identical. Differences between the analgesic sensitivity of standard cutaneous measures of pain and pain-induced functional deficits have been described previously for other outcomes used to test pain interference on physical function, such as inflammation-induced weight bearing differences or wheel running depression (reviewed in Cobos and Portillo-Salido, 2013).

We also tested the effects of S1RA (in the absence of morphine) on nociceptive heat pain, inflammatory tactile allodynia and grip strength deficits induced by inflammation. S1RA did not alter nociceptive heat pain, as previously reported for this and other sigma-1 antagonists (e.g., Chien and Pasternak, 1994, 1995; Tejada et al., 2014, 2017). Here we show that this sigma-1 antagonist was able to markedly ameliorate sensory hypersensitivity during mild inflammation, as previously reported (Parenti et al., 2014; Gris et al., 2015; Tejada et al., 2018), but it was devoid of effect when inflammation was more prominent (at a higher dose of CFA). We previously reported a clear relationship between ankle thickness and the volume of CFA administered (Montilla-García et al., 2017). We needed to use a higher dose of CFA in our study because the decreases in grip strength induced by lower doses of this compound were too small to reliably assess the effects of analgesic drugs, as we previously reported (Montilla-García et al., 2017). Therefore, the experimental conditions used here to induce inflammatory allodynia were too restrictive to detect the antiallodynic effects induced by sigma-1 antagonism. Despite the absence of effect of S1RA on inflammatory tactile allodynia during this more prominent inflammation, here we show that S1RA was able to partially ameliorate grip strength deficits induced by inflammation, which again indicates that the sensitivity to drug effects differs between tactile allodynia and grip strength deficits. We have previously shown that both nociceptive heat pain and tactile allodynia during inflammation in our experimental conditions are sensitive to the *in vivo* ablation of transient receptor potential vanilloid (TRPV1)-expressing neurons by resiniferatoxin (Montilla-García et al., 2017, 2018). However, grip strength deficits during inflammation are insensitive to resiniferatoxin treatment (Montilla-García et al., 2017). These results indicate that the neurobiological mechanisms involved in grip strength deficits during inflammation and in the behavioral tests of cutaneous sensitivity explored here are different. Therefore, the effect of S1RA on grip strength deficits in mice with inflammation may be due to sigma-1 actions in other pain pathways unrelated to those involved in heat nociceptive pain or inflammatory tactile allodynia.

In this study we show that the systemic administration of S1RA was able to enhance morphine antinociception to contact heat stimulation, in agreement with previous reports which used other types of nociceptive heat stimulus (reviewed in Sánchez-Fernández et al., 2017). We show that S1RA markedly potentiated the antiallodynic effect of morphine in mice with inflammation. To our knowledge this is the first reported evidence that sigma-1 antagonism enhances the effect of an opioid drug in a pathological pain model. The enhancement by S1RA of the effects of morphine on nociceptive heat pain and inflammatory tactile allodynia was abolished by the administration of the sigma-1 agonist PRE-084, which argues in favor of an action mediated by sigma-1 receptors in these S1RA-induced effects. Despite the evident increase in the effects of morphine on nociceptive heat pain and inflammatory tactile allodynia noted above, and despite the greater sensitivity of grip strength deficits to the effects of S1RA when administered alone (in the absence of morphine), we show that S1RA was not able to potentiate the effects of morphine on grip strength deficits induced by inflammation. This result further supports the notion that different neurobiological mechanisms are involved in grip strength deficits and cutaneous pain.

We also explored the modulation of morphine analgesic tolerance by S1RA, given that this unavoidable opioid effect is a substantial drawback to the use of opioid analgesics (Morgan and Christie, 2011). We found that when S1RA was administered to morphine-tolerant mice, it was able to rescue the effect of morphine on nociceptive pain in response to contact heat stimulus, in agreement with previous studies that used nociceptive heat stimulation (Vidal-Torres et al., 2013; Rodríguez-Muñoz et al., 2015). We also show that S1RA was able to rescue the effects of morphine on inflammatory tactile allodynia. The rescue of morphine tolerance by this sigma-1 antagonist in heat nociception or inflammatory tactile allodynia was abolished by the administration of PRE-084, which again argues in favor of a role for an action mediated by sigma-1 receptors in the effects induced by S1RA. The association of S1RA and morphine administered on the day of the behavioral evaluation to morphine-tolerant animals also induced a clear recovery of grip strength deficits. It is worth pointing out the possibility that not all the effect detected in morphine-tolerant animals that received S1RA + morphine on the day of the experiment were due to the rescue of morphine tolerance; given that S1RA had a slight but significant effect on grip strength in mice with inflammation, this might have contributed to the effect observed. We show that this effect of S1RA + morphine in tolerant animals was reversed not only by the administration of PRE-084, but also by the administration of (+)-pentazocine, another selective sigma-1 agonist (Cobos et al., 2008), which further supports the selectivity of the effects induced by S1RA.

These results on the rescue of morphine tolerance by S1RA cannot be explained by pharmacokinetic interactions that might increase the level of morphine or its major murine metabolite morphine-3-glucuronide (Pasternak and Pan, 2013), since we found that the levels of these compounds remained unaltered after acute S1RA administration in tolerant animals. Our

results point instead to pharmacodynamic interactions between sigma-1 antagonism and opioid effects. Interestingly, plasma levels of S1RA in our mice were similar to plasma levels of this drug found in humans after oral S1RA treatment at therapeutic doses (Abadias et al., 2013; Bruna et al., 2018). To study whether the administration of S1RA was able to prevent the development of morphine tolerance, we administered this sigma-1 antagonist during an escalating morphine dosage regimen (but not on the day of the behavioral evaluation). We found that, as previously reported, the repeated, preemptive administration S1RA failed to prevent tolerance to the effects of morphine on a nociceptive heat stimulus (Vidal-Torres et al., 2013). In addition, sigma-1 antagonism also failed to prevent tolerance to the antiallodynic effect of morphine during inflammation. The repeated administration of S1RA did not alter grip strength in morphine-tolerant animals with inflammation, although surprisingly, it completely prevented the development of tolerance to the effect of morphine on grip strength deficits. Therefore, the effects induced by S1RA in the preemptive protocol cannot be attributed to the effects of this compound alone. Interestingly, we found that at the time of the behavioral tests, the levels of morphine or morphine-3-glucuronide remained unaltered in S1RA-treated mice and there was no remaining S1RA in either plasma or brain tissues. These results indicate that S1RA, when repeatedly administered with morphine, is able to induce protective effects against the development of tolerance.

It has been suggested that sigma-1 antagonism both potentiates opioid analgesia and diminish morphine tolerance by decreasing the inhibition of  $\mu$ -opioid receptors by *N*-methyl-D-aspartate receptor (NMDAR) activity (Rodríguez-Muñoz et al., 2015). Because S1RA failed to enhance the effect of morphine on grip strength deficits during inflammation in non-tolerant mice but was able to successfully prevent morphine tolerance in this outcome, the mechanisms for opioid potentiation by sigma-1 receptors appear to be dissociated from the effects on opioid tolerance, at least in this measure of pain-induced functional impairment.

It has been reported that the sigma-1 antagonists S1RA and BD-1063 prevent paclitaxel-induced neuropathic pain (Nieto et al., 2012, 2014), which points to broader neuroprotective effects of sigma-1 antagonism. However, it remains unclear why this prevention of morphine tolerance by S1RA affects only grip strength deficits but not heat nociception or inflammatory tactile allodynia. Although the mechanisms of cutaneous sensitivity have been extensively explored for decades, little is known about the mechanisms of pain-induced functional impairment, which may not fully overlap (Cobos and Portillo-Salido, 2013; Montilla-García et al., 2017; Negus, 2018). Similarly, the mechanisms of opioid analgesic tolerance might also depend on the pain measure used. Regardless of the exact mechanisms involved in the differential results obtained in grip strength deficits and the other two pain measures explored in the present study, in light of our results it is clear that they are not fully equivalent.

Interestingly, neither the acute administration of morphine nor the acute or repeated administration of S1RA were able

to alter CFA-induced inflammatory edema. The results with S1RA are in agreement with a previous study showing that this sigma-1 antagonist did not alter carrageenan-induced inflammatory edema (Gris et al., 2014; Tejada et al., 2014). Therefore, taking into account the amelioration of grip strength deficits by the drugs tested here but their lack of effects on inflammatory edema, our results suggest that their effects on grip strength are not attributable to improved grip strength resulting from reduced swelling around the joints or tendons, and that swelling *per se* does not prevent movement. Furthermore, grip strength is classically used to assess neurotoxicity in rodents, and is included in the Irwin screen (Irwin, 1968; Mattsson et al., 1996), which is ingrained in the pharmaceutical industry as the first tier of preclinical testing to detect drug-induced neurotoxic effects (Moser, 2011). We show that morphine or S1RA (administered acutely or repeatedly), as well as the acute administration of PRE-084, did not alter grip strength in animals without inflammation, suggesting that the doses used in our study did not alter normal motor function. Taken together, our results suggest that the drugs tested here exert their effects through pain modulation rather than through unspecific effects on inflammation or motor performance.

Although von Frey testing, the behavioral assay currently used most widely in preclinical pain research, is undoubtedly useful to detect sensory alterations in patients with neuropathy (e.g., Bennett, 2001; Bouhassira et al., 2005; Moharic et al., 2012), it is almost never used in other human pain conditions such as rheumatic disease. Therefore, although von Frey testing has been established as the standard in preclinical pain testing, it is not a widely used pain measure in patients with non-neuropathic chronic painful diseases. On the other hand, grip strength has been widely and routinely evaluated for decades as a functional measure in patients with joint inflammation caused by rheumatic disease (e.g., Bijlsma et al., 1987; Pincus and Callahan, 1992; Lee, 2013), and it is known to correlate with pain (Callahan et al., 1987; Fraser et al., 1999; Overend, T. J. et al., 1999). In fact, one set of consensus-based recommendations advocates measuring physical function as one of the main outcomes in clinical trials of pain treatments (Dworkin et al., 2008). In light of the differences we observed in the effects of sigma-1 receptors on opioid analgesia and tolerance, as reflected in grip strength tests and the measures of cutaneous sensitivity explored in the present study, we believe measures of physical functioning merit inclusion in the standard repertoire of behavioral tests in preclinical laboratories, to better approximate the human pain phenotype in preclinical pain research.

We conclude that sigma-1 receptors play a pivotal role in the control of morphine analgesia and tolerance, albeit in a manner dependent on the type of painful stimulus explored. These findings may have important therapeutic implications for the use of sigma-1 antagonists as opioid adjuvants. In addition, the results we obtained for grip strength deficit as a surrogate pain measure were not equivalent to those seen when standard measures of cutaneous sensitivity were used. Further studies are needed to fully understand the mechanisms through which pain interferes with physical function.



## AUTHOR CONTRIBUTIONS

EC designed the research. ÁM-G, MT, MR-C, SY, and IB-C performed the research. ÁM-G, MT, SY, and DZ analyzed the data. ÁM-G, MT, MR-C, SY, IB-C, DZ, and EC, wrote the manuscript. All authors read and approved the final version of the manuscript.

## FUNDING

MT was supported by a postdoctoral grant from the University of Granada. MR-C and IB-C were supported by FPU grants from the Spanish Ministry of Economy and Competitiveness (MINECO). This study was partially supported by the Spanish Ministry of Economy and Competitiveness (Grants SAF2013-47481P and SAF2016-80540-R), the Junta de Andalucía (Grant CTS109), and

FEDER funds. This research was done in partial fulfillment of the requirements for the doctoral thesis defended by ÁM-G in the Ph.D. Program in Biomedicine.

## ACKNOWLEDGMENTS

The authors acknowledge Prof. José Manuel Baeyens for his useful comments and thank K. Shashok for improving the use of English in the manuscript.

## SUPPLEMENTARY MATERIAL

The Supplementary Material for this article can be found online at: <https://www.frontiersin.org/articles/10.3389/fphar.2019.00136/full#supplementary-material>

## REFERENCES

- Abadias, M., Escriche, M., Vagué, A., Sust, M., and Encina, G. (2013). Safety, tolerability and pharmacokinetics of single and multiple doses of a novel sigma-1 receptor antagonist in three randomized phase I studies. *Br. J. Clin. Pharmacol.* 75, 103–117. doi: 10.1111/j.1365-2125.2012.04333.x
- Bennett, M. (2001). The LANSS pain scale: the leeds assessment of neuropathic symptoms and signs. *Pain* 92, 147–157. doi: 10.1016/S0304-3959(00)00482-6
- Bijlsma, J. W., Huber-Bruning, O., and Thijssen, J. H. (1987). Effect of oestrogen treatment on clinical and laboratory manifestations of rheumatoid arthritis. *Ann. Rheum. Dis.* 46, 777–779. doi: 10.1136/ard.46.10.777
- Bouhassira, D., Attal, N., Alchaar, H., Boureau, F., Brochet, B., Bruxelle, J., et al. (2005). Comparison of pain syndromes associated with nervous or somatic lesions and development of a new neuropathic pain diagnostic questionnaire (DN4). *Pain* 114, 29–36. doi: 10.1016/j.pain.2004.12.010
- Bruna, J., Videla, S., Argvriou, A. A., Velasco, R., Villoria, J., Santos, C., et al. (2018). Efficacy of a novel sigma-1 receptor antagonist for oxaliplatin-induced neuropathy: a randomized, double-blind, placebo-controlled phase iia clinical trial. *Neurotherapeutics* 15, 178–189. doi: 10.1007/s13311-017-0572-5
- Callahan, L. F., Brooks, R. H., Summey, J. A., and Pincus, T. (1987). Quantitative pain assessment for routine care of rheumatoid arthritis patients, using a pain scale based on activities of daily living and a visual analog pain scale. *Arth. Rheum.* 30, 630–636. doi: 10.1002/art.1780300605
- Chandran, P., Pai, M., Blomme, E. A., Hsieh, G. C., Decker, M. W., and Honore, P. (2009). Pharmacological modulation of movement-evoked pain in a rat model of osteoarthritis. *Eur. J. Pharmacol.* 613, 39–45. doi: 10.1016/j.ejphar.2009.04.009
- Chaplan, S. R., Bach, F. W., Pogrel, J. W., Chung, J. M., and Yaksh, T. L. (1994). Quantitative assessment of tactile allodynia in the rat paw. *J. Neurosci. Methods* 53, 55–63. doi: 10.1016/0165-0270(94)90144-9
- Chien, C. C., and Pasternak, G. W. (1994). Selective antagonism of opioid analgesia by a sigma system. *J. Pharmacol. Exp. Ther.* 271, 1583–1590.
- Chien, C. C., and Pasternak, G. W. (1995). Sigma antagonists potentiate opioid analgesia in rats. *Neurosci. Lett.* 190, 137–139. doi: 10.1016/0304-3940(95)11504-P
- Cobos, E. J., Entrena, J. M., Nieto, F. R., Cendán, C. M., and Del, P. E. (2008). Pharmacology and therapeutic potential of sigma1 receptor ligands. *Curr. Neuropharmacol.* 6, 344–366. doi: 10.2174/157015908787386113
- Cobos, E. J., Nickerson, C. A., Gao, F., Chandran, V., Bravo-Caparrós, I., González-Cano, R., et al. (2018). Mechanistic differences in neuropathic pain modalities revealed by correlating behavior with global expression profiling. *Cell Rep.* 22, 1301–1312. doi: 10.1016/j.celrep.2018.01.006
- Cobos, E. J., and Portillo-Salido, E. (2013). "Bedside-to-bench" behavioral outcomes in animal models of pain: beyond the evaluation of reflexes. *Curr. Neuropharmacol.* 11, 560–591. doi: 10.2174/1570159X113119990041
- Dworkin, R. H., Turk, D. C., Wyrwich, K. W., Beaton, D., Cleeland, C. S., Farrar, J. T., et al. (2008). Interpreting the clinical importance of treatment outcomes in chronic pain clinical trials: IMMPACT recommendations. *J. Pain* 9, 105–121. doi: 10.1016/j.jpain.2007.09.005
- Fraser, A., Vallow, J., Preston, A., and Cooper, R. G. (1999). Predicting 'normal' grip strength for rheumatoid arthritis patients. *Rheumatology* 38, 521–528. doi: 10.1093/rheumatology/38.6.521
- González-Cano, R., Merlos, M., Baeyens, J. M., and Cendán, C. M. (2013).  $\sigma 1$  receptors are involved in the visceral pain induced by intracolonic administration of capsaicin in mice. *Anesthesiology* 118, 691–700. doi: 10.1097/ALN.0b013e318280a60a
- Gris, G., Cobos, E. J., Zamanillo, D., and Portillo-Salido, E. (2015). Sigma-1 receptor and inflammatory pain. *Inflamm. Res.* 64, 377–381. doi: 10.1007/s00011-015-0819-8
- Gris, G., Merlos, M., Vela, J. M., Zamanillo, D., Portillo-Salido, E. (2014). S1RA, a selective sigma-1 receptor antagonist, inhibits inflammatory pain in the carrageenan and complete freund's adjuvant models in mice. *Behav. Pharmacol.* 25, 226–235. doi: 10.1097/FBP.0000000000000038
- Hayashi, T., and Su, T. P. (2004). Sigma-1 receptor ligands: potential in the treatment of neuropsychiatric disorders. *CNS Drugs* 18, 269–284. doi: 10.2165/00023210-200418050-00001
- Helfert, S. M., Reimer, M., Höper, J., and Baron, R. (2015). Individualized pharmacological treatment of neuropathic pain. *Clin. Pharmacol. Ther.* 97, 135–142. doi: 10.1002/cpt.19
- Irwin, S. (1968). Comprehensive observational assessment: ia. a systematic, quantitative procedure for assessing the behavioral and physiologic state of the mouse. *Psychopharmacologia* 13, 222–257. doi: 10.1007/BF00401402
- Lee, Y. C. (2013). Effect and treatment of chronic pain in inflammatory arthritis. *Curr. Rheumatol. Rep.* 15:300. doi: 10.1007/s11926-012-0300-4
- Mattsson, J. L., Spencer, P. J., and Albee, R. R. (1996). A performance standard for clinical and functional observational battery examinations of rats. *J. Am. Coll. Toxicol.* 15, 239–254. doi: 10.3109/10915819609008716
- Menéndez, L., Lastra, A., Hidalgo, A., and Baamonde, A. (2002). Unilateral hot plate test: a simple and sensitive method for detecting central and peripheral hyperalgesia in mice. *J. Neurosci. Methods* 113, 91–97. doi: 10.1016/S0165-0270(01)00483-6
- Mogil, J. S., Chesler, E. J., Wilson, S. G., Juraska, J. M., and Sternberg, W. F. (2000). Sex differences in thermal nociception and morphine antinociception in rodents depend on genotype. *Neurosci. Biobehav. Rev.* 24, 375–389. doi: 10.1016/S0149-7634(00)00015-4
- Moharic, M., Vidmar, G., and Burger, H. (2012). Sensitivity and specificity of von frey's hairs for the diagnosis of peripheral neuropathy in patients with type 2 diabetes mellitus. *J. Diabetes Compl.* 26, 319–322. doi: 10.1016/j.jdiacomp.2012.04.008
- Montilla-García, A., Perazzoli, G., Tejada, M. A., Gonzalez-Cano, R., Sánchez-Fernández, C., Cobos, E. J., and Baeyens, J. M. (2018). Modality-specific peripheral antinociceptive effects of mu-opioid agonists on heat and mechanical

- stimuli: contribution of sigma-1 receptors. *Neuropharmacology* 135, 328–342. doi: 10.1016/j.neuropharm.2018.03.025
- Montilla-García, A., Tejada, M. A., Perazzoli, G., Entrena, J. M., Portillo-Salido, E., Fernández-Segura, E., et al. (2017). Grip strength in mice with joint inflammation: a rheumatology function test sensitive to pain and analgesia. *Neuropharmacology* 125, 231–242. doi: 10.1016/j.neuropharm.2017.07.029
- Morgan, M. M., and Christie, M. J. (2011). Analysis of opioid efficacy, tolerance, addiction and dependence from cell culture to human. *Br. J. Pharmacol.* 164, 1322–1334. doi: 10.1111/j.1476-5381.2011.01335.x
- Moser, V. C. (2011). Functional assays for neurotoxic testing. *Toxicol. Pathol.* 39, 36–45. doi: 10.1177/0192623310385255
- Negus, S. S. (2018). Addressing the opioid crisis: the importance of choosing translational endpoints in analgesic drug discovery. *Trends Pharmacol. Sci.* 39, 327–330. doi: 10.1016/j.tips.2018.02.002
- Nieto, F. R., Cendán, C. M., Cañizares, F. J., Cubero, M. A., Vela, J. M., Fernández-Segura, E., and Baeyens, J. M. (2014). Genetic inactivation and pharmacological blockade of sigma-1 receptors prevent paclitaxel-induced sensory-nerve mitochondrial abnormalities and neuropathic pain in mice. *Mol. Pain* 10:11. doi: 10.1186/1744-8069-10-11
- Nieto, F. R., Cendán, C. M., Sánchez-Fernández, C., Cobos, E. J., Entrena, J. M., Tejada, M. A., et al. (2012). Role of sigma-1 receptors in paclitaxel-induced neuropathic pain in mice. *J. Pain* 13, 1107–1121. doi: 10.1016/j.jpain.2012.08.006
- Overend, T. J., Wuori-Fearn, J. L., Kramer, J. F., and MacDermid, J. C. (1999). Reliability of a patient-rated forearm evaluation questionnaire for patients with lateral epicondylitis. *J. Hand Ther.* 12, 31–37. doi: 10.1016/S0894-1130(99)80031-3
- Parenti, C., Marrazzo, A., Aricò, G., Cantarella, G., Prezzavento, O., Ronsisvalle, S., et al. (2014). Effects of a selective sigma 1 antagonist compound on inflammatory pain. *Inflammation* 37, 261–266. doi: 10.1007/s10753-013-9736-6
- Pasternak, G. W., and Pan, Y. X. (2013). Mu opioids and their receptors: evolution of a concept. *Pharmacol. Rev.* 65, 1257–1317. doi: 10.1124/pr.112.007138
- Pincus, T., and Callahan, L. F. (1992). Rheumatology function tests: grip strength, walking time, button test and questionnaires document and predict longterm morbidity and mortality in rheumatoid arthritis. *J. Rheumatol.* 19, 1051–1057.
- Rodríguez-Muñoz, M., Sánchez-Blázquez, P., Herrero-Labrador, R., Martínez-Murillo, R., Merlos, M., Vela, J. M., and Garzón, J. (2015). The sigma1 receptor engages the redox-regulated HINT1 protein to bring opioid analgesia under NMDA receptor negative control. *Antioxid. Redox. Signal* 22, 799–818. doi: 10.1089/ars.2014.5993
- Romero, L., Merlos, M., and Vela, J. M. (2016). Antinociception by sigma-1 receptor antagonists: central and peripheral effects. *Adv. Pharmacol.* 75, 179–215. doi: 10.1016/bs.apha.2015.11.003
- Romero, L., Zamanillo, D., Nadal, X., Sánchez-Arroyos, R., Rivera-Arconada, I., Dordal, A., et al. (2012). Pharmacological properties of SIRA, a new sigma-1 receptor antagonist that inhibits neuropathic pain and activity-induced spinal sensitization. *Br. J. Pharmacol.* 166, 2289–2306. doi: 10.1111/j.1476-5381.2012.01942.x
- Salaffi, F., Carotti, M., Gasparini, S., Intorcchia, M., and Grassi, W. (2009). The health-related quality of life in rheumatoid arthritis, ankylosing spondylitis, and psoriatic arthritis: a comparison with a selected sample of healthy people. *Health Qual. Life Outcomes* 7:25. doi: 10.1186/1477-7525-7-25
- Sánchez-Fernández, C., Entrena, J. M., Baeyens, J. M., and Cobos, E. J. (2017). Sigma-1 receptor antagonists: a new class of neuromodulatory analgesics. *Adv. Exp. Med. Biol.* 964, 109–132. doi: 10.1007/978-3-319-50174-1-9
- Sánchez-Fernández, C., Montilla-García, A., González-Cano, R., Nieto, F. R., Romero, L., Artacho-Cordón, A., et al. (2014). Modulation of peripheral mu-opioid analgesia by sigma1 receptors. *J. Pharmacol. Exp. Ther.* 348, 32–45. doi: 10.1124/jpet.113.208272
- Sánchez-Fernández, C., Nieto, F. R., González-Cano, R., Artacho-Cordón, A., Romero, L., Montilla-García, A., et al. (2013). Potentiation of morphine-induced mechanical antinociception by sigma(1) receptor inhibition: role of peripheral sigma(1) receptors. *Neuropharmacology* 70, 348–358. doi: 10.1016/j.neuropharm.2013.03.002
- Stein, C., Clark, J. D., Oh, U., Vasko, M. R., Wilcox, G. L., Overland, A. C., et al. (2009). Peripheral mechanisms of pain and analgesia. *Brain Res. Rev.* 60, 90–113. doi: 10.1016/j.brainresrev.2008.12.017
- Stubbs, D., Krebs, E., Bair, M., Damush, T., Wu, J., Sutherland, J., and Kroenke, K. (2010). Sex differences in pain and pain-related disability among primary care patients with chronic musculoskeletal pain. *Pain Med.* 11, 232–239. doi: 10.1111/j.1526-4637.2009.00760.x
- Tejada, M. A., Montilla-García, A., Cronin, S. J., Cikes, D., Sánchez-Fernández, C., González-Cano, R., et al. (2017). Sigma-1 receptors control immune-driven peripheral opioid analgesia during inflammation in mice. *Proc. Natl. Acad. Sci. U. S. A.* 114, 8396–8401. doi: 10.1073/pnas.1620068114
- Tejada, M. A., Montilla-García, A., González-Cano, R., Bravo-Caparrós, I., Ruiz-Cantero, M. C., Nieto, F. R., and Cobos, E. J. (2018). Targeting immune-driven opioid analgesia by sigma-1 receptors: opening the door to novel perspectives for the analgesic use of sigma-1 antagonists. *Pharmacol. Res.* 131, 224–230. doi: 10.1016/j.phrs.2018.02.008
- Tejada, M. A., Montilla-García, A., Sánchez-Fernández, C., Entrena, J. M., Perazzoli, G., Baeyens, J. M., and Cobos, E. J. (2014). Sigma-1 receptor inhibition reverses acute inflammatory hyperalgesia in mice: role of peripheral sigma-1 receptors. *Psychopharmacology* 231, 3855–3869. doi: 10.1007/s00213-014-3524-3
- Unruh, A. M. (1996). Gender variations in clinical pain experience. *Pain* 65, 123–167. doi: 10.1016/0304-3959(95)00214-6
- Vela, J. M., Merlos, M., and Almansa, C. (2015). Investigational sigma-1 receptor antagonists for the treatment of pain. *Exp. Opin. Investig. Drugs* 24, 883–896. doi: 10.1517/13543784.2015.1048334
- Vidal-Torres, A., de la Puente, B., Rocasalbas, M., Tourino, C., Bura, S. A., Fernández-Pastor, B., et al. (2013). Sigma-1 receptor antagonism as opioid adjuvant strategy: enhancement of opioid antinociception without increasing adverse effects. *Eur. J. Pharmacol.* 711, 63–72. doi: 10.1016/j.ejphar.2013.04.018
- Zamanillo, D., Romero, L., Merlos, M., and Vela, J. M. (2013). Sigma 1 receptor: a new therapeutic target for pain. *Eur. J. Pharmacol.* 716, 78–93. doi: 10.1016/j.ejphar.2013.01.068

**Conflict of Interest Statement:** The authors declare that the research was conducted in the absence of any commercial or financial relationships that could be construed as a potential conflict of interest.

Copyright © 2019 Montilla-García, Tejada, Ruiz-Cantero, Bravo-Caparrós, Yeste, Zamanillo and Cobos. This is an open-access article distributed under the terms of the Creative Commons Attribution License (CC BY). The use, distribution or reproduction in other forums is permitted, provided the original author(s) and the copyright owner(s) are credited and that the original publication in this journal is cited, in accordance with accepted academic practice. No use, distribution or reproduction is permitted which does not comply with these terms.



# Allosteric Modulators of Sigma-1 Receptor: A Review

Edijs Vavers<sup>1\*</sup>, Liga Zvejniece<sup>1</sup>, Tangui Maurice<sup>2</sup> and Maija Dambrova<sup>1</sup>

<sup>1</sup> Laboratory of Pharmaceutical Pharmacology, Latvian Institute of Organic Synthesis, Riga, Latvia, <sup>2</sup> MMDN, University of Montpellier, INSERM, EPHE, UMR-S1198, Montpellier, France

## OPEN ACCESS

### Edited by:

Salvatore Salomone,  
Università degli Studi di Catania, Italy

### Reviewed by:

Nadezhda A. German,  
Texas Tech University Health Sciences  
Center, United States  
Pilar Sánchez-Blázquez,  
Spanish National Research Council  
(CSIC), Spain  
Arnold Eino Ruoho,  
University of Wisconsin School of  
Medicine and Public Health,  
United States

### \*Correspondence:

Edijs Vavers  
edijs.vavers@farm.osi.lv

### Specialty section:

This article was submitted to  
Experimental Pharmacology and Drug  
Discovery,  
a section of the journal  
Frontiers in Pharmacology

Received: 14 December 2018

Accepted: 22 February 2019

Published: 19 March 2019

### Citation:

Vavers E, Zvejniece L, Maurice T and  
Dambrova M (2019) Allosteric  
Modulators of Sigma-1 Receptor: A  
Review. *Front. Pharmacol.* 10:223.  
doi: 10.3389/fphar.2019.00223

Allosteric modulators of sigma-1 receptor (Sig1R) are described as compounds that can increase the activity of some Sig1R ligands that compete with (+)-pentazocine, one of the classic prototypical ligands that binds to the orthosteric Sig1R binding site. Sig1R is an endoplasmic reticulum membrane protein that, in addition to its promiscuous high-affinity ligand binding, has been shown to have chaperone activity. Different experimental approaches have been used to describe and validate the activity of allosteric modulators of Sig1R. Sig1R-modulatory activity was first found for phenytoin, an anticonvulsant drug that primarily acts by blocking the voltage-gated sodium channels. Accumulating evidence suggests that allosteric Sig1R modulators affect processes involved in the pathophysiology of depression, memory and cognition disorders as well as convulsions. This review will focus on the description of selective and non-selective allosteric modulators of Sig1R, including molecular structure properties and pharmacological activity both *in vitro* and *in vivo*, with the aim of providing the latest overview from compound discovery approaches to eventual clinical applications. In this review, the possible mechanisms of action will be discussed, and future challenges in the development of novel compounds will be addressed.

**Keywords:** sigma-1 receptor (Sig1R), allosteric modulator, phenytoin, E1R, SOMCL-668, SKF83959, OZP002, fenfluramine

## INTRODUCTION

The International Union of Basic and Clinical Pharmacology included sigma receptor in its list of receptors only in 2013 as a ligand-regulated non-opioid intracellular receptor (Alexander et al., 2013). Two pharmacologically distinct subtypes of sigma receptor, namely, sigma-1 receptor (Sig1R) and sigma-2 receptor (Sig2R), have been identified (Hellewell and Bowen, 1990; Quirion et al., 1992; Hellewell et al., 1994). Sig2R is known also as endoplasmic reticulum-resident transmembrane protein TMEM97 (Alon et al., 2017) involved in the regulation of cholesterol homeostasis and cell differentiation (Bartz et al., 2009; Haller et al., 2012). Number of selective Sig1R and Sig2R ligands have been described confirming significant differences in the pharmacological regulation of these subtypes. Thus, far no allosteric modulators of Sig2R have been reported.

Sig1R is an integral membrane-bound protein that is found in the nuclear membrane and endoplasmic reticulum and mitochondria-associated membrane (Mori et al., 2013; Mavlyutov et al., 2015; Su et al., 2016). Sig1R is expressed in both the CNS and peripheral tissues (Su and Junien, 1994). Sig1R is widely distributed in the brain, and it concentrates in specific areas involved in memory, emotion and sensory and motor functions (Alonso et al., 2000; Cobos et al., 2008). Sig1R,

as described by its functional nature, is a chaperone protein and a unique cell protein modulator [reviewed in (Su et al., 2016)] that can amplify or reduce the signaling initiated when interacting with target proteins (Hayashi and Su, 2007; Zamanillo et al., 2012; Rodríguez-Muñoz et al., 2015). Therefore, Sig1R demonstrates properties that can be attributed to both chaperone proteins and receptors. However, the notion that allosteric modulators of Sig1R are identified is an additional argument for the “receptor” view of Sig1R.

Allosteric regulation is the regulation of protein activity by binding an effector molecule at a site other than the orthosteric or active site of a protein (**Figure 1**). The binding of allosteric modulators to a target protein induces a conformational change in the protein structure and changes the activity of orthosteric ligands (**Figure 1**). Allosteric modulators can be positive or negative effectors (PAMs or NAMs, respectively). PAMs increase the activity of the ligand, while NAMs block it (**Figure 1**). To date phenytoin, some benzazepine derivatives and stereoisomers of methylphenylpiracetam have been reported as PAMs of Sig1R while NAMs of Sig1R have not yet been described. The definition of allosteric Sig1R modulators might be artificial due to a lack of information on the orthosteric binding site for Sig1R. It is thought that the orthosteric binding site for Sig1R ligands is the binding site of (+)-SKF-10,047 and (+)-pentazocine, benzomorphan compounds that were the first identified to bind to Sig1R with high affinity and selectivity (Martin et al., 1976; Su, 1982). Thus, allosteric modulators of Sig1R are described as compounds that can increase the activity of Sig1R ligands that compete with [ $^3$ H](+)-pentazocine for binding to Sig1R.

At the moment, two compounds, the Sig1R and muscarinic receptor mixed agonist ANAVEX<sup>TM</sup> 2-73 (ANAVEX Life Sciences, ClinicalTrials.gov Identifier: NCT02244541) and the Sig1R antagonist E-52862 (ESTEVE, EudraCT number: 2012-000400-14) are being tested in clinical trials for the treatment of Alzheimer’s disease and neuropathic pain, respectively, thus

justifying the importance of Sig1R as a valid molecular target for clinical applications. Compared to widely used agonists and antagonists, allosteric modulators are less studied but are highly promising due to their advantageous clinical applications.

In recent years, significant progress has been achieved in the discovery, optimization and preclinical development of allosteric Sig1R modulators. These compounds can provide new advances in developing novel drugs, drug leads and research tools for Sig1R and have potential utility for the treatment of multiple human disorders. Accumulating evidence suggests that allosteric Sig1R modulators affect processes involved in the pathophysiology of depression, memory and cognition disorders as well as convulsions, and thus can provide novel strategies for the treatment of neurological disorders.

This review summarizes the literature and data on all known Sig1R allosteric modulators, including discovery and development, *in vitro* and *in vivo* pharmacological activities and discussion on allosteric regulation of Sig1R.

## DISCOVERY OF ALLOSTERIC SIG1R MODULATORS

The first evidence indicating that a compound demonstrates allosteric activity on Sig1R came from radioligand binding studies. The first drug discovered as an allosteric modulator of Sig1R was phenytoin (diphenylhydantoin, **Figure 2**). Phenytoin has been used in clinical practice as an anti-convulsant since 1930 (Merritt and Putnam, 1984; Yaari et al., 1986). The anti-convulsant mechanism of phenytoin is the selective blockage of neuronal voltage-dependent sodium channels (Yaari et al., 1986). Over the course of competition binding studies, it was shown that phenytoin can increase the binding of [ $^3$ H]dextromethorphan ([ $^3$ H]DM) (Craviso and Musacchio, 1983) and [ $^3$ H](+)-3-(3-hydroxyphenyl)-N-propylpiperidine ([ $^3$ H](+)-3-PPP) in the guinea pig brain (Musacchio et al., 1989).

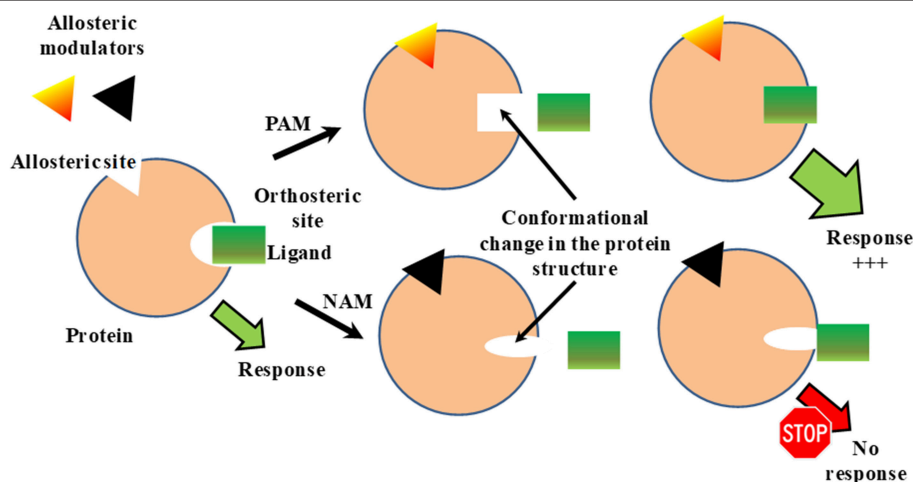
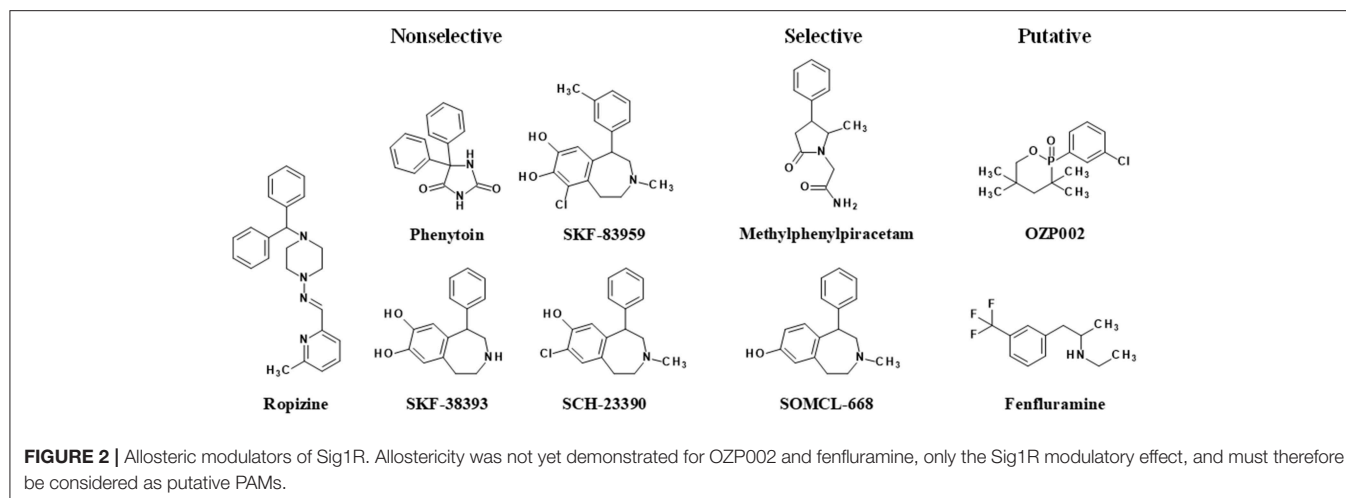


**FIGURE 1 |** Classical model for allosteric regulation of receptor. PAM, positive allosteric modulation; NAM, negative allosteric modulation. This Figure has been modified from Vavters (2017).





These results were the first showing that phenytoin allosterically modulated the binding of prototypic sigma site ligands. Very rapidly, phenytoin sensitivity was even considered an intrinsic characteristic of the sigma-1 subtype of sigma sites, not shared by sigma-2 (Quirion et al., 1992). Sig1R were indeed defined mainly through their high-affinity sites for the dextrorotatory isomers of benzomorphans and their sensitivity to phenytoin. Moreover, similar to phenytoin, ropizine (SC-13504), an anti-convulsant benzhydryl piperazine (**Figure 2**), induced a marked concentration-dependent increase in the binding of [ $^3$ H]DM (Musacchio et al., 1988) and [ $^3$ H](+)-3-PPP (Musacchio et al., 1989). It was shown that the non-narcotic anti-tussive nescapine can dose-dependently potentiate the binding of [ $^3$ H]DM in guinea pig brainstem homogenate (Craviso and Musacchio, 1983). In addition, hydrastine demonstrated similar activity on the binding of [ $^3$ H]DM (Craviso and Musacchio, 1983). However, to date, nescapine and hydrastine have not been demonstrated to modulate the binding of more selective Sig1R ligands such as [ $^3$ H](+)-pentazocine and are considered only putative allosteric Sig1R modulators.

Later, compound SR31747A (N-cyclohexyl-N-ethyl-3-(3-chloro-4-cyclohexylphenyl)propen-2-ylamine hydrochloride) was also proposed to act as an allosteric modulator of peripheral sigma binding sites (Paul et al., 1994). Although SR31747A modulated the activity of Sig1R ligands *in vivo* and *in vitro*, the use of radiolabeled [ $^3$ H]SR31747A demonstrated that SR31747A binds specifically, saturably and reversibly to rat spleen membranes and human lymphocytes at a single class of high-affinity sites, which were clearly different from the [ $^3$ H](+)-pentazocine and [ $^3$ H](+)-3-PPP binding sites (Paul et al., 1994). A few years later, the purified amino acid sequence of the [ $^3$ H]SR31747A binding site was found to be a nuclear membrane protein related to a fungal C8-C7 sterol isomerase; additionally, this protein, which was called SR31747A-binding protein, was encoded by the ERG2 gene (Jbilo et al., 1997). The exact molecular mechanism of SR31747A has not been fully described thus far, but SR31747A is currently not considered an allosteric Sig1R modulator.

In 2013, more than two decades after the discovery of the positive allosteric Sig1R modulatory activity of phenytoin, it was shown that the atypical dopamine D<sub>1</sub> receptor agonist SKF83959 (3-methyl-6-chloro-7,8-hydroxy-1-[3-methylphenyl]-2,3,4,5-tetrahydro-1H-3-benzazepine) and its analogs SKF38393 and SCH23390 act as allosteric Sig1R modulators (Guo et al., 2013; **Figure 2**). These compounds could enhance the binding activity of [ $^3$ H](+)-pentazocine in brain and/or liver tissues, shift the saturation curve toward the left, and decrease the dissociation rate in binding kinetic analysis (Guo et al., 2013). At the same time another allosteric Sig1R modulator, methylphenylpiracetam (2-(5-methyl-2-oxo-4-phenyl-pyrrolidin-1-yl)-acetamide), was described (Veinberg et al., 2013; **Figure 2**). The activity of E1R, a 4R,5S-isomer of methylphenylpiracetam, was profiled using commercially available screening assays, which showed that the compound selectively modulates Sig1R activity but does not affect the other investigated neuronal receptors and ion channels (Zvejniece et al., 2014). The following detailed *in vitro* studies, in which more selective Sig1R ligands were used, provided solid evidence that E1R is a PAM of Sig1R (Zvejniece et al., 2014). Sig1R is the only molecular target described thus far that accounts for the pharmacological activity of E1R. Therefore, E1R is considered the first known selective allosteric Sig1R modulator. Later, several chemical derivatives of SKF83959 were synthesized to find a selective Sig1R allosteric modulator and to exclude the potential involvement of other receptors. One of these newly synthesized compounds, called SOMCL-668 (**Figure 2**), did not exhibit affinity for human dopamine D<sub>1</sub>, D<sub>2</sub>, D<sub>3</sub>, serotonin 5-HT<sub>1A</sub>, or 5-HT<sub>2A</sub> receptors (Zhang et al., 2014) but did show potent allosteric modulating activity at Sig1R (Guo et al., 2015). Therefore, SOMCL-668 has also been proposed as a selective allosteric Sig1R modulator.

Recently, a novel oxazaphosphinane compound derived from hydroxybupropion, was described (Volle et al., 2010). (±)-2-(3-chlorophenyl)-3,3,5,5-tetramethyl-2-oxo-[1,4,2]-oxazaphosphinane (OZP002) did not inhibit [ $^3$ H](+)-pentazocine binding to Sig1R, as did bupropion

or hydroxybupropion (Ritz and George, 1997), but rather moderately increased it. However, the drug did potentiate Sig1R agonist-induced antidepressant and anti-amnesic effects in wild-type mice but not in Sig1R-knock-out animals, and the effects were prevented by a Sig1R antagonist NE-100 suggesting a Sig1R positive modulatory effect (Maurice et al., 2017). Finally, fenfluramine (N-ethyl- $\alpha$ -methyl-3-(trifluoromethyl)-benzeneethanamine), a potent serotonin releaser activating multiple 5-HT receptor subtypes (Fuller et al., 1988), has been described for its positive modulatory activity at Sig1R (Maurice et al., 2018). Beyond serotonin, fenfluramine also binds Sig1R with high nanomolar affinity for Sig1R. However, in functional assays, fenfluramine potentiated the (+)-SKF-10,047-induced increase in the twitch contraction amplitude and the Sig1R/binding immunoglobulin protein (BiP) dissociation induced by the Sig1R agonist PRE-084, suggesting a positive modulatory action at Sig1R (Maurice et al., 2018).

The list of identified or suspected Sig1R positive modulators is presently being extended, and they present effective pharmacological activity that is closely related *in vivo* to that of orthosteric agonists. However, the different chemical structures of the identified compounds suggest a complex mode of action and clear specificities among the drugs.

## THE PHARMACOLOGICAL ACTIVITIES OF ALLOSTERIC SIG1R MODULATORS

### Phenytoin

The allosteric modulation of sigma recognition sites by phenytoin has been demonstrated by the ability of phenytoin to stimulate the binding of various tritiated Sig1R agonists (Musacchio et al., 1988; McCann and Su, 1991; Chaki et al., 1996; Cobos et al., 2005), to slow dissociation from sigma sites and to shift sigma sites from a low-affinity state to a high-affinity state (DeHaven-Hudkins et al., 1993). A detailed comparison of the effects of phenytoin on the binding of [ $^3$ H](+)-pentazocine and [ $^3$ H]NE-100 using saturation and kinetics assays showed that phenytoin acts as PAM and can negatively modulate the binding of [ $^3$ H]NE-100 by decreasing the specific binding and increasing the dissociation rate from Sig1R (Cobos et al., 2006), demonstrating significant allosteric effects on the Sig1R ligand binding to Sig1R.

Phenytoin has been used in the clinic against various types of epileptiform seizures for more than 80 years (Santulli et al., 2016). The mechanism by which phenytoin exerts its anti-seizure activity is primarily related to the inhibition of voltage-gated sodium channels (Tunnicliff, 1996). Phenytoin has been reported to reduce increases in extracellular  $K^+$  concentration in neuroblastoma cells (Nobile and Lagostena, 1998) and inhibit both  $Na^+$  (Rush and Elliott, 1997) and T-type  $Ca^{2+}$  currents in isolated dorsal root ganglia (Todorovic and Lingle, 1998). Phenytoin was shown to block the decrease in extracellular  $Ca^{2+}$  concentration effected by repetitive stimulation of pyramidal cells in hippocampal slices (Yaari et al., 1986). In rat cerebral synaptosomes phenytoin has been shown to increase the activity of  $Na^+$ - $K^+$ -ATPase (Festoff and Appel, 1968). Phenytoin is known to block  $Na^+$  influx through sodium channels and the

binding of [ $^3$ H]phenytoin to these channels is inhibited by sodium channel blockers (Tunnicliff, 1996). It has been shown that Sig1R is involved in the regulation of sodium channels (Johannessen et al., 2009), however it has not been clearly demonstrated that the effects of phenytoin on sodium channels are Sig1R specific, and the *in vivo* pharmacological effects of phenytoin are not Sig1R related. Therefore, phenytoin is a non-selective allosteric modulator of Sig1R.

### Ropizine (SC-13504)

Ropizine was shown to increase the binding of [ $^3$ H]DM and [ $^3$ H](+)-3-PPP in guinea pig brains (Musacchio et al., 1988, 1989). The allosteric effects of ropizine on [ $^3$ H]DM binding are fully apparent at 10-fold lower concentrations than those of phenytoin (Musacchio et al., 1988). Ropizine has been shown to possess anti-convulsant activity in mice (Craig, 1967), cats (Edmonds and Stark, 1974) and dogs (Edmonds et al., 1978). It has been shown that ropizine is similar in efficacy to phenytoin in maximal electroshock-induced seizures (Novack et al., 1979), while it has limited anti-convulsant activity against chemically induced seizures (Edmonds et al., 1978, 1979). Ropizine is more active and potent than phenytoin in antagonizing the after discharges produced by cortical or hippocampal stimulation in cats (Joy and Edmonds, 1974). Data in the literature about the mechanism of action of ropizine are scarce (Table 1). It has been shown that ropizine inhibits magnesium-dependent ATPase activity in rat brain synaptosomes (Gilbert and Wyllie, 1976). Direct involvement of Sig1R in this pharmacological activity has not been demonstrated, and thus, ropizine is considered a non-selective allosteric modulator of Sig1R.

### Methylphenylpiracetam (E1R)

The Sig1R site was the only site that E1R was discovered to target in *in vitro* pharmacological profiling assays, which included a number of ion channels, G protein-coupled receptors and CNS transporters (Zvejniec et al., 2014). The selected *in vitro* assays revealed that E1R did not bind directly to Sig1R but rather acted as a PAM of the receptor and enhanced the binding of an unselective sigma receptor radioligand [ $^3$ H]DTG. E1R potentiated the contractions of rat vas deferens in the presence of the selective Sig1R agonist PRE-084 but not in the presence of the Sig2R agonist PB-28 (Zvejniec et al., 2014). In addition, E1R enhanced the effect of PRE-084 on the BDK-induced [ $Ca^{2+}$ ] $_i$  increase, thus confirming its Sig1R positive allosteric modulatory effect *in vitro*.

E1R successfully alleviated scopolamine-induced cognitive impairment in mice, as assessed using passive avoidance and spontaneous alternation (Y-maze) tests. The effects of E1R were antagonized by the selective Sig1R antagonist NE-100, thus confirming the Sig1R modulatory activity of E1R *in vivo*. E1R demonstrated dose-dependent anti-convulsant effects on pentylenetetrazole (PTZ)- and bicuculline (BIC)-induced seizures at doses of 10 and 50 mg/kg (Vavers et al., 2017; Tables 1, 3). To verify that Sig1R was involved in the anti-convulsant activity of E1R, the selective Sig1R antagonist NE-100 was used. The administration of NE-100 (5 mg/kg) before E1R (10 mg/kg) significantly restored the tonic seizure threshold to

**TABLE 1** | Summary of *in vivo* effects of allosteric Sig1R modulators.

Compound	Dose, mg/kg (route of administration)	Effect <i>in vivo</i>	Animal model (species)	Molecular target	References
Phenytoin*	5–20 (i.p.)	Anti-seizure activity/*anti-epileptic drug	Maximal electroshock-induced seizures (mice)	Voltage-gated sodium channels	Jones et al., 1981; Reviewed in Tunnickliff, 1996
	20, 40 (p.o.)	Anti-seizure activity	Ischemia-induced epilepsy (rats)		Edmonds et al., 1996
Ropizine (SC-13504)	2, 4 (i.v.)	Anti-seizure activity	Penicillin-induced epileptogenic foci (cats)	N/A	Edmonds and Stark, 1974
	4, 6 (i.v.)	Anti-seizure activity	Photosensitive epilepsy (baboons)	Magnesium-dependent ATPase	Meldrum et al., 1976
	3, 300 (p.o.)	Anti-seizure activity	Partially kindled hippocampal seizures (rats)	N/A	Albertson et al., 1978
	2.5 (ED <sub>50</sub> )	Anti-seizure activity	Maximal electroshock-induced seizures (rats)	N/A	Edmonds et al., 1979
SKF-83959	0.5 (i.p.)	Anti-Parkinson activity	6-OHDA-induced Parkinson's disease model (rats)	Dopamine D <sub>1</sub> receptor	Zhang et al., 2007
	0.5, 1 (i.p.)		6-OHDA-induced Parkinson's disease model (rats)		Zhen et al., 2005
	2, 4, 8 (i.p.)	Anti-depressant activity	Tail suspension test; forced swimming test (mice)	SERT/NET/DAT	Fang et al., 2013
	0.5, 1 (i.p., 10 days)		Chronic social defeat stress model (mice)	Dopamine D <sub>5</sub> receptor	Jiang et al., 2015
	10, 20, 40 (i.p.)	Anti-seizure activity	PTZ-induced seizures; kainic acid-induced <i>status epilepticus</i> (mice)	Sig1R	Guo et al., 2015
	1 (i.p., 11 days)	Anti-tumor activity	S.c. injection of GH3 and SCG7901 cancer cells (mice)	Dopamine D <sub>5</sub> receptor	Leng et al., 2017
	0.5, 1 (i.p.)	Memory improvement	Scopolamine-induced learning deficits (mice)	Dopamine D <sub>1</sub> -D <sub>2</sub> receptor heteromer	Sheng et al., 2018
SCH-23390	0.1–0.3 (i.p.)	Anti-seizure activity	Pilocarpine-induced seizures (rats)	Dopamine D <sub>1</sub> receptor	Barone et al., 1992
	0.8 (i.p.)		Pilocarpine-induced seizures (mice)		Burke et al., 1990
	0.5 (i.p.)		Soman-induced seizures (guinea pigs)		Bourne et al., 2001
SKF-38393	1, 5, 10 (s.c.)	Anti-seizure activity	PTZ-induced seizures (mice)	Dopamine D <sub>1</sub> receptor	Ogren and Pakh, 1993
	5 (i.p.)	Memory improvement	Maternal deprivation-induced memory deficiency (rats)	Dopamine D <sub>1</sub> receptor	Lejeune et al., 2013
SOMCL-668	40 (i.p.)	Anti-seizure activity	PTZ-induced seizures; kainic acid-induced <i>status epilepticus</i> (mice)	Sig1R	Guo et al., 2015
	10, 20 (i.p.)	Anti-depressant activity	Forced swimming test; tail suspension test; sucrose preference test (mice)	Sig1R	Wang et al., 2016
E1R	1, 5, 10 (i.p.)	Memory improvement	Scopolamine-induced learning deficits (mice)	Sig1R	Zvejniece et al., 2014
	10, 50 (i.p.)	Anti-seizure activity	PTZ- and BIC-induced seizures (mice)	Sig1R	Vavers et al., 2017
OZP002	10, 30 (i.p.)	Anti-depressant-like activity	Forced swimming test (mice)	Sig1R	Maurice et al., 2017
	0.1, 0.3 (i.p.)	Anti-amnesic activity	Scopolamine-induced learning deficits; i.c.v. injection of amyloid Aβ <sub>25–35</sub> peptide; APP <sub>Swe</sub> mice (mice)	Sig1R	
	0.7 (i.p.)	Neuroprotection	I.c.v. injection of amyloid Aβ <sub>25–35</sub> peptide (mice)	Sig1R	
Fenfluramine (ZX008)*	3 nmol (i.c.v.)	Anti-seizure activity	I.c.v. injection of NMDA (mice)	Serotonin 5-HT <sub>2A</sub> receptor, Sig1R	Rodríguez-Muñoz et al., 2018
	0.3, 1 (i.p.)	Anti-amnesic effect	Dizocilpine-induced learning deficits (mice)	Sig1R	Maurice et al., 2018
	10, 30 (i.p.)	Anti-depressant-like activity	Forced swimming test (mice)	Serotonin 5-HT <sub>1A</sub> receptor, Sig1R	Maurice et al., 2018

\*Drug used in clinics; i.v., intravenous; i.p., intraperitoneal; s.c., subcutaneous; i.c.v., intracerebroventricular; Sig1R, sigma-1 receptor.

the basal level and therefore showed that the anti-seizure effect of E1R was mediated through Sig1R activity (Vavers et al., 2017). The pharmacological activity of E1R demonstrates that it is a selective PAM of Sig1R.

## Benzazepine Derivatives

### SKF83959, SCH23390, SKF38393

SKF83959 is an atypical D<sub>1</sub> agonist (Downes and Waddington, 1993; Deveney and Waddington, 1995). Previously, it was shown that SKF83959 also exerted many D<sub>1</sub> receptor-independent pharmacological effects. For example, SKF83959 suppressed excitatory synaptic transmission and voltage-activated Na<sup>+</sup> current in rat hippocampus (Chu et al., 2011), inhibited the delayed rectifier potassium channel in primary culture neurons (Chen et al., 2009), and promoted the spontaneous release of glutamate in the rat somatosensory cortical neurons (Chu et al., 2010). The activity of SKF83959 was related to Sig1R based on the pharmacological activity of SKF83959 and similarities of the pharmacophore with some other Sig1R ligands. SKF-83959 increased the binding of [<sup>3</sup>H](+)-pentazocine to Sig1R in the brain and liver tissues and showed that SKF-83959 is PAM of Sig1R (Guo et al., 2013). SKF83959 has been shown to inhibit the generation of intracellular reactive oxygen species and the expression of tumor necrosis factor  $\alpha$ , interleukin-1 $\beta$ , and cytokine-inducible nitric oxide synthase in lipopolysaccharide-stimulated mouse brain microglial BV2 cells (Wu et al., 2015). These effects of SKF83959 were blocked by Sig1R antagonists BD-1047 and BD1063 (Wu et al., 2015). In the same study, it was shown that in a [<sup>3</sup>H](+)-pentazocine binding assay, SKF83959 enhanced the binding activity of dehydroepiandrosterone (DHEA), a neurosteroid acting as a Sig1R agonist, by shifting the DHEA binding curve to the left. In addition, SKF83959 enhanced the anti-inflammatory effect of exogenous DHEA in a synergistic manner, which was dependent on Sig1R (Wu et al., 2015), thus showing that the anti-inflammatory effects of SKF83959 are due to positive allosteric Sig1R modulator activity in cells.

The anti-convulsant effects of SKF83959 at doses of 20 and 40 mg/kg in PTZ- and kainic acid-induced seizures were demonstrated to be mediated by modulating Sig1R (Guo et al., 2015, **Tables 1, 3**). The anti-convulsant effects of SKF83959 were blocked by the selective Sig1R antagonist BD-1047 at a dose of 1 mg/kg (Guo et al., 2015). SKF83959 has also demonstrated significant anti-Parkinson, anti-depressant, anti-tumor and memory-improving activity, which is associated with activity at dopamine receptors and regulation of dopamine reuptake (summarized in **Table 1**). In addition, it has been shown that SKF83959 inhibits voltage-gated sodium channels in cultured striatal neurons via the D<sub>1</sub>-like receptor-phosphatidylinositol-PKC pathway (Ma et al., 2015) and inhibits dopamine-sensitive adenylyl cyclase activity (Downes and Waddington, 1993), which are responsible for some additional *in vivo* activities not related to Sig1R.

SKF83959 analogs, such as SCH22390 and SKF38393, also have shown similar allosteric effects on Sig1R in liver tissue using [<sup>3</sup>H](+)-pentazocine (Guo et al., 2013). It was shown that SCH23390 affords protection against pinacolylmethylphosphonofluoridate-evoked electrical and

motor seizure activity by inhibiting D<sub>1</sub> receptor (Bourne and Fosbraey, 2000) but, similar to SKF83959, does not demonstrate anti-seizure activity in a PTZ-induced seizure model (Guo et al., 2015). SCH23390 is considered a highly potent D<sub>1</sub> antagonist (Hyttel, 1983) and demonstrates moderately high affinity for the 5-HT<sub>2</sub> and 5-HT<sub>1C</sub> receptors as well (Hicks et al., 1984). In contrast, SKF38393 is a selective D<sub>1</sub> agonist (Molloy and Waddington, 1984), and the *in vivo* pharmacological activity of SKF38393 is D<sub>1</sub> receptor dependent (**Table 1**). Overall, SKF83959 and its analogs SCH22390 and SKF38393 are non-selective allosteric modulators of Sig1R.

### SOMCL-668

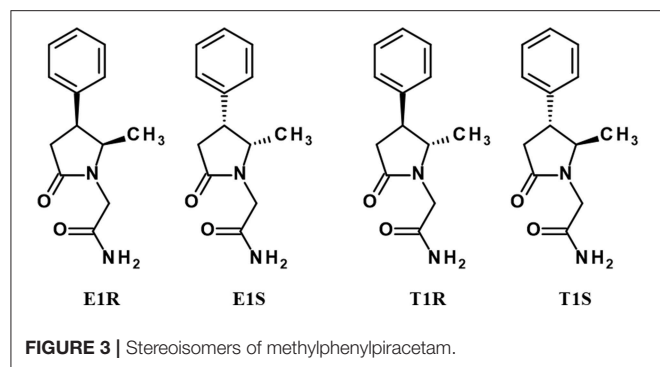
SOMCL-668 has demonstrated selective allosteric modulating activity on Sig1R (Guo et al., 2015). In the [<sup>3</sup>H](+)-pentazocine binding assay, SOMCL-668 shifted the saturation curve toward the left and significantly decreased the dissociation constant of the radioligand (Guo et al., 2015). SOMCL-668 synergized the effect of (+)-SKF-10,047 on Sig1R dissociation from binding immunoglobulin protein, which was further confirmed by immunoprecipitation and the plasma membrane translocation assay (Wang et al., 2016). SOMCL-668 increased the phosphorylation of glycogen synthase kinase-3 $\beta$  (GSK3 $\beta$ ) on the Ser<sup>9</sup> epitope and potentiated the agonist (+)-SKF-10,047-increased phosphorylation of (Ser<sup>9</sup>)-GSK3 $\beta$  in the hippocampus of mice and in hippocampal neuronal HT-22 cells, which was abolished by pretreatment with the Sig1R antagonist BD-1047 or by the knockdown of Sig1R in HT-22 cells (Wang et al., 2016). SOMCL-668 also significantly potentiated (+)-SKF-10,047-stimulated neurite growth and the production of BDNF (Wang et al., 2016), and the effect was Sig1R dependent.

The selective Sig1R allosteric modulator SOMCL-668 has been tested for its potential anti-depressant activity (Wang et al., 2016). SOMCL-668 at doses of 10 and 20 mg/kg significantly decreased the immobility time of mice in the forced-swimming and tail suspension tests, and these effects were blocked by the BD-1047 (Wang et al., 2016). In addition, daily administration of SOMCL-668 at a dose of 10 mg/kg for 1 week significantly reversed the decrease in the sucrose preference in the chronic mild stress model in mice (Wang et al., 2016). SOMCL-668 at a dose of 40 mg/kg also raised the seizure threshold in the maximal electroshock seizure test and prolonged the latencies to the clonus and generalized tonic-clonic convulsions as well as the survival time in the PTZ-induced seizure model (Guo et al., 2015). In kainic acid-induced *status epilepticus* SOMCL-668 prolonged the latency to seizure, lowered the average severity of seizure and shortened the duration of seizure (Guo et al., 2015). Moreover, the Sig1R antagonist BD-1047 at a dose of 1 mg/kg abolished the anti-seizure activity of SOMCL-668, indicating that its effect was Sig1R dependent (Guo et al., 2015; **Table 1**). Only Sig1R has been demonstrated to be involved in the pharmacological activities of SOMCL-668; therefore SOMCL-668 is considered a selective PAM of Sig1R.

### OZP002

The oxazaphosphinane compound did not inhibit [<sup>3</sup>H](+)-pentazocine binding to sigma sites, but it did induce Sig1R receptor-like effects *in vivo* and potentiated the behavioral





efficacy of Sig1R agonists. OZP002 had an antidepressant effect in the forced swimming test at 10 mg/kg and potentiated the effect of the Sig1R agonist igmesine at 5 mg/kg. These effects were blocked by coinjection of the Sig1R antagonist NE-100 or were absent in Sig1R-knock-out mice (Maurice et al., 2017). OZP002 prevented scopolamine-induced learning and memory impairments (spontaneous alternation or passive avoidance) at 0.1–0.3 mg/kg, and these effects were blocked not only by NE-100 but also, interestingly, by the  $\alpha 7$  nicotinic acetylcholine receptor antagonist methyllycaconitine (Maurice et al., 2017). Moreover, the compound was analyzed for its neuroprotective activity in a pharmacological model of Alzheimer's disease, induced in mice by intracerebroventricular injection of oligomerized amyloid A $\beta_{25-35}$  peptide, and in APP<sup>Swe</sup> mice after a 2-months treatment. OZP002 prevented learning deficits in both models and decreased the expression levels of several markers of apoptosis, neuroinflammation and oxidative stress (Maurice et al., 2017). The drug therefore clearly acted as a Sig1R positive modulator and showed *in vivo* pharmacological activity closely related to that of Sig1R agonists, combining pharmacological efficacy, selectivity and therapeutic safety.

## Fenfluramine (ZX008)

Fenfluramine has recently been shown in 2 phase 3 studies to have anti-convulsant activity in a childhood epilepsy condition, Dravet syndrome (Polster, 2018). It acts as a 5-HT agonist by interacting with 5-HT<sub>1D</sub>, 5-HT<sub>2A</sub>, and 5-HT<sub>2C</sub> receptors (Sourbron et al., 2016). The drug also interacts with Sig1R at nanomolar concentrations (Martin et al., 2017). In the Sig1R/BiP dissociation assay, it did not promote Sig1R/BiP dissociation but rather potentiated the effect of the Sig1R agonist PRE-084, suggesting a positive modulatory activity. The (+)-isomer of fenfluramine but not (–)-fenfluramine attenuated dizocilpine-induced deficits in a similar manner as PRE-084 (Maurice et al., 2018). It must be noted that the racemate and individual isomers of fenfluramine-related compound norfenfluramine did not affect dizocilpine-amnesia but rather prevented the PRE-084 effect, suggesting Sig1R antagonism. Combination between low doses of fenfluramine or (+)-fenfluramine and PRE-084 followed by calculation of combination indexes (Zhao et al., 2010; Maurice, 2016) showed that most combinations led to

synergistic effects. Fenfluramine, as well as its active isomer (+)-fenfluramine, behaved *in vitro* and *in vivo* as Sig1R positive modulators. The drug is therefore a mixed 5-HT releaser/5-HT agonist and Sig1R modulator. Moreover, as the neuromodulatory role of Sig1R on neurotransmitter release, receptor activation and regulation of numerous ionophores is well-described, Sig1R modulation must be considered in the potential mechanism of action of its anti-convulsant activity demonstrated for Dravet syndrome (Polster, 2018).

## COMPARISON OF THE EFFECTS OF ALLOSTERIC SIG1R MODULATORS

### Stereochemistry of Allosteric Sig1R Modulators

A number of Sig1R ligands contains chiral centers in their molecular structures, which indicates that compounds are optically active and that there are possibly different stereoisomers of the same molecule, which also corresponds to different pharmacological activities for the same molecules. Geometric isomers of ropizine in *cis* and *trans* forms are possible, but the molecule of ropizine is not optically active. Additionally, phenytoin is not an optically active compound due to the lack of chiral atoms in the molecular structure. Methylphenylpiracetam is a complex molecule in terms of its stereochemistry. There are two chiral centers in the molecular structure of methylphenylpiracetam; therefore, it is possible to isolate four individual stereoisomers, which are denoted E1R, T1R, E1S, and T1S (reviewed in Veinberg et al., 2015; Figure 3).

SKF83959 is a racemate that consists of the R-(+)- and S-(–)-enantiomers MCL-202 and MCL-201, respectively (Desai et al., 2007). The R-(+)- and S-(–)-enantiomers are also possible for SKF38393, SCH23390, and SOMCL-668 (Figure 4).

All stereoisomers of methylphenylpiracetam are known to act as PAMs of Sig1R (Veinberg et al., 2013). In an *ex vivo* test the enantiomers with the R-configuration at the C-4 chiral center in the 2-pyrrolidone ring (E1R and T1R) were found to be more effective PAMs of Sig1R than their optical antipodes (Veinberg et al., 2013), showing that some stereo selectivity is possible also for allosteric Sig1R modulators.

The Sig1R modulatory activity of changes in the activity of Sig1R ligands induced by different enantiomers of benzazepine derivatives has not been compared. It would be interesting to compare the allosteric modulatory activity on Sig1R regarding the stereochemical properties of benzazepine derivatives. For example, it has been shown that the D<sub>1</sub> receptor binding site favors the R-enantiomers of the D<sub>1</sub> receptor-selective benzazepines over the corresponding S-enantiomers (Kebabian, 1988), which is true for both the D<sub>1</sub> agonist SKF38393 and the D<sub>1</sub> antagonist SCH23390 (Kebabian, 1988). In addition, the stereo selectivity of the R-isomer of SCH23390 for blockade of D<sub>1</sub> receptors *in vivo* has been demonstrated (Ongini et al., 1987). In the case of benzazepine derivatives, Sig1R selectivity over dopamine receptors could depend on the pharmacological activity of individual isomers. However, this dependence has not been demonstrated so far.

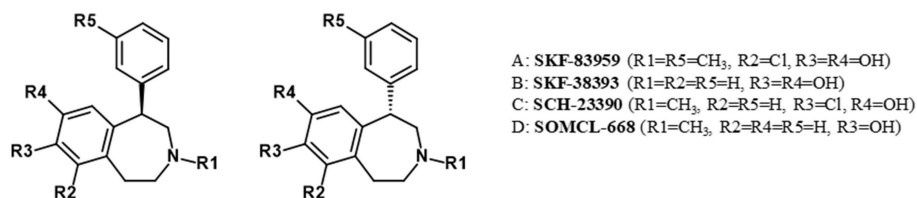


FIGURE 4 | Enantiomers of benzazepine analogs.

The structure-activity relationship for fenfluramine is rather clear since the positive modulator activity of the drug originates from only the dextrorotatory isomer (+)-fenfluramine. In all behavioral responses analyzed, the racemate behaved as (+)-fenfluramine, suggesting chiral binding of the drug to the yet unidentified, modulatory binding site on Sig1R.

### In vitro Effects

No screening assay is available for allosteric modulators of Sig1R. Therefore, different *in vitro* assays and *in vivo* pharmacological approaches have been used to describe and validate the activity of allosteric Sig1R modulators. For comparison, the Sig1R-related *in vitro* activities of allosteric Sig1R modulators are summarized in Table 2.

The allosteric modulatory activity of phenytoin has previously been described in rat and guinea pig brains (DeHaven-Hudkins et al., 1993; Cobos et al., 2006; Guo et al., 2013), rat livers (McCann and Su, 1991), and mice lung tissues (Lever et al., 2015). In turn, it has been shown that phenytoin could modulate Sig1R ligand binding in rat brain tissue but not in rat liver tissue (Guo et al., 2013, Table 2). For example, SCH23390 and SKF38393 modulated the binding of [ $^3H$ ](+)-pentazocine only in liver tissues, while no detectable effects were observed in brain tissues (Guo et al., 2013). In the same study, SKF83959 was shown to allosterically modulate the binding of [ $^3H$ ](+)-pentazocine in both rat brain and liver tissues (Guo et al., 2013). The different effects of these Sig1R allosteric modulators in rat and guinea pig brain tissues have been described previously and could be explained by the variation in the size of the binding site between the two species (Klein and Musacchio, 1992). It seems that not only different species but also different tissues from the same animal species can respond differently to allosteric Sig1R modulators. SKF83959 and its analogs failed to change the binding activity of [ $^3H$ ](+)-pentazocine at Sig1R in human embryonic kidney (HEK)293 cells that stably expressed the Sig1R (Guo et al., 2013). The lack of binding modulatory activity of [ $^3H$ ](+)-pentazocine in HEK293 cells was also observed for phenytoin (Guo et al., 2013). Although [ $^3H$ ](+)-pentazocine displayed similar affinity for Sig1R in transfected HEK293 cells and rat brain tissues, the absence of allosteric modulation of Sig1R in the constructed system *in vitro* could be attributed to differences in Sig1R structure, cellular contents, or auxiliary proteins (Guo et al., 2013), which should be taken into account when studying mechanisms of Sig1R *in vitro*.

Above described issues rise number of questions in the understanding of molecular mechanisms of allosteric Sig1R modulators. Why allosteric modulatory activity of compounds has been observed in one type of tissues and/or animal species but not in the others? Is that because of the structure differences between compounds? Could it be because of different Sig1R structures, conformation states or even tissue specific Sig1R subtypes? Are there species specific Sig1R? It should be noted that some observed allosteric effects on Sig1R were shown after administration of allosteric modulator in high concentrations (Table 2). Thereby, how Sig1R-specific is the activity of allosteric modulators? Are there other proteins involved in the activity of compounds? What is the influence of endogenous compounds? Future studies must be focused to answer these questions. Nevertheless, it is clear that allosteric Sig1R modulators could be used as pharmacological tools to increase the global understanding of the physiological function of Sig1R and its interaction with ligands. Also the Sig1R-related *in vivo* activities of allosteric Sig1R modulators are very promising to reach clinical advantages.

### Anti-seizure Activity

All allosteric Sig1R modulators demonstrate anti-seizure activity. However, the anti-seizure activity is not associated directly with Sig1R for most of allosteric Sig1R modulators (Table 3).

It was demonstrated that the anti-seizure effect of E1R, SOMCL-668, and SKF83959 was blocked by the Sig1R selective antagonists NE-100 and BD-1047 (Guo et al., 2015; Vavers et al., 2017), while the anti-seizure effect of phenytoin was not blocked by BD-1047 (Guo et al., 2015). Moreover, anti-seizure effect of phenytoin is related to the inhibition of voltage-gated sodium channels (Tunnicliff, 1996). At the same time, it was shown that SCH23390, an analog of SKF83959, does not affect PTZ-induced seizures (Guo et al., 2015). Rather, SCH23390 has been shown to modulate seizures evoked by the subcutaneous administration of the cholinesterase inhibitor pinacolylmethylphosphonofluoridate and this activity was demonstrated to be D<sub>1</sub> receptor dependent (Bourne et al., 2001). Current knowledge indicates that not all PAMs of Sig1R possess anti-seizure activities and that the anti-seizure effects are not always regulated by Sig1R.

### Memory Improvement

Among all the positive allosteric Sig1R modulators described, E1R, OZP002, and fenfluramine showed Sig1R-dependent memory-improving effects (Zvejniece et al., 2014; Maurice et al.,

**TABLE 2 |** The comparison of *in vitro* allosteric effects of Sig1R modulators.

Compound	[ $\mu$ M]	Activity	Sig1R ligand	Tissues/cells (species)	References
Phenytoin	10–100	Increases the binding	[ $^3$ H]DM	Brain tissues (guinea pig)	Craviso and Musacchio, 1983; Musacchio et al., 1988, 1989
	10–100	Increases the binding	[ $^3$ H](+)-3-PPP	Brain tissues (guinea pig)	Musacchio et al., 1989
	300	Increases the binding	[ $^3$ H](+)-SKF-10,047	Brain tissues (guinea pig)	Karbon et al., 1991
	300	Increases the binding	[ $^3$ H](+)-SKF-10,047	Liver tissues (rat)	McCann and Su, 1991
	0.1–250	Increases the binding	[ $^3$ H](+)-Pentazocine	Brain tissues (guinea pig)	DeHaven-Hudkins et al., 1993; Cobos et al., 2005, 2006
	100–10,000	Increases the binding	[ $^3$ H](+)-Pentazocine	Brain tissues (rat)	Guo et al., 2013
	1,000	Increases the binding affinity of dm	[ $^3$ H](+)-Pentazocine	Lung tissues (mice)	Lever et al., 2015
	100	No effect	[ $^3$ H]DM	Liver tissues (guinea pig)	Craviso and Musacchio, 1983
	0.0001–100	No effect	[ $^3$ H](+)-Pentazocine	Brain tissues (rat)	Zvejniec et al., 2014
	1–10,000	No effect	[ $^3$ H](+)-Pentazocine	Liver tissues (rat)	Guo et al., 2013
	10, 100	No effect	[ $^3$ H](+)-Pentazocine	Constructed HEK293 cells	
	10, 100/300	No effect	[ $^3$ H]DTG	Brain tissues (guinea pig/ rat)	Karbon et al., 1991; Guo et al., 2013
	0.1–250	Decreases the binding	[ $^3$ H]NE-100	Brain tissues (guinea pig)	Cobos et al., 2006
	10, 100	No effect	[ $^3$ H]Progesterone	Brain and liver tissues (rat)	Guo et al., 2013
Ropizine (SC-13504)	0.1–10	Increases the binding	[ $^3$ H]DM	Brain tissues (guinea pig)	Musacchio et al., 1988, 1989; Klein and Musacchio, 1992
	0.1–10	Increases the binding	[ $^3$ H](+)-3-PPP	Brain tissues (guinea pig)	Musacchio et al., 1989; Klein and Musacchio, 1990, 1992
SKF83959	0.1–100	Increases the binding	[ $^3$ H](+)-Pentazocine	Brain and liver tissues (rat)	Guo et al., 2013
	0.1–10	Increases the binding affinity of DHEA	[ $^3$ H](+)-Pentazocine	Brain tissues (rat)	Wu et al., 2015
	0.1	Enhances the anti-inflammatory effect on LPS induced inflammation	DHEA	Microglial BV-2 cells (mice)	
	1	Enhances the anti-inflammatory effect on LPS induced inflammation	PRE-084	Microglial BV-2 cells (mice)	
	10, 100	No effect	[ $^3$ H](+)-Pentazocine	Constructed HEK293 cells	Guo et al., 2013
	10, 100	No effect	[ $^3$ H]Progesterone	Brain and liver tissues (rat)	
	10, 100	No effect	[ $^3$ H]DTG	Brain and liver tissues (rat)	
SCH23390	0.1–100	Increases the binding	[ $^3$ H](+)-Pentazocine	Liver tissues (rat)	Guo et al., 2013
	0.001–100	No effect	[ $^3$ H](+)-Pentazocine	Brain tissues (rat)	
	10, 100	No effect	[ $^3$ H](+)-Pentazocine	Constructed HEK293 cells	
	10, 100	No effect	[ $^3$ H]Progesterone	Brain and liver tissues (rat)	
	10, 100	No effect	[ $^3$ H]DTG	Brain and liver tissues (rat)	
SKF38393	0.1–100	Increases the binding	[ $^3$ H](+)-Pentazocine	Liver tissues (rat)	Guo et al., 2013
	0.001–100	No effect	[ $^3$ H](+)-Pentazocine	Brain tissues (rat)	
	10, 100	No effect	[ $^3$ H](+)-Pentazocine	Constructed HEK293 cells	
	10, 100	No effect	[ $^3$ H]Progesterone	Brain and liver tissues (rat)	
	10, 100	No effect	[ $^3$ H]DTG	Brain and liver tissues (rat)	
SOMCL-668	100	Increases the binding	[ $^3$ H](+)-Pentazocine	Brain tissues (rat)	Guo et al., 2015
	10	Enhances the translocation of Sig1R from BiP	(+)-SKF-10,047	Hippocampal neuronal HT-22 cells (mice)	Wang et al., 2016
	10	Enhances stimulated neurite growth and BDNF secretion	(+)-SKF-10,047	Primary cortical/hippocampal neurons (mice)	
E1R	10	Increases the binding	[ $^3$ H]DTG	Jurkat cells (human)	Zvejniec et al., 2014
	0.0001–100	No effect	[ $^3$ H](+)-Pentazocine	Brain tissues (rat)	
	10	Enhances the activity on electrically stimulated contractions	PRE-084	<i>vasa deferentia</i> (rat)	Veinberg et al., 2013; Zvejniec et al., 2014
	10	No effect	PB-28	<i>vasa deferentia</i> (rat)	Zvejniec et al., 2014

(Continued)

TABLE 2 | Continued

Compound	[μM]	Activity	Sig1R ligand	Tissues/cells (species)	References
	10	Enhances the activity on the BDK-induced [Ca <sup>2+</sup> ] <sub>i</sub> increase	PRE-084	NG108-15 cells (rat and mice)	
OZP002	1	No effect	[ <sup>3</sup> H]DTG	Jurkat cells (human)	Maurice et al., 2017
	1–30	Increases the binding	[ <sup>3</sup> H](+)-Pentazocine	Jurkat cells (human)	
Fenfluramine (ZX008)	0.0001–100	Inhibits the binding	[ <sup>3</sup> H]DTG	Jurkat cells (human)	Martin et al., 2017
	0.0001–100	Inhibits the binding	[ <sup>3</sup> H](+)-Pentazocine	Jurkat cells (human)	Maurice et al., 2018
	3–10	Enhances agonist-induced activity on electrically stimulated contractions	(+)-SKF-10,047	<i>vasa deferentia</i> (guinea pig)	
	1–10	Enhances the translocation of Sig1R from BiP	PRE-084	CHO cells	

2017, 2018). E1R, however, is the only modulator showing dose-dependent memory-improving activity in drug-naïve animals (Zvejniece et al., 2014). E1R and OZP002 successfully alleviated scopolamine-induced cognitive impairment in mice, as assessed using passive avoidance and spontaneous alternation tests (Zvejniece et al., 2014; Maurice et al., 2017). The effects were antagonized by the selective Sig1R antagonist NE-100, thus confirming the Sig1R modulatory activity of E1R *in vivo*. Moreover, fenfluramine showed anti-amnesic effects in mice treated with the non-competitive NMDA receptor antagonist dizocilpine (Maurice et al., 2018). This activity has long been described for Sig1R agonists (Maurice et al., 1994a,b) and is usually considered a potential activity test confirming the Sig1R agonist or antagonist activity of selective drugs. Finally, OZP002 showed anti-amnesic effects against learning deficits induced by amyloid Aβ<sub>25–35</sub> peptide, a pharmacological model of symptomatic efficacy in Alzheimer’s disease (Maurice et al., 1998). Some memory improvement activities have also been demonstrated for benzazepines SKF83959 and SKF38393. For example, administration of SKF83959 significantly improved scopolamine-induced memory impairments in the passive avoidance task, spontaneous alternation test, and place learning task in the Morris water maze task in mice (Sheng et al., 2018; Table 1). SKF38393 has been shown to improve temporal order memory performance in maternally deprived rats (Lejeune et al., 2013; Table 1). However, the effects of SKF83959 and SKF38393 on memory are dopamine receptor-mediated, and the involvement of Sig1R in the memory improvement of these compounds has not been demonstrated. In contrast to E1R treatment, treatment with phenytoin triggered memory impairment during the passive avoidance task (Reeta et al., 2009). Treatment of epilepsy with phenytoin has been shown to induce learning and memory deficits in patients as well (Mishra and Goel, 2015). Sig1R-related memory-improving activity could be specific for selective allosteric Sig1R modulators such as E1R and SOMCL-668. However, it has not been demonstrated that SOMCL-668 improves memory and cognition through a Sig1R-related pathway. Therefore, to date, the Sig1R-related memory-improving activity is specific only for E1R, OZP002, and fenfluramine.

Anti-depressant Activity

To date, SOMCL-668, OZP002 and fenfluramine have shown anti-depressant activity, which has been demonstrated to be Sig1R specific. The anti-depressant activity of SKF-83959 was shown to be regulated through other mechanisms (Table 1). It has been described that stereoisomers of methylphenylpiracetam, including E1R, did not induce any significant effects on the depressive condition in mice (Vavers et al., 2015). In the case of phenytoin, major depression as a complication of phenytoin intoxication has been described (Levkovitch et al., 1993). Therefore, anti-depressant activity seems to be shared by but not specific to allosteric modulators of Sig1R.

ALLOSTERIC MODULATION OF SIG1R

There are no clearly defined molecular mechanisms that could fully describe the function of Sig1R and the activity of Sig1R ligands. Thus, it is more difficult to describe the activity of allosteric modulators, which do not compete with orthosteric Sig1R ligands for binding in the active site of Sig1R but rather enhance the activity of Sig1R agonists. The crystal structure of Sig1R shows that the ligand-binding domain in the protein is highly conserved, and how ligands enter and exit this site remains unclear (Schmidt et al., 2016). The binding site for allosteric Sig1R modulators is probably located outside the orthosteric ligand-binding domain. Since allosteric modulators are compounds that induce a conformational change within the protein structure, PAMs should reorganize the Sig1R protein in a way that would allow agonists to freely enter the ligand-binding site. It has been discussed previously that phenytoin might induce a conformational change in the Sig1R and thus enhance the affinity of the orthosteric ligand [<sup>3</sup>H](+)-pentazocine for its binding site on Sig1R (Cobos et al., 2006), which fits classic description of the activity of allosteric modulators (Figure 6). However, it is not clear how allosteric modulators of Sig1R can distinguish between agonists and antagonists and then selectively enhance the activity of agonists, even though the agonists and antagonists sometimes contain the same structural moieties.

Classical models for allosteric modulation might not be attributed to allosteric modulation of Sig1R. Several previous



**TABLE 3 |** Sig1R-dependent anti-seizure activity of allosteric Sig1R modulators.

Compound	Dose, mg/kg	Seizure model	Effects	References
SKF83959	2	Maximal electroshock seizure threshold test	No significant effect	Guo et al., 2015
	10		Increased the seizure threshold	
	20			
	40			
	2	PTZ (80 mg/kg, s.c.)	No significant effect	
	10		No significant effect	
	20		Prolonged the latencies of clonic and generalized clonic-tonic seizures, survival time, and significantly lowered seizure scores	
	40			
	2	Kainic acid (30 mg/kg, i.p.)	No significant effect	
	10		No significant effect	
	20		No significant effect	
	40		Significantly reduced seizure incidence, prolonged the latency to seizures, and shortened the duration of seizures	
SOMCL-668	40	Maximal electroshock seizure threshold test	Increased the seizure threshold	Guo et al., 2015
	40	PTZ (80 mg/kg, s.c.)	Prolonged the latency time to the generalized clonic-tonic seizures and survival time	
	40	Kainic acid (30 mg/kg, i.p.)	Prolonged the latency time and shortened the duration of seizures	
E1R	10	PTZ (i.v. infusion)	Increased the threshold for clonic and tonic seizures	Vavers et al., 2017
	50			
	10	BIC (i.v. infusion)	No significant effect	
	50		Increased the threshold for clonic and tonic seizures	
	75	NE-100 (75 mg/kg, i.p.)*	Significantly reduced generalized seizure count and average behavioral score	
Fenfluramine (ZX008)	Maximum Tolerable Concentration	Homozygous <i>scn1a</i> mutant zebrafish larvae	Decreased epileptiform activity	Sourbron et al., 2017
	3 nmol	NMDA (i.c.v. administration)	Reduced rearing, hypermotility-circling, clonic convulsions, tonic seizures, and death	Rodríguez-Muñoz et al., 2018
	500 μM	Low Mg <sup>2+</sup>	Blockade of early and late epileptiform activity	Gentsch et al., 2000

\*NE-100 induced seizures in 100% of animals at a dose of 75 mg/kg (Vavers et al., 2017). Phenytoin, ropizine, SCH23390, and SKF38393 are not included in the table because the seizure modulating activities of these compounds are not shown to be significantly blocked by the selective Sig1R ligands.

experiments support the conclusion that in ligand binding, Sig1R functions as an oligomer (Schuster et al., 1995; Chu et al., 2013; Gromek et al., 2014). Therefore, oligomerization is a key functional property of the Sig1R that may be linked to ligand efficacy [Schmidt et al., 2016; reviewed in Chu and Ruoho (2016)] and could explain how ligands can regulate the activity of Sig1R (Figure 6). Sig1R ligands may regulate the activity of the receptor interaction with client proteins by altering the oligomeric/monomeric receptor ratio and favoring the oligomeric states (Mishra et al., 2015). It has been shown that the Sig1R agonist (+)-pentazocine increased the relative ratio of dimers and monomers, while the inhibitor haloperidol increased the incidence of higher oligomeric forms (Chu and Ruoho, 2016). This observation indicates that higher oligomeric forms of Sig1R might be

functionally inactive (Figure 5A). Since all Sig1R allosteric modulators known thus far are PAMs and enhance the activity of Sig1R agonists, they might modulate Sig1R by stabilizing the agonist state of the receptor, providing an increase in the dimeric (Figure 5B) and/or monomeric (Figure 5C) protein forms.

Sig1R has already been described as a chaperone that modulates other receptor systems through heteromeric protein-protein interactions (Navarro et al., 2013; Pabba, 2013; Moreno et al., 2014; Su et al., 2016). Therefore, it is possible that heteromeric complexes formed by Sig1R and its target proteins could be regulated by allosteric modulators of Sig1R (Figure 6). Allosteric Sig1R modulators could serve as a bridge between Sig1R and its target proteins. The “molecular glue” concept was first discovered by observing the mechanism of action

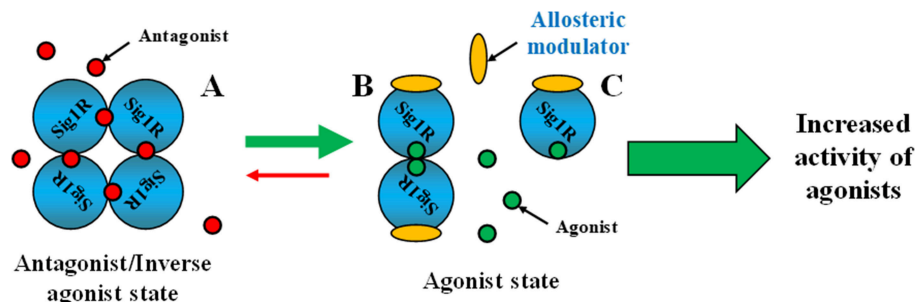


**FIGURE 5 |** Stabilization of the agonist state of Sig1R by PAMs. A model showing possible mechanisms of Sig1R ligand activity. **(A)** Oligomeric form. For the agonist state, **(B,C)** represent the dimeric and monomeric forms of Sig1R, respectively. This Figure has been modified from (Chu and Ruoho, 2016).

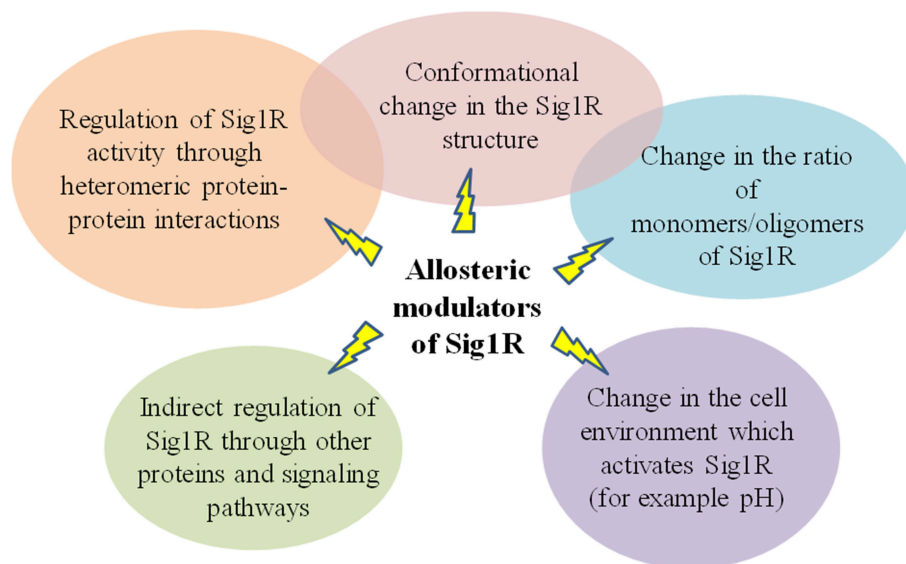


**FIGURE 6 |** Summary of possible mechanisms of allosteric modulators of Sig1R.

of natural products that promote immunomodulatory ternary complex formation (Che et al., 2018), and recently, some compounds of synthetic origin have been reported to induce novel protein-protein interactions [reviewed in (Che et al., 2018)]. The “molecular glue” principle could be attributed not only to heteromeric protein-protein interactions but also to homomeric Sig1R interactions and could explain how allosteric modulators could increase the number of Sig1R in the agonist state conformation, thus increasing the activity of Sig1R agonists.

It has been shown that compounds that bind to allosteric site of protein may activate the receptor in the absence of agonist (Schwartz and Holst, 2007). This condition, known as allosteric agonism, could explain the direct pharmacological effects of allosteric modulators of Sig1R observed both *in vitro* and *in vivo* (Zvejniece et al., 2014; Guo et al., 2015; Wang et al., 2016; Maurice et al., 2017, 2018). “Superagonism” or ago-allosteric modulation also could be one of the possible descriptions of the modulatory activity of allosteric Sig1R ligands.

An ago-allosteric modulator acts as both an agonist and an enhancer of agonist potency and provides “superagonism,” which would result in an efficacy >100% (Schwartz and Holst, 2007). One example of ago-allosteric modulatory activity could be the published *in vitro* effects of E1R (Zvejniece et al., 2014). It was shown that both selective Sig1R agonist PRE-084 and allosteric modulator E1R increased the BDK-induced  $[Ca^{2+}]_i$  increase, while the combination of both compounds resulted in an even more pronounced cellular response (Zvejniece et al., 2014). The similar “superagonism” could also be attributed to SOMCL-668. Both the allosteric Sig1R modulator SOMCL-668 and Sig1R agonist (+)-SKF-10,047 increased P(Ser<sup>9</sup>)-GSK-3 $\beta$  in hippocampal neuronal HT-22 cells, while the (+)-SKF-10,047-increased phosphorylation was potentiated by SOMCL-668 (Wang et al., 2016). While “superagonism” could be attributed only to some *in vitro* effects of E1R and SOMCL-668, it cannot be concluded that allosteric Sig1R modulators are superagonists. In addition, the direct pharmacological effects of allosteric Sig1R modulators could be explained by the

presence of a possible endogenous agonists of Sig1R. N,N-dimethyltryptamine is considered as one of the most active endogenous Sig1R agonists identified thus far (Fontanilla et al., 2009; Su et al., 2009). Very recently, it was shown that also choline acts as an endogenous ligand (Brailoiu et al., 2019). However, to date no study has demonstrated the enhancement of endogenous agonist activity by known allosteric modulators of Sig1R. The acidity or alkalinity of a studied system is another issue that should be considered when evaluating possible mechanisms of allosteric Sig1R modulators (Figure 6) because it has been shown that pH by itself changes the activity of Sig1R ligands. Binding of ligands to Sig1R is pH dependent and is enhanced at higher pH (Largent et al., 1987). [<sup>3</sup>H](+)-Pentazocine binding to C6 glioma cell membranes was progressively increased at pH = 8.0 compared to buffer at pH = 7.0 and pH = 7.4 (Vilner et al., 1995). In addition, it was discovered that the pH of the medium markedly affected the activity of the Sig1R compounds in C6 glioma cells (Vilner et al., 1995). Increasing the pH from the range 7.2–7.4 to 8.3–8.5 caused a marked leftward shift in the dose curves for all active Sig1R compounds, while lowering the pH generally decreased the ability of sigma compounds to change cell morphology (Vilner et al., 1995). As it is known, all of the allosteric Sig1R modulators induce the same effect, which means an increase in the binding and activity of Sig1R ligands. Can allosteric modulators of Sig1R change the intracellular pH? Interestingly, it was previously demonstrated that a phenytoin-induced increase in the binding affinity of [<sup>3</sup>H]DM to brain homogenate is more marked at pH = 7.4 than at pH = 8.3 (Musacchio et al., 1988). Phenytoin is a weak acid with a pKa of approximately pH = 8.3. Therefore, at pH = 7.4 the concentration of unionized phenytoin is almost doubled, which may explain why phenytoin is much more potent at pH 7.4 (Musacchio et al., 1988). This finding demonstrates that pH plays a significant role in the process that determines the interaction between Sig1R ligands and receptors. Protonation or deprotonation of amino acids due to different pH could explain the change in the structure of Sig1R and therefore the change in the binding affinity of ligands to Sig1R. What is the role of allosteric modulators in these processes? In a number of structure-activity relationship studies, only agonists or antagonists have been used for evaluation of possible ligand-protein interactions. Additionally, no NMR data are available where allosteric modulators have been used to describe their molecular interaction with Sig1R. Most likely, three or more component systems (allosteric modulator-Sig1R-agonist and/or antagonist) must be applied to understand the interaction with Sig1R at the protein level. Detailed studies on allosteric Sig1R modulators at the protein level would be necessary to increase the global understanding of the interaction with the receptor and activity of Sig1R ligands.

## KEY ISSUES

### Characterization of Binding Site

The binding site(s) for Sig1R allosteric modulators is(are) not identified. The binding dynamics in the

Sig1R for allosteric compounds must be confirmed and characterized.

## Screening System

No screening assay is available for allosteric modulators of Sig1R and must be developed and validated. Notably, modulation of the agonist-induced dissociation of Sig1R from BiP *in vitro* must be confirmed with all already identified modulators.

## Stereoselectivity

The use of enantiomerically pure compounds is necessary to provide detailed evaluation of the *in vitro* and *in vivo* effects of allosteric Sig1R modulators. Comparison of all allosteric Sig1R modulators in the same experimental setup should be performed.

## *In vivo* Proof of the Sig1R-Related Mechanism of Action

There is a lack of *in vivo* studies combining Sig1R agonists and allosteric Sig1R modulators to confirm the allosteric modulatory activity of a compound at Sig1R. *In vitro* concentrations and therapeutic doses *in vivo* should be comparable.

## CONCLUSION

Allosteric pharmacology, that is, the design of drugs targeting sites topographically different from the orthosteric ligand binding site, is innovative approach to drug discovery. Allosteric modulation of Sig1R is an emerging and important target for designing novel drugs. A number of issues must be answered regarding the mechanisms of action and possible clinical applications of allosteric Sig1R modulators. More detailed classification of Sig1R ligands is inevitably necessary, and the development of new screening assay methods focused on ligand characterization is highly important to advance the understanding of the role of Sig1R and its allosteric modulators. Nevertheless, during the last 6 years, a large step forward in the understanding of allosteric modulation of Sig1R has been made. The first selective allosteric Sig1R modulators have been identified, which offer a basis for the discovery of novel and selective Sig1R compounds and increase knowledge of the impact of Sig1R regulation in living organisms, thereby providing novel treatment possibilities for various CNS-related diseases.

## AUTHOR CONTRIBUTIONS

EV and LZ wrote the manuscript in consultation with TM and MD. TM provided additional information on OZP002 and fenfluramine. All authors discussed the data and commented on the manuscript. MD supervised the manuscript.

## FUNDING

This review article was supported by the European Regional Development Fund Project No. 1.1.1.1/16/A/292.

## REFERENCES

- Albertson, T. E., Peterson, S. L., and Stark, L. G. (1978). Effects of phenobarbital and SC-13504 on partially kindled hippocampal seizures in rats. *Exp. Neurol.* 61, 270–280. doi: 10.1016/0014-4886(78)90246-7
- Alexander, S. P. H., Benson, H. E., Faccenda, E., Pawson, A. J., Sharman, J. L., McGrath, J. C., et al. (2013). The concise guide to pharmacology 2013/14: overview. *Br. J. Pharmacol.* 170, 1449–1458. doi: 10.1111/bph.12444
- Alon, A., Schmidt, H. R., Wood, M. D., Sahn, J. J., Martin, S. F., and Kruse, A. C. (2017). Identification of the gene that codes for the  $\sigma 2$  receptor. *Proc. Natl. Acad. Sci. U. S. A.* 114, 7160–7165. doi: 10.1073/pnas.1705154114
- Alonso, G., Phan, V., Guillemain, I., Saunier, M., Legrand, A., Anoa, M., et al. (2000). Immunocytochemical localization of the sigma1 receptor in the adult rat central nervous system. *Neuroscience* 97, 155–170. doi: 10.1016/S0306-4522(00)00014-2
- Barone, P., Palma, V., de Bartolomeis, A., Cicarelli, G., and Campanella, G. (1992). Dopaminergic regulation of epileptic activity. *Neurochem. Int.* 20(Suppl.) 245S–249S. doi: 10.1016/0197-0186(92)90246-N
- Bartz, F., Kern, L., Erz, D., Zhu, M., Gilbert, D., Meinhof, T., et al. (2009). Identification of cholesterol-regulating genes by targeted RNAi screening. *Cell Metab.* 10, 63–75. doi: 10.1016/j.cmet.2009.05.009
- Bourne, J. A., and Fosbraey, P. (2000). Novel method of monitoring electroencephalography at the site of microdialysis during chemically evoked seizures in a freely moving animal. *J. Neurosci. Methods* 99, 85–90. doi: 10.1016/S0165-0270(00)00217-X
- Bourne, J. A., Fosbraey, P., and Halliday, J. (2001). SCH 23390 affords protection against soman-evoked seizures in the freely moving guinea-pig: a concomitant neurochemical, electrophysiological and behavioural study. *Neuropharmacology* 40, 279–288. doi: 10.1016/S0028-3908(00)00136-2
- Brailoiu, E., Chakraborty, S., Brailoiu, G. C., Zhao, P., Barr, J. L., Ilies, M. A., et al. (2019). Choline is an intracellular messenger linking extracellular stimuli to IP(3)-evoked  $\text{Ca}^{2+}$  signals through sigma-1 receptors. *Cell Rep.* 26, 330–337.e4. doi: 10.1016/j.celrep.2018.12.051
- Burke, K., Chandler, C. J., Starr, B. S., and Starr, M. S. (1990). Seizure promotion and protection by D-1 and D-2 dopaminergic drugs in the mouse. *Pharmacol. Biochem. Behav.* 36, 729–733. doi: 10.1016/0091-3057(90)90068-S
- Chaki, S., Okuyama, S., Ogawa, S., Tanaka, M., Muramatsu, M., Nakazato, A., et al. (1996). Solubilization and characterization of binding sites for [ $^3\text{H}$ ]NE-100, a novel and potent sigma 1 ligand, from guinea pig brain. *Life Sci.* 59, 1331–1340. doi: 10.1016/0024-3205(96)00458-4
- Che, Y., Gilbert, A. M., Shanmugasundaram, V., and Noe, M. C. (2018). Inducing protein-protein interactions with molecular glues. *Bioorg. Med. Chem. Lett.* 28, 2585–2592. doi: 10.1016/j.bmcl.2018.04.046
- Chen, X.-Q., Zhang, J., Neumeyer, J. L., Jin, G.-Z., Hu, G.-Y., Zhang, A., et al. (2009). Arylbenzazepines are potent modulators for the delayed rectifier  $\text{K}^+$  channel: a potential mechanism for their neuroprotective effects. *PLoS ONE* 4:e5811. doi: 10.1371/journal.pone.0005811
- Chu, H.-Y., Wu, Q., Zhou, S., Cao, X., Zhang, A., Jin, G.-Z., et al. (2011). SKF83959 suppresses excitatory synaptic transmission in rat hippocampus via a dopamine receptor-independent mechanism. *J. Neurosci. Res.* 89, 1259–1266. doi: 10.1002/jnr.22653
- Chu, H.-Y., Yang, Z., Zhao, B., Jin, G.-Z., Hu, G.-Y., and Zhen, X. (2010). Activation of phosphatidylinositol-linked D1-like receptors increases spontaneous glutamate release in rat somatosensory cortical neurons *in vitro*. *Brain Res.* 1343, 20–27. doi: 10.1016/j.brainres.2010.04.043
- Chu, U. B., Ramachandran, S., Hajipour, A. R., and Ruoho, A. E. (2013). Photoaffinity labeling of the sigma-1 receptor with N-[3-(4-nitrophenyl)propyl]-N-dodecylamine: evidence of receptor dimers. *Biochemistry* 52, 859–868. doi: 10.1021/bi301517u
- Chu, U. B., and Ruoho, A. E. (2016). Biochemical pharmacology of the sigma-1 receptor. *Mol. Pharmacol.* 89, 142–153. doi: 10.1124/mol.115.101170
- Cobos, E., Entrena, J., Nieto, F., Cendan, C., and Pozo, E. (2008). Pharmacology and therapeutic potential of sigma1 receptor ligands. *Curr. Neuropharmacol.* 6, 344–366. doi: 10.2174/157015908787386113
- Cobos, E. J., Baeyens, J. M., and Del Pozo, E. (2005). Phenytoin differentially modulates the affinity of agonist and antagonist ligands for  $\sigma 1$  receptors of guinea pig brain. *Synapse* 55, 192–195. doi: 10.1002/syn.20103
- Cobos, E. J., Lucena, G., Baeyens, J. M., and Del Pozo, E. (2006). Differences in the allosteric modulation by phenytoin of the binding properties of the sigma1 ligands [ $^3\text{H}$ ](+)-pentazocine and [ $^3\text{H}$ ]NE-100. *Synapse* 59, 152–161. doi: 10.1002/syn.20230
- Craig, C. R. (1967). Anticonvulsant properties of some benzhydryl piperazine and benzhydryl piperidine compounds. *Arch. Int. Pharmacodyn. Ther.* 165, 328–336.
- Craviso, G. L., and Musacchio, J. M. (1983). High-affinity dextromethorphan binding sites in guinea pig brain. II. Competition experiments. *Mol. Pharmacol.* 23, 629–640.
- DeHaven-Hudkins, D. L., Ford-Rice, F. Y., Allen, J. T., and Hudkins, R. L. (1993). Allosteric modulation of ligand binding to [ $^3\text{H}$ ](+)-pentazocine-defined sigma recognition sites by phenytoin. *Life Sci.* 53, 41–48. doi: 10.1016/0024-3205(93)90609-7
- Desai, R. I., Neumeyer, J. L., Paronis, C. A., Nguyen, P., and Bergman, J. (2007). Behavioral effects of the R-(+)- and S-(-)-enantiomers of the dopamine D(1)-like partial receptor agonist SKF 83959 in monkeys. *Eur. J. Pharmacol.* 558, 98–106. doi: 10.1016/j.ejphar.2006.11.042
- Deveney, A. M., and Waddington, J. L. (1995). Pharmacological characterization of behavioural responses to SKF 83959 in relation to “D1-like” dopamine receptors not linked to adenylyl cyclase. *Br. J. Pharmacol.* 116, 2120–2126.
- Downes, R. P., and Waddington, J. L. (1993). Grooming and vacuous chewing induced by SKF 83959, an agonist of dopamine “D1-like” receptors that inhibits dopamine-sensitive adenylyl cyclase. *Eur. J. Pharmacol.* 234, 135–136.
- Edmonds, H. L., Bellin, S. I., Chen, F. C., and Hegreberg, G. A. (1978). Anticonvulsant properties of ropizine in epileptic and nonepileptic beagle dogs. *Epilepsia* 19, 139–146. doi: 10.1111/j.1528-1157.1978.tb05024.x
- Edmonds, H. L., Jiang, Y. D., Zhang, P. Y., and Shank, R. P. (1996). Anticonvulsant activity of topiramate and phenytoin in a rat model of ischemia-induced epilepsy. *Life Sci.* 59, PL127–PL131. doi: 10.1016/0024-3205(96)00379-7
- Edmonds, H. L., and Stark, L. G. (1974). Penicillin-induced epileptogenic foci—II: the anticonvulsant and neuropharmacological effects of SC-13504 in the cat. *Neuropharmacology* 13, 269–277. doi: 10.1016/0028-3908(74)90077-X
- Edmonds, H. L., Stark, L. G., Stark, D. M., McCormack, C. R., Sylvester, D. M., and Bellin, S. I. (1979). The anticonvulsant activity of ropizine in the rat. *J. Pharmacol. Exp. Ther.* 208, 236–242.
- Fang, X., Guo, L., Jia, J., Jin, G., Zhao, B., Zheng, Y., et al. (2013). SKF83959 is a novel triple reuptake inhibitor that elicits anti-depressant activity. *Acta Pharmacol. Sin.* 34, 1149–1155. doi: 10.1038/aps.2013.66
- Festoff, B. W., and Appel, S. H. (1968). Effect of diphenylhydantoin on synaptosome sodium-potassium-ATPase. *J. Clin. Invest.* 47, 2752–2758. doi: 10.1172/JCI105956
- Fontanilla, D., Johannessen, M., Hajipour, A. R., Cozzi, N. V., Jackson, M. B., and Ruoho, A. E. (2009). The hallucinogen N,N-dimethyltryptamine (DMT) is an endogenous sigma-1 receptor regulator. *Science* 323, 934–937. doi: 10.1126/science.1166127
- Fuller, R. W., Snoddy, H. D., and Robertson, D. W. (1988). Mechanisms of effects of d-fenfluramine on brain serotonin metabolism in rats: uptake inhibition versus release. *Pharmacol. Biochem. Behav.* 30, 715–721. doi: 10.1016/0091-3057(88)90089-5
- Gentsch, K., Heinemann, U., Schmitz, B., and Behr, J. (2000). Fenfluramine blocks low- $\text{Mg}^{2+}$ -induced epileptiform activity in rat entorhinal cortex. *Epilepsia* 41, 925–928. doi: 10.1111/j.1528-1157.2000.tb00273.x
- Gilbert, J. C., and Wyllie, M. G. (1976). Effects of anticonvulsant and convulsant drugs on the ATPase activities of synaptosomes and their components. *Br. J. Pharmacol.* 56, 49–57. doi: 10.1111/j.1476-5381.1976.tb06958.x
- Gromek, K. A., Suchy, F. P., Meddaugh, H. R., Wrobel, R. L., LaPointe, L. M., Chu, U. B., et al. (2014). The oligomeric states of the purified sigma-1 receptor are stabilized by ligands. *J. Biol. Chem.* 289, 20333–20344. doi: 10.1074/jbc.M113.537993
- Guo, L., Chen, Y., Zhao, R., Wang, G., Friedman, E., Zhang, A., et al. (2015). Allosteric modulation of sigma-1 receptors elicits anti-seizure activities. *Br. J. Pharmacol.* 172, 4052–4065. doi: 10.1111/bph.13195
- Guo, L., Zhao, J., Jin, G., Zhao, B., Wang, G., Zhang, A., et al. (2013). SKF83959 is a potent allosteric modulator of sigma-1 receptor. *Mol. Pharmacol.* 83, 577–586. doi: 10.1124/mol.112.083840



- Haller, J. L., Panyutin, I., Chaudhry, A., Zeng, C., Mach, R. H., and Frank, J. A. (2012). Sigma-2 receptor as potential indicator of stem cell differentiation. *Mol. Imaging Biol.* 14, 325–335. doi: 10.1007/s11307-011-0493-3
- Hayashi, T., and Su, T.-P. (2007). Sigma-1 receptor chaperones at the ER-mitochondrion interface regulate  $\text{Ca}^{2+}$  signaling and cell survival. *Cell* 131, 596–610. doi: 10.1016/j.cell.2007.08.036
- Hellewell, S. B., and Bowen, W. D. (1990). A sigma-like binding site in rat pheochromocytoma (PC12) cells: decreased affinity for (+)-benzomorphans and lower molecular weight suggest a different sigma receptor form from that of guinea pig brain. *Brain Res.* 527, 244–253. doi: 10.1016/0006-8993(90)91143-5
- Hellewell, S. B., Bruce, A., Feinstein, G., Orringer, J., Williams, W., and Bowen, W. D. (1994). Rat liver and kidney contain high densities of sigma 1 and sigma 2 receptors: characterization by ligand binding and photoaffinity labeling. *Eur. J. Pharmacol.* 268, 9–18. doi: 10.1016/0922-4106(94)90115-5
- Hicks, P. E., Schoemaker, H., and Langer, S. Z. (1984). 5HT-receptor antagonist properties of SCH23390 in vascular smooth muscle and brain. *Eur. J. Pharmacol.* 105, 339–342. doi: 10.1016/0014-2999(84)90628-9
- Hyttel, J. (1983). SCH 23390 - the first selective dopamine D-1 antagonist. *Eur. J. Pharmacol.* 91, 153–154. doi: 10.1016/0014-2999(83)90381-3
- Jbilo, O., Vidal, H., Paul, R., De Nys, N., Bensaid, M., Silve, S., et al. (1997). Purification and characterization of the human SR 31747A-binding protein. A nuclear membrane protein related to yeast sterol isomerase. *J. Biol. Chem.* 272, 27107–27115. doi: 10.1074/jbc.272.43.27107
- Jiang, B., Wang, F., Yang, S., Fang, P., Deng, Z.-F., Xiao, J.-L., et al. (2015). SKF83959 produces antidepressant effects in a chronic social defeat stress model of depression through BDNF-TrkB pathway. *Int. J. Neuropsychopharmacol.* 18:pyu096. doi: 10.1093/ijnp/pyu096
- Johannessen, M., Ramachandran, S., Riemer, L., Ramos-Serrano, A., Ruoho, A. E., and Jackson, M. B. (2009). Voltage-gated sodium channel modulation by  $\sigma$ -receptors in cardiac myocytes and heterologous systems. *Am. J. Physiol. Physiol.* 296, C1049–C1057. doi: 10.1152/ajpcell.00431.2008
- Jones, G. L., Amato, R. J., Wimbish, G. H., and Peyton, G. A. (1981). Comparison of anticonvulsant potencies of cyphenamide, carbamazepine, and phenytoin. *J. Pharm. Sci.* 70, 618–620. doi: 10.1002/jps.2600700611
- Joy, R. M., and Edmonds, H. L. (1974). The antagonism of hippocampal and cortical afterdischarge by SC-13504, a new anticonvulsant. *Neuropharmacology* 13, 145–157. doi: 10.1016/0028-3908(74)90102-6
- Karbon, E. W., Naper, K., and Pontecorvo, M. J. (1991). [ $^3\text{H}$ ]DTG and [ $^3\text{H}$ ](+)-3-PPP label pharmacologically distinct sigma binding sites in guinea pig brain membranes. *Eur. J. Pharmacol.* 193, 21–27. doi: 10.1016/0014-2999(91)90195-V
- Kebabian, J. W. (1988). “The D-1 dopamine receptor,” in *Central D1 Dopamine Receptors*, ed M. J. Goldstein (New York, NY: Springer), 19–31.
- Klein, M., and Musacchio, J. M. (1990). Computer-assisted analysis of dextromethorphan and (+)-3-(3-hydroxyphenyl)-N-(1-propyl)piperidine binding sites in rat brain. Allosteric effects of ropizine. *Life Sci.* 47, 1625–1634. doi: 10.1016/0024-3205(90)90367-Z
- Klein, M., and Musacchio, J. M. (1992). High-affinity dextromethorphan and (+)-3-(3-hydroxyphenyl)-N-(1-propyl)piperidine binding sites in rat brain. Allosteric effects of ropizine. *J. Pharmacol. Exp. Ther.* 260, 990–999.
- Largent, B. L., Wikström, H., Gundlach, A. L., and Snyder, S. H. (1987). Structural determinants of sigma receptor affinity. *Mol. Pharmacol.* 32, 772–784.
- Lejeune, S., Dourmap, N., Martres, M.-P., Giros, B., Daugé, V., and Naudon, L. (2013). The dopamine D1 receptor agonist SKF 38393 improves temporal order memory performance in maternally deprived rats. *Neurobiol. Learn. Mem.* 106, 268–273. doi: 10.1016/j.nlm.2013.10.005
- Leng, Z. G., Lin, S. J., Wu, Z. R., Guo, Y. H., Cai, L., Shang, H. B., et al. (2017). Activation of DRD5 (dopamine receptor D5) inhibits tumor growth by autophagic cell death. *Autophagy* 13, 1404–1419. doi: 10.1080/15548627.2017.1328347
- Lever, J. R., Litton, T. P., and Ferguson-Cantrell, E. A. (2015). Characterization of pulmonary sigma receptors by radioligand binding. *Eur. J. Pharmacol.* 762, 118–126. doi: 10.1016/j.ejphar.2015.05.026
- Levkovitch, Y., Abramovitch, Y., and Nizan, I. (1993). [Dilantin toxicity as a possible cause of major depression]. *Harefuah* 124, 762–4, 795.
- Ma, J., Long, L.-H., Hu, Z.-L., Zhang, H., Han, J., Ni, L., et al. (2015). Activation of D1-like receptor-dependent phosphatidylinositol signal pathway by SKF83959 inhibits voltage-gated sodium channels in cultured striatal neurons. *Brain Res.* 1615, 71–79. doi: 10.1016/j.brainres.2015.04.030
- Martin, P., Gammaitoni, A., Farfel, G., Boyd, B., and Galer, B. (2017). 663. An examination of the mechanism of action of fenfluramine in dravet syndrome: a look beyond serotonin. *Biol. Psychiatry* 81, S268–S269. doi: 10.1016/j.biopsych.2017.02.1072
- Martin, W. R., Eades, C. G., Thompson, J. A., Huppler, R. E., and Gilbert, P. E. (1976). The effects of morphine- and nalorphine- like drugs in the nondependent and morphine-dependent chronic spinal dog. *J. Pharmacol. Exp. Ther.* 197, 517–532.
- Maurice, T. (2016). Protection by sigma-1 receptor agonists is synergic with donepezil, but not with memantine, in a mouse model of amyloid-induced memory impairments. *Behav. Brain Res.* 296, 270–278. doi: 10.1016/j.bbr.2015.09.020
- Maurice, T., Farfel, G., Boyd, B., Gammaitoni, A., Galer, B., and Martin, P. (2018). Fenfluramine is a sigma-1 receptor positive modulator in mice. *Soc. Neurosci. Abstr.* 692.
- Maurice, T., Hiramatsu, M., Itoh, J., Kameyama, T., Hasegawa, T., and Nabeshima, T. (1994a). Behavioral evidence for a modulating role of sigma ligands in memory processes. I. Attenuation of dizocilpine (MK-801)-induced amnesia. *Brain Res.* 647, 44–56. doi: 10.1016/0006-8993(94)91397-8
- Maurice, T., Su, T. P., Parish, D. W., Nabeshima, T., and Privat, A. (1994b). PRE-084, a sigma selective PCP derivative, attenuates MK-801-induced impairment of learning in mice. *Pharmacol. Biochem. Behav.* 49, 859–869. doi: 10.1016/0091-3057(94)90235-6
- Maurice, T., Su, T. P., and Privat, A. (1998). Sigma1 receptor agonists and neurosteroids attenuate B25-35-amyloid peptide-induced amnesia in mice through a common mechanism. *Neuroscience* 83, 413–428. doi: 10.1016/S0306-4522(97)00405-3
- Maurice, T., Volle, J. N., Strehaiano, M., Pereira, C., Laborde, C., Virieux, D., et al. (2017). A novel phoshinolactone compound, OZP002, positive modulator of  $\sigma$ 1 receptors, is neuroprotective in non-transgenic and transgenic mouse models of Alzheimer's disease. *Soc. Neurosci. Abstr.* 127.
- Mavlyutov, T. A., Epstein, M., and Guo, L.-W. (2015). Subcellular localization of the sigma-1 receptor in retinal neurons - an electron microscopy study. *Sci. Rep.* 5:10689. doi: 10.1038/srep10689
- McCann, D. J., and Su, T. P. (1991). Solubilization and characterization of haloperidol-sensitive (+)-[ $^3\text{H}$ ]SKF-10,047 binding sites (sigma sites) from rat liver membranes. *J. Pharmacol. Exp. Ther.* 257, 547–554.
- Meldrum, B. S., Smyth, M. R., Franklin-Smyth, W., and Clifford, J. M. (1976). The relationship between the anticonvulsant properties of SC-13504 and its plasma levels, measured by polarography, in baboons with photosensitive epilepsy. *Psychopharmacology* 51, 59–64. doi: 10.1007/BF00426322
- Merritt, H. H., and Putnam, T. J. (1984). Landmark article Sept 17, 1938: Sodium diphenyl hydantoinate in the treatment of convulsive disorders. *JAMA* 251, 1062–1067.
- Mishra, A., and Goel, R. K. (2015). Comparative behavioral and neurochemical analysis of phenytoin and valproate treatment on epilepsy induced learning and memory deficit: search for add on therapy. *Metab. Brain Dis.* 30, 951–958. doi: 10.1007/s11011-015-9650-8
- Mishra, A. K., Mavlyutov, T., Singh, D. R., Biener, G., Yang, J., Oliver, J. A., et al. (2015). The sigma-1 receptors are present in monomeric and oligomeric forms in living cells in the presence and absence of ligands. *Biochem. J.* 466, 263–271. doi: 10.1042/BJ20141321
- Molloy, A. G., and Waddington, J. L. (1984). Dopaminergic behaviour stereospecific promoted by the D1 agonist R-SKF 38393 and selectively blocked by the D1 antagonist SCH 23390. *Psychopharmacology* 82, 409–410. doi: 10.1007/BF00427697
- Moreno, E., Moreno-Delgado, D., Navarro, G., Hoffmann, H. M., Fuentes, S., Rosell-Vilar, S., et al. (2014). Cocaine disrupts histamine H3 receptor modulation of dopamine D1 receptor signaling:  $\sigma$ 1-D1-H3 receptor complexes as key targets for reducing cocaine's effects. *J. Neurosci.* 34, 3545–3558. doi: 10.1523/JNEUROSCI.4147-13.2014
- Mori, T., Hayashi, T., Hayashi, E., and Su, T.-P. (2013). Sigma-1 receptor chaperone at the ER-mitochondrion interface mediates the mitochondrion-ER-nucleus signaling for cellular survival. *PLoS ONE* 8:e76941. doi: 10.1371/journal.pone.0076941



- Musacchio, J. M., Klein, M., and Paturzo, J. J. (1989). Effects of dextromethorphan site ligands and allosteric modifiers on the binding of (+)-[3H]3-(3-hydroxyphenyl)-N-(1-propyl)piperidine. *Mol. Pharmacol.* 35, 1–5.
- Musacchio, J. M., Klein, M., and Santiago, L. J. (1988). High affinity dextromethorphan binding sites in guinea pig brain: further characterization and allosteric interactions. *J. Pharmacol. Exp. Ther.* 247, 424–431.
- Navarro, G., Moreno, E., Bonaventura, J., Brugarolas, M., Farré, D., Aguinaga, D., et al. (2013). Cocaine inhibits dopamine D2 receptor signaling via sigma-1-D2 receptor heteromers. *PLoS ONE* 8:e61245. doi: 10.1371/journal.pone.0061245
- Nobile, M., and Lagostena, L. (1998). A discriminant block among K<sup>+</sup> channel types by phenytoin in neuroblastoma cells. *Br. J. Pharmacol.* 124, 1698–1702. doi: 10.1038/sj.bjp.0702035
- Novack, G. D., Stark, L. G., and Peterson, S. L. (1979). Anticonvulsant effects of benzhydryl piperazines on maximal electroshock seizures in rats. *J. Pharmacol. Exp. Ther.* 208, 480–484.
- Ogren, S. O., and Pakh, B. (1993). Effects of dopamine D1 and D2 receptor agonists and antagonists on seizures induced by chemoconvulsants in mice. *Pharmacol. Toxicol.* 72, 213–220. doi: 10.1111/j.1600-0773.1993.tb01639.x
- Ongini, E., Caporali, M. G., Massotti, M., and Sagratella, S. (1987). SCH 23390 and its S-enantiomer stereoselectively prevent EEG and behavioral activation induced by dopamine agonists in the rabbit. *Pharmacol. Biochem. Behav.* 26, 715–718. doi: 10.1016/0091-3057(87)90602-2
- Pabba, M. (2013). The essential roles of protein–protein interaction in sigma-1 receptor functions. *Front. Cell. Neurosci.* 7:50. doi: 10.3389/fncel.2013.00050
- Paul, R., Lavastre, S., Floutard, D., Floutard, R., Canat, X., Casellas, P., et al. (1994). Allosteric modulation of peripheral sigma binding sites by a new selective ligand: SR 31747. *J. Neuroimmunol.* 52, 183–192. doi: 10.1016/0165-5728(94)90112-0
- Polster, T. (2018). Individualized treatment approaches: fenfluramine, a novel antiepileptic medication for the treatment of seizures in Dravet syndrome. *Epilepsy Behav.* doi: 10.1016/j.yebeh.2018.08.021. [Epub ahead of print].
- Quirion, R., Bowen, W. D., Itzhak, Y., Junien, J. L., Musacchio, J. M., Rothman, R. B., et al. (1992). A proposal for the classification of sigma binding sites. *Trends Pharmacol. Sci.* 13, 85–86. doi: 10.1016/0165-6147(92)90030-A
- Reeta, K. H., Mehla, J., and Gupta, Y. K. (2009). Curcumin is protective against phenytoin-induced cognitive impairment and oxidative stress in rats. *Brain Res.* 1301, 52–60. doi: 10.1016/j.brainres.2009.09.027
- Ritz, M. C., and George, F. R. (1997). Cocaine toxicity: concurrent influence of dopaminergic, muscarinic and sigma receptors in mediating cocaine-induced lethality. *Psychopharmacology* 129, 311–321. doi: 10.1007/s002130050198
- Rodríguez-Muñoz, M., Sánchez-Blázquez, P., and Garzón, J. (2018). Fenfluramine diminishes NMDA receptor-mediated seizures via its mixed activity at serotonin 5HT<sub>2A</sub> and type 1 sigma receptors. *Oncotarget* 9, 23373–23389. doi: 10.18632/oncotarget.25169
- Rodríguez-Muñoz, M., Sánchez-Blázquez, P., Herrero-Labrador, R., Martínez-Murillo, R., Merlos, M., Vela, J. M., et al. (2015). The  $\sigma$ 1 receptor engages the redox-regulated HINT1 protein to bring opioid analgesia under NMDA receptor negative control. *Antioxid. Redox Signal.* 22, 799–818. doi: 10.1089/ars.2014.5993
- Rush, A. M., and Elliott, J. R. (1997). Phenytoin and carbamazepine: differential inhibition of sodium currents in small cells from adult rat dorsal root ganglia. *Neurosci. Lett.* 226, 95–98. doi: 10.1016/S0304-3940(97)00258-9
- Santulli, L., Coppola, A., Balestrini, S., and Striano, S. (2016). The challenges of treating epilepsy with 25 antiepileptic drugs. *Pharmacol. Res.* 107, 211–219. doi: 10.1016/j.phrs.2016.03.016
- Schmidt, H. R., Zheng, S., Gurpinar, E., Koehl, A., Manglik, A., and Kruse, A. C. (2016). Crystal structure of the human  $\sigma$ 1 receptor. *Nature* 532, 527–530. doi: 10.1038/nature17391
- Schuster, D. I., Arnold, F. J., and Murphy, R. B. (1995). Purification, pharmacological characterization and photoaffinity labeling of sigma receptors from rat and bovine brain. *Brain Res.* 670, 14–28. doi: 10.1016/0006-8993(94)01123-Y
- Schwartz, T. W., and Holst, B. (2007). Allosteric enhancers, allosteric agonists and ago-allosteric modulators: where do they bind and how do they act? *Trends Pharmacol. Sci.* 28, 366–373. doi: 10.1016/j.tips.2007.06.008
- Sheng, G., Zhang, J., Gao, S., Gu, Y., Jiang, B., and Gao, Q. (2018). SKF83959 has protective effects in the scopolamine model of dementia. *Biol. Pharm. Bull.* 41, 427–434. doi: 10.1248/bpb.b17-00877
- Sourbron, J., Schneider, H., Kecskés, A., Liu, Y., Buening, E. M., Lagae, L., et al. (2016). serotonergic modulation as effective treatment for dravet syndrome in a zebrafish mutant model. *ACS Chem. Neurosci.* 7, 588–598. doi: 10.1021/acschemneuro.5b00342
- Sourbron, J., Smolders, I., de Witte, P., and Lagae, L. (2017). Pharmacological analysis of the anti-epileptic mechanisms of fenfluramine in scn1a mutant zebrafish. *Front. Pharmacol.* 8:191. doi: 10.3389/fphar.2017.00191
- Su, T.-P., Hayashi, T., and Vaupel, D. B. (2009). When the endogenous hallucinogenic trace amine N,N-dimethyltryptamine meets the sigma-1 receptor. *Sci. Signal.* 2:pe12. doi: 10.1126/scisignal.261pe12
- Su, T.-P., Su, T.-C., Nakamura, Y., and Tsai, S.-Y. (2016). The sigma-1 receptor as a pluripotent modulator in living systems. *Trends Pharmacol. Sci.* 37, 262–278. doi: 10.1016/j.tips.2016.01.003
- Su, T. P. (1982). Evidence for sigma opioid receptor: binding of [<sup>3</sup>H]SKF-10047 to etorphine-inaccessible sites in guinea-pig brain. *J. Pharmacol. Exp. Ther.* 223, 284–290.
- Su, T. P., and Junien, J. L. (1994). “Sigma receptors in the central nervous system and the periphery,” in *Sigma Receptors*, ed Y. Itzhak (London: Academic Press), 21–44.
- Todorovic, S. M., and Lingle, C. J. (1998). Pharmacological properties of T-type Ca<sup>2+</sup> current in adult rat sensory neurons: effects of anticonvulsant and anesthetic agents. *J. Neurophysiol.* 79, 240–252. doi: 10.1152/jn.1998.79.1.240
- Tunnicliffe, G. (1996). Basis of the antiseizure action of phenytoin. *Gen. Pharmacol.* 27, 1091–1097. doi: 10.1016/S0306-3623(96)00062-6
- Vavers, E. (2017). *Discovery of E1R: A Novel Positive Allosteric Modulator of Sigma-1 Receptor*. Ph.D. thesis. Riga Stradins University, Riga.
- Vavers, E., Svalbe, B., Lauberte, L., Stonans, I., Misane, I., Dambrova, M., et al. (2017). The activity of selective sigma-1 receptor ligands in seizure models *in vivo*. *Behav. Brain Res.* 328, 13–18. doi: 10.1016/j.bbr.2017.04.008
- Vavers, E., Zvejniece, L., Veinberg, G., Svalbe, B., Domracheva, I., Vilskersts, R., et al. (2015). Novel positive allosteric modulators of sigma-1 receptor. *Springerplus* 4:P51. doi: 10.1186/2193-1801-4-S1-P51
- Veinberg, G., Vavers, E., Orlova, N., Kuznecovs, J., Domracheva, I., Vorona, M., et al. (2015). Stereochemistry of phenylpiracetam and its methyl derivative: improvement of the pharmacological profile. *Chem. Heterocycl. Compd.* 51, 601–606. doi: 10.1007/s10593-015-1747-9
- Veinberg, G., Vorona, M., Zvejniece, L., Vilskersts, R., Vavers, E., Liepinsh, E., et al. (2013). Synthesis and biological evaluation of 2-(5-methyl-4-phenyl-2-oxopyrrolidin-1-yl)-acetamide stereoisomers as novel positive allosteric modulators of sigma-1 receptor. *Bioorganic Med. Chem.* 21, 2764–2771. doi: 10.1016/j.bmc.2013.03.016
- Vilner, B. J., de Costa, B. R., and Bowen, W. D. (1995). Cytotoxic effects of sigma ligands: sigma receptor-mediated alterations in cellular morphology and viability. *J. Neurosci.* 15, 117–134. doi: 10.1523/JNEUROSCI.15-01-00117.1995
- Volle, J. N., Filippini, D., Krawczyk, B., Kaloyanov, N., Van der Lee, A., Maurice, T., et al. (2010). Drug discovery: phosphinolactone, *in vivo* bioisostere of the lactol group. *Org. Biomol. Chem.* 8, 1438–1444. doi: 10.1039/b919345f
- Wang, Y., Guo, L., Jiang, H.-F., Zheng, L.-T., Zhang, A., and Zhen, X.-C. (2016). Allosteric modulation of sigma-1 receptors elicits rapid antidepressant activity. *CNS Neurosci. Ther.* 22, 368–377. doi: 10.1111/cns.12502
- Wu, Z., Li, L., Zheng, L.-T., Xu, Z., Guo, L., and Zhen, X. (2015). Allosteric modulation of sigma-1 receptors by SKF83959 inhibits microglia-mediated inflammation. *J. Neurochem.* 134, 904–914. doi: 10.1111/jnc.13182
- Yaari, Y., Selzer, M. E., and Pincus, J. H. (1986). Phenytoin: mechanisms of its anticonvulsant action. *Ann. Neurol.* 20, 171–184. doi: 10.1002/ana.410200202
- Zamanillo, D., Portillo-Salido, E., Vela, J. M., and Romero, L. (2012). “Sigma-1 receptor chaperone: pharmacology and therapeutic perspectives,” in *Therapeutic Targets: Modulation, Inhibition, and Activation*, eds L. M. Botana and M. Loza (Hoboken, NJ: Wiley), 225–278.
- Zhang, H., Ma, L., Wang, F., Chen, J., and Zhen, X. (2007). Chronic SKF83959 induced less severe dyskinesia and attenuated L-DOPA-induced dyskinesia in 6-OHDA-lesioned rat model of Parkinson's disease. *Neuropharmacology* 53, 125–133. doi: 10.1016/j.neuropharm.2007.04.004

- Zhang, J., Huang, J., Song, Z., Guo, L., Cai, W., Wang, Y., et al. (2014). Structural manipulation on the catecholic fragment of dopamine D(1) receptor agonist 1-phenyl-N-methyl-benzazepines. *Eur. J. Med. Chem.* 85, 16–26. doi: 10.1016/j.ejmech.2014.07.059
- Zhao, L., Au, J. L.-S., and Wientjes, M. G. (2010). Comparison of methods for evaluating drug-drug interaction. *Front. Biosci.* 2, 241–249.
- Zhen, X., Goswami, S., and Friedman, E. (2005). The role of the phosphatidylinositol-linked D dopamine receptor in the pharmacology of SKF83959. *Pharmacol. Biochem. Behav.* 80, 597–601. doi: 10.1016/j.pbb.2005.01.016
- Zvejniece, L., Vavers, E., Svalbe, B., Vilskersts, R., Domracheva, I., Vorona, M., et al. (2014). The cognition-enhancing activity of E1R, a novel positive allosteric modulator of sigma-1 receptors. *Br. J. Pharmacol.* 171, 761–771. doi: 10.1111/bph.12506

**Conflict of Interest Statement:** TM is co-inventor on the patent (PCT/EP2017/060129) describing OZP002 and received consultancy fees and research contracts from Zogenix Inc. The company had no role in the writing of this review.

The remaining authors declare that the research was conducted in the absence of any commercial or financial relationships that could be construed as a potential conflict of interest.

Copyright © 2019 Vavers, Zvejniece, Maurice and Dambrova. This is an open-access article distributed under the terms of the Creative Commons Attribution License (CC BY). The use, distribution or reproduction in other forums is permitted, provided the original author(s) and the copyright owner(s) are credited and that the original publication in this journal is cited, in accordance with accepted academic practice. No use, distribution or reproduction is permitted which does not comply with these terms.



# Molecular Interplay Between the Sigma-1 Receptor, Steroids, and Ion Channels

Sara L. Morales-Lázaro<sup>1\*</sup>, Ricardo González-Ramírez<sup>2</sup> and Tamara Rosenbaum<sup>1</sup>

<sup>1</sup> Departamento de Neurociencia Cognitiva, División de Neurociencias, Instituto de Fisiología Celular, Universidad Nacional Autónoma de México, Ciudad de México, Mexico, <sup>2</sup> Departamento de Biología Molecular e Histocompatibilidad, Hospital General Dr. Manuel Gea González, Secretaría de Salud, Ciudad de México, Mexico

## OPEN ACCESS

### Edited by:

Tangui Maurice,  
INSERM U1198 Mécanismes  
Moléculaires dans les Démences  
Neurodégénératives, France

### Reviewed by:

Olivier Soriani,  
Centre National de la Recherche  
Scientifique (CNRS), France  
Carmela Parenti,  
Università degli Studi di Catania, Italy

### \*Correspondence:

Sara L. Morales-Lázaro  
saraluzm@ifc.unam.mx

### Specialty section:

This article was submitted to  
Experimental Pharmacology  
and Drug Discovery,  
a section of the journal  
Frontiers in Pharmacology

**Received:** 20 January 2019

**Accepted:** 03 April 2019

**Published:** 24 April 2019

### Citation:

Morales-Lázaro SL,  
González-Ramírez R and  
Rosenbaum T (2019) Molecular  
Interplay Between the Sigma-1  
Receptor, Steroids, and Ion Channels.  
Front. Pharmacol. 10:419.  
doi: 10.3389/fphar.2019.00419

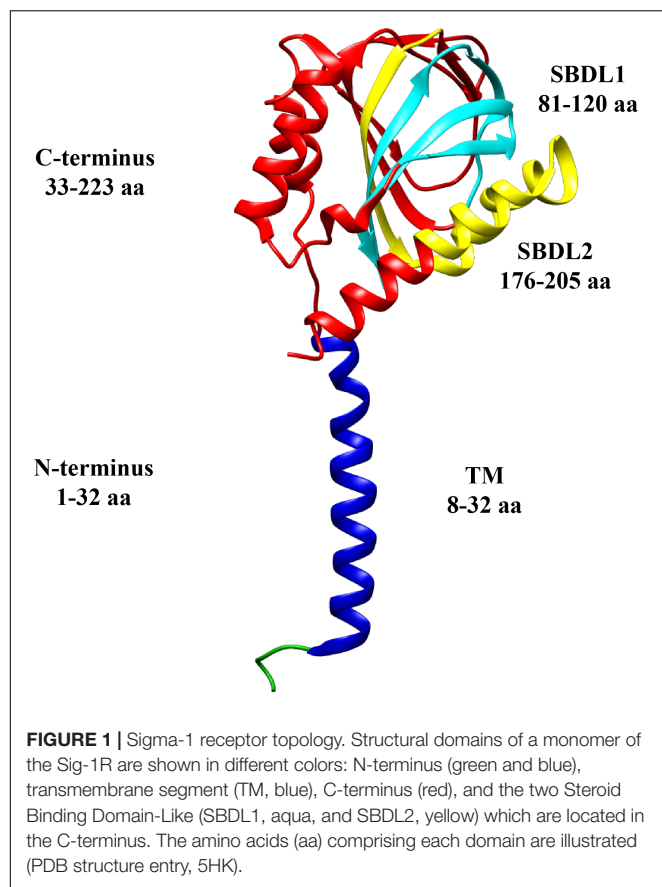
Cell excitability is tightly regulated by the activity of ion channels that allow for the passage of ions across cell membranes. Ion channel activity is controlled by different mechanisms that change their gating properties, expression or abundance in the cell membrane. The latter can be achieved by forming complexes with a diversity of proteins like chaperones such as the Sigma-1 receptor (Sig-1R), which is one with unique features and exhibits a role as a ligand-operated chaperone. This molecule also displays high intracellular mobility according to its activation level since, depletion of internal  $\text{Ca}^{+2}$  stores or the presence of specific ligands, produce Sig-1R's mobilization from the endoplasmic reticulum toward the plasma membrane or nuclear envelope. The function of the Sig-1R as a chaperone is regulated by synthetic and endogenous ligands, with some of these compounds being a steroids and acting as key endogenous modifiers of the actions of the Sig-1R. There are cases in the literature that exemplify the close relationship between the actions of steroids on the Sig-1R and the resulting negative or positive effects on ion channel function/abundance. Such interactions have been shown to importantly influence the physiology of mammalian cells leading to changes in their excitability. The present review focuses on describing how the Sig-1R regulates the functional properties and the expression of some sodium, calcium, potassium, and TRP ion channels in the presence of steroids and the physiological consequences of these interplays at the cellular level are also discussed.

**Keywords:** Sig-1R, ion channels, steroids, NMDA – receptor, TRPV1, voltage-gated ion channel, progesterone

## INTRODUCTION

The Sigma-1 receptor (Sig-1R) is a protein mainly localized to the endoplasmic reticulum (ER), where it functions as a ligand-operated chaperone (Hayashi and Su, 2003, 2007). The first studies related to Sig-1R incorrectly classified it as an opioid-type receptor (Martin et al., 1976; Su, 1982), although, Sig-1R displays high affinity for (+)-benzomorphans (such as (+)-SKF 10047) and not for the negative enantiomers of these compounds (Tam, 1983; Largent et al., 1987).

It was also hypothesized that its structure contained two transmembrane segments (Hayashi and Su, 2007; Aydar et al., 2016), however, the recent crystallographic structure for Sig-1R, shows only one transmembrane segment (Schmidt et al., 2016; **Figure 1**). The C-terminus of Sig-1R was also elucidated by crystallography, and it was proposed to be located facing toward the cell cytoplasm (Schmidt et al., 2016). Nonetheless, *in vivo* experiments later suggested that it is found facing the lumen of the ER (Mavlyutov et al., 2018).



The high affinity of Sig-1R for dextrorotatory isomers of specific opiate benzomorphans like (+) pentazocine (Tam and Cook, 1984; Prezzavento et al., 2017), was exploited to purify it from guinea pig liver and characterize it as a ~25 kDa protein (Hanner et al., 1996). It was determined that its sequence shares no homology with any other mammalian protein, that it contains a typical ER-retention signal within the N-terminus and, initial hydrophobicity analysis, provided the first sign of the presence of a single transmembrane segment (Hanner et al., 1996). Also, it was defined that the C-terminus of this receptor (residues 33–223) contains the ligand binding-sites (Kruse, 2017), two steroid-like binding domains (SBDL1-2) (Pal et al., 2007) and the chaperone domain (Figure 1; Hayashi and Su, 2007; Ortega-Roldan et al., 2013). Another essential feature of Sig-1R is its intracellular mobility, although it is mostly localized to the mitochondria-associated membrane (MAM) of the ER (a domain with high cholesterol content; Hayashi and Su, 2007), it still exhibits movement toward the plasma membrane and nuclear envelope (Hayashi and Su, 2003). Under basal conditions, Sig-1R forms complexes with another ER resident protein, BiP (or Gpr78) and calcium depletion from the ER derives in the dissociation of these two proteins. Then, Sig-1R becomes available to perform its chaperone functions by contributing to the stability of targets proteins, such as the inositol triphosphate (IP3) receptor (IP3R) and others, as will be here discussed (Hayashi and Su, 2007).

An important property of the function of this receptor is its regulation by synthetic and endogenous ligands (Hayashi and Su, 2004; Table 1). According to the physiological responses that these ligands elicit, they can play a role as agonists by potentiating some physiological responses or by normalizing alterations produced during some pathological conditions. On the other hand, antagonists block these effects. For example, PRE084 is considered to be a Sig-1R agonist since it improves learning impairments induced by MK-801 (a non-competitive antagonist of NMDA receptors), while this effect is suppressed by a Sig-1R antagonist, haloperidol (Maurice et al., 1994). Another example of this is the psychomotor responsiveness induced by cocaine, which is Sig-1R-dependent, an effect that is prevented by the co- or pre-administration of Sig-1R antagonists (Kourrich et al., 2013).

It has been reported that some ligands allow for the dissociation of the Sig-1R/BiP complexes, facilitating the interaction of Sig-1R with other proteins (for example, ion channels), similar to what is described above for calcium (Hayashi and Su, 2007). Examples of ligands that promote the dissociation of Sig-1R from BiP are (+)-pentazocine, (+)-SKF 10047, PRE084, fluoxetine and cocaine (Hayashi and Su, 2007). In contrast, other Sig-1R ligands can preserve it in a silent state, either associated with BiP or by producing its oligomerization (Hayashi and Su, 2007; Mishra et al., 2015). Compounds representative of the latter are haloperidol, methamphetamine and NE-100 (Hayashi and Su, 2007; Mishra et al., 2015).

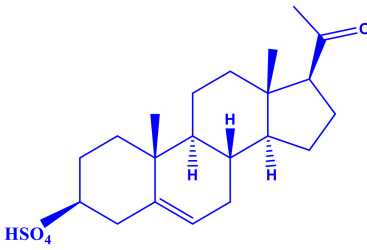
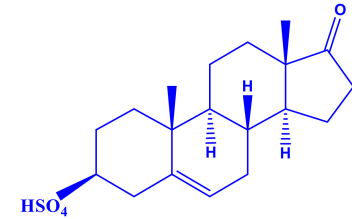
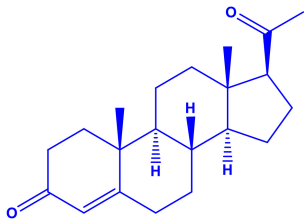
Interestingly, most of the endogenous ligands for Sig-1R are steroids (Su et al., 1988; Maurice et al., 1996). Among them are steroids synthesized in the nervous system (neurosteroids) that modulate the physiology of neuronal tissues (Corpechot et al., 1981). Neurosteroids such as pregnenolone-sulfate (PREG-S) and dehydroepiandrosterone sulfate (DHEA-S) have a role as Sig-1R agonists (Maurice et al., 1998; Table 1). Conversely, progesterone is an endogenous antagonist of this receptor, that displays the highest affinity for Sig-1R, as compared to the other steroid-type ligands (Su et al., 1988; Maurice et al., 1998; Table 1). On the other hand, testosterone, a steroid whose specific actions on Sig-1R are still unclear, only shows a partial affinity for the receptor (Su et al., 1988). In addition, cholesterol, the precursor of all steroids, can regulate Sig-1R through its binding to the C-terminus of Sig-1R (Palmer et al., 2007).

Altogether, the use of Sig-1R ligands has allowed establishing its role in neuroprotection, neurogenesis, pain, addiction, neurodegenerative and cardiovascular diseases (reviewed in Tsai et al., 2009). This review article will focus on our current understanding of how the interactions between Sig-1R and steroids regulate some ion channels such as voltage-gated potassium and sodium channels, NMDA receptors and TRP channels as well as on the resulting physiological effects of such interactions (Figure 2).

## ION CHANNELS

An early event of evolution was the appearance of a plasma membrane that functioned as a barrier to separate and protect

**TABLE 1** | Steroid Sig-1R ligands that regulate some ion channels.

Effect on Sig-1R	Name	Structure	Ion Channel Target
Agonist	Pregnenolone Sulfate $K_i = 3.196 \pm 0.823$		(-) L-type channels (+) NMDAr
	DHEA Sulfate $K_i = 15.126 \pm 7.69$		(-) $Na_v$ channels (+) NMDAr
Antagonist	Progesterone $K_i = 0.175 \pm 0.55$		(-) TRPV1 channels (+) $Na_{v1.5}$ channels* (-) NMDAr** (-) hERG channels***

$K_i$  ( $\mu M$ ) are indicated below the steroid name and represent the concentration of steroids necessary to inhibit in vitro binding of (+)-[3H]-SKF 10047 to brain homogenates (Su et al., 1988; Maurice et al., 1996). The column on the right indicates the ion channel that is the target of the steroid's actions through modulation of Sig-1R. (+) and (-) indicate the type of effect reported. \*Progesterone prevents the inhibitory effects of DMT on  $Na_{v1.5}$  channels. \*\*Progesterone disrupts the interaction between Sig-1R and NMDAr. \*\*\*This effect has not been directly demonstrated.

the interior of cells from changes in the external conditions. This lipid barrier also allows for the separation of charges between the extracellular and intracellular regions, serving as a shelter for pore-forming proteins that allow for selective passage of ions from one side to the other which, in turn, results in the generation of a membrane potential (Hille, 2001). Some of these proteins, called voltage-gated ion channels (VGICs; i.e.,  $Na_v$ ,  $K_v$ , and  $Ca_v$ ), open their pores to ion conduction (sodium, potassium and calcium) in response to electrical changes, a phenomenon which is possible thanks to a voltage-sensitive domain that modulates the gating properties of these channels (Hille, 2001). Other channels are specifically activated by ligands (i.e., *N*-methyl-D-aspartate or NMDA receptors), which directly bind to certain regions of the channels modulating their gating (Hille, 2001). Also, there are polymodal ion channels, such as the Transient Receptor Potential or TRP channels, that are activated by several stimuli including those of thermal, chemical and osmotic natures (Li, 2017).

Different mechanisms can regulate the functions of ion channels that include specific pore blockers or modifiers of their gating properties (chemical compounds/toxins; Hille, 2001), post-translational modifications (phosphorylation, glycosylation) and interactions with other proteins, such as Sig-1R, among others.

Although several reports illustrate the regulation of ion channels by Sig-1R and its synthetic Sig-1R ligands, few studies

have conclusively shown that endogenous Sig-1R ligands, such as steroids, modulate its interaction with some ion channels. Thus, examples of the latter will be discussed below.

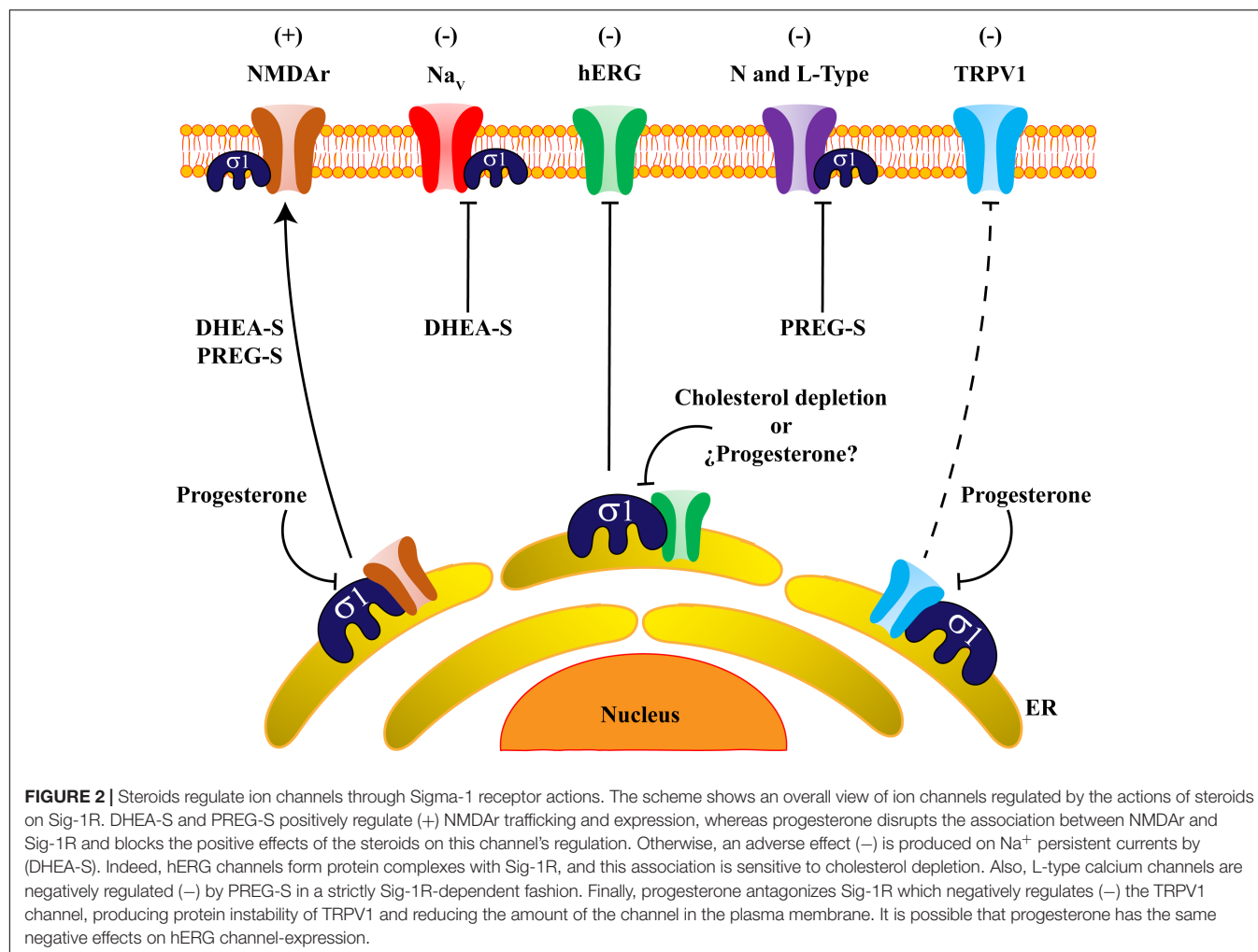
## STEROID-TYPE COMPOUNDS AS REGULATORS OF $Na_v$ CHANNELS THROUGH SIG-1R

Voltage-gated sodium ( $Na_v$ ) channels are molecular complexes primordial to cell depolarization in all excitable cells (Hille, 2001). They are constituted by  $\alpha$  and  $\beta$  subunits (pore-forming and accessory subunits, respectively) and nine different  $Na_v$  channels have been identified ( $Na_{v1.1-1.9}$ ) (Dhar Malhotra et al., 2001).

To date, it has been demonstrated that Sig-1R interacts with  $Na_{v1.5}$  channels. These channels are expressed in the brain regulating neuronal excitation (Wu et al., 2002) and in cardiac tissue shaping the action potential in the heart (Veerman et al., 2015).

Balasuriya and collaborators demonstrated the association between Sig-1R and  $Na_{v1.5}$  channels. They performed assays using HEK293 cells transiently expressing both, Sig-1R and  $Na_{v1.5}$  channels, and determined, through atomic force microscopy (AFM) experiments, that Sig-1R directly interacts with  $Na_{v1.5}$  tetramers with a 4-fold symmetry (Balasuriya et al., 2012).





This molecular association is disrupted by some of Sig-1R's synthetic ligands (haloperidol and pentazocine).

The physiological importance of the Sig-1R interaction with Na<sub>v1.5</sub> channels is exemplified in studies performed with some breast cancer cell lines, such as MDA-MB-231. This cell line constitutively expresses Sig-1R and Na<sub>v1.5</sub>, where it has been shown that they form a protein complex (Aydar et al., 2016). The knockdown of Sig-1R expression reduces Na<sub>v1.5</sub> channels surface levels in this cancer breast cell line (Aydar et al., 2016), and the physiological consequence of this is a decrease in cell adhesion. This is a clear example of the importance of the Sig-1R/Nav1.5 protein complex in regulating the metastatic behavior of these cancer cells (Aydar et al., 2016).

Other studies have shown that the endogenous hallucinogen N,N-dimethyltryptamine (DMT) (Saavedra and Axelrod, 1972), is a ligand of Sig-1R (Fontanilla et al., 2009). DMT has been shown to reduce the activation of Na<sub>v1.5</sub> channels expressed in HEK293 cells and neonatal cardiac myocytes (Fontanilla et al., 2009). Effects of this Sig-1R agonist on Na<sup>+</sup> currents are strictly dependent upon Sig-1R expression since they are scarce in cells expressing low levels of Sig-1R, such as in the COS-7 cell line (Johannessen et al., 2009).

As for steroids and the roles of Sig-1R on the regulation of Na<sub>v</sub> channels, it has been shown that DHEA-S negatively impacts on the function of persistent Na<sup>+</sup> currents. It is known that the increase of this type of currents leads to hyperexcitability of cells expressing these channels (Deng and Klyachko, 2016). The effects of DHEA-S on persistent Na<sup>+</sup> currents were evaluated in rat medial prefrontal cortex slices and were examined before and after DHEA-S perfusion (4.5 min) (Cheng et al., 2008). Whole-cell patch clamp recordings showed that DHEA-S reduces persistent Na<sup>+</sup> currents an action mimicked by carbetapentane citrate (a Sig-1R agonist) and blocked by Sig-1R antagonist (i.e., haloperidol) (Cheng et al., 2008). Although a change in the overall excitability of the tissue in question would have been expected in the presence of DHEA-S, this was not observed and the reasons for this remain unclear. Nonetheless, it has been suggested by the authors of this study that, such a lack of change in the tissue's excitability in the presence of DHEA-S, may be due to a positive effect of this compound on other molecular targets. This would lead to neutralization of the negative regulation of persistent Na<sup>+</sup> currents by DHEA-S and a neutral effect on neuronal excitability (Cheng et al., 2008).

Moreover, it has been suggested that the regulation of persistent  $\text{Na}^+$  currents by DHEA-S, is probably relevant under pathological conditions such as brain ischemia. Under this scenario, negative regulation of persistent  $\text{Na}^+$  currents by DHEA-S, through the actions of Sig-1R, would lead to a decrease in neuronal excitability, resulting in a neuroprotective effect. It has been proposed that DHEA-S may be a desirable candidate for therapeutic approaches directed toward relieving induced cerebral ischemia infarction (Yabuki et al., 2015).

In summary, there are only a few evidences showing the direct relationship between Sig-1R, steroids and  $\text{Na}_v$  channels. Nonetheless, available studies suggest that the negative role of synthetic Sig-1R ligands on  $\text{Na}^+$  currents are similar to those promoted by steroidal Sig-1R agonists (i.e., DHEA-S) (**Figure 2**).

## **K<sub>v</sub> CHANNELS ARE FUNCTIONAL TARGETS OF THE ACTIONS OF CHOLESTEROL ON SIG-1R**

The generation of action potentials depends upon a fine-tuned coordination of different electrical phases, among which is repolarization. Through this process, the membrane potential is returned to negative voltage values to ensure that an excitable cell can respond to new stimuli. For repolarization to occur, the activation of voltage-gated  $\text{K}^+$  channels ( $\text{K}_v$ ) is essential (Hille, 2001; Kandel et al., 2012).

It has been shown that Sig-1R forms complexes with these ion channels regulating their function or abundance in the plasma membrane. Ligands of Sig-1R highly regulate the formation of some of these complexes. For instance, coimmunoprecipitation assays have demonstrated that Sig-1R is associated to  $\text{K}_{v1.4}$  in posterior pituitary nerve terminals from rat and also in *Xenopus* oocytes with heterologous expression of Sig-1R and  $\text{K}_{v1.4}$  channels (Aydar et al., 2002). In the latter, whole-cell recordings showed that (+)-SKF 10047, downregulates  $\text{K}_{v1.4}$  channel outward currents, indicating a negative role of Sig-1R on the function of these proteins (Aydar et al., 2002).

Conversely, cocaine triggers the dissociation of Sig-1R from BiP, leading to its interaction with  $\text{K}_{v1.2}$  and facilitating channel translocation to the plasma membrane. As a result of this,  $\text{K}_{v1.2}$  function is positively regulated, resulting in neuronal hypoactivity (Kourrich et al., 2013). These results highlight the physiological consequence of a cocaine-induced long-lasting association of these two proteins by which, an enduring experience-dependent plasticity phenomenon, occurs. This also pinpoints a mechanism that can shape neuronal and behavioral responses to cocaine, as suggested by Kourich and collaborators.

Despite the lack of direct experimental evidences showing the effects of steroids on the association of Sig-1R with  $\text{K}_v$  channels, some reports have demonstrated a possible interplay between them. For example, patch clamp experiments performed in the K562 leukemic cell line, which endogenously expresses Sig-1R and hERG channels (a  $\text{K}_v$  channel also expressed in cardiac tissues), showed that hERG currents are inhibited by igmesine and (+) pentazocine (both of which are Sig-1R ligands).

In addition, silencing of Sig-1R using shRNA-based strategies, also demonstrated reduced hERG current-densities without affecting hERG-channel transcription, but rather by decreasing the amount of the mature form of the channel on the plasma membrane of the cells (Crottes et al., 2011).

It has also been reported that progesterone alters hERG-channel expression. By using HEK293 cells stably-expressing hERG channels and whole-cell voltage clamp recordings, it has been demonstrated that progesterone decreases hERG current-density. This effect was also observed in an hERG-channel endogenous expression system of rat neonatal cardiac myocytes (Wu et al., 2011). Confocal microscopy and western blot analysis of surface proteins showed that progesterone decreases the amount of the mature form of hERG-channel proteins in the plasma membrane and induces channel accumulation in the ER. Moreover, using filipin cell-staining techniques, it was shown that treatment with progesterone produces disruption of cholesterol homeostasis, impairing adequate hERG-channel folding and traffic to the Golgi compartment (Wu et al., 2011). Since progesterone is a Sig-1R antagonist, it could be hypothesized that these effects are produced through a disruption of the Sig-1R and hERG protein complexes. Alternatively, this could be the result of an alteration of cholesterol homeostasis, affecting the function or localization of Sig-1R. The consequences of both possibilities are an improper folding and traffic of hERG channels; thus, the overall effect of progesterone is negative regulation of channel expression in the plasma membrane (**Figure 2**).

Additionally, AFM imaging and homogenous time-resolved fluorescence experiments, have demonstrated that Sig-1R interacts with hERG channels with a 4-fold symmetry in the plasma membrane of HEK293 cells stably transfected with both proteins (Balasuriya et al., 2014). This is a similar scenario to the that reported for the formation of protein complexes between Sig-1R and  $\text{Na}_{v1.5}$  channels (Balasuriya et al., 2012). Interestingly, this association is independent of Sig-1R's ligands but susceptible to cholesterol depletion (Balasuriya et al., 2014). Accordingly, it has been suggested that Sig-1R ligands can displace cholesterol from its binding site altering the distribution of the receptor in the cell and profoundly impacting on its association with other proteins (Palmer et al., 2007).

This experimental evidence suggests that Sig-1R supports a suitable assembly and folding of immature hERG channels in order to enable them to exit from the ER. Thus, it follows that progesterone and cholesterol affect Sig-1R actions and reduce hERG channel maturation.

Similar results have been obtained for SK3 channels, the small-conductance calcium-activated potassium channels, for which expression of these proteins is regulated by the cellular content of Sig-1R and cholesterol (Gueguinou et al., 2017). The molecular silencing of Sig-1R or the use of igmesine (a Sig-1R ligand) decreases the amount of SK3 channels localized to lipid-enriched nanodomains in breast cells. This, in turn, results in a reduction in the migration of these cancer cells (Gueguinou et al., 2017). Thus, these findings emphasize an interesting area of research in which, the regulation of Sig-1R activity, may be an alternative to control the metastatic potential of certain types of cancers where

the levels of Sig-1R are upregulated (i.e., colorectal or breast cancers) (Gueguinou et al., 2017).

## REGULATION OF $Ca_v$ CHANNELS THROUGH SIG-1R'S ACTIVATION

Voltage-gated calcium channels ( $Ca_v$ ) are the main transducers of membrane potential changes (Hille, 2001). Their activation produces the influx of  $Ca^{+2}$  ions to the cell, where they function as second messengers to activate different cell signaling pathways, leading to diverse physiological consequences.  $Ca_v$  channels are constituted by pore-forming subunits,  $\alpha_1$  (similar to  $Na_v$  channels) and by accessory subunits ( $\alpha_2\delta$ ,  $\beta$ , and  $\gamma$ ), which are necessary for a suitable function and expression of these channels. According to the types of  $Ca^{+2}$  currents that they generate, these proteins are classified as L-, N-, P/Q-, R-, and T-type calcium channels (reviewed in Catterall, 2000).

So far, there is interesting evidence about the interactions between  $Ca_v$  channels and Sig-1R. In this respect, the data show that Sig-1R activation by different synthetic agonists, negatively influences  $Ca_v$  channels functions, as shown in isolated intracardiac neurons of neonatal rats (Zhang and Cuevas, 2002). In this experimental model,  $Ca_v$  channel inactivation rates are increased, and the steady-state voltage-dependences of activation and inactivation are shifted to negative potentials.

The adverse effects of Sig-R ligands on  $Ca_v$  channel function have also been observed in cholinergic interneurons from the rat striatum. Here, agonists of Sig-1R such as (+)-SKF 10047 and PRE-084, inhibit N-type calcium currents and, as it would be expected, BD1047, a Sig-1R antagonist obliterates this phenomenon. FRET and coimmunoprecipitation experiments demonstrated that N-type channels and Sig-1R form protein-complexes when these proteins are expressed in HEK293 cells. The authors of this study proposed that Sig-1R agonists produce a conformational change in these protein complexes that negatively regulates N-type channels (Zhang et al., 2017).

Likewise, the negative roles of Sig-1R ligands on  $Ca_v$  channels have been observed in primary neuronal cultures from the hippocampus, where SA4503 (a Sig-1R agonist), inhibits N- and L-Type currents, producing an increase in axonal outgrowth (Li et al., 2017).

As for L-type ion channels, these have been shown to co-localize with Sig-1R in retinal ganglion cells (Mueller et al., 2013). Likewise, physical interactions between these proteins have also been demonstrated through coimmunoprecipitation assays in these cells (Tchedre et al., 2008).

Furthermore, an interplay between L-Type channels, Sig-1R and the neurosteroid, PREG-S, has been reported (Sabeti et al., 2007). This was evaluated using electrophysiological recordings from CA1 neurons of rat hippocampal slices perfused with PREG-S before and during the induction of long-term potentiation (LTP) of excitatory transmission. The data demonstrated that LTP increased in slices subjected to PREG-S perfusion. Suitably, nimodipine, an antagonist of L-type calcium

channels, blocked PREG-S-induced LTP. Additionally, perfusion of PREG-S and BD1047, also blocked LTP in hippocampal slices, strongly supporting the role of PREG-S acting through Sig-1R in this process (Sabeti et al., 2007). Thus, in this neuronal context, regulation of the function of L-type channels confers synaptic plasticity (Figure 2).

## REGULATION OF NMDA RECEPTORS BY NEUROSTEROID MOLECULES AND SIG-1R

The N-methyl-D-aspartate receptor (NMDAr) is a heterotetrameric ionotropic receptor formed by the assembly of two NR1 and two NR2 or NR3 subunits. NMDAr functions as a channel permeable to  $Ca^{+2}$ , its activation is produced by the binding of two different ligands (glutamate and glycine), profoundly impacting on neuronal plasticity, memory and learning processes (reviewed in Hansen et al., 2018).

Regulation of NMDAr by Sig-1R ligands has been extensively reported and, positive effects on their function, strongly correlate to Sig-1R's activation. A pioneering study by Monnet and collaborators demonstrated that a synthetic Sig-1R agonist potentiated neuronal activation induced by NMDAr in CA3 dorsal hippocampal neurons, an effect that was reverted by haloperidol (Monnet et al., 1990). Positive NMDAr regulation by Sig-1R's agonists leads to an improvement in learning and memory since it has been shown that PRE084, attenuates the impairment of learning in mice treated with an NMDAr antagonist (Maurice et al., 1994). A recent study showed that memory deficits produced in mice where brain ischemia was induced, were improved by the use of Sig-1R agonists while they were worsened by antagonism of the NR2 subunits (Xu et al., 2017).

Recently, a direct interaction between Sig-1R and the NR1 subunit of NMDAr has been revealed *in vitro* through the use of AFM imaging. Proximity-ligation assays also confirmed this interaction, supporting an *in vivo* association between these proteins (Balasuriya et al., 2013). This protein-complex is disrupted by some Sig-1R ligands such as BD1063, cannabidiol and progesterone, as demonstrated by pull-down assays (Rodriguez-Munoz et al., 2018). In addition, it has also been shown that the NR2 subunit of NMDAr is positively regulated by Sig-1R agonists, producing an upregulation in NR2-protein-expression and increasing traffic of NR2 to the plasma membrane (Pabba et al., 2014; Figure 3A). Finally, it has been shown that Sig-1R knockout mice display decreases in NMDAr-mediated currents and that these animals exhibit deficiencies in neurogenesis at the hippocampal dentate gyrus (Sha et al., 2013). These data suggest that Sig-1R activation positively influences NMDAr function during memory and learning processes.

Effects of steroid-type Sig-1R ligands on NMDAr functions have also been reported. For example, rats subjected to intraperitoneal injection of dizocilpine, (a competitive antagonist of NMDAr), exhibit spatial working and memory deficits. These effects are attenuated by DHEA-S and PREG-S or by a SA4503, all of which are Sig-1R agonists (Figure 3B). In contrast, progesterone or NE-100 (both of which constitute

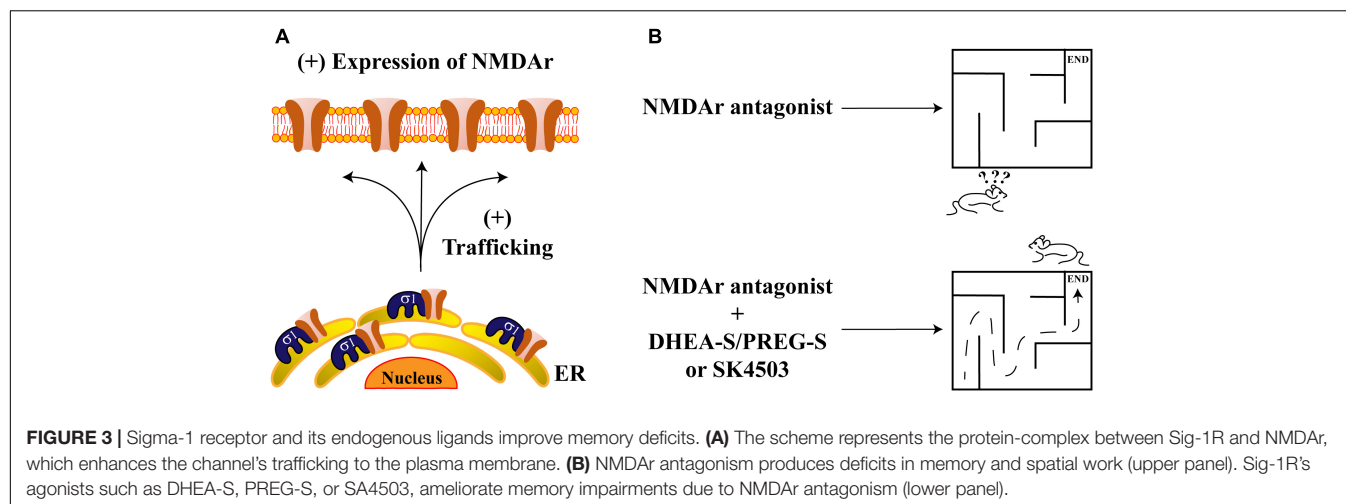


**FIGURE 3 |** Sigma-1 receptor and its endogenous ligands improve memory deficits. **(A)** The scheme represents the protein-complex between Sig-1R and NMDAr, which enhances the channel's trafficking to the plasma membrane. **(B)** NMDAr antagonism produces deficits in memory and spatial work (upper panel). Sig-1R's agonists such as DHEA-S, PREG-S, or SA4503, ameliorate memory impairments due to NMDAr antagonism (lower panel).

Sig-1R antagonists), block the ameliorative effects of DHEA-S and PREG-S on dizocilpine-induced memory deficits (Zou et al., 2000).

Similarly, some brain ischemia animal models display impairment of LTP at the hippocampal CA1 area, an effect that is prevented by DHEA-S. On the contrary, NE100 and progesterone revert the positive actions of DHEA-S in this model (Li et al., 2006). Finally, the protective effects of DHEA-S on spatial memory have also been reported and have demonstrated that they are dependent upon Sig-1R's actions (Li et al., 2009).

## TRPV1: THE FIRST TRP CHANNEL SHOWN TO BE REGULATED BY SIG-1R

Transient Receptor Potential (TRP) ion channels allow for the influx of cations in a non-selective fashion. These proteins possess four subunits, giving rise to functional tetramers (reviewed in Ramsey et al., 2006). According to their structural features, these channels have been classified into seven subfamilies: TRPA (ankyrin), TRPC (canonical), TRPM (melastatin), TRPML (mucolipin), TRPN (no-mechanoreceptor potential C), TRPP (polycystic) and TRPV (vanilloid) (reviewed in Li, 2017). Several of the members of these subfamilies are implicated in the transduction of thermal, chemical and osmotic stimuli.

TRPV1 channels have been extensively studied for their roles in pain. They are mainly expressed by nociceptors (A $\delta$  and C-Fibers) where they are essential for the transduction of noxious signals. These channels are activated by high temperatures ( $\geq 42^\circ\text{C}$ ), irritant compounds (capsaicin, resiniferatoxin, allicin, etc.) (Caterina et al., 1997; Salazar et al., 2008) and by changes in extra- and intracellular pH (acid and basic, respectively) (Caterina et al., 1997; Jordt et al., 2000; Dhaka et al., 2009). Additionally, TRPV1's activation can also be achieved by some endogenous compounds released during inflammation or tissue injury, such as lysophosphatidic acid (LPA) (Nieto-Posadas et al., 2011), among other endogenous agonists (reviewed in Morales-Lázaro et al., 2013). Since TRPV1 exhibits a pivotal role in painful signal transduction, this channel has become a pharmacological

target with several research groups around the world focusing on ways to regulate its function to relieve certain types of pain.

So far, several synthetic compounds and some of a natural origin (i.e., oleic acid) (Morales-Lázaro et al., 2016), have been described as negative regulators of TRPV1's activation. However, few studies have revealed alternative ways to regulate TRPV1's functions, including manipulating the abundance of this channel in the plasma membrane of nociceptors. Just recently, our group described that Sig-1R is a crucial molecular target that can regulate the amount of TRPV1 channels localized to the plasma membrane of cells, without affecting channel transcription (Ortiz-Renteria et al., 2018). This constituted the first report for a TRP channel as being regulated by Sig-1R, highlighting the role of a direct interaction between TRPV1 and Sig-1R in pain.

In this study, we found that a synthetic ligand of Sig-1R, BD1063, decreased TRPV1 protein levels in mice dorsal root ganglia (DRG) and HEK293 cells transiently expressing TRPV1. This effect was mimicked by the knockdown of Sig-1R expression in TRPV1-expressing HEK293 cells. Furthermore, progesterone also produced down-regulation of TRPV1 expression, as demonstrated by western blot assays. Worth noting is that the effects of progesterone on TRPV1 expression were found to be independent of its classical nuclear receptors (Ortiz-Renteria et al., 2018).

Also, whole-cell recordings showed that Sig-1R knockdown and the addition of BD1063 or progesterone to cell cultures, reduced the current-densities evoked by capsaicin, indicating that negative regulation of Sig-1R (either by reducing Sig-1R expression or using its antagonists), decreased the amount of TRPV1 localized to the plasma membrane. This negative effect on TRPV1 expression was prevented through the inhibition of proteasomal degradation, suggesting that Sig-1R is necessary for TRPV1 protein stability and confirms an independent effect of a transcriptional mechanism (Ortiz-Renteria et al., 2018).

Besides, we established a direct association between Sig-1R and the TRPV1 channel through coimmunoprecipitation and FRET experiments. We found that Sig-1R interacts with the transmembrane domain of TRPV1, similarly, to what had been previously reported for K<sub>v1.3</sub> ion channels (Kinoshita



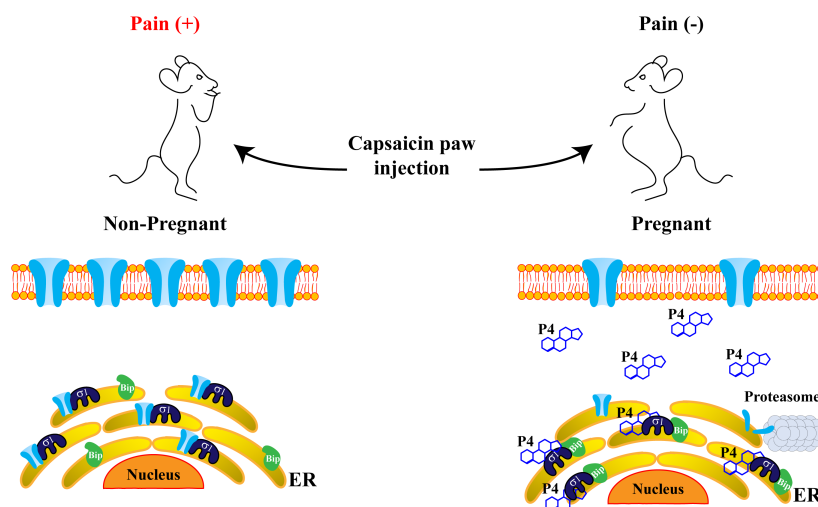


**FIGURE 4 |** Progesterone attenuates pain-related behavior through disruption of the Sig-1R/TRPV1 complex. Sig-1R and TRPV1 channels are physically associated in the endoplasmic reticulum (ER), improving TRPV1 stability and resulting in suitable TRPV1 expression in the plasma membrane, where the channel transduces painful signals. Consequently, non-pregnant mice display pain behaviors in response to capsaicin paw-injection (left). However, in pregnant mice (right), when progesterone levels considerably increase, the formation of the complex between Sig-1R and the Binding immunoglobulin protein (BiP), is promoted. This maintains Sig-1R in a sequestered state and blocks its association with the TRPV1 channel, improving protein instability and avoiding degradation through the proteasomal pathway. Thus, TRPV1 protein levels in the plasma membrane decrease, leading to an increased pain threshold in response to capsaicin in pregnant mice.

et al., 2012). Interestingly, this protein-complex was sensitive to Sig-1R ligands, since BD1063 and progesterone decreased the association between TRPV1 and Sig-1R. Furthermore, by confocal microscopy analysis, we observed that this protein-protein association is most prominent at the ER compartment and occurs less at the level of the plasma membrane. Together, all of these evidences pointed to a role of Sig-1R in conferring protein stability during the biogenesis of the channel, with Sig-1R preventing the misfolding of TRPV1 and avoiding its degradation by the proteasomal system (Figure 4).

Since, progesterone is the steroid with higher affinity for Sig-1R, its interactions with this receptor and the physiological consequences of such interplays have been a subject of focus in pregnancy, a physiological phase where progesterone levels are high (Bergeron et al., 1999). With this in mind, we explored if pain thresholds in response to capsaicin were different between non- and pregnant mice. The results indicated that, during pregnancy, pain-like behavior in response to the TRPV1 agonist was significantly decreased in mice, as compared to their non-pregnant counterparts (Figure 4). This led us to conclude that elevated levels of progesterone, such as those found during pregnancy, could confer protection against painful situations through the disruption of the protein complex between Sig-1R and TRPV1. This, in turn, would result in the downregulation of TRPV1's levels in the plasma membrane, ultimately decreasing the pain threshold associated with TRPV1's activation (Figure 4).

Several sources in the literature, together with our findings, have highlighted Sig-1R as a protein widely associated with nociception. For example, it has been reported that Sig-1R knockout mice, exhibit endurance to pain and mechanical allodynia induced by formalin and capsaicin, respectively (Cendan et al., 2005; Entrena et al., 2009).

Since Sig-1R is expressed in DRG neurons (Mavlyutov et al., 2016) and in specific regions of the spinal cord (Alonso et al., 2000), its actions are relevant at the pre and post-synaptic levels (reviewed in Romero et al., 2016). Thus, its roles in pain responses must involve more than one molecular target. For instance, several reports show that Sig-1R agonists induce and maintain central sensitization during painful states (Romero et al., 2012; Entrena et al., 2016; Choi et al., 2017). Some of Sig-1R's effects are through the upregulation or phosphorylation of the NR1 subunit of the NMDAR that lead to neuronal overexcitability (Roh et al., 2010). Conversely, antagonists of Sig-1R prevent or decrease pain in some neuropathic pain animal models since these compounds inhibit the upregulation of NR1 (Zhu et al., 2015). Besides it has been demonstrated that DHEA-S and PREG-S positively regulate the activity of P2X receptors resulting in the potentiation of the mechanical allodynia induced through these receptors (Kwon et al., 2016).

In conclusion, Sig-1R is essential for regulating peripheral and central sensitization by interacting with various molecular targets such as TRPV1 channels, P2X channels, NMDAR and it is possible that several other proteins involved in these processes, will be identified in the future.

## Progesterone as a Prototypical Endogenous Ligand of Sig-1R

Up to this point, we have emphasized findings that link the actions of Sig-1R and steroids to the function of ion channels. It is important to stress that, the steroid concentrations used in most of the experiments here described, are well above the reported physiological range.



The low affinity of steroids to Sig-1R justifies the use of high concentrations of steroid ligands in different experimental systems. For example, a study by Su et al. (1988) showed that progesterone competes ( $K_i = 268$  nM) with [H3](+)-SKF 10047 for the binding site in Sig-1R and exhibits higher affinity for this receptor. However, other steroids are required at much higher concentrations than those of progesterone to displace [H3](+)-SKF 10047 (Su et al., 1988). Nevertheless, this progesterone concentration is still too high to be normally circulating in blood but, in pregnancy, the circulating levels of this steroids can rise to 400 nM (Neill et al., 1969), reaching concentrations high enough to regulate Sig-1R.

In agreement with the results obtained by Su et al. (1988), Maurice et al. (1996) showed that progesterone displaces the binding of (+)-SKF 10047 to rat brain homogenates with a  $K_i$  of 175 nM. They showed that [H3](+)-SKF 10047 binding is significantly reduced in the hippocampus and the cortex from pregnant mice, as compared to non-pregnant female or male mice (Maurice et al., 1996).

These findings, together with ours where we showed that pregnant female mice display high pain-thresholds as compared to unpregnant mice (Ortiz-Renteria et al., 2018), suggesting that high circulating progesterone levels in pregnancy are enough to modify pain thresholds in mice.

Recently, a new high-affinity Sig-1R selective radiotracer ( $[^{18}\text{F}]$  FPS) has been developed. This compound has been used to perform PET studies in Rhesus monkeys showing high uptake of the radiotracer in brain regions where there are moderate densities of Sig-1R (Mach et al., 2005). Interestingly, animals pre-injected with progesterone displayed a significant reduction in the uptake of the radiotracer in the brain of the monkeys, confirming that progesterone displaces the radiotracer from Sig-1R's binding sites (Mach et al., 2005). In addition, this radiotracer was used to perform *in vitro* binding assays in rat forebrain homogenates showing that progesterone inhibits the binding of the radiotracer to Sig-1R. Notably, the  $K_i$  for progesterone is of 36 nM, a concentration of progesterone achieved during the luteal phase of the menstrual cycle (Neill et al., 1969). This finding further strengthens the notion that low progesterone levels also play a role in the activity of Sig-1R and that this steroid functions as an endogenous ligand of this receptor (Waterhouse et al., 2007).

## CONCLUSION

Regulation of ion channel physiology has been a subject of intense research for several decades. The implications of such modifications of ion channel function are extremely diverse and

important, and they are exemplified by the roles that these proteins play under normal physiological conditions but also in pathophysiological scenarios. Not only do these essential proteins regulate muscle contraction, neuronal excitability, and hormonal secretion but changes in their expression and function during pathological conditions lead to severe diseases such as epilepsy, diabetes, ataxia, pain, itch, etc. For many years, studies have focused on identifying molecular targets of synthetic and naturally-produced agents to regulate the activity of ion channels.

In addition to the identification of chemicals that specifically bind to members of different ion channel families to alter their biophysical properties, research groups have also focused on determining how protein-protein interactions regulate these. Among the proteins that can bind and change ion channel function and expression are chaperones and their roles and the consequences of their misfunctions are being studied in several diseases (Broadley and Hartl, 2009). The Sig-1R has been shown to play essential roles for the adequate function of several types of cells (Tsai et al., 2009), including those that are electrically excitable and hence express ion channels. Thus, from these studies and those discussed here, it is evident that a mechanism by which we may regulate ion channel physiology is through tools that allow us to manipulate the interactions between Sig-1R and these other proteins if this was to be possible without other severe consequences. But utmost important is that, by studying the interactions of Sig-1R with ion channels, we have gained valuable knowledge on how this receptor regulates ion channels. In turn, this has also helped us understand the physiological consequences of modifying the interplays between Sig-1R and ion channels for the function of the cells where these proteins are expressed.

## AUTHOR CONTRIBUTIONS

All authors listed have made a substantial, direct and intellectual contribution to the work, and approved it for publication.

## FUNDING

This work was supported by grants from Dirección General de Asuntos del Personal Académico (DGAPA)-Programa de Apoyo a Proyectos de Investigación e Innovación Tecnológica (PAPIIT) grant IN206819 and Estímulos a Investigaciones Médicas Miguel Alemán Valdés to SLM-L and Consejo Nacional de Ciencia y Tecnología (CONACyT) grant A1-S-8760, CONACyT Fronteras en la Ciencia No. 77 and DGAPA-PAPIIT grant IN200717 to TR.

## REFERENCES

- Alonso, G., Phan, V., Guillemain, I., Saunier, M., Legrand, A., Anoa, M., et al. (2000). Immunocytochemical localization of the sigma(1) receptor in the adult rat central nervous system. *Neuroscience* 97, 155–170.
- Aydar, E., Palmer, C. P., Klyachko, V. A., and Jackson, M. B. (2002). The sigma receptor as a ligand-regulated auxiliary potassium channel subunit. *Neuron* 34, 399–410.
- Aydar, E., Stratton, D., Fraser, S. P., Djamgoz, M. B., and Palmer, C. (2016). Sigma-1 receptors modulate neonatal Nav1.5 ion channels in breast cancer cell lines. *Eur. Biophys. J.* 45, 671–683.
- Balasuriya, D., D'Sa, L., Talker, R., Dupuis, E., Maurin, F., Martin, P., et al. (2014). A direct interaction between the sigma-1 receptor and the hERG voltage-gated  $\text{K}^+$  channel revealed by atomic force microscopy and homogeneous time-resolved fluorescence (HTRF<sup>(R)</sup>). *J. Biol. Chem.* 289, 32353–32363. doi: 10.1074/jbc.M114.603506

- Balasuriya, D., Stewart, A. P., Crottes, D., Borgese, F., Soriani, O., and Edwardson, J. M. (2012). The sigma-1 receptor binds to the Nav1.5 voltage-gated Na<sup>+</sup> channel with 4-fold symmetry. *J. Biol. Chem.* 287, 37021–37029. doi: 10.1074/jbc.M112.382077
- Balasuriya, D., Stewart, A. P., and Edwardson, J. M. (2013). The sigma-1 receptor interacts directly with GluN1 but not GluN2A in the GluN1/GluN2A NMDA receptor. *J. Neurosci.* 33, 18219–18224. doi: 10.1523/JNEUROSCI.3360-13.2013
- Bergeron, R., de Montigny, C., and Debonnel, G. (1999). Pregnancy reduces brain sigma receptor function. *Br. J. Pharmacol.* 127, 1769–1776. doi: 10.1038/sj.bjp.0702724
- Broadley, S. A., and Hartl, F. U. (2009). The role of molecular chaperones in human misfolding diseases. *FEBS Lett.* 583, 2647–2653. doi: 10.1016/j.febslet.2009.04.029
- Caterina, M. J., Schumacher, M. A., Tominaga, M., Rosen, T. A., Levine, J. D., and Julius, D. (1997). The capsaicin receptor: a heat-activated ion channel in the pain pathway. *Nature* 389, 816–824. doi: 10.1038/39807
- Catterall, W. A. (2000). Structure and regulation of voltage-gated Ca<sup>2+</sup> channels. *Annu. Rev. Cell Dev. Biol.* 16, 521–555. doi: 10.1146/annurev.cellbio.16.1.521
- Cendan, C. M., Pujalte, J. M., Portillo-Salido, E., Montoliu, L., and Baeyens, J. M. (2005). Formalin-induced pain is reduced in sigma(1) receptor knockout mice. *Eur. J. Pharmacol.* 511, 73–74. doi: 10.1016/j.ejphar.2005.01.036
- Cheng, Z. X., Lan, D. M., Wu, P. Y., Zhu, Y. H., Dong, Y., Ma, L., et al. (2008). Neurosteroid dehydroepiandrosterone sulphate inhibits persistent sodium currents in rat medial prefrontal cortex via activation of sigma-1 receptors. *Exp. Neurol.* 210, 128–136. doi: 10.1016/j.expneurol.2007.10.004
- Choi, S. R., Moon, J. Y., Roh, D. H., Yoon, S. Y., Kwon, S. G., Choi, H. S., et al. (2017). Spinal D-serine increases PKC-dependent GluN1 phosphorylation contributing to the sigma-1 receptor-induced development of mechanical allodynia in a mouse model of neuropathic pain. *J. Pain* 18, 415–427. doi: 10.1016/j.jpain.2016.12.002
- Corpechot, C., Robel, P., Axelsson, M., Sjövall, J., and Baulieu, E. E. (1981). Characterization and measurement of dehydroepiandrosterone sulfate in rat brain. *Proc. Natl. Acad. Sci. U.S.A.* 78, 4704–4707.
- Crottes, D., Martial, S., Rapetti-Mauss, R., Pisani, D. F., Loriol, C., Pellissier, B., et al. (2011). Sig1R protein regulates hERG channel expression through a post-translational mechanism in leukemic cells. *J. Biol. Chem.* 286, 27947–27958. doi: 10.1074/jbc.M111.226738
- Deng, P. Y., and Klyachko, V. A. (2016). Increased persistent sodium current causes neuronal hyperexcitability in the entorhinal cortex of *fmr1* knockout mice. *Cell Rep.* 16, 3157–3166. doi: 10.1016/j.celrep.2016.08.046
- Dhaka, A., Uzzell, V., Dubin, A. E., Mathur, J., Petrus, M., Bandell, M., et al. (2009). TRPV1 is activated by both acidic and basic pH. *J. Neurosci.* 29, 153–158. doi: 10.1523/JNEUROSCI.4901-08.2009
- Dhar Malhotra, J., Chen, C., Rivolta, I., Abriel, H., Malhotra, R., Mattei, L. N., et al. (2001). Characterization of sodium channel alpha- and beta-subunits in rat and mouse cardiac myocytes. *Circulation* 103, 1303–1310.
- Entrena, J. M., Cobos, E. J., Nieto, F. R., Cendan, C. M., Gris, G., Del Pozo, E., et al. (2009). Sigma-1 receptors are essential for capsaicin-induced mechanical hypersensitivity: studies with selective sigma-1 ligands and sigma-1 knockout mice. *Pain* 143, 252–261. doi: 10.1016/j.pain.2009.03.011
- Entrena, J. M., Sanchez-Fernandez, C., Nieto, F. R., Gonzalez-Cano, R., Yeste, S., Cobos, E. J., et al. (2016). Sigma-1 receptor agonism promotes mechanical allodynia after priming the nociceptive system with capsaicin. *Sci. Rep.* 6:37835. doi: 10.1038/srep37835
- Fontanilla, D., Johannessen, M., Hajipour, A. R., Cozzi, N. V., Jackson, M. B., and Ruoho, A. E. (2009). The hallucinogen N,N-dimethyltryptamine (DMT) is an endogenous sigma-1 receptor regulator. *Science* 323, 934–937. doi: 10.1126/science.1166127
- Gueguinou, M., Crottes, D., Chantome, A., Rapetti-Mauss, R., Potier-Cartreau, M., Clarysse, L., et al. (2017). The SigmaR1 chaperone drives breast and colorectal cancer cell migration by tuning SK3-dependent Ca<sup>2+</sup> homeostasis. *Oncogene* 36, 3640–3647. doi: 10.1038/onc.2016.501
- Hanner, M., Moebius, F. F., Flandorfer, A., Knaus, H. G., Striessnig, J., Kempner, E., et al. (1996). Purification, molecular cloning, and expression of the mammalian sigma1-binding site. *Proc. Natl. Acad. Sci. U.S.A.* 93, 8072–8077.
- Hansen, K. B., Yi, F., Perszyk, R. E., Furukawa, H., Wollmuth, L. P., Gibb, A. J., et al. (2018). Structure, function, and allosteric modulation of NMDA receptors. *J. Gen. Physiol.* 150, 1081–1105. doi: 10.1085/jgp.201812032
- Hayashi, T., and Su, T. P. (2003). Sigma-1 receptors (sigma(1) binding sites) form raft-like microdomains and target lipid droplets on the endoplasmic reticulum: roles in endoplasmic reticulum lipid compartmentalization and export. *J. Pharmacol. Exp. Ther.* 306, 718–725. doi: 10.1124/jpet.103.051284
- Hayashi, T., and Su, T. P. (2004). Sigma-1 receptor ligands: potential in the treatment of neuropsychiatric disorders. *CNS Drugs* 18, 269–284.
- Hayashi, T., and Su, T. P. (2007). Sigma-1 receptor chaperones at the ER-mitochondrion interface regulate Ca<sup>2+</sup> signaling and cell survival. *Cell* 131, 596–610. doi: 10.1016/j.cell.2007.08.036
- Hille, B. (2001). *Ionic Channels of Excitable Membranes*. Sunderland, MA: Sinauer.
- Johannessen, M., Ramachandran, S., Riemer, L., Ramos-Serrano, A., Ruoho, A. E., and Jackson, M. B. (2009). Voltage-gated sodium channel modulation by sigma-receptors in cardiac myocytes and heterologous systems. *Am. J. Physiol. Cell Physiol.* 296, C1049–C1057. doi: 10.1152/ajpcell.00431.2008
- Jordt, S. E., Tominaga, M., and Julius, D. (2000). Acid potentiation of the capsaicin receptor determined by a key extracellular site. *Proc. Natl. Acad. Sci. U.S.A.* 97, 8134–8139. doi: 10.1073/pnas.100129497
- Kandel, E. R., Schwartz, J. H., Jessell, T. M., and Siegelbaum, S. A. (2012). *Principles of Neural Science*, 5th Edn. New York, NY: McGraw-Hill Education.
- Kinoshita, M., Matsuoka, Y., Suzuki, T., Mirrieles, J., and Yang, J. (2012). Sigma-1 receptor alters the kinetics of Kv1.3 voltage gated potassium channels but not the sensitivity to receptor ligands. *Brain Res.* 1452, 1–9. doi: 10.1016/j.brainres.2012.02.070
- Kourrich, S., Hayashi, T., Chuang, J. Y., Tsai, S. Y., Su, T. P., and Bonci, A. (2013). Dynamic interaction between sigma-1 receptor and Kv1.2 shapes neuronal and behavioral responses to cocaine. *Cell* 152, 236–247. doi: 10.1016/j.cell.2012.12.004
- Kruse, A. (2017). Structural insights into sigma1 function. *Handb. Exp. Pharmacol.* 244, 13–25. doi: 10.1007/164\_2016\_95
- Kwon, S. G., Yoon, S. Y., Roh, D. H., Choi, S. R., Choi, H. S., Moon, J. Y., et al. (2016). Peripheral neurosteroids enhance P2X receptor-induced mechanical allodynia via a sigma-1 receptor-mediated mechanism. *Brain Res. Bull.* 121, 227–232. doi: 10.1016/j.brainresbull.2016.02.012
- Largent, B. L., Wikstrom, H., Gundlach, A. L., and Snyder, S. H. (1987). Structural determinants of sigma receptor affinity. *Mol. Pharmacol.* 32, 772–784.
- Li, D., Zhang, S. Z., Yao, Y. H., Xiang, Y., Ma, X. Y., Wei, X. L., et al. (2017). Sigma-1 receptor agonist increases axon outgrowth of hippocampal neurons via voltage-gated calcium ions channels. *CNS Neurosci. Ther.* 23, 930–939. doi: 10.1111/cns.12768
- Li, H. (2017). TRP channel classification. *Adv. Exp. Med. Biol.* 976, 1–8. doi: 10.1007/978-94-024-1088-4\_1
- Li, Z., Cui, S., Zhang, Z., Zhou, R., Ge, Y., Sokabe, M., et al. (2009). DHEA-neuroprotection and -neurotoxicity after transient cerebral ischemia in rats. *J. Cereb. Blood Flow Metab.* 29, 287–296. doi: 10.1038/jcbfm.2008.118
- Li, Z., Zhou, R., Cui, S., Xie, G., Cai, W., Sokabe, M., et al. (2006). Dehydroepiandrosterone sulfate prevents ischemia-induced impairment of long-term potentiation in rat hippocampal CA1 by up-regulating tyrosine phosphorylation of NMDA receptor. *Neuropharmacology* 51, 958–966. doi: 10.1016/j.neuropharm.2006.06.007
- Mach, R. H., Gage, H. D., Buchheimer, N., Huang, Y., Kuhner, R., Wu, L., et al. (2005). N-[18F]4'-fluorobenzylpiperidin-4-yl-(2-fluorophenyl) acetamide ([18F]FBFPA): a potential fluorine-18 labeled PET radiotracer for imaging sigma-1 receptors in the CNS. *Synapse* 58, 267–274. doi: 10.1002/syn.20207
- Martin, W. R., Eades, C. G., Thompson, J. A., Huppler, R. E., and Gilbert, P. E. (1976). The effects of morphine- and nalorphine- like drugs in the nondependent and morphine-dependent chronic spinal dog. *J. Pharmacol. Exp. Ther.* 197, 517–532.
- Maurice, T., Roman, F. J., and Privat, A. (1996). Modulation by neurosteroids of the in vivo (+)-[3H]SKF-10,047 binding to sigma 1 receptors in the mouse forebrain. *J. Neurosci. Res.* 46, 734–743.
- Maurice, T., Su, T. P., Parish, D. W., Nabeshima, T., and Privat, A. (1994). PRE-084, a sigma selective PCP derivative, attenuates MK-801-induced impairment of learning in mice. *Pharmacol. Biochem. Behav.* 49, 859–869.

- Maurice, T., Su, T. P., and Privat, A. (1998). Sigma1 (sigma 1) receptor agonists and neurosteroids attenuate B25-35-amyloid peptide-induced amnesia in mice through a common mechanism. *Neuroscience* 83, 413–428.
- Mavlyutov, T. A., Duellman, T., Kim, H. T., Epstein, M. L., Leese, C., Davletov, B. A., et al. (2016). Sigma-1 receptor expression in the dorsal root ganglion: Reexamination using a highly specific antibody. *Neuroscience* 331, 148–157. doi: 10.1016/j.neuroscience.2016.06.030
- Mavlyutov, T., Chen, X., Guo, L., and Yang, J. (2018). APEX2- tagging of Sigma 1-receptor indicates subcellular protein topology with cytosolic N-terminus and ER luminal C-terminus. *Protein Cell* 9, 733–737.
- Mishra, A. K., Mavlyutov, T., Singh, D. R., Biener, G., Yang, J., Oliver, J. A., et al. (2015). The sigma-1 receptors are present in monomeric and oligomeric forms in living cells in the presence and absence of ligands. *Biochem. J.* 466, 263–271. doi: 10.1042/BJ20141321
- Monnet, F. P., Debonnel, G., Junien, J. L., and De Montigny, C. (1990). N-methyl-D-aspartate-induced neuronal activation is selectively modulated by sigma receptors. *Eur. J. Pharmacol.* 179, 441–445.
- Morales-Lazaro, S. L., Llorente, I., Sierra-Ramirez, F., Lopez-Romero, A. E., Ortiz-Renteria, M., Serrano-Flores, B., et al. (2016). Inhibition of TRPV1 channels by a naturally occurring omega-9 fatty acid reduces pain and itch. *Nat. Commun.* 7:13092. doi: 10.1038/ncomms13092
- Morales-Lazaro, S. L., Simon, S. A., and Rosenbaum, T. (2013). The role of endogenous molecules in modulating pain through transient receptor potential vanilloid 1 (TRPV1). *J. Physiol.* 591, 3109–3121. doi: 10.1113/jphysiol.2013.251751
- Mueller, B. H. II, Park, Y., Daudt, D. R. III, Ma, H. Y., Akopova, I., Stankowska, D. L., et al. (2013). Sigma-1 receptor stimulation attenuates calcium influx through activated L-type voltage gated calcium channels in purified retinal ganglion cells. *Exp. Eye Res.* 107, 21–31. doi: 10.1016/j.exer.2012.11.002
- Neill, J. D., Johansson, E. D., and Knobil, E. (1969). Patterns of circulating progesterone concentrations during the fertile menstrual cycle and the remainder of gestation in the rhesus monkey. *Endocrinology* 84, 45–48.
- Nieto-Posadas, A., Picazo-Juarez, G., Llorente, I., Jara-Oseguera, A., Morales-Lazaro, S., Escalante-Alcalde, D., et al. (2011). Lysophosphatidic acid directly activates TRPV1 through a C-terminal binding site. *Nat. Chem. Biol.* 8, 78–85. doi: 10.1038/nchembio.712
- Ortega-Roldan, J. L., Ossa, F., and Schnell, J. R. (2013). Characterization of the human sigma-1 receptor chaperone domain structure and binding immunoglobulin protein (BiP) interactions. *J. Biol. Chem.* 288, 21448–21457. doi: 10.1074/jbc.M113.450379
- Ortiz-Renteria, M., Juarez-Contreras, R., Gonzalez-Ramirez, R., Islas, L. D., Sierra-Ramirez, F., Llorente, I., et al. (2018). TRPV1 channels and the progesterone receptor Sig-1R interact to regulate pain. *Proc. Natl. Acad. Sci. U.S.A.* 115, E1657–E1666. doi: 10.1073/pnas.1715972115
- Pabba, M., Wong, A. Y., Ahlskog, N., Hristova, E., Biscaro, D., Nassrallah, W., et al. (2014). NMDA receptors are upregulated and trafficked to the plasma membrane after sigma-1 receptor activation in the rat hippocampus. *J. Neurosci.* 34, 11325–11338. doi: 10.1523/JNEUROSCI.0458-14.2014
- Pal, A., Hajipour, A. R., Fontanilla, D., Ramachandran, S., Chu, U. B., Mavlyutov, T., et al. (2007). Identification of regions of the sigma-1 receptor ligand binding site using a novel photoprobe. *Mol. Pharmacol.* 72, 921–933. doi: 10.1124/mol.107.038307
- Palmer, C. P., Mahen, R., Schnell, E., Djamgoz, M. B., and Aydar, E. (2007). Sigma-1 receptors bind cholesterol and remodel lipid rafts in breast cancer cell lines. *Cancer Res.* 67, 11166–11175.
- Prezzavento, O., Arena, E., Sanchez-Fernandez, C., Turnaturi, R., Parenti, C., Marrazzo, A., et al. (2017). (+)- and (–)-Phenazocine enantiomers: evaluation of their dual opioid agonist/sigma1 antagonist properties and antinociceptive effects. *Eur. J. Med. Chem.* 125, 603–610. doi: 10.1016/j.ejmech.2016.09.077
- Ramsey, I. S., Delling, M., and Clapham, D. E. (2006). An introduction to TRP channels. *Annu. Rev. Physiol.* 68, 619–647. doi: 10.1146/annurev.physiol.68.040204.100431
- Rodriguez-Munoz, M., Onetti, Y., Cortes-Montero, E., Garzon, J., and Sanchez-Blazquez, P. (2018). Cannabidiol enhances morphine antinociception, diminishes NMDA-mediated seizures and reduces stroke damage via the sigma 1 receptor. *Mol. Brain* 11:51.
- Roh, D. H., Yoon, S. Y., Seo, H. S., Kang, S. Y., Moon, J. Y., Song, S., et al. (2010). Sigma-1 receptor-induced increase in murine spinal NR1 phosphorylation is mediated by the PKCalpha and epsilon, but not the PKCzeta, isoforms. *Neurosci. Lett.* 477, 95–99. doi: 10.1016/j.neulet.2010.04.041
- Romero, L., Merlos, M., and Vela, J. M. (2016). Antinociception by sigma-1 receptor antagonists: central and peripheral effects. *Adv. Pharmacol.* 75, 179–215. doi: 10.1016/bs.apha.2015.11.003
- Romero, L., Zamanillo, D., Nadal, X., Sanchez-Arroyos, R., Rivera-Arconada, I., Dordal, A., et al. (2012). Pharmacological properties of S1RA, a new sigma-1 receptor antagonist that inhibits neuropathic pain and activity-induced spinal sensitization. *Br. J. Pharmacol.* 166, 2289–2306. doi: 10.1111/j.1476-5381.2012.01942.x
- Saavedra, J. M., and Axelrod, J. (1972). Psychotomimetic N-methylated tryptamines: formation in brain in vivo and in vitro. *Science* 175, 1365–1366.
- Sabeti, J., Nelson, T. E., Purdy, R. H., and Gruol, D. L. (2007). Steroid pregnenolone sulfate enhances NMDA-receptor-independent long-term potentiation at hippocampal CA1 synapses: role for L-type calcium channels and sigma-receptors. *Hippocampus* 17, 349–369. doi: 10.1002/hipo.20273
- Salazar, H., Llorente, I., Jara-Oseguera, A., Garcia-Villegas, R., Munari, M., Gordon, S. E., et al. (2008). A single N-terminal cysteine in TRPV1 determines activation by pungent compounds from onion and garlic. *Nat. Neurosci.* 11, 255–261. doi: 10.1038/nn2056
- Schmidt, H. R., Zheng, S., Gurbinar, E., Koehl, A., Manglik, A., and Kruse, A. C. (2016). Crystal structure of the human sigma1 receptor. *Nature* 532, 527–530. doi: 10.1038/nature17391
- Sha, S., Qu, W. J., Li, L., Lu, Z. H., Chen, L., Yu, W. F., et al. (2013). Sigma-1 receptor knockout impairs neurogenesis in dentate gyrus of adult hippocampus via down-regulation of NMDA receptors. *CNS Neurosci. Ther.* 19, 705–713. doi: 10.1111/cns.12129
- Su, T. P. (1982). Evidence for sigma opioid receptor: binding of [3H]SKF-10047 to etorphine-inaccessible sites in guinea-pig brain. *J. Pharmacol. Exp. Ther.* 223, 284–290.
- Su, T. P., London, E. D., and Jaffe, J. H. (1988). Steroid binding at sigma receptors suggests a link between endocrine, nervous, and immune systems. *Science* 240, 219–221.
- Tam, S. W. (1983). Naloxone-inaccessible sigma receptor in rat central nervous system. *Proc. Natl. Acad. Sci. U.S.A.* 80, 6703–6707.
- Tam, S. W., and Cook, L. (1984). Sigma opiates and certain antipsychotic drugs mutually inhibit (+)-[3H] SKF 10,047 and [3H]haloperidol binding in guinea pig brain membranes. *Proc. Natl. Acad. Sci. U.S.A.* 81, 5618–5621.
- Tchedre, K. T., Huang, R. Q., Dibas, A., Krishnamoorthy, R. R., Dillon, G. H., and Yorio, T. (2008). Sigma-1 receptor regulation of voltage-gated calcium channels involves a direct interaction. *Invest. Ophthalmol. Vis. Sci.* 49, 4993–5002. doi: 10.1167/iovs.08-1867
- Tsai, S., Hayashi, T., Mori, T., and Su, T. P. (2009). Sigma-1 receptor chaperones and diseases. *Cent. Nerv. Syst. Agents Med. Chem.* 9, 184–189.
- Veeraman, C. C., Wilde, A. A., and Lodder, E. M. (2015). The cardiac sodium channel gene SCN5A and its gene product Nav1.5: role in physiology and pathophysiology. *Gene* 573, 177–187. doi: 10.1016/j.gene.2015.08.062
- Waterhouse, R. N., Chang, R. C., Atuehene, N., and Collier, T. L. (2007). In vitro and in vivo binding of neuroactive steroids to the sigma-1 receptor as measured with the positron emission tomography radioligand [18F]FPS. *Synapse* 61, 540–546. doi: 10.1002/syn.20369
- Wu, L., Nishiyama, K., Hollyfield, J. G., and Wang, Q. (2002). Localization of Nav1.5 sodium channel protein in the mouse brain. *Neuroreport* 13, 2547–2551. doi: 10.1097/01.wnr.0000052322.62862.a5
- Wu, Z. Y., Yu, D. J., Soong, T. W., Dawe, G. S., and Bian, J. S. (2011). Progesterone impairs human ether-a-go-go-related gene (HERG) trafficking by disruption of intracellular cholesterol homeostasis. *J. Biol. Chem.* 286, 22186–22194. doi: 10.1074/jbc.M110.198853
- Xu, Q., Ji, X. F., Chi, T. Y., Liu, P., Jin, G., Chen, L., et al. (2017). Sigma-1 receptor in brain ischemia/reperfusion: possible role in the NR2A-induced pathway to regulate brain-derived neurotrophic factor. *J. Neurol. Sci.* 376, 166–175. doi: 10.1016/j.jns.2017.03.027
- Yabuki, Y., Shinoda, Y., Izumi, H., Ikuno, T., Shioda, N., and Fukunaga, K. (2015). Dehydroepiandrosterone administration improves memory deficits following transient brain ischemia through sigma-1 receptor stimulation. *Brain Res.* 1622, 102–113. doi: 10.1016/j.brainres.2015.05.006
- Zhang, H., and Cuevas, J. (2002). Sigma receptors inhibit high-voltage-activated calcium channels in rat sympathetic and parasympathetic neurons. *J. Neurophysiol.* 87, 2867–2879. doi: 10.1152/jn.2002.87.6.2867

- Zhang, K., Zhao, Z., Lan, L., Wei, X., Wang, L., Liu, X., et al. (2017). Sigma-1 receptor plays a negative modulation on N-type calcium channel. *Front. Pharmacol.* 8:302. doi: 10.3389/fphar.2017.00302
- Zhu, S., Wang, C., Han, Y., Song, C., Hu, X., and Liu, Y. (2015). Sigma-1 receptor antagonist BD1047 reduces mechanical allodynia in a rat model of bone cancer pain through the inhibition of Spinal NR1 phosphorylation and microglia activation. *Mediators Inflamm.* 2015:265056. doi: 10.1155/2015/265056
- Zou, L. B., Yamada, K., Sasa, M., Nakata, Y., and Nabeshima, T. (2000). Effects of sigma(1) receptor agonist SA4503 and neuroactive steroids on performance in a radial arm maze task in rats. *Neuropharmacology* 39, 1617–1627.

**Conflict of Interest Statement:** The authors declare that the research was conducted in the absence of any commercial or financial relationships that could be construed as a potential conflict of interest.

Copyright © 2019 Morales-Lázaro, González-Ramírez and Rosenbaum. This is an open-access article distributed under the terms of the Creative Commons Attribution License (CC BY). The use, distribution or reproduction in other forums is permitted, provided the original author(s) and the copyright owner(s) are credited and that the original publication in this journal is cited, in accordance with accepted academic practice. No use, distribution or reproduction is permitted which does not comply with these terms.



# Supraspinal and Peripheral, but Not Intrathecal, $\sigma_1$ R Blockade by S1RA Enhances Morphine Antinociception

Alba Vidal-Torres, Begoña Fernández-Pastor, Alicia Carceller, José Miguel Vela, Manuel Merlos\* and Daniel Zamanillo\*

Drug Discovery and Preclinical Development, Esteve Pharmaceuticals, Parc Científic Barcelona, Barcelona, Spain

## OPEN ACCESS

### Edited by:

Stephen Timothy Safrany,  
Royal College of Surgeons in Ireland,  
Bahrain

### Reviewed by:

Hsiang-en Wu Wu,  
National Institute on Drug Abuse  
(NIDA), United States  
Mahmoud Al-Khrasani,  
Semmelweis University, Hungary

### \*Correspondence:

Manuel Merlos  
mmerlos@esteva.com  
Daniel Zamanillo  
dzamanillo@esteva.com

### Specialty section:

This article was submitted to  
Experimental Pharmacology  
and Drug Discovery,  
a section of the journal  
Frontiers in Pharmacology

**Received:** 23 January 2019

**Accepted:** 03 April 2019

**Published:** 24 April 2019

### Citation:

Vidal-Torres A,  
Fernández-Pastor B, Carceller A,  
Vela JM, Merlos M and Zamanillo D  
(2019) Supraspinal and Peripheral,  
but Not Intrathecal,  $\sigma_1$ R Blockade by  
S1RA Enhances Morphine  
Antinociception.  
Front. Pharmacol. 10:422.  
doi: 10.3389/fphar.2019.00422

Sigma-1 receptor ( $\sigma_1$ R) antagonism increases the effects of morphine on acute nociceptive pain. S1RA (E-52862) is a selective  $\sigma_1$ R antagonist widely used to study the role of  $\sigma_1$ Rs. S1RA alone exerted antinociceptive effect in the formalin test in rats and increased noradrenaline levels in the spinal cord, thus accounting for its antinociceptive effect. Conversely, while systemic S1RA failed to elicit antinociceptive effect by itself in the tail-flick test in mice, it did potentiate the antinociceptive effect of opioids in this acute pain model. The present study aimed to investigate the site of action and the involvement of spinal noradrenaline on the potentiation of opioid antinociception by S1RA on acute thermal nociception using the tail-flick test in rats. Local administration was performed after intrathecal catheterization or intracerebroventricular and rostroventral medullar (RVM) cannulae implantation. Noradrenaline levels in the spinal cord were evaluated using the concentric microdialysis technique in awake, freely-moving rats. Systemic or supraspinal administration of S1RA alone, while having no effect on antinociception, enhanced the effect of morphine in rats. However, spinal S1RA administration did not potentiate the antinociceptive effect of morphine. Additionally, the peripherally restricted opioid agonist looperamide was devoid of antinociceptive effect but produced antinociception when combined with S1RA. Neurochemical studies revealed that noradrenaline levels in the dorsal horn of the spinal cord were not increased at doses exerting potentiation of the antinociceptive effect of the opioid. In conclusion, the site of action of  $\sigma_1$ R for opioid modulation on acute thermal nociception is located at the peripheral and supraspinal levels, and the opioid-potentiating effect is independent of the spinal noradrenaline increase produced by S1RA.

**Keywords:** sigma-1 receptor, S1RA, morphine, nociceptive pain, antinociceptive effect, concentric microdialysis

## INTRODUCTION

The sigma-1 receptor ( $\sigma_1$ R) has been described as the first ligand-regulated molecular chaperone located at the endoplasmic reticulum and plasma membranes whose activity is regulated in an agonist-antagonist manner. The  $\sigma_1$ R is expressed in key areas for pain control and there is cumulative evidence supporting an involvement of the  $\sigma_1$ R mainly in two kinds of pain conditions: (1) those involving sensitization, e.g., after sensitization with capsaicin or formalin or following nerve injury where  $\sigma_1$ R antagonists by themselves inhibit pain behaviors in the absence of opioids



(Romero et al., 2012; Vidal-Torres et al., 2014; Gris et al., 2016); and (2) in acute pain conditions after the application of mechanical (paw pressure test) or thermal (tail-flick and hot plate tests) nociceptive stimuli, where  $\sigma_1$ R antagonists by themselves fail to modify the nociceptive thresholds but enhance opioid-induced antinociception (Sánchez-Fernández et al., 2013; Vidal-Torres et al., 2013; Merlos et al., 2017; Sánchez-Fernández et al., 2017).

S1RA (also known as MR309 or E-52862) is a  $\sigma_1$ R antagonist with high affinity for  $\sigma_1$ R, good  $\sigma_1/\sigma_2$  selectivity ratio ( $>550$ ), and selectivity against a panel of 170 receptors, enzymes, transporters, and ion channels (Romero et al., 2012). We previously reported that co-administration of S1RA with several opioids used in clinics results in an enhancement of the antinociception but not of undesired opioid-induced phenomena such as the development of analgesic tolerance, physical dependence, or inhibition of gastrointestinal transit. Moreover, S1RA restored morphine antinociception in tolerant mice and reversed the reward effects of morphine (Vidal-Torres et al., 2013). S1RA has been recently developed as a first-in-class analgesic drug. It has shown good safety and tolerability profiles after single and multiple doses in healthy humans in phase I clinical trials (Abadias et al., 2013); S1RA has also shown promising results in phase II clinical trial for neuropathic pain (Bruna et al., 2018).

Regarding the site of action, recent studies demonstrated that S1RA exerts by itself an antinociceptive effect after spinal, supraspinal and peripheral administration in the formalin-induced pain model in rats (Vidal-Torres et al., 2014), and also after peripheral administration in carrageenan-induced pain models in mice (Gris et al., 2014; Tejada et al., 2014; Gris et al., 2015). Recent information advocates that modulation by  $\sigma_1$ R ligands of opioid antinociception occurs at the peripheral level, as shown in the paw pressure mechanical acute model (Sánchez-Fernández et al., 2014; Tejada et al., 2018). In contrast, available information also shows that this modulation on opioid antinociception occurs at the supraspinal level in the acute thermal nociception test in mice (Mei and Pasternak, 2002; Mei and Pasternak, 2007).

At the neurochemical level, S1RA increased noradrenaline (NA) levels in the dorsal horn of the spinal cord after intraplantar injection of formalin. Accordingly, intrathecal pre-treatment with the selective  $\alpha_2$ -adrenoceptor ( $\alpha_2$ -AR) antagonist idazoxan blocked the antinociceptive effect of S1RA (Vidal-Torres et al., 2014). No studies addressing this issue are available in relation to the opioid potentiating effect.

To gain further insight into the mechanisms underlying the modulatory effect of  $\sigma_1$ R on opioid antinociception, we selected S1RA as a tool compound because it is one of the most characterized selective  $\sigma_1$ R antagonists and the only one that has been evaluated in clinical trials with an intended indication for pain relief. S1RA efficacy in combination with morphine was studied by using different routes of administration in the tail-flick acute thermal nociceptive pain model in rats. The possible involvement of spinal NA in the potentiating effect was also investigated by using the concentric microdialysis technique in awake, freely-moving rats.

## MATERIALS AND METHODS

### Animals

All animal husbandry and experimental procedures complied with the European guidelines for the protection of animals used for experimental and other scientific purposes (Council Directive of 22 September 2010, 2010/63/EU), and were approved by the local Ethics Committee. The results are reported in accordance with the ARRIVE guidelines for reporting experiments involving animals (McGrath et al., 2010). Male Wistar rats weighing 230–330 g (Charles River, France) were used. Naïve animals were housed in groups of four and housed individually after surgery. They had free access to food and water and were kept in controlled laboratory conditions with temperature at  $21 \pm 1^\circ\text{C}$  and a light-dark cycle of 12 h (lights on at 7:00 a.m.). Experiments were carried out in a soundproof, air-regulated experimental room during the light phase. Each animal was used in a single experiment only.

### Drugs and Drug Administration

Morphine hydrochloride was obtained from the Spanish Drug Agency (Agencia Española de Medicamentos y Productos Sanitarios, Area Estupefacientes (Madrid, Spain)). Loperamide hydrochloride and naloxone-methiodide were obtained from Sigma-Aldrich. 4- (2- (5- methyl-1- (naphthalen-2- yl)- 1H-pyrazol-3- yloxy) ethyl) morpholine hydrochloride (S1RA; E-52862) (Díaz et al., 2012) was synthesized at Esteve Pharmaceuticals (Barcelona, Spain). Morphine (2.5, 5, and 10 mg/kg), naloxone-methiodide (4 mg/kg) and S1RA (10, 20, 40, and 80 mg/kg) were dissolved in 0.5% hydroxypropyl-methylcellulose (HPMC) (Sigma-Aldrich), and loperamide (1, 2, and 4 mg/kg) was dissolved in HPMC containing 0.5% Tween 80 and was administered intraperitoneally (i.p.) at 2 mL/kg. Naloxone-methiodide was administered 5 min prior to loperamide and S1RA. Baseline responses were always obtained prior to treatment administration. For intrathecal (i.t., volume: 10  $\mu\text{L}$ ), intracerebroventricular (i.c.v., volume: 10  $\mu\text{L}$  bilaterally) and rostroventral medulla (RVM, volume: 1  $\mu\text{L}$ ) administrations, S1RA (80, 160, or 320  $\mu\text{g}$ ) was dissolved in cerebrospinal fluid (CSF, Perfusion Fluid CNS, CMA) and co-administered with systemic morphine (i.p., 2.5 or 5 mg/kg). I.t. and i.c.v. S1RA doses were selected based on a previous study where S1RA showed antinociceptive effects in the formalin-induced pain model (Vidal-Torres et al., 2014). Doses are expressed as the salt forms of the drugs.

### Antinociceptive Assay (Tail-Flick Test)

To evaluate the acute antinociceptive effects of the drugs and their combination, the nociceptive responses to acute thermal (heat) stimulation were assessed by the tail-flick test as previously described (D'Amour and Smith, 1941). Briefly, animals were gently restrained with a cloth to orient their tails toward the source of heat of the tail-flick apparatus (Panlab, Barcelona, Spain). A noxious beam of light was focused on the tail about 5 cm from the tip, and the tail-flick latency (TFL, latency to remove the tail as of the onset of the radiant heat stimulus)

was recorded automatically to the nearest 0.1 s. The intensity of the radiant heat source was adjusted to yield baseline latencies between 2 and 4 s and a cut-off time was set at 10 s to avoid heat-related tail damage.

The effect of treatments on TFL was calculated by the formula  $\% \text{Antinociception} = ((\text{Individual test latency} - \text{Individual baseline latency}) / (\text{Cut-off latency} - \text{Individual baseline latency})) \times 100$ . When appropriate, the ED<sub>50</sub> value was estimated from the dose-response curve.

## Intrathecal Catheterization and Administration

Catheterization of the spinal subarachnoid space was conducted as previously described (Storkson et al., 1996; Pogatzki et al., 2000) with i.t. catheters (No. 0007740, Alzet) under anaesthesia with pentobarbital (i.p., 60 mg/kg, 2 mL/kg). The lower dorsal pelvic area corresponding to vertebral L3-S3 was shaved and prepared with povidone-iodine. A midline longitudinal skin incision was made (2–3 cm) and the space between the lumbar vertebrae L5 and L6 was punctured with a 22G hypodermic needle. Tail-flick or hind paw retraction indicated an i.t. position. A 28G PU catheter (10 cm length, 0.36 mm OD; 0.18 mm ID, Alzet) reinforced with a teflon-coated stainless steel stylet was advanced cranially 4 cm through the needle to reach the L4-L5 medullar area. The needle and the stylet were removed and the catheter was withdrawn so that 5 cm extended outside of the lumbar muscles. Superglue-3 gel (Loctite®) was used to fix the catheter to the fascia. The distal end of the 28G PU catheter was connected with super glue to an 8 cm tube (0.84 mm OD; 0.36 mm ID) ended with an Alzet connection (1.02 mm OD; 0.61 mm ID). The catheter was tunneled under the skin to the cervical region, flushed with CSF and sealed with a cautery pen. The skin was then closed and animals were allowed to recover in individual cages for 7 days. Catheterized rats had no detectable motor deficits. S1RA or CSF were injected i.t. with a 50 µL Hamilton syringe at a volume of 10 µL over a period of 20 s, followed by 20 µL of CSF to flush the catheter. At the end of the experiment, the animals were killed by CO<sub>2</sub> inhalation, 10 µL of fast green was injected i.t., and the level and side position of the catheter tip were confirmed. Epidural catheterizations (15%) were discarded and only i.t. catheters were considered.

## Intracerebroventricular and RVM Cannulae Implantation and Administration

Bilateral i.c.v. administration guide cannulae (26 GA, 0.46 mm OD, 0.24 mm ID, 5 mm long, Plastics One) or a RVM administration guide cannulae (26 GA 20 mm, C315G/SPC, Plastics One) were stereotactically implanted in rats anaesthetized with pentobarbital (i.p., 60 mg/kg, 2 mL/kg). With the incisor bar set at 0 or –5 mm, the coordinates from bregma were –0.8 AP, –1.6 L, and –3.5 DV; or –10.8 AP, 0.0 L, and –4.3 DV (from the dura mater) for i.c.v. and RVM, respectively. Stainless steel guide cannulae were secured to the skull with two anchor screws and dental acrylic. Animals were housed in individual

cages, disinfected daily with povidone-iodine and allowed 6–7 days to recover from surgery. In RVM-implanted rats, 18 h prior to the test, after removing the dummy cannulae (Plastics One), an internal cannula (33 GA, C315IA/SP, Plastics One) extending 6 mm past the guide cannula was introduced under isoflurane anaesthesia. S1RA or CSF were injected i.c.v. with a 10 µL Hamilton syringe at a volume of 5 µL (per cannula) over a period of 20 s, followed by 1.8 µL of CSF to flush the cannula. S1RA or CSF were injected RVM with a 5 µL Hamilton syringe at a volume of 1 µL over a period of 20 s, followed by 1.8 µL of CSF to flush the cannula. After experimental testing, the animals were killed by CO<sub>2</sub> inhalation and fast green was injected for cannula placement examination. Only animals with correct cannula placements (100% in i.c.v. implantation and 90% in RVM implantation) were included in data analyses.

## Microdialysis Surgical Procedures/Microdialysis Probe Implantation in Spinal Cord

Rats were anaesthetized with chloral hydrate (i.p., 440 mg/kg) and placed on a David Kopf stereotaxic frame. The dorsal zone corresponding to the thoracic vertebra (Th13) was shaved and prepared with povidone-iodine. An incision was made along the dorsal midline such that the muscle overlaying the Th13 and the first lumbar vertebra (L1) could be removed. Th13 was then immobilized on the horizontal plane by using a transverse process clamp and a burr hole was made in the dorsal surface. The exposed dura mater was then carefully opened and a microdialysis probe of concentric design (CMA/11) was inserted into the spinal cord at an angle of 45° from the vertical plane. The microdialysis probes (exposed tip 2.0 mm × 0.24 mm) were implanted into the medial DH of the L4 lumbar region of the spinal cord. The probe was fixed by applying superglue-3 gel (Loctite®) and dental cement around the probe and by a stainless steel anchorage screw located in the Th13 vertebra. The skin was then closed and rats were allowed to recover overnight, one per cage, with free access to food and water. Only implanted rats showing normal behavior after the recovery period (no walking dysfunction, normal weakened extension withdrawal reflex of the hind limb, no reduced toe spread, normal food and water intake, no piloerection or apparent stress signals) were considered in the study, and were used only once. At the end of the experiment, the animals were killed by CO<sub>2</sub> inhalation and spinal cords were dissected out for histological examination to verify that microdialysis probes were correctly implanted. Only animals with correct probe placements (90%) were included in data analyses.

## Sample Collection in Awake Rats

Around 20 h after probe implantation, rats were placed individually in a system for freely moving animals. The dialysis probes were connected to a CMA microdialysis system, then perfused with CSF perfusion fluid at 1.5 µL min<sup>-1</sup> flow rate, and consecutive samples were collected into vials every 15 min. The probe was perfused for 1 h for stabilization of baseline NA release. This was followed by a 90 min period for baseline

sample collection. Animals received systemic (i.p.) morphine (5 and 10 mg/kg) or vehicle + systemic (i.p.) S1RA (40 and 80 mg/kg) or vehicle and were perfused for 180 min. Dialysis sampling was performed separately in groups of rats other than those used for tail-flick assessment of operated animals in order to avoid excessive rat handling likely to interfere with NA level determination.

## Analytical Procedures

Dialysate samples were assayed for NA content by reversed-phase high-performance liquid chromatography (HPLC) coupled with electrochemical detection. The mobile phase was 75 mM phosphate buffer (pH 6) containing 0.35 mM octanesulfonic acid and 0.2 mM ethylenediamine tetra-acetic acid (EDTA) with 25% of methanol. Separation was carried out with a Gemini C18 110A (3  $\mu$ m) column, connected to a Waters 2465 electrochemical detector at 35°C and operated at a flow rate of 0.2 mL/min. Detection was performed by oxidation at 0.45 V. Values were not corrected for *in vitro* recovery through the dialysis probe.

## Statistical Analysis

Data were expressed as means  $\pm$  S.E.M. The mean values of four dialysate samples obtained before treatment administration were considered as the 100% baseline values. The extracellular NA concentration of dialysate samples collected during an experiment were normalized as percentage of the baseline values. Treatment groups were compared with appropriate control groups using one-way or two-way ANOVA analysis of variance followed by the Newman-Keuls multiple comparison test or followed by the Bonferroni *post hoc* test, respectively, as appropriate. ED<sub>50</sub> values were determined using a four-parameter logistic equation (sigmoidal dose-response curve, variable slope) with the top or bottom fixed (DeLean et al., 1978). The ED<sub>50</sub> was defined as the dose that produced 50% of the maximum possible effect. Drug effects were expressed as area under the curve (AUC) within the same subject, as calculated using the linear trapezoidal method and were compared to vehicle using one-way ANOVA followed by Newman-Keuls multiple comparison test. In all cases the level of statistical significance was set at  $P < 0.05$ . ED<sub>50</sub> values with 95% confidence intervals (CI), calculation of the area under the curve (AUC) and statistical analyses were computed using GraphPad Prism version 5 software (San Diego, CA, United States).

## RESULTS

### Systemic S1RA Enhanced the Antinociceptive Effect of Systemic Morphine in the Tail-Flick Test in Rats

We first investigated the antinociceptive effects elicited by the systemic co-administration of an opioid with a  $\sigma_1$ R antagonist in the tail-flick test in rats. To this purpose, tail-flick latencies were assessed over time following co-administration of morphine (2.5 mg/kg, i.p.) + S1RA (40 mg/kg, i.p.) (Figure 1A). Two-way ANOVA (time  $\times$  treatment) revealed a treatment effect

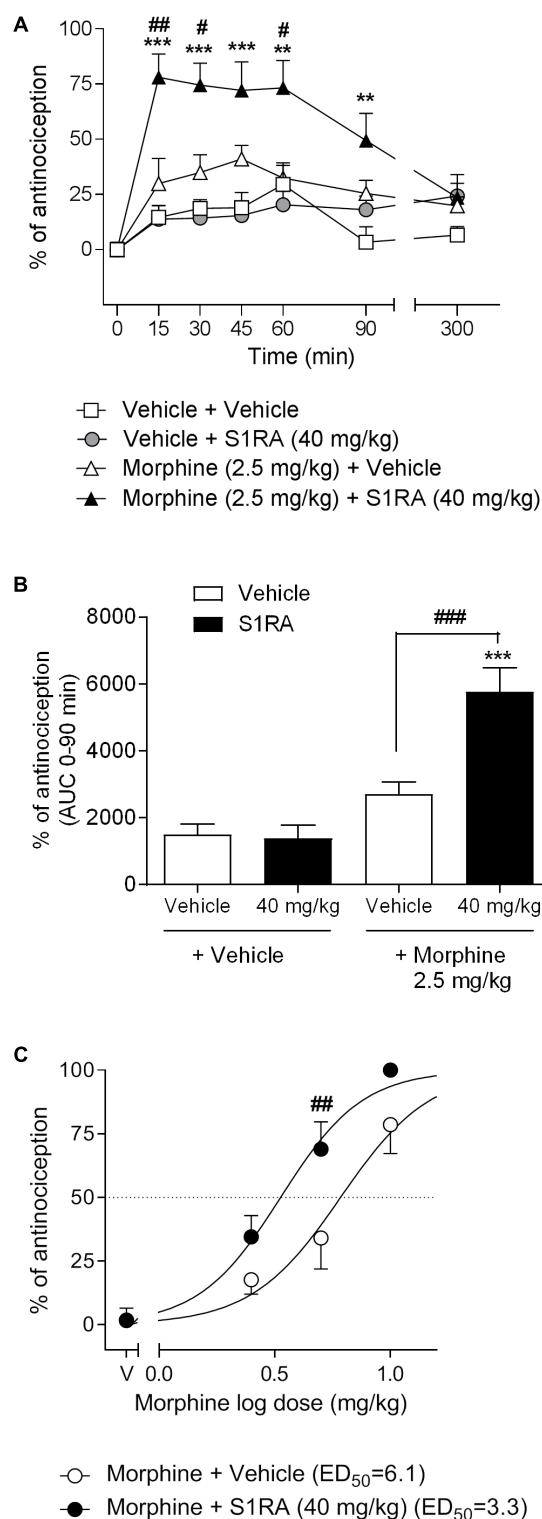


**FIGURE 1 |** Effects of systemic co-administration of S1RA with morphine in the tail-flick test in rats. **(A)** Rats received morphine (2.5 mg/kg, i.p.), S1RA (40 mg/kg, i.p.), their combination or respective vehicles, and the tail-flick latency was evaluated over time. Note that the enhancement of the antinociceptive effect was clearly observed 15 min post-treatment and

(Continued)



**FIGURE 1 | Continued**

lasted up to 90 min post-treatment. Each point and vertical line represents the mean  $\pm$  S.E.M. percentage of antinociception ( $n = 9$ –10 per group). Two-way ANOVA (time  $\times$  treatment) of 0–300 min interval evaluation was performed.  $^{**}P < 0.01$ ,  $^{***}P < 0.001$  vs. respective baseline values;  $^{\#}P < 0.05$ ,  $^{\#\#}P < 0.01$  vs. morphine group (Bonferroni *post hoc* test). **(B)** AUC of 0–90 min interval evaluation.  $^{***}P < 0.001$  vs. vehicle+vehicle group;  $^{***}P < 0.001$  vs. morphine+vehicle group (Newman–Keuls multiple comparison test *post one-way* ANOVA). **(C)** Rats received increasing doses of morphine (i.p.) or vehicle + a fixed dose of S1RA (40 mg/kg, i.p.) or vehicle, and the tail-flick latency was evaluated 30 min later. Note that S1RA increased the morphine antinociceptive effect. Each point and vertical line represents the mean  $\pm$  S.E.M. percentage of antinociception ( $n = 8$ –10 per group). Two-way ANOVA (dose  $\times$  treatment) was performed.  $^{**}P < 0.01$  vs. morphine 5 mg/kg+vehicle group (Bonferroni *post hoc* test).

$F(3, 34) = 17.37$ ,  $P < 0.001$ , 0–300 min. In vehicle + vehicle treated rats, the tail-flick latencies did not change significantly from the baseline values over the entire period of time (300 min). Morphine (2.5 mg/kg, i.p.) exerted a discrete, non-significant antinociceptive effect during the first 60 min post-treatment whereas S1RA (40 mg/kg, i.p.) was devoid of antinociceptive effect at any evaluated timepoint. Co-administration of S1RA with morphine produced a significant increase in the tail-flick latency over time, with maximum effect at 15–60 min post-treatment and return to baseline 300 min post-treatment (**Figure 1A**). AUC analysis revealed a significant enhancement of antinociception ( $P < 0.001$ ) in the co-treated group as compared to the morphine-treated group (**Figure 1B**).

To further assess the potentiation of the antinociceptive effect, we next combined different doses of morphine (2.5, 5, and 10 mg/kg, i.p.) with a fixed dose of S1RA (40 mg/kg, i.p.) and tail-flick latencies were evaluated 30 min after co-administration. The combination induced a shift to the left of the dose-response curve of morphine, resulting in an enhancement of the antinociceptive potency of the opioid by a factor of 1.8. The  $ED_{50}$ 's were 6.1 (95% CI, 4.8–7.8) and 3.3 (95% CI, 2.7–4.1) mg/kg for morphine alone and morphine plus 40 mg/kg of S1RA, respectively (**Figure 1C**). Two-way ANOVA (dose  $\times$  treatment) revealed a treatment effect  $F(1, 36) = 12.94$ ,  $P < 0.001$ . The morphine dose that produced a higher enhancement by S1RA was 5 mg/kg and was therefore the first dose selected for the next set of experiments.

### S1RA and Morphine Systemically Co-administered Failed to Modify Spinal Noradrenaline (NA) Levels

We previously reported that S1RA (80 mg/kg) increased NA levels in the dorsal horn of the spinal cord and that this effect correlated well with the antinociceptive effect of S1RA in the formalin-induced pain model (Vidal-Torres et al., 2014). Here we address whether S1RA enhancement of opioid antinociception is associated with a potentiation of the increase in NA spinal levels (studied in naïve or in implanted animals, respectively).

Two-way ANOVA (time  $\times$  treatment) revealed a treatment effect  $F(2, 10) = 12.14$ ,  $P < 0.01$ , –45–180 min (**Figure 2A**). Vehicle-treated animals showed stable NA spinal levels. NA spinal levels increased following i.p. administration of S1RA at

80 mg/kg (171% vs. baseline (100%) was found 30 min post-administration), but not at 40 mg/kg (**Figure 2A**). However, both doses of S1RA were devoid of antinociceptive effects at 30 min post-administration when administered alone (**Figure 2B**). Two-way ANOVA (time  $\times$  treatment) revealed a treatment effect  $F(2, 11) = 7.84$ ,  $P < 0.01$ , –45–180 min (**Figure 2C**). However, 30 min after i.p. administration of 5 and 10 mg/kg of morphine, NA spinal levels did not significantly differ from baseline values (114 and 115%, respectively), although significantly increased levels were attained 60 min post-administration (**Figure 2C**). Interestingly, both morphine doses resulted in an antinociceptive effect ( $P < 0.05$  and  $P < 0.001$ , respectively) 30 min post-administration (**Figure 2D**). Two-way ANOVA (time  $\times$  treatment) revealed that there was no treatment effect  $F(3, 17) = 2.68$ ,  $P$  ns, –45–180 min (**Figure 2E**). The combination of S1RA (40 mg/kg) and morphine (5 mg/kg) enhanced antinociception (**Figure 2F**), but did not significantly modify extracellular NA levels vs. baseline (133%) (**Figure 2E**).

### Intrathecal S1RA Failed to Enhance the Antinociceptive Effect of Systemic Morphine in the Tail-Flick Test in Rats

We have previously shown that i.t. administration of 160 and 320  $\mu$ g of S1RA dose-dependently reduced formalin-induced flinching but not licking/lifting behaviors. In order to investigate whether spinal  $\sigma_1$ R antagonism is involved in the modulation of opioid antinociception, rats were i.t. administered with S1RA in combination with systemic morphine. Two-way ANOVA (time  $\times$  treatment) revealed a treatment effect  $F(3, 31) = 3.40$ ,  $P < 0.05$ , 0–120 min (**Figure 3A**). S1RA administered alone by i.t. route at 160 and 320  $\mu$ g was inactive in the tail-flick test. Morphine (5 mg/kg, i.p.) exerted significant antinociceptive effects ( $P < 0.001$ ) 30 min post-administration, but S1RA (320  $\mu$ g) co-administered i.t. was unable to increase its analgesic effect (**Figure 3A**). Two-way ANOVA (time  $\times$  treatment) revealed no treatment effect  $F(3, 24) = 0.81$ ,  $P$  ns, 0–120 min (**Figure 3C**). A lower morphine dose (2.5 mg/kg) was also not enhanced by S1RA (160  $\mu$ g) (**Figure 3C**). AUC analysis confirmed no enhancement of morphine antinociception in co-treated vs. morphine-treated groups (**Figures 3B,D**).

### Intracerebroventricular but Not Rostroventral Medullar S1RA Enhanced the Antinociceptive Effect of Systemic Morphine in the Tail-Flick Test in Rats

We had previously shown that 320  $\mu$ g of i.c.v. S1RA significantly reduced formalin-induced pain behaviors. Here we assessed whether supraspinal  $\sigma_1$ R antagonism potentiates morphine antinociception. Two-way ANOVA (time  $\times$  treatment) revealed a treatment effect  $F(3, 30) = 6.05$ ,  $P < 0.01$ , 0–120 min. S1RA (320  $\mu$ g) administered i.c.v. and systemic morphine (5 mg/kg, i.p.) did not significantly modify tail-flick latencies in i.c.v.-implanted rats when both compounds were administered alone. However, their combination resulted in a significant enhancement ( $P < 0.05$ ) of the antinociception at 15 and 30 min post-administration (**Figure 4A**). AUC analysis revealed

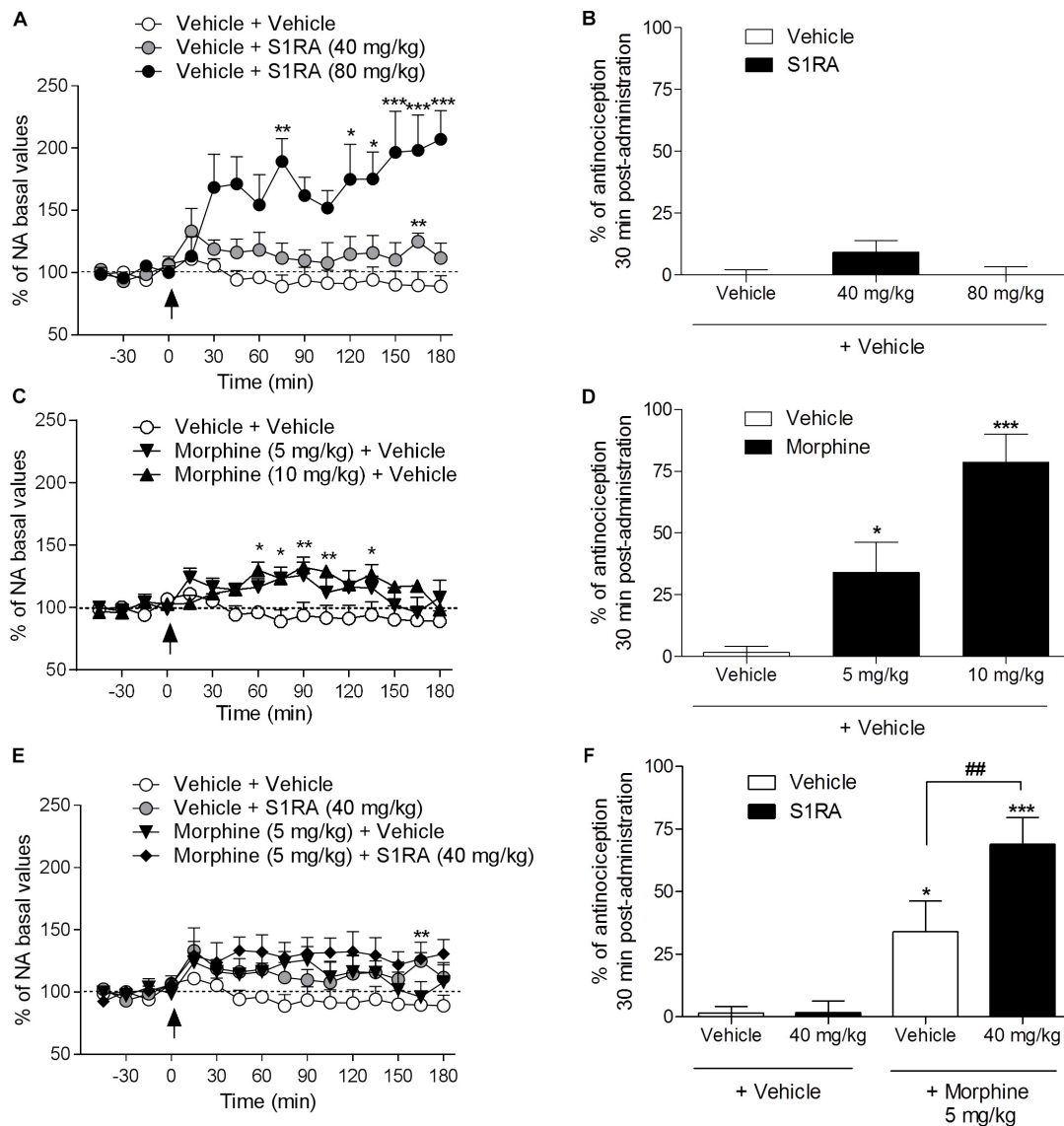


**FIGURE 2 |** Behavioral antinociceptive effects and noradrenaline (NA) levels in the dorsal horn of the spinal cord following systemic S1RA, morphine and their combination in rats. Implanted rats received i.p. S1RA (40 and 80 mg/kg) or vehicle (**A**), i.p. morphine (5 and 10 mg/kg) or vehicle (**C**), or the combination of morphine (5 mg/kg) and S1RA (40 mg/kg) (**E**), and were perfused for 180 min to evaluate the effect on extracellular concentration of NA in the dorsal horn of the spinal cord. Two-way ANOVA (time  $\times$  treatment) of  $-45$ – $180$  min interval evaluation was performed. Dots are means  $\pm$  S.E.M. values and are expressed as percentages of the respective baseline values ( $n = 4$ – $8$  per group).  $*P < 0.05$ ,  $**P < 0.01$ ,  $***P < 0.001$  vs. respective baseline value (Bonferroni *post hoc* test). Naïve rats received the same treatments and 30 min later tail-flick latencies were evaluated and the percentage of antinociception elicited by treatments was calculated (**B,D,F**). Note that S1RA at 80 mg/kg increased NA levels (**A**) but failed to produce an antinociceptive effect (**B**). In contrast, 5 and 10 mg/kg of morphine, although they did not change NA levels 30 min post-administration (**C**), resulted in antinociception (**D**). The combination of S1RA (40 mg/kg) and morphine (5 mg/kg) failed to significantly modify NA values (**E**) but enhanced antinociception (**F**). Each point and vertical line represents the mean  $\pm$  S.E.M. percentage of antinociception ( $n = 8$ – $10$  per group).  $*P < 0.05$ ,  $***P < 0.001$  vs. respective vehicle+vehicle group;  $##P < 0.01$  vs. vehicle+morphine 5 mg/kg group (Newman-Keuls multiple comparison test *post one-way ANOVA*).

a significant enhancement of antinociception ( $P < 0.01$ ) in co-treated vs. morphine-treated groups (**Figure 4B**).

RVM was reported to be a key area for opioid modulation by some  $\sigma_1$ R ligands (Mei and Pasternak, 2007). To further explore the supraspinal site for  $\sigma_1$ R-mediated potentiation of opioid antinociception, we investigated the involvement of the RVM in such a potentiation. To this purpose, intra-RVM

administration of S1RA (80  $\mu$ g) was combined with systemic morphine (2.5 and 5 mg/kg, i.p.). Two-way ANOVA (time  $\times$  treatment) revealed a treatment effect  $F(3, 23) = 4.45$ ,  $P < 0.05$ , 0–120 min only in **Figure 5A**. RVM microinjection of S1RA (80  $\mu$ g) alone exerted a significant pronociceptive effect in the tail-flick test at 15 and 30 min post-administration. Morphine at 2.5 mg/kg i.p. was devoid of effect (**Figure 5C**) but exhibited a



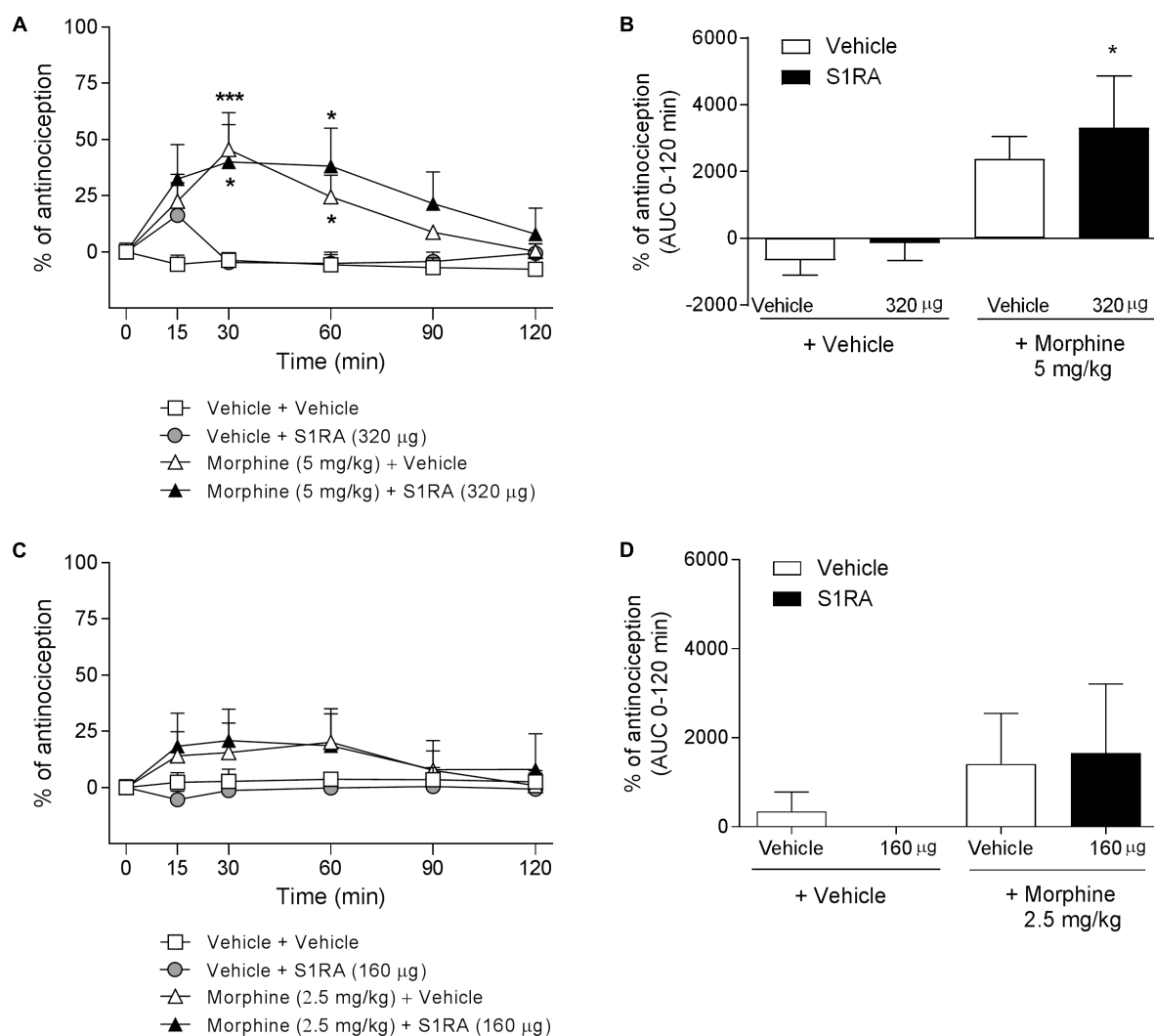


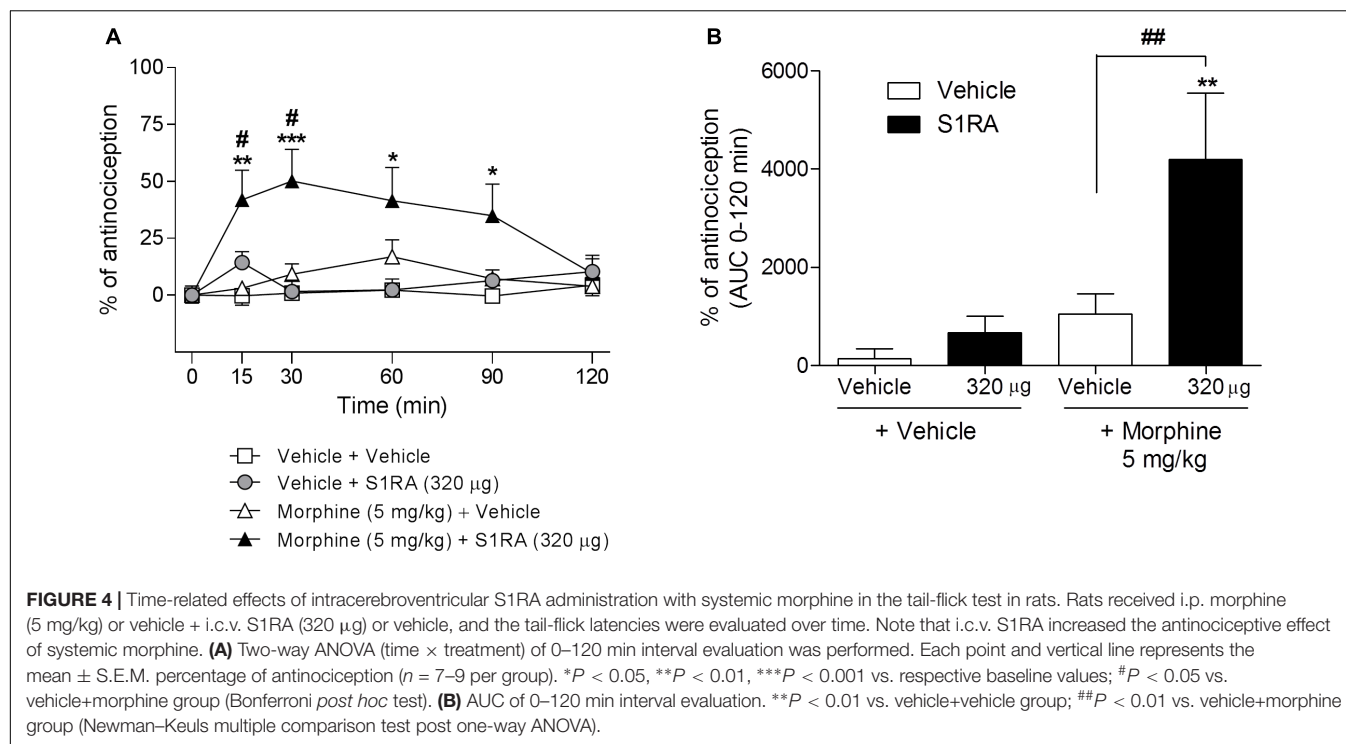
**FIGURE 3 |** Time-related effects of intrathecal S1RA administration with systemic morphine in the tail-flick test in rats. Rats received i.p. morphine (2.5 or 5 mg/kg) or vehicle + i.t. S1RA (160 or 320 µg) or vehicle, and the tail-flick latencies were assessed over time. **(A,C)** Two-way ANOVA (time  $\times$  treatment) of 0–120 min interval evaluation were performed. Each point and vertical line represents the mean  $\pm$  S.E.M. percentage of antinociception ( $n = 5–10$  per group). \* $P < 0.05$ , \*\*\* $P < 0.001$  vs. respective baseline values (Bonferroni *post hoc* test). Note that morphine elicited a significant antinociceptive effect (30 and 60 min post-administration) and that this effect was not increased by i.t. S1RA. **(B,D)** AUC of 0–120 min interval evaluation. \* $P < 0.05$  vs. vehicle+vehicle group; ns vs. morphine+vehicle group (Newman–Keuls multiple comparison test post one-way ANOVA).

significant antinociceptive effect at 30 min post-treatment when administered at 5 mg/kg i.p. ( $P < 0.05$ ) (**Figure 5A**). When S1RA (80 µg, intra-RVM) and morphine (2.5 and 5 mg/kg, i.p.) were combined, no significant change vs. the effect exerted by morphine alone was observed. AUC analysis revealed no significant enhancement of antinociception in co-treated vs. morphine-treated groups (**Figures 5B,D**).

### Systemic S1RA Enhanced the Antinociceptive Effect of Systemic Loperamide in the Tail-Flick Test in Rats

In order to address the involvement of  $\sigma_1$ R in opioid antinociception at the periphery, different doses of the

peripheral  $\mu$ -opioid agonist loperamide (1, 2, and 4 mg/kg, i.p.) were co-administered with a fixed dose of S1RA (40 mg/kg, i.p.) in the tail-flick test in rats. Two-way ANOVA (time  $\times$  treatment) revealed a treatment effect  $F(7, 49) = 4.90$ ,  $P < 0.001$ , 0–120 min. Loperamide alone did not elicit significant antinociceptive responses but did dose-dependently elicit antinociception when combined with S1RA over time, with maximum effect observed at 30 min post-treatment (**Figures 6A,B**). In another set of confirmatory experiments, animals were only measured at baseline and 30 min after loperamide and S1RA co-administration, and the effect was assessed in the presence of the peripherally acting  $\mu$ -opioid receptor antagonist naloxone-methiodide. Pre-treatment with naloxone-methiodide (4 mg/kg, i.p.)



blocked the potentiating effect of the loperamide + S1RA combination (Figure 6C).

## DISCUSSION

The present study demonstrated that supraspinal and peripheral, but not spinal, S1RA administration enhances opioid antinociception and that such a potentiating effect occurs without a concomitant increase in spinal NA release, in contrast to what is described for the formalin-induced pain model (Vidal-Torres et al., 2014).

The acute tail-flick response to nociceptive thermal (heat) stimulation was used to assess the potentiating effect of S1RA on opioid antinociception in rats. Systemic S1RA (40 mg/kg) had no antinociceptive effect when given alone but significantly increased the antinociceptive effect induced by morphine (2.5 mg/kg) up to 90 min post-administration. An ED<sub>50</sub> ratio value of 1.8 was obtained for morphine alone and in combination with S1RA (40 mg/kg) 30 min after administration. This value was similar to that previously obtained for S1RA in mice (2.4) and for haloperidol in rats (2) (Chien and Pasternak, 1994; Vidal-Torres et al., 2013).

Because we previously argued that S1RA modulates the analgesic effect in the formalin test by increasing spinal NA levels (Vidal-Torres et al., 2014), we dialysed the dorsal horn of the spinal cord after co-administration of morphine and S1RA at doses exerting antinociceptive effects. This technique allowed us to study spinal neurochemical modulation at the dorsal horn level in awake, freely-moving rats (Vidal-Torres et al., 2012). Subactive doses of S1RA and morphine, when

combined, enhanced opioid antinociception in the tail-flick test, but failed to modify NA concentrations vs. baseline. In fact, morphine induced a dose-dependent antinociceptive effect without concomitantly increasing NA spinal levels, and S1RA (80 mg/kg) *per se* increased spinal NA levels but failed to evoke antinociceptive effects in the tail-flick test. Therefore, opioid antinociception and potentiation of opioid antinociception did not correlate well with an enhancement of NA levels in the dorsal horn of the spinal cord. This fact discards the change in spinal NA levels as a key mechanism underlying opioid antinociception and  $\sigma_1$ R antagonism-mediated potentiation of opioid antinociception in the spinal reflex tail-flick response to an acute thermal stimulation. This contrasts with the previous findings suggesting that increased NA levels lie behind the antinociceptive effect of S1RA in the formalin test (Vidal-Torres et al., 2014). Therefore, we might difference two S1RA-mediated mechanisms of action for analgesia depending of the spinal NA involvement. However, caution should be exerted when interpreting and extrapolating these results, as the involvement of spinal NA seems to differ depending on the nature of the painful stimuli and the outcome measure of the response. In addition, it cannot be discarded an involvement of other neurotransmitters (serotonin, endogenous opioid peptides. . .) in the  $\sigma_1$ R antagonism on opioid analgesia in the descending pain control pathway.

The site of action of  $\sigma_1$ R modulation of opioid analgesia was addressed in a few studies using non-selective sigma compounds at the supraspinal and spinal levels (Mei and Pasternak, 2002, 2007; Marrazzo et al., 2006; Tseng et al., 2011) and more recently using S1RA at the peripheral level (Tejada et al., 2017, 2018). In the present study we took advantage of using the selective  $\sigma_1$ R antagonist S1RA to investigate the contribution of

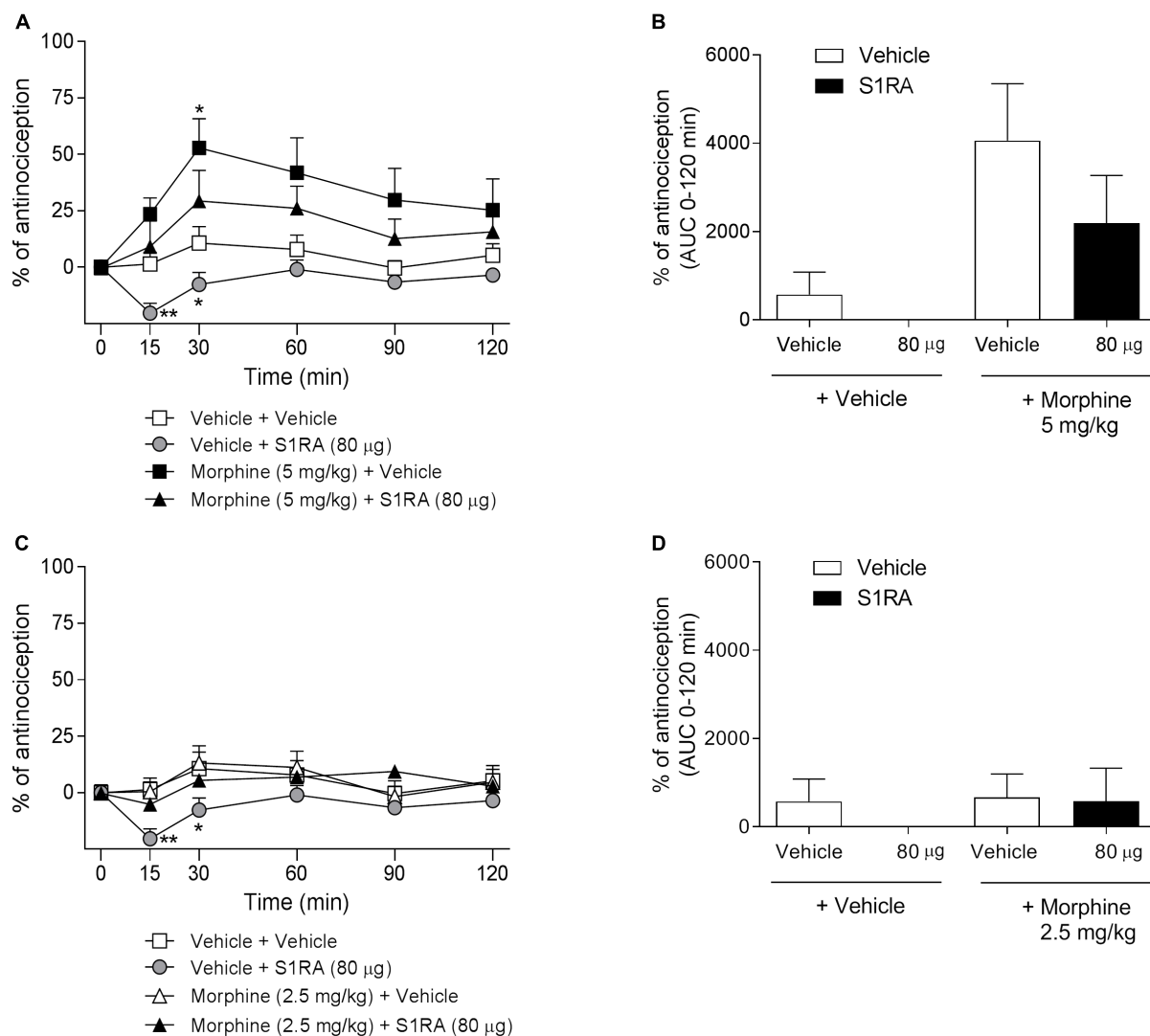


**FIGURE 5 |** Time-related effects of rostroventral medulla S1RA administration with systemic morphine in the tail-flick test in rats. Rats received i.p. morphine (2.5 or 5 mg/kg) or vehicle + RVM S1RA (80 µg) or vehicle, and the TFL was evaluated over time. **(A,C)** Two-way ANOVA (time × treatment) of 0–120 min interval evaluation was performed. Note that morphine exhibited significant antinociceptive effects (30 min post-administration) that were not increased by RVM S1RA. Each point and vertical line represents the mean ± S.E.M. percentage of antinociception ( $n = 6–8$  per group). \* $P < 0.05$ , \*\* $P < 0.01$  vs. respective baseline values (Bonferroni *post hoc* test). **(B,D)** AUC of 0–120 min interval evaluation. ns vs. vehicle+morphine group (Newman-Keuls multiple comparison test post one-way ANOVA).

peripheral, spinal and supraspinal  $\sigma_1$ R blockade on morphine antinociception enhancement in the tail-flick acute thermal nociceptive pain model in rats.

Firstly, we found that i.t. and i.c.v. S1RA treatment alone failed to produce antinociception in the tail-flick test at the same doses inducing clear-cut antinociceptive effects in the formalin-induced pain model (Vidal-Torres et al., 2014). These results are not surprising given that systemic S1RA by itself did not produce antinociceptive effects in the tail-flick test, and are consistent with previous studies reporting that  $\sigma_1$ R antagonism elicits antinociception in sensitizing conditions but does not affect perception of normal nociceptive stimuli (e.g., perception of thermal stimulation in the tail-flick test) (de la Puente et al., 2009; Nieto et al.,

2012; Romero et al., 2012). I.t. S1RA attenuated the flinching behavior (phases I and II) but not the lifting/licking response in the formalin test. These results in the formalin test can be reconciled if we consider that the lifting/licking response requires supraspinal integration, whereas the flinching behavior is essentially a spinal response that does not require the integrative action of higher brain centers. Accordingly,  $\sigma_1$ R antagonists acting locally at the spinal cord level seem to modulate the spinal reflex output but not motor neuron responses integrating descending, supraspinally processed outputs. While this fits well with data in the formalin test, i.t. S1RA did not inhibit the tail withdrawal response in the tail-flick test, which is also considered to be a spinal response (Irwin, 1962). Differences in the nociceptive

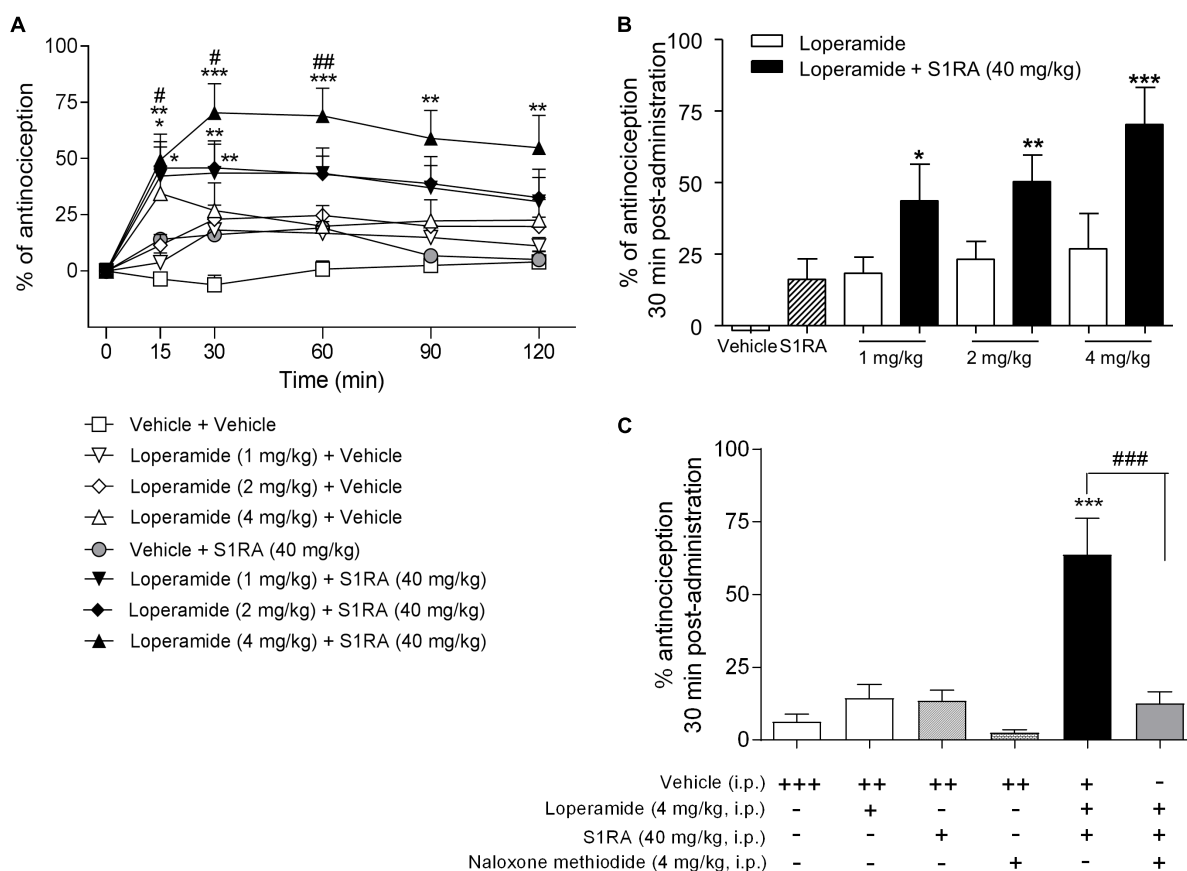


**FIGURE 6 |** Time-related effects of systemic S1RA administration with systemic loperamide in the tail-flick test in rats. **(A)** Rats received i.p. loperamide (1, 2, and 4 mg/kg) or vehicle + i.p. S1RA (40 mg/kg) or vehicle, and the tail-flick latencies were evaluated over time. Two-way ANOVA (time  $\times$  treatment) of 0–120 min interval evaluation was performed. Note that loperamide effects were enhanced by systemic S1RA. Each point and vertical line represents the mean  $\pm$  S.E.M. percentage of antinociception ( $n = 6$ –10 per group).  $*P < 0.05$ ,  $**P < 0.01$ ,  $***P < 0.001$  vs. vehicle-treated group;  $\#P < 0.05$ ,  $\#\#P < 0.01$  vs. corresponding loperamide dose (Bonferroni *post hoc* test). **(B)** Effects at 30 min post-administration.  $*P < 0.05$ ,  $**P < 0.01$ ,  $***P < 0.001$  vs. vehicle-treated group (Newman-Keuls multiple comparison test post one-way ANOVA). **(C)** Animals were pre-treated with i.p. naloxone-methiodide (4 mg/kg) 5 min prior to i.p. loperamide (4 mg/kg) and i.p. S1RA (40 mg/kg), and evaluated at 30 min post-administration. Note that enhancement of the loperamide effect by S1RA was blocked by naloxone-methiodide. Each point and vertical line represent the mean  $\pm$  S.E.M. percentage of antinociception ( $n = 8$ –12 per group).  $***P < 0.001$  vs. vehicle (+++) group;  $\#\#\#P < 0.001$  vs. loperamide+S1RA+vehicle group (Newman-Keuls multiple comparison test post one-way ANOVA). +, ++, +++ represents the number of administrations; - means no administration.

stimuli (thermal vs. chemical), which recruit different spinal pathways/mechanisms being differentially regulated (or not regulated at all) by  $\sigma_1$ R, could provide an explanation. In this regard, i.t. administration of the  $\sigma_1$ R antagonist BD-1047 is known to attenuate mechanical allodynia but not thermal hyperalgesia in a neuropathic pain model (Roh et al., 2008). Alternatively, the difference could be related to the duration of the stimulus, as thermal stimulation in the tail-flick test evokes immediate withdrawal/guarding responses whereas formalin-induced pain, even in phase I, lasts for several minutes, and thus some degree of sensitization may occur. This wider operating window gives  $\sigma_1$ R antagonists, which are known to inhibit spinal wind-up sensitization phenomena (Romero et al., 2012; Mazo et al., 2015), the opportunity to exert their effect.

Secondly, our results revealed that i.c.v. but not i.t. administration of S1RA in combination with systemic morphine

enhanced morphine antinociception in the co-treated group as compared to the morphine-treated group. The lack of effect of i.t. administration on opioid antinociception might be related to the poor co-expression of both targets in the same spinal cord region: the dorsal horn expresses high levels of opioids receptors but not  $\sigma_1$ R which is highly expressed in the ventral horn of the spinal cord (Mavlyutov et al., 2016). These effects of i.c.v. and i.t. administration of S1RA on opioid antinociception are consistent with those previously described by Mei and Pasternak in mice (Mei and Pasternak, 2002). They found diminished systemic morphine antinociception when the  $\sigma_1$ R agonist (+)pentazocine was given i.c.v., but no effect of (+)pentazocine against morphine when both were given spinally. Similarly, down-regulation of supraspinal  $\sigma_1$ R using an antisense approach potentiated systemic and i.c.v. morphine effects (Mei and Pasternak, 2002). The supraspinal regional localization relevant to  $\sigma_1$ R-mediated modulation of opioid antinociception is only beginning to be

clarified. PAG, LC, and RVM, areas where  $\sigma_1$ R is expressed (Walker et al., 1992), are relevant morphine-sensitive sites (Rossi et al., 1993, 1994). Morphine antinociception was lowered by co-administration of low doses of (+)-pentazocine in all three regions (although PAG was far less sensitive than the others), thus implying a highly sensitive  $\sigma_1$  system. Only RVM seems to have a tonic  $\sigma_1$  activity based upon the ability of the  $\sigma_1$ R antagonist haloperidol and the antisense treatment to enhance morphine actions (Mei and Pasternak, 2007). Nevertheless, S1RA (80  $\mu$ g) administered into the RVM failed to increase the tail-flick latency when given alone and also failed to enhance the effects of systemic morphine. These results suggest that the  $\sigma_1$ R system in this brainstem region (RVM) does not enhance systemic morphine antinociception in the tail-flick test. In contrast to the study by Mei and Pasternak (2007), in which morphine was microinjected together with the  $\sigma_1$ R ligand, in our experiment morphine was administered systemically. In addition, S1RA when given alone into the RVM produced a slight decrease in the tail-flick latency at 15 and 30 min after the administration in our experimental conditions. Therefore, we cannot discard that the short-term pronociceptive effect of S1RA could be a reason why S1RA did not potentiate morphine antinociception. This makes this area especially interesting for further studies to understand the physiological consequences of a possible pronociceptive action of the S1RA when given in the RVM.

Finally, we showed that  $\sigma_1$ R plays an important role on peripheral opioid-mediated acute thermal antinociception. We tested the effects of S1RA on the modulation of analgesia by using the peripherally acting  $\mu$ -opioid agonist loperamide (Heykants et al., 1974; Schinkel et al., 1996). Loperamide (1, 2, and 4 mg/kg) was devoid of antinociceptive effects in the tail-flick in rats, in agreement with previous reports (Menéndez et al., 2005; Sevostianova et al., 2005) and consistent with the view that analgesic effects of opioids on acute pain are primarily mediated through receptors located in the central nervous system (Yaksh and Rudy, 1978; McNally, 1999). Interestingly, systemic loperamide produced a marked antinociceptive effect when combined with S1RA (40 mg/kg). The recruitment of peripheral opioid receptors in the antinociception produced by loperamide in the presence of S1RA was confirmed by its sensitivity to the reversion by the peripherally restricted opioid antagonist naloxone methiodide (Russell et al., 1982). Therefore, the tonically active anti-opioid sigma-1 system, previously described by Pasternak, works not only at central levels, but also at peripheral sites. In fact, the density of  $\sigma_1$ Rs in the DRG was found to be much higher than in brainstem areas or in the dorsal spinal cord (Sánchez-Fernández et al., 2014), pointing to a prominent role for peripheral  $\sigma_1$ Rs in pain modulation. In fact, the administration of a  $\sigma_1$ R antagonist was sufficient to unmask the opioid effect of loperamide, a peripherally restricted mu opioid agonist commonly used as antidiarrheal drug. The molecular mechanism of the interaction between  $\sigma_1$ Rs and the mu opioid receptor was recently elucidated. Sigma-1 antagonism increases mu-opioid signaling through a complex regulation of the interaction between NMDA receptors and mu-opioid receptors, two of the main protein targets of  $\sigma_1$ Rs (Rodríguez-Muñoz et al., 2015). Although the specific

role of  $\sigma_1$ R on pain modulation at the periphery has not been extensively studied, our results are in agreement with those recently reported by Cobos and coworkers, where S1RA and other  $\sigma_1$ R antagonists did not modify nociceptive thresholds when administered locally at the periphery (intraplantarly) but did potentiate opioid mechanical antinociception. Interestingly, the sigma-1 tonic inhibitory actions on peripheral opioid seem to be limited to the mechanical stimuli because  $\sigma_1$ R inhibition did not potentiate other peripherally-mediated opioid effects, such as constipation, or peripheral opioid antinociception to heat stimuli (Sánchez-Fernández et al., 2014, 2017; Montilla-García et al., 2018). It has also been described that  $\sigma_1$ R antagonists alone exert remarkable antinociceptive effects at the periphery in conditions involving inflammation by modulating the analgesic effects of endogenous opioid produced by immune cells at the periphery (Tejada et al., 2017, 2018). Interestingly, loperamide alone produces peripheral analgesia also in inflammatory pain conditions (Khalefa et al., 2012). Altogether, the antagonism on  $\sigma_1$ R at the periphery may be used as a local adjuvant strategy to enhance peripheral  $\mu$ -opioid analgesia while avoiding the undesirable central opioid-mediated side effects, thus increasing the opioid benefit-to-risk ratio.

## CONCLUSION

In conclusion, the studies herein suggest that the  $\sigma_1$ R antagonism enhances opioid antinociception in acute thermal pain conditions by the sum/integration of supraspinal and peripheral effects, through a mechanism independent of spinal NA levels.

## ETHICS STATEMENT

All animal husbandry and experimental procedures complied with the European guidelines for the protection of animals used for experimental and other scientific purposes (Council Directive of 22 September 2010, 2010/63/EU), and were approved by the local Ethics Committee.

## AUTHOR CONTRIBUTIONS

AV-T, BF-P, and DZ designed and conducted the research. AV-T, AC, and BF-P performed the experiments. AV-T, JV, MM, and DZ wrote the main manuscript text. All authors analyzed the results and reviewed the manuscript.

## FUNDING

The study has been supported by the Spanish Ministry of Economy, Industry and Competitiveness through the Centre for the Development of Industrial Technology (CDTI, IDI20130943). This study was partially funded by a Doctoral Research Grant awarded to AV-T by the Generalitat de Catalunya (AGAUR).



## REFERENCES

- Abadias, M., Escriche, M., Vagué, A., Sust, M., and Encina, G. (2013). Safety, tolerability and pharmacokinetics of single and multiple doses of a novel sigma-1 receptor antagonist in three randomized phase I studies. *Br. J. Clin. Pharmacol.* 75, 103–117. doi: 10.1111/j.1365-2125.2012.04333.x
- Bruna, J., Videla, S., Argyriou, A. A., Velasco, R., Villoria, J., Santos, C., et al. (2018). Efficacy of a novel sigma-1 receptor antagonist for oxaliplatin-induced neuropathy: a randomized, double-blind, placebo-controlled phase IIa clinical trial. *Neurotherapeutics* 15, 178–189. doi: 10.1007/s13311-017-0572-5
- Chien, C. C., and Pasternak, G. W. (1994). Selective antagonism of opioid analgesia by a sigma system. *J. Pharmacol. Exp. Ther.* 271, 1583–1590.
- D'Amour, F. E., and Smith, D. L. (1941). A method for determining loss of pain sensation. *J. Pharmacol. Exp. Ther.* 72, 74–79.
- de la Puente, B., Nadal, X., Portillo-Salido, E., Sánchez-Arroyos, R., Ovalle, S., Palacios, G., et al. (2009). Sigma-1 receptors regulate activity-induced spinal sensitization and neuropathic pain after peripheral nerve injury. *Pain* 145, 294–303. doi: 10.1016/j.pain.2009.05.013
- DeLean, A., Munson, P. J., and Rodbard, D. (1978). Simultaneous analysis of families of sigmoidal curves: application to bioassay, radioligand assay, and physiological dose-response curves. *Am. J. Physiol.* 235, E97–E102.
- Díaz, J. L., Cuberes, R., Berrocal, J., Contijoch, M., Christmann, U., Fernández, A., et al. (2012). Synthesis and biological evaluation of the 1-arylpyrazole class of sigma(1) receptor antagonists: identification of 4-[2-[5-methyl-1-(naphthalen-2-yl)-1H-pyrazol-3-yloxy]ethyl]morpholine (S1RA, E-52862). *J. Med. Chem.* 55, 8211–8224. doi: 10.1021/jm3007323
- Gris, G., Cobos, E. J., Zamanillo, D., and Portillo-Salido, E. (2015). Sigma-1 receptor and inflammatory pain. *Inflamm. Res.* 64, 377–381. doi: 10.1007/s00011-015-0819-8
- Gris, G., Merlos, M., Vela, J. M., Zamanillo, D., and Portillo-Salido, E. (2014). S1RA, a selective sigma-1 receptor antagonist, inhibits inflammatory pain in the carrageenan and complete Freund's adjuvant models in mice. *Behav. Pharmacol.* 25, 226–235. doi: 10.1097/fbp.0000000000000038
- Gris, G., Portillo-Salido, E., Aubel, B., Darbaky, Y., Deseure, K., Vela, J. M., et al. (2016). The selective sigma-1 receptor antagonist E-52862 attenuates neuropathic pain of different aetiology in rats. *Sci. Rep.* 6:24591. doi: 10.1038/srep24591
- Heykants, J., Michiels, M., Knaeps, A., and Brugmans, J. (1974). Loperamide (R 18 553), a novel type of antidiarrheal agent. Part 5: the pharmacokinetics of loperamide in rats and man. *Arzneimittelforschung* 24, 1649–1653.
- Irwin, S. (1962). Drug screening and evaluative procedures: current approaches do not provide the information needed for properly predicting drug effects in man. *Science* 136, 123–128. doi: 10.1126/science.136.3511.123
- Khalefa, B. I., Shaqura, M., Al-Khrasani, M., Fürst, S., Mousa, S. A., and Schäfer, M. (2012). Relative contributions of peripheral versus supraspinal or spinal opioid receptors to the antinociception of systemic opioids. *Eur. J. Pain* 16, 690–705. doi: 10.1002/j.1532-2149.2011.00070.x
- Marrazzo, A., Parenti, C., Scavo, V., Ronsisvalle, S., Scoto, G. M., and Ronsisvalle, G. (2006). In vivo evaluation of (+)-MR200 as a new selective sigma ligand modulating MOR, DOP and KOP supraspinal analgesia. *Life Sci.* 78, 2449–2453. doi: 10.1016/j.lfs.2005.10.005
- Mavlyutov, T. A., Duellman, T., Kim, H. T., Epstein, M. L., Leese, C., Davletov, B. A., et al. (2016). Sigma-1 receptor expression in the dorsal root ganglion: reexamination using a highly specific antibody. *Neuroscience* 331, 148–157. doi: 10.1016/j.neuroscience.2016.06.030
- Mazo, I., Roza, C., Zamanillo, D., Merlos, M., Vela, J. M., and López-García, J. A. (2015). Effects of centrally acting analgesics on spinal segmental reflexes and wind-up. *Eur. J. Pain* 19, 1012–1020. doi: 10.1002/ejp.629
- McGrath, J. C., Drummond, G. B., McLachlan, E. M., Kilkeny, C., and Wainwright, C. L. (2010). Guidelines for reporting experiments involving animals: the ARRIVE guidelines. *Br. J. Pharmacol.* 160, 1573–1576. doi: 10.1111/j.1476-5381.2010.00873.x
- McNally, G. P. (1999). Pain facilitatory circuits in the mammalian central nervous system: their behavioral significance and role in morphine analgesic tolerance. *Neurosci. Biobehav. Rev.* 23, 1059–1078. doi: 10.1016/s0149-7634(99)00040-8
- Mei, J., and Pasternak, G. W. (2002). Sigma1 receptor modulation of opioid analgesia in the mouse. *J. Pharmacol. Exp. Ther.* 300, 1070–1074. doi: 10.1124/jpet.300.3.1070
- Mei, J., and Pasternak, G. W. (2007). Modulation of brainstem opiate analgesia in the rat by sigma 1 receptors: a microinjection study. *J. Pharmacol. Exp. Ther.* 322, 1278–1285. doi: 10.1124/jpet.107.121137
- Menéndez, L., Lastra, A., Meana, A., Hidalgo, A., and Baamonde, A. (2005). Analgesic effects of loperamide in bone cancer pain in mice. *Pharmacol. Biochem. Behav.* 81, 114–121. doi: 10.1016/j.pbb.2005.02.007
- Merlos, M., Romero, L., Zamanillo, D., Plata-Salamán, C., and Vela, J. M. (2017). Sigma-1 receptor and pain. *Handb. Exp. Pharmacol.* 244, 131–161. doi: 10.1007/164\_2017\_9
- Montilla-García, A., Perazzoli, G., Tejada, M. A., González-Cano, R., Sánchez-Fernández, C., Cobos, E. J., et al. (2018). Modality-specific peripheral antinociceptive effects of  $\mu$ -opioid agonists on heat and mechanical stimuli: contribution of sigma-1 receptors. *Neuropharmacology* 135, 328–342. doi: 10.1016/j.neuropharm.2018.03.025
- Nieto, F. R., Cerdán, C. M., Sánchez-Fernández, C., Cobos, E. J., Entrena, J. M., Tejada, M. A., et al. (2012). Role of sigma-1 receptors in paclitaxel-induced neuropathic pain in mice. *J. Pain* 13, 1107–1121. doi: 10.1016/j.jpain.2012.08.006
- Pogatzki, E. M., Zahn, P. K., and Brennan, T. J. (2000). Lumbar catheterization of the subarachnoid space with a 32-gauge polyurethane catheter in the rat. *Eur. J. Pain* 4, 111–113. doi: 10.1053/eupj.1999.0157
- Rodríguez-Muñoz, M., Sánchez-Blázquez, P., Herrero-Labrador, R., Martínez-Murillo, R., Merlos, M., Vela, J. M., et al. (2015). The  $\sigma_1$  receptor engages the redox-regulated HINT1 protein to bring opioid analgesia under NMDA receptor negative control. *Antioxid. Redox Signal.* 22, 799–818. doi: 10.1089/ars.2014.5993
- Roh, D. H., Kim, H. W., Yoon, S. Y., Seo, H. S., Kwon, Y. B., Kim, K. W., et al. (2008). Intrathecal injection of the sigma(1) receptor antagonist BD1047 blocks both mechanical allodynia and increases in spinal NR1 expression during the induction phase of rodent neuropathic pain. *Anesthesiology* 109, 879–889. doi: 10.1097/ALN.0b013e3181895a83
- Romero, L., Zamanillo, D., Nadal, X., Sánchez-Arroyos, R., Rivera-Arconada, I., Dordal, A., et al. (2012). Pharmacological properties of S1RA, a new sigma-1 receptor antagonist that inhibits neuropathic pain and activity-induced spinal sensitization. *Br. J. Pharmacol.* 166, 2289–2306. doi: 10.1111/j.1476-5381.2012.01942.x
- Rossi, G., Pan, Y. X., Cheng, J., and Pasternak, G. W. (1994). Blockade of morphine analgesia by an antisense oligodeoxynucleotide against the mu receptor. *Life Sci.* 54, L375–L379.
- Rossi, G. C., Pasternak, G. W., and Bodnar, R. J. (1993). Synergistic brainstem interactions for morphine analgesia. *Brain Res.* 624, 171–180. doi: 10.1016/0006-8993(93)90075-x
- Russell, J., Bass, P., Goldberg, L. I., Schuster, C. R., and Merz, H. (1982). Antagonism of gut, but not central effects of morphine with quaternary narcotic antagonists. *Eur. J. Pharmacol.* 78, 255–261. doi: 10.1016/0014-2999(82)90026-7
- Sánchez-Fernández, C., Entrena, J. M., Baeyens, J. M., and Cobos, E. J. (2017). Sigma-1 receptor antagonists: a new class of neuromodulatory analgesics. *Adv. Exp. Med. Biol.* 964, 109–132. doi: 10.1007/978-3-319-50174-1\_9
- Sánchez-Fernández, C., Montilla-García, Á., González-Cano, R., Nieto, F. R., Romero, L., Artacho-Cordón, A., et al. (2014). Modulation of peripheral mu-opioid analgesia by sigma1 receptors. *J. Pharmacol. Exp. Ther.* 348, 32–45. doi: 10.1124/jpet.113.208272
- Sánchez-Fernández, C., Nieto, F. R., González-Cano, R., Artacho-Cordón, A., Romero, L., Montilla-García, Á., et al. (2013). Potentiation of morphine-induced mechanical antinociception by sigma-1 receptor inhibition: role of peripheral sigma-1 receptors. *Neuropharmacology* 70, 348–358. doi: 10.1016/j.neuropharm.2013.03.002
- Schinkel, A. H., Wagenaar, E., Mol, C. A., and van, D. L. (1996). P-glycoprotein in the blood-brain barrier of mice influences the brain penetration and pharmacological activity of many drugs. *J. Clin. Invest.* 97, 2517–2524. doi: 10.1172/jci118699
- Sevostianova, N., Danysz, W., and Bernal, A. Y. (2005). Analgesic effects of morphine and loperamide in the rat formalin test: interactions with NMDA

- receptor antagonists. *Eur. J. Pharmacol.* 525, 83–90. doi: 10.1016/j.ejphar.2005.10.010
- Storkson, R. V., Kjorsvik, A., Tjolsen, A., and Hole, K. (1996). Lumbar catheterization of the spinal subarachnoid space in the rat. *J. Neurosci. Methods* 65, 167–172. doi: 10.1016/0165-0270(95)00164-6
- Tejada, M. A., Montilla-García, A., Cronin, S. J., Cikes, D., Sánchez-Fernández, C., González-Cano, R., et al. (2017). Sigma-1 receptors control immune-driven peripheral opioid analgesia during inflammation in mice. *Proc. Natl. Acad. Sci. U.S.A.* 114, 8396–8401. doi: 10.1073/pnas.1620068114
- Tejada, M. A., Montilla-García, A., Sánchez-Fernández, C., Entrena, J. M., Perazzoli, G., Baeyens, J. M., et al. (2014). Sigma-1 receptor inhibition reverses acute inflammatory hyperalgesia in mice: role of peripheral sigma-1 receptors. *Psychopharmacology* 231, 3855–3869. doi: 10.1007/s00213-014-3524-3
- Tejada, M. A., Montilla-García, A., González-Cano, R., Bravo-Caparrós, I., Ruiz-Cantero, M. C., Nieto, F. R., et al. (2018). Targeting immune-driven opioid analgesia by sigma-1 receptors: opening the door to novel perspectives for the analgesic use of sigma-1 antagonists. *Pharmacol. Res.* 131, 224–230. doi: 10.1016/j.phrs.2018.02.008
- Tseng, L. F., Hogan, Q. H., and Wu, H. E. (2011). (+)-Morphine attenuates the (-)-morphine-produced tail-flick inhibition via the sigma-1 receptor in the mouse spinal cord. *Life Sci.* 89, 875–877. doi: 10.1016/j.lfs.2011.09.018
- Vidal-Torres, A., Carceller, A., Zamanillo, D., Merlos, M., Vela, J. M., and Fernández-Pastor, B. (2012). Evaluation of formalin-induced pain behavior and glutamate release in the spinal dorsal horn using in vivo microdialysis in conscious rats. *J. Pharmacol. Sci.* 120, 129–132. doi: 10.1254/jphs.12105sc
- Vidal-Torres, A., de la Puente, B., Rocasbalbas, M., Touriño, C., Andreea, B. S., Fernández-Pastor, B., et al. (2013). Sigma-1 receptor antagonism as opioid adjuvant strategy: enhancement of opioid antinociception without increasing adverse effects. *Eur. J. Pharmacol.* 711, 63–72. doi: 10.1016/j.ejphar.2013.04.018
- Vidal-Torres, A., Fernández-Pastor, B., Carceller, A., Vela, J. M., Merlos, M., and Zamanillo, D. (2014). Effects of the selective sigma-1 receptor antagonist S1RA on formalin-induced pain behavior and neurotransmitter release in the spinal cord in rats. *J. Neurochem.* 129, 484–494. doi: 10.1111/jnc.12648
- Walker, J. M., Bowen, W. D., Goldstein, S. R., Roberts, A. H., Patrick, S. L., Hohmann, A. G., et al. (1992). Autoradiographic distribution of [3H](+)-pentazocine and [3H]1,3-di-o-tolylguanidine (DTG) binding sites in guinea pig brain: a comparative study. *Brain Res.* 581, 33–38. doi: 10.1016/0006-8993(92)90340-f
- Yaksh, T. L., and Rudy, T. A. (1978). Narcotic analgesics: CNS sites and mechanisms of action as revealed by intracerebral injection techniques. *Pain* 4, 299–359. doi: 10.1016/0304-3959(77)90145-2

**Conflict of Interest Statement:** The authors of this article are employees of Esteve Pharmaceuticals.

Copyright © 2019 Vidal-Torres, Fernández-Pastor, Carceller, Vela, Merlos and Zamanillo. This is an open-access article distributed under the terms of the Creative Commons Attribution License (CC BY). The use, distribution or reproduction in other forums is permitted, provided the original author(s) and the copyright owner(s) are credited and that the original publication in this journal is cited, in accordance with accepted academic practice. No use, distribution or reproduction is permitted which does not comply with these terms.



# Blockade of the Sigma-1 Receptor Relieves Cognitive and Emotional Impairments Associated to Chronic Osteoarthritis Pain

Mireia Carcolé<sup>1</sup>, Daniel Zamanillo<sup>2</sup>, Manuel Merlos<sup>2</sup>, Begoña Fernández-Pastor<sup>2</sup>, David Cabañero<sup>1†</sup> and Rafael Maldonado<sup>1\*†</sup>

<sup>1</sup> Neuropharmacology Laboratory, Department of Experimental and Health Sciences, Pompeu Fabra University, Barcelona, Spain, <sup>2</sup> Drug Discovery and Preclinical Development, Laboratories Esteve, Barcelona Science Park, Barcelona, Spain

## OPEN ACCESS

### Edited by:

Enrique José Cobos,  
University of Granada, Spain

### Reviewed by:

Filipa Pinto-Ribeiro,  
University of Minho, Portugal  
Fani Moreira Neto,  
Universidade do Porto, Portugal

### \*Correspondence:

Rafael Maldonado  
rafael.maldonado@upf.edu

<sup>†</sup>These authors have contributed  
equally to this work

### Specialty section:

This article was submitted to  
Experimental Pharmacology  
and Drug Discovery,  
a section of the journal  
Frontiers in Pharmacology

**Received:** 22 January 2019

**Accepted:** 12 April 2019

**Published:** 03 May 2019

### Citation:

Carcolé M, Zamanillo D,  
Merlos M, Fernández-Pastor B,  
Cabañero D and Maldonado R (2019)  
Blockade of the Sigma-1 Receptor  
Relieves Cognitive and Emotional  
Impairments Associated to Chronic  
Osteoarthritis Pain.  
Front. Pharmacol. 10:468.  
doi: 10.3389/fphar.2019.00468

Osteoarthritis is the most common musculoskeletal disease worldwide, often characterized by degradation of the articular cartilage, chronic joint pain and disability. Cognitive dysfunction, anxiety and depression are common comorbidities that impact the quality of life of these patients. In this study, we evaluated the involvement of sigma-1 receptor ( $\sigma$ 1R) on the nociceptive, cognitive and emotional alterations associated with chronic osteoarthritis pain. Monosodium iodoacetate (MIA) was injected into the knee of Swiss-albino CD1 mice to induce osteoarthritis pain, which then received a repeated treatment with the  $\sigma$ 1R antagonist E-52862 or its vehicle. Nociceptive responses and motor performance were assessed with the von Frey and the Catwalk gait tests. Cognitive alterations were evaluated using the novel object recognition task, anxiety-like behavior with the elevated plus maze and the zero-maze tests, whereas depressive-like responses were determined using the forced swimming test. We also studied the local effect of the  $\sigma$ 1R antagonist on cartilage degradation, and its central effects on microglial reactivity in the medial prefrontal cortex. MIA induced mechanical allodynia and gait abnormalities that were prevented by the chronic treatment with the  $\sigma$ 1R antagonist. E-52862 also reduced the memory impairment and the depressive-like behavior associated to osteoarthritis pain. Interestingly, the effect of E-52862 on depressive-like behavior was not accompanied by a modification of anxiety-like behavior. The pain-relieving effects of the  $\sigma$ 1R antagonist were not due to a local effect on the articular cartilage, since E-52862 treatment did not modify the histological alterations of the knee joints. However, E-52862 induced central effects revealed by a reduction of the cortical microgliosis observed in mice with osteoarthritis pain. These findings show that  $\sigma$ 1R antagonism inhibits mechanical hypersensitivity, cognitive deficits and depressive-like states associated with osteoarthritis pain in mice. These effects are associated with central modulation of glial activity but are unrelated to changes in cartilage degradation. Therefore, targeting the  $\sigma$ 1R with E-52862 represents a promising pharmacological approach with effects on multiple aspects of chronic osteoarthritis pain that may go beyond the strict inhibition of nociception.

**Keywords:** osteoarthritis, pain, sigma-1 receptor, cognition, depression, microglia, medial prefrontal cortex

## INTRODUCTION

Osteoarthritis is one of the most prevalent chronic diseases and represents a major socio-economic burden worldwide (Johnson and Hunter, 2014; Puig-Junoy and Ruiz Zamora, 2015). It is a complex disease of the whole joint defined by progressive destruction of articular cartilage (Sutton et al., 2009; Zhang et al., 2013). Its most problematic symptoms are pain and loss of joint function, and current pharmacological therapies are limited and generally directed to relief pain. However, osteoarthritis pain is frequently accompanied by co-morbid affective manifestations, such as anxiety and depression (Axford et al., 2010; Goldenberg, 2010; Sharma et al., 2016), and by cognitive alterations including memory dysfunction, which contribute to an overall impairment of the quality of life (Moriarty et al., 2011; Moriarty and Finn, 2014). These co-morbid alterations could in turn aggravate pain perception and contribute to the establishment of chronic osteoarthritis pain (Villemure and Bushnell, 2009). In this context, treatments that simultaneously control the nociceptive, affective and cognitive manifestations could represent an efficient therapeutical approach for chronic osteoarthritis pain.

Sigma-1 receptor ( $\sigma$ 1R) is a ligand-regulated chaperone that interacts with a large number of receptors and ion channels (Su and Hayashi, 2003; Hayashi and Su, 2007; Tsai et al., 2009) and has widespread distribution in the nervous system (Harada et al., 1994; Alonso et al., 2000; Kitaichi et al., 2000). Preclinical studies have implicated this receptor in several neurological disorders, such as addiction (Matsumoto et al., 2002; Maurice et al., 2002), schizophrenia (Hayashi et al., 2011) neurodegenerative disorders (Maurice et al., 1998; Francardo et al., 2014) or depression (Urani et al., 2001; Skuza and Rogó, 2003; Lucas et al., 2008).  $\sigma$ 1R has also been proposed as an effective therapeutic target in several models of chronic pain (Entrena et al., 2009; Nieto et al., 2012; Romero et al., 2012; Gris et al., 2014; Tejada et al., 2014). However, these studies do not assess the participation of the  $\sigma$ 1R on the emotional or cognitive alterations that can develop after the induction of persistent pain (La Porta et al., 2015, 2016; Negrete et al., 2017). Thus, it remains to be determined whether  $\sigma$ 1R ligands could be effective relieving chronic osteoarthritis pain together with its co-morbid cognitive and affective impairments.

The prefrontal cortex plays a crucial role in emotional processing (Gusnard et al., 2001; Etkin et al., 2011), cognitive functions (Phelps et al., 2004) and modulation of pain perception (Apkarian et al., 2004, 2005; Metz et al., 2009). Clinical studies have observed functional and structural abnormalities in the prefrontal cortex of patients suffering from chronic pain (Apkarian et al., 2004; Seminowicz et al., 2011). Such anatomical alterations have also been observed in animal models of neuropathic pain, where a decreased volume of the prefrontal cortex was found in correlation with anxiety-like behavior (Seminowicz et al., 2009). Several studies have also revealed the important role of microglial cells in the adaptative changes occurring in the central nervous system during chronic pain, leading to the persistence of pain manifestations (Racz et al., 2008). The role of microglia on chronic pain has been revealed in the spinal cord (Racz et al., 2008), and supraspinal activation of

microglia is also partly responsible for the structural, functional, and molecular neuroplasticity associated with pathological pain (Boadas-Vaello et al., 2017). In fact, it has been proposed that microglial alterations in cortical regions underlie pain-induced emotional and cognitive impairments (Panigada and Gosselin, 2011). Therefore, targeting microglial reactivity in these areas could be an appropriate strategy to treat the affective and memory disturbances observed in chronic pain conditions. Interestingly,  $\sigma$ 1R is highly expressed in microglia (Gekker et al., 2006) where it exerts a modulatory function (Peviani et al., 2014; Moritz et al., 2015). Therefore, it would be important to elucidate the possible role of  $\sigma$ 1R on cortical microgliosis associated to chronic osteoarthritis pain.

Here we assessed the effect of the  $\sigma$ 1R antagonist E-52862, also named S1RA (Romero et al., 2012; Gris et al., 2014) and MR309 (Castany et al., 2018), on the nociceptive, cognitive and emotional alterations observed in the monosodium iodoacetate (MIA) model of osteoarthritis pain in mice. To determine whether E-52862 exerts its effects through a local participation of  $\sigma$ 1R on the knee joint, we analyzed levels of cartilage degradation through histological assessment. In addition, we evaluated possible central neuroplastic effects of the  $\sigma$ 1R antagonist by determining microglial density and morphology in the medial prefrontal cortex.

## MATERIALS AND METHODS

### Animals

Swiss albino male mice (Charles River, Lyon, France) 8–12 weeks old were used in all the experiments. Mice weighted 22–24 g at the beginning of the experiments and were housed in groups of 3–4 with free access to water and food. The housing conditions were maintained at  $21 \pm 1^\circ\text{C}$  and  $55 \pm 10\%$  relative humidity in a controlled light/dark cycle (light on between 8:00 a.m. and 8:00 p.m.). During the weekly home cage replacement, the nest and an ounce of the old bedding were kept to reduce stress, and it was scheduled for days without any behavioral testing to avoid interferences. Six to 8 animals were used for each experimental group for behavioral testing, and 5–7 animals for the histological scoring, using a total of 53 mice. All experimental procedures and animal husbandry were conducted following the ARRIVE (Animal Research: Reporting *In Vivo* Experiments) guidelines and according to the ethical principles of the International Association for the Study of Pain (I.A.S.P.) for the evaluation of pain in conscious animals (Zimmermann, 1986) and the European Parliament and the Council Directive (2010/63/EU), and were approved by the Animal Care and Use Committees of the PRBB and *Departament de Territori i Habitatge* of Generalitat de Catalunya. All the experiments were performed under blinded conditions.

### Intra-Articular Injection of MIA

Osteoarthritis pain was induced in mice briefly anesthetized with isoflurane (2% v/v) vaporized in oxygen. The joint was shaved and flexed at a  $90^\circ$  angle and 10  $\mu\text{L}$  of MIA (10 mg/mL, Sigma, United Kingdom) dissolved in sterile saline (NaCl 0.9%) were



intra-articularly injected with a 30-gauge needle. Control mice received the same volume of sterile saline.

## Nociceptive Behavior

Hypersensitivity to punctate stimuli (von Frey filaments), which will be referred as mechanical allodynia throughout the text, was used as outcome measure of osteoarthritis pain. For this purpose, hind paw withdrawal response to von Frey filament stimulation was assessed (Chaplan et al., 1994). Briefly, animals were placed in Plexiglas cylinders (20 cm high, 9 cm diameter) positioned on a grid surface through which calibrated von Frey filaments (North Coast Medical, United States) were applied following the up-down paradigm, as previously reported (Chaplan et al., 1994). The 0.4-g filament was used first, and the strength of the next filament was decreased or increased according to the response following this sequence 0.07, 0.16, 0.4, 0.6, 1.0, 2.0. The 2.0-g filament was used as a cut-off. The mechanical threshold (in grams) was then calculated with the up-down Excel program (Dixon, 1965). Animals were habituated for 3 consecutive days (2 h per day) to the von Frey environment before the baseline measurements and for 1 h before testing to allow appropriate behavioral immobility. Clear paw withdrawal, shaking or licking was considered as nociceptive response. Both ipsilateral and contralateral hind paws were tested. Only ipsilateral responses are shown, since contralateral sides showed no significant differences.

## Gait Analysis

We used the Catwalk automated gait analysis (Noldus, Netherlands) to assess the effects of osteoarthritis pain on gait (Vrinten and Hamers, 2003; Ferland et al., 2011). Each mouse was placed individually in the Catwalk walkway, which consists of a glass plate (100 cm × 15 cm × 0.6 cm) plus two Plexiglas walls, spaced 5 cm apart. Mice were allowed to walk freely and traverse from one side to the other of the walkway glass plate. The recordings were carried out when the room was completely dark. A pair of infrared beams spaced 90 cm apart were used to detect mouse arrival and to control (start/stop) data acquisition. LED light from an enhanced fluorescent lamp was emitted inside the glass plate and completely internally reflected. Where mice paws made contact with the glass plate, light was reflected down, and the illuminated contact areas were recorded with a high-speed color video camera. The camera was positioned underneath the glass plate connected to a computer that run the Catwalk software 9.1. The software regarded a run as compliant if the animal did not show a maximum speed variation greater than 40%. Three compliant runs (trial) were recorded for each animal and time point. The software automatically labeled all the areas containing pixels above the set thresholds. These areas were identified and assigned to the respective paws. Data were segmented to only take into account sequences with a minimum number of 10 consecutive steps per run and an average speed between 20 and 90 cm/s. Print area (complete surface area contacted by the paw during a stance phase), maximal contact area (maximum area of a paw that comes into contact with the glass plate), swing (duration in sec of no contact of a paw with the glass plate) and duty cycle (duration in sec of contact of a

paw with the glass plate as percentage of a whole step cycle) were analyzed. A ratio between right and left hind paws was calculated.

## Cognitive Behavior

Object recognition memory was assessed with the V-maze (Panlab, Barcelona, Spain) to measure cognitive performance, as previously described (Puighermanal et al., 2009; Saravia et al., 2019). V-maze consisted on an apparatus made of black plexiglass with two corridors (30 cm long × 4.5 cm wide) set in V with a 90° angle and 15 cm-high walls. This task consists of 3 sessions of 9 min each (habituation, training and test). On day 1, mice were<sup>1</sup> habituated to the empty maze. On the 2nd day, mice were put back and 2 identical objects were presented at the end of each of the corridors. Mice were placed again in the maze 24 h later and one of the familiar objects was replaced with a novel object. Time exploring each of the 2 objects (novel and familiar) was recorded. A discrimination index [(time exploring the novel object – time exploring the familiar)/(time exploring novel + familiar) \* 100] was used as outcome measure of cognitive behavior. High values of discrimination represent good recognition memory. Total time of exploration of the 2 objects was used as a measure of locomotor activity.

## Affective Behavior

The elevated plus maze was used to evaluate anxiety 11 days after saline or MIA injection. It was performed in a black Plexiglas apparatus with 4 arms (29 cm long × 5 cm wide), 2 open and 2 closed, set in cross from a neutral square (5 cm × 5 cm) elevated 30 cm above the floor and indirectly illuminated from the top (40–50 lux in the open arms/4–6 lux in the close arms). 5-min test sessions were performed, and the latency to the first entrance to the open arms and the percentage of entries and time spent in the open arms were used as a measure of anxiety-like behavior (Cruz et al., 1994). Mice were habituated to the testing room for 1 h before starting the evaluation, and the equipment was carefully cleaned between subjects.

The elevated zero maze was used as additional measure of anxiety-like behavior 21 days after saline or MIA injection. Mice were placed in a black Plexiglas apparatus with a round shape, where 2 quarters of the maze were closed by walls (20 cm-high) and elevated 30 cm above the floor. Sessions were 5 min long, and the latency to the open quadrants and the percentage of time spent in the open parts was determined (Shepherd et al., 1994). Mice were habituated to the testing room for 1 h before starting the evaluation, and the equipment was carefully cleaned between subjects.

The forced swimming test was used to evaluate depressive-like behavior 25 days after saline/MIA (Porsolt et al., 1977). Mice were placed for 6 min into transparent Plexiglas cylinders (17.5 cm high and 12.5 cm diameter) filled with 15 cm of water at 22 ± 2°C. The percentage of time of immobility was assessed for the last 4 min. Immobility was considered when the animal made no movements in order to escape (swimming, climbing the walls).

<sup>1</sup>[https://www.ebi.ac.uk/gxa/genes/ENSG00000147955?bs=%7B%22homo%20sapiens%22%3A%5B%22ORGANISM\\_PART%22%5D%7D&ds=%7B%22kingdom%22%3A%5B%22animals%22%5D%7D#baseline](https://www.ebi.ac.uk/gxa/genes/ENSG00000147955?bs=%7B%22homo%20sapiens%22%3A%5B%22ORGANISM_PART%22%5D%7D&ds=%7B%22kingdom%22%3A%5B%22animals%22%5D%7D#baseline)



Mice were habituated to the testing room for 1 h before starting the evaluation, the equipment was carefully cleaned, and the water was changed between subjects.

## Experimental Protocol

Animals were carefully handled and habituated to the von Frey environment for 3 consecutive days before the baseline measurement. The day following baseline nociceptive assessment, MIA or saline was injected into the knee joint. Mice were intraperitoneally treated twice a day (10 a.m. and 06 p.m.) with either vehicle or E-52862 (20 mg/kg) from the 1st day after the intra-knee injection to the end of the experiment on day 25. Mechanical sensitivity was evaluated 5 and 19 days after the intra-articular injection with the von Frey test, and at days 6 and 12 with the Catwalk gait test. Nociceptive assessments were performed 30 min after drug administration. Cognitive and affective behavior were also analyzed. For this purpose, the elevated plus maze was performed 11 days after intra-knee injection, the novel object recognition task at days 13, 14, and 15 (habituation, training, and test), the zero-maze at day 21 and the forced swimming test at day 25 after MIA/saline. The late anxiety-like behavior was assessed with a different test from the early evaluation to avoid the well-reported one-trial tolerance to the behavioral test (File et al., 1990; Holmes and Rodgers, 1998). The days of the evaluation of affective behavior, E-52862-treated mice received vehicle instead of the  $\sigma$ 1R antagonist 30 min before the test to avoid acute effects of the drug, and E-52862 was administered after the test to continue the repeated treatment. An additional group of vehicle-treated mice received a single dose of E-52862 before the novel object recognition task. Tissue for immunofluorescence analysis was extracted on day 26 and  $12 \pm 1$  h after the last drug administration.

## Drugs

The selective  $\sigma$ 1R antagonist E-52862 [(4-[5-methyl-1-(2-naphthalenyl)-1H-pyrazol-3-yl]oxy]ethyl morpholine hydrochloride] was developed and supplied by Laboratories Esteve (Barcelona, Spain). E-52862 was dissolved in an aqueous solution (0.5% hydroxypropylmethyl cellulose, HPMC; Sigma-Aldrich) and administered by intraperitoneal route at a volume of 10 ml/kg 30 min before behavioral testing.

## Histology

### Knee Joint Isolation

A separate group of mice was intra-knee injected with saline or MIA and intraperitoneally repeatedly treated with vehicle or E-52862. Mice were sacrificed by cervical dislocation 29 days after the experimental induction of osteoarthritis pain. The ipsilateral knee joints were subsequently removed, post-fixed 48 h in 4% paraformaldehyde, and then cryopreserved in 30% sucrose solution at 4°C.

### Histological Preparation

The fixed knee joints were decalcified in Osteomoll (Merck, Germany) for 6–7 h and left overnight in 30% sucrose solution. The joints were subsequently embedded in gelatine (7.5%) and frozen in cold 2-methyl-butane. Coronal 16- to 18- $\mu$ m sections

were cut in a cryostat from the frontal plane toward the back of each joint and mounted on gelatinized slides (6–7 slides with 10 sections each). All the serial sections were stained with the Safranin O-Fast Green staining protocol. Briefly, after hydrating sections with decreasing concentrations of ethanol, sections were stained with haematoxylin (Merck, Germany) and subsequently with 0.002% Fast Green (Sigma, Spain) and 0.2% Safranin O (Merck, Germany) solutions. The sections were finally dehydrated and cleared with increasing ethanol concentrations and xylene, then mounted with Eukitt (O. Kindler, Germany) and a covering glass. All the stained sections were viewed with a 10 $\times$  objective using a Leica DMR microscope equipped with a Leica DFC 300 FX digital camera. Nine images of the obtained sections spanning the central load-bearing region of the knee were taken for both medial and lateral sides of each joint (18 total images per joint) and used for histological scoring.

### Histological Scoring

A semiquantitative scoring system for murine histopathology, the OARSI score (Glasson et al., 2010) was applied and adapted to our experimental conditions (Figure 2C). All 4 quadrants of the knee joint were evaluated: medial femoral condyle (MFC), lateral femoral condyle (LFC), medial tibial plateau (MTP), and lateral tibial plateau (LTP). A score from 0 to 6 was given to each quadrant of 9 serial sections per animal, having a total of 36 values per animal. The final histological scores were expressed as the sum of all the individual values and the average summed score for each experimental group was calculated. The same observer scored all the histological changes and was blinded to the specimen samples.

### Tissue Isolation

On day 26 after osteoarthritis induction, both MIA and saline mice were deeply anesthetized by intraperitoneally injection (0.2 ml/10 g of body weight) of a mixture of ketamine (100 mg/kg) and xylazine (20 mg/kg) prior to intracardiac perfusion of 4% PFA in 0.1 M  $\text{Na}_2\text{HPO}_4/\text{NaH}_2\text{PO}_4$  buffer, pH 7.5, delivered with a peristaltic pump at 22 ml per min for 2 min. Brains were removed and post-fixed overnight at 4°C in the same fixative solution. Then, brains were transferred to a solution of 30% sucrose in PB 0.1 M and kept at 4°C. Coronal brain sections (30  $\mu$ m) containing the prelimbic and infralimbic prefrontal cortex were obtained with a microtome (Leica) and kept in a solution of 5% sucrose PB 0.1 M at 4°C until processed for immunofluorescence analysis.

### Immunofluorescence

Free-floating slices were rinsed in PB 0.1 M and blocked in a solution containing 3% normal goat serum and 0.3% Triton X-100 in PB 0.1 M during 2 h at room temperature. The slices were incubated overnight at 4°C with the primary antibody anti-Iba-1 (1:500, rabbit, Wako). The next day, after 3 rinses in PB 0.1 M, sections were incubated for 2 h at room temperature with the secondary antibody AlexaFluor-555 goat anti-rabbit (1:1000, Life Technologies). Then, slices were

rinsed 3 times and mounted with Fluoromount onto glass slides coated with gelatine.

## Immunofluorescence Image Analysis

The stained sections were analyzed with the 40 $\times$  objective and 1 $\times$  zoom using a confocal microscope (Leica TCS SP5 STED). A z-stack image of 30  $\mu$ m with 0.5 depth intervals was obtained from every slice. Density<sup>2</sup> and cell architecture of microglia was examined using the ImageJ analysis software. The perimeter of microglial soma was measured using the tool “Freehand line” and the option “Analyze and Measure.” Four images per brain area of 6 animals per group were analyzed.

## Statistical Analysis

A 3-way repeated measure analysis of variance (ANOVA) with surgery and treatment as between-subject factors and day as within-subject factor was used to analyze von Frey and gait data. 2-way ANOVA (surgery and treatment) was used to analyze affective behavioral data, as well as the histological scoring from the joint, and 1-way ANOVA was used to analyze the cognitive behavior. In all comparisons, Fisher Least Significant Difference (LSD) *post hoc* analysis was applied when appropriate (significant interaction between factors). STATISTICA 6.0 (StatSoft, Inc., Tulsa, OK, United States) software was used. The differences were considered statistically significant when the *P*-value was below 0.05 (Supplementary Table S1).

## RESULTS

### The $\sigma$ 1R Antagonist E-52862 Reverses Mechanical Hypersensitivity Associated to Osteoarthritis Pain

To evaluate the effect of E-52862 on mechanical hypersensitivity associated to osteoarthritis pain, mice were intraperitoneally treated twice a day with either vehicle or E-52862 (20 mg/kg) from the 1st day after MIA injection until the end of the experiment (day 25). Von Frey test was performed before and 5 and 19 days after MIA injection, and gait analysis was evaluated at 6 and 12 days (Figure 1A). MIA injection induced a persistent mechanical hypersensitivity in vehicle-treated mice ( $p < 0.001$  vs. saline mice, days 5 and 19). Conversely, this decrease in mechanical thresholds was absent in mice treated with E-52862 ( $p < 0.001$  vs. MIA vehicle mice, days 5 and 19) (Figure 1B). Gait analysis also showed MIA-induced alterations on walking patterns that were partly reversed by E-52862. Mice injected with MIA and treated with vehicle showed a significant decrease of the print area ( $p < 0.01$  vs. saline; Figure 1C) and maximal contact area ( $p < 0.05$  vs. saline; Figure 1D) at both time points tested. These alterations were not observed when MIA-injected mice were treated with E-52862 (Figures 1C,D). No significant effects were observed in the swing for any of the experimental groups (Figure 1E), however, a trend toward a decreased duty

cycle was observed in MIA mice treated with vehicle ( $p = 0.08$  vs. saline; Figure 1F). Therefore, blocking the  $\sigma$ 1R produced a relief of mechanical pain associated to the injection of MIA that was also reflected into a normalization of gait function.

### MIA Injection Into the Knee Produces Cartilage Degradation Insensitive to the $\sigma$ 1R Antagonist E-52862

Monosodium iodoacetate is a chondrocyte glycolytic inhibitor which produces chondrocyte death and damage in the entire joint space. We determined the level of cartilage degeneration through proteoglycan staining 29 days after the intra-knee injection (Figure 2A). MIA injected mice had a clear increase on the OARSI score when compared to saline mice ( $p < 0.001$ ; Figure 2B), and no significant effect of the E-52862 treatment (20 mg/kg, twice daily during 25 days) was found. Therefore, joint damage was not significantly prevented by the blockade of  $\sigma$ 1R.

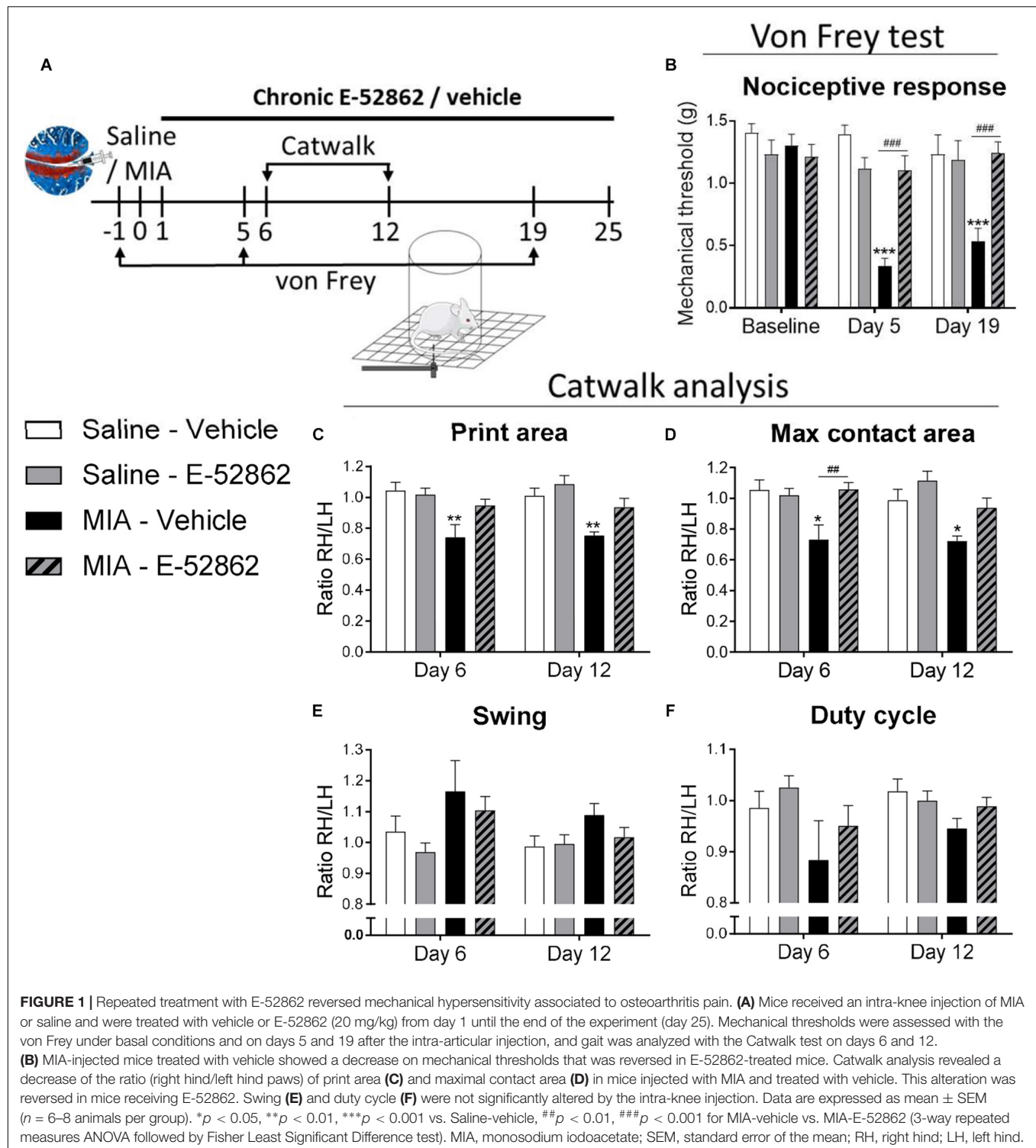
### Acute and Chronic Blockade of $\sigma$ 1R Avoid Osteoarthritis-Induced Cognitive Impairment

Chronic pain is often accompanied by memory dysfunction. Therefore, we analyzed the effect of chronic treatment with E-52862 (20 mg/kg, twice daily during 25 days) over recognition memory in the osteoarthritis model (Figure 3A). The novel object recognition task performed 15 days after MIA/saline injection showed a significant decrease on the discrimination index of MIA-injected mice treated with vehicle ( $p < 0.001$  vs. saline). This cognitive impairment was avoided after the chronic treatment with E-52862 ( $p < 0.05$  vs. MIA vehicle; Figure 3B). Interestingly, MIA-injected mice receiving a single acute dose of the  $\sigma$ 1R antagonist (20 mg/kg) 30 min before the test also showed an improvement on the discrimination index ( $p < 0.001$  vs. MIA vehicle) (Figure 3B). All groups of mice showed similar total exploration times, suggesting normal locomotor activity in this paradigm regardless of the surgery or the treatments (Figure 3C). Therefore, the impairment of recognition memory caused by chronic osteoarthritis pain was improved after chronic or acute blockade of  $\sigma$ 1R.

### E-52862 Decreases Depressive-Like Behaviour Associated to Osteoarthritis Pain

Anxiety and depressive-like behavior were assessed to determine whether E-52862 (20 mg/kg, twice daily during 25 days) could modulate emotional-like states associated to osteoarthritis pain (Figure 4A). It has been proposed that the initial stages of osteoarthritis pain are associated with inflammatory processes, whereas later stages involve neuropathic components, which may differentially affect the emotional manifestations. Thus, early and late anxiety-like behavior was assessed in our model. Early anxiety was evaluated 11 days after intra-knee injection in the elevated plus maze. No differences were found between saline- and MIA-injected mice in the latency to entry to the open arms, and the percentage of time and entries to the open arms, regardless

<sup>2</sup><https://www.proteinatlas.org/ENSG00000147955-SIGMAR1/tissue>



of the treatment received (Figures 4B–D). On the other hand, despite the latency to the open quadrants of the zero-maze was not altered (Figure 4E), mice with osteoarthritis pain showed late anxiety-like behavior reflected in a significant decrease of the time spent in the open arms of the zero-maze ( $p < 0.001$  vs. saline), also regardless of the treatment. Thus, E-52862 did

not normalize the anxiogenic-like responses induced by MIA (Figure 4F). Depressive-like behavior was analyzed in the forced swimming test 25 days after the intra-articular injection. In this paradigm, mice with osteoarthritis pain receiving vehicle showed a significant increase on immobility time ( $p < 0.05$  vs. saline; Figure 4G). Chronic E-52862 administration prevented such an



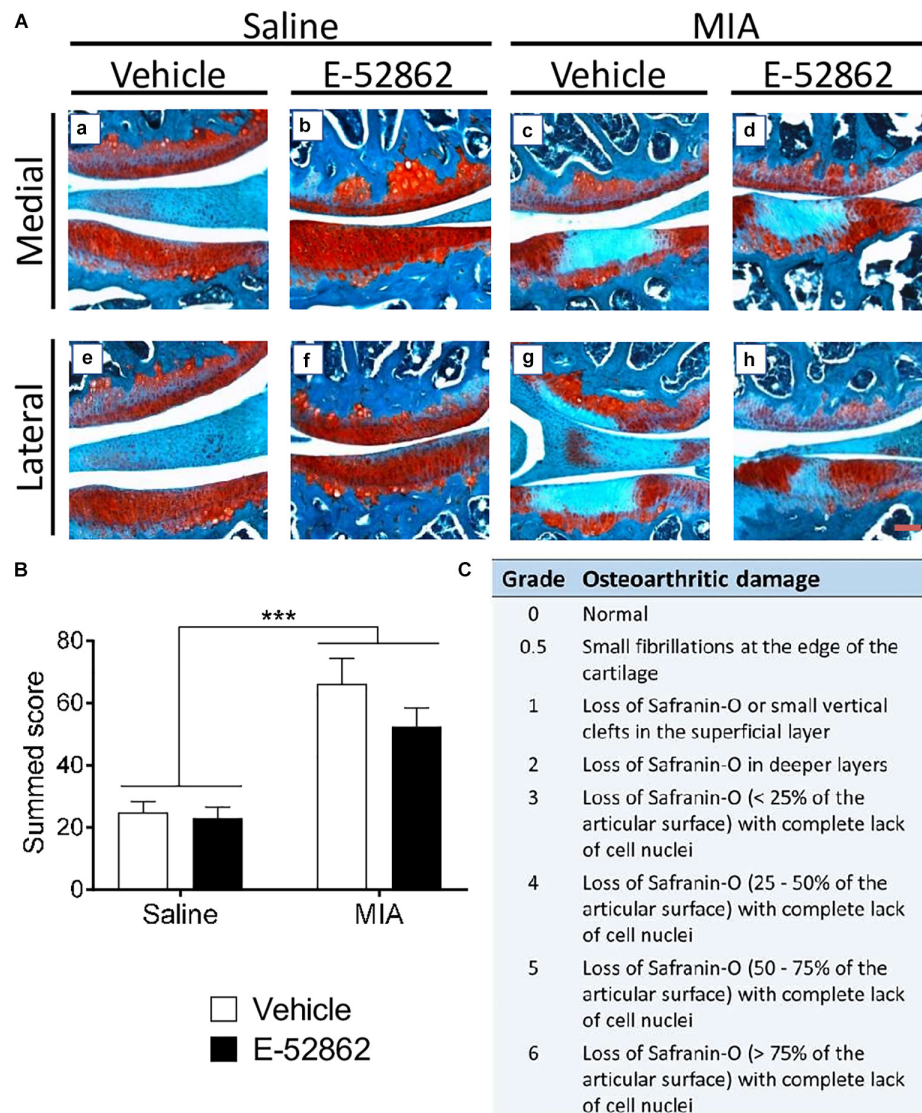


**FIGURE 2 |** Histological knee alterations in mice injected with MIA were not prevented by the chronic treatment with E-52862. Ipsilateral knees of saline and MIA mice were obtained 29 days after intra-articular injection in mice receiving vehicle or E-52862 treatment. **(A)** Medial and lateral sides of the joints are represented, showing the femur condyle (above) and the tibial plateau (below). **(B)** The injection of MIA produced cartilage degeneration revealed by an increased OARSI score. Treatment with E-52862 (20 mg/kg, twice daily during 25 days) did not prevent the joint damage. **(C)** The semiquantitative scoring system for joint histopathology. The scores for each image are (first value represents femur condyle and second value represents tibial plateau): **(a)** 1, 0.5; **(b)** 0.5, 0; **(c)** 2, 5; **(d)** 2, 5; **(e)** 2, 0.5; **(f)** 0, 0.5; **(g)** 3, 6; **(h)** 2, 3. Data are expressed as the mean  $\pm$  SEM ( $n = 5-7$  animals per group). Scale bar: 100  $\mu$ m. \*\*\* $p < 0.001$  for saline vs. MIA (2-way ANOVA). MIA, monosodium iodoacetate; SEM, standard error of the mean.

increase in despair-like behavior ( $p < 0.01$  vs. MIA vehicle; **Figure 4G**). Therefore, anxiety-like behavior was not sensitive to  $\sigma$ 1R antagonism, whereas MIA-induced depressive-like behavior was prevented after E-52862 treatment.

### E-52862 Modulates Microglial Expression in the Medial Prefrontal Cortex

A possible central role of  $\sigma$ 1R modulating microglial activity was assessed through quantification of the density of microglial

cells and the perimeter of the somas in the prelimbic and infralimbic areas of the medial prefrontal cortex (**Figure 5**). The analysis of the cellular density showed a significant increase on the total number of microglial cells in the prelimbic and the infralimbic areas of mice with osteoarthritis pain receiving vehicle ( $p < 0.001$  vs. saline) (**Figures 5A,C,D,F**). Repeated administration of the  $\sigma$ 1R antagonist (20 mg/kg, twice daily during 25 days) significantly reduced the microglial density in both cortical areas ( $p < 0.01$  vs. MIA vehicle; **Figures 5A,C,D,F**). MIA-injected mice had an increase of the perimeter of microglial cells in the infralimbic ( $p < 0.05$ ;

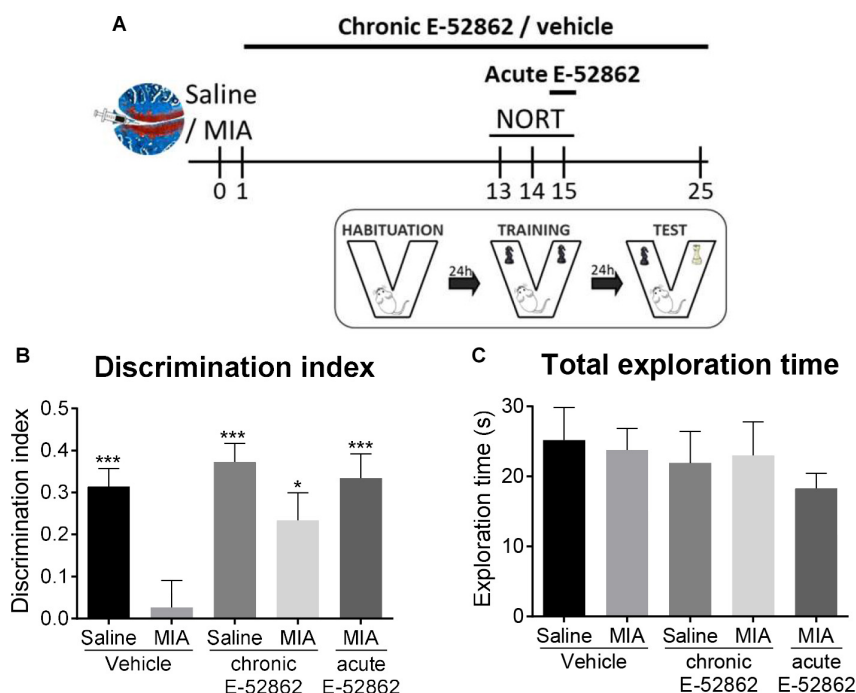


**FIGURE 3 |** Acute and chronic treatments with E-52862 improved the cognitive deficits induced by MIA injection. **(A)** Saline or MIA-injected mice treated with vehicle or E-52862 (20 mg/kg, twice daily during 25 days) were evaluated for recognition memory 15 days after the intra-knee injection in the novel object recognition test (NORT). **(B)** Mice with osteoarthritis pain treated with vehicle showed decreased discrimination index indicating a memory impairment. Acute and chronic treatment with E-52862 reversed the cognitive deficits induced by MIA. **(C)** Animals revealed similar total exploration times regardless of the surgery or the treatment. Data are expressed as mean  $\pm$  SEM ( $n = 6$ –8 animals per group). \* $p < 0.05$ , \*\*\* $p < 0.001$  vs. MIA-vehicle (1-way ANOVA followed by Fisher least significant difference test). MIA, monosodium iodoacetate; SEM, standard error of the mean.

Figure 5E), but not in the prelimbic area (Figure 5B) when compared to saline-injected mice. This increase was not significantly affected by the treatment with E-52862. Therefore, E-52862 modulated the density of microglial cells in the medial prefrontal cortices without affecting microglia activation.

## DISCUSSION

The present study reveals the involvement of the  $\sigma$ 1R in the nociceptive, emotional and cognitive alterations associated with osteoarthritis pain in mice. Mechanical allodynia and gait impairments induced by MIA injection were partly prevented by chronic administration of the  $\sigma$ 1R antagonist E-52862. This treatment also inhibited the cognitive deficits and depressive-like behavior of mice with osteoarthritis pain, although anxiogenic-like responses were not modified. Modulation of the pain-induced behavioral alterations by E-52862 was not due to an inhibition of joint damage produced by MIA, and there was a concomitant decrease on MIA-induced microgliosis in the medial prefrontal cortex.

$\sigma$ 1R is highly expressed in key areas for pain control (Alonso et al., 2000; Bangaru et al., 2013). Behavioral studies have shown analgesic efficacy of the  $\sigma$ 1R antagonist E-52862 in acute (Romero et al., 2012; Gris et al., 2014; Tejada et al.,

2014) and chronic (Gris et al., 2014) models of inflammatory pain, and in neuropathic pain models induced by partial sciatic nerve ligation (Romero et al., 2012), chemotherapy (Nieto et al., 2012), or streptozotocin-induced diabetes (Gris et al., 2016). However, the role of  $\sigma$ 1R has not been previously assessed in models of osteoarthritis pain, one of the most prevalent and disabling chronic pain conditions. We showed that E-52862 inhibited both mechanical hypersensitivity and gait alterations in the MIA model of osteoarthritis pain. Gait alterations could be associated to structural modifications of the joint or to the increased mechanical sensitivity (Boettger et al., 2009). Previous studies using the antigen-induced arthritis model in rats suggested that specific gait parameters, such as the angle between the paws, were exclusively influenced by the structural damage of the joint as indicated by its correlation with cartilage destruction (Boettger et al., 2009). However, other parameters, such as the paw print area, represent good measures of pain (Boettger et al., 2009). The correlation with mechanical allodynia would be in agreement with previous work showing that nerve-injured rats with decreased mechanical thresholds to punctate stimulation had also altered walking patterns (Vrinten and Hamers, 2003). In the same line, the MIA model of osteoarthritis pain in rodents showed that celecoxib and morphine reduced mechanical allodynia and gait abnormalities (Ferland et al., 2011; Ferreira-Gomes et al., 2012), suggesting that both parameters are associated in this



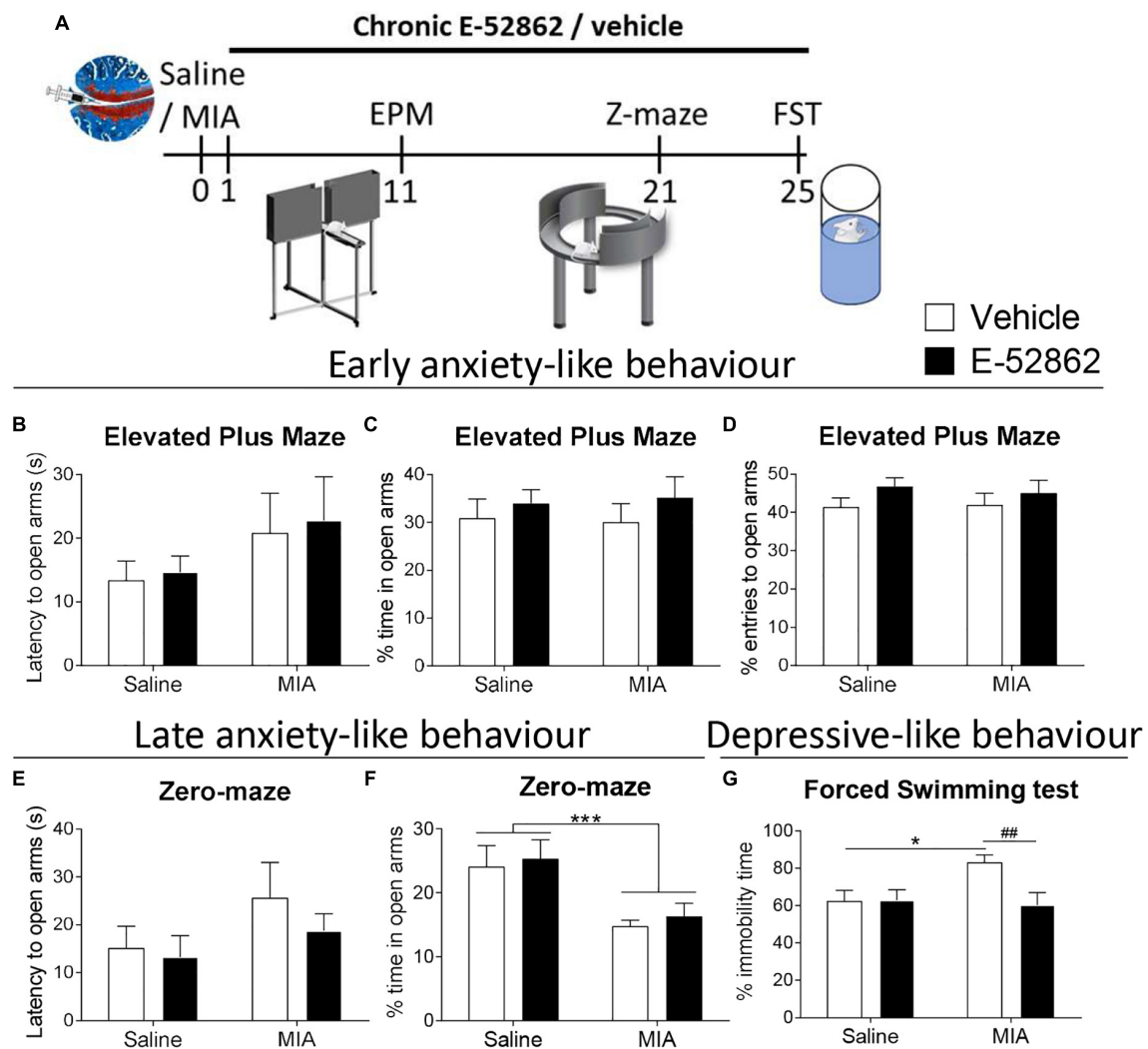


**FIGURE 4 |** E-52862 treatment reduced depressive-like behavior, but not anxiety-like responses associated with chronic osteoarthritis pain. **(A)** Emotional manifestations of osteoarthritis pain were assessed in saline- or MIA-injected mice after repeated administration with vehicle or E-52862 (20 mg/kg, twice daily during 25 days) to saline or MIA-injected mice. Anxiety-like behavior was evaluated on day 11 after the intra-knee injection with the elevated plus maze (EPM), and at day 21 in the zero-maze (Z-maze), while depressive-like behavior was determined in the forced-swimming test (FST) on day 25. The latency to enter in the open arms **(B)**, and the percentage of time **(C)** and entries **(D)** to the open arms of the EPM showed no significant differences between groups. At day 21, no significant differences were observed in the latency to the open quadrants of the zero-maze **(E)**, whereas mice injected with MIA and treated with vehicle spent less time in the open parts **(F)**. This increase on late anxiety-like behavior was not modified by E-52862 treatment. **(G)** Mice with osteoarthritis pain receiving vehicle showed increased immobility time, which was reversed by E-52862 treatment. Data are expressed as mean  $\pm$  SEM ( $n = 6-8$  animals per group). For **(D)**: \*\*\* $p < 0.001$  for saline vs. MIA (two-way ANOVA). For **(E)**: \* $p < 0.05$  for saline – vehicle vs. MIA – vehicle, \*\* $p < 0.01$  for MIA – vehicle vs. MIA – E-52862 (two-way ANOVA). MIA, monosodium iodoacetate; SEM, standard error of the mean.

chronic pain model. Such correlation has also been described in higher order mammals with osteoarthritis pain (Haussler et al., 2007; Frost-Christensen et al., 2008; Moreau et al., 2011; Cake et al., 2013). Thus, the reduction of the paw print area and the maximal contact area parameters observed in our study in osteoarthritic mice were probably a consequence of an unwillingness of the animal to bear weight on the injured limb, while the normalization of such parameters after E-52862 treatment might be related to reduced pain perception. In agreement, the effect of E-52862 on the walking patterns of mice with osteoarthritis was not accompanied by

a normalization of the structural alterations observed in the histological assessments. This absence of effect on cartilage damage is in agreement with the low expression levels of  $\sigma$ 1R in chondrocytes and bone marrow when compared to its expression in the peripheral and central nervous system<sup>1,2</sup>. The relief of mechanical hypersensitivity and pain-associated comorbidities after the treatment with E-52862 coexisted with the cartilage degradation, in agreement with the widely recognized fact that the presence and severity of joint pain poorly correlates with structural joint damage in osteoarthritis patients (Lawrence et al., 1966; Dieppe, 2004). Thus, the pain-relieving

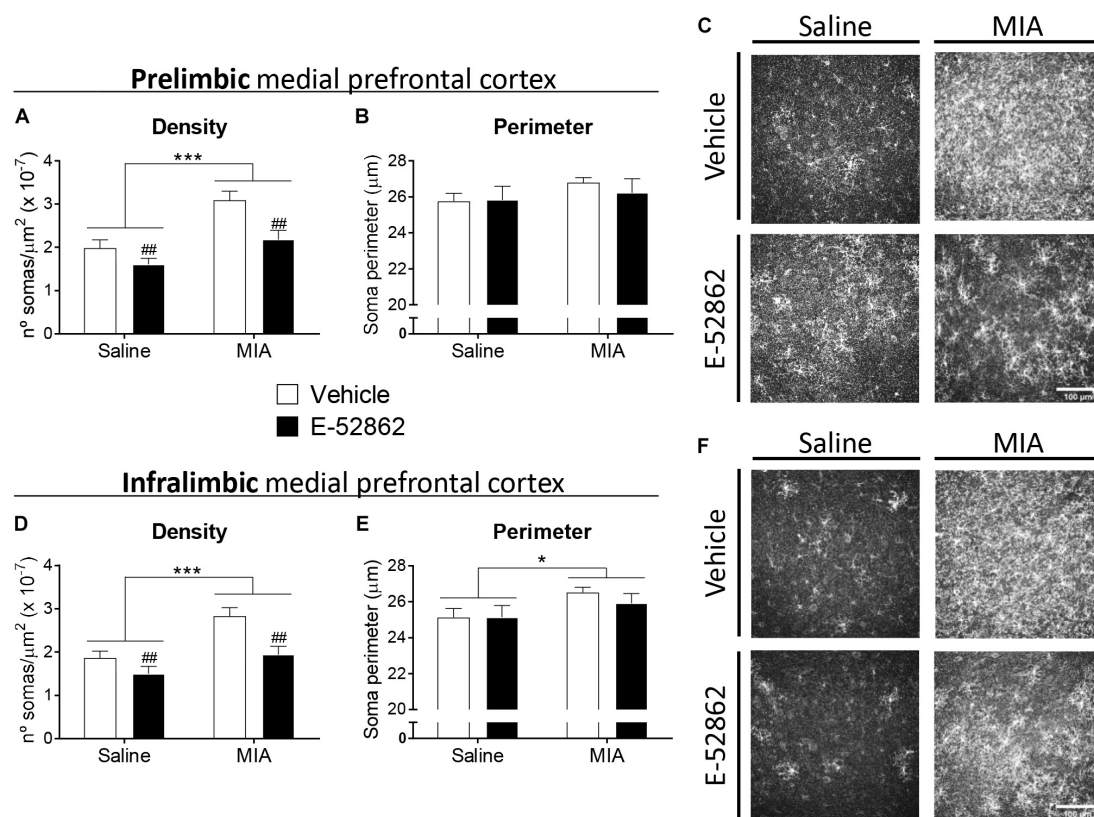


**FIGURE 5 |** E-52862 decreased pain-induced microgliosis in the medial prefrontal cortex. Microglial cells were detected in the prelimbic and infralimbic areas of the medial prefrontal cortex (mPFC) of saline and MIA injected mice after the repeated treatment with vehicle or the  $\sigma$ 1R antagonist E-52862 (20 mg/kg, twice daily during 25 days). Mice with osteoarthritis pain treated with vehicle showed an increased density of microglial cells in the prelimbic (**A**) and the infralimbic areas (**D**). This microgliosis was normalized by the treatment with E-52862 (**A,D**). MIA-injected mice revealed larger perimeters of the soma of microglial cells in the infralimbic (**E**), but not in the prelimbic area (**B**). Treatment with E-52862 did not modify this alteration (**E**). (**C,F**) Representative images of all groups are shown. Data are expressed as the mean  $\pm$  SEM ( $n = 7$  animals per group). Scale bar: 100  $\mu\text{m}$ . \* $p < 0.05$ , \*\*\* $p < 0.001$  for saline vs. MIA, <sup>##</sup> $p < 0.01$  for vehicle vs. E-52862 (two-way ANOVA). MIA, monosodium iodoacetate; SEM, standard error of the mean.

effects of the  $\sigma$ 1R antagonist probably rely on a modulatory role on the nervous system and are independent of the site of the primary lesion.

We observed a cognitive deficit associated to osteoarthritis induced by MIA, which was significantly reduced by the repeated administration of E-52862. Our result suggests that the blockade of  $\sigma$ 1R plays a protective role in this long-term memory impairment produced by chronic pain. Previous studies also showed impaired memory function in other chronic pain models (Zhao et al., 2006; Kodama et al., 2011) and specifically during MIA-induced joint pain (La Porta et al., 2015; Negrete et al., 2017). Selective  $\sigma$ 1R ligands failed to modify learning, consolidation or retention phases of the mnemonic process when administered to naïve animals (Hashimoto et al., 2007; Antonini et al., 2011), but  $\sigma$ 1R activation reduced cognitive deficits associated with schizophrenia (Hashimoto et al., 2007), Alzheimer disease (Maurice et al., 1998; Antonini et al., 2011) or scopolamine treatment (Hiramatsu et al., 2002). In contrast, we observed that  $\sigma$ 1R blockade reversed the memory impairment induced after MIA injection. The

overlap between the neuroanatomical substrates implicated in both pain control and cognitive functions provides information about the development of memory deficits in patients with chronic pain (Moriarty et al., 2011). However, the precise causal mechanisms underlying the pain-related cognitive impairment are still unclear, and the role of the  $\sigma$ 1R on this specific type of memory deficits has not been studied. Our data suggest that  $\sigma$ 1R antagonists are efficient improving cognitive functions under a chronic pain state.

We obtained increased anxiety-like responses after the intra-knee injection of MIA, as previously reported in other murine models of inflammatory (Schellinck et al., 2003; Chen et al., 2013) and neuropathic pain (Benbouzid et al., 2008; Matsuzawa-Yanagida et al., 2008; La Porta et al., 2016). Anxiety-like behavior was present 3 weeks after MIA, but not at earlier time points (11 days). Previous studies suggested that persistent pain may trigger alterations in brain areas involved in affective responses, which over time may lead to emotional comorbidities including anxiety and depressive-like behavior (Narita et al., 2006; Suzuki et al., 2007;

Seminowicz et al., 2009; Sellmeijer et al., 2018). In agreement, 25 days after the intra-knee injection of MIA depressive-like responses were observed in animals with osteoarthritis pain, as in previous studies investigating inflammatory and neuropathic pain (Hasnie et al., 2007; Suzuki et al., 2007; Norman et al., 2010; Negrete et al., 2017). Depressive-like responses were abolished after chronic administration of E-52862, although anxiety-like behavior was not modified with this  $\sigma$ 1R antagonist. These results are in line with previous works studying affective behavior in  $\sigma$ 1R knockout mice. In these studies,  $\sigma$ 1R knockouts exhibited increased immobility in the forced swimming test, but normal anxiety-like behavior (Sabino et al., 2009), suggesting distinct roles of the receptor modulating depressive and anxiety responses. Common neuroplastic changes associated with chronic pain and emotional disorders were proposed as important routes for the onset and reciprocal aggravation of both pathologies (Sheng et al., 2017). Consequently, analgesic drugs such as opioids (Mague et al., 2003; Tenore, 2008) or benzodiazepines (Vollenweider et al., 2011) have been proposed as a treatment for chronic pain-induced depression, and antidepressants like selective serotonin reuptake inhibitors (SSRIs) (Tasmuth et al., 2002; Gebhardt et al., 2016) or tricyclic antidepressants (Rowbotham et al., 2005; Kopsky and Keppel Hesselink, 2012) exhibited antinociceptive effects under chronic pain conditions. The interest of  $\sigma$ 1R ligands for the treatment of depressive states raised from the observation that several antidepressants had moderate to high affinity for  $\sigma$ 1R sites (Schmidt et al., 1989; Itzhak et al., 1991; Narita et al., 1996). While some SSRIs such as fluvoxamine or venlafaxine have shown agonism for  $\sigma$ 1R, others like sertraline may act as antagonists (Ishima et al., 2014). Moreover, the antidepressant efficacy of  $\sigma$ 1R ligands may depend on the affective status of the animal, since the selective  $\sigma$ 1R agonist PRE-084 reduced depressive-like behavior in adrenalectomized mice but lacked effect in naïve animals (Urani et al., 2001).

We observed an increased microgliosis in the medial prefrontal cortex produced by the injection of MIA. This result agrees with a previous study showing increases of microglial density in the infralimbic cortex of nerve-injured rats (Chu Sin Chung et al., 2017; Xu et al., 2017). Other brain areas such as the amygdala, periaqueductal gray (PAG) or hippocampus, have also shown increased gliosis during chronic pain conditions (Humo et al., 2019). Interestingly, a recent study on neuropathic pain showed enhanced expression of microglial markers in the prefrontal cortex accompanied by depressive-like behavior. Chronic minocycline attenuated both microglial activation and depressive-like responses (Xu et al., 2017). Previous studies have shown that the  $\sigma$ 1R antagonist BD1047 attenuated microglial activation in the spinal cord in a model of bone cancer pain (Zhu et al., 2015), but the effect of  $\sigma$ 1R on supraspinal microglia has not been assessed in chronic pain models. Our data show that  $\sigma$ 1R antagonist E-52862 significantly reduced the density of microglia in medial prefrontal cortices of mice with osteoarthritis pain. This effect was not accompanied by a reduction of anxiety-like behavior, suggesting that

this affective disturbance is not directly related to cortical microgliosis. However, these anatomical changes correlated with the cognitive performance and the depressive-like behavior, pointing toward an involvement of cortical microglia on both pain comorbidities. Therefore,  $\sigma$ 1R-regulated cortical microgliosis might be crucial for the manifestation of cognitive and emotional alterations often present in chronic pain conditions. Indeed, antidepressant drugs such as SSRIs also have activity modulating microgliosis and reducing microglial production of tumor necrosis factor  $\alpha$  and nitric oxide (Chung et al., 2011; Tynan et al., 2012). It is well known that  $\sigma$ 1R modulates several signal transduction pathways, including the production of ATP, reactive oxygen species or mitogen-activated protein kinases (MAPK) (Zamanillo et al., 2013; Hayashi, 2015; Zhao et al., 2017). All these molecules have been identified as effective signals for microglial migration and activation (Biber et al., 2007; Fan et al., 2017), suggesting an indirect modulatory role of  $\sigma$ 1R. In agreement,  $\sigma$ 1R activation by methamphetamine induces a microgliosis that involves generation of reactive oxygen species and activation of the MAPK pathway (Chao et al., 2017).

The present study reveals that E-52862 alleviates the nociceptive, cognitive and emotional manifestations associated to chronic osteoarthritis pain. We provide evidence showing that the effect of  $\sigma$ 1R over these manifestations of chronic pain is not associated to local changes in articular damage but is accompanied by modulation of microglial activity in the medial prefrontal cortex. Our data highlight the blockade of  $\sigma$ 1R as an interesting pharmacological strategy for the simultaneous management of multiple aspects of chronic osteoarthritis pain.

## ETHICS STATEMENT

All experimental procedures and animal husbandry were conducted following the ARRIVE (Animal Research: Reporting *In Vivo* Experiments) guidelines and according to the ethical principles of the International Association for the Study of Pain (I.A.S.P.) for the evaluation of pain in conscious animals (Zimmermann, 1986) and the European Parliament and the Council Directive (2010/63/EU), and were approved by the Animal Care and Use Committees of the PRBB and Departament de Territori i Habitatge of Generalitat de Catalunya.

## AUTHOR CONTRIBUTIONS

All authors listed have made a substantial, direct and intellectual contribution to the work, and approved it for publication.

## ACKNOWLEDGMENTS

We acknowledge the financial support of the European Commission (FP7, NeuroPain #2013-602891), the Catalan Government (AGAUR, #SGR2017-669), the Spanish Instituto

de Salud Carlos III (RTA, #RD16/0017/0020), and AGAUR (ICREA Academia Award 2015). MC is the recipient of an Industrial Doctorate contract from the Catalan Government and Laboratorios Esteve (AGAUR, #2014-DI-040). Partial support from FEDER funds is also acknowledged.

## REFERENCES

- Alonso, G., Phan, V., Guillemain, I., Saunier, M., Legrand, A., Anoa, M., et al. (2000). Immunocytochemical localization of the sigma(1) receptor in the adult rat central nervous system. *Neuroscience* 97, 155–170. doi: 10.1016/s0306-4522(00)00014-2
- Antonini, V., Marrazzo, A., Kleiner, G., Coradazzi, M., Ronsisvalle, S., Prezzavento, O., et al. (2011). Anti-amnesic and neuroprotective actions of the sigma-1 receptor agonist (-)-MR22 in rats with selective cholinergic lesion and amyloid infusion. *J. Alzheimers Dis.* 24, 569–586. doi: 10.3233/JAD-2011-101794
- Apkarian, A. V., Bushnell, M. C., Treede, R.-D., and Zubieta, J.-K. (2005). Human brain mechanisms of pain perception and regulation in health and disease. *Eur. J. Pain* 9, 463–463. doi: 10.1016/j.ejpain.2004.11.001
- Apkarian, A. V., Sosa, Y., Sonty, S., Levy, R. M., Harden, R. N., Parrish, T. B., et al. (2004). Chronic back pain is associated with decreased prefrontal and thalamic gray matter density. *J. Neurosci.* 24, 10410–10415. doi: 10.1523/JNEUROSCI.2541-04.2004
- Axford, J., Butt, A., Heron, C., Hammond, J., Morgan, J., Alavi, A., et al. (2010). Prevalence of anxiety and depression in osteoarthritis: use of the hospital anxiety and depression scale as a screening tool. *Clin. Rheumatol.* 29, 1277–1283. doi: 10.1007/s10067-010-1547-7
- Bangaru, M. L., Weihsrauch, D., Tang, Q.-B., Zoga, V., Hogan, Q., and Wu, H. (2013). Sigma-1 receptor expression in sensory neurons and the effect of painful peripheral nerve injury. *Mol. Pain* 9:47. doi: 10.1186/1744-8069-9-47
- Benbouzid, M., Pallage, V., Rajalu, M., Waltsperger, E., Doridot, S., Poisbeau, P., et al. (2008). Sciatic nerve cuffing in mice: a model of sustained neuropathic pain. *Eur. J. Pain* 12, 591–599. doi: 10.1016/j.ejpain.2007.10.002
- Biber, K., Neumann, H., Inoue, K., and Boddeke, H. W. G. M. (2007). Neuronal “On” and “Off” signals control microglia. *Trends Neurosci.* 30, 596–602. doi: 10.1016/j.tins.2007.08.007
- Boadas-Vaello, P., Homs, J., Reina, F., Carrera, A., and Verdú, E. (2017). Neuroplasticity of supraspinal structures associated with pathological pain. *Anat. Rec.* 300, 1481–1501. doi: 10.1002/ar.23587
- Boettger, M. K., Weber, K., Schmidt, M., Gajda, M., Bräuer, R., and Schaible, H.-G. (2009). Gait abnormalities differentially indicate pain or structural joint damage in monoarticular antigen-induced arthritis. *Pain* 145, 142–150. doi: 10.1016/j.pain.2009.06.006
- Cake, M. A., Read, R. A., Corfield, G., Daniel, A., Burkhardt, D., Smith, M. M., et al. (2013). Comparison of gait and pathology outcomes of three meniscal procedures for induction of knee osteoarthritis in sheep. *Osteoarthr. Cartil.* 21, 226–236. doi: 10.1016/j.joca.2012.10.001
- Castany, S., Gris, G., Vela, J. M., Verdú, E., and Boadas-Vaello, P. (2018). Critical role of sigma-1 receptors in central neuropathic pain-related behaviours after mild spinal cord injury in mice. *Sci. Rep.* 8:3873. doi: 10.1038/s41598-018-22217-9
- Chao, J., Zhang, Y., Du, L., Zhou, R., Wu, X., Shen, K., et al. (2017). Molecular mechanisms underlying the involvement of the sigma-1 receptor in methamphetamine-mediated microglial polarization. *Sci. Rep.* 7:11540. doi: 10.1038/s41598-017-11065-8
- Chaplan, S. R., Bach, F. W., Pogrel, J. W., Chung, J. M., and Yaksh, T. L. (1994). Quantitative assessment of tactile allodynia in the rat paw. *J. Neurosci. Methods* 53, 55–63. doi: 10.1016/0165-0270(94)90144-9
- Chen, J., Song, Y., Yang, J., Zhang, Y., Zhao, P., Zhu, X.-J., et al. (2013). The contribution of TNF-α in the amygdala to anxiety in mice with persistent inflammatory pain. *Neurosci. Lett.* 541, 275–280. doi: 10.1016/j.neulet.2013.02.005
- Chu Sin, Chung, P., Panigada, T., Cardis, R., Decosterd, I., and Gosselin, R.-D. (2017). Peripheral nerve injury induces a transitory microglial reaction in the rat infralimbic cortex. *Neurosci. Lett.* 655, 14–20. doi: 10.1016/j.neulet.2017.06.037
- Chung, Y. C., Kim, S. R., Park, J.-Y., Chung, E. S., Park, K. W., Won, S. Y., et al. (2011). Fluoxetine prevents MPTP-induced loss of dopaminergic neurons by inhibiting microglial activation. *Neuropharmacology* 60, 963–974. doi: 10.1016/j.neuropharm.2011.01.043
- Cruz, A. P., Frei, F., and Graeff, F. G. (1994). Ethopharmacological analysis of rat behavior on the elevated plus-maze. *Pharmacol. Biochem. Behav.* 49, 171–176. doi: 10.1016/0091-3057(94)90472-3
- Dieppe, P. A. (2004). Relationship between symptoms and structural change in osteoarthritis. What are the important targets for osteoarthritis therapy? *J. Rheumatol. Suppl.* 70, 50–53.
- Dixon, W. J. (1965). The up-and-down method for small samples. *J. Am. Stat. Assoc.* 60, 967–978. doi: 10.1080/01621459.1965.10480843
- Entrena, J. M., Cobos, E. J., Nieto, F. R., Cendán, C. M., Gris, G., Del Pozo, E., et al. (2009). Sigma-1 receptors are essential for capsaicin-induced mechanical hypersensitivity: Studies with selective sigma-1 ligands and sigma-1 knockout mice. *Pain* 143, 252–261. doi: 10.1016/j.pain.2009.03.011
- Etkin, A., Egner, T., and Kalisch, R. (2011). Emotional processing in anterior cingulate and medial prefrontal cortex. *Trends Cogn. Sci.* 15, 85–93. doi: 10.1016/j.tics.2010.11.004
- Fan, Y., Xie, L., and Chung, C. Y. (2017). Signaling pathways controlling microglia chemotaxis. *Mol. Cells* 40, 163–168. doi: 10.14348/molcells.2017.0011
- Ferland, C. E., Laverty, S., Beaudry, F., and Vachon, P. (2011). Gait analysis and pain response of two rodent models of osteoarthritis. *Pharmacol. Biochem. Behav.* 97, 603–610. doi: 10.1016/j.pbb.2010.11.003
- Ferreira-Gomes, J., Adães, S., Mendonça, M., and Castro-Lopes, J. M. (2012). Analgesic effects of lidocaine, morphine and diclofenac on movement-induced nociception, as assessed by the knee-bend and cat walk tests in a rat model of osteoarthritis. *Pharmacol. Biochem. Behav.* 101, 617–624. doi: 10.1016/j.pbb.2012.03.003
- File, S. E., Mabbutt, P. S., and Hitchcott, P. K. (1990). Characterisation of the phenomenon of “one-trial tolerance” to the anxiolytic effect of chlordiazepoxide in the elevated plus-maze. *Psychopharmacology* 102, 98–101. doi: 10.1007/bf02245751
- Francardo, V., Bez, F., Wieloch, T., Nissbrandt, H., Ruscher, K., and Cenci, M. A. (2014). Pharmacological stimulation of sigma-1 receptors has neurorestorative effects in experimental parkinsonism. *Brain* 137, 1998–2014. doi: 10.1093/brain/awu107
- Frost-Christensen, L. N., Mastbergen, S. C., Vianen, M. E., Hartog, A., DeGroot, J., Voorhout, G., et al. (2008). Degeneration, inflammation, regeneration, and pain/disability in dogs following destabilization or articular cartilage grooving of the stifle joint. *Osteoarthr. Cartil.* 16, 1327–1335. doi: 10.1016/j.joca.2008.03.013
- Gebhardt, S., Heinzel-Gutenbrunner, M., and König, U. (2016). Pain relief in depressive disorders. *J. Clin. Psychopharmacol.* 36, 658–668. doi: 10.1097/JCP.0000000000000604
- Gekker, G., Hu, S., Sheng, W. S., Rock, R. B., Lokensgard, J. R., and Peterson, P. K. (2006). Cocaine-induced HIV-1 expression in microglia involves sigma-1 receptors and transforming growth factor-beta1. *Int. Immunopharmacol.* 6, 1029–1033. doi: 10.1016/j.intimp.2005.12.005
- Glasson, S. S., Chambers, M. G., Van Den Berg, W. B., and Little, C. B. (2010). The OARSI histopathology initiative – recommendations for histological assessments of osteoarthritis in the mouse. *Osteoarthr. Cartil.* 18, S17–S23. doi: 10.1016/j.joca.2010.05.025
- Goldenberg, D. L. (2010). The interface of pain and mood disturbances in the rheumatic diseases. *Semin. Arthritis Rheum.* 40, 15–31. doi: 10.1016/j.semarthrit.2008.11.005
- Gris, G., Merlos, M., Vela, J. M., Zamanillo, D., and Portillo-Salido, E. (2014). SIRA, a selective sigma-1 receptor antagonist, inhibits inflammatory pain in the carrageenan and complete Freund’s adjuvant models in mice. *Behav. Pharmacol.* 25, 226–235. doi: 10.1097/FBP.0000000000000038

## SUPPLEMENTARY MATERIAL

The Supplementary Material for this article can be found online at: <https://www.frontiersin.org/articles/10.3389/fphar.2019.00468/full#supplementary-material>



- Gris, G., Portillo-Salido, E., Aubel, B., Darbaky, Y., Deseure, K., Vela, J. M., et al. (2016). The selective sigma-1 receptor antagonist E-52862 attenuates neuropathic pain of different aetiology in rats. *Sci. Rep.* 6:24591. doi: 10.1038/srep24591
- Gusnard, D. A., Akbudak, E., Shulman, G. L., and Raichle, M. E. (2001). Medial prefrontal cortex and self-referential mental activity: Relation to a default mode of brain function. *Proc. Natl. Acad. Sci. U.S.A.* 98, 4259–4264. doi: 10.1073/pnas.071043098
- Harada, Y., Hara, H., and Sukamoto, T. (1994). Receptor binding profiles of KB-5492, a novel anti-ulcer agent, at sigma receptors in guinea-pig brain. *Eur. J. Pharmacol.* 256, 321–328. doi: 10.1016/0014-2999(94)90558-4
- Hashimoto, K., Fujita, Y., and Iyo, M. (2007). Phencyclidine-induced cognitive deficits in mice are improved by subsequent subchronic administration of flunitrazepam: role of sigma-1 receptors. *Neuropsychopharmacology* 32, 514–521. doi: 10.1038/sj.npp.1301047
- Hasnie, F. S., Wallace, V. C. J., Hefner, K., Holmes, A., and Rice, A. S. C. (2007). Mechanical and cold hypersensitivity in nerve-injured C57BL/6J mice is not associated with fear-avoidance- and depression-related behaviour. *Br. J. Anaesth.* 98, 816–822. doi: 10.1093/bja/aem087
- Hausser, K. K., Hill, A. E., Frisbie, D. D., and McIlwraith, C. W. (2007). Determination and use of mechanical nociceptive thresholds of the thoracic limb to assess pain associated with induced osteoarthritis of the middle carpal joint in horses. *Am. J. Vet. Res.* 68, 1167–1176. doi: 10.2460/ajvr.68.11.1167
- Hayashi, T. (2015). Sigma-1 receptor: the novel intracellular target of neuropsychopharmacological drugs. *J. Pharmacol. Sci.* 127, 2–5. doi: 10.1016/j.jphs.2014.07.001
- Hayashi, T., and Su, T.-P. (2007). Sigma-1 receptor chaperones at the ER-mitochondrion interface regulate Ca(2+) signaling and cell survival. *Cell* 131, 596–610. doi: 10.1016/j.cell.2007.08.036
- Hayashi, T., Tsai, S.-Y., Mori, T., Fujimoto, M., and Su, T.-P. (2011). Targeting ligand-operated chaperone sigma-1 receptors in the treatment of neuropsychiatric disorders. *Expert Opin. Ther. Targets* 15, 557–577. doi: 10.1517/14728222.2011.560837
- Hiramatsu, M., Hoshino, T., Kameyama, T., and Nabeshima, T. (2002). Involvement of kappa-opioid and sigma receptors in short-term memory in mice. *Eur. J. Pharmacol.* 453, 91–98. doi: 10.1016/s0014-2999(02)02388-9
- Holmes, A., and Rodgers, R. J. (1998). Responses of swiss-webster mice to repeated plus-maze experience: further evidence for a qualitative shift in emotional state? *Pharmacol. Biochem. Behav.* 60, 473–488. doi: 10.1016/s0091-3057(98)00008-2
- Humo, M., Lu, H., and Yalcin, I. (2019). The molecular neurobiology of chronic pain-induced depression. *Cell Tissue Res.* [Epub ahead of print].
- Ishima, T., Fujita, Y., and Hashimoto, K. (2014). Interaction of new antidepressants with sigma-1 receptor chaperones and their potentiation of neurite outgrowth in PC12 cells. *Eur. J. Pharmacol.* 727, 167–173. doi: 10.1016/j.ejphar.2014.01.064
- Itzhak, Y., Stein, I., Zhang, S. H., Kassim, C. O., and Cristante, D. (1991). Binding of sigma-ligands to C57BL/6 mouse brain membranes: effects of monoamine oxidase inhibitors and subcellular distribution studies suggest the existence of sigma-receptor subtypes. *J. Pharmacol. Exp. Ther.* 257, 141–148.
- Johnson, V. L., and Hunter, D. J. (2014). The epidemiology of osteoarthritis. *Best Pract. Res. Clin. Rheumatol.* 28, 5–15. doi: 10.1016/j.berh.2014.01.004
- Kitaichi, K., Chabot, J. G., Moebius, F. F., Flandorfer, A., Glossmann, H., and Quirion, R. (2000). Expression of the purported sigma(1) (sigma(1)) receptor in the mammalian brain and its possible relevance in deficits induced by antagonism of the NMDA receptor complex as revealed using an antisense strategy. *J. Chem. Neuroanat.* 20, 375–387. doi: 10.1016/s0891-0618(00)00106-x
- Kodama, D., Ono, H., and Tanabe, M. (2011). Increased hippocampal glycine uptake and cognitive dysfunction after peripheral nerve injury. *Pain* 152, 809–817. doi: 10.1016/j.pain.2010.12.029
- Kopsky, D. J., and Keppel Hesselink, J. M. (2012). High doses of topical amitriptyline in neuropathic pain: two cases and literature review. *Pain Pract.* 12, 148–153. doi: 10.1111/j.1533-2500.2011.00477.x
- La Porta, C., Bura, S. A., Llorente-Onandia, J., Pastor, A., Navarrete, F., García-Gutiérrez, M. S., et al. (2015). Role of the endocannabinoid system in the emotional manifestations of osteoarthritis pain. *Pain* 156, 2001–2012. doi: 10.1097/j.pain.0000000000000260
- La Porta, C., Lara-Mayorga, I. M., Negrete, R., and Maldonado, R. (2016). Effects of pregabalin on the nociceptive, emotional and cognitive manifestations of neuropathic pain in mice. *Eur. J. Pain* 20, 1454–1466. doi: 10.1002/ejp.868
- Lawrence, J. S., Bremner, J. M., and Bier, F. (1966). Osteo-arthritis. Prevalence in the population and relationship between symptoms and x-ray changes. *Ann. Rheum. Dis.* 25, 1–24. doi: 10.1136/annrheumdis00506-0006
- Lucas, G., Rymar, V. V., Sadikot, A. F., and Debonnel, G. (2008). Further evidence for an antidepressant potential of the selective sigma1 agonist SA 4503: electrophysiological, morphological and behavioural studies. *Int. J. Neuropsychopharmacol.* 11, 485–495. doi: 10.1017/S1461145708008547
- Mague, S. D., Pliakas, A. M., Todtenkopf, M. S., Tomasiewicz, H. C., Zhang, Y., Stevens, W. C., et al. (2003). Antidepressant-like effects of kappa-opioid receptor antagonists in the forced swim test in rats. *J. Pharmacol. Exp. Ther.* 305, 323–330. doi: 10.1124/jpet.102.046433
- Matsumoto, R. R., McCracken, K. A., Pouw, B., Zhang, Y., and Bowen, W. D. (2002). Involvement of sigma receptors in the behavioral effects of cocaine: evidence from novel ligands and antisense oligodeoxynucleotides. *Neuropharmacology* 42, 1043–1055. doi: 10.1016/s0028-3908(02)00056-4
- Matsuzawa-Yanagida, K., Narita, M., Nakajima, M., Kuzumaki, N., Niikura, K., Nozaki, H., et al. (2008). Usefulness of antidepressants for improving the neuropathic pain-like state and pain-induced anxiety through actions at different brain sites. *Neuropsychopharmacology* 33, 1952–1965. doi: 10.1038/sj.npp.1301590
- Maurice, T., Martin-Fardon, R., Romieu, P., and Matsumoto, R. R. (2002). Sigma(1) (sigma(1)) receptor antagonists represent a new strategy against cocaine addiction and toxicity. *Neurosci. Biobehav. Rev.* 26, 499–527. doi: 10.1016/s0149-7634(02)00017-9
- Maurice, T., Su, T. P., and Privat, A. (1998). Sigma1 (sigma 1) receptor agonists and neurosteroids attenuate B25-35-amyloid peptide-induced amnesia in mice through a common mechanism. *Neuroscience* 83, 413–428. doi: 10.1016/s0306-4522(97)00405-3
- Metz, A. E., Yau, H.-J., Centeno, M. V., Apkarian, A. V., and Martina, M. (2009). Morphological and functional reorganization of rat medial prefrontal cortex in neuropathic pain. *Proc. Natl. Acad. Sci. U.S.A.* 106, 2423–2428. doi: 10.1073/pnas.0809897106
- Moreau, M., Rialland, P., Pelletier, J.-P., Martel-Pelletier, J., Lajeunesse, D., Boileau, C., et al. (2011). Tiludronate treatment improves structural changes and symptoms of osteoarthritis in the canine anterior cruciate ligament model. *Arthritis Res. Ther.* 13:R98. doi: 10.1186/ar3373
- Moriarty, O., and Finn, D. P. (2014). Cognition and pain. *Curr. Opin. Support. Palliat. Care* 8, 130–136. doi: 10.1097/SPC.0000000000000054
- Moriarty, O., McGuire, B. E., and Finn, D. P. (2011). The effect of pain on cognitive function: A review of clinical and preclinical research. *Prog. Neurobiol.* 93, 385–404. doi: 10.1016/j.pneurobio.2011.01.002
- Moritz, C., Berardi, F., Abate, C., and Peri, F. (2015). Live imaging reveals a new role for the sigma-1 (σ1) receptor in allowing microglia to leave brain injuries. *Neurosci. Lett.* 591, 13–18. doi: 10.1016/j.neulet.2015.02.004
- Narita, M., Kuzumaki, N., Narita, M., Kaneko, C., Hareyama, N., Miyatake, M., et al. (2006). Chronic pain-induced emotional dysfunction is associated with astrogliosis due to cortical delta-opioid receptor dysfunction. *J. Neurochem.* 97, 1369–1378. doi: 10.1111/j.1471-4159.2006.03824.x
- Narita, N., Hashimoto, K., Tomitaka, S., and Minabe, Y. (1996). Interactions of selective serotonin reuptake inhibitors with subtypes of sigma receptors in rat brain. *Eur. J. Pharmacol.* 307, 117–119. doi: 10.1016/0014-2999(96)00254-3
- Negrete, R., García Gutiérrez, M. S., Manzanares, J., and Maldonado, R. (2017). Involvement of the dynorphin/KOR system on the nociceptive, emotional and cognitive manifestations of joint pain in mice. *Neuropharmacology* 116, 315–327. doi: 10.1016/j.neuropharm.2016.08.026
- Nieto, F. R., Cendán, C. M., Sánchez-Fernández, C., Cobos, E. J., Entrena, J. M., Tejada, M. A., et al. (2012). Role of sigma-1 receptors in paclitaxel-induced neuropathic pain in mice. *J. Pain* 13, 1107–1121. doi: 10.1016/j.jpain.2012.08.006
- Norman, G. J., Karelina, K., Zhang, N., Walton, J. C., Morris, J. S., and DeVries, A. C. (2010). Stress and IL-1β contribute to the development of depressive-like behavior following peripheral nerve injury. *Mol. Psychiatry* 15, 404–414. doi: 10.1038/mp.2009.91

- Panigada, T., and Gosselin, R.-D. (2011). Behavioural alteration in chronic pain: Are brain glia involved? *Med. Hypotheses* 77, 584–588. doi: 10.1016/j.mehy.2011.06.036
- Peviani, M., Salvaneschi, E., Bontempi, L., Petese, A., Manzo, A., Rossi, D., et al. (2014). Neuroprotective effects of the Sigma-1 receptor (S1R) agonist PRE-084, in a mouse model of motor neuron disease not linked to SOD1 mutation. *Neurobiol. Dis.* 62, 218–232. doi: 10.1016/j.nbd.2013.10.010
- Phelps, E. A., Delgado, M. R., Nearing, K. I., and LeDoux, J. E. (2004). Extinction learning in humans. *Neuron* 43, 897–905. doi: 10.1016/j.neuron.2004.08.042
- Porsolt, R. D., Bertin, A., and Jalfre, M. (1977). Behavioral despair in mice: a primary screening test for antidepressants. *Arch. Int. Pharmacodyn. Ther.* 229, 327–336.
- Puighermanal, E., Marsicano, G., Busquets-Garcia, A., Lutz, B., Maldonado, R., and Ozaita, A. (2009). Cannabinoid modulation of hippocampal long-term memory is mediated by mTOR signaling. *Nat. Neurosci.* 12, 1152–1158. doi: 10.1038/nn.2369
- Puig-Junoy, J., and Ruiz Zamora, A. (2015). Socio-economic costs of osteoarthritis: a systematic review of cost-of-illness studies. *Semin. Arthritis Rheum.* 44, 531–541. doi: 10.1016/j.semarthrit.2014.10.012
- Racz, I., Nadal, X., Alferink, J., Banos, J. E., Rehnelt, J., Martin, M., et al. (2008). Crucial role of CB2 cannabinoid receptor in the regulation of central immune responses during neuropathic pain. *J. Neurosci.* 28, 12125–12135. doi: 10.1523/JNEUROSCI.3400-08.2008
- Romero, L., Zamanillo, D., Nadal, X., Sánchez-Arroyos, R., Rivera-Arconada, I., Dordal, A., et al. (2012). Pharmacological properties of S1RA, a new sigma-1 receptor antagonist that inhibits neuropathic pain and activity-induced spinal sensitization. *Br. J. Pharmacol.* 166, 2289–2306. doi: 10.1111/j.1476-5381.2012.01942.x
- Rowbotham, M. C., Reisner, L. A., Davies, P. S., and Fields, H. L. (2005). Treatment response in antidepressant-naïve postherpetic neuralgia patients: double-blind, randomized trial. *J. Pain* 6, 741–746. doi: 10.1016/j.jpain.2005.07.001
- Sabino, V., Cottone, P., Parylak, S. L., Steardo, L., and Zorrilla, E. P. (2009). Sigma-1 receptor knockout mice display a depressive-like phenotype. *Behav. Brain Res.* 198, 472–476. doi: 10.1016/j.bbr.2008.11.036
- Saravia, R., Ten-Blanco, M., Grande, M. T., Maldonado, R., and Berrendero, F. (2019). Anti-inflammatory agents for smoking cessation? Focus on cognitive deficits associated with nicotine withdrawal in male mice. *Brain. Behav. Immun.* 75, 228–239. doi: 10.1016/j.bbi.2018.11.003
- Schellinck, H. M., Stanford, L., and Darrah, M. (2003). Repetitive acute pain in infancy increases anxiety but does not alter spatial learning ability in juvenile mice. *Behav. Brain Res.* 142, 157–165. doi: 10.1016/s0166-4328(02)00406-0
- Schmidt, A., Lebel, L., Koe, B. K., Seeger, T., and Heym, J. (1989). Sertraline potently displaces (+)-[3H]3-PPP binding to sigma sites in rat brain. *Eur. J. Pharmacol.* 165, 335–336. doi: 10.1016/0014-2999(89)90734-6
- Sellmeijer, J., Mathis, V., Hugel, S., Li, X.-H., Song, Q., Chen, Q.-Y., et al. (2018). Hyperactivity of anterior cingulate cortex areas 24a/24b drives chronic pain-induced anxiodepressive-like consequences. *J. Neurosci.* 38, 3102–3115. doi: 10.1523/JNEUROSCI.3195-17.2018
- Seminowicz, D. A., Laferriere, A. L., Millicamps, M., Yu, J. S. C.,Coderre, T. J., and Bushnell, M. C. (2009). MRI structural brain changes associated with sensory and emotional function in a rat model of long-term neuropathic pain. *Neuroimage* 47, 1007–1014. doi: 10.1016/j.neuroimage.2009.05.068
- Seminowicz, D. A., Wideman, T. H., Naso, L., Hatami-Khoroushahi, Z., Fallatah, S., Ware, M. A., et al. (2011). Effective treatment of chronic low back pain in humans reverses abnormal brain anatomy and function. *J. Neurosci.* 31, 7540–7550. doi: 10.1523/JNEUROSCI.5280-10.2011
- Sharma, A., Kudesia, P., Shi, Q., and Gandhi, R. (2016). Anxiety and depression in patients with osteoarthritis: impact and management challenges. *Open Access Rheumatol.* 8, 103–113. doi: 10.2147/OARRR.S93516
- Sheng, J., Liu, S., Wang, Y., Cui, R., and Zhang, X. (2017). The link between depression and chronic pain: neural mechanisms in the brain. *Neural Plast.* 2017:9724371. doi: 10.1155/2017/9724371
- Shepherd, J. K., Grewal, S. S., Fletcher, A., Bill, D. J., and Dourish, C. T. (1994). Behavioural and pharmacological characterisation of the elevated "zero-maze" as an animal model of anxiety. *Psychopharmacology* 116, 56–64. doi: 10.1007/bf02244871
- Skuza, G., and Rogóz, Z. (2003). Sigma1 receptor antagonists attenuate antidepressant-like effect induced by co-administration of 1,3 di-otolylguanidine (DTG) and memantine in the forced swimming test in rats. *Pol. J. Pharmacol.* 55, 1149–1152.
- Su, T.-P., and Hayashi, T. (2003). Understanding the molecular mechanism of sigma-1 receptors: towards a hypothesis that sigma-1 receptors are intracellular amplifiers for signal transduction. *Curr. Med. Chem.* 10, 2073–2080. doi: 10.2174/0929867033456783
- Sutton, S., Clutterbuck, A., Harris, P., Gent, T., Freeman, S., Foster, N., et al. (2009). The contribution of the synovium, synovial derived inflammatory cytokines and neuropeptides to the pathogenesis of osteoarthritis. *Vet. J.* 179, 10–24. doi: 10.1016/j.tvjl.2007.08.013
- Suzuki, T., Amata, M., Sakaue, G., Nishimura, S., Inoue, T., Shibata, M., et al. (2007). Experimental neuropathy in mice is associated with delayed behavioral changes related to anxiety and depression. *Anesth. Analg.* 104, 1570–1577. doi: 10.1213/01.ane.0000261514.19946.66
- Tasmuth, T., Härtel, B., and Kalso, E. (2002). Venlafaxine in neuropathic pain following treatment of breast cancer. *Eur. J. Pain* 6, 17–24. doi: 10.1053/eujp.2001.0266
- Tejada, M. A., Montilla-García, A., Sánchez-Fernández, C., Entrena, J. M., Perazzoli, G., Baeyens, J. M., et al. (2014). Sigma-1 receptor inhibition reverses acute inflammatory hyperalgesia in mice: role of peripheral sigma-1 receptors. *Psychopharmacology* 231, 3855–3869. doi: 10.1007/s00213-014-3524-3
- Tenore, P. L. (2008). Psychotherapeutic benefits of opioid agonist therapy. *J. Addict. Dis.* 27, 49–65. doi: 10.1080/10550880802122646
- Tsai, S.-Y., Hayashi, T., Mori, T., and Su, T.-P. (2009). Sigma-1 receptor chaperones and diseases. *Cent. Nerv. Syst. Agents Med. Chem.* 9, 184–189. doi: 10.2174/1871524910909030184
- Tynan, R. J., Weidenhofer, J., Hinwood, M., Cairns, M. J., Day, T. A., and Walker, F. R. (2012). A comparative examination of the anti-inflammatory effects of SSRI and SNRI antidepressants on LPS stimulated microglia. *Brain Behav. Immun.* 26, 469–479. doi: 10.1016/j.bbi.2011.12.011
- Urani, A., Roman, F. J., Phan, V. L., Su, T. P., and Maurice, T. (2001). The antidepressant-like effect induced by sigma(1)-receptor agonists and neuroactive steroids in mice submitted to the forced swimming test. *J. Pharmacol. Exp. Ther.* 298, 1269–1279.
- Villemure, C., and Bushnell, M. C. (2009). Mood influences supraspinal pain processing separately from attention. *J. Neurosci.* 29, 705–715. doi: 10.1523/JNEUROSCI.3822-08.2009
- Vollenweider, I., Smith, K. S., Keist, R., and Rudolph, U. (2011). Antidepressant-like properties of α2-containing GABAA receptors. *Behav. Brain Res.* 217, 77–80. doi: 10.1016/j.bbr.2010.10.009
- Vrinten, D. H., and Hamers, F. F. T. (2003). “CatWalk” automated quantitative gait analysis as a novel method to assess mechanical allodynia in the rat; a comparison with von Frey testing. *Pain* 102, 203–209. doi: 10.1016/s0304-3959(02)00382-2
- Xu, N., Tang, X.-H., Pan, W., Xie, Z.-M., Zhang, G.-F., Ji, M.-H., et al. (2017). Spared nerve injury increases the expression of microglia M1 markers in the prefrontal cortex of rats and provokes depression-like behaviors. *Front. Neurosci.* 11:209. doi: 10.3389/fnins.2017.0209
- Zamanillo, D., Romero, L., Merlos, M., and Vela, J. M. (2013). Sigma 1 receptor: a new therapeutic target for pain. *Eur. J. Pharmacol.* 716, 78–93. doi: 10.1016/j.ejphar.2013.01.068
- Zhang, R.-X., Ren, K., and Dubner, R. (2013). Osteoarthritis pain mechanisms: basic studies in animal models. *Osteoarthritis Cartil.* 21, 1308–1315. doi: 10.1016/j.joca.2013.06.013
- Zhao, J., Mysona, B. A., Wang, J., Gonsalvez, G. B., Smith, S. B., and Bollinger, K. E. (2017). Sigma 1 receptor regulates ERK activation and promotes survival of optic nerve head astrocytes. *PLoS One* 12:e0184421. doi: 10.1371/journal.pone.0184421

- Zhao, M.-G., Ko, S. W., Wu, L.-J., Toyoda, H., Xu, H., Quan, J., et al. (2006). Enhanced presynaptic neurotransmitter release in the anterior cingulate cortex of mice with chronic pain. *J. Neurosci.* 26, 8923–8930. doi: 10.1523/JNEUROSCI.2103-06.2006
- Zhu, S., Wang, C., Han, Y., Song, C., Hu, X., and Liu, Y. (2015). Sigma-1 receptor antagonist BD1047 reduces mechanical allodynia in a rat model of bone cancer pain through the inhibition of spinal NR1 phosphorylation and microglia activation. *Med. Inflamm.* 2015, 1–11. doi: 10.1155/2015/265056
- Zimmermann, M. (1986). Ethical considerations in relation to pain in animal experimentation. *Acta Physiol. Scand. Suppl.* 554, 221–233.

**Conflict of Interest Statement:** The authors declare that the research was conducted in the absence of any commercial or financial relationships that could be construed as a potential conflict of interest.

The handling Editor declared a past co-authorship with several of the authors.

Copyright © 2019 Carcolé, Zamanillo, Merlos, Fernández-Pastor, Cabañero and Maldonado. This is an open-access article distributed under the terms of the Creative Commons Attribution License (CC BY). The use, distribution or reproduction in other forums is permitted, provided the original author(s) and the copyright owner(s) are credited and that the original publication in this journal is cited, in accordance with accepted academic practice. No use, distribution or reproduction is permitted which does not comply with these terms.



# Anti-tumor Efficacy Assessment of the Sigma Receptor Pan Modulator RC-106. A Promising Therapeutic Tool for Pancreatic Cancer

## OPEN ACCESS

### Edited by:

Tanguy Maurice,  
INSERM U1198 Mécanismes  
Moléculaires dans les Démences  
Neurodégénératives, France

### Reviewed by:

Franck Borgese,  
INSERM U1091 Institut de Biologie  
de Valrose, France  
Elia Ranzato,  
University of Eastern Piedmont, Italy

### \*Correspondence:

Anna Tesei  
anna.tesei@irst.emr.it  
Simona Collina  
simona.collina@unipv.it

† These authors have contributed  
equally to this work

### Specialty section:

This article was submitted to  
Experimental Pharmacology  
and Drug Discovery,  
a section of the journal  
Frontiers in Pharmacology

**Received:** 22 January 2019

**Accepted:** 17 April 2019

**Published:** 14 May 2019

### Citation:

Tesei A, Cortesi M, Pignatta S,  
Arienti C, Dondio GM, Bigogno C,  
Malacrida A, Miloso M, Meregalli C,  
Chiorazzi A, Carozzi V, Cavaletti G,  
Rui M, Marra A, Rossi D and Collina S  
(2019) Anti-tumor Efficacy  
Assessment of the Sigma Receptor  
Pan Modulator RC-106. A Promising  
Therapeutic Tool for Pancreatic  
Cancer. *Front. Pharmacol.* 10:490.  
doi: 10.3389/fphar.2019.00490

Anna Tesei<sup>1\*†</sup>, Michela Cortesi<sup>1†</sup>, Sara Pignatta<sup>1</sup>, Chiara Arienti<sup>1</sup>,  
Giulio Massimo Dondio<sup>2</sup>, Chiara Bigogno<sup>2</sup>, Alessio Malacrida<sup>3</sup>, Mariarosaria Miloso<sup>3</sup>,  
Cristina Meregalli<sup>3</sup>, Alessia Chiorazzi<sup>3</sup>, Valentina Carozzi<sup>3</sup>, Guido Cavaletti<sup>3</sup>, Marta Rui<sup>4</sup>,  
Annamaria Marra<sup>4</sup>, Daniela Rossi<sup>4</sup> and Simona Collina<sup>4\*</sup>

<sup>1</sup> Biosciences Laboratory, Istituto Scientifico Romagnolo per lo Studio e la Cura dei Tumori (IRCCS), Meldola, Italy, <sup>2</sup> Aphad S.r.l., Milan, Italy, <sup>3</sup> Experimental Neurology Unit, School of Medicine and Surgery, Milan Center for Neuroscience, University of Milano-Bicocca, Monza, Italy, <sup>4</sup> Department of Drug Sciences, Medicinal Chemistry and Pharmaceutical Technology Section, University of Pavia, Pavia, Italy

**Introduction:** Pancreatic cancer (PC) is one of the most lethal tumor worldwide, with no prognosis improvement over the past 20-years. The silent progressive nature of this neoplasia hampers the early diagnosis, and the surgical resection of the tumor, thus chemotherapy remains the only available therapeutic option. Sigma receptors (SRs) are a class of receptors proposed as new cancer therapeutic targets due to their over-expression in tumor cells and their involvement in cancer biology. The main localization of these receptors strongly suggests their potential role in ER unfolded protein response (ER-UPR), a condition frequently occurring in several pathological settings, including cancer. Our group has recently identified **RC-106**, a novel pan-SR modulator with good *in vitro* antiproliferative activities toward a panel of different cancer cell lines. In the present study, we investigated the *in vitro* properties and pharmacological profile of **RC-106** in PC cell lines with the aim to identify a potential lead candidate for the treatment of this tumor.

**Methods:** Pancreatic cancer cell lines Panc-1, Capan-1, and Capan-2 have been used in all experiments. S1R and TMEM97/S2R expression in PC cell lines was quantified by Real-Time qRT-PCR and Western Blot experiments. MTS assay was used to assess the antiproliferative effect of **RC-106**. The apoptotic properties of **RC-106** was evaluated by TUNEL and caspase activation assays. GRP78/BiP, ATF4, and CHOP was quantified to evaluate ER-UPR. Proteasome activity was investigated by a specific fluorescent-based assay. Scratch wound healing assay was used to assess **RC-106** effect on cell migration. In addition, we delineated the *in vivo* pharmacokinetic profile and pancreas distribution of **RC-106** in male CD-1 mice.

**Results:** Panc-1, Capan-1, and Capan-2 express both SRs. **RC-106** exerts an antiproliferative and pro-apoptotic effect in all examined cell lines. Cells exposure to



**RC-106** induces the increase of the expression of ER-UPR related proteins, and the inhibition of proteasome activity. Moreover, **RC-106** is able to decrease PC cell lines motility. The *in vivo* results show that **RC-106** is more concentrated in pancreas than plasma.

**Conclusion:** Overall, our data evidenced that the pan-SR modulator **RC-106** is an optimal candidate for *in vivo* studies in animal models of PC.

**Keywords:** Pancreatic cancer, pan-sigma receptor modulators, endoplasmic reticulum stress, unfolded protein response, proteasome inhibition

## INTRODUCTION

Pancreatic cancer remains one of the most lethal tumor types for both men and women and, it represents the 11th most common cancer worldwide (Ilic and Ilic, 2016). WCRF reported that in 2018 there were 460,000 new cases, which mainly affected developed countries (Weledji et al., 2016). For this type of tumor, beneficial pharmaceutical approaches result challenging to develop, since the etiology as well as the triggering factors associated with PC remain undefined (Kim and Ahuja, 2015). Relying on the negative prognosis – the average 5-year survival rate is 6% or less (Siegel et al., 2014) – and on the lack of a concrete cure, PC urgently requires effective therapeutic strategies.

Over the past few decades, SRs, have been widely associated with aging- and mitochondria-associated disorders, such as Parkinson's and Alzheimer's disease and cancer (Martin et al., 1976; Su, 1982; Vaupel, 1983; Quirion et al., 1987; Maurice and Lockhart, 1997; Skuza, 2003; Peviani et al., 2014; Collina et al., 2017a,b). Moreover, although no endogenous SRs ligands have ever been found, and the specific role played by this orphan receptor family in cell biology has yet to be clarified, SRs are considered as potential therapeutic targets for neurodegenerative diseases and cancer. Accumulating evidence strongly suggests a pivotal role of these proteins in ER-UPR pathways, whose activation is frequently detected in many solid tumors (Shuda et al., 2003; Corazzari et al., 2017). In particular, the triggering of the UPR machinery in cancer is the result of neoplastic cells spreading in unfavorable environments characterized by hypoxia, low pH, high levels of ROS and inadequate glucose and amino acid supply, conditions that could compromise the correct ER protein folding. Under such stress conditions, SRs are activated to allow the cells survival, as broadly demonstrated by the direct

involvement of S1R in UPR pathways (Hayashi, 2015; Penke et al., 2017). The decrease of  $\text{Ca}^{++}$  ion level in ER, the accumulation of misfolded or aggregated protein within the ER, the rise of ROS level due to stress conditions promote the exit of S1R from a dormant state and its activation as chaperon protein. Accordingly, the correct  $\text{Ca}^{++}$  signaling from the ER to the mitochondria, the transmission of the ER stress signal to the nucleus and the consequent increase of antistress and antioxidant proteins production are guaranteed (Hayashi and Su, 2007; Mori et al., 2013; Wang et al., 2015).

Only recently S2R has been cloned and its identity as TMEM97 has been postulated (Alon et al., 2017). TMEM97 is a transmembrane protein involved in cholesterol homeostasis, and its dysregulation has been associated to ER stress and to activation of the UPR, thus causing cellular lipid accumulation (Colgan et al., 2011). Notably, UPR is classically related to the maintenance of cellular homeostasis in secretory cells (i.e., pancreatic and immune cells), where the high demand for protein synthesis and secretion leads to proteostasis and cellular stress (Hetz, 2012; Moore and Hollien, 2012). Indeed, pancreatic cells have high hormone and enzyme secretory functions and possess highly developed ER. The role of ER stress in PC pathobiology and inflammation has been increasingly recognized as an important factor in tumorigenesis and chemoresistance (Yadav et al., 2014). Nonetheless, PC is extremely rich in stroma, is hypoxic and deficient in metabolites (Vasseur et al., 2010). A similar behavior can be found when cells grow under chronic metabolic stress conditions, favoring the activation of adaptive mechanisms, such as UPR and autophagy (Kondo et al., 2005; Moenner et al., 2007) the latter frequently associated to SR overexpression (Zeng et al., 2012; Mir et al., 2013). Altogether, these findings pointed out SRs as potential targets useful for inhibiting UPR machinery in PC.

Our research team is active in the SR modulation and recently we identified compound **RC-106** endowed with pan-SR modulatory activity (S1R antagonist and S2R agonist profile) and *in vitro* antiproliferative properties toward a panel of cancer cell lines (i.e., Capan-2, MDA-MB 231, PC3, and U87) (Rui et al., 2016; Rossi et al., 2017). These encouraging results led us to further investigate its potential in PC treatment. After preparing **RC-106** in a suitable amount to support the whole study, we deepened its antitumor properties and evaluated its capability to interfere with ER stress conditions. Lastly preliminary PK and biodistribution studies have been performed, to verify if **RC-106** is able to reach the target tissue.

**Abbreviations:** ATCC, American Type Culture Collection; ATF4, activating transcription factor 4; CHOP, C/EBP homologous protein; CTR, control; DMSO, dimethyl sulfoxide; ER, endoplasmic reticulum; ESI, electrospray ionization; FC, flash chromatography; FITC, fluorescein isothiocyanate; GAPDH, glyceraldehyde 3-phosphate dehydrogenase; GRP78, 78-kDa glucose regulated protein; HPRT-1, hypoxanthine phosphoribosyltransferase 1; IS, internal standard; LC, liquid chromatography; MAM, mitochondria associated ER membrane; M-PER, Mammalian Protein Extraction Reagent; MRM, multiple reaction monitoring; MS, mass spectrometry; NMR, nuclear magnetic resonance; OD, optical density; PBS, phosphate buffered saline; PC, Pancreatic cancer; PK, pharmacokinetic; QC, quality control; RCCS, rotary cell culture system; ROS, reactive oxygen species; S1R, sigma 1 receptor; S2R, sigma 2 receptor; SD, standard deviation; SRs, sigma receptors; TdT, terminal deoxynucleotidyl transferase; TLC, thin layer chromatography; TMEM97, transmembrane protein 97; UFLC, ultra-fast liquid chromatography; UPLC, ultra performance liquid chromatography; UPR, unfolded protein response; UV, ultraviolet; WCRF, World Cancer Research Fund.

## MATERIALS AND METHODS

### RC-106 Synthesis

Reagents and solvents for synthesis were obtained from Sigma-Aldrich (Italy). Solvents were purified according to the guidelines in Purification of Laboratory Chemicals. Melting points were measured on SMP3 Stuart Scientific apparatus and are uncorrected. For FT-IR analysis a Spectrum One PerkinElmer spectrophotometer equipped with a MIRacle™ ATR device was used. The IR spectra were scanned over wavenumber range of 4000–650  $\text{cm}^{-1}$  with a resolution of 4  $\text{cm}^{-1}$ . Analytical thin-layer chromatography (TLC) was carried out on silica gel precoated glass backed plates (Fluka Kieselgel 60 F254, Merck); visualized by UV radiation, acidic ammonium molybdate (IV), or potassium permanganate. FC was performed with Silica Gel 60 (particle size 230e400 mesh, purchased from Merck). Proton NMR spectra were recorded on Bruker Avance 400 spectrometer operating at 400 MHz.  $^{13}\text{C}$  NMR spectra were recorded on 500 MHz spectrometer, operating at 125 MHz, with complete proton decoupling. UPLC-UV-ESI/MS analyses were carried out on a Acquity UPLC Waters LCQ FLEET system using an ESI source operating in positive ion mode, controlled by ACQUITY PDA and 4 MICRO (Waters). Analyses were run on a ACQUITY BEH C18 (50 mm  $\times$  2.1 mm, 1.7 mm) column, at room temperature, with gradient elution (solvent A: water containing 0.1% of formic acid; solvent B: methanol containing 0.1% of formic acid; gradient: 10% B in A to 100% B in 3 min, followed by isocratic elution 100% B for 1.5 min, return to the initial conditions in 0.2 min) at a flow rate of 0.5  $\text{mL min}^{-1}$ . Detailed synthetic procedure and characterization of intermediates and RC-106 are reported in the **Supplementary Material**.

### Cell Cultures

#### 2D Cell Culture

Pancreatic adenocarcinoma Panc-1, Capan-1, and Capan-2, cell lines were purchased by the ATCC. All cell lines were grown in culture medium composed of DMEM/Ham's F12 (1:1; Euroclone) supplemented with fetal calf serum (10%; Euroclone), glutamine (2 mM; Euroclone), and insulin (10  $\mu\text{g/mL}$ ; Sigma-Aldrich, St. Louis, MO, United States). All experiments were performed on cells in the exponential growth phase and checked periodically for mycoplasma contamination by MycoAlert™ Mycoplasma Detection Kit (Lonza, Basel, Switzerland).

#### 3D-Cell Culture

Spheroids were obtained as previously described (Zanoni et al., 2016). Briefly, a rotatory cell culture system RCCS (Synthecon Inc., Houston, TX, United States) was used. The rotary systems were placed inside a humidified 37°C, 5%  $\text{CO}_2$  incubator and all procedures were performed in sterile conditions. Single cell suspensions of about  $1 \times 10^6$  cells/ml of Panc-1 were placed in the 50 mL rotating chamber at an initial speed of 12 rpm. Speed was increased as cells formed aggregates to avoid sedimentation. The culture medium was changed every 4 days and tumor spheroids with an equivalent diameter ranging from about 500–1300  $\mu\text{m}$

were obtained in around 15 days. After formation, spheroids were transferred into a 96-well low-attachment culture plates (Corning Inc., Corning, NY, United States; one spheroid/well), containing 100  $\mu\text{L}$  of fresh culture medium per well.

### Cell Viability Assays

#### MTS Assay

Cytotoxicity was assayed using CellTiter 96® AQueous One Solution Cell Proliferation Assay (Promega, Milan, Italy). Cells were seeded onto a 96-well plate at a density of  $3 \times 10^3$  cells per well. Cell lines were exposed to increasing concentrations of the drug, ranging from 0.1 to 100  $\mu\text{M}$ . The effect of the drug was evaluated after 24, 48, and 72 h of continued exposure. Two independent experiments were performed in octuplicate. The OD of treated and untreated cells was determined at a wavelength of 490 nm using a fluorescence plate reader.

Dose response curves were created by Excel software.  $\text{IC}_{50}$  values were determined graphically from the plot.

#### CellTiter-Glo® 3D

Cell viability of Panc-1 spheroids was measured using a 3D cell viability assay (Promega, Milan, Italy). Briefly, homogeneous spheroids were removed from the 96-well low-attachment culture plate and placed separately in single wells of a 96-well opaque culture plate (BD Falcon). CellTiter-Glo® 3D reagent was added to each well and the luminescence signal was read after 30 min with the GloMax® bioluminescent reader (Promega).

### Analysis of Morphological Parameters of 3D Tumor Spheroids

The analysis of morphological parameters were performed as previously described (Piccinini et al., 2017). Briefly, an inverted Olympus IX51 microscope (Olympus Corporation, Tokyo, Japan), equipped with a Nikon Digital Sight DS-Vi1 camera (CCD vision sensor, square pixels of 4.4  $\mu\text{m}$  side length, 1600  $\times$  1200 pixel resolution, 8-bit gray level; Nikon Instruments, Spa. Florence, Italy) was used to take images and for morphological analyses. The open-source ReViSM software tools was used to achieve morphological 3D, such as volume and sphericity, and to select morphologically homogeneous spheroids. For the experiments, Panc-1 spheroids characterized by spherical shape and by a diameter size ranging from 500 to 600  $\mu\text{m}$  were selected.

### Real Time RT-PCR

Total cellular RNA was extracted using TRIzol reagent (Life technologies) in accordance with manufacturer's instruction and quantified using the Nanodrop MD-1000 spectrophotometer system. Reverse transcription reactions were performed in 20  $\mu\text{L}$  of nuclease free water containing 400 ng of total RNA using iScript cDNA Synthesis kit (Bio-Rad Laboratories, Hercules, CA). Real-Time PCR was run using 7500 Fast Real-Time PCR system (Applied Biosystems) and TaqMan assays to detect the expression of SIGMAR1, TMEM97, GRP78/BiP, ATF4, and CHOP genes.

Reactions were carried out in triplicate at a final volume of 20  $\mu\text{L}$  containing 40 ng of cDNA template, TaqMan universal PCR Master Mix (2X), and selected TaqMan assays (20X).

Samples were maintained at 50°C for 2 min, then at 95°C for 10 min followed by 40 amplification cycles at 95°C for 15 s, and at 60°C for 30 s.

The amount of mRNA was normalized to the endogenous genes GAPDH and HPRT-1.

## TUNEL Assay

TUNEL assay was performed as previously described (Tesei et al., 2007). Briefly, cells were fixed in 1% formaldehyde in PBS on ice for 15 min, suspended in 70% ice cold ethanol and stored overnight at 20°C. Cells were then washed twice in PBS and re-suspended in PBS containing 0.1% Triton X-100 for 5 min at 48°C. Thereafter, samples were incubated in 50 µL of solution containing TdT and FITC conjugated dUTP deoxynucleotides 1:1 (Roche Diagnostic GmbH, Mannheim, Germany) in a humidified atmosphere for 90 min at 37°C in the dark, washed in PBS, counterstained with propidium iodide (2.5 µg/mL, MP Biomedicals, Verona, Italy) and RNase (10 kU/mL, Sigma-Aldrich) for 30 min at 48°C in the dark and analyzed by flow cytometry. Flow cytometric analysis was performed using a FACS Canto flow cytometer (Becton Dickinson, San Diego, CA, United States). Data acquisition and analysis were performed using FACSDiva software (Becton Dickinson). Samples were run in triplicate and 10,000 events were collected for each replicate.

## Western Blot

Western Blot were performed as previously described (Arienti et al., 2016). Briefly, Cell proteins were extracted with M-PER (Thermo Fisher Scientific) supplemented with Halt Protease Phosphatase Inhibitor Cocktail (Thermo Fisher Scientific).

Mini-PROTEANTGX<sup>TM</sup> precast gels (4–20% and any kD; BIO-RAD) were run using Mini-PROTEAN Tetra electrophoresis cells and then electroblotted by Trans-Blot Turbo<sup>TM</sup> Mini PVDF Transfer Packs (BIORAD). The unoccupied membrane sites were blocked with T-TBS 1X (Tween 0.1%) and 5% non-fat dry milk to prevent non-specific binding of antibodies and probed with specific primary antibodies overnight at 4°C. This was followed by incubation with the respective secondary antibodies. The antibody-antigen complexes were detected with Immun-Star<sup>TM</sup> WesternC<sup>TM</sup> kit (BIO-RAD).

The following primary antibodies were used: anti-sigma receptor (S18): sc-22948 (Santa Cruz Biotechnology inc.), anti-TMEM97, anti-caspase-3, and anti-caspase-9. Anti-vinculin (sc-5573) from Santa Cruz Biotechnology and anti-actin from Sigma Aldrich Inc., were used as housekeeping. Quantity One Software was used for analysis.

## Proteasome Activity Assay

Cells were seeded in 6-well plates at density of  $250 \times 10^3$  cells/well. Cells were treated with increasing concentration of RC-106 and after 24 h total protein extracts were obtained: cells were washed 2 times with PBS and lysed with 100 µL of lysis buffer (Hepes 5 mM pH 7.5, NaCl 150 mM, Glycerol 10%, Triton X100 1%, MgCl<sub>2</sub> 1.5 mM, EGTA 5 mM). Protein concentration of samples was quantified using Bradford method. Proteasome activity was quantified as described below.

Proteasome solution was composed by 40 µg of proteins, 10 µL of 10X proteasome buffer (Hepes pH 7.5 250 mM, EDTA pH 8.0 5 mM, NP-40 0.5%, SDS 0.01%) and 10 µL of 10 mM proteasome substrate (N-Succinyl-Leu-Leu-Val-Tyr-7-Amido-4-Methylcoumarin, 7.6 mg/mL; Sigma-Aldrich, United States). 100 µL of proteasome solution was loaded in wells of a black 96-well plate. The plate was then incubated at 37°C for 2 h and the fluorescence was measured in a microplate reader (excitation 380 nm, emission 460 nm; BMG-Labtech, Germany).

## Migration Scratch Wound Healing Assay

Cells were seeded in a 6-well plate and were incubated at 37°C until confluence of 90–100% was reached. Culture medium was then replaced by serum free medium. After 24 h, a scratch was made on cell monolayer using a plastic tip and wells were washed 2 times with PBS to remove detached cells and debris. Culture medium, with or without RC-106, was added to each well. Micrographs of the scratches were taken at 0 h, immediately after the scratch, and at 24, 48, and 72 h. Cell migration area was quantified using IMAGEJ software.

## Pharmacokinetic and Pancreas Distribution Studies

### Animals and Biological Matrix Preparation

The experiments were performed in agreement with the Italian Law D. L.vo 4 marzo 2014, n. 26. The treatments involved male CD-1 mice and a unique number on the tail identified each animal. Mice were housed, in groups of four, in cages suitable for the species. After 5 days of adaptation to the local housing conditions, animals were housed in a single, exclusive, air-conditioned room to provide a minimum of 15 air changes/hour. The environmental controls were set to maintain the temperature at around 22°C and the relative humidity within the range 50 to 60%, along with an approximate 12:12 h light/dark cycle automatically controlled. Food (Mucedola Standard GLP diet) and water were available *ad libitum* throughout the entire duration of the study. All animals were weighted on the day of the treatment.

Mice ( $n = 4/\text{time point}$ ) received an intraperitoneal administration (i.p., 10 mL/kg) of RC-106 at 10 mg/kg. CD-1 male mice were exsanguinated under anesthesia (isoflurane) from the aorta at the following time points: 5, 10, 30, 120, 240, and 480 min. Blood samples were collected in tubes containing heparin, gently mixed and immediately placed on ice. Afterward, they have been centrifuged ( $3500 \times g$ , at 4°C for 15 min), the obtained plasma has been collected and transferred to individually labeled tubes and frozen at  $-20^\circ\text{C}$  until the analysis. Plasma samples were used for quantification of RC-106. Pancreas was taken by surgical resection after 20 min from the last treatment, washed in saline, dried on paper, weighted and frozen at  $-20^\circ\text{C}$ . The organ was homogenized using a Velp OV5 homogenizer with 20 mM ammonium formate buffer in a ratio of 1 g of tissue per 10 mL of buffer.

### Sample Preparation

20 mg/mL stock solution (s.s.) of RC-106 was prepared by dissolving the compound in DMSO. 1 mL of 5% Tween80 in H<sub>2</sub>O



was slowly added to 500  $\mu\text{L}$  of s.s. under stirring. Then 8.5 mL of water was gently spiked to obtain the 1 mg/mL formulation of **RC-106**.

Standard curves of **RC-106** were prepared for plasma and pancreas homogenate, and analyzed together with each QC and unknown sample set. For the PK and pancreas distribution sample analysis, plasma and pancreas homogenate samples (50  $\mu\text{L}$ ) were spiked in 200  $\mu\text{L}$  of IS in MeOH (0.1  $\mu\text{g/mL}$  of **RC-33**), followed by 2 min vortex mixing. Samples were centrifuged and transferred in UFLC vials. 5  $\mu\text{L}$  aliquots of the collected samples were injected into the LC-MS/MS system. Standard calibration graphs were constructed by linear least-squares regression analysis on the analyte/IS area ratio plotted against sample concentration. Calibration ranges were from 5 to 1000 ng/mL for plasma, and from 5 to 500 ng/mL for pancreas homogenate. Accuracy values were determined in triplicates at three different concentrations (high, medium, and low) in the range of linearity of the calibration curves.

### LC-MS/MS Conditions

Analyses were acquired on a Shimadzu AC20 UFLC system interfaced with an API 3200 Triple Quadrupole detector (AB Sciex). Data acquisition and control were performed using the Analyst<sup>TM</sup> 6.1 (Applied Biosystems) Software. A Phenomenex Gemini-NX C18 (50 mm  $\times$  2 mm, 5  $\mu\text{m}$ ) column was selected to carry out the analytical evaluations. A gradient method was set up (**Supplementary Table S1**) and it provided the employment of water and methanol, both containing 0.1% of formic acid, at a flow rate of 0.3 mL/min. The LC eluate was directly introduced into the MS interface using the ESI in the positive ion mode. The MRM transitions  $m/z$  181.2 were tracked (**Supplementary Table S2**).

## RESULTS

### Chemistry

We studied an easy to handle synthetic route suitable to dispose of **RC-106** in a g-scale amount. The synthetic route is outlined in **Scheme 1**. Briefly, a Heck reaction between 4-bromobiphenyl and

(*E*)-ethyl crotonate, using Palladium acetate microencapsulated in polyurea matrix (Pd EnCat<sup>®</sup>) as catalyst allowed to obtain the  $\alpha,\beta$ -unsaturated ester (*E*)-**1** which was easily reduced to give allyl alcohol (*E*)-**2**, and then converted into **RC-106** according to Frøyen and Juvvik (1995). The use of Pd EnCat<sup>®</sup> simplified the work-up procedure and more important avoided the heavy metal contamination of the product, which could compromise the *in vitro* and *in vivo* studies.

### Cell Biology

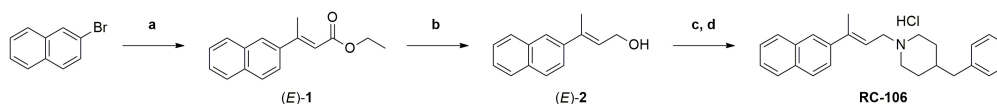
#### SRs Expression in Pancreatic Adenocarcinoma

We explored the expression of S1R and TMEM97/S2R genes in a panel of cell lines representative of pancreatic adenocarcinoma. The expression of S1R and TMEM97/S2R was evaluated in cells derived both from primary tumor and metastatic site (i.e., liver), characterized by different doubling time and different mutational status of p53, KRAS, P16/CDKN2A, and SMAD 4 (**Table 1**), the major driver-genes involved in the pathogenesis of PC (Sipos et al., 2003).

The expression level of SRs was determined by Real-Time qRT-PCR. We used cervix adenocarcinoma HeLa as reference sample, because of its high expression of both S1R and TMEM97/S2R (Bartz et al., 2009; Ebrahimi-Fakhari et al., 2015; Miki et al., 2015). All analyzed cell lines express SRs and no correlation between the tumor site and the expression level of both targets, as well as respect to the mutational status of p53 and KRAS was evidenced. In particular, S1R was expressed at similar levels in the PC cell lines. Conversely, differences about the expression of TMEM97/S2R have been evidenced in the three cell lines investigated, with the highest expression in Capan-1 (4-fold respect to the control line) and the lowest in Capan-2 cells (**Figure 1**). Basing on these results, we took into account the three cell lines to perform the biological evaluation.

#### *In vitro* Cytotoxic Activity

We evaluated the *in vitro* cytotoxic activity of **RC-106** by MTS assay. Cells were treated for 24, 48, and 72 h with increasing concentrations, ranging from 0.1 to 100  $\mu\text{M}$ . **RC-106** was effective in all cell lines tested independently from the exposure time (IC<sub>50</sub> values ranging from 33 to 57  $\mu\text{M}$ , **Figure 2A**).



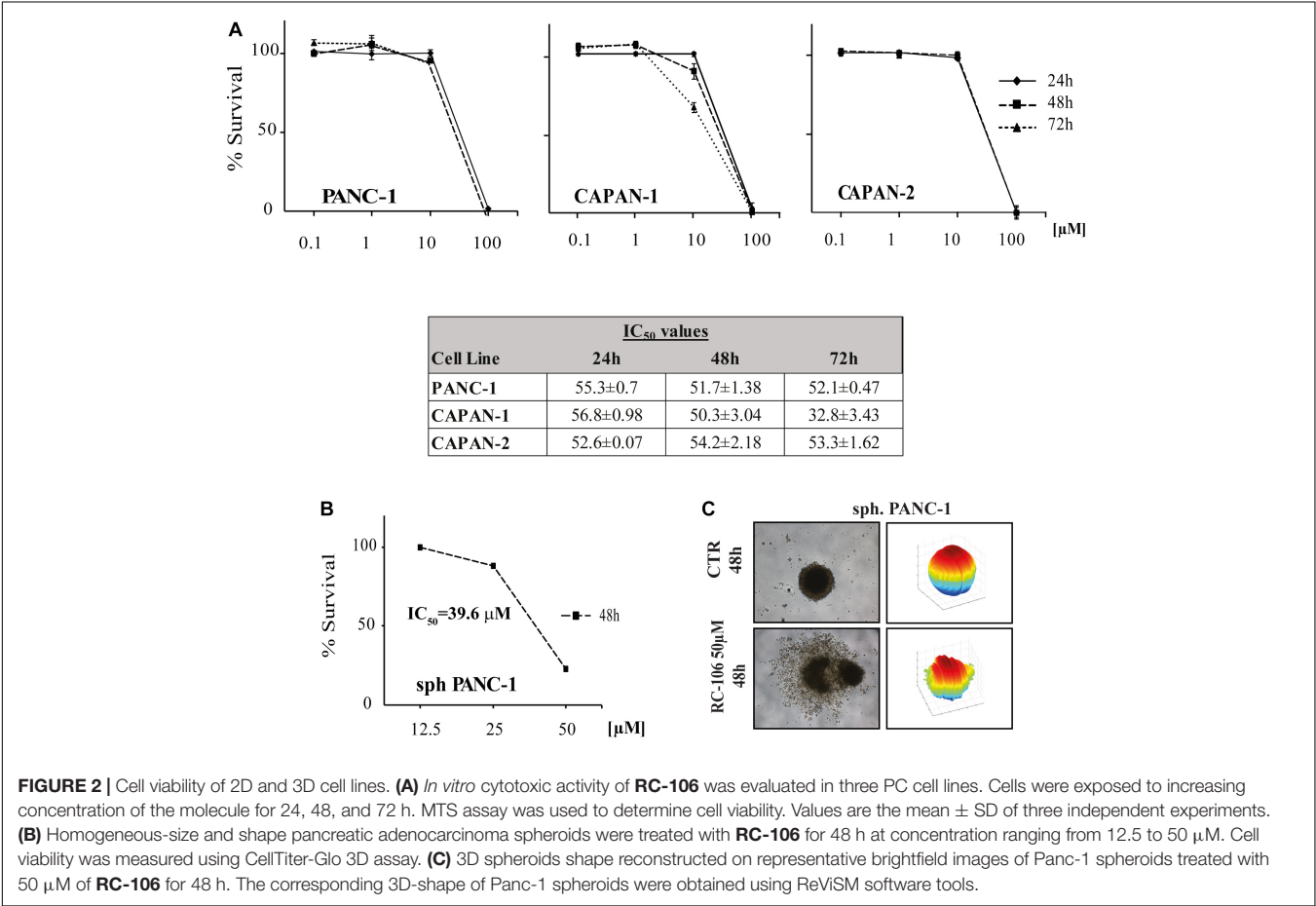
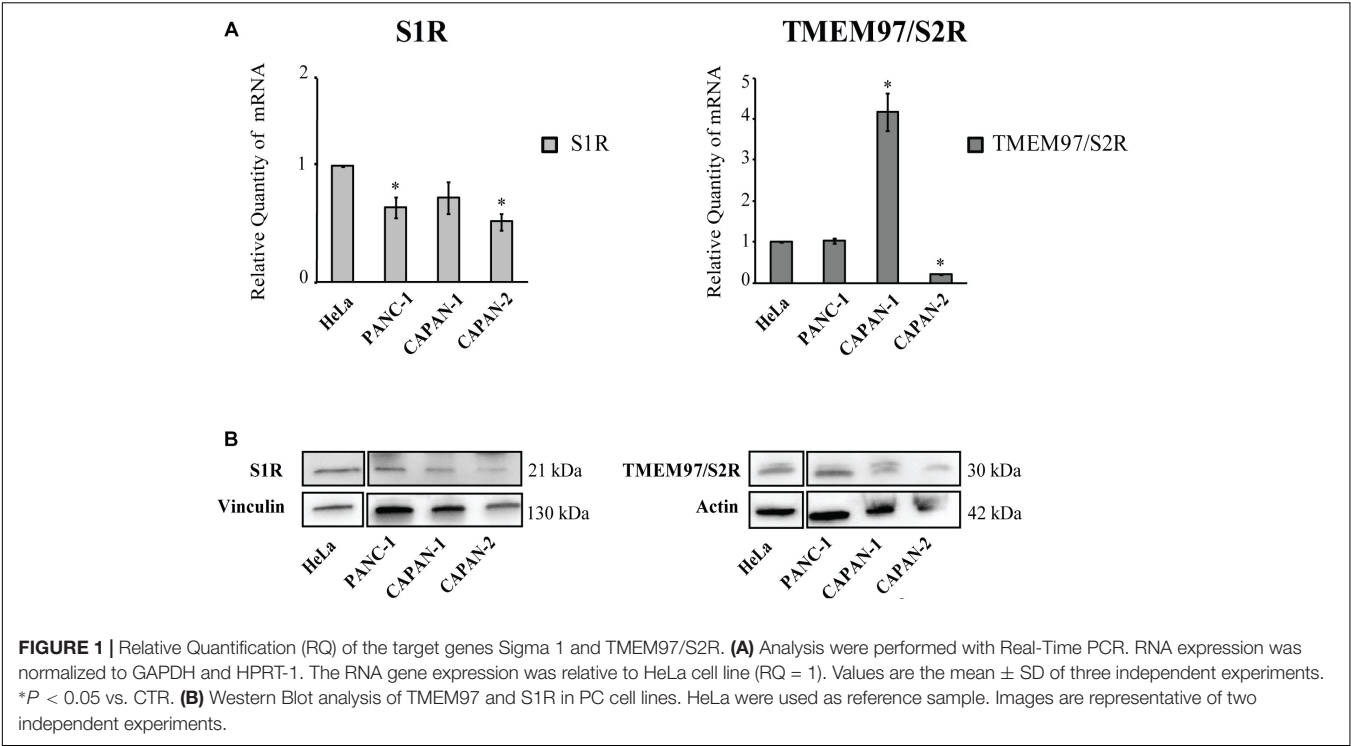
**SCHEME 1** | Synthesis of **RC-106**. Reagents and conditions: **(a)** (*E*)-ethyl crotonate, Pd EnCat<sup>®</sup> 40, TEAC, NaOAc, DMF anhydrous, N<sub>2</sub> atm., 105°C; **(b)** LiAlH<sub>4</sub> (1M in THF), Et<sub>2</sub>O anhydrous, N<sub>2</sub> atm., 0°C; **(c)** Ph<sub>3</sub>P, NBS, N<sub>2</sub>, -15/18°C; **(d)** 4-benzylpiperidine, Et<sub>3</sub>N, N<sub>2</sub> atm., from -15/–18°C to r.t.

**TABLE 1** | Pancreatic ductal adenocarcinoma cell lines characterization.

	Site	Doubling time	p53	KRAS	P16/CDKN2A	SMAD 4
Panc-1	Primary tumor	52 h	Mut	Mut	Mut	WT
Capan-1	Liver metastasis	38 h	Mut	Mut	Mut	Mut
Capan-2	Primary tumor	96 h	WT	Mut	Mut	N.d

All cell lines were purchased from ATCC.





Encouraged by these results, we investigated the capability of **RC-106** to penetrate three dimensional structures mimicking tumor micronodules of about 500–600  $\mu\text{m}$  in diameter. Panc-1 cells grown as 3D spheroids were treated with increasing concentrations of **RC-106** (12.5–50  $\mu\text{M}$  for 48 h, **Figure 2B**). The results obtained with Panc-1 spheroids with a diameter up to 600  $\mu\text{m}$  ( $\text{IC}_{50}$  = 39.55  $\mu\text{M}$ , **Figures 2B,C**) are in line with those observed in 2D culture.

### Pro-apoptotic Effect

The apoptotic properties of **RC-106** was evaluated by TUNEL assay. The exposure time (48 h) and the drug concentration (50  $\mu\text{M}$ ) have been chosen according to the data resulting from cell viability assay. TUNEL assay showed a significant induction of apoptosis in treated samples compared to the untreated controls, with a percentage of apoptotic cells ranging from 53.25%  $\pm$  4.7 (Panc-1) to 78.55%  $\pm$  5.6 (Capan-1) (**Figure 3A**). Hence, we investigated the activation of caspase cascade by Western Blot analysis, treating cells with **RC-106** at different exposure times. We found that both caspases 3 and 9 were cleaved, in all cell lines after the treatment, indicating the activation of the intrinsic apoptotic pathway. To sum up, **RC-106** was able to activate both caspases in all the considered cell lines,

but after different exposure times and concentrations. In detail, in Panc-1 and Capan-2 cell lines this event occurred after an exposure of 48 h to **RC-106** at 25  $\mu\text{M}$  concentration, whereas in Capan-1 cell line after 12 h at 50  $\mu\text{M}$  concentration (**Figure 3B**).

### ER Stress and Unfolded Protein Response

The expression of the ER stress master proteins GRP78/BiP, ATF4, and CHOP, commonly used for the detection of UPR activation (Samali et al., 2010), was analyzed by Real-Time qRT-PCR. In general, the mRNA expression of all the investigated ER markers highly increased after the exposure to 50  $\mu\text{M}$  of **RC-106**. In the two cell lines derived from primitive pancreatic tumor, Panc-1 and Capan-2, the trend is similar. In particular, GRP78/BiP and ATF4 mRNA levels increased after 24 h of treatment, while CHOP mRNA levels considerably increased after 12 h, then slightly declined after 24 h (**Figure 4A**). The highest increase in expression of CHOP was individuated in Capan-2 (70 fold higher than untreated cells). A different behavior was observed for the metastatic cell line Capan-1, where a faster switch-off of all ER markers was evidenced already starting from 12 h after the beginning of treatment.

All the cell lines were treated with increasing concentrations of **RC-106** (20–100  $\mu\text{M}$ ) to evaluate *in vitro* **RC-106** proteasome

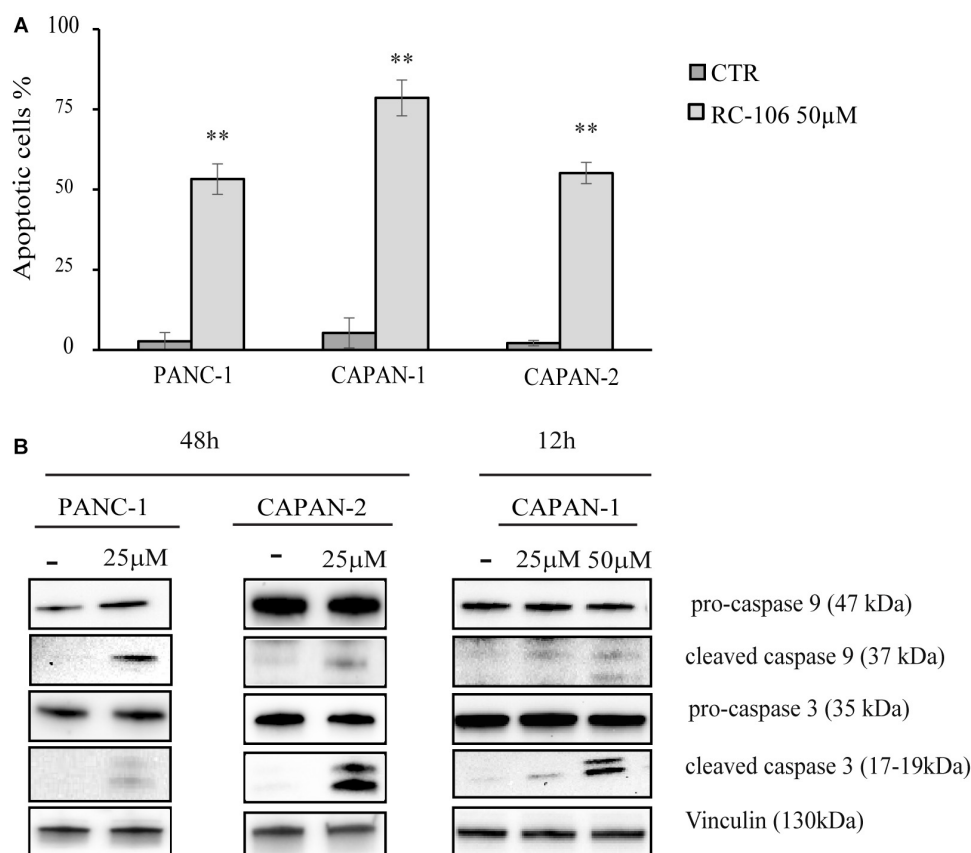


**FIGURE 3 |** Apoptosis analysis. **(A)** TUNEL assay performed on Panc-1, Capan-1, and Capan-2 cell lines. Cells were treated with **RC-106** 50  $\mu\text{M}$  for 48 h. Values are the mean  $\pm$  SD of three independent experiments. **\*\*** $P$  < 0.01 vs. CTR. **(B)** Western Blot analysis of caspase 3 and 9 activation after 48 h treatment with **RC-106** 25  $\mu\text{M}$  (Panc-1 and Capan-2) and after 12 h treatment with **RC-106** 50  $\mu\text{M}$  (Capan-1). Images are representative of two independent experiments.

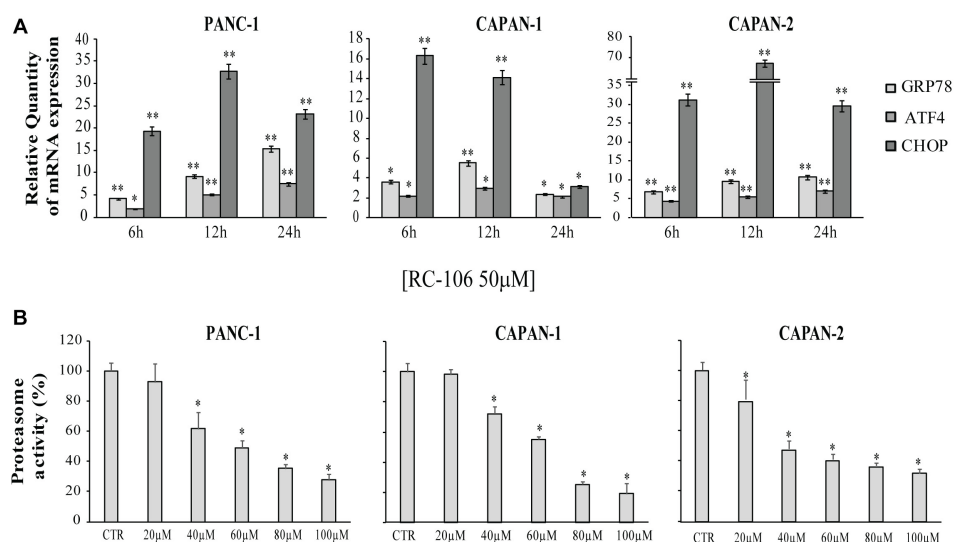


**FIGURE 4 |** Relative Quantification (RQ) of the ER stress and UPR marker genes. **(A)** GRP78, ATF4, and CHOP mRNA expression levels were measured after a treatment with **RC-106** 50 μM for 6, 12, and 24 h. Analysis were performed with Real-Time PCR. RNA expression was normalized to GAPDH and HPRT-1. In each time point tested the RNA gene expression was relative to the corresponding untreated control (RQ = 1). Values are the mean ± SD of three independent experiments. (\* $P < 0.05$  vs. CTR; \*\* $P < 0.01$  vs. CTR). **(B)** Graphs represent the proteasome activity of PANC-1, Capan-1, and Capan-2, treated with increasing concentration of **RC-106** (20–100 μM) for 24 h. Data are expressed as the average percentage ± SD of at least three independent experiments and are compared to untreated controls (CTR 100%; \* $P < 0.05$  vs. CTR).

effect. After 24 h of treatment, **RC-106** was able to reduce proteasome activity in a dose dependent manner in all the PC investigated (**Figure 4B**). Capan-2 resulted the most sensible cell line as showed by the lowest concentration used to inhibit proteasome activity (20 μM). Instead the greatest proteasome inhibition is observed in Capan-1 cells but at highest concentration used (100 μM).

### Cell Migration

Scratch wound healing assay was performed to assess the effect of **RC-106** on cell migration. After the scratch, cells were treated with increasing concentration of **RC-106** (20–60 μM) and cell migration was evaluated after 24, 48, and 72 h. Capan-1 untreated cells migrated normally to refill the scratch present on cell monolayer. Cell migration was significantly reduced after 48 h

of treatment with **RC-106** ( $c = 20$  μM). Conversely, **RC-106** at concentrations of 40 and 60 μM reduced cell migration already after 24 h of treatment, whereas at major times these concentrations resulted too toxic, promoting cellular death. Capan-2 untreated cells migrated normally and continued to fill the empty space of the scratch for all considered times. **RC-106** 20 and 40 μM significantly reduced Capan-2 cells migration ability after 48 and 72 h of treatment. **RC-106** 60 μM is too toxic and, as for Capan-1 cells, it was not possible to quantify cell migration inhibition at 48 and 72 h. Panc-1 untreated cells migrated only for the first 24 h, then they slow down and stop migration. **RC-106** reduced Panc-1 cell migration in a dose dependent manner, but only in cells treated with 60 μM, migration was significantly reduced for all considered time points (**Figure 5**).

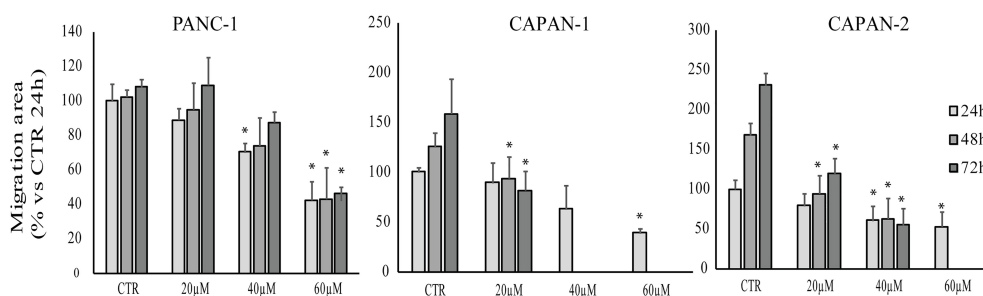


**FIGURE 5 |** Effect of **RC-106** on Capan-1, Capan-2, and Panc-1 cell migration. Migration area of cells was quantified after 24, 48, and 72 h of treatment with increasing concentrations of **RC-106** (20–60 μM). Data are expressed as the average percentage ± SD of at least three independent experiments and are compared to controls (CTR, 100%; \* $P < 0.05$  vs. respective CTR).

## In vivo Pharmacokinetic and Pancreas Distribution Studies

We investigated the *in vivo* PK profile and pancreas distribution of **RC-106** in male CD-1 mice. Basing on our experience, we developed a rapid and sensitive UFLC-MS/MS method for detecting and quantifying **RC-106** in biological matrices (Rossi et al., 2013; Marra et al., 2016a,b). Briefly, chromatographic elutions were achieved on a reverse phase column and eluting under a gradient conditions (**Supplementary Table S1**). LC eluates were directly introduced into the MS interface using the ESI source and detected in positive ion mode (**Supplementary Table S2**). According to the structure of **RC-106**, parent ion  $m/z$  356.5 and product ion  $m/z$  181.2 – MRM transitions – were monitored during the analyses. Quantification of **RC-106** in plasma or pancreas homogenate were performed by generating 7 concentrations-calibration curves (5–1000 ng/mL for plasma, and 5–500 ng/mL for pancreas homogenate), employing **RC-33** as IS, 0.1  $\mu\text{g/mL}$  in MeOH. Accordingly, concentrations of **RC-106** at each time point were extrapolated from the corresponding calibration curve. The developed method resulted suitable to separate **RC-106** from endogenous interferences. Afterward, CD-1 male mice received intraperitoneal administration at a concentration of 10 mg/kg. Plasma PK parameters are listed in **Supplementary Table S3**. **RC-106** showed a maximal concentration ( $C_{\text{max}}$ ) in plasma of 973.3 ng/mL ( $T_{\text{max}}$  of 5 min) with an area under the curve ( $\text{AUC}_{0-t}$ ) of 67986.7 ng/mL\*min (**Figure 6** and **Supplementary Table S4**). Interestingly, **RC-106** reached high concentrations also in pancreas with  $\text{AUC}_{0-t}$  of 1729315.7 ng/mL\*min, thus showing  $\text{AUC}_{0-t}$  pancreas/ $\text{AUC}_{0-t}$  plasma of about 25 times (**Figure 6** and **Supplementary Table S4**).

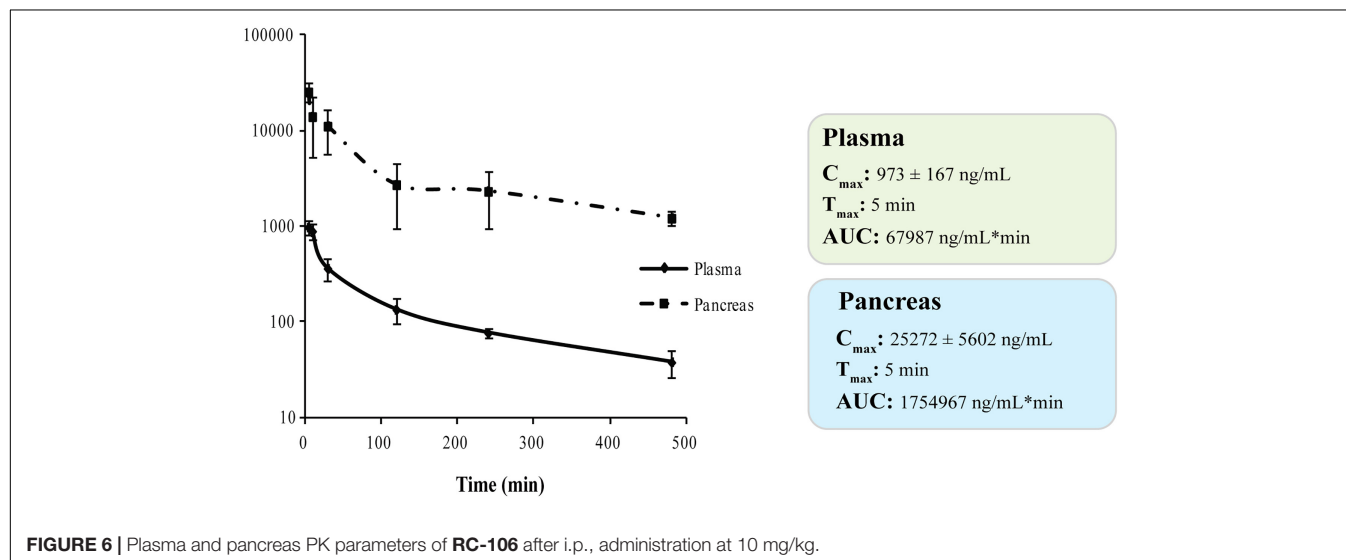
## DISCUSSION

Chemotherapy is the only therapeutic strategy effective in counteracting PC. Nevertheless, the pharmaceutical panorama

counts very few effective molecules, since the etiology of this tumor is still elusive and specific therapeutic targets have not been identified yet. Recently, our research team highlighted that the PC cell lines express both S1R and S2R/TMEM97. Therefore, molecules acting *via* SRs pathway may play a positive role in counteracting PC. In the present work, we deepened the *in vitro* properties of the pan-SR modulator **RC-106** and evaluated its PK profile to define its potential as *lead* compound.

Pancreatic cancer cell lines Panc-1, Capan-1, and Capan-2, harboring a mutational status representative of clinical tumors and expressing both SRs, have been selected to delineate the *in vitro* **RC-106** profile, and used in all the experiments. The cytotoxicity tests clearly showed that **RC-106** exerts a strong antiproliferative and pro-apoptotic action in all considered cell lines, with  $\text{IC}_{50}$  values in the micromolar range. To straighten these data, we exploit the 3D cell culture spheroids, an *in vitro* model mimicking *in vivo* features, thus providing better read-outs for drug screening (Carragher et al., 2018). The analysis of 3D morphological parameters of Panc-1 cells, the only able to grow as 3D structure, showed a complete disaggregation of spheroid organization and cytoarchitecture, thus confirming both the strong cytotoxic activity of **RC-106** and its good penetration capability.

The cytotoxic activity of **RC-106** seems to be mostly attributable to the induction of the intrinsic apoptotic pathways. Herein, we focused on the failure of the adaptive response to restore protein-folding homeostasis. In fact, when UPR is inadequate to restore ER proteostasis, the pathway alternates its signaling toward a terminal UPR, leading to cellular death. To study the role of SRs in ER stress, we measured the expression of the key factors GRP78/BiP, ATF4, and CHOP. In detail, GRP78/BiP is one of the best characterized ER chaperones (Lee, 2005), whereas ATF4 and CHOP are both markers for the shift of the UPR signaling into the alternate signaling program called the “terminal UPR” (Oyadomari and Mori, 2004; Maly and Papa, 2014; Hetz and Papa, 2018).





The cellular exposure to **RC-106** induces a relevant increase of the considered key regulators of ER stress, being GRP78/BiP, ATF4, and CHOP overexpressed. To sum up, results of our experiments demonstrated that the antitumor activity of **RC-106** is related to the triggering of the “terminal UPR,” confirming the key role of SRs as ER Stress gatekeepers (Tesei et al., 2018). It is worth noting that some compounds able to activate the terminal “UPR” have already reached the clinic for the treatment of several neoplasia, including PC (Hetz et al., 2013; Wang et al., 2018). Among them, bortezomib an inhibitor of proteasome enzyme complex (Chen et al., 2011) deserve to be mentioned, even if its therapeutic use is hampered by its toxic side effects (Field-Smith et al., 2006; Chen et al., 2011; Kharel et al., 2018). Since previous works reported that the silencing or the presence of loss-of-function mutations of S1R lead to an imbalance of protein degradation (Fukunaga et al., 2015; Dreser et al., 2017; Kim, 2017), we extent the evaluation to proteasome inhibition activity. **RC-106** resulted able to inhibit the proteasome activity in all the examined cell lines in a dose dependent manner. As a last step of cell biology investigation, we performed the scratch wound healing assay suitable for estimating the local spreading of cancer cells in the tissues/organs. The results showed that **RC-106** is able to decrease PC cell motility in a dose dependent manner, suggesting its therapeutic efficacy also in advanced disease.

Taken together the aforementioned results suggest **RC-106** as a valuable candidate for the treatment of PC. Considering that tissue distribution in target organ is at the core of drug discovery and development process, having a direct impact on pharmacology, we conclude our study performing PK and pancreas distribution evaluations. The results show that **RC-106** is 25 times more concentrated in pancreas than plasma, reaching a concentration similar or even higher ( $C_{max}$  about 70  $\mu$ M) than those required to be effective in all the *in vitro* experiments considered in this work.

## CONCLUSION

Pancreatic cancer treatment is one of the most relevant challenges that the scientific community will have to face in the 21st century. Although novel approaches for PC have been recently proposed, chemotherapy still remains the only effective option to mitigate and counteract the devastating outcome. We herein

propose **RC-106**, a pan-SR modulator with S1R antagonist and S2R agonist profile discovered by our research team, as a valuable compound for *in vivo* investigation. Obtained results clearly demonstrated that it is effective against PC, *via* apoptotic pathways, driven by both SR modulation and proteasome complex inhibition. We also deepen the mechanism of action, studying the role played by SR as ER gatekeepers. The so-obtained results demonstrated that **RC-106** is able to modulate UPR in response to ER stress, enhancing the expression of GRP78/BiP, ATF4, and CHOP. Furthermore, **RC-106** affected not only the viability of PC lines, but also their metastatic potential. Not last in importance, our lead compound it is able to reach the target tissue.

In conclusion, basing on pharmacological and PK profile we suggest the pan-SR modulator **RC-106**, as an optimal candidate for proof of concept *in vivo* studies in animal models of PC.

## ETHICS STATEMENT

Autorizzazione ministeriale 433/2016-PR: the procedures were authorized by the national authority (Istituto Superiore di Sanità, authorization number 433/2016-PR) and adhered to all the applicable institutional and governmental guidelines for the treatment of laboratory animals (Italian D.L.vo n. 26/2014).

## AUTHOR CONTRIBUTIONS

AT and SC: conceptualization. AT, MM, GD, DR, and SC: experimental design and methodology. MC, SP, CA, AIM, CM, AC, VC, MR, and AnM: investigation. MC, AIM, MR, and AnM: writing-original draft preparation. AT, MC, GD, MM, MR, and SC: writing-review and editing. AT, GC, and SC: supervision. AT and SC: project administration. All authors contributed to manuscript revision, and read and approved the submitted version.

## SUPPLEMENTARY MATERIAL

The Supplementary Material for this article can be found online at: <https://www.frontiersin.org/articles/10.3389/fphar.2019.00490/full#supplementary-material>

## REFERENCES

- Alon, A., Schmidt, H. R., Wood, M. D., Sahn, J. J., Martin, S. F., and Kruse, A. C. (2017). Identification of the gene that codes for the  $\sigma 2$  receptor. *Proc. Natl. Acad. Sci. U.S.A.* 114, 7160–7165. doi: 10.1073/pnas.1705154114
- Arienti, C., Zannoni, M., Pignatta, S., Del Rio, A., Carloni, S., Tebaldi, M., et al. (2016). Preclinical evidence of multiple mechanisms underlying trastuzumab resistance in gastric cancer. *Oncotarget* 7, 18424–18439. doi: 10.18632/oncotarget.7575
- Bartz, F., Kern, L., Erz, D., Zhu, M., Gilbert, D., Meinhof, T., et al. (2009). Identification of cholesterol-regulating genes by targeted RNAi screening. *Cell Metab.* 10, 63–75. doi: 10.1016/j.cmet.2009.05.009
- Carragher, N., Piccinini, F., Tesei, A., Trask, O. J., Bickle, M., and Horvath, P. (2018). Concerns, challenges and promises of high-content analysis of 3D cellular models. *Nat. Rev. Drug Discov.* 17:606. doi: 10.1038/nrd.2018.99
- Chen, D., Frezza, M., Schmitt, S., Kanwar, J., and Dou, Q. P. (2011). Bortezomib as the first proteasome inhibitor anticancer drug: current status and future perspectives. *Curr. Cancer Drug Targets* 11, 239–253.
- Colgan, S. M., Al-Hashimi, A. A., and Austin, R. C. (2011). Endoplasmic reticulum stress and lipid dysregulation. *Expert Rev. Mol. Med.* 13:e4. doi: 10.1017/S1462399410001742
- Collina, S., Bignardi, E., Rui, M., Rossi, D., Gaggeri, R., Zamagni, A., et al. (2017a). Are sigma modulators an effective opportunity for cancer treatment?

- A patent overview (1996-2016). *Expert Opin. Ther. Pat.* 27, 565–578. doi: 10.1080/13543776.2017.1276569
- Collina, S., Rui, M., Stotani, S., Bignardi, E., Rossi, D., Curti, D., et al. (2017b). Are sigma receptor modulators a weapon against multiple sclerosis disease? *Future Med. Chem.* 9, 2029–2051. doi: 10.4155/fmc-2017-0122
- Corazzari, M., Gagliardi, M., Fimia, G. M., and Piacentini, M. (2017). Endoplasmic reticulum stress, unfolded protein response, and cancer cell fate. *Front. Oncol.* 7:78. doi: 10.3389/fonc.2017.00078
- Dreser, A., Vollrath, J. T., Sechi, A., Johann, S., Roos, A., Yamoah, A., et al. (2017). The ALS-linked E102Q mutation in Sigma receptor-1 leads to ER stress-mediated defects in protein homeostasis and dysregulation of RNA-binding proteins. *Cell Death Differ.* 24, 1655–1671. doi: 10.1038/cdd.2017.88
- Ebrahimi-Fakhari, D., Wahlster, L., Bartz, F., Werenbeck-Ueding, J., Praggastis, M., Zhang, J., et al. (2015). Reduction of TMEM97 increases NPC1 protein levels and restores cholesterol trafficking in Niemann-pick type C1 disease cells. *Hum. Mol. Genet.* 25, 3588–3599. doi: 10.1093/hmg/ddw204
- Field-Smith, A., Morgan, G. J., and Davies, F. E. (2006). Bortezomib (Velcade) in the treatment of multiple myeloma. *Ther. Clin. Risk Manag.* 2, 271–279. Available at: <http://www.ncbi.nlm.nih.gov/pubmed/18360602> (accessed January 11, 2019).
- Froyen, P., and Juvvik, P. (1995). One-pot synthesis of secondary or tertiary amines from alcohols and amines via alkoxyphosphonium salts. *Tetrahedron Lett.* 36, 9555–9558.
- Fukunaga, K., Shinoda, Y., and Tagashira, H. (2015). The role of SIGMAR1 gene mutation and mitochondrial dysfunction in amyotrophic lateral sclerosis. *J. Pharmacol. Sci.* 127, 36–41. doi: 10.1016/j.jphs.2014.12.012
- Hayashi, T. (2015). Sigma-1 receptor: the novel intracellular target of neuropsychotropic drugs. *J. Pharmacol. Sci.* 127, 2–5. doi: 10.1016/j.jphs.2014.07.001
- Hayashi, T., and Su, T. P. (2007). Sigma-1 receptor chaperones at the ER-mitochondrion interface regulate Ca<sup>2+</sup> signaling and cell survival. *Cell* 131, 596–610. doi: 10.1016/j.cell.2007.08.036
- Hetz, C. (2012). The unfolded protein response: controlling cell fate decisions under ER stress and beyond. *Nat. Rev. Mol. Cell Biol.* 13, 89–102. doi: 10.1038/nrm3270
- Hetz, C., Chevet, E., and Harding, H. P. (2013). Targeting the unfolded protein response in disease. *Nat. Rev. Drug Discov.* 12, 703–719. doi: 10.1038/nrd3976
- Hetz, C., and Papa, F. R. (2018). The unfolded protein response and cell fate control. *Mol. Cell* 69, 169–181. doi: 10.1016/j.molcel.2017.06.017
- Ilic, M., and Ilic, I. (2016). Epidemiology of pancreatic cancer. *World J. Gastroenterol.* 22, 9694–9705. doi: 10.3748/wjg.v22.i44.9694
- Kharel, P., Uprety, D., Chandra, A. B., Hu, Y., Belur, A. A., and Dhakal, A. (2018). Bortezomib-induced pulmonary toxicity: a case report and review of literature. *Case Rep. Med.* 2018, 1–5. doi: 10.1155/2018/2913124
- Kim, F. J. (2017). Introduction to sigma proteins: evolution of the concept of sigma receptors. *Handb. Exp. Pharmacol.* 244, 1–11. doi: 10.1007/164\_2017\_41
- Kim, V. M., and Ahuja, N. (2015). Early detection of pancreatic cancer. *Chin. J. Cancer Res.* 27, 321–331. doi: 10.3978/j.issn.1000-9604.2015.07.03
- Kondo, Y., Kanzawa, T., Sawaya, R., and Kondo, S. (2005). The role of autophagy in cancer development and response to therapy. *Nat. Rev. Cancer* 5, 726–734. doi: 10.1038/nrc1692
- Lee, A. S. (2005). The ER chaperone and signaling regulator GRP78/BiP as a monitor of endoplasmic reticulum stress. *Methods* 35, 373–381. doi: 10.1016/j.jymeth.2004.10.010
- Maly, D. J., and Papa, F. R. (2014). Druggable sensors of the unfolded protein response. *Nat. Chem. Biol.* 10, 892–901. doi: 10.1038/nchembio.1664
- Marra, A., Rossi, D., Maggi, L., Corana, F., Mannucci, B., Peviani, M., et al. (2016a). Development of easy-to-use reverse-phase liquid chromatographic methods for determining PRE-084, RC-33 and RC-34 in biological matrices. The first step for in vivo analysis of sigma1 receptor agonists. *Biomed. Chromatogr.* 30, 645–651. doi: 10.1002/bmc.3609
- Marra, A., Rossi, D., Pignataro, L., Bigogno, C., Canta, A., Oggioni, N., et al. (2016b). Toward the identification of neuroprotective agents: g-scale synthesis, pharmacokinetic evaluation and CNS distribution of (R)-RC-33, a promising SIGMA1 receptor agonist. *Future Med. Chem.* 8, 287–295. doi: 10.4155/fmc.15.191
- Martin, W. R., Eades, C. G., Thompson, J. A., Huppler, R. E., and Gilbert, P. E. (1976). The effects of morphine- and nalorphine- like drugs in the nondependent and morphine-dependent chronic spinal dog. *J. Pharmacol. Exp. Ther.* 197, 517–532.
- Maurice, T., and Lockhart, B. P. (1997). Neuroprotective and anti-amnesic potentials of sigma ( $\sigma$ ) receptor ligands. *Prog. Neuropsychopharmacol. Biol. Psychiatry* 21, 69–102. doi: 10.1016/S0278-5846(96)00160-1
- Miki, Y., Tanji, K., Mori, F., and Wakabayashi, K. (2015). Sigma-1 receptor is involved in degradation of intranuclear inclusions in a cellular model of huntington's disease. *Neurobiol. Dis.* 74, 25–31. doi: 10.1016/j.nbd.2014.11.005
- Mir, S. U. R., Schwarze, S. R., Jin, L., Zhang, J., Friend, W., Miriyala, S., et al. (2013). Progesterone receptor membrane component 1/Sigma-2 receptor associates with MAP1LC3B and promotes autophagy. *Autophagy* 9, 1566–1578. doi: 10.4161/auto.25889
- Moenner, M., Pluquet, O., Bouchecareilh, M., and Chevet, E. (2007). Integrated endoplasmic reticulum stress responses in cancer. *Cancer Res.* 67, 10631–10634. doi: 10.1158/0008-5472.CAN-07-1705
- Moore, K. A., and Hollien, J. (2012). The unfolded protein response in secretory cell function. *Annu. Rev. Genet.* 46, 165–183. doi: 10.1146/annurev-genet-110711-155644
- Mori, T., Hayashi, T., Hayashi, E., and Su, T. P. (2013). Sigma-1 receptor chaperone at the ER-mitochondrion interface mediates the mitochondrion-ER-nucleus signaling for cellular survival. *PLoS One* 8:e76941. doi: 10.1371/journal.pone.0076941
- Oyadomari, S., and Mori, M. (2004). Roles of CHOP/GADD153 in endoplasmic reticulum stress. *Cell Death Differ.* 11, 381–389. doi: 10.1038/sj.cdd.4401373
- Penke, B., Fulop, L., Szucs, M., and Frecska, E. (2017). The role of sigma-1 receptor, an intracellular chaperone in neurodegenerative diseases. *Curr. Neuropharmacol.* 16, 97–116. doi: 10.2174/1570159X15666170529104323
- Peviani, M., Salvaneschi, E., Bontempi, L., Petese, A., Manzo, A., Rossi, D., et al. (2014). Neuroprotective effects of the Sigma-1 receptor (S1R) agonist PRE-084, in a mouse model of motor neuron disease not linked to SOD1 mutation. *Neurobiol. Dis.* 62, 218–232. doi: 10.1016/j.nbd.2013.10.010
- Piccinini, F., Tesei, A., Zanoni, M., and Bevilacqua, A. (2017). ReViMS: software tool for estimating the volumes of 3-D multicellular spheroids imaged using a light sheet fluorescence microscope. *Biotechniques* 63, 227–229. doi: 10.2144/000114609
- Quirion, R., Chicheportiche, R., Contreras, P. C., Johnson, K. M., Lodge, D., William Tam, S., et al. (1987). Classification and nomenclature of phencyclidine and sigma receptor sites. *Trends Neurosci.* 10, 444–446. doi: 10.1016/0166-2236(87)90094-4
- Rossi, D., Pedrali, A., Gaggeri, R., Marra, A., Pignataro, L., Laurini, E., et al. (2013). Chemical, pharmacological, and in vitro metabolic stability studies on enantiomerically pure RC-33 compounds: promising neuroprotective agents acting as  $\sigma$ 1 receptor agonists. *ChemMedChem* 8, 1514–1527. doi: 10.1002/cmdc.201300218
- Rossi, D., Rui, M., Di Giacomo, M., Schepmann, D., Wünsch, B., Monteleone, S., et al. (2017). Gaining in pan-affinity towards sigma 1 and sigma 2 receptors. SAR studies on arylalkylamines. *Bioorg. Med. Chem.* 25, 11–19. doi: 10.1016/j.bmc.2016.10.005
- Rui, M., Rossi, D., Marra, A., Paolillo, M., Schinelli, S., Curti, D., et al. (2016). Synthesis and biological evaluation of new aryl-alkyl(alkenyl)-4-benzylpiperidines, novel sigma receptor (SR) modulators, as potential anticancer-agents. *Eur. J. Med. Chem.* 124, 649–665. doi: 10.1016/j.ejmech.2016.08.067
- Samali, A., Fitzgerald, U., Deegan, S., and Gupta, S. (2010). Methods for monitoring endoplasmic reticulum stress and the unfolded protein response. *Int. J. Cell Biol.* 2010:830307. doi: 10.1155/2010/830307
- Shuda, M., Kondoh, N., Imazeki, N., Tanaka, K., Okada, T., Mori, K., et al. (2003). Activation of the ATF6, XBP1 and grp78 genes in human hepatocellular carcinoma: a possible involvement of the ER stress pathway in hepatocarcinogenesis. *J. Hepatol.* 38, 605–614. doi: 10.1016/S0
- Siegel, R., Ma, J., Zou, Z., and Jemal, A. (2014). Cancer statistics, 2014. *CA Cancer J. Clin.* 64, 9–29. doi: 10.3322/caac.21208
- Sipos, B., Möser, S., Kalthoff, H., Török, V., Löhr, M., and Klöppel, G. (2003). A comprehensive characterization of pancreatic ductal carcinoma cell lines:

- towards the establishment of an in vitro research platform. *Virchows Arch.* 442, 444–452. doi: 10.1007/s00428-003-0784-4
- Skuza, G. (2003). Potential antidepressant activity of sigma ligands. *Pol. J. Pharmacol.* 55, 923–934.
- Su, T. P. (1982). Evidence for sigma opioid receptor: binding of [3H]SKF-10047 to etorphine-inaccessible sites in guinea-pig brain. *J. Pharmacol. Exp. Ther.* 223, 284–290.
- Tesei, A., Cortesi, M., Zamagni, A., Arienti, C., Pignatta, S., Zannoni, M., et al. (2018). Sigma receptors as endoplasmic reticulum stress “gatekeepers” and their modulators as emerging new weapons in the fight against cancer. *Front. Pharmacol.* 9:711. doi: 10.3389/fphar.2018.00711
- Tesei, A., Rosetti, M., Ulivi, P., Fabbri, F., Medri, L., Vannini, I., et al. (2007). Study of molecular mechanisms of pro-apoptotic activity of NCX 4040, a novel nitric oxide-releasing aspirin, in colon cancer cell lines. *J. Transl. Med.* 5:52. doi: 10.1186/1479-5876-5-52
- Vasseur, S., Tomasini, R., Tournaire, R., and Iovanna, J. L. (2010). Hypoxia induced tumor metabolic switch contributes to pancreatic cancer aggressiveness. *Cancers* 2, 2138–2152. doi: 10.3390/cancers2042138
- Vaupel, D. B. (1983). Naltrexone fails to antagonize the sigma effects of PCP and SKF 10,047 in the dog. *Eur. J. Pharmacol.* 92, 269–274.
- Wang, J., Shanmugam, A., Markand, S., Zorrilla, E., Ganapathy, V., and Smith, S. B. (2015). Sigma 1 receptor regulates the oxidative stress response in primary retinal Müller glial cells via NRF2 signaling and system x, the Na-independent glutamate-cystine exchanger. *Free Radic. Biol. Med.* 86, 25–36. doi: 10.1016/j.freeradbiomed.2015.04.009
- Wang, M., Law, M. E., Castellano, R. K., and Law, B. K. (2018). The unfolded protein response as a target for anticancer therapeutics. *Crit. Rev. Oncol. Hematol.* 127, 66–79. doi: 10.1016/j.critrevonc.2018.05.003
- Weledji, E. P., Enoworock, G., Mokake, M., and Sinju, M. (2016). How grim is pancreatic cancer? *Oncol. Rev.* 10:294. doi: 10.4081/oncol.2016.294
- Yadav, R. K., Chae, S.-W., Kim, H.-R., and Chae, H. J. (2014). Endoplasmic reticulum stress and cancer. *J. Cancer Prev.* 19, 75–88. doi: 10.15430/JCP.2014.19.2.75
- Zannoni, M., Piccinini, F., Arienti, C., Zamagni, A., Santi, S., Polico, R., et al. (2016). 3D tumor spheroid models for in vitro therapeutic screening: a systematic approach to enhance the biological relevance of data obtained. *Sci. Rep.* 6:19103. doi: 10.1038/srep19103
- Zeng, C., Rothfuss, J., Zhang, J., Chu, W., Vangveravong, S., Tu, Z., et al. (2012). Sigma-2 ligands induce tumour cell death by multiple signalling pathways. *Br. J. Cancer* 106, 693–701. doi: 10.1038/bjc.2011.602

**Conflict of Interest Statement:** The authors declare that the research was conducted in the absence of any commercial or financial relationships that could be construed as a potential conflict of interest.

Copyright © 2019 Tesei, Cortesi, Pignatta, Arienti, Dondio, Bigogno, Malacrida, Miloso, Meregalli, Chiorazzi, Carozzi, Cavaletti, Rui, Marra, Rossi and Collina. This is an open-access article distributed under the terms of the Creative Commons Attribution License (CC BY). The use, distribution or reproduction in other forums is permitted, provided the original author(s) and the copyright owner(s) are credited and that the original publication in this journal is cited, in accordance with accepted academic practice. No use, distribution or reproduction is permitted which does not comply with these terms.



# Trends in Sigma-1 Receptor Research: A 25-Year Bibliometric Analysis

Luz Romero\* and Enrique Portillo-Salido\*

Drug Discovery and Preclinical Development, Esteve Pharmaceuticals, Parc Científic de Barcelona, Barcelona, Spain

**Purpose:** There are previous reviews focused on Sigma-1 receptor but no bibliometric studies examining this field as a whole. This article aims to present a global view of Sigma-1 receptor research and its intellectual structure.

**Methods:** We used bibliometric indicators of a basic nature as well as techniques for the visualization and analysis of networks of scientific information extracted from Scopus database.

**Results:** In total, 1,102 articles from 1992 to 2017 were identified. The growth in the production of articles is not constant over time, with periods of stagnation of approximately 5 years. Only 247 authors have five or more publications. The authors appear grouped in relatively independent clusters, thus suggesting a low level of collaborations between those dedicated to the Sigma-1 receptor. The United States was the country with the highest production followed by Japan and Germany. Spain, Japan, and Italy showed the highest per million inhabitants ratio. The highest citation/article ratio was reached in France, United States, and Canada. The leading institutions were the University of Münster, the National Institutes of Health, ESTEVE, and INSERM. The top authors in number of publications were Wünsch-B, Schepmann-D, and Maurice-T. Hayashi-T, Su-TP and Bowen-WD showed the highest citations per article. The article by Hayashi-T and Su-TP in Cell (2007) describing the Sigma-1 receptor as a chaperone protein is the top cited reference. Cluster labeling from author co-citation analysis shows that research has been focused on specific diseases such as addiction, neuroprotection and neurodegenerative diseases, psychiatric disorders, and pain. High-frequency terms in author keywords suggest that the research efforts in some areas such as neuroimaging, cocaine addiction or psychiatric disorders have declined over time, while others such as neurodegenerative diseases or pain are currently most popular.

**Perspective:** A greater involvement of the scientific community, with an increase in the scientific production related to Sigma-1, is desirable. Additional boost needed to improve research performance is likely to come from combining data from different laboratories to overcome the limitations of individual approaches. The resulting maps are a useful and attractive tool for the Sigma-1 receptor research community, as they reveal the main lines of exploration at a glance.

**Keywords:** sigma-1 receptor, bibliometrics, scopus, VOSviewer, co-occurrence analysis, co-citation analysis, co-authorship analysis

## OPEN ACCESS

### Edited by:

Ebru Aydar,  
University College London,  
United Kingdom

### Reviewed by:

Elena Martín-García,  
Universidad Pompeu Fabra, Spain  
Zaida Chinchilla-Rodríguez,  
Spanish National Research Council  
(CSIC), Spain

### \*Correspondence:

Luz Romero  
lromero@esteva.com  
Enrique Portillo-Salido  
eportillo@esteva.com

### Specialty section:

This article was submitted to  
Experimental Pharmacology and Drug  
Discovery,  
a section of the journal  
Frontiers in Pharmacology

**Received:** 27 February 2019

**Accepted:** 06 May 2019

**Published:** 24 May 2019

### Citation:

Romero L and Portillo-Salido E (2019)  
Trends in Sigma-1 Receptor  
Research: A 25-Year Bibliometric  
Analysis. *Front. Pharmacol.* 10:564.  
doi: 10.3389/fphar.2019.00564



## INTRODUCTION

The Sigma-1 receptor is considered a unique ligand-operated chaperone protein which regulates protein folding/degradation, ER/oxidative stress, and cell survival (Hayashi, 2015). Sigma-1 receptor ligands have long been expected to serve as drugs for the treatment of human diseases such as neurodegenerative disorders, depression, chronic pain, drug abuse, retinal disease, and cancer (Cobos et al., 2008; Katz et al., 2017; Kim and Maher, 2017; Maurice and Gogvadze, 2017a,b; Merlos et al., 2017a,b; Sabino et al., 2017; Sanchez-Fernandez et al., 2017; Smith et al., 2018). Two subtypes of Sigma receptors have been identified, Sigma-1 and Sigma-2 (Hellewell et al., 1994). Confused with opioid receptors for many years due to the cross-reactivity of some ligands (Martin et al., 1976; Tam, 1983), the Sigma-1 receptor (also known as Sigma1, Sig1R,  $\sigma$ 1 receptor, and several other names) was first cloned in 1996 from guinea pig liver (Hanner et al., 1996), and later from mouse kidney, human cell lines, rat brain, and mouse brain (Kekuda et al., 1996; Seth et al., 1997, 1998). The Sigma-2 receptor (Sigma2, Sig2R,  $\sigma$ 2 receptor) was cloned very recently from calf liver (Alon et al., 2017) and identified as transmembrane protein 97 (TMEM97). Very recently, the first crystal structure of the full-length human Sig-1R was reported in a complex with two different ligands, PD144418 and 4-IBP (Schmidt et al., 2016). As shows in the **Figure 1**, representing a chronological view of these important milestones, the research on Sigma-1 receptor has evolved since the cloning of the receptor. The Sigma-1 receptor shares no homology with any mammalian protein (Hanner et al., 1996). It is widely distributed in peripheral organs and different areas of the central nervous system involved in memory, emotion, sensory and motor function (Wolfe et al., 1989; Brust et al., 2014). The generation of the Sigma-1 knockout mice in 2003 contributed to better understand the *in vivo* role of Sigma-1 receptors (Langa et al., 2003). The concept of the Sigma-1 receptor has evolved significantly over the past decades. Today, it seems clear that the Sigma-1 is not a traditional receptor. It is considered to be a non-G-protein coupled, non-ionotropic intracellular chaperone at the endoplasmic reticulum (ER) that modulates  $\text{Ca}^{2+}$ -signaling (Hayashi and Su, 2007; Kim, 2017; Penke et al., 2018). Nevertheless, we are only just beginning to understand what the Sigma-1 protein does and how it works.

The most popular methods to study the function of a specific protein mainly include molecular, cellular and pharmacological approaches, and bioinformatic analysis. However, very few researchers utilize systematic bibliometric analytical approaches to study a specific protein or gene. Bibliometric analysis is a widely used quantitative method to examine the knowledge structure and development in research fields (Portillo-Salido, 2010; Guler et al., 2016; Munoz-Ecija et al., 2017). It is widely used in various areas to estimate the productivity of institutions, countries, and authors; and identify international collaborations and geographic distributions (Chinchilla-Rodríguez et al., 2015). More recently it is being used to explore research hotspots and frontiers in specific fields such as diseases (Zhou et al., 2018), materials (Vargas-Quesada et al., 2017), genes/proteins/targets (Zongyi et al., 2016; Lu et al., 2018; Zhao et al., 2018), and drugs (Sweileh et al., 2016; Hernandez-Vasquez et al.,

2018; Zyoud et al., 2018). To our knowledge, no previous bibliometric analysis on Sigma-1 receptor has been published. When searching for the term “sigma-1 receptor” in the Scopus or Pubmed scientific databases, the first two references that appear are from Basile et al. (1992a,b). Previously, the more general term “sigma receptor” was used for many years but the use of this generic term progressively declined when, 4 years after Basile’s articles, the Sigma-1 receptor was cloned. In the current study, we performed a bibliometric analysis to qualitatively and quantitatively specifically evaluate the Sigma-1 receptor studies until 2017. We take advantage of new visualization techniques based on bibliometric analysis of scientific publications to better approach the research focused on Sigma-1 receptor in the last 25 years. Our objectives were to describe the scientific outputs of Sigma-1 receptor research and identify trends and hotspots. The main questions that became our guidelines for analysis were:

1. How vast and varied is Sigma-1 receptor research output?
2. What are the main research areas in which the role of Sigma-1 receptor has been explored?
3. What were the most influential authors and publications in Sigma-1 receptor research?
4. What was the level of collaboration between the Sigma-1 receptor research community?

## METHODS

### Study Design

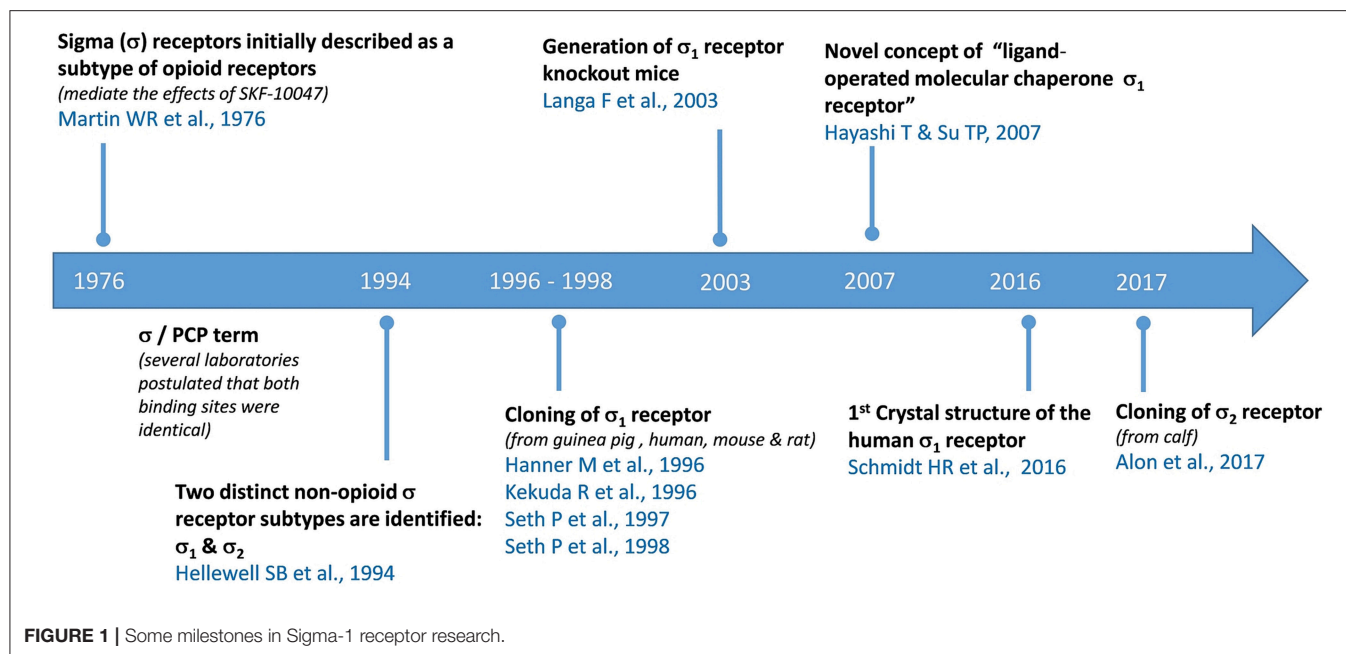
A bibliometric analysis using documents published until December 2017 in journals indexed in Scopus (<https://www.scopus.com/>) was performed. While there are a variety of document types, only articles were included.

### Source of Information

Scopus (Elsevier BV Company, USA) is the largest abstract and citation database of scientific peer-review literature, including more than 22,000 titles from international publishers. We decided to use this database because it includes all MEDLINE documents and other characteristics, such as country of all authors and citations per document—this information being relevant to this study (Falagas et al., 2008; Kulkarni et al., 2009; Agarwal et al., 2016).

### Search Strategy

A literature search was conducted by the authors in Scopus for publications on a single day, May 15, 2018, and used the following search: [TITLE-ABS-KEY (“Sigma-1 receptor”) OR TITLE-ABS-KEY (“SigmaR1”) OR TITLE-ABS-KEY (“Sigma type 1”) OR TITLE-ABS-KEY (“Sig1r”) OR TITLE-ABS-KEY (“Sigma1 receptor”) OR TITLE-ABS-KEY (“Sigma-1 agonist”) OR TITLE-ABS-KEY (“Sigma-1 antagonist”) OR TITLE-ABS-KEY (“Sigma-1 ligand”) OR TITLE-ABS-KEY (“Sigma1 agonist”) OR TITLE-ABS-KEY (“Sigma1 antagonist”) OR TITLE-ABS-KEY (“Sigma1 ligand”) OR TITLE-ABS-KEY (“Sigma1-binding”)] AND DOCTYPE (ar) AND PUBYEAR < 2018 AND [LIMIT-TO (LANGUAGE, “English”)]. The validity of the search strategy was tested by manually reviewing the retrieved articles.



## Data Analysis

All data were collected by the authors and downloaded in csv format. The data were imported to Microsoft Excel 2013 and quantitatively and qualitatively analyzed. Some data had to be standardized because documents mistakenly attributed to the domain of author name and affiliation were detected. Therefore, standardization was carried out manually by the authors. Different outputs were extracted from Scopus, including annual research, countries, journals, authors, institutions, and citation frequency. The annual publications and average citations per year per publication, the relationship between the average number of times cited per paper and the number of years since its publication was calculated. The mean number of citations per publication (CPP), including article lifespan for all 1,102 articles and for those with more than 150 citations was also analyzed. For journal analysis we used Bradford's law as a bibliometric indicator for the dispersion of scientific information. This law first described by Samuel C. Bradford in 1934 is to show the distribution of the scientific literature in a particular discipline, and Bradford proposed a model of concentric zones of productivity (Bradford zones) with decreasing density of information that can be used to identify the "core" journals in a field (Brookes, 1969; Desai et al., 2018). One formulation is that if journals in a field are sorted by the number of articles into three zones, each with approximately one-third of all articles, then the number of journals in each zone will be proportional to 1:n:n<sup>2</sup>. We also summarized the number of journal articles and percentage of total, cumulative number of articles published by the journals and percentage of Sigma-1 receptor articles, SCImago Journal Rank (SJR), CiteScore, best quartile, and categories.

To analyse the impact factor of the journals we used CiteScore and SCImago Journal Rank (SJR) from Scopus. CiteScore is a new

journal metric recently launched by Elsevier which is similar to the Journal Impact Factor (Journal Citations Reports, Clarivate Analytics). CiteScore is the number of citations received by a journal in 1 year to documents published in the 3 previous years, divided by the number of documents indexed in Scopus published in those same 3 years (see [https://service.elsevier.com/app/answers/detail/a\\_id/14880/supporthub/scopus/](https://service.elsevier.com/app/answers/detail/a_id/14880/supporthub/scopus/) for details). SCImago Journal Rank indicator expresses the average number of weighted citations received in the selected year by the documents published in the selected journal in the three previous years. Citation weighting depends on subject field and prestige of the citing serial (see <https://www.scimagojr.com/> for further details). The contributions of countries were evaluated based on paper and citation numbers, and the research output of each country was adjusted according to population size (<http://www.worldbank.org/>). For author and cited reference analysis, the top 15 productive and cited authors on Sigma-1 receptor research, along with their h-index, period of activity, and number and citations per article was analyzed. The research areas (e.g., Neuroscience, Medicine, Chemistry, etc.) were defined as described in SCOPUS.

## Visualization Maps

Several visualization tools for bibliometrics have been developed and are now frequently used, including Vosviewer, Citespace, Bicom, and BibExcel (Chen, 2004). These tools have been developed to help researchers create knowledge maps, evaluate the collective state of the art about a subject, and identify hotspots in a research field. The two most common methods are co-occurrence and co-citation analysis. Co-occurrence analysis helps researchers identify the hot topics and trends in a discipline. If two words co-occur frequently in an article, they may have a closer relationship than other pairs of words. The citations in

an article can provide important insight into what is currently known about a given topic. The most common method to acquire this information is by co-citation analysis: two papers that are both cited by a third article have a co-citation relationship. The strength of this relationship between articles can help researchers identify the intellectual base of the discipline, research frontiers, important authors, and other relevant bibliometric information (Chen, 2004; Vargas-Quesada et al., 2017).

We used VOSviewer version 1.6.9 for viewing and creating the desired bibliometric maps (<http://www.vosviewer.com/>; Leiden University, Netherlands; van Eck and Waltman, 2010). It is a software tool for building and depicting networks based on bibliometric data. It features a text mining instrument that can be used to depict co-occurrence networks of terms extracted from any part of scientific literature. The terms maps were used to explore trends and active growth areas. To explore the knowledge structure and main lines of Sigma-1 receptor research, we selected Author Keywords as the unit of analysis; their co-occurrence was, as we mentioned before, the unit of measurement (full counting). When two different keywords were used to define the same concept, normalization was applied (for instance the different variants used for the term “positron emission tomography” were normalized to “PET”). Country co-authorship, author co-authorship and author co-citation were also presented as network visualization maps. In VOSviewer maps, the size of the label and the circle of an item are determined by the weight of the item. The higher its weight, the larger its label, and circle. The color of an item is determined by the cluster to which the item belongs. Lines between items represent links. By default, at most 1,000 lines

are displayed and represent the 1,000 strongest links between items. The distance between two items in the visualization approximately indicates the relatedness of the items in terms of co-authorship, co-occurrence, citation, bibliographic coupling, or co-citation links.

## Research Ethics

The data were downloaded from Scopus; these being secondary data, no interaction with animal or human subjects was involved.

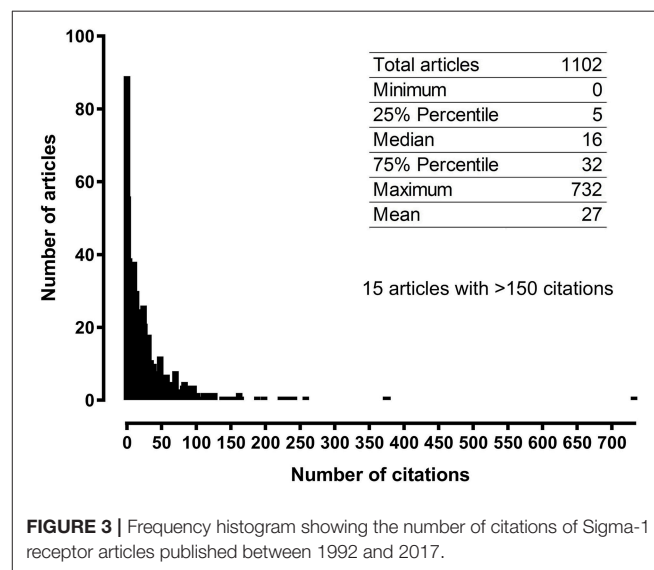


**FIGURE 3 |** Frequency histogram showing the number of citations of Sigma-1 receptor articles published between 1992 and 2017.

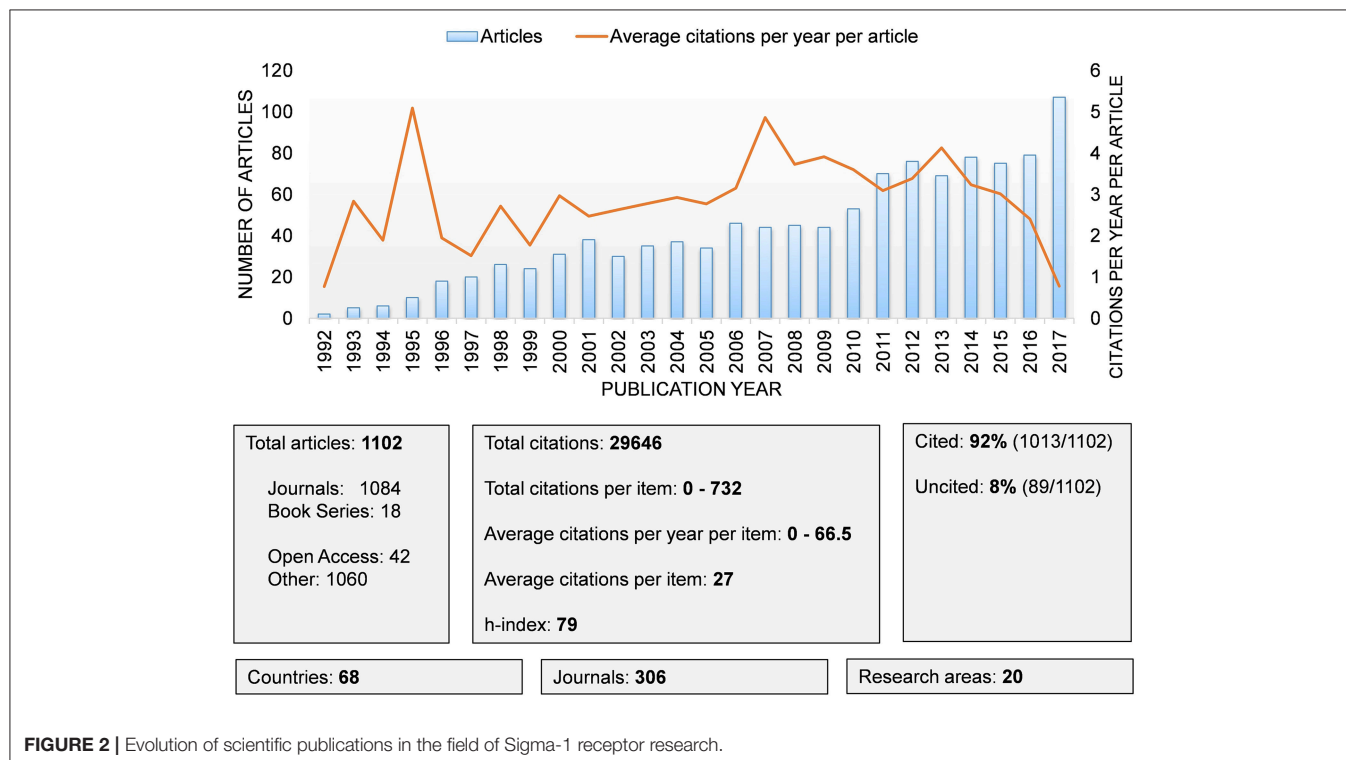


**FIGURE 2 |** Evolution of scientific publications in the field of Sigma-1 receptor research.

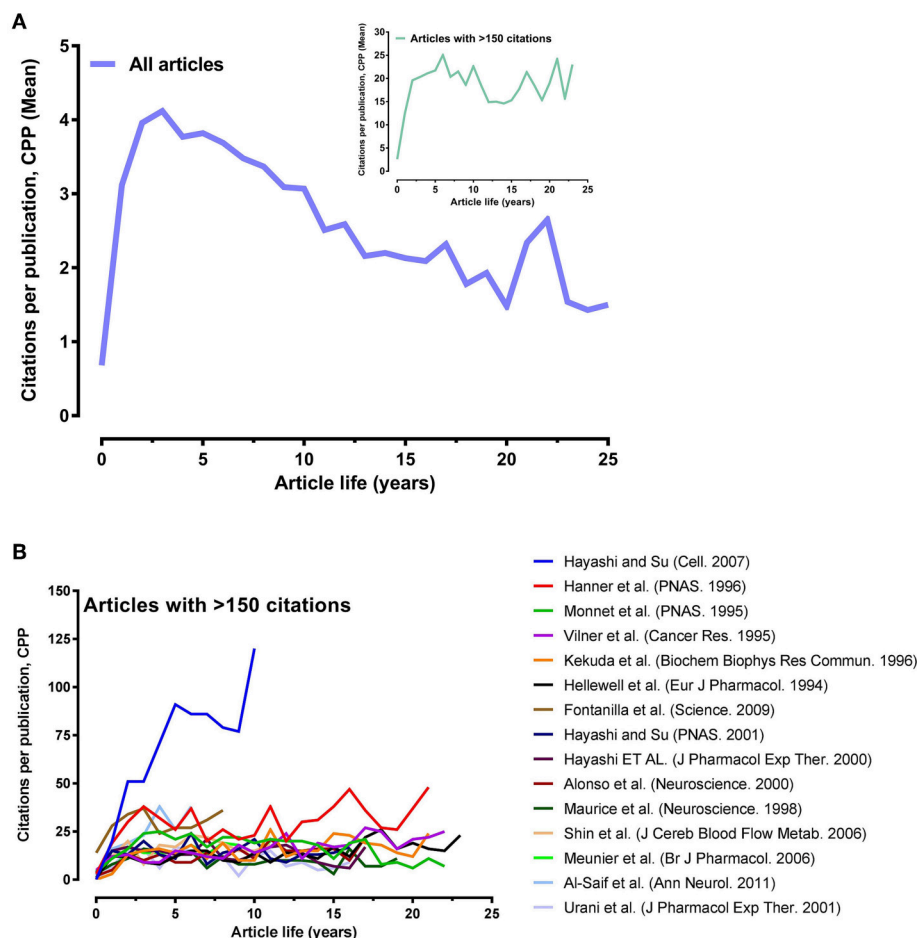


**FIGURE 4 |** Variations of citations per publication (CPP) with article lifespan. **(A)** Mean CPP with article lifespan for all 1102 articles and for those with more than 150 citations (insert graph). **(B)** CPP values of each highly cited article over the years.

There were no ethical questions about the data. Approval by an ethics committee was not necessary.

## RESULTS AND DISCUSSION

### Analysis of Publication Outputs and Citations

Annual publications and average citations per year per publication on the Sigma-1 receptor are summarized in **Figure 2**. From 1992 to 2017, there were 1,102 publications on the Sigma-1 receptor, including 1,084 articles published in Journals and 18 Book Series. While the annual number of publications increased over time, growth rate fluctuations were observed. Thus, the distribution of publications can be divided into different time stages. Sigma-1 receptor research was initiated in 1992–1995, with increased research in 1996–2001; twice as many publications were found in 2001 (38 articles) vs. 1996 (18 articles). As compared to the past 5 years (1996–2001), the publication growth rate suddenly decreased in the period of 2001–2009 (1.2-fold). From 2009 to 2012 the growth rate partially recovered again

(1.73-fold). Finally, there was no growth in the number of articles from 2012 to 2016. Interestingly, the last year analyzed (2017) reached a peak of 107 publications, which represent the largest increase in the number of articles with respect to previous year. The sum of all citation numbers is 29,646. Thus, the average citation value was 27 per paper and the h-index was 79. A total of 3,531 authors in 2,697 organizations from 68 countries were found. When analyzing the average number of citations per year per published item since 1992, the 10 articles published in 1995 and the 44 articles published in 2007 reached peaks of 5.09 and 4.86 citations per year, respectively. These citation peaks were due to three articles that were frequently cited: (Monnet et al., 1995) (16.35); (Vilner et al., 1995) (16.26); (Hayashi and Su, 2007) (66.55) (discussed below).

**Figure 3** shows the histogram of the citation data for all Sigma-1 receptor papers. Among all 1,102 Sigma-1 related articles in the pool indexed in the Scopus publication database, 89 papers (~8% of the pool) had no citations at all, 86% received fewer than 50 citations, and 75% received fewer than 32 citations. The median research paper on the Sigma-1 receptor



received 16 citations, and only 15 articles received more than 150 citations. The most highly cited paper was cited 732 times (discussed below).

The citation of an article usually follows a time course. The article lifespan demonstrates the influence of the article on scientific research. The impact of normal publications increases during the first years after publication, peaks after 3–5 years and then decreases over time (Costas et al., 2011). **Figure 4** shows the citation pattern of the Sigma-1 receptor publications, i.e., the relationship between the average number of times cited per paper and the number of years since its publication. **Figure 4A** shows the mean number of citations per publication (CPP), including article lifespan for all 1102 articles and for those with more than 150 citations (insert graph). CPP values for all 1102 articles significantly increased over the first 2 years, peaked in the 3rd year (CPP ~4) and declined thereafter. Only 15 papers received more than 150 citations. These articles were published between 1995 and 2011. CPP values from these highly cited articles also significantly increased over the first 2 years but peaked only in

the 6th year (CPP ~25). The mean number of citations for the 15 most cited articles was ~261 times.

Citation frequency curves of individual articles can exhibit one of the following patterns: 1) initially much praised work, 2) basic recognized work, 3) scarcely reflected work, 4) well-received but later erroneous qualified work, and 5) genius work (Avramescu, 1979). **Figure 4B** illustrates the CPP values of each highly cited article over the years. Two types of citing patterns can be observed, including basic recognized work and one genius work. The article published by Hayashi and Su (2007), the genius work, stands out prominently. It is the most highly cited recent article and does not seem to have reached its peak yet, as evidenced by the steady CPP value increase over the years. The other 14 highly cited articles had lower CPP values and remained essentially constant.

## Journal Analysis

More than 300 scholarly journals have published articles on Sigma-1 research. Bradford's law of scattering is a pattern first described by Samuel C. Bradford in 1934 that estimates the exponentially diminishing returns of extending a search for references in science journals, and that can be used to identify the "core" journals in a field (Brookes, 1969; Desai et al., 2018). One formulation is that if journals in a field are sorted by the number of articles into three zones, each with approximately one-third of all articles, then the number of journals in each zone will be proportional to  $1:n:n^2$ . **Table 1** shows the Bradford zones of scattering for Sigma-1 receptor literature. Our sample from 1992 to 2017 includes 306 journals. Of these, 170 journals have published only 1 paper on the Sigma-1 receptor. **Table 1** lists the nucleus and the successive zones of journals. Three zones, each

**TABLE 1 |** Bradford's Law of Scattering for journals that published articles on Sigma-1 receptor research from 1992 to 2017.

	<i>n</i>	<i>n/N (%)</i>
Zone 1	11	3.6
Zone 2	44	14.4
Zone 3	251	82.0

Each zone represents about 33% of the total articles (1,102); *n*, the number of journals in each zone; *N*, the number of all journals (306).

**TABLE 2 |** The 15 most active journals that published articles on Sigma-1 receptor research from 1992 to 2017.

Journal	Sigma-1 articles	%	Total articles in the journal	%	CiteScore 2017	SJR 2017	Best quartile	Categories
Eur. J. Pharmacol.	73	7	24,529	0.3	3.18	1.06	Q1	Pharmacology
J. Med. Chem.	56	5	22,665	0.2	6.25	2.57	Q1	Drug Discovery; Molecular Medicine
J. Pharmacol. Exp. Ther.	47	4	22,048	0.2	3.70	1.59	Q1	Pharmacology; Molecular Medicine
Bioorg. Med. Chem.	38	3	13,358	0.3	2.90	0.87	Q1	Pharmaceutical Science; Organic Chemistry
Bioorg. Med. Chem. Lett.	25	2	25,609	0.1	2.53	0.81	Q1	Pharmaceutical Science
Neuropharmacology	24	2	9,520	0.3	4.65	2.04	Q1	Pharmacology; Cellular and Molecular Neuroscience
Nucl. Med. Biol.	24	2	3,024	0.8	2.12	0.70	Q1	Radiology Nuclear Medicine and imaging
Br. J. Pharmacol.	24	2	20,003	0.1	5.97	2.60	Q1	Pharmacology
Synapse	23	2	3,300	0.7	2.18	0.97	Q3	Cellular and Molecular Neuroscience
Psychopharmacology	17	2	12,924	0.1	3.05	1.49	Q2	Pharmacology
Pharmacol. Biochem. Behav.	17	2	12,227	0.1	3.02	1.15	Q1	Behavioral Neuroscience
Eur. J. Med. Chem.	17	2	9,381	0.2	4.63	1.27	Q1	Pharmacology; Organic Chemistry; Drug Discovery
Brain Res.	16	1	51,636	0.03	3.02	1.40	Q1	Clinical Neurology
PLoS ONE	16	1	183,064	0.01	3.01	1.16	Q1	General Agricultural and Biological Sciences; General Biochemistry, Genetics and Molecular Biology
Adv. Exp. Med. Biol.	15	1	7,168	0.2	1.67	0.87	Q2	General Biochemistry, Genetics and Molecular Biology

publishing approximately 33% (367 articles) of the total Sigma-1 receptor articles (1,102 articles), constitute the most specific subdivisions. We found that 3.6% (11 journals) of the journals that published articles on Sigma-1 research were distributed in zone 1, 14% (44 journals) were distributed in zone 2, and 82% (251 journals) were distributed in zone 3, which had a lower influence than zone 1 or 2 (**Table 1**).

To more closely examine the leading journals, **Table 2** lists the number of journal articles in descending order and percentage of total, cumulative number of articles published by the journal from 1992 to 2017 and percentage of Sigma-1 receptor articles, CiteScore, SCImago Journal Rank (SJR), best journal quartile, and categories. We used CiteScore and SJR from Scopus as an indicator of the publication's repercussion. As indicated in **Table 2**, the core Sigma-1 receptor literature concentrates on a small number of Pharmacology, Drug Discovery and Chemistry related journals. Others categories are Radiology Nuclear Medicine and Imaging, Neurosciences, Biochemistry, and Biology. Out of the top 15 journals analyzed, the European Journal of Pharmacology (CiteScore2017: 3.18, SJR2017: 1.06, 73 articles, 7%) ranks first in the number of Sigma-1 receptor publications, followed by the Journal of Medicinal Chemistry (CiteScore2017: 6.25, SJR2017: 2.75, 56 articles, 5%) and

the Journal of Pharmacology and Experimental Therapeutics (CiteScore2017: 3.70, SJR: 1.59, 47 articles, 4%). These three journals published 16% of the total articles. Additionally, Nuclear Medicine and Biology (CiteScore2017: 2.12; SJR2017: 0.70) devoted 24 articles (0.8% of its publications) to Sigma-1 research, followed by Synapse (CiteScore2017: 2.18; SJR2017: 0.97, 23 articles, 0.7% of its publications). As compared to other journals, articles on Sigma-1 research were more likely to be accepted by these active journals. The 15 most active journals (80% in Quartile 1; 13% in Quartile 2; 7% in Quartile 3) published approximately the 40% of the Sigma-1 receptor articles.

All 15 most active journals have a CiteScore ranging from 1.67 (Advances in Experimental Medicine and Biology) to 6.25 (Journal of Medicinal Chemistry). The top journals with a CiteScore > 5 (2/15; 13% of the top journals) published 7% of the total number of Sigma-1-related articles. The top journals with CiteScore 3–5 (8/15; 53% of the top journals) published 21% of the total number of Sigma-1-related articles. The top journals with CiteScore < 3 (5/15; 33% of the top journals) published 10% of the total number of Sigma-1-related articles. In summary, when comparing the rate of Sigma-1 receptor articles medium-CiteScore journals (CiteScore 3–5) to that of all journals (rate of journals with CiteScore > 10, 0.7%; CiteScore 5–10, 3.1%;

**TABLE 3 |** Top countries, country institutions and institution authors with more publications on Sigma-1 receptor research from 1992 to 2017.

Country	Articles	Citations	h-Index	Citations per article	Articles per million inhabitants	Top country institution (top institution author)	Institution articles	%	Main research area of the institution in Sigma-1 field
United States	405	13,634	63	34	1.2	National Institutes of Health (Su, T.P.)	65	16	Drug addiction
Japan	228	5,660	43	25	1.8	Tokyo Metropolitan Institute of Gerontology (Ishiwata, K.)	35	15	Neuroimaging/PET
Germany	103	937	27	9	1.2	University of Münster (Wünsch, B.)	67	65	Chemistry
Italy	98	1,944	25	20	1.6	University of Catania (Prezzavento, O.)	29	30	Chemistry; Neuroprotection; Memory; Pain, ...
China	85	1,009	20	12	0.1	Nanjing Medical University (Chen, L.)	23	27	Neuropsychiatric disorders; Neuroprotection, ...
France	84	4,719	40	56	1.3	INSERM (Maurice, T.)	45	54	Cognition; Neuroprotection
Spain	83	1,877	28	23	1.8	ESTEVE (Vela, J.M.)	48	58	Pain
South Korea	33	727	18	22	0.6	Seoul National University (Roh, D.H. & Yoon, S.Y.)	21	64	Pain
United Kingdom	33	882	19	27	0.5	University of East Anglia (Duncan, G. & Wang, L.)	5	15	Eye
						University of Cambridge (Balasuriya, D. & Edwardson, J.M.)	5	15	Neurobiology; Protein-protein interaction
Australia	27	477	13	18	1.1	University of Sydney (Kassiou, M.)	12	44	Chemistry
Canada	22	722	15	33	0.6	McGill University (Debonnel, G.)	8	36	Depression
Poland	22	414	12	19	0.6	Polish Academy of Sciences (Skuza, G.)	17	77	Depression

CiteScore 3–5, 8.8%; and CiteScore < 3, 87.4%) (<https://www.scopus.com/sources>), Sigma-1 receptor articles were relatively intensively published in medium CiteScore journals.

## Country, Institution, and International Collaboration Analysis

The top countries, country institutions and institution authors with more publications on Sigma-1 receptor research from 1992 to 2017 are shown in **Table 3**. Sigma-1 receptor publications were produced by countries from different world geographies, including countries outside Europe and North America. The United States was the country with the highest production with 405 (37%) documents, followed by Japan and Germany with 228 (21%) and 103 (9%) documents, respectively. Spain (1.8), Japan (1.8) and Italy (1.6) showed the highest per million inhabitants ratio. The United States had the highest h-index of 63, followed by Japan (h-index 43) and France (h-index 40). The highest citation/article ratio was reached in France (56), United States (34) and Canada (33). The leading institutions were the University of Münster (67; 65% of Germany documents), the National Institutes of Health (65; 16% of The United States documents), ESTEVE (48; 58% of Spain documents) and INSERM (45; 54% of France documents). The main research area within these four institutions was related to chemistry, drug addiction, pain, and cognition/neuroprotection, respectively.

Nineteen companies published 119 articles (11% of the total articles) (**Table 4**). Out of 19 companies publishing about the Sigma-1 receptor, 2 companies contributed 63% of the papers. The most productive company was ESTEVE (now Esteve Pharmaceuticals) with 48 publications, followed by Santen Pharmaceutical, which contributed 27 articles until 2004, thus suggesting that they are not currently active in Sigma-1 receptor research. Santen Pharmaceutical is the originator company of Cutamesine (SA-4503), a Sigma-1 receptor denoted as agonist/activator that was under development for the treatment of amyotrophic lateral sclerosis, age-related macular degeneration, acute ischemic stroke, major depressive disorder, traumatic brain injury, multiple sclerosis, stroke, and retinitis pigmentosa. While the drug was tested in phase II in patients with major depressive disorders and in patients recovering from stroke, its development was terminated for the given conditions. Currently, M's science corporation (under license from Santen) is supposedly developing cutamesine for the potential treatment of amyotrophic lateral sclerosis and retinitis pigmentosa as more suitable target diseases (Source: <https://pharma.globaldata.com/>). Esteve Pharmaceuticals is currently active in the development of Sigma-1 receptor antagonists/inhibitors for the treatment of neuropathic pain (Source: <https://www.esteve.com/en/hboxresearch-development>).

We used VOSviewer to visualize the network map of country co-authorship (international collaboration) for Sigma-1 receptor publications. Distribution maps provide valuable information and help researchers identify potential collaborators. The largest set of connected countries consists of 26 countries in 7 clusters. **Figure 5** illustrates the collaborative network of countries publishing more than five documents (26 of the 68

**TABLE 4 |** Companies that publish on Sigma-1 receptor research.

Company	Country	Total publications	Corresponding publications	Publication years
ESTEVE	Spain	48	26	1999–2017
Santen Pharmaceutical	Japan	27	13	1997–2004
Hamamatsu Photonics	Japan	7	1	2003–2017
Sanofi-Synthelabo	France	6	4	1997–2003
Mitsui Pharmaceuticals	Japan	4	2	1999–2001
Nihon Schering (formerly Mitsui)	Japan	4	4	2001–2002
Taisho Pharmaceutical	Japan	4	4	1999–2004
UCB Pharma /UCB Research	Belgium/ United States	3	2	2004–2013
Nensius Research	Denmark	2	2	2011–2013
Teva Pharmaceutical Industries	Israel	2	2	2016–2017
Merck Research Laboratories	United States	2	1	1994–2007
NitroMed	United States	2	1	1999–2004
Anavex Life Sciences	Greece	2	0	2007–2013
Servier	France	1	1	1998
Newron Pharmaceuticals	Italy	1	1	2000
BioNeuroFar	Italy	1	1	2007
PerkinElmer Health Sciences	United States	1	1	2012
Daya Drug Discoveries	United States	1	1	2014
Corden Pharma Switzerland	Switzerland	1	1	2016

countries). Clusters are formed by the frequency of co-occurring terms representing each country, the more often the terms tend to co-occur they get colored into clusters. The size of circles represents the number of publications of the country and the thickness of lines depicts the size of collaboration. For example, the link strength (collaboration) between the United States and Japan was 20 and it represents a thick line. On the other hand, the line between the United States and India had a link strength of 2. Countries with similar color form one cluster. The blue cluster shows collaborative links between the largest circles of the United States, Japan (green color) and Italy representing authors affiliated to these countries. The United States collaborated the most with other countries worldwide. Other international researchers who collaborated the most with the United States researchers were from South Korea, France, Italy, and China. Spain is associated with France (red color), and to a lesser extent other countries such as the United Kingdom and Canada. The

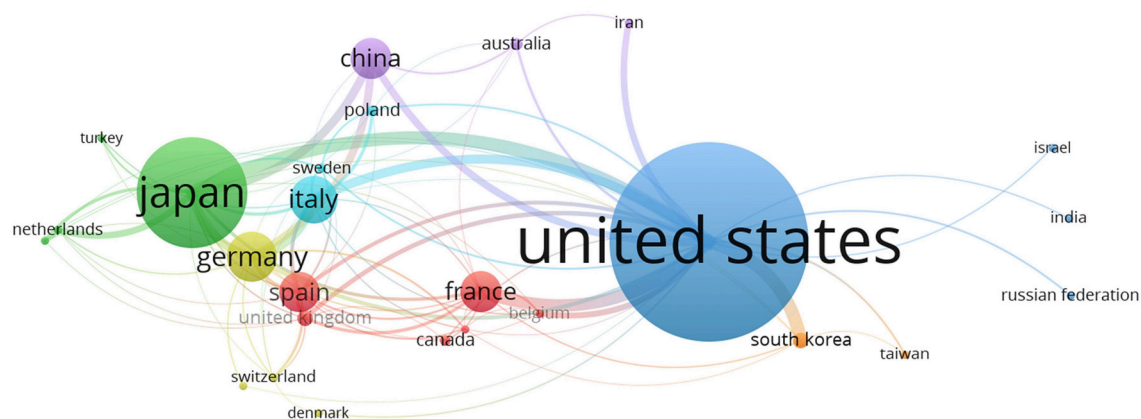


**FIGURE 5 |** VOSviewer network visualization map of country co-authorship (international collaboration) for Sigma-1 receptor publications, 1992–2017. Twenty-six out of the 68 countries had at least 5 publications; the largest set of connected countries consists of 26 countries in 7 clusters.

**TABLE 5 |** The 15 most active authors in Sigma-1 receptor research from 1992 to 2017.

Author	Articles	Document h-index	Citations	Citations per article	Year of 1st-last Sigma-1 publication
Wünsch, B.	73	23	1,267	17	2001–2017
Schepmann, D.	57	19	856	15	2006–2017
Maurice, T.	45	30	2,642	59	1996–2016
Ishiwata, K.	36	19	987	27	1998–2016
Su, T.P.	34	25	2,991	88	1998–2017
Mach, R.H.	29	16	780	27	1995–2016
Hayashi, T.	27	24	2,669	99	1995–2015
Ruoho, A.E.	27	17	1,013	38	2007–2017
Hashimoto, K.	26	14	777	30	1997–2003
Matsumoto, R.R.	26	15	632	24	1997–2017
Vela, J.M.	26	16	607	23	2003–2017
Bowen, W.D.	25	20	1,553	62	1993–2016
Matsuno, K.	25	19	1,086	43	1995–2004
Brust, P.	24	13	344	14	2008–2017
Zamarrillo, D.	22	16	741	34	2000–2016

purple cluster is leaded by China collaborating with Japan and the United States.

## Author and Cited Reference Analysis

The 1,102 articles on the Sigma-1 receptor were drafted by more than 3,000 authors. **Table 5** presents the top 15 productive and cited authors on Sigma-1 receptor research, along with their h-index, period of activity, and number and citations per article. **Table 6** shows the 15 most frequently cited references. Eleven out of the 15 most frequently cited articles were published in journals with a high impact factor (CiteScore > 7). Hayashi-T and Su-TP (Cell. 2007) is the top cited reference (732 citations, 66.5 citations per year). Each of the 15 most active authors contributed at least 22 articles to Sigma-1 research. Wünsch (73

articles), who mainly participated in chemistry-related papers, ranks first, followed by Schepmann-D (57 articles), who is a coauthor in the Wünsch's articles, and by Maurice-T (45 articles), who mainly focused on the role and applications of Sigma-1 receptor and ligands to cognitive/behavioral diseases. Most of the productive authors were also the most cited ones, with some particularities. Wünsch, who is the most productive, ranks thirteenth in terms of citations per article. Most cited authors were Hayashi-T and Su-TP, who had the most cited publication in the field of the Sigma-1 receptor (**Table 6** and **Figure 4B**). Their paper identified the Sigma-1 receptor as a novel “ligand-operated” chaperone and characterized the important role played by the Sigma-1 receptor in endoplasmic reticulum-mitochondrial interorganelle  $\text{Ca}^{2+}$  signaling and also in cell survival. These two authors have two more articles among the most cited ones (Hayashi and Su, 2001; Kourrich et al., 2013; **Table 6**) which demonstrated that Sigma-1 receptor modulation of different proteins contribute to the effects of cocaine, neurosteroids and other drugs by regulating intracellular  $\text{Ca}^{2+}$  signaling. The third most cited author is Bowen-WD, who ranks twelfth in number of articles, followed by Maurice-T, who also ranks third in number of articles. Maurice-T also scores first in h-index (h-index = 30). As shown in **Table 6**, Bowen-WD contributed an early article, which is among the most cited ones, describing the expression of Sigma-1 and Sigma-2 receptors in a wide variety of human and rodent tumor cell lines (Vilner et al., 1995). A paper authored by Maurice-T describing the involvement of the Sigma-1 receptor in the anti-amnesic and neuroprotective effects of donepezil in a mouse model of Alzheimer's disease in mice is also among the most cited (Meunier et al., 2006) (**Table 6**). The paper by Schmidt et al. (2016), published in Nature and reporting the crystal structure of the human  $\sigma_1$  receptor, ranks second and is followed by a paper in Science by Fontanilla et al. (2009) in terms of average citations per year. Schmidt-HR showed the overall architecture, oligomerization state and molecular basis for ligand recognition of the Sigma-1 receptor, and Fontanilla-D described N,N-dimethyltryptamine (DMT), which has shown hallucinogenic properties, as an endogenous Sigma-1 receptor



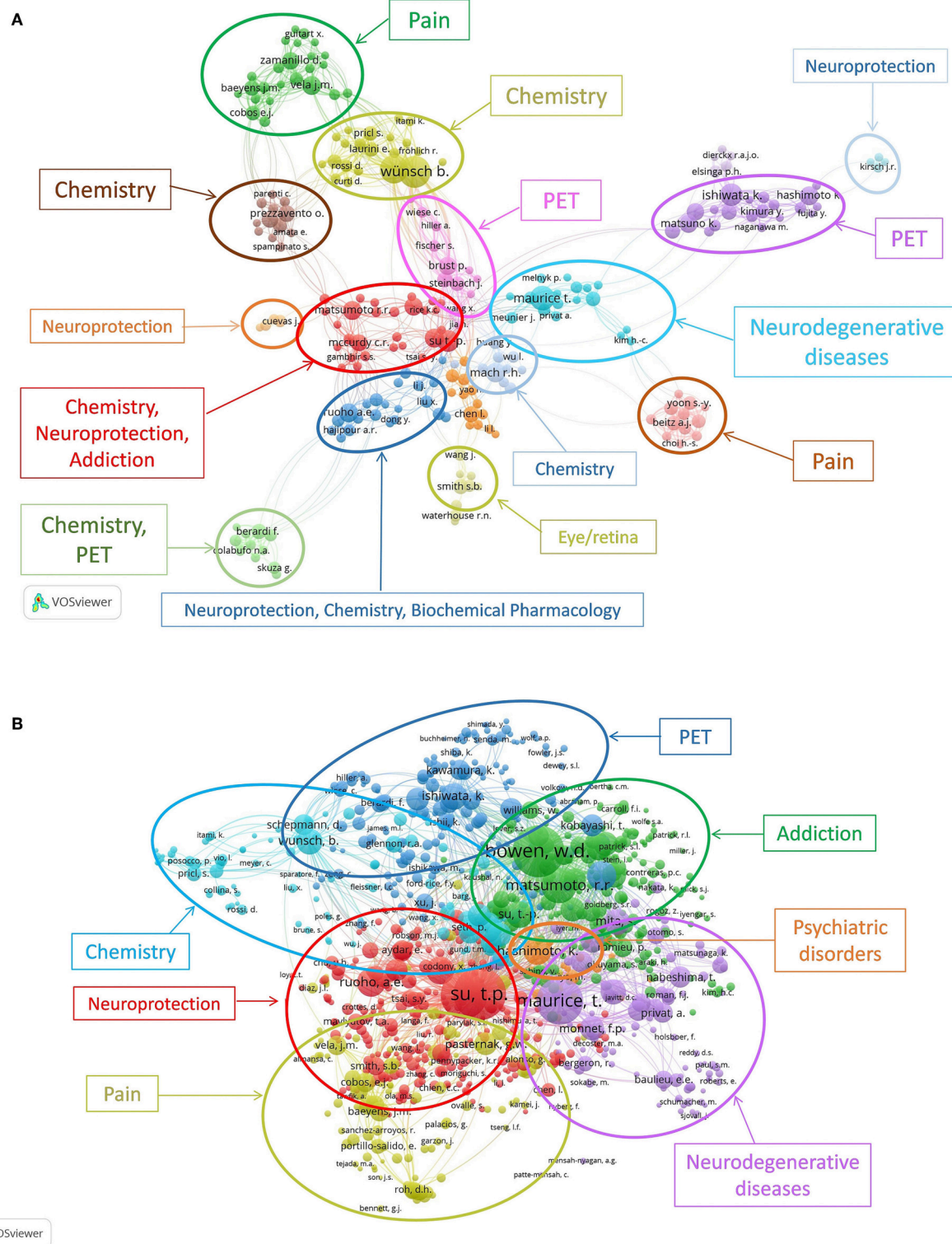
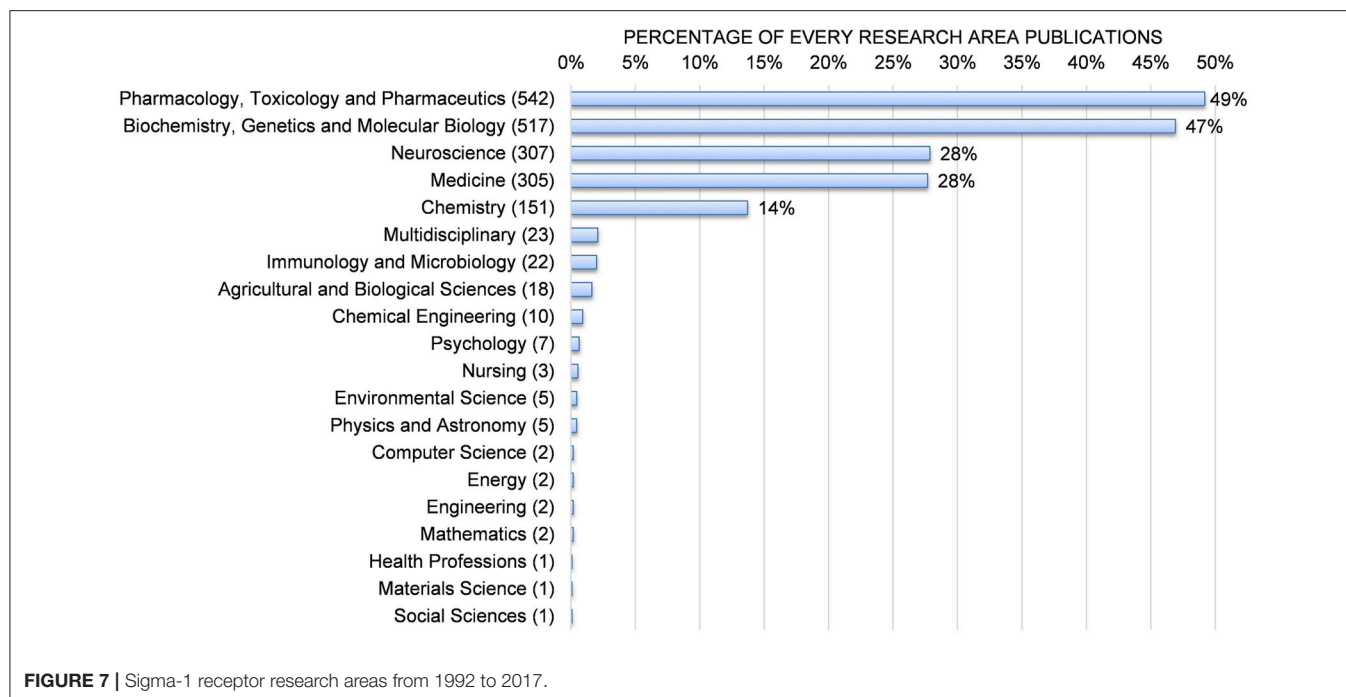


**TABLE 6 |** The 15 most frequently cited references in Sigma-1 receptor research from 1992 to 2017.

References	Average citations per year	Total citations	Title	Journal	CiteScore 2017	SJR 2017
Hayashi and Su, 2007	66.5	732	Sigma-1 Receptor Chaperones at the ER-Mitochondrion Interface Regulate $\text{Ca}^{2+}$ Signaling and Cell Survival	Cell. 2007 Nov 2;131(3):596–610.	21.99	25.14
Schmidt et al., 2016	35.0	70	Crystal structure of the human $\sigma 1$ receptor	Nature. 2016 Apr 28;532(7600):527–30.	14.59	17.87
Hanner et al., 1996	29.7	653	Purification, molecular cloning, and expression of the mammalian sigma1-binding site	Proc Natl Acad Sci U S A. 1996 Jul 23;93(15):8072–7.	8.59	6.09
Fontanilla et al., 2009	28.7	258	The hallucinogen N,N-dimethyltryptamine (DMT) is an endogenous sigma-1 receptor regulator	Science. 2009 Feb 13;323(5916):934–7.	15.85	14.14
Hedskog et al., 2013	23.6	118	Modulation of the endoplasmic reticulum-mitochondria interface in Alzheimer's disease and related models	Proc Natl Acad Sci U S A. 2013 May 7;110(19):7916–21.	8.59	6.09
Al-Saif et al., 2011	23.1	162	A mutation in sigma-1 receptor causes juvenile amyotrophic lateral sclerosis	Ann Neurol. 2011 Dec;70(6):913–9.	7.62	5.71
Kourrich et al., 2013	16.8	84	Dynamic interaction between sigma-1 receptor and Kv1.2 shapes neuronal and behavioral responses to cocaine	Cell. 2013 Jan 17;152(1–2):236–47.	21.99	25.14
Monnet et al., 1995	16.3	376	Neurosteroids, via $\sigma$ receptors, modulate the [ $^3\text{H}$ ]norepinephrine release evoked by N-methyl-D-aspartate in the rat hippocampus	Proc Natl Acad Sci U S A. 1995 Apr 25;92(9):3774–8.	8.59	6.09
Vilner et al., 1995	16.3	374	Sigma-1 and Sigma-2 Receptors Are Expressed in a Wide Variety of Human and Rodent Tumor Cell Lines	Cancer Res. 1995 Jan 15;55(2):408–13.	7.35	4.26
Shin et al., 2006	15.7	188	Vasoconstrictive neurovascular coupling during focal ischemic depolarizations	J Cereb Blood Flow Metab. 2006 Aug;26(8):1018–30.	5.07	2.56
Kekuda et al., 1996	15.0	331	Cloning and functional expression of the human type 1 sigma receptor (hSigmaR1)	Biochem Biophys Res Commun. 1996 Dec 13;229(2):553–8.	2.62	1.09
Francardo et al., 2014	14.5	58	Pharmacological stimulation of sigma-1 receptors has neurorestorative effects in experimental parkinsonism	Brain. 2014 Jul;137(Pt 7):1998–2014.	7.43	5.86
Hayashi and Su, 2001	13.9	236	Regulating ankyrin dynamics: Roles of sigma-1 receptors	Proc Natl Acad Sci U S A. 2001 Jan 16;98(2):491–6.	8.59	6.09
Hellewell et al., 1994	13.8	330	Rat liver and kidney contain high densities of sigma 1 and sigma 2 receptors: characterization by ligand binding and photoaffinity labeling	Eur J Pharmacol. 1994 Jun 15;268(1):9–18.	3.18	1.06
Meunier et al., 2006	13.7	164	The anti-amnesic and neuroprotective effects of donepezil against amyloid B 25–35 peptide-induced toxicity in mice involve an interaction with the $\sigma 1$ receptor	Br J Pharmacol. 2006 Dec;149(8):998–1012.	5.97	2.60

regulator. Other highly cited articles on Sigma-1 focused on the role of Sigma-1 in a number of diseases with important medical needs such as Alzheimer's disease (Hedskog et al., 2013), amyotrophic lateral sclerosis (Al-Saif et al., 2011), cancer (Vilner et al., 1995), and Parkinson disease (Francardo et al., 2014). Finally, two articles on Sigma-1 receptor cloning and expression (Hanner et al., 1996; Kekuda et al., 1996) and one on Sigma-1 and Sigma-2 receptor characterization (Hellewell et al., 1994) also appear as highly cited in **Table 6**.

Citation networks have been applied to information science analysis. Here, VOSviewer was also used to analyse author citations in Sigma-1 research. VOSviewer is primarily intended to be used for bibliometric network analysis. The program can be used to create maps of publications, authors or journals based on a citation, co-citation, or bibliographic coupling network, or to create keyword maps based on a co-occurrence network. Two network visualization maps provided by VOSviewer are shown in **Figure 6**. In the co-authorship analysis (**Figure 6A**)



the relatedness of items is determined based on the number of co-authored documents. Each node represents an author with at least five publications, the node label is the last name of the author, and the node size indicates the number of published articles. The link connecting two nodes stands for the cooperative relationship between two authors, and the thickness of the link stands for the intensity of cooperation. Another important information regarding authors is the degree of co-citation. Author co-citation analysis measures the number of times a particular group of authors was cited together within the collection (van Eck and Waltman, 2017). In the co-citation analysis (**Figure 6B**) the relatedness of items is determined based on the number of times they are cited together. Each node represents an author with at least 20 citations, the node label is the last name of the author, and edges represent citation relations. When co-authorship analysis was performed (**Figure 6A**), 247 out of the 3,529 authors had at least 5 publications, and the largest set of connected authors consists of 224 authors in 16 clusters. An inspection of the publications from each cluster allows displaying the main area for each research group. There are several independent clusters working in the same area. For instance, there are six clusters publishing articles on “Chemistry,” four clusters on “Neuroprotection,” three clusters on “PET,” two clusters on “Pain,” and one cluster related to those publishing mainly in “Addiction.”

The co-citation analysis by author included 51,564 cited authors, of which 1,291 were cited at least 20 times (**Figure 6B**); the largest set of authors with greatest total link strength selected consists of 1,000 authors in 7 clusters. In this case, each color represents a community of authors within the same subject of interest, and authors within a cluster represent a set of strongly connected authors in terms of co-citation relations. These

clusters, as can be seen from **Figure 6B** relate to “Chemistry,” “PET,” “Neuroprotection,” “Addiction,” “Neurodegenerative diseases,” “Psychiatric disorders,” and “Pain.” These clusters point toward the pivotal scholars whose works were cited in the references of our collection and who contributed to build on each field studied (**Figure 6B**).

## Research Area Analysis

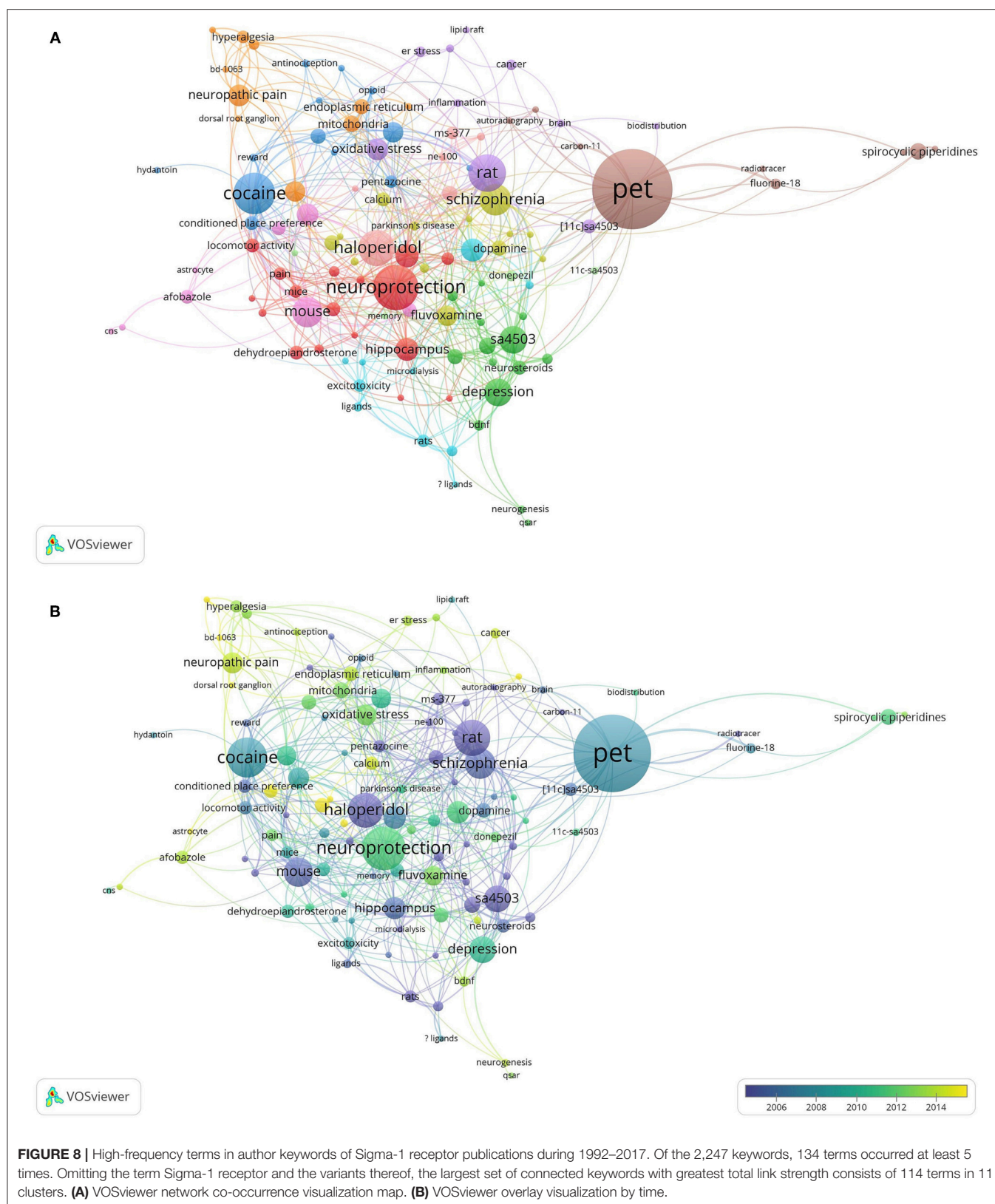
Research on the Sigma-1 receptor occurred in 20 special research areas. These 20 research areas, appearing in publications of Sigma-1 receptor research from 1992 to 2017, are shown in **Figure 7**. Here, the research areas (e.g., Neuroscience, Medicine, Chemistry, etc.) were defined as described in SCOPUS. “Pharmacology, Toxicology and Pharmaceutics” and “Biochemistry, Genetics, and Molecular Biology” accounted for the largest number of publications (49 and 47%, respectively), followed by “Neuroscience” (28%), “Medicine” (28%), and “Chemistry” (14%).

## Keyword Co-occurrence Cluster Analysis

The topics involved in Sigma-1 receptor research can be outlined in the keywords assigned to each article. Keywords have as their main objective to provide rapid access to scientific works and are highly effective in terms of bibliometric analysis when investigating the knowledge structure of scientific fields (Zhang et al., 2016; Vargas-Quesada et al., 2017). Keywords provide a reasonable description of research hotspots (attention by a number of scientific researchers focused on a set of related research problems and concepts).

In the present study, VOSviewer was used to create a knowledge map of keyword co-occurrence with 114 terms in 11 clusters (**Figure 8**) and to identify the top 25 keywords





in Sigma-1 research articles from 1992 to 2017, according to occurrences and citation counts, and ordered by average publication year (**Figure 9**). The top 5 keywords were “Positron

Emission Tomography (PET),” “Neuroprotection,” “Cocaine,” “Rat,” and “Haloperidol” (**Figure 9**). High-frequency terms in author keywords such as “Learning and Memory” (2004),



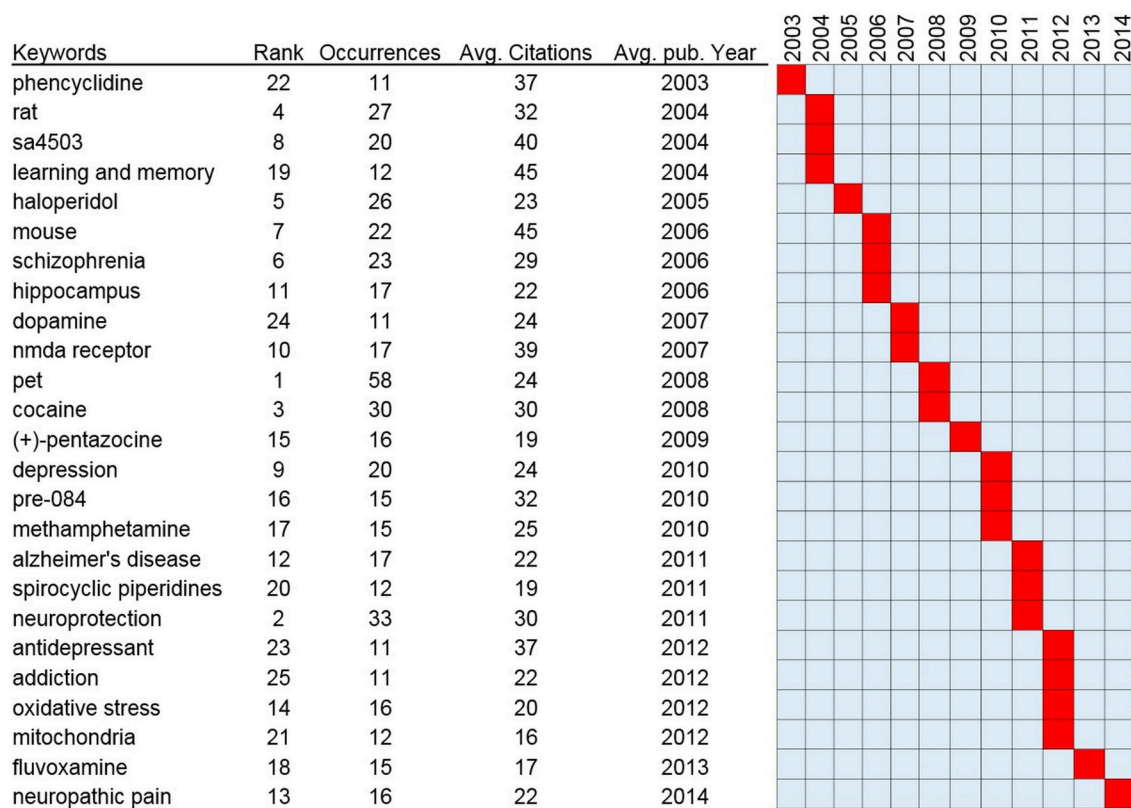


**FIGURE 9 |** Top 25 keywords with strongest occurrences and average citations in articles related to Sigma-1 receptor research.

“Schizophrenia” (2006), “Positron Emission Tomography” (2008), “Cocaine” (2008), and “Depression” (2010) were found in the early years, as compared to terms such as “Alzheimer’s disease” (2011), “Neuroprotection” (2011), “Addiction” (2012), and “Neuropathic Pain” (2014) in more recent years (**Figure 8B**).

## CONCLUSIONS

In this work, the global scientific outputs of Sigma-1 receptor research, its main research lines and its evolution are studied for the first time by means of bibliometric indicators of a basic nature and modern information visualization techniques. The resulting maps are a useful and attractive tool for the Sigma-1 receptor research community, as they reveal the main lines of exploration at a glance. The global view provided by our study shows that researchers have intended to explore the potential involvement of Sigma-1 receptors in some specific physiological processes and diseases. The hope that the modulation of the Sigma-1 receptor could be a therapeutic strategy is likely driving the Sigma-1 research community. Consistent with this, intensive activity has been carried out in the area of Medicinal Chemistry to obtain selective ligands that could be developed as drugs in the future. According to our analysis, the main diseases in which the Sigma-1 receptors have been explored include addiction, neuroprotection and neurodegenerative diseases, psychiatric disorders, and pain. Keyword co-occurrence analysis suggests that the research efforts

made in some indications such as those in cocaine (addiction), learning and memory or depression/schizophrenia/ haloperidol (psychiatric conditions) have declined over time, while others such as those focusing on neuroprotection/Alzheimer’s disease (neurodegenerative diseases) or pain are currently most popular. Early studies on psychiatric disorders, learning and memory or cocaine did not translate into marketed drugs, and hopes now seem to be placed on studies relating to neurodegenerative diseases and pain. Leaving aside the well-known low success in transforming basic research into new drugs with a clear therapeutic potential and difficulties related to drug discovery programs (Paul et al., 2010), the lack of selective Sigma-1 ligands approved for use in humans could be the result of insufficient research effort/interest by the scientific community, including biopharmaceutical companies. In fact, only 247 authors have five or more publications and the growth in the production of articles is not constant over time, with periods of stagnation of approximately 5 years. The authors appear grouped in relatively independent clusters, thus suggesting a low level of collaboration between those devoted to the Sigma-1 receptor. Furthermore, as evidenced by the number of recent articles, only one pharmaceutical company, developing selective Sigma-1 receptor drug ligands, is currently actively publishing in the field. Additionally, the very nature of the Sigma-1 receptor may also be influencing the low success in transforming basic research into new drugs with a clear therapeutic potential. It is common in

papers to describe the Sigma-1 receptor as an “enigmatic protein whose molecular mechanism of action remains elusive.” The most cited article we found in this bibliometric analysis (Hayashi and Su, 2007) proposed that the Sigma-1 receptor acts as a molecular chaperone and therefore is not a traditional receptor. Chaperones ensure that all proteins obtain their correct folding and functionalities in the right localization at the right time. They recognize and bind their protein clients in conformational ensembles that are locally highly dynamic and interconvert, while in other cases clients bind in unique conformations (Hiller, 2019). Thus, to transform basic research into new drugs with a clear therapeutic potential, the intrinsic difficulty when trying to understand the mysteries of this unique ligand-regulated molecular chaperone should be considered in drug discovery programs.

In summary, a greater interest and involvement of the scientific community for this enigmatic chaperone, accompanied by a parallel increase in the scientific production would help, hopefully in coming years, to the discovery of new functions and deepening in those already known. Additional boost needed to improve research performance are likely to come from new conceptual frameworks and breakthrough discoveries derived from recent and future advances in the “chaperone field,” and from collaborative, synergistic initiatives by combining resources and knowhow from different laboratories to overcome the

limitations of the individual approaches. This study may provide a valuable basis for identifying important topics for future research, and create opportunities for collaboration between research groups with complementary scientific interest in the field of Sigma-1 receptor.

## DATA AVAILABILITY

The datasets generated for this study are available on request to the corresponding author.

## AUTHOR CONTRIBUTIONS

EP-S and LR designed the study, performed the search, analyzed the data, and wrote the paper.

## FUNDING

This work was a part of activities in R&D projects IDI20150914 and IDI20150915 supported by the Spanish Ministerio de Economía y Competitividad (MINECO), through the Centro para el Desarrollo Tecnológico Industrial (CDTI), co-financed by the European Union through the European Regional Development Fund (ERDF; Fondo Europeo de Desarrollo Regional, FEDER).

## REFERENCES

- Agarwal, A., Durairajanayagam, D., Tatagari, S., Esteves, S. C., Harlev, A., Henkel, R., et al. (2016). Bibliometrics: tracking research impact by selecting the appropriate metrics. *Asian J. Androl.* 18, 296–309. doi: 10.4103/1008-682x.171582
- Alon, A., Schmidt, H. R., Wood, M. D., Sahn, J. J., Martin, S. F., and Kruse, A. C. (2017). Identification of the gene that codes for the sigma2 receptor. *Proc. Natl. Acad. Sci. U S A.* 114, 7160–7165. doi: 10.1073/pnas.1705154114
- Alonso, G., Phan, V., Guillemain, I., Saunier, M., Legrand, A., Anol, M., et al. (2000). Immunocytochemical localization of the sigma(1) receptor in the adult rat central nervous system. *Neuroscience* 97, 155–170. doi: 10.1016/s0306-4522(00)00014-2
- Al-Saif, A., Al-Mohanna, F., and Bohlega, S. (2011). A mutation in sigma-1 receptor causes juvenile amyotrophic lateral sclerosis. *Ann. Neurol.* 70, 913–919. doi: 10.1002/ana.22534
- Avramescu, A. (1979). Actuality and obsolescence of scientific literature. *J. Am. Soc. Inf. Sci. Technol.* 30, 296–303.
- Basile, A. S., Paul, I. A., and de Costa, B. (1992a). Differential effects of cytochrome P-450 induction on ligand binding to sigma receptors. *Eur. J. Pharmacol.* 227, 95–98.
- Basile, A. S., Paul, I. A., Mirchevich, A., Kuijpers, G., and De Costa, B. (1992b). Modulation of (+)-[3H]pentazocine binding to guinea pig cerebellum by divalent cations. *Mol. Pharmacol.* 42, 882–889.
- Brookes, B. C. (1969). Bradford's law and the bibliography of science. *Nature* 224, 953–956.
- Brust, P., Deuther-Conrad, W., Lehmkuhl, K., Jia, H., and Wunsch, B. (2014). Molecular imaging of sigma1 receptors *in vivo*: current status and perspectives. *Curr. Med. Chem.* 21, 35–69. doi: 10.2174/09298673113209990214
- Chen, C. (2004). Searching for intellectual turning points: progressive knowledge domain visualization. *Proc. Natl. Acad. Sci. U S A.* 101, 5303–5310. doi: 10.1073/pnas.0307513100
- Chinchilla-Rodríguez, Z., Zacca-González, G., Vargas-Quesada, B., and Moya-Angón, F. (2015). Latin American scientific output in Public Health: combined analysis using bibliometric, socioeconomic and health indicators. *Scientometrics* 102, 609–628. doi: 10.1007/s11192-014-1349-9
- Cobos, E. J., Entrena, J. M., Nieto, F. R., Cendan, C. M., and Del Pozo, E. (2008). Pharmacology and therapeutic potential of sigma(1) receptor ligands. *Curr. Neuropharmacol.* 6, 344–366. doi: 10.2174/157015908787386113
- Costas, R., van Leeuwen, T. N., and van Raan, A. F. (2011). The “Mendel syndrome” in science: durability of scientific literature and its effects on bibliometric analysis of individual scientists. *Scientometrics* 89, 177–205. doi: 10.1007/s11192-011-0436-4
- Desai, N., Veras, L., and Gosain, A. (2018). Using Bradford's law of scattering to identify the core journals of pediatric surgery. *J. Surg. Res.* 229, 90–95. doi: 10.1016/j.jss.2018.03.062
- Falagas, M. E., Pitsouni, E. I., Malietzis, G. A., and Pappas, G. (2008). Comparison of PubMed, Scopus, Web of Science, and Google Scholar: strengths and weaknesses. *FASEB J.* 22, 338–342. doi: 10.1096/fj.07-9492LSF
- Fontanilla, D., Johannessen, M., Hajipour, A. R., Cozzi, N. V., Jackson, M. B., and Ruoho, A. E. (2009). The hallucinogen N,N-dimethyltryptamine (DMT) is an endogenous sigma-1 receptor regulator. *Science* 323, 934–937. doi: 10.1126/science.1166127
- Francardo, V., Bez, F., Wieloch, T., Nissbrandt, H., Ruscher, K., and Cenci, M. A. (2014). Pharmacological stimulation of sigma-1 receptors has neurorestorative effects in experimental parkinsonism. *Brain* 137 (Pt 7), 1998–2014. doi: 10.1093/brain/awu107
- Guler, A. T., Waaijer, C. J., and Palmblad, M. (2016). Scientific workflows for bibliometrics. *Scientometrics* 107, 385–398. doi: 10.1007/s11192-016-1885-6
- Hanner, M., Moebius, F. F., Flandorfer, A., Knaus, H. G., Striessnig, J., Kempner, E., et al. (1996). Purification, molecular cloning, and expression of the mammalian sigma1-binding site. *Proc. Natl. Acad. Sci. U S A.* 93, 8072–8077.
- Hayashi, T. (2015). Sigma-1 receptor: the novel intracellular target of neuropsychopharmacological drugs. *J. Pharmacol. Sci.* 127, 2–5. doi: 10.1016/j.jphs.2014.07.001
- Hayashi, T., and Su, T. P. (2001). Regulating ankyrin dynamics: roles of sigma-1 receptors. *Proc. Natl. Acad. Sci. U S A.* 98, 491–496. doi: 10.1073/pnas.021413698

- Hayashi, T., and Su, T. P. (2007). Sigma-1 receptor chaperones at the ER-mitochondrion interface regulate  $\text{Ca}^{2+}$  signaling and cell survival. *Cell* 131, 596–610. doi: 10.1016/j.cell.2007.08.036
- Hedskog, L., Pinho, C. M., Filadi, R., Ronnback, A., Hertwig, L., Wiehager, B., et al. (2013). Modulation of the endoplasmic reticulum-mitochondria interface in Alzheimer's disease and related models. *Proc. Natl. Acad. Sci. U S A.* 110, 7916–7921. doi: 10.1073/pnas.1300677110
- Hellewell, S. B., Bruce, A., Feinstein, G., Orringer, J., Williams, W., and Bowen, W. D. (1994). Rat liver and kidney contain high densities of sigma 1 and sigma 2 receptors: characterization by ligand binding and photoaffinity labeling. *Eur. J. Pharmacol.* 268, 9–18.
- Hernandez-Vasquez, A., Alarcon-Ruiz, C. A., Bendezu-Quispe, G., Comande, D., and Rosselli, D. (2018). A bibliometric analysis of the global research on biosimilars. *J. Pharmaceut. Pol. Pract.* 11:6. doi: 10.1186/s40545-018-0133-2
- Hiller, S. (2019). Chaperone-bound clients: the importance of being dynamic. *Trends Biochem. Sci.* doi: 10.1016/j.tibs.2018.12.005
- Katz, J. L., Hiranita, T., Hong, W. C., Job, M. O., and McCurdy, C. R. (2017). A role for sigma receptors in stimulant self-administration and addiction. *Handb. Exp. Pharmacol.* 244, 177–218. doi: 10.1007/164\_2016\_94
- Kekuda, R., Prasad, P. D., Fei, Y. J., Leibach, F. H., and Ganapathy, V. (1996). Cloning and functional expression of the human type 1 sigma receptor (hSigmaR1). *Biochem. Biophys. Res. Commun.* 229, 553–558. doi: 10.1006/bbrc.1996.1842
- Kim, F. J. (2017). Introduction to sigma proteins: evolution of the concept of sigma receptors. *Handb. Exp. Pharmacol.* 244, 1–11. doi: 10.1007/164\_2017\_41
- Kim, F. J., and Maher, C. M. (2017). Sigma1 pharmacology in the context of cancer. *Handb. Exp. Pharmacol.* 244, 237–308. doi: 10.1007/164\_2017\_38
- Kourrich, S., Hayashi, T., Chuang, J. Y., Tsai, S. Y., Su, T. P., and Bonci, A. (2013). Dynamic interaction between sigma-1 receptor and Kv1.2 shapes neuronal and behavioral responses to cocaine. *Cell* 152, 236–247. doi: 10.1016/j.cell.2012.12.004
- Kulkarni, A. V., Aziz, B., Shams, I., and Busse, J. W. (2009). Comparisons of citations in Web of Science, Scopus, and Google Scholar for articles published in general medical journals. *JAMA* 302, 1092–1096. doi: 10.1001/jama.2009.1307
- Langa, F., Codony, X., Tovar, V., Lavado, A., Gimenez, E., Cozar, P., et al. (2003). Generation and phenotypic analysis of sigma receptor type I (sigma 1) knockout mice. *Eur. J. Neurosci.* 18, 2188–2196. doi: 10.1046/j.1460-9568.2003.02950.x
- Lu, K., Yu, S., Sun, D., Xing, H., An, J., Kong, C., et al. (2018). Scientometric Analysis of SIRT6 Studies. *Med. Sci. Monitor* 24, 8357–8371. doi: 10.12659/msm.913644
- Martin, W. R., Eades, C. G., Thompson, J. A., Huppler, R. E., and Gilbert, P. E. (1976). The effects of morphine- and nalorphine- like drugs in the nondependent and morphine-dependent chronic spinal dog. *J. Pharmacol. Exp. Therapeut.* 197, 517–532.
- Maurice, T., and Gogvadze, N. (2017a). Role of sigma1 receptors in learning and memory and Alzheimer's disease-type dementia. *Adv. Exp. Med. Biol.* 964, 213–233. doi: 10.1007/978-3-319-50174-1\_15
- Maurice, T., and Gogvadze, N. (2017b). Sigma-1 (sigma1) receptor in memory and neurodegenerative diseases. *Handb. Exp. Pharmacol.* 244, 81–108. doi: 10.1007/164\_2017\_15
- Maurice, T., Su, T. P., and Privat, A. (1998). Sigma1 (sigma 1) receptor agonists and neurosteroids attenuate B25-35-amyloid peptide-induced amnesia in mice through a common mechanism. *Neuroscience* 83, 413–428.
- Merlos, M., Burgueno, J., Portillo-Salido, E., Plata-Salaman, C. R., and Vela, J. M. (2017a). Pharmacological modulation of the sigma 1 receptor and the treatment of pain. *Adv. Exp. Med. Biol.* 964, 85–107. doi: 10.1007/978-3-319-50174-1\_8
- Merlos, M., Romero, L., Zamanillo, D., Plata-Salaman, C., and Vela, J. M. (2017b). Sigma-1 Receptor and Pain. *Handb. Exp. Pharmacol.* 244, 131–161. doi: 10.1007/164\_2017\_9
- Meunier, J., Ieni, J., and Maurice, T. (2006). The anti-amnesic and neuroprotective effects of donepezil against amyloid beta25-35 peptide-induced toxicity in mice involve an interaction with the sigma1 receptor. *Br. J. Pharmacol.* 149, 998–1012. doi: 10.1038/sj.bjp.0706927
- Monnet, F. P., Mahe, V., Robel, P., and Baulieu, E. E. (1995). Neurosteroids, via sigma receptors, modulate the [3H]norepinephrine release evoked by N-methyl-D-aspartate in the rat hippocampus. *Proc. Natl. Acad. Sci. U S A.* 92, 3774–3778.
- Munoz-Ecija, T., Vargas-Quesada, B., and Chinchilla-Rodriguez, Z. (2017). Identification and visualization of the intellectual structure and the main research lines in nanoscience and nanotechnology at the worldwide level. *J. Nanoparticle Res.* 19:62. doi: 10.1007/s11051-016-3732-3
- Paul, S. M., Mytelka, D. S., Dunwiddie, C. T., Persinger, C. C., Munos, B. H., Lindborg, S. R., et al. (2010). How to improve R&D productivity: the pharmaceutical industry's grand challenge. *Nat. Rev. Drug Discov.* 9, 203–214. doi: 10.1038/nrd3078
- Penke, B., Fulop, L., Szucs, M., and Frecska, E. (2018). The role of sigma-1 receptor, an intracellular chaperone in neurodegenerative diseases. *Curr. Neuropharmacol.* 16, 97–116. doi: 10.2174/1570159x15666170529104323
- Portillo-Salido, E. F. (2010). A bibliometric analysis of research in psychopharmacology by psychology departments (1987–2007). *Spanish J. Psychol.* 13, 503–515. doi: 10.1017/s1138741600004054
- Sabino, V., Hicks, C., and Cottone, P. (2017). Sigma receptors and substance use disorders. *Adv. Exp. Med. Biol.* 964, 177–199. doi: 10.1007/978-3-319-50174-1\_13
- Sanchez-Fernandez, C., Entrena, J. M., Baeyens, J. M., and Cobos, E. J. (2017). Sigma-1 receptor antagonists: a new class of neuromodulatory analgesics. *Adv. Exp. Med. Biol.* 964, 109–132. doi: 10.1007/978-3-319-50174-1\_9
- Schmidt, H. R., Zheng, S., Gurpinar, E., Koehl, A., Manglik, A., and Kruse, A. C. (2016). Crystal structure of the human sigma1 receptor. *Nature* 532, 527–530. doi: 10.1038/nature17391
- Seth, P., Fei, Y. J., Li, H. W., Huang, W., Leibach, F. H., and Ganapathy, V. (1998). Cloning and functional characterization of a sigma receptor from rat brain. *J. Neurochem.* 70, 922–931.
- Seth, P., Leibach, F. H., and Ganapathy, V. (1997). Cloning and structural analysis of the cDNA and the gene encoding the murine type 1 sigma receptor. *Biochem. Biophys. Res. Commun.* 241, 535–540. doi: 10.1006/bbrc.1997.7840
- Shin, H. K., Dunn, A. K., Jones, P. B., Boas, D. A., Moskowitz, M. A., and Ayata, C. (2006). Vasoconstrictive neurovascular coupling during focal ischemic depolarizations. *J. Cereb. Blood Flow Metab.* 26, 1018–1030. doi: 10.1038/sj.jcbfm.9600252
- Smith, S. B., Wang, J., Cui, X., Mysona, B. A., Zhao, J., and Bollinger, K. E. (2018). Sigma 1 receptor: a novel therapeutic target in retinal disease. *Prog. Retinal Eye Res.* 67, 130–149. doi: 10.1016/j.preteyeres.2018.07.003
- Sweilch, W. M., Shraim, N. Y., Zyoud, S. H., and Al-Jabi, S. W. (2016). Worldwide research productivity on tramadol: a bibliometric analysis. *SpringerPlus* 5:1108. doi: 10.1186/s40064-016-2801-5
- Tam, S. W. (1983). Naloxone-inaccessible sigma receptor in rat central nervous system. *Proc. Natl. Acad. Sci. U S A.* 80, 6703–6707.
- Urani, A., Roman, F. J., Phan, V. L., Su, T. P., and Maurice, T. (2001). The antidepressant-like effect induced by sigma(1)-receptor agonists and neuroactive steroids in mice submitted to the forced swimming test. *J. Pharmacol. Exp. Therapeut.* 298, 1269–1279.
- van Eck, N. J., and Waltman, L. (2010). Software survey: VOSviewer, a computer program for bibliometric mapping. *Scientometrics* 84, 523–538. doi: 10.1007/s11192-009-0146-3
- van Eck, N. J., and Waltman, L. (2017). Citation-based clustering of publications using CitNetExplorer and VOSviewer. *Scientometrics* 111, 1053–1070. doi: 10.1007/s11192-017-2300-7
- Vargas-Quesada, B., Chinchilla-Rodríguez, Z., and Rodríguez, N. (2017). Identification and visualization of the intellectual structure in graphene research. *Front. Res. Metrics Anal.* 2:7. doi: 10.3389/frma.2017.00007
- Vilner, B. J., John, C. S., and Bowen, W. D. (1995). Sigma-1 and sigma-2 receptors are expressed in a wide variety of human and rodent tumor cell lines. *Cancer Res.* 55, 408–413.
- Wolfe, S. A. Jr., Culp, S. G., and De Souza, E. B. (1989). Sigma-receptors in endocrine organs: identification, characterization, and autoradiographic localization in rat pituitary, adrenal, testis, and ovary. *Endocrinology* 124, 1160–1172. doi: 10.1210/endo-124-3-1160
- Zhang, J., Yu, Q., Zheng, F., Long, C., Lu, Z., and Duan, Z. (2016). Comparing keywords plus of WOS and author keywords: a case study of patient

- adherence research. *J. Assoc. Info. Sci. Technol.* 67, 967–972. doi: 10.1002/asi.23437
- Zhao, D., Li, J., Seehus, C., Huang, X., Zhao, M., Zhang, S., et al. (2018). Bibliometric analysis of recent sodium channel research. *Channels* 12, 311–325. doi: 10.1080/19336950.2018.1511513
- Zhou, H., Tan, W., Qiu, Z., Song, Y., and Gao, S. (2018). A bibliometric analysis in gene research of myocardial infarction from 2001 to 2015. *PeerJ*. 6:e4354. doi: 10.7717/peerj.4354
- Zongyi, Y., Dongying, C., and Baifeng, L. (2016). Global regulatory T-cell research from 2000 to 2015: a bibliometric analysis. *PLoS ONE* 11:e0162099. doi: 10.1371/journal.pone.0162099
- Zyoud, S. H., Waring, W. S., Al-Jabi, S. W., and Sweileh, W. M. (2018). Bibliometric profile of global scientific research on digoxin toxicity (1849–2015). *Drug Chem. Toxicol.* 3, 1–7. doi: 10.1080/01480545.2018.1518453

**Conflict of Interest Statement:** LR and EP-S are employees of ESTEVE Pharmaceuticals.

Copyright © 2019 Romero and Portillo-Salido. This is an open-access article distributed under the terms of the Creative Commons Attribution License (CC BY). The use, distribution or reproduction in other forums is permitted, provided the original author(s) and the copyright owner(s) are credited and that the original publication in this journal is cited, in accordance with accepted academic practice. No use, distribution or reproduction is permitted which does not comply with these terms.





# A New Pharmacophore Model for the Design of Sigma-1 Ligands Validated on a Large Experimental Dataset

Rosalía Pascual\*, Carmen Almansa, Carlos Plata-Salamán and José Miguel Vela

ESTEVE Pharmaceuticals S.A., Drug Discovery and Preclinical Development, Barcelona, Spain

## OPEN ACCESS

### Edited by:

Enrique José Cobos,  
University of Granada, Spain

### Reviewed by:

Pramod C. Nair,  
Flinders University, Australia  
Rajnish Kumar,  
Karolinska Institute (KI), Sweden

### \*Correspondence:

Rosalía Pascual  
rpascual@esteve.com

### Specialty section:

This article was submitted to  
Experimental Pharmacology  
and Drug Discovery,  
a section of the journal  
Frontiers in Pharmacology

Received: 04 February 2019

Accepted: 24 April 2019

Published: 31 May 2019

### Citation:

Pascual R, Almansa C,  
Plata-Salamán C and Vela JM (2019)  
A New Pharmacophore Model  
for the Design of Sigma-1 Ligands  
Validated on a Large Experimental  
Dataset. *Front. Pharmacol.* 10:519.  
doi: 10.3389/fphar.2019.00519

The recent publication of the  $\sigma$ 1R crystal structure is an important cornerstone for the derivation of more accurate activity prediction models. We report here a comparative study involving a set of more than 25,000 structures from our internal database that had been screened for  $\sigma$ 1R affinity. Using the recently published crystal structure, 5HK1, two new pharmacophore models were generated. The first one, **5HK1-Ph.A**, was obtained by an algorithm that identifies the most important receptor-ligand interactions including volume restrictions enforced by the atomic structure of the recognition site. The second, **5HK1-Ph.B**, resulted from a manual edition of the first one by the fusion of two hydrophobic (HYD) features. Finally, we also docked the database using a high throughput docking technique and scored the resulting poses with seven different scoring functions. Statistical performance measures were obtained for the two models, comparing them with previously published  $\sigma$ 1R pharmacophores (Hit Rate, sensitivity, specificity, and Receiver Operator Characteristic) and **5HK1-Ph.B** emerged as the best one in discriminating between active and inactive compounds, with a ROC-AUC value above 0.8 and enrichment values above 3 at different fractions of screened samples. **5HK1-Ph.B** also showed better results than the direct docking, which may be due to the rigidity of the crystal structure in the docking process (i.e., feature tolerances in the pharmacophore model). Additionally, the impact of the HYD interactions and the penalty for desolvating ligands with polar atoms may be not adequately captured by scoring functions, whereas HYD groups filling up such regions of the binding site are entailed in the pharmacophore model. Altogether, using annotated data from a large and diverse compound collection together with crystal structure information provides a sound basis for the generation and validation of predictive models to design new molecules.

**Keywords:** sigma-1, crystal structure, 5HK1, pharmacophore model, docking, virtual screening

## INTRODUCTION

The sigma-1 receptor ( $\sigma$ 1R) is an intracellular chaperone protein, expressed in CNS regions and known to regulate  $\text{Ca}^{2+}$  signaling and cell survival. The  $\sigma$ 1R gene encodes a 24 kDa protein of 223 amino acids anchored to the endoplasmic reticulum (ER) and plasma membranes (Maurice and Su, 2009). The  $\sigma$ 1R sequence has no homology with other mammalian proteins and is structurally and

**Abbreviations:** 2/3D, 2/3-Dimensional; EF, Enrichment Factor; HR, Hit Rate; HYD, Hydrophobic; HBA, Hydrogen Bond Acceptor; PI, Positive Ionizable; AR, Aromatic Ring; HYD-AR, Hydrophobic Aromatic; ROC, Receiver Operator Characteristic; ROC-AUC, Area under the ROC curve;  $\sigma$ 1R, Sigma-1-Receptor; TRP, Sensitivity; TNR, Specificity; ECFP, extended connectivity fingerprints; FCFP, functional class fingerprints.

functionally different from other target classes. The  $\sigma$ 1R is also unique in that it exerts molecular chaperone activity and interacts with diverse proteins to modulate their functions. Accordingly, the  $\sigma$ 1R is involved in many physiological functions, including inter-organelle signaling (Su et al., 2010). Its activity can be regulated by ligands in an agonist/antagonist manner (Hayashi et al., 2011). Just as examples, the  $\sigma$ 1R modulates opioid analgesia through physical protein-protein interactions, with  $\sigma$ 1R antagonists enhancing and  $\sigma$ 1R agonists inhibiting the antinociceptive effect of opioids, and  $\sigma$ 1R antagonists reproduce the pain-protective phenotype of  $\sigma$ 1R knockout mice when administered to wild-type mice (Zamanillo et al., 2013).

Until its recent crystallization, little was known about the  $\sigma$ 1R 3-dimensional (3D) structure and the rational design of  $\sigma$ 1R modulators mostly relied on ligand-based approaches. Based on a series of diphenylalkylamines, a first 2D-pharmacophore model (Glennon-Ph) for the  $\sigma$ 1R was designed in the early 90's (Glennon et al., 1994) consisting in a positive ionizable (PI) group (i.e., a basic amino group) and two opposite hydrophobic (HYD) regions at 2.5–3.9 Å and 6–10 Å without any angle constrain (**Figure 1**). This qualitative model has been very useful as a guide to medicinal chemists for the design of new ligands. In 2004, a Sybyl 3D-pharmacophore model (Gund-Ph) was derived based on the alignment of PD144418, spipethiane, haloperidol and (+)-pentazocine (Gund et al., 2004). It consists in an aromatic region and a nitrogen atom that acts as hydrogen bond acceptor, as primary requirement for binding, and a polar feature representing an oxygen or sulfur atom as secondary binding interaction. In 2005, Langer's group developed a 3D-pharmacophore model (Langer-Ph) based upon 23 structurally diverse molecules with  $\sigma$ 1R  $K_i$  values between 10 pM and 100  $\mu$ M (Laggner et al., 2005). The model was generated with the HypoGen algorithm of Catalyst (Catalyst 4.9, 2003) and it consists in one PI and four HYD features (**Figure 1**). The model is in good agreement with Glennon's one but lacks the secondary polar binding region of Gund-Ph. Another HypoGen derived model (Zampieri-Ph) was published in 2009 using a series of 31 benzo[d]oxazol-2(3H)-one derivatives (Zampieri et al., 2009). The model contains one hydrogen bond acceptor (HBA), two hydrophobic aromatic features (HYD-AR), one HYD feature and one PI group. It is also in agreement with Glennon-Ph concerning distances among the PI feature and any HYD group, but it includes an additional polar/hydrogen bond acceptor feature as hypothesized by Gund. Langer-Ph and Zampieri-Ph share feature type and number (except for the additional HBA and the differentiation of one HYD to aliphatic HYD). Reported distances from the PI group to HYD features are similar, but not so much as it regards to their disposition and angles. Using the MOE Pharmacophore Elucidation routine, Wünsch's group aligned a training set of 66 spirocyclic derivatives to generate an additional pharmacophore model (Oberdorf-Ph) with four annotation points: aromatic, HYD, PI and HBA (Oberdorf et al., 2010). In 2012, another  $\sigma$ 1R 5-features model for a series of 32 N-substituted azahexacyclododecanols was developed using the Phase program provided in Maestro (Banister et al., 2012). Its composition of HYD, PI and HBA features is in accordance

with previous published models, but again with particular pairwise distances and angles. In summary, all the available pharmacophoric models share the presence of a PI and several HYD features with variations in distances and angles, and all of them, except Glenon's and Langer's ones include the presence of a polar group.

The first  $\sigma$ 1R homology model was published in 2011 by Pricl's group (Laurini et al., 2011). It was built taking as reference non-overlapping segments of four crystalized proteins with  $\geq 30\%$  sequence identities to the  $\sigma$ 1R. The N-terminal domain (residues 1–16) was built *de novo* and the four fragments were joined, generating and ranking alternative models for the loop portions in each junction zone. This initial 3D model was then subjected to refinement by molecular dynamics and a putative binding site was identified. The refined  $\sigma$ 1R homology model was then used for docking and binding affinity determination of a series of bioactive ligands and reference  $\sigma$ 1R ligands via the MM/PBSA methodology, as well as for the design of new ligands and their ranking for receptor affinity (Laurini et al., 2012, 2013). Later on, another  $\sigma$ 1R homology model was published, with results based on only the cold-active aminopeptidase, (PDB code 3CIA), also used by Pricl's group among template structures, wherein two distinct but closely proximal binding sites were suggested from docking studies of pentacycloundecylamines using MOE (Geldenhuys et al., 2013).

In 2016, the first crystal structure of the human  $\sigma$ 1R was published in complex with two ligands, PD144418 and 4-IBP (Schmidt et al., 2016). More recently the same group reported co-crystallization with additional compounds (Schmidt et al., 2018). The crystal structure shows an overall trimeric receptor arrangement, with a single transmembrane helix in each protomer, and each protomer binding a single ligand molecule. The single-pass transmembrane architecture was surprising in view of the widely accepted two-pass transmembrane architecture, compatible with or suggested from fluorescent tags and immunocytochemistry (Aydar et al., 2002; Hayashi and Su, 2007), radioiodinated photoprobe (Fontanilla et al., 2008) or solution circular dichroism-nuclear magnetic resonance (Ortega-Roldan et al., 2015) studies, although a single transmembrane segment close to the N-terminus and coded by exon 2 had already been suggested from the very beginning by hydropathy analysis of the amino acid sequence (Hanner et al., 1996; Kekuda et al., 1996; Seth et al., 1997; Prasad et al., 1998).

Taking advantage of the information and resolution provided by the X-ray crystallographic structure, we explored its contribution to the prediction of binding affinities in virtual screening conditions compared to previous pharmacophore models. To this aim we developed two new  $\sigma$ 1R pharmacophore models using the structural information revealed by the crystal structure, which was also used for docking studies in several conditions. Additionally we reproduced most of the published  $\sigma$ 1R pharmacophore models and compared their performance in front of a fraction of our chemical database, experimentally assayed for  $\sigma$ 1R affinity, containing more than 25,000 unique structures. To the best of our knowledge this is the first time that such a large compound dataset is used for establishing the predictive value of  $\sigma$ 1R models.

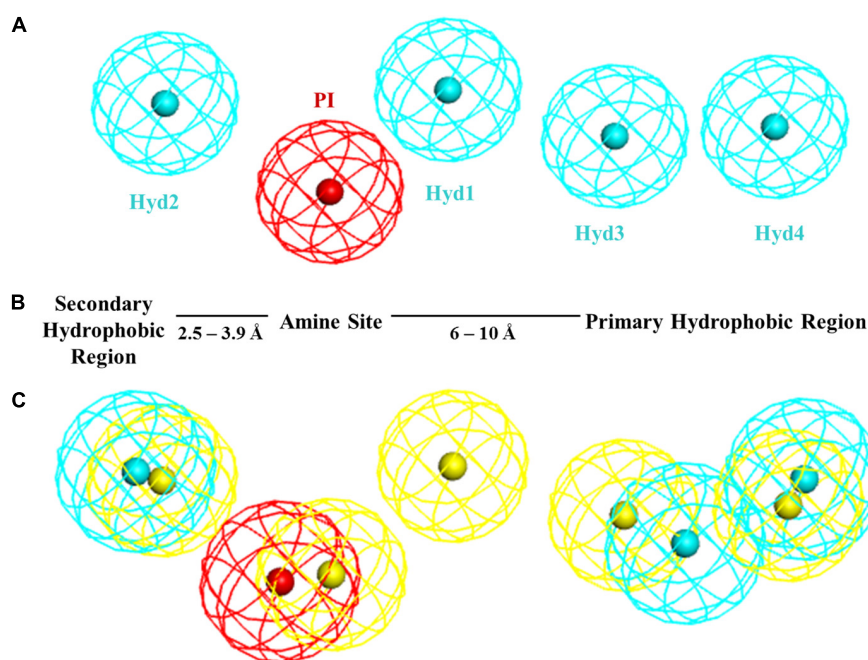


**FIGURE 1 | (A)** Langer-Ph. **(B)** Glennon-Ph. **(C)** Comparison of **5HK1-Ph.A** (without exclusion spheres) with Langer-Ph (yellow).

## MATERIALS AND METHODS

### Protein Preparation

The recently crystalized  $\sigma$ 1R structure (PDB = 5HK1) was prepared using Discovery Studio 16 (Dassault Systèmes BIOVIA, 2016a). Sulfate ions and oleoyl-glycerol molecules were removed, as well as all waters, since no key water molecules were observed within the binding site. Incomplete side chains were added, the structure was typed with the CHARMM forcefield and atoms were ionized according to the predicted pK at pH = 7.4, using the ‘calculate protein ionization and residue pK’ protocol. The charge of Asp126 was set to zero, allowing a hydrogen bond with the charged Glu172 as previously hypothesized (Schmidt et al., 2016). Subunit B of the trimeric structure was selected for further calculation as it shows the lowest average isotropic displacement. However, very similar results should be obtained using any of the other two subunits, as the RMSD of the 3 subunits superimposed by C-alpha pairs of residues within 5 Å distance to the ligand has a value of 0.25 between chains A and B and of 0.18 between chains B and C (RMSD superimposed using the whole chains is a bit higher due to the different bending of the helices).

### Ligand Databases Collection and Preparation

All in-house characterized compounds for  $\sigma$ 1R binding together with their data were retrieved from ESTEVE’s internal Activity Base database (IDBS, 2016). This made up a total of 25,676 unique structures. Compounds were obtained in the neutral form, as salts had been already striped in the registration process. Then a 3D multiconformational database was built

with Catalyst as implemented in Discovery Studio 2016, using the BEST methodology (Smellie et al., 1995; Kirchmair et al., 2006). 3D conformational generation was launched from Pipeline Pilot 2016 (Dassault Systèmes BIOVIA, 2016b). Special attention was given to correctly retain the stereochemical information of the compounds. Both chirality options were included in the conformation generation process for racemic mixtures. In the case of enantiomeric mixtures with grouped stereocenters, Catalyst is not able to take the stereochemistry-related information into account for conformer generation. Hence, different 3D entries for each of those compounds with the stereochemical combination defined by the stereo-groups were created, generating conformations specifically for each of them and joining them afterward with the same compound identifier. Compounds with fused cyclopropyl groups as well as some substituted cyclobutyl derivatives cannot be treated by the BEST algorithm. In this case conformations were built by systematic search using a default torsion increment of 60 for sp<sup>3</sup>-sp<sup>3</sup> and sp<sup>3</sup>-sp<sup>2</sup> bonds and of 180 for sp<sup>2</sup>-sp<sup>2</sup>, followed by minimization using the MMFF force field. The final database generated, consisting of 3,707,672 conformers, was used as input for pharmacophoric screening.

Additionally a second multiconformational database of the same compounds, but ionized, was built. To do so, basic pK<sub>a</sub> constants were calculated for all compounds using both ACD-classic and ACD-Galas (ACD/Labs, 2014). A Pipeline Pilot protocol was designed to generate a pool of different ionization states for each compound, by protonating basic points with pK<sub>a</sub> values above 5 or unprotonating acidic points below 5 successively on the previous state, and adding the resulting ionized structure to the pool. The protocol was run for the



ACD-classic and ACD-Galas generated values, and both output structures were merged and duplicate ionization states removed. Finally, the same procedure described above was followed, obtaining a new database with 7,573,004 conformers.

For the purpose of this work, structures were classified as actives when their  $K_i$  value was equal or under 1  $\mu$ M (18.6% of the samples; 4766 structures) or as inactives in the contrary cases or when  $K_i$  values had not been determined because their percentage inhibition at 1  $\mu$ M was under 50% (81.4% of the samples; 20,910 structures).

## Pharmacophore Generation

The receptor-ligand pharmacophore generator job implemented in Discovery Studio 16 was run on the prepared subunit B of the  $\sigma$ 1R with the co-crystallized ligand PD144418 to obtain **5HK1-Ph.A**. The algorithm (Sutter et al., 2011) generates pharmacophore models from the features that correspond to the receptor-ligand interactions, identifying in a first step all ligand features and pruning then those features that do not match the protein-ligand interactions. It additionally places as well excluded volumes to represent the steric aspect of the protein. **5HK1-Ph.B** was built modifying **5HK1-Ph.A** in the Discovery Studio interface using the available pharmacophore edition functionalities, specifically the averaging, the tolerance edition tool, and the feature customization functionality which was used to exclude certain substructures from the amidine and guanidine default mapping definition of PI that did not show basicity following the prediction of both ACD-classic and ACD-Galas (ACD/Labs, 2014). Langer-Ph, developed in Catalyst, now included in the Discovery Studio platform, was reproduced thanks to the definitions, coordinates, tolerances and weights included in its publication (Laggner et al., 2005). Zampieri-Ph and Banister-Ph were reproduced deriving the feature positions that fulfill the published distances and angles and setting a default constrain radius of 1.6 Å for the features. In the case of Zampieri-Ph, the angle of the projection point of the HBA feature was not reported, thus no location constrain was set for that projection point to avoid filtering out any hits of the original Zampieri-Ph. Regarding Banister-Ph, although it was built with the Phase program, Catalyst equivalent features were set for the different pharmacophoric points. In the case of the HBA and the Aromatic Ring (AR) features, as no directionality information was described, again the projection points of those features were left without location constrains. Gund-Ph, originally built using the Sybyl package, was reproduced in Discovery Studio using the given coordinate points (Gund et al., 2004). To be as accurate as possible in replicating the original features, the default tail definition of the Catalyst HBA feature was modified, accepting only the mapping to nitrogen atoms. Thus, the new HBA feature could be used to map the nitrogen location and the provided projection point of the hydrogen bond between the nitrogen and the receptor. To solve the issue of two normal vectors defining the AR, and understanding them as an attempt to map a pi-pi stacking from both sites of the ring, two Catalyst pharmacophores were built: one with the projection point on one side and the other with the projection on the other, requiring the fitting of both pharmacophores at the same time. Again a default constrain radius of 1.6 Å was set for all features

except for the HBA projection point where the default radius is 2.2 Å. Oberdorf-Ph could not be reproduced, as no distances, angles or feature coordinates were provided by the authors.

## Screening Methods

The generated multiconformational database with 3,707,672 conformers was screened with the Ligand Pharmacophore Mapping protocol launched from the Pipeline Pilot 2016 interface (Dassault Systèmes BIOVIA, 2016b), where each conformation was mapped separately and only the best mapping solution was returned for each of them, keeping finally only the mapped conformation with the best FitValue for each compound. Further, typical virtual screening conditions were used in the calculation: the omission of any feature was not allowed, and both rigid fit between each ligand conformation and the pharmacophore, as well as flexible fit, where slight conformational modifications are allowed to better fit the pharmacophore, were applied. In the case of the Langer-Ph, the published affinity prediction conditions were also used for screening, using the published weights and setting in this case the maximum number of omitted features to any. In the case of Gund-Ph to achieve the double directionality of the aromatic feature, we screened compounds first with a pharmacophore having the AR pointing to the direction of Tyr103, as determined after the pharmacophore-receptor alignment: Gund-up-Ph, and then we filtered the resulting conformations in place and without fitting, with a second pharmacophore equal to Gund-up-Ph but with the inverted projection point of AR.

For the docking studies, the LibDock program (Diller and Merz, 2001; Rao et al., 2007) implemented in Discovery Studio 16 was used, taking the prepared subunit B of the 5HK1 structure and the generated multi-conformational database of ionized compounds. A Site Sphere of 10 Å centered on the crystallized PD144418 ligand was defined and the docking grid was calculated using 1000 hotspots. No minimum cut-off value was set for the LibDockScore and up to 100 ligand poses could be saved for each ligand, but a filter requiring a charge interaction of the output poses with Glu172 was established to lower the number of possible solutions, as this interaction is the strongest interaction found in the crystallized structure (Schmidt et al., 2016) and mutation of Glu172 has been proven to abolish binding (Seth et al., 2001). Additionally, to ensure a proper orientation of the ligand, a hydrogen bond as part of the electrostatic salt-bridge interaction was also required (Bissantz et al., 2010). Finally poses with unfavorable interactions were filtered out. The remaining LibDock settings were left to their default values, and to score the resulting poses, the following seven scoring functions as implemented in Discovery Studio 16 were used: LigScore1, LigScore2 (Krammer et al., 2005), PLP1, PLP2 (Gehlhaar et al., 1995), Jain (Jain, 1996), PMF (Muegge and Martin, 1999), and PMF04 (Muegge, 2006).

## Human Sigma-1 Receptor Radioligand Assay

The binding properties of the 25,676 compounds to human  $\sigma$ 1R were studied in transfected HEK-293 membranes using [ $^3$ H](+)-pentazocine (Perkin Elmer, NET-1056) as the



radioligand. The assay was carried out with 7  $\mu$ g of membrane suspension, [ $^3$ H]-(+)-pentazocine (5 nM) in either absence or presence of either buffer or 10  $\mu$ M haloperidol for total and non-specific binding, respectively. Binding buffer contained Tris-HCl (50 mM, at pH 8). Plates were incubated at 37°C for 120 min. After the incubation period, the reaction mix was transferred to MultiScreen HTS, FC plates (Millipore), filtered and plates were washed (3 times) with ice-cold Tris-HCl (10 mM, pH 7.4). Filters were dried and counted at approximately 40% efficiency in a MicroBeta scintillation counter (Perkin-Elmer) using EcoScint liquid scintillation cocktail. The distribution of activities obtained is indicated in **Table 1**.

## Evaluation of Screening Performance

For evaluating the effectiveness of the different models, well-known metrics were used. The Enrichment Factor ( $EF^{x\%}$ ) measures the density of active compounds that can be found at a given fraction of the model-ordered database in comparison to a random selection. It is calculated by Equation (1), where  $Actives^{x\%}_{Selected}$  is the number of active compounds found at top x% of the database screened, following the model ranking;  $N^{x\%}_{Selected}$  is the number of compounds at top x% of the database;  $Actives_{Total}$  is the number of active ligands in entire database; and  $N_{total}$  is the number of compounds in the entire database. A major drawback of the Enrichment Factor, that turns it unsuitable for comparison of screening performance among different databases, is its dependency on the ratio between active and inactive compounds. However,

it allows a ranking of different models for the same database (Truchon and Bayly, 2007).

$$EF^{x\%} = \frac{Actives^{x\%}_{Selected}/N^{x\%}_{Selected}}{Actives_{Total}/N_{total}} \quad (1)$$

The Hit Rate ( $HR^{x\%}$ ) corresponds to the ratio of known hits found within the top x% and it is defined as the quotient of the real EF and the ideal EF (Hamza et al., 2012).

Sensitivity (TPR) is the fraction of correctly identified active compounds within the selected top x%.

Specificity (TNR) is the fraction of correctly identified inactive compounds within that x%.

The Receiver Operator Characteristic (ROC) curve plots sensitivity (true positive rate) versus specificity at all possible selection thresholds (Fawcett, 2006). The area under its curve (ROC-AUC) is a practical and objective way of measuring the performance of screening models, being independent of the balance of active and inactive compounds present in the database. ROC-AUC values range from 0.0 to 1.0, with 0.5 meaning random selection.

## Similarity Calculations

Extended-Connectivity Fingerprints (Rogers and Hahn, 2010), Functional-Class Fingerprints and MDL public keys (Durant et al., 2002) as implemented in Pipeline Pilot were used as structural descriptors. All pairwise Tanimoto distances among compounds of each set were calculated and statistical values and histogram frequencies were obtained with implemented protocols.

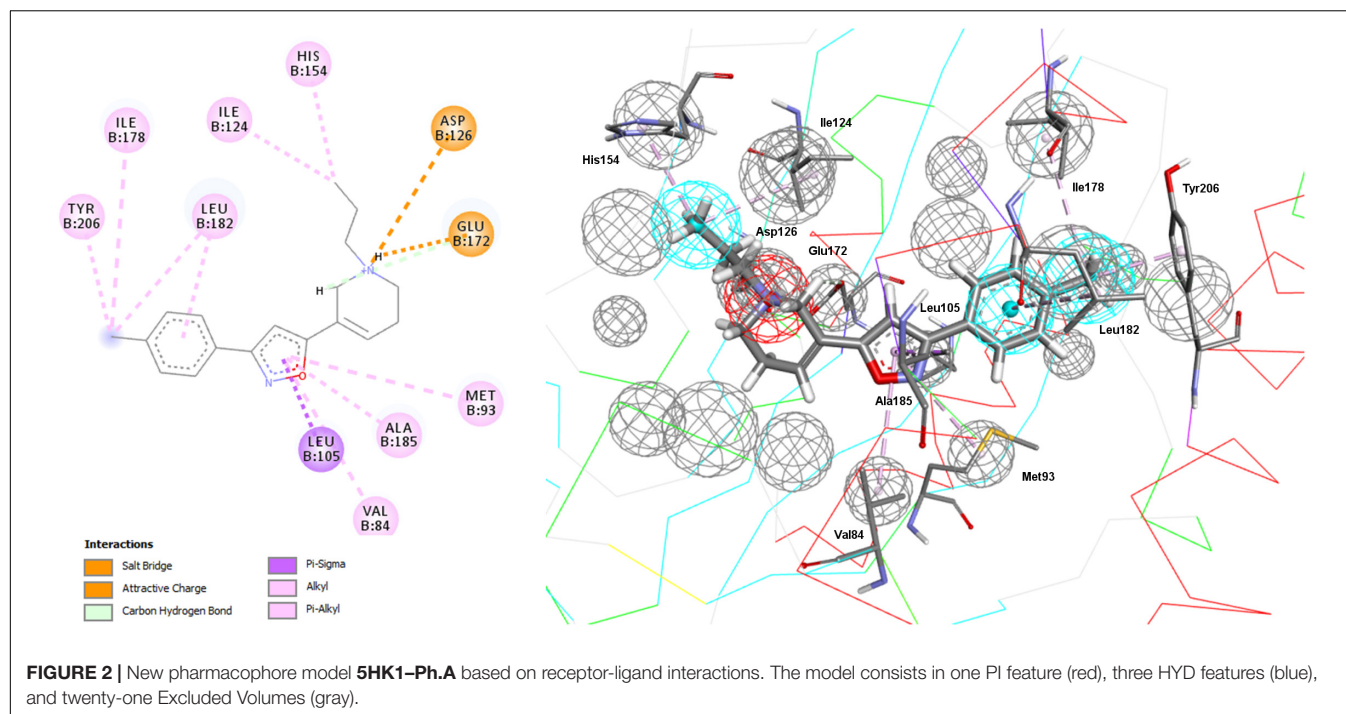
## RESULTS

As a first step, a new  $\sigma$ 1R pharmacophore model based on the receptor-ligand interactions observed in the 5HK1 crystal structure was automatically built. Only four out of the ten pharmacophoric features present in PD144418 were chosen by the algorithm as being the most characteristic and selective ones. Those were one PI feature and three HYD features, two on one side of the PI with distances from 7 to 13 Å and one on the other side at  $3.7 \text{ Å} \pm 0.8 \text{ Å}$ . The PI feature stands for the ionic interaction between the amine of PD144418 and Glu172 and Asp126; the HYD on one side for the hydrophobic interaction of the propyl chain with Ile124 and His154; and the two other HYD features for the interactions of the phenyl ring and the methyl with Leu182, Tyr206, and Ile178. These features together with the excluded volumes constituted the new  $\sigma$ 1R pharmacophore model **5HK1-Ph.A** (**Figure 2**).

Comparing **5HK1-Ph.A** with previously described models, we found that it perfectly matched the distances of Glennon-Ph. Langer-Ph just differed by having one additional HYD feature, while distances and angles were almost in perfect overlap with the new model (an RMS displacement of 1.1 Å if disregarding the additional HYD1 feature, **Figure 1**). This supports the feasibility of building ligand-based global models that account for receptor interactions, as well as HypoGen's model building power when a

**TABLE 1** | Experimentally determined  $\sigma$ 1R affinity range distribution of compounds in the dataset of 25,676 unique structures used for virtual screening and validation of the different models.

$\sigma$ 1R affinity range, Ki (nM)	#compounds
<50	1620
50–100	707
100–150	430
150–200	298
200–250	235
250–300	165
300–350	110
350–400	114
400–450	127
450–500	99
500–550	91
550–600	96
600–650	93
650–700	120
700–750	135
750–800	107
800–850	84
850–900	50
900–950	54
950–1000	31
>1000	20,910



proper diverse training set with a wide activity range is selected. The fact that the additional HYD feature present in Langer-Ph (HYD1) was not necessary for  $\sigma$ 1R binding, and could be replaced by other non-hydrophobic chemical groups, had already been observed for some of our  $\sigma$ 1R ligand families. For example, in a series of 4-aminotriazole derivatives (Díaz et al., 2015), the HYD1 feature was reported not to be covered by high affinity ligands; instead, triazole nitrogen atoms were present in that region.

To further determine whether HYD1 and its position may be dispensable (although it can account for the interaction of particular compound families), Langer-Ph was displaced and positioned into the  $\sigma$ 1R active site in two different ways. As a first option the within Discovery Studio available pharmacophore alignment algorithm was used. The second strategy entailed a rigid fitting of PD144418 into the pharmacophore, allowing the omission of one feature, followed by the displacement of the fitted structure to its crystallographic position, displacing at the same time the pharmacophore itself. In both cases, HYD1 turned out to be located directly over Tyr103. This implies that the conformation of a ligand that fulfills the geometrical disposition of the five features that make up the Langer-Ph would be positioned in a way that would at least initially clash with the crystallized  $\sigma$ 1R (Figure 3).

Going over to the remaining pharmacophore models that have in common the presence of an additional polar feature, Gund-Ph differed mainly by the absence of a HYD feature next to the PI and by the so-called secondary binding region defined by the presence of an oxygen or sulfur atom. After a rigid fit of Gund-Ph to the crystallized PD144418 model, we found that the AR did coincide with one of the HYD features of **5HK1-Ph.A** (Figure 4). Looking at the receptor, we observed that Tyr103 was actually pi-stacking with the phenyl ring of the ligand, thus

the aromatic feature in this position captured a ligand-receptor interaction, although only in one direction, since there was no other aromatic ring facing the phenyl from the other site. As for the directionality of the hydrogen bond established by the nitrogen, it reflected the interaction of the basic amine that may receive a hydrogen atom from either Glu172 or Asp126. In comparison to Langer-Ph, there was no HYD feature on the other site of the PI. Finally, the polar feature, defined in this case by the presence of an oxygen or sulfur atom, can be found in ligands such as PD144418, which was among those used to derive the pharmacophore, but it did not reflect a binding interaction, as the oxygen of the isoxazole ring does not show any polar interaction with the receptor.

Regarding Zampieri-Ph, no more than two features could be aligned simultaneously to **5HK1-Ph.A** when using the pharmacophore alignment algorithm. Only one of the solutions remained within the binding site region delimited by the exclusion volumes after the alignment, but in this case the location of the HBA would partially collapse with Tyr103 and the crystallized PD144418 would not fulfill more than two features in that disposition (Figure 5). On the other hand, a rigid fit of PD144418 was only achieved allowing the omission of two features, and when displacing the solution that mapped the PI feature to the crystallographic position of the ligand, space constraints could be observed for the non-fitted HYD and HYD-AR features of the pharmacophore.

Finally, all Banister-Ph features were mapped by PD144418 except for the HBA, although with a considerable low FitValue (Figure 6). An HBA in the specified position might represent a second polar interaction with Glu172, but this interaction was particular to the chemistry used to derive the model and does not seem to be always required for binding. The HYD feature

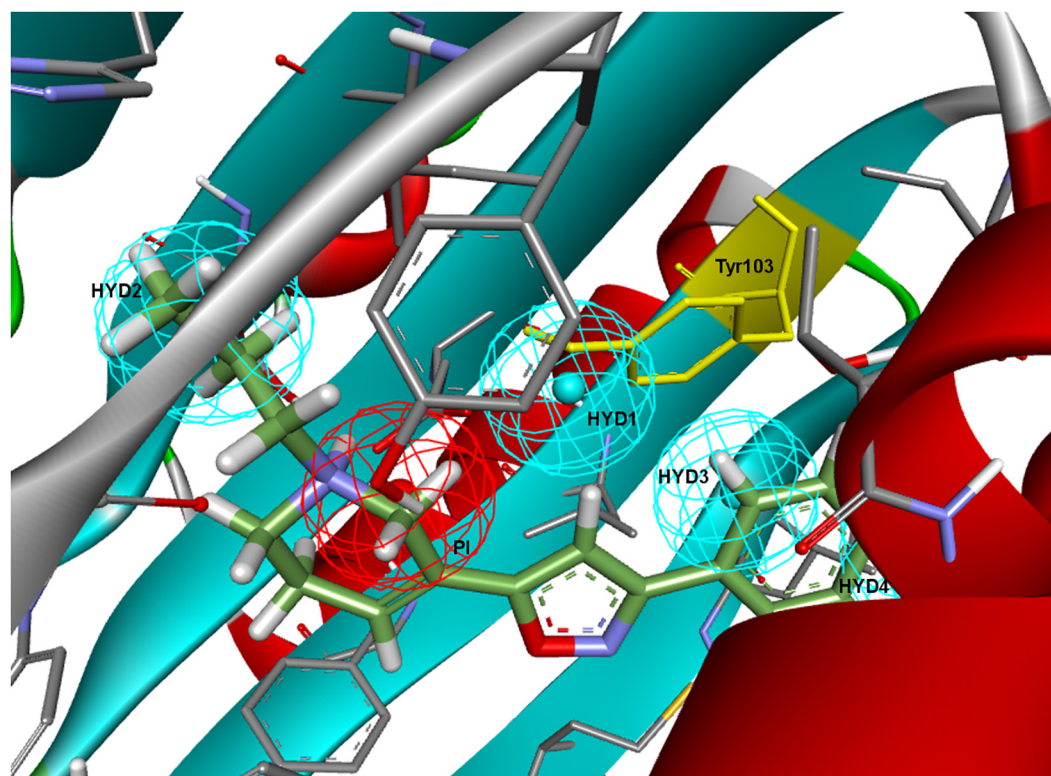


**FIGURE 3** | Langer-Ph positioned in the active site of the  $\sigma$ 1R. Note that HYD1 collapses with Tyr103 (in yellow).

next to the PI having an equivalent location to **5HK1-Ph.A** or to Langer-Ph was missing, but instead a second HYD that might stand for interactions with other hydrophobic aminoacids (Phe107) was found.

Visualizing the five pharmacophore models overlapped in the  $\sigma$ 1R binding site (**Figure 7**), we can conclude that they all have identified the important ionic interaction (PI), and coincide in placing a HYD or HYD aromatic site that has turned out to be the space defined by residues Tyr103, Leu105, Leu95, Tyr206, Leu182, and Ala185 and delimited by helices  $\alpha$ 4 and  $\alpha$ 5. More ambiguity was observed in the location of the other HYD region, which is not defined in Gund-Ph and has different placements in Banister's and Zampieri's models. Only Langer-Ph and the new structure-derived **5HK1-Ph.A** place it at the bottom of the  $\beta$ -barrel, near Asp126. Regarding the polar feature present in three of the models, it might likely reflect regions where a polar group can be tolerated rather than necessary interactions for binding.

In order to experimentally validate and test the performance of the different models, a 3D multiconformational database of 25,676 unique structures was built. They belong to ESTEVE's internal compound library and have been characterized over the years for  $\sigma$ 1R binding (displacement of [ $^3$ H]-(+)-pentazocine in HEK-293 membranes transfected with human  $\sigma$ 1R (DeHaven-Hudkins et al., 1992)). The compound dataset comprises compounds within all the affinity ranges, as indicated in **Table 1**. It is worth noting that almost half of the compounds considered

active for the  $\sigma$ 1R ( $K_i < 1 \mu\text{M}$ ) are high affinity compounds with  $K_i < 100 \text{ nM}$ .

The resulting multiconformational database (3,707,672 conformers) was screened with the five pharmacophore models applying both rigid and flexible fit. In the case of Langer-Ph, affinity prediction conditions were also tested. In the case of Gund-Ph two options were considered: compounds fulfilling just the directionality of the aromatic feature pointing to Tyr103 (Gund-up-Ph) and compounds with an aromatic feature accessible from both sites, which corresponds to the original definition (Gund-Ph). We then calculated for all the models the sensitivity, specificity, enrichment values and hit rates at 1, 5, and 10% of the database, and the area under the ROC curve (ROC-AUC). Results are displayed in **Table 2** and **Figure 8**. Gund's and Zampieri's models failed to discriminate actives from inactives, having ROC-AUC values scarcely above 0.5. Both Gund-Ph and Gund-up-Ph were equally unsatisfactory, probably due to the model simplicity, since both active and inactive compounds were equally able to fit the pharmacophore (high sensitivity and low specificity values), both with similar FitValues translating in enrichment factors around 1. Zampieri-Ph, on the contrary, had a low true positive rate, suggesting that the hypothesized features in the specified arrangement were not fulfilled by a high percentage of  $\sigma$ 1R binders. The very low enrichment factors tending to 1 already at the 10% of the ranked compounds indicates that inactive compounds suited the model almost as



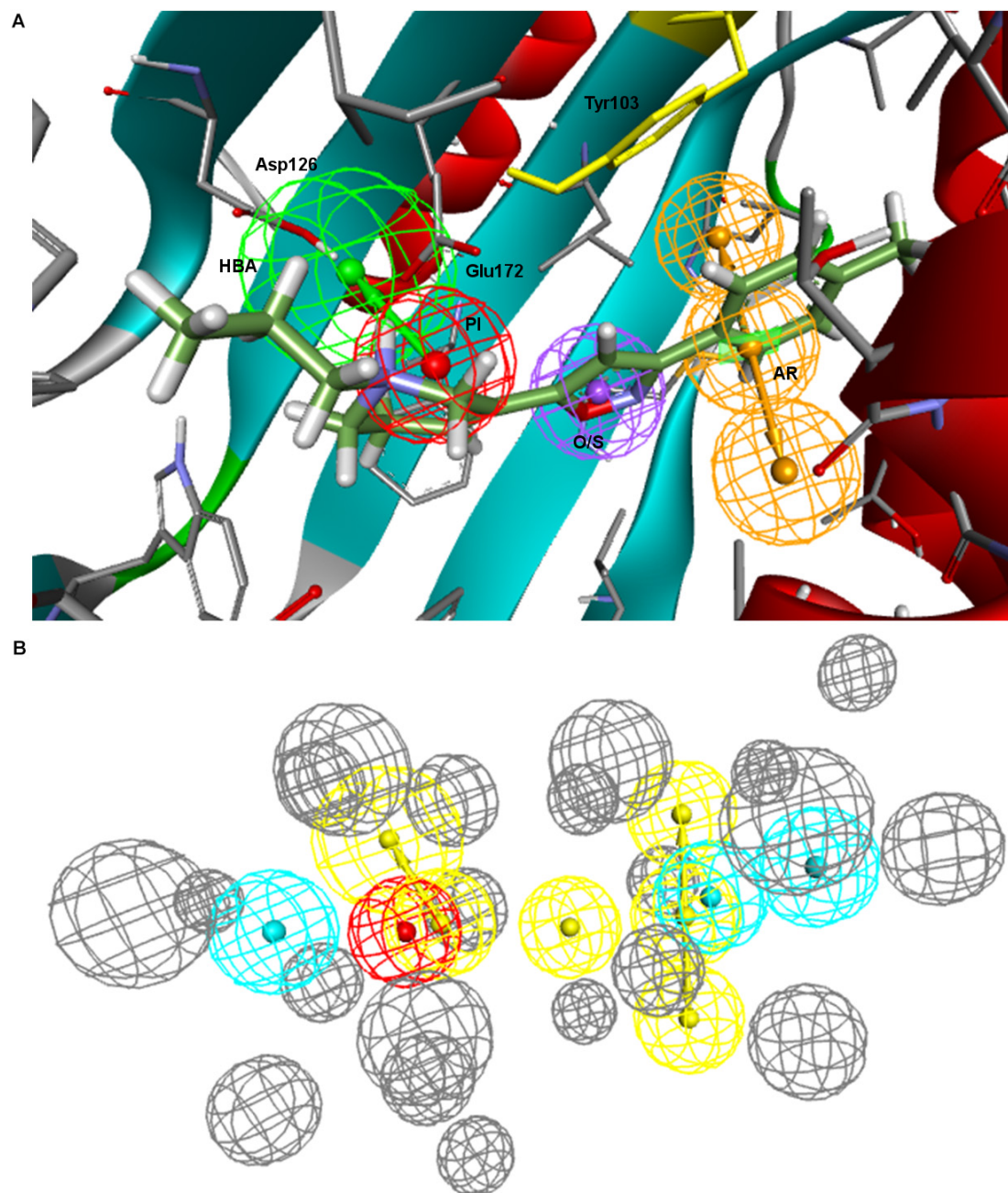


**FIGURE 4 | (A)** Gund-Ph positioned in the active site of the s1R by rigid ligand alignment. The AR features capture the pi-stacking with Tyr103, but there is no aromatic side chain on the other side for the interaction on the opposite direction; **(B)** Gund-Ph (yellow) overlapped with **5HK1-Ph.A**.

well as active ones. Both facts, together with the difficulties in the pharmacophore-receptor alignment, may indicate that the lack of success shown by ROC-AUC values was due to a feature disposition that does not geometrically map the key  $\sigma$ 1R-ligand interactions.

On the other hand, Langer-Ph, Banister-Ph and the new **5HK1-Ph.A** behaved approximately equal in discriminating active versus inactive compounds, either by applying rigid or flexible fit, with an almost equal poor to fair accuracy based

on ROC-AUC values around 0.7. They differed, however, in their sensitivity to specificity ratio. Banister-Ph had a high sensitivity, being able to recover around 80% of the hits, but at the cost of selecting many false positive compounds. Although the final area under the ROC curve was quite fair, enrichment factors up to 10% of the ranked compounds were barely above one. Accordingly, the presence of the features in the reported positions with a tolerance radius of 1.6 Å seems to be common to active compounds and fair enough to



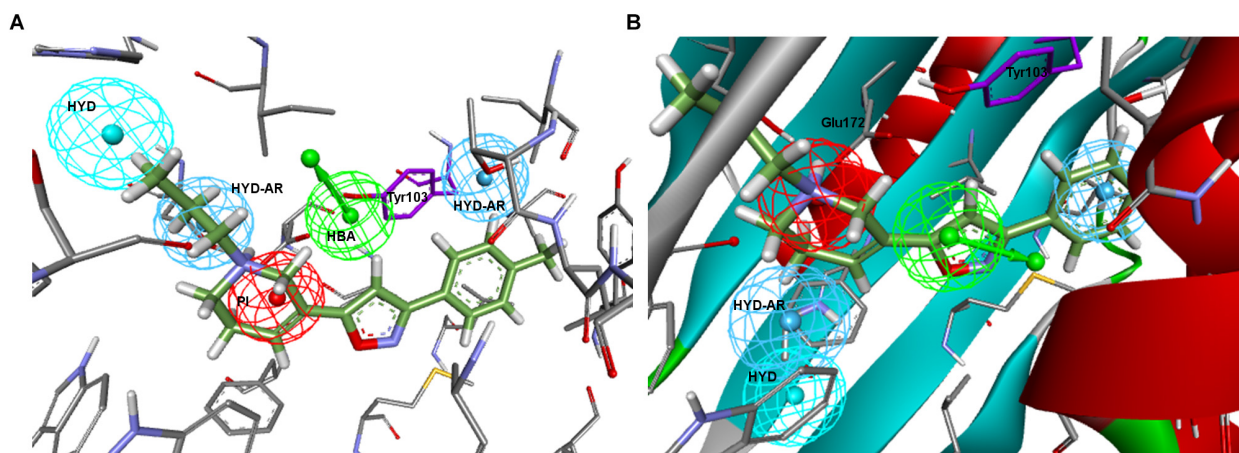


**FIGURE 5 | (A)** Zampieri-Ph place in the  $\sigma$ 1R binding site resulting from alignment with **5HK1-Ph.A**. HBA collapses partially with Tyr103 and the crystallized PD144418 does not fulfill more than 2 features; **(B)** Placement resulting from the rigid fit of PD144418 to Zampieri-Ph and displacement of the whole set to the crystallographic position of the ligand. Space constraints can be observed for the non-fitted HYD and HYD-AR features.

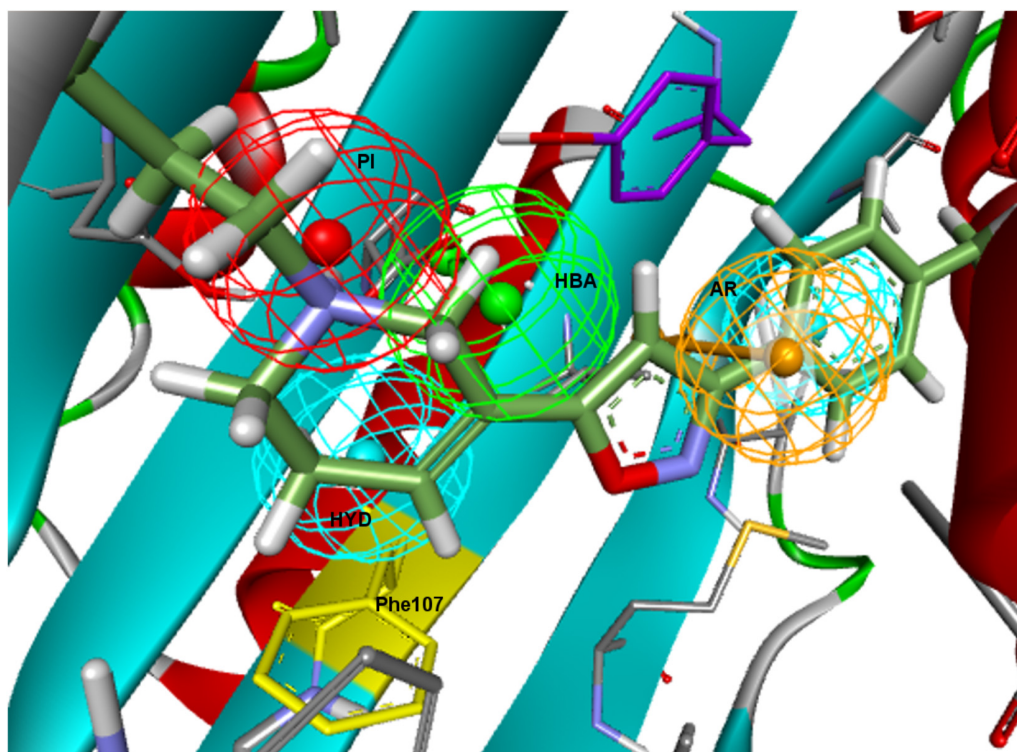


**FIGURE 6 |** Banister-Ph positioned in the binding site by rigid ligand-fit and displacement. The HYD under the PI might stand for interactions with other HYD aminoacids, mainly with Phe107 (in yellow).

distinguish them from inactive, but the predictability is low when considering only compounds with the best adjustments to reported distances and angles. Oppositely, Langer-Ph and **5HK1-Ph.A** managed high specificity values, with lower though acceptable true positive rates and enrichment factors between 2 and 3. Thus, both models were able to differentiate between actives and inactive, both globally and considering only best

fitting compounds. In fact, **5HK1-Ph.A** surpassed Langer-Ph in enrichment and hit rate values, with an average hit rate above fifty percent up to a 10% of ranked compounds, meaning that five to six out of each 10 compounds selected by the model show affinity for the  $\sigma$ 1R. In general, flexible fits seemed to perform slightly better in terms of ROC-AUC but not when looking at enrichment factors. This small difference may be

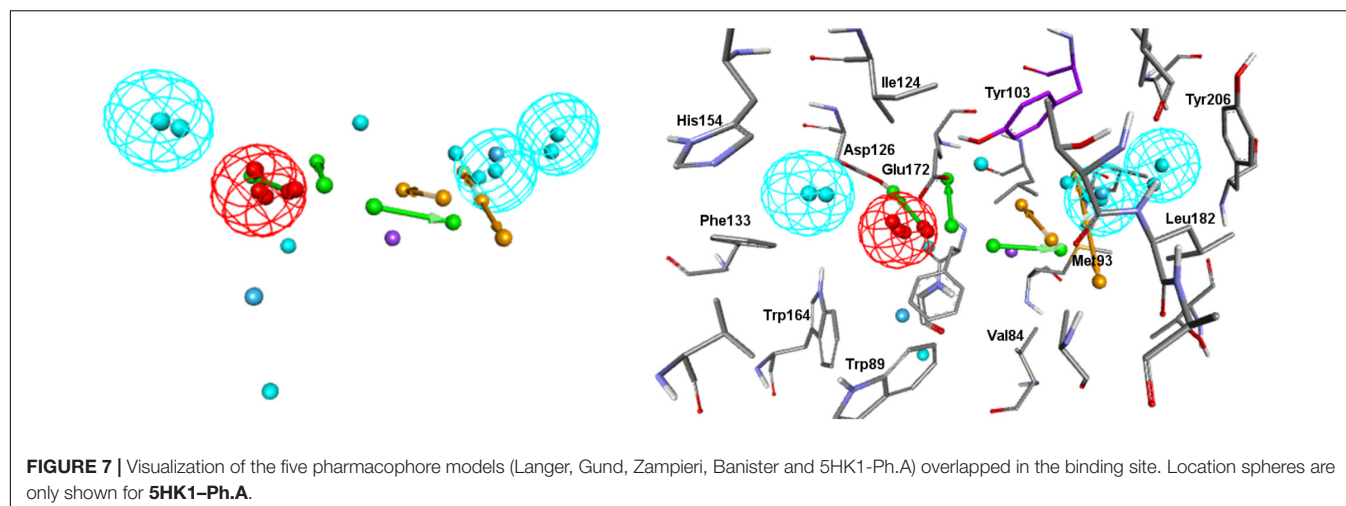


**TABLE 2 |** Area under the ROC curve, sensitivity, specificity, enrichment factors and hit rates at 1%, 5% and 10% of screened compounds using six different pharmacophore models, with both rigid and flexible fit.

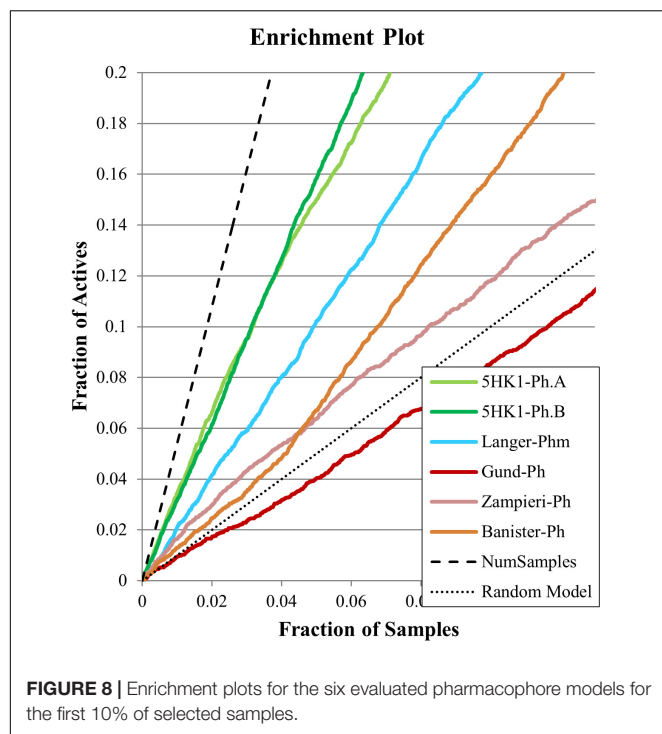
	ROC AUC	Sensitivity (TPR)	Specificity (TNR)	EF1%	EF5%	EF10%	HR1%	HR5%	HR10%
<b>5HK1-Ph.A</b>	0.65	0.45	0.84	3.44	3.00	2.66	63.8	55.6	49.3
<b>5HK1-Ph.A flex.</b>	0.66	0.5	0.80	3.40	2.79	2.43	63.1	51.7	45.1
<b>Langer-Ph</b>	0.67	0.53	0.80	2.10	2.04	2.04	38.9	37.8	37.8
<b>Langer-Ph flex.</b>	0.71	0.65	0.76	2.41	2.15	2.10	44.7	39.9	38.9
<b>Langer-Ph AffPred.<sup>a</sup></b>	0.73			1.97	1.93	1.91	36.5	35.8	35.4
<b>Gund-Ph</b>	0.52	0.71	0.34	0.94	0.81	0.85	17.5	14.9	15.8
<b>Gund-Ph flex.</b>	0.51	0.74	0.33	0.90	0.99	0.88	16.7	18.4	16.3
<b>Gund-up-Ph</b>	0.52	0.78	0.31	0.92	0.88	0.88	17.1	16.3	16.3
<b>Gund-up-Ph flex.</b>	0.52	0.8	0.3	0.82	0.84	0.91	15.2	15.6	16.9
<b>Zampieri-Ph</b>	0.51	0.16	0.87	1.66	1.28	1.18	30.8	23.7	21.9
<b>Zampieri-Ph flex.</b>	0.52	0.21	0.83	1.68	1.33	1.15	31.2	24.7	21.3
<b>Banister-Ph</b>	0.71	0.79	0.63	1.30	1.34	1.60	24.1	24.9	29.7
<b>Banister-Ph flex.</b>	0.76	0.82	0.61	1.30	1.16	1.35	24.1	21.5	25.0
<b>5HK1-Ph.B</b>	0.85	0.94	0.63	3.17	3.17	3.10	58.8	58.8	57.5
<b>5HK1-Ph.B flex.</b>	0.83	0.95	0.59	2.43	2.67	2.56	45.1	49.5	47.5

<sup>a</sup>In the case of Langer-Ph affinity prediction conditions have also been tested.

due to the higher number of compounds fitting the model thanks to this flexibility, conferring some advantage over random at higher fractions of selected compounds. Finally, Langer-Ph under affinity prediction conditions showed comparable results to Langer-Ph using a flexible fit.

Taking into consideration the binding site region (mainly built by amino acids exerting apolar interactions with the ligand) and receptor-ligand interactions automatically retrieved in the **5HK1-Ph.A**, we suspected that the two contiguous HYD features could be due to the nature of the ligand complexed in the crystal structure rather than to a real requisite for  $\sigma$ 1R binding. Therefore we decided to modify **5HK1-Ph.A** in order to average the two mentioned HYD features into a new one, placed at their center. This was done by increasing the tolerance to 3 Å to allow the fitting of any compound amenable to HYD interactions at that region, but without exceeding the surface delimited by the excluded volumes. Further, the tolerance of the

HYD feature at the other site of the PI group was increased to 2.2 Å, which approximately corresponds to the available receptor cavity, and excluded volumes were left the same. Additionally the PI feature was customized to exclude certain substructures from the amidine and guanidine default PI definition. With all these parameters a new pharmacophore, **5HK1-Ph.B**, was generated (**Figure 9**) and used to screen the same 3D multiconformational database applying again both rigid and flexible fit. The new results and statistical measures can be found as well in **Table 2** and **Figure 8**. We found that by merging the two HYD features sensitivity increased to optimal values (around 0.95), which means that **5HK1-Ph.B** is able to recognize almost all binders and without a substantial decrease, neither in precision nor in specificity, in comparison to the previous models. The higher sensitivity translated into a ROC-AUC value above 0.8, indicating a good statistical accuracy. Rigid fit surpassed flexible fit. Further enrichment factors and hit rates of the new models



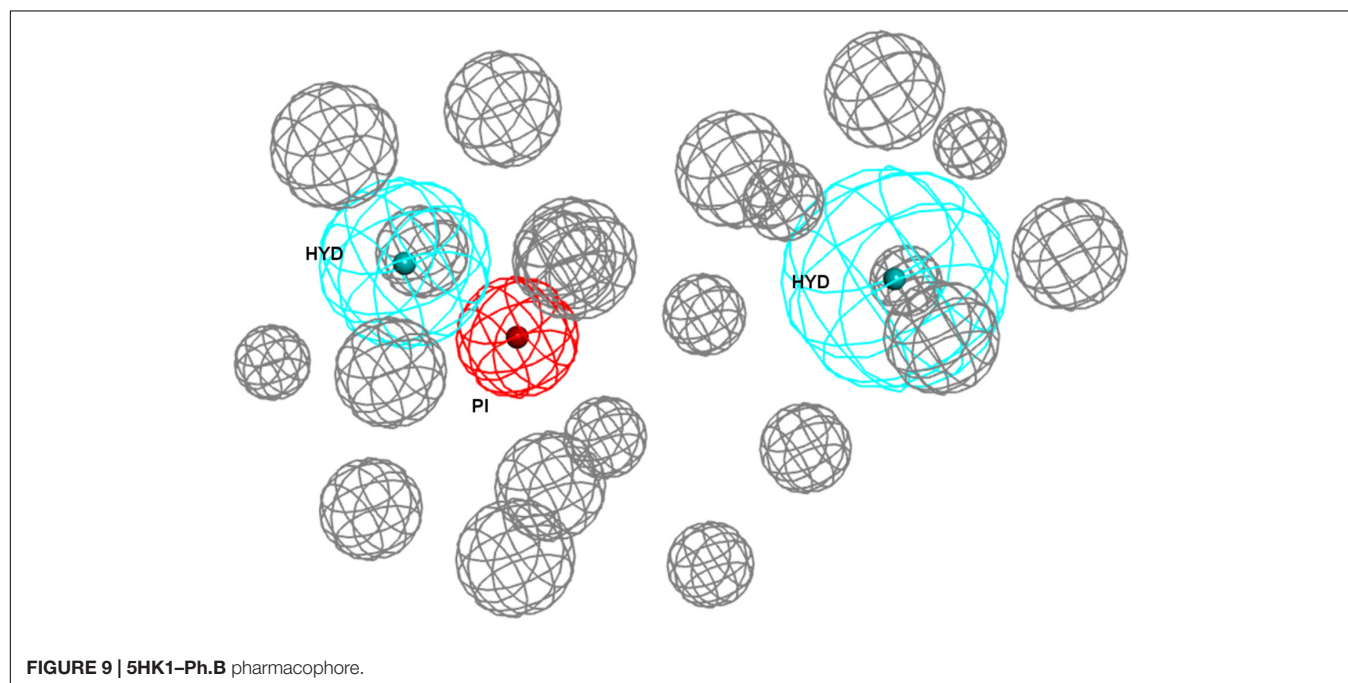
at screening percentages below 10% of the database are quite comparable to the best ones obtained previously. This leaves **5HK1-Ph.B** as the best  $\sigma$ 1R pharmacophore model among those assayed in this study in light of our internal, experimental *in vitro* data.

In addition to the pharmacophore models it was deemed interesting to perform a docking-based virtual screening using

the coordinates of the crystal  $\sigma$ 1R structure. For that purpose the 25,676 compounds were ionized for pH values greater than 5 to generate a new conformational database with 7,573,004 conformers that were docked using LibDock (Diller and Merz, 2001; Rao et al., 2007) as described in the experimental section. As shown in **Table 3**, the docking process was able to differentiate active from inactive compounds with fair ROC-AUC values around 0.77 for the different scoring functions, providing better sensitivity than specificity. That is, it generated more false positives than false negatives. The main difference among the scoring functions was found in enrichment values in the first 10% of ranked compounds, where -PMF04, LigScore2\_Dreiding and Jain achieved the higher values. With the best scored pose of  $\sigma$ 1R ligands (obtained with -PMF04), receptor-ligand interaction analysis was performed (**Figure 10**). It can be appreciated that, together with Glu172, other aminoacids such as Met93, Tyr103, Phe107, Tyr120, Leu182, and Ala185 are important for ligand recognition.

When comparing pharmacophore-based and docking-based screenings, pharmacophore search using **5HK1-Ph.B** outperformed docking results in all evaluated parameters. **5HK1-Ph.A** also showed a better performance than docking when looking at enrichment values, although with an opposite sensitivity-specificity profile. This may be due to the rigidity of the crystal structure in the docking process, as opposed to the feature tolerances in the pharmacophore model. Additionally, the importance of the HYD interactions characteristic of the  $\sigma$ 1R and the penalty for desolvating ligands with polar atoms may be not well captured by the tested scoring functions, whereas the pharmacophore model directly requires HYD groups to fill those regions up.

Finally, to assess the value of the **5HK1-Ph.B** model not only in terms of effectiveness but also in its potential

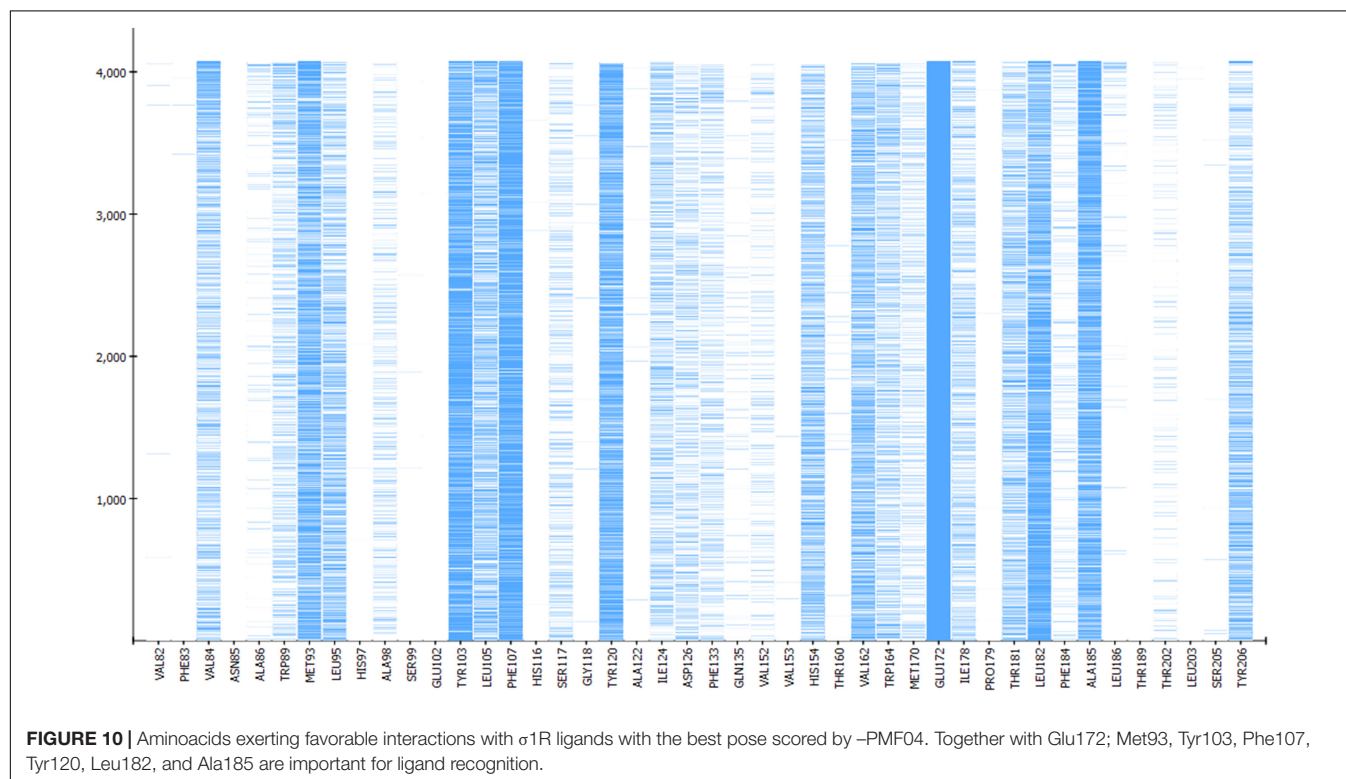




**TABLE 3 |** Area under the ROC curve, sensitivity, specificity, enrichment factors and hit rates at 1, 5, and 10% of ranked compounds after docking and scoring by seven different scoring functions.

	ROC-AUC	EF <sup>1%</sup>	EF <sup>5%</sup>	EF <sup>10%</sup>	HR <sup>1%</sup>	HR <sup>5%</sup>	HR <sup>10%</sup>
-PLP1	0.77	1.74	1.99	2.18	32.3	36.9	40.3
-PLP2	0.77	1.72	2.1	2.14	31.9	38.9	39.7
-PMF	0.76	1.3	1.72	1.9	24.1	31.9	35.2
-PMF04	0.77	2.81	2.34	2.27	52.1	43.4	42.1
Jain	0.78	1.87	2.3	2.4	34.7	42.7	44.5
LigScore1_Dreiding	0.74	1.51	1.6	1.82	28	29.7	33.8
LigScore2_Dreiding	0.75	2.62	2.36	2.2	48.6	43.8	40.8

–PMF04 shows the best results throughout the different indicators. Sensitivity (TPR): 0.85 Specificity (TNR): 0.59.

**FIGURE 10 |** Aminoacids exerting favorable interactions with  $\sigma$ 1R ligands with the best pose scored by –PMF04. Together with Glu172; Met93, Tyr103, Phe107, Tyr120, Leu182, and Ala185 are important for ligand recognition.

to capture diversity, we calculated all pairwise Tanimoto similarities for different subgroups of compounds, as depicted in **Table 4** and **Figure 11**. Three structural descriptors were used: Extended-Connectivity Fingerprints and Functional-Class Fingerprints with diameters four and six (that is maximal distance in bond length considered for the generation of the atom-centered substructural features encoded), and the MDL public keys implemented in Pipeline Pilot. Out of those pairwise distances, the average, median and mode distance values were also determined. Four subgroups were devised: (i) all the 25,676 compounds in the library; (ii) all the active compounds; (iii) the first 10% of selected compounds by the **5HK1-Ph.B** model; and (iv) the true active compounds within this 10%. As reference values for a selection of analogs we considered 88 active analogs of the  $\sigma$ 1R antagonist in clinical development (S1RA; E52862) (Díaz et al., 2012) as well as the first 88 ranked compounds by the **5HK1-Ph.B** model. We first found that calculated

distances of both Extended-Connectivity and Functional-Class fingerprints with diameter six exhibited slightly greater distances than those calculated with diameter four, and both of them returned higher values than those determined using MDL Public Keys. Interestingly, however, the same conclusions can be drawn with all of them: active compounds among the library are very diverse, with average, median and mode distances quite close to those exhibited by the whole library, which confirms the structural variety of  $\sigma$ 1R binders. The same degree of diversity was also observed for the first 10% compounds selected by the **5HK1-Ph.B** model, considering actives and inactives or only active compounds among the selected. In fact, statistical values obtained for the true positives among this 10% were almost equal to the values obtained for all the actives in the library. It is remarkable that the first 88 active compounds ranked by the model were able to reach high average distances, whereas the 88 analogs of S1RA showed clearly lower values. This reinforces the



**TABLE 4 |** Average ( $\mu$ ), median ( $M_e$ ), and mode ( $M_o$ ) pairwise Tanimoto distance values for five different subgroups: 88 analogs of the lead compound S1RA (E52862); the first 10% of selected compounds by the 5HK1-Ph.B model; the true active compounds within this 10%; all database compounds; all active compounds in the database.

	ECFP_6			ECFP_4			FCFP_6			FCFP_4			MDLPublicKeys		
	$\mu$	$M_e$	$M_o$	$\mu$	$M_e$	$M_o$	$\mu$	$M_e$	$M_o$	$\mu$	$M_e$	$M_o$	$\mu$	$M_e$	$M_o$
S1RA Analogs (88)	0.63	0.66	0.67	0.55	0.56	0.50	0.57	0.59	0.50	0.45	0.45	0.50	0.18	0.17	0.11
First 88 actives	0.85	0.87	0.89	0.82	0.84	0.86	0.82	0.85	0.86	0.76	0.78	0.75	0.42	0.44	0.50
First 10%	0.87	0.87	0.88	0.83	0.84	0.83	0.84	0.85	0.83	0.77	0.78	0.80	0.45	0.46	0.50
TP in the 10%	0.86	0.87	0.88	0.83	0.84	0.83	0.83	0.84	0.83	0.76	0.77	0.75	0.45	0.47	0.50
All database	0.89	0.89	0.89	0.86	0.87	0.86	0.86	0.87	0.86	0.82	0.82	0.80	0.52	0.52	0.50
All actives	0.86	0.87	0.88	0.82	0.84	0.83	0.83	0.84	0.83	0.76	0.77	0.75	0.45	0.46	0.50

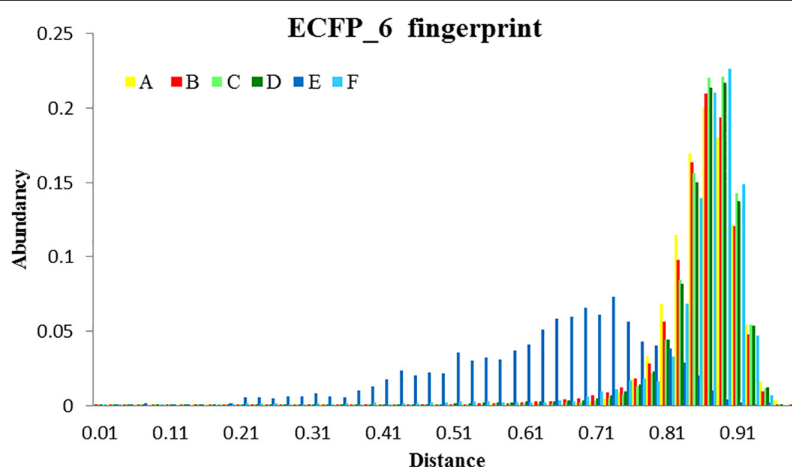


**FIGURE 11 |** Analysis of the diversity of the compounds with  $\sigma$ 1R affinity compared to the diversity of the whole database and compared as well with the diversity shown by the analogs of a lead compound. The diversity obtained by the pharmacophore selection (C) is comparable to that of the whole database (A). A, All library compounds; B, Active compounds in the library; C, first 10% of selected compounds by the 5HK1-Ph.B model; D, True positives within this 10%; E, 88 analogs of S1RA (E52862); F, First 88 ranked compounds by the 5HK1-Ph.B model.

mentioned ability of 5HK1-Ph.B to discriminate binders even when there are high structural differences among them.

## DISCUSSION

After the publication of the  $\sigma$ 1R crystal structure, a new avenue was open for the derivation of accurate models, either by generating new receptor-ligand derived pharmacophore models or by using it for docking studies. In order to show how this information could help in the design of new  $\sigma$ 1R ligands we decided to use it for the generation of new pharmacophoric models of general applicability. Two models were developed: The first one, 5HK1-Ph.A, was obtained by an algorithm that identifies the most important receptor-ligand interactions including as well excluded volumes based on atom location on the protein. The second, 5HK1-Ph.B, resulted from a manual edition of the first one mainly by merging two HYD features that we thought match the particular structure of one co-crystallized ligand more than specific requirements of the binding site.

In order to compare these new models with the information provided by previously published  $\sigma$ 1R pharmacophore models

(Langer-Ph, Gund-Ph, Zampieri-Ph, Banister-Ph), we carried out a study involving a set of 25,676 structures of our internal database that had been experimentally screened for  $\sigma$ 1R affinity in a binding assay of [ $^3$ H]-(+)-pentazocine displacement and displayed a wide range of activities and structural diversity.

All the pharmacophoric models assessed identified the important ionic interaction (PI) of ligands with Glu172 and placed a HYD or HYD aromatic site in the same region that turned out to be the space defined by residues Tyr103, Leu105, Leu95, Tyr206, Leu182, and Ala185 and delimited by helices  $\alpha$ 4 and  $\alpha$ 5. More ambiguity was observed in the location of the other HYD region, which is not defined in Gund-Ph and has different placements in Banister's and Zampieri's models. Only Langer-Ph and the new structure-derived 5HK1-Ph.A and 5HK1-Ph.B place it at the bottom of the  $\beta$ -barrel, near Asp126.

Finally, we also docked the ionized database using a high throughput docking technique and scored the resulting poses with seven different scoring functions. With the best scored pose of  $\sigma$ 1R ligands obtained with the best scoring function (-PMF04), receptor-ligand interaction analysis was performed and it was determined that, together with Glu172, other aminoacids such

as Met93, Tyr103, Phe107, Tyr120, Leu182, and Ala185 are important for ligand recognition.

Statistical performance measures were obtained with all the models generated, including Hit Rate (ratio of known hits found within the top x%), sensitivity (fraction of correctly identified active compounds), specificity (fraction of correctly identified inactive compounds) and the area under the Receiver Operator Characteristic Curve (ROC-AUC, which plots the true positive rate against the false positive rate at descending model's scores). When comparing all these parameters throughout the different models, **5HK1-Ph.B** emerged as the best model to discriminate between active and inactive compounds, with a ROC-AUC value above 0.8 and enrichment values above 3 at different fractions of screened samples. This means that **5HK1-Ph.B** could be used with the highest confidence in relation to any of the previously available models either in the design of new  $\sigma$ 1R ligands or in the virtual screening of large compound collections, where an increased hit-rate ratio is expected.

When comparing pharmacophore-based with docking-based screening, the receptor derived pharmacophore **5HK1-Ph.B** showed better results than the direct docking to the receptor. The superior performance of the pharmacophore screening is not absolutely unexpected as it has already been reported for other targets (Chen et al., 2009) and could be explained by the rigidity of the crystal structure in the docking process, that could be implicitly compensated by the feature tolerances in the pharmacophore model. Additionally, HYD interactions are very relevant in the  $\sigma$ 1R binding region and the penalty for desolvating ligands with polar atoms could be not well captured by the docking scoring functions. On the contrary, the pharmacophore model directly requires HYD groups to fill up those regions of the binding site.

It is important to note that  $\sigma$ 1R binds a remarkable variety of small molecules with high affinity (<100 nM), as already shown in the literature (Almansa and Vela, 2014). The results reported here were obtained using an internal database of drug-like as well as CNS-oriented molecules with experimentally determined affinities using a homogenous procedure, both for active and inactive compounds. Many of them were generated in the context of Medicinal Chemistry  $\sigma$ 1R programs and hence the database contains many diverse scaffolds where small modifications within congeneric series may abolish activity. This situation is not frequently encountered since models are usually generated or validated based on one or a few chemical families active on the target, in front of assumed inactives or decoys obtained by diversity selection of drug-like compounds (Réau et al., 2018). Altogether, the use of a large and diverse compound collection together with accurate structural information provides a sound basis for the generation and validation of predictive models to design new molecules.

While writing this manuscript, a 3D-QSAR model for a pooled dataset of known  $\sigma$ 1R antagonists from five structurally diverse chemical families, with 147 compounds for model development and 33 compounds for model validation, has been published (Peng et al., 2018). Interestingly, the X-ray crystal structure of the human  $\sigma$ 1R in complex with PD144418 was used to derive the pharmacophore model needed for the structural

alignment of the compounds. With this alignment procedure, a predictive 3D-QSAR model for  $\sigma$ 1R antagonists was obtained and further validated by virtually screening the DrugBank database of FDA approved drugs. Two approved drugs with high and previously unknown  $\sigma$ 1R affinities were identified (diphenhydramine and phenyltoloxamine;  $K_i$  = 58 and 160 nM, respectively). Despite the constrained applicability domain of 3D-QSAR to the range of binding affinities and chemical space of the training set ligands, the publication demonstrates as well the success in the use of the X-ray structure for model development, allowing the identification of new drug leads prior to the resource-demanding tasks of chemical synthesis and experimental biological evaluation.

Finally, it is important to note that classification of  $\sigma$ 1R ligands as agonists or antagonists has been often based on their opposing or counteracting effects on biological systems including cell lines, primary cultures and animals (Cobos et al., 2008; Maurice and Su, 2009; Entrena et al., 2016). Little is known in terms of specific structural features or specific receptor conformations when agonists or antagonists are bound. Ligand-mediated conformational changes distinctive for agonist and antagonist ligands were observed when some reference  $\sigma$ 1R ligands were assayed in a  $\sigma$ 1R fluorescence resonance energy transfer (FRET)-based biosensor (Gómez-Soler et al., 2014). FRET data also support distinctive interactions as some  $\sigma$ 1R antagonists stabilize high-molecular-weight oligomers, while certain agonists suppress oligomerization (Mishra et al., 2015). However, the agonist-bound crystallizes similarly to the antagonist-bound  $\sigma$ 1R, and the overall conformation of the receptor does not significantly differ, except for a 1.8 Å shift of helix  $\alpha$ 4 found when compared the (+)-pentazocine-bound relative to the PD 144418-bound structure (Schmidt et al., 2018). Thus, current structural data are insufficient to comment substantively on the impact of identified receptor-ligand interactions on the functional nature of assayed ligands. This will doubtless be an important area for future research. Going further, elucidation of distinct ligand-driven conformations and regulation of homo-/heteromerization states is poised to be an important area for  $\sigma$ 1R structural biology. Importantly, the advent of structural data now allows more rational construct design and analysis for computational work.

## AUTHOR CONTRIBUTIONS

The manuscript was written through contributions of all authors. All authors have given approval to the final version of the manuscript.

## FUNDING

This work was a part of activities in R&D projects IDI20150914 and IDI20150915 supported by the Spanish Ministerio de Economía y Competitividad (MINECO), through the Centro para el Desarrollo Tecnológico Industrial (CDTI), co-financed by the European Union through the European Regional Development Fund (ERDF; Fondo Europeo de Desarrollo Regional, FEDER).

## REFERENCES

- ACD/Labs (2014). *ACD/Structure Elucidator, Version 2018.1*. Toronto, ON: Advanced Chemistry Development, Inc. Available at: <https://www.acdlabs.com/company/reference.php> (accessed May, 2019).
- Almansa, C., and Vela, J. M. (2014). Selective sigma-1 receptor antagonists for the treatment of pain. *Future Med. Chem.* 6, 1179–1199. doi: 10.4155/fmc.14.54
- Aydar, E., Palmer, C. P., Klyachko, V. A., and Jackson, M. B. (2002). The sigma receptor as a ligand-regulated auxiliary potassium channel subunit. *Neuron* 34, 399–410. doi: 10.1016/S0896-6273(02)00677-3
- Banister, S. D., Manoli, M., Doddareddy, M. R., Hibbs, D. E., and Kassiou, M. (2012). A  $\sigma$ 1 receptor pharmacophore derived from a series of N-substituted 4-azahexacyclo[5.4.1.0<sub>2,6</sub>.0<sub>3,10</sub>.0<sub>5,9</sub>.0<sub>8,11</sub>]dodecan-3-ols (AHDs). *Bioorgan. Med. Chem. Lett.* 22, 6053–6058. doi: 10.1016/j.bmcl.2012.08.046
- Bissantz, C., Kuhn, B., and Stahl, M. (2010). A medicinal chemist's guide to molecular interactions. *J. Med. Chem.* 53, 5061–5084. doi: 10.1021/jm100112j
- Catalyst 4.9 (2003). *Catalyst 4.9*. San Diego, CA: Accelrys.
- Chen, Z., Li, H. L., Zhang, Q. J., Bao, X. G., Yu, K. Q., Luo, X. M., et al. (2009). Pharmacophore-based virtual screening versus docking-based virtual screening: a benchmark comparison against eight targets. *Acta Pharmacol. Sin.* 30, 1694–1708. doi: 10.1038/aps.2009.159
- Cobos, E. J., Entrena, J. M., Nieto, F. R., Cendán, C. M., and Del Pozo, E. (2008). Pharmacology and therapeutic potential of sigma(1) receptor ligands. *Curr. Neuropharmacol.* 6, 344–366. doi: 10.2174/157015908787386113
- Dassault Systèmes BIOVIA (2016a). *Discovery Studio*, 16. San Diego, CA: Dassault Systèmes BIOVIA.
- Dassault Systèmes BIOVIA (2016b). *Pipeline Pilot* 16. San Diego, CA: Dassault Systèmes BIOVIA.
- DeHaven-Hudkins, D. L., Fleissner, L. C., and Ford-Rice, F. Y. (1992). Characterization of the binding of [3H](+)-pentazocine to recognition sites in guinea pig brain. *Eur. J. Pharmacol.* 227, 371–378. doi: 10.1016/0922-4106(92)90153-M
- Díaz, J. L., Christmann, U., Fernandez, A., Torrens, A., Port, A., Pascual, R., et al. (2015). Synthesis and structure–activity relationship study of a new series of selective  $\sigma$ 1 receptor ligands for the treatment of pain: 4-aminotriazoles. *J. Med. Chem.* 58, 2441–2451. doi: 10.1021/jm501920g
- Díaz, J. L., Cuberes, R., Berrocal, J., Contijoch, M., Christmann, U., Fernánde, A., et al. (2012). Synthesis and biological evaluation of the 1-arylpyrazole class of  $\sigma$ 1 receptor antagonists: identification of 4-[2-[5-methyl-1-(naphthalen-2-yl)-1H-pyrazol-3-yl]oxy]ethylmorpholine (S1RA, E-52862). *J. Med. Chem.* 55, 8211–8224. doi: 10.1021/jm3007323
- Diller, D. J., and Merz, K. M. Jr. (2001). High throughput docking for library design and library prioritization. *Proteins* 43, 113–124.
- Durant, J. L., Leland, B., Henry, D. R., and Nourse, J. G. (2002). Reoptimization of MDL keys for use in drug discovery. *J. Chem. Inf. Comput. Sci.* 42, 1273–1280. doi: 10.1021/ci010132r
- Entrena, J. M., Sánchez-Fernández, C., Nieto, F. R., González-Cano, R., Yeste, S., Cobos, E. J., et al. (2016). Sigma-1 receptor agonism promotes mechanical allodynia after priming the nociceptive system with capsaicin. *Sci Rep.* 6:37835. doi: 10.1038/srep37835
- Fawcett, T. (2006). An introduction to ROC analysis. *Pattern Recogn. Lett.* 27, 861–874. doi: 10.1016/j.patrec.2005.10.010
- Fontanilla, D., Hajipour, A. R., Pal, A., Chu, U. B., Arbabian, M., and Ruoho, A. E. (2008). Probing the steroid-binding domain-like I (SBDLI) of the sigma-1 receptor binding site using N-substituted photoaffinity labels. *Biochemistry* 47, 7205–7217. doi: 10.1021/bi800564j
- Gehlhaar, D. K., Verkhivker, G. M., Rejto, P. A., Sherman, C. J., Fogel, D. B., Fogel, L. J., et al. (1995). Molecular recognition of the inhibitor AG-1343 by HIV-1 protease: conformationally flexible docking by evolutionary programming. *Chem. Biol.* 2, 317–324. doi: 10.1016/1074-5521(95)90050-0
- Geldenhuys, W. J., Novotny, N., Malan, S. F., and Van der Schyf, C. J. (2013). 3D-QSAR and docking studies of pentacycloundecylamines at the sigma-1 ( $\sigma$ 1) receptor. *Bioorgan. Med. Chem. Lett.* 223, 1707–1711. doi: 10.1016/j.bmcl.2013.01.069
- Glennon, R. A., Ablordeppay, S. Y., Ismael, A. M., El-Ashmawy, M. B., Fischer, J. B., and Howie, K. B. (1994). Structural features important for sigma.1 receptor binding. *J. Med. Chem.* 37, 1214–1219. doi: 10.1021/jm00034a020
- Gómez-Soler, M., Fernández-Dueñas, V., Portillo-Salido, E., Pérez, P., Zamanillo, D., Vela, J. M., et al. (2014). Predicting the antinociceptive efficacy of  $\sigma$ (1) receptor ligands by a novel receptor fluorescence resonance energy transfer (FRET) based biosensor. *J. Med. Chem.* 57, 238–242. doi: 10.1021/jm401529t
- Gund, T. M., Floyd, J., and Jung, D. (2004). Molecular modeling of sigma 1 receptor ligands: a model of binding conformational and electrostatic considerations. *J. Mol. Graph. Model.* 22, 221–230. doi: 10.1016/j.jmkgm.2003.08.001
- Hamza, A., Wei, N., and Zhan, C. (2012). Ligand-based virtual screening Approach using a new scoring function. *J. Chem. Inf. Model.* 52, 963–974. doi: 10.1021/ci200617d
- Hanner, M., Moebius, F. F., Flandorfer, A., Knaus, H. G., Striessnig, J., Kempner, E., et al. (1996). Purification, molecular cloning, and expression of the mammalian sigma1-binding site. *Proc. Natl. Acad. Sci. U.S.A.* 93, 8072–8077. doi: 10.1073/pnas.93.15.8072
- Hayashi, T., and Su, T. P. (2007). Sigma-1 receptor chaperones at the ER-mitochondrion interface regulate Ca(2+) signaling and cell survival. *Cell* 131, 596–610. doi: 10.1016/j.cell.2007.08.036
- Hayashi, T., Tsai, S. Y., Mori, T., Fujimoto, M., and Su, T. P. (2011). Targeting ligandoperated chaperone sigma-1 receptors in the treatment of neuropsychiatric disorders. *Expert Opin. Ther. Targets* 15, 557–577. doi: 10.1517/14728222.2011.560837
- IDBS (2016). *Activity Base*. Available at: <http://www.idbs.com> (accessed May, 2019).
- Jain, A. N. (1996). Scoring noncovalent protein-ligand interactions: a continuous differentiable function tuned to compute binding affinities. *J. Comput. Aided Mol. Design* 10, 427–440. doi: 10.1007/BF00124474
- Kekuda, R., Prasad, P. D., Fei, Y. J., Leibach, F. H., and Ganapathy, V. (1996). Cloning and functional expression of the human type 1 sigma receptor (hSigmaR1). *Biochem. Biophys. Res. Commun.* 229, 553–558. doi: 10.1006/bbrc.1996.1842
- Kirschmair, J., Wolber, G., Laggner, C., and Langer, T. (2006). Comparative performance assessment of the conformational model generators omega and catalyst: a large-scale survey on the retrieval of protein-bound ligand conformations. *J. Chem. Inf. Model.* 46, 1848–1861. doi: 10.1021/ci060084g
- Krammer, A., Kirchhoff, P. D., Jiang, X., Venkatachalam, C. M., and Waldman, M. (2005). LigScore: a novel scoring function for predicting binding affinities. *J. Mol. Graph. Model.* 23, 395–407. doi: 10.1016/j.jmkgm.2004.11.007
- Laggner, C., Schieferer, C., Fiechtner, B., Poles, G., Hoffmann, R. D., Glossmann, H., et al. (2005). Discovery of high-affinity ligands of  $\sigma$ 1 receptor, ERG2, and emopamil binding protein by pharmacophore modeling and virtual Screening. *J. Med. Chem.* 48, 4754–4764. doi: 10.1021/jm049073
- Laurini, E., Dal Col, V., Mamolo, M. G., Zampieri, D., Posocco, P., Fermeiglia, M., et al. (2011). Homology model and docking based virtual screening for ligands of the  $\sigma$ 1 receptor. *ACS Med. Chem. Lett.* 2, 834–839. doi: 10.1021/ml2001505
- Laurini, E., Dal Col, V., Wünsch, B., and Pricl, S. (2013). Analysis of the molecular interactions of the potent analgesic S1RA with the  $\sigma$  receptor. *Bioorgan. Med. Chem. Lett.* 10, 2868–2871. doi: 10.1016/j.bmcl.2013.03.087
- Laurini, E., Marson, D., Dal Col, V., Fermeiglia, M., Mamolo, M. G., Zampieri, D., et al. (2012). Another brick in the wall. Validation of the  $\sigma$ 1 receptor 3D model by computer-assisted design, synthesis, and activity of new  $\sigma$ 1 ligands. *Mol. Pharm.* 9, 3107–3126. doi: 10.1021/mp300233y
- Maurice, T., and Su, T. P. (2009). The pharmacology of sigma-1 receptors. *Pharmacol. Ther.* 124, 195–206. doi: 10.1016/j.pharmthera.2009.07.001
- Mishra, A. K., Mavlyutov, T., Singh, D. R., Biener, G., Yang, J., Oliver, J. A., et al. (2015). The sigma-1 receptors are present in monomeric and oligomeric forms in living cells in the presence and absence of ligands. *Biochem. J.* 466, 263–271. doi: 10.1042/BJ20141321
- Muegge, I. (2006). PMF scoring revisited. *J. Med. Chem.* 49, 5895–5902. doi: 10.1021/jm050038s
- Muegge, I., and Martin, Y. C. (1999). A general and fast scoring function for protein-ligand interactions: a simplified potential approach. *J. Med. Chem.* 42, 791–894. doi: 10.1021/jm980536j
- Oberdorf, C., Schmidt, T. J., and Wünsch, B. (2010). 5D-QSAR for spirocyclic sigma1 receptor ligands by Quasar receptor surface modeling. *Eur. J. Med. Chem.* 45, 3116–3124. doi: 10.1016/j.ejmech.2010.03.048
- Ortega-Roldán, J. L., Ossa, F., Amin, N. T., and Schnell, J. R. (2015). Solution NMR studies reveal the location of the second transmembrane domain of the

- human sigma-1 receptor. *FEBS Lett.* 589, 659–665. doi: 10.1016/j.febslet.2015.01.033
- Peng, Y., Dong, H., and Welsh, W. J. (2018). Comprehensive 3D-QSAR model predicts binding affinity of structurally diverse sigma 1 receptor ligands. *J. Chem. Inf. Model.* 59, 486–497. doi: 10.1021/acs.jcim.8b00521
- Prasad, P. D., Li, H. W., Fei, Y. J., Ganapathy, M. E., Fujita, T., Plumley, L. H., et al. (1998). Exon-intron structure, analysis of promoter region, and chromosomal localization of the human type 1 sigma receptor gene. *J. Neurochem.* 70, 443–451. doi: 10.1046/j.1471-4159.1998.70020443.x
- Rao, S. N., Head, M. S., Kulkarni, A., and Lalonde, J. M. (2007). Validation studies of the site-directed docking program LibDock. *J. Chem. Inf. Model.* 47, 2159–2171. doi: 10.1021/ci6004299
- Réau, M., Langenfeld, F., Zagury, J. F., Lagarde, N., and Montes, M. (2018). Decoys selection in benchmarking datasets: overview and perspectives. *Front. Pharmacol.* 9:11. doi: 10.3389/fphar.2018.00011
- Rogers, D., and Hahn, M. (2010). Extended-connectivity fingerprints. *J. Chem. Inf. Model.* 50, 742–754. doi: 10.1021/ci100050t
- Schmidt, H. R., Betz, R. M., Dror, R. O., and Kruse, A. C. (2018). Structural basis for  $\sigma$ 1 receptor ligand recognition. *Nat. Struct. Mol. Biol.* 25, 981–987. doi: 10.1038/s41594-018-0137-2
- Schmidt, H. R., Zheng, S., Gurpinar, E., Koehl, A., Manglik, A., and Kruse, A. C. (2016). Crystal structure of the human  $\sigma$ 1 receptor. *Nature* 532, 527–530. doi: 10.1038/nature17391
- Seth, P., Ganapathy, M. E., Conway, S. J., Bridges, C. D., Smith, S. B., Casellas, P., et al. (2001). Expression pattern of the type 1 sigma receptor in the brain and identity of critical anionic amino acid residues in the ligand-binding domain of the receptor. *Biochim. Biophys. Acta* 1540, 59–67. doi: 10.1016/S0167-4889(01)00117-3
- Seth, P., Leibach, F. H., and Ganapathy, V. (1997). Cloning and structural analysis of the cDNA and the gene encoding the murine type 1 sigma receptor. *Biochem. Biophys. Res. Commun.* 241, 535–540. doi: 10.1006/bbrc.1997.7840
- Smellie, A., Teig, S. L., and Towbin, P. (1995). Poling: promoting conformational variation. *J. Comp. Chem.* 16, 171–187. doi: 10.1002/jcc.540160205
- Su, T. P., Hayashi, T., Maurice, T., Buch, S., and Ruoho, A. E. (2010). The sigma-1 receptor chaperone as an inter-organelle signaling modulator. *Trends Pharmacol. Sci.* 31, 557–566. doi: 10.1016/j.tips.2010.08.007
- Sutter, J., Li, J., Maynard, A. J., Goupil, A., Luu, A., and Nadassy, K. (2011). New features that improve the pharmacophore tools from Accelrys. *Curr. Comput. Aided Drug Des.* 7, 173–180. doi: 10.2174/157340911796504305
- Truchon, J. F., and Bayly, C. I. (2007). Evaluating virtual screening methods: good and bad metrics for the “early recognition”. *Problem. J. Chem. Inf. Model.* 47, 488–508. doi: 10.1021/ci600426e
- Zamanillo, D., Romero, L., Merlos, M., and Vela, J. M. (2013). Sigma1 receptor: a new therapeutic target for pain. *Eur. J. Pharmacol.* 716, 78–93. doi: 10.1016/j.ejphar.2013.01.068
- Zampieri, D., Mamolo, M. G., Laurini, E., Florio, C., Zanette, C., Fermeglia, M., et al. (2009). Synthesis, biological evaluation, and three-dimensional in silico pharmacophore model for  $\sigma$ 1 receptor ligands based on a series of substituted benzo-[d]oxazol-2(3H)-one derivatives. *J. Med. Chem.* 52, 5380–5393. doi: 10.1021/jm900366z

**Conflict of Interest Statement:** All authors are full-time employees of ESTEVE Pharmaceuticals S.A.

The handling Editor declared a past co-authorship with one of the authors JV.

Copyright © 2019 Pascual, Almansa, Plata-Salamán and Vela. This is an open-access article distributed under the terms of the Creative Commons Attribution License (CC BY). The use, distribution or reproduction in other forums is permitted, provided the original author(s) and the copyright owner(s) are credited and that the original publication in this journal is cited, in accordance with accepted academic practice. No use, distribution or reproduction is permitted which does not comply with these terms.





# Ligands Exert Biased Activity to Regulate Sigma 1 Receptor Interactions With Cationic TRPA1, TRPV1, and TRPM8 Channels

Elsa Cortés-Montero<sup>1</sup>, Pilar Sánchez-Blázquez<sup>1</sup>, Yara Onetti<sup>1</sup>, Manuel Merlos<sup>2</sup> and Javier Garzón<sup>1\*</sup>

<sup>1</sup> Laboratory of Neuropharmacology, Department of Translational Neuroscience, Cajal Institute, CSIC, Madrid, Spain, <sup>2</sup> Drug Discovery & Preclinical Development, Esteve, Barcelona, Spain

## OPEN ACCESS

### Edited by:

Ebru Aydar,  
University College London,  
United Kingdom

### Reviewed by:

Sudarshan Rajagopal,  
Duke University Health System,  
United States  
Shelley J. Russek,  
Boston University, United States

### \*Correspondence:

Javier Garzón  
jgarzon@cajal.csic.es

### Specialty section:

This article was submitted to  
Experimental Pharmacology  
and Drug Discovery,  
a section of the journal  
Frontiers in Pharmacology

**Received:** 05 December 2018

**Accepted:** 17 May 2019

**Published:** 12 June 2019

### Citation:

Cortés-Montero E,  
Sánchez-Blázquez P, Onetti Y,  
Merlos M and Garzón J (2019)  
Ligands Exert Biased Activity  
to Regulate Sigma 1 Receptor  
Interactions With Cationic TRPA1,  
TRPV1 and TRPM8 Channels.  
Front. Pharmacol. 10:634.  
doi: 10.3389/fphar.2019.00634

The sigma 1 receptor ( $\sigma$ 1R) and the mu-opioid receptor (MOR) regulate the transient receptor potential (TRP) V1 calcium channel. A series of proteins are involved in the cross-regulation between MORs and calcium channels like the glutamate *N*-methyl-D-aspartate receptor (NMDAR), including the histidine triad nucleotide-binding protein 1 (HINT1), calmodulin (CaM), and the  $\sigma$ 1R. Thus, we assessed whether similar mechanisms also apply to the neural TRP ankyrin member 1 (TRPA1), TRP vanilloid member 1 (TRPV1), and TRP melastatin member 8 (TRPM8). Our results indicate that  $\sigma$ 1R and CaM bound directly to cytosolic regions of these TRPs, and this binding increased in the presence of calcium. By contrast, the association of HINT1 with these TRPs was moderately dependent on calcium. The  $\sigma$ 1R always competed with CaM for binding to the TRPs, except for its binding to the TRPA1 C-terminal where  $\sigma$ 1R binding cooperated with that of CaM. However,  $\sigma$ 1R dampened HINT1 binding to the TRPA1 N-terminal. When the effect of  $\sigma$ 1R ligands was addressed, the  $\sigma$ 1R agonists PRE084 and pregnenolone sulfate enhanced the association of the  $\sigma$ 1R with the TRPM8 N-terminal and TRPV1 C-terminal in the presence of physiological calcium, as seen for the  $\sigma$ 1R–NMDAR interactions. However, these agonists dampened  $\sigma$ 1R binding to the TRPA1 and TRPV1 N-terminal domains, and also to the TRPA1 C-terminal, as seen for  $\sigma$ 1R–binding immunoglobulin protein (BiP) interactions in the endoplasmic reticulum (ER). By contrast, the  $\sigma$ 1R antagonists progesterone and S1RA reduced the association of  $\sigma$ 1R with TRPA1 and TRPV1 C-terminal regions, as seen for the  $\sigma$ 1R–NMDAR interactions. Conversely, they enhanced the  $\sigma$ 1R interaction with the TRPA1 N-terminal, as seen for  $\sigma$ 1R–BiP interactions, whereas they barely affected the association of  $\sigma$ 1R with the TRPV1 N-terminal. Thus, depending on the calcium channel and the cytosolic region examined, the  $\sigma$ 1R agonists pregnenolone sulfate and PRE084 opposed or collaborated with the  $\sigma$ 1R antagonists progesterone and S1RA to disrupt or promote such interactions. Through the use of cloned cytosolic regions of selected TRP calcium channels, we were able to demonstrate that  $\sigma$ 1R ligands exhibit biased activity to regulate particular  $\sigma$ 1R interactions with other

proteins. Since  $\sigma$ 1Rs are implicated in essential physiological processes, exploiting such ligand biases may represent a means to develop more selective and efficacious pharmacological interventions.

**Keywords:** type 1 sigma receptor, transient receptor potential ankyrin member 1, transient receptor potential melastatin member 8, transient receptor potential vanilloid member 1, calmodulin, histidine triad nucleotide-binding protein 1, ligand bias, *N*-methyl-D-aspartate receptor

## INTRODUCTION

The sigma 1 receptor ( $\sigma$ 1R) is a 223-amino-acid polypeptide that is widely distributed in different tissues and cell compartments. In nervous tissue, the  $\sigma$ 1R is located in areas implicated in nociception and pain control, such as the spinal cord ganglia, substantia gelatinosa of the dorsal horn, and brainstem (Kitaichi et al., 2000; Su et al., 2010). Initially, the  $\sigma$ 1,  $\mu$ , and  $\kappa$  receptors in the neural plasma membrane were pharmacologically classified as opioid receptors (Martin et al., 1976). However, the absence of a G-protein-coupled receptor (GPCR) structure and regulated transduction distanced the  $\sigma$ 1R from the opioid receptor family (Su et al., 1988; Su et al., 2010). Nevertheless, the  $\sigma$ 1R maintains a relationship with the opioid system, where it exerts a tonic anti-opioid effect (Mei and Pasternak, 2002) and modulates the activity-induced sensitization of nociceptive pathways (Cobos et al., 2008; Maurice and Su, 2009; Diaz et al., 2009). Thus, certain  $\sigma$ 1R ligands enhance the antinociceptive effects of clinically relevant  $\mu$ -opioid receptor (MOR) opioids such as morphine, fentanyl, oxycodone, codeine, buprenorphine, and tramadol (Mei and Pasternak, 2002; Diaz et al., 2009; Sánchez-Fernández et al., 2014). However, although other  $\sigma$ 1R ligands do not alter opioid-induced analgesia, they dampen antagonist-mediated effects. Thus, the  $\sigma$ 1R ligands that enhance MOR analgesia are referred to as antagonists, and those that reduce opioid analgesia and/or oppose the effects of antagonists are classified as agonists.

Under normal conditions,  $\sigma$ 1R antagonists do not alter mechanical or thermal thresholds but instead decrease the perception of pain caused by nociceptive sensitization or by pathological states, such as neuropathy, inflammation, or ischemic pain (Kim et al., 2006; Roh et al., 2008; Romero et al., 2012). Recent research has revealed the presence of  $\sigma$ 1Rs in the MOR environment. The cytosolic C-terminus of MOR binds to the histidine triad nucleotide-binding protein 1 (HINT1) protein, facilitating the interactions of the  $\sigma$ 1R and glutamate *N*-methyl-D-aspartate receptor (NMDAR) with the MOR (Rodríguez-Muñoz et al., 2015a). In this context, the  $\sigma$ 1R cooperates with the HINT1 protein to bring the NMDAR under control of the MOR (Rodríguez-Muñoz et al., 2015b). Indeed, activation of the MOR promotes calcium permeation through the NMDAR, which is regulated by the competitive binding of the  $\sigma$ 1R and calmodulin (CaM) to the regulatory cytosolic C1 region of the NMDAR NR1 subunit. Upon  $\sigma$ 1R depletion, HINT1 also reduces the inhibitory binding of calcium-activated CaM to the NMDAR NR1 subunit. Therefore, the MOR activates and regulates the function of ionotropic NMDAR calcium channels through the interactions between  $\sigma$ 1R, HINT1, and CaM where the calcium-dependent

binding of  $\sigma$ 1Rs to NMDARs can predominate over the interactions with CaM and HINT1. This observation prompted us to investigate whether other calcium channels may also be regulated by these  $\sigma$ 1R-mediated mechanisms.

Different classes of channels in the ER and plasma membrane dynamically control intracellular calcium levels. In the present study, we focus on the transient receptor potential (TRP) channel family, homotetrameric calcium channels with variable cytosolic N- and C-terminal regions that contain diverse regulatory protein binding domains and motifs (Owsianik et al., 2006). CaM binds to the cytosolic N- and C-terminal regions of TRPV1 in a calcium-dependent manner (Numazaki et al., 2003; Rosenbaum et al., 2004), as well as to the C-terminus of TRPA1 (Hasan et al., 2017). In fact, by modulating the gating of the calcium influx, CaM participates in the mechanism regulating TRP activity (Numazaki et al., 2003; Lishko et al., 2007; Sarria et al., 2011; Hasan et al., 2017). In addition, pharmacological interventions targeting  $\sigma$ 1R alter TRPV1 expression, with  $\sigma$ 1R antagonists downregulating TRPV1 channels in the plasma membrane of sensory neurons (Ortiz-Renteria et al., 2018). Moreover, MOR and TRPV1 channels are co-precipitated when exogenously expressed in cultured cells (Scherer et al., 2017). While nerve damage provoked by peripheral inflammation enhances TRPA1 levels in dorsal root ganglia (DRG) neurons (Obata et al., 2005), TRPV1 levels increase in undamaged sensory connections (Hudson et al., 2001), facilitating the transmission of nociceptive information and thereby contributing to the resulting pain response. Thus, similar to NMDARs, TRP channels play roles in several pain-related pathological conditions, including inflammatory, neuropathic, visceral, and dental pain, as well as in pain associated with cancer (Patapoutian et al., 2009; Julius, 2013; Mickle et al., 2015). Evidence for these roles has mainly been obtained using specific antagonists of individual nociceptive TRP channels in animal models of pain-related pathologies, such as by inducing these pathologies in mice through the genetic deletion/alteration of individual nociceptive TRP channels (Caterina et al., 2000; Davis et al., 2000; Katsura et al., 2006). These studies have led to the development of a new generation of analgesics that target the TRP sensors for heat, cold, and irritants (Kaneko and Szallasi, 2014).

Three TRPs belonging to different subfamilies and expressed at the spinal level and in the brain fulfilled our criteria to be included in a comparative study with the neural NMDAR. The TRP ankyrin member 1 (TRPA1), TRP vanilloid member 1 (TRPV1), and TRP melastatin member 8 (TRPM8) belong to the so-called thermo TRP channels that participate in detecting temperature changes and integrating different noxious stimuli (Julius, 2013). TRPA1 is a non-selective calcium channel activated by multiple stimuli,

including harmful cold temperatures, acids, and numerous chemical pollutants (Jordt et al., 2004). The TRPM8 channel plays a physiological role in detecting low temperature (10–33°C), and it is over-expressed in sensory neurons after nerve injury or inflammation; TRPM8 also participates in cold allodynia and hyperalgesia (Xing et al., 2007). TRPV1 is also a non-selective calcium channel that is activated by noxious temperatures (>43°C), an acidic pH, and vanilloid compounds. TRPV1 expression is upregulated in response to acute inflammation (Camprubi-Robles et al., 2009) and in conditions of chronic pain, and the activity of this TRP is potentiated by pro-algetic mediators released during inflammation and tissue injury (Huang et al., 2006). In addition, TRPA1 receptors are coexpressed with TRPV1 channels in C-fiber sensory neurons (Fajardo et al., 2008), and they seem to fulfill crucial roles in neuronal and nonneuronal neuropathic pain.

Accordingly, we addressed whether the cloned N- and C-terminal cytosolic regions of these TRP channels participate in direct and calcium-dependent interactions with the  $\sigma$ 1R and the MOR-related HINT1 protein. Because calcium-dependent binding of CaM to cytosolic regions of these TRPs has previously been mapped, we addressed its possible interference in the interaction with  $\sigma$ 1Rs. Given the differences that ligands exhibit on the interactions of  $\sigma$ 1Rs with BiP in the ER and with NR1 subunits of the NMDAR, we also analyzed their profiles in the interactions of  $\sigma$ 1Rs with the cytosolic regions of the TRPs selected. We observed that  $\sigma$ 1R interacts with the N- or C-terminus of these TRPs in a calcium-dependent manner, and most relevantly,  $\sigma$ 1R ligands exhibit a biased activity to disrupt or promote the interaction of  $\sigma$ 1Rs with the TRP domains.

## MATERIALS AND METHODS

### Recombinant Protein Expression

The coding region of the full-length murine  $\sigma$ 1R (AF004927), HINT1 (NM\_008248), and the N- and C-terminal regions of TRPA1 (NP\_808449; residues 1–721 and 961–1125), TRPV1 (NP\_542437; residues 1–433 and 680–839), and TRPM8 (NP\_599013; residues 1–639) were amplified by reverse transcription polymerase chain reaction (RT-PCR) using total RNA isolated from the mouse brain as the template. Specific primers containing an upstream Sgf I restriction site and a downstream Pme I restriction site were used, as described previously (Rodríguez-Muñoz et al., 2015b). The PCR products were cloned downstream of the glutathione S-transferase (GST)/HaloTag® coding sequence (Flexi® Vector, Promega, Spain) and the tobacco etch virus protease (TEV) protease site, and when sequenced, the proteins were identical to the GenBank™ sequences. The vector was introduced into the *Escherichia coli* BL21 (KRX #L3002, Promega), and clones were selected on solid medium containing ampicillin. After 3 h of induction at room temperature (RT), in the presence of 1 mM isopropyl  $\beta$ -D-1-thiogalactopyranoside (IPTG) and 0.1% Rhamnose, the cells were collected by centrifugation and maintained at –80°C. The fusion proteins were purified under native conditions on GStrap FF columns (#17-5130-01, GE Healthcare, Spain) or with HaloLink Resin (#G1915, Promega). When necessary, the fusion proteins retained were cleaved on the column with ProTEV protease

(#V605A, Promega) and further purification was achieved by high-resolution ion exchange (#780-0001Enrich Q, BioRad, Spain). Sequences were confirmed by automated capillary sequencing. Recombinant calmodulin (CaM, #208694) was purchased at Merck-Millipore (Spain).

### In Vitro Interactions Between Recombinant Proteins: Pull-Down of Recombinant Proteins and the Effect of Drugs on the Sigma 1 Receptor–Transient Receptor Potential Interactions

Having demonstrated that the  $\sigma$ 1R and HINT1 do not bind to GST (#Z02039; GenScript Co., USA) (see **Supplementary Figure 1**) (Sánchez-Blázquez et al., 2012), we assessed the association of GST-free  $\sigma$ 1Rs or HINT1 with the GST-tagged TRP cytosolic sequences. The N- and C-terminal domains of TRP were immobilized through covalent attachment to N-Hydroxysuccinimide (NHS)-activated Sepharose 4 fast flow (4FF, #17-0906-01; GE) according to the manufacturer's instructions. Recombinant  $\sigma$ 1R (200 nM) was then incubated with either NHS-blocked Sepharose 4FF (negative control) or with the immobilized TRP sequence (100 nM) in 200  $\mu$ L of a buffer containing 50 mM Tris–HCl (pH 7.5) and 0.2% 3-[(3-choleamidopropyl)dimethylammonio]-1-propanesulfonate (CHAPS), and in the presence or absence of 3 mM CaCl<sub>2</sub>. In pilot assays, we found that the TRP– $\sigma$ 1R association was maximal after 30 min incubation and that, in this period, the drugs could also promote stable changes in this association. The samples were mixed by rotation for 30 min at RT, and the  $\sigma$ 1Rs bound to TRP-Sepharose 4FF were recovered by centrifugation and washed three times. This protocol was also carried out to assess the TRP–HINT1 or TRP–CaM associations, or the competition between HINT1/CaM and higher concentrations of  $\sigma$ 1R to bind to the TRPs. To study whether the drugs used provoked changes in the TRP– $\sigma$ 1R association, the agarose-attached TRP– $\sigma$ 1R complexes were incubated for a further 30 min at RT with rotation in the presence of increasing concentrations of the drugs and in a final reaction volume of 300  $\mu$ L of 50 mM Tris–HCl (pH 7.5), 3 mM CaCl<sub>2</sub> and 0.2% CHAPS. In this assay,  $\sigma$ 1R ligands dissolved in aqueous solutions display calcium- and concentration-dependent activity, altering the  $\sigma$ 1R–TRP associations. If an organic solvent was required to incorporate the drug under study, such as dimethyl sulfoxide (DMSO) for pregnenolone sulfate, the DMSO had to remain below 1% in the assay buffer. Agarose pellets containing the bound proteins were obtained by centrifugation, and they were washed thrice in the presence of 3 mM CaCl<sub>2</sub> and then solubilized in 2 $\times$  Laemmli buffer, analyzing the  $\sigma$ 1R/HINT1/CaM content in Western blots. The compounds studied were as follows: progesterone (#P7556, Sigma-Aldrich, Spain), pregnenolone sulfate (#P162, Sigma-Aldrich), S1RA (#16279, Cayman Chemical, USA), and PRE084 (#0589, Tocris Bioscience, UK) (see **Supplementary Figure 2**).

The  $\sigma$ 1R/HINT1/CaM bound to the Sepharose-TRP sequences were resolved with Sodium dodecyl sulfate–polyacrylamide gel electrophoresis (SDS-PAGE) in 4–12% Bis–Tris gels (#NP0341, Invitrogen, Fisher Scientific, Spain), with 2-(N-morpholino)ethanesulfonic acid SDS (ME SDS) as the running buffer (#NP0002, Invitrogen). The proteins were transferred onto

0.2- $\mu$ m Polyvinylidene difluoride (PVDF) membranes (#162-0176; BioRad) and probed overnight at 6°C with primary antibodies diluted in Tris-buffered saline (pH 7.7) (TBS) + 0.05% Tween 20 (TTBS): anti- $\sigma$ 1R (#42-3300, Invitrogen), anti-CaM (#05-173, Merck-Millipore), or the anti-HINT1 antibody produced in rabbits against the peptide sequence GYRMVVNEGADGGG (aa 93–106; Immunostep, Spain). All primary antibodies were detected using the appropriate horseradish-peroxidase-conjugated secondary antibodies. Thus, the blot areas containing the corresponding sizes of the cloned target proteins were selected for image capture and analysis. The Western blot images were visualized by chemiluminescence (#170-5061; BioRad) and recorded on an ImageQuant™ LAS 500 (GE). For each blot, the area containing the target cloned protein was typically selected. The device automatically captures the selected area and the associated software automatically calculated the optimal exposure time to provide the strongest possible signal from which the rest of the signals could be accurately quantified. For each group of immunosignals derived from the same cloned protein, the area of the strongest signal was used to determine the average optical density of the pixels within the object area/mm<sup>2</sup> of all the signals (AlphaEase FC software). The gray values of the means were then normalized within the 8 bit/256 gray levels [(256 – computed value)/computed value].

## Statistical Analyses

The signals from the Western blot were expressed as the change relative to the controls, which were assigned an arbitrary value of 1. Statistical analyses were performed using the Sigmaplot/SigmaStat v.14 package [statistical package for the social sciences (SPSS) Science Software, Erkrath, Germany], and the level of significance was considered as  $p < 0.05$ . The data were analyzed using one-way ANOVA followed by Dunnett multiple comparisons against the control group.

## RESULTS

### Interactions Between Sigma 1 Receptor, Calmodulin, and Histidine Triad Nucleotide-Binding Protein 1 with the N- and C-terminal Cytosolic Domains of Transient Receptor Potential Ankyrin Member 1/Melastatin Member 8/Vanilloid Member 1

The activation of CaM by calcium provides a mechanism to rapidly regulate different signaling pathways and protein activities, such as TRP cationic permeation. Protein analysis (DNASTAR NovaFold v15, Madison, USA) suggests the presence of CaM-binding motifs in the cytosolic sequences of the studied TRPs (Yap et al., 2000), and indeed, we identified a stable calcium-dependent interaction between CaM and the N- and C-terminal regions of TRPA1 (Figure 1A). The  $\sigma$ 1R exhibited binding to both cytosolic regions of the TRPA1 channel, which increased considerably in the presence of 3 mM CaCl<sub>2</sub>. In contrast, the HINT1 protein interacted with the N-terminal but not the C-terminal domain of TRPA1. The formation of HINT1-TRPA1 complexes was moderately dependent on the calcium concentration (Figure 1A);

importantly, the binding of the  $\sigma$ 1R to the TRPA1 N-terminal domain prevented the binding of the HINT1 protein (Figure 1B). Although  $\sigma$ 1R and CaM bind to the N- and C-terminal cytosolic regions of TRPA1,  $\sigma$ 1R and CaM only compete for binding to the TRPA1 N-terminal domain (Figure 1B), whereas  $\sigma$ 1R substantially enhanced the binding of CaM to the TRPA1 C-terminus (Figure 1C). Thus,  $\sigma$ 1R competes with CaM and HINT1 for binding to the N-terminal domain of TRPA1.

A putative CaM-binding site was predicted in the TRPM8 N-terminal but not the C-terminal domain, and this binding was confirmed in our *in vitro* assays with the cloned proteins. Indeed, we detected the calcium-dependent binding of CaM,  $\sigma$ 1R, and HINT1 to the N-terminus of TRPM8 (Figure 2A). In the absence of calcium, HINT1 interacted with the channel; the  $\sigma$ 1R and CaM were virtually undetectable. The  $\sigma$ 1R competed with CaM, but not with HINT1, for binding to the N-terminal region of TRPM8 (Figure 2B). Regarding the TRPV1 channel, its N-terminal ankyrin repeat domain and short distal C-terminal segment contained putative CaM-binding motifs. The  $\sigma$ 1R, CaM, and, to a lesser extent, HINT1 all interacted with TRPV1, and their binding increased in the presence of 3 mM CaCl<sub>2</sub> (Figure 3A). Similar to TRPA1, HINT1 bound to the N-terminal domain of TRPV1, but not to its C-terminus, although it did not apparently affect the binding of  $\sigma$ 1R to this N-terminal region of TRPV1 (Figure 3B). However, the binding of  $\sigma$ 1R hindered the interaction between CaM and the TRPV1 N- and C-terminal sequences (Figure 3B and C).

### Ligands of Sigma 1 Receptor Modify the Formation of the Sigma 1 Receptor–Transient Receptor Potential Ankyrin Member 1/Melastatin Member 8/Vanilloid Member 1 Complexes

For comparison with other reports, we will refer to the  $\sigma$ 1R ligands as agonists and antagonists, based on their effects on the analgesic assays with morphine in rodents (Mei and Pasternak, 2002). In the presence of 3 mM CaCl<sub>2</sub>, the agonist pregnenolone sulfate blocked the interactions of the  $\sigma$ 1R with both the N- and C-terminal domains of TRPA1 (Figure 4). Conversely, the antagonist progesterone enhanced the interaction of the  $\sigma$ 1R with the N-terminal domain of TRPA1, while reducing its binding to the TRPA1 C-terminus. Pregnenolone sulfate also reduced the binding of the  $\sigma$ 1R to the TRPV1 N-terminus, while substantially increasing the association of the  $\sigma$ 1R with TRPV1 C-terminus and TRPM8 N-terminal sequence. Progesterone slightly augmented the interaction of  $\sigma$ 1R with the TRPV1 N-terminal domain, while reducing  $\sigma$ 1R binding to the TRPV1 C-terminus and TRPM8 N-terminus. The effects of neurosteroids on the interactions of  $\sigma$ 1R with the three TRPs were mostly reproduced by exogenous ligands of this receptor. Thus, the selective antagonist S1RA modulated these associations to a similar extent as pregnenolone, and with the exception of TRPV1 N-terminus, the agonist PRE084 also reproduced the effects of pregnenolone sulfate (Figure 4). These data are summarized in Table 1. Conversely, the ligands that promote or did not alter the association of  $\sigma$ 1R with TRP domains reduced the disruptive effects of other ligands on these  $\sigma$ 1R–TRP complexes. For example, the interaction between pregnenolone sulfate and PRE084 at



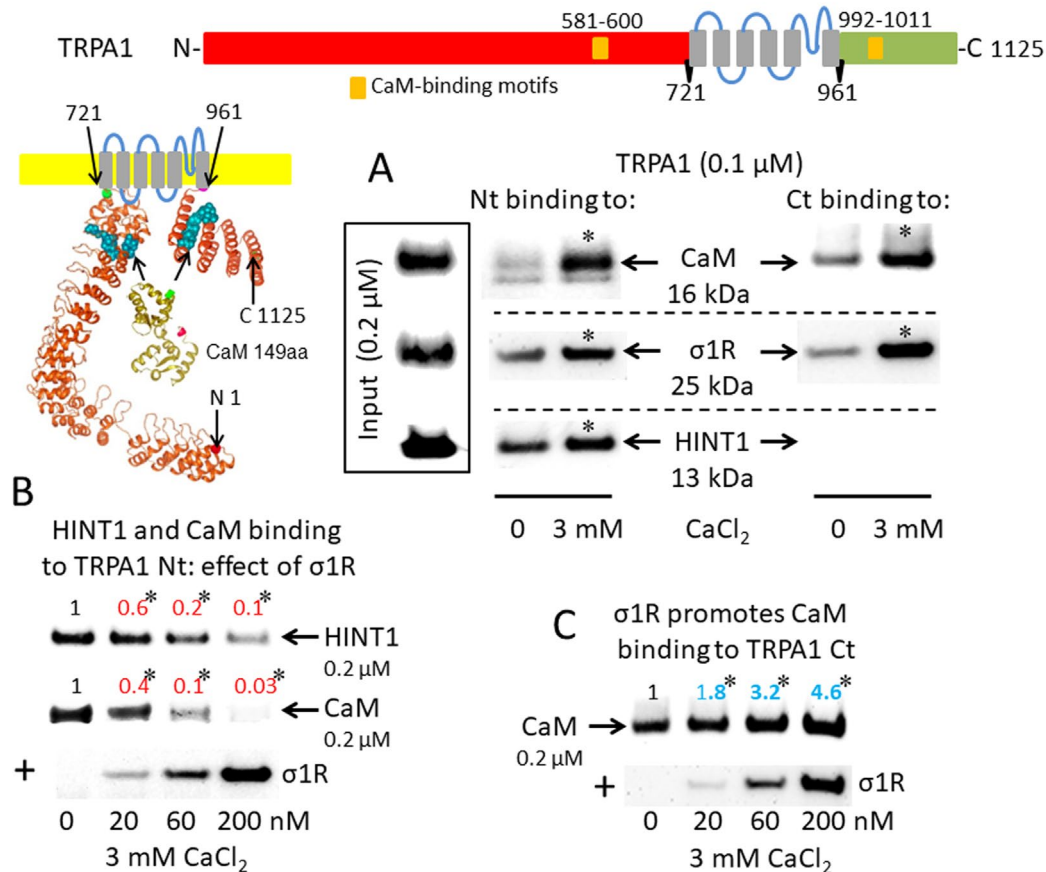


**FIGURE 1 |** Sigma 1 receptor (σ1R), histidine triad nucleotide-binding protein 1 (HINT1), and calmodulin (CaM) binding to the transient receptor potential ankyrin member 1 (TRPA1) calcium channel. The TRP structural models shown were predicted by Novafold (DNASTAR Inc., Madison, WI, USA). Linear model: the N- and C-terminal cytosolic sequences are red and green, respectively, and the six transmembrane domains are in gray. Ribbon model: The 3D structure of N- and C-terminal sequences is shown; the CaM-binding motifs are indicated by blue spheres. **(A)** The *in vitro* interactions of the σ1R, CaM, and HINT1 with TRPA1 were evaluated in co-precipitation assays. Recombinant N- and C-terminal regions of TRPA1 (100 nM) were co-incubated in the presence and absence of 3 mM CaCl<sub>2</sub>, with the input of 200 nM CaM, σ1R, and HINT1. The TRPA1 N-terminus (aa 1–721) or the TRPA1 C-terminus (aa 961–1125) were immobilized by covalent attachment to NHS-activated Sepharose. Prey proteins alone did not bind to the blocked NHS-Sepharose (negative control). **(B and C)** Competition assays between the σ1R and CaM or HINT1 for binding to the N- and C-terminal regions of TRPA1. After incubation in 3 mM CaCl<sub>2</sub>, the TRPA1-bound proteins were detached and resolved by SDS-PAGE chromatography, and analyzed in Western blots. The assays were repeated at least twice, producing comparable results. For the interactions with increased concentrations of the σ1R (up to 200 nM), the data are shown relative to that obtained in the absence of the σ1R, with the control group arbitrary assigned a value of 1. \*Significant differences with respect to the control group, ANOVA and Dunnett multiple comparisons vs. control group,  $p < 0.05$ . Representative blots are shown.

the TRPV1 N-terminus is of particular interest. Both ligands are considered agonists but pregnenolone sulfate weakened the σ1R–TRPV1 interaction at the N-terminus more effectively than PRE084. Hence, PRE084 diminished the capacity of pregnenolone sulfate to disrupt this particular σ1R interaction (Figure 5).

## DISCUSSION

This molecular *in vitro* study demonstrates the physical interactions of σ1R with N- and C-terminal domains of the TRPA1, TRPM8, and TRPV1 calcium channels, and the dependence of its binding on calcium levels. Notably, calcium regulates σ1R binding to TRPs and also its interactions with the BiP protein in the ER (Hayashi and Su, 2007) and the NR1 C1 subunit of

the NMDAR (Rodríguez-Muñoz et al., 2015a; Rodríguez-Muñoz et al., 2015b). Increases in calcium levels always promote the σ1R interaction with third partner signaling proteins, while calcium depletion reduces these associations. In the case of σ1R, a ligand-operated chaperone, depending on the interacting protein, BiP or NR1 C1, the same σ1R ligand either promotes the disruption of the complex or prevents the disrupting activities of other ligands. In this context, the present study confirmed the disparate activities of σ1R ligands to regulate the interactions of this chaperone with the cytosolic domains of the TRPA1, TRPM8, and TRPV1 channels. Based on all these observations, calcium emerges as the main known physiological regulator of σ1R chaperone activity. In this context, the regulation of σ1R interactions by endogenous molecules, such as steroids, *N,N*-dimethyltryptamine, sphingosine, monoglycosylated ceramide,

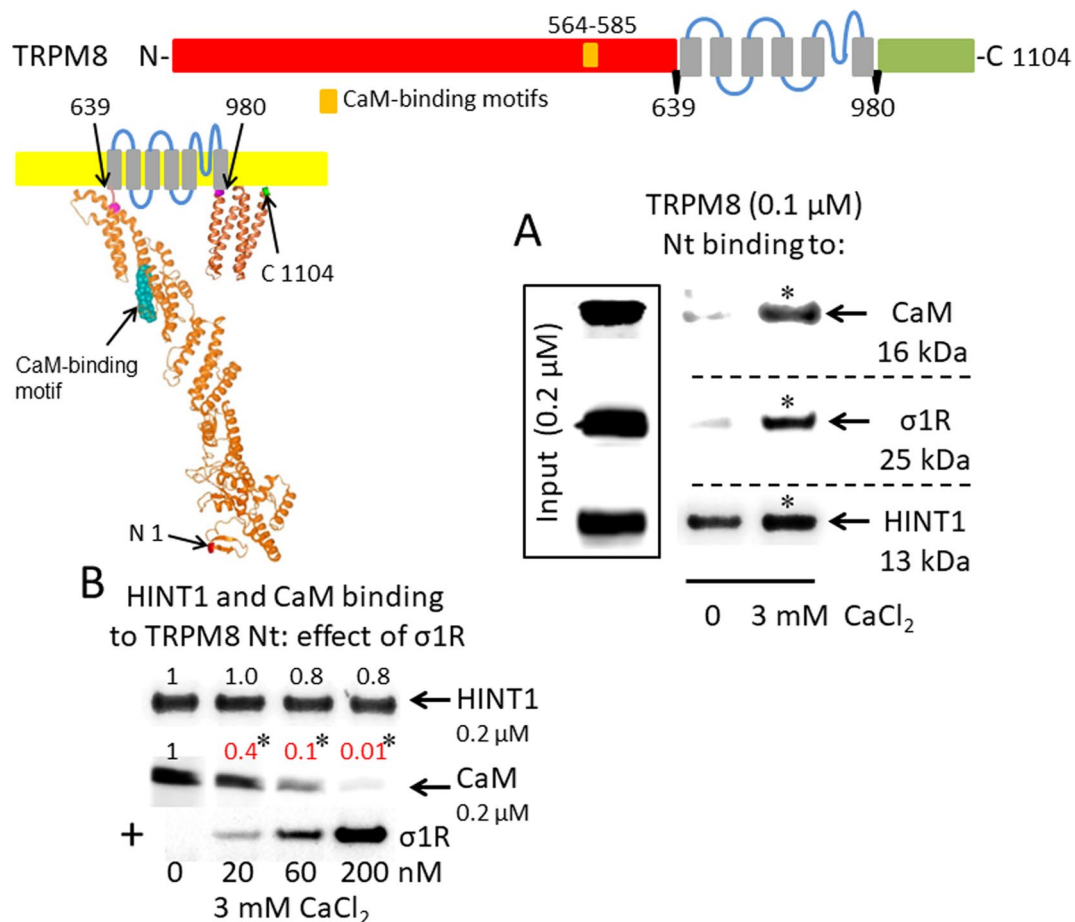


**FIGURE 2 |**  $\sigma$ 1R, HINT1, and CaM binding to the transient receptor potential melastatin member 8 (TRPM8) calcium channel. **(A)** Interactions between the  $\sigma$ 1R, CaM, and HINT1 with the TRPM8 N-terminus (aa 1–639). Recombinant TRPM8 N-terminus (100 nM) was incubated with CaM,  $\sigma$ 1R, and HINT1 (200 nM) in the presence or absence of 3 mM CaCl<sub>2</sub>. **(B)** Competition experiments to evaluate the interference of  $\sigma$ 1R binding with that of CaM and HINT1 to the TRPM8 N-terminus (details as in Figure 1).

etc. (Hayashi, 2015), as well as exogenous compounds has attracted increasing pharmacological interest.

As described for the NMDAR (Ehlers et al., 1996), the calcium-activated CaM also reduces calcium permeation through TRP channels (Numazaki et al., 2003; Rosenbaum et al., 2004; Sarria et al., 2011; Hasan et al., 2017). The computer-predicted CaM-binding cytosolic regions in TRPA1, TRPM8, and TRPV1 coincided with the sites previously reported through mutation and sequence deletion assays (Numazaki et al., 2003; Rosenbaum et al., 2004; Hasan et al., 2017). The CaM binding motifs in NR1 C1 subunits overlap with the binding sites of the  $\sigma$ 1R (Rodríguez-Muñoz et al., 2015b). Our observations also suggest that a similar phenomenon occurs in the TRPV1 N- and C-terminal regions and TRPA1 and TRPM8 N-termini. The TRPA1 C-terminus exhibit noticeable CaM binding, even in the absence of calcium, and this CaM binding motif must be located close to the  $\sigma$ 1R binding site; thus, the chaperone positively influences CaM binding, suggesting a dual regulatory role for CaM in the function of this TRP. Indeed, at low calcium levels, CaM binds to TRPA1 C-terminus and increases calcium permeation through the channel; however, when calcium

concentrations increase over a certain level, CaM, probably by binding to the N-terminus, desensitizes the TRPA1 channel (Hasan et al., 2017). Similar to the  $\sigma$ 1R, ATP/Phosphatidylinositol 4,5-bisphosphate (PIP<sub>2</sub>) also prevents the desensitizing effect of CaM binding to the TRPV1 channel (Lishko et al., 2007); however, biochemical data addressing the possible competence of their binding to the receptor are unavailable. Regarding the physiological relevance of the present study, the  $\sigma$ 1R always prevented CaM binding to the TRPs at matched concentrations, with the exception of the TRPA1 C-terminus, where  $\sigma$ 1R binding cooperated with CaM binding. Since the  $\sigma$ 1R negatively regulates the inhibitory effect of CaM on NMDAR function (Rodríguez-Muñoz et al., 2015b), a similar mechanism may regulate TRP activity. The binding of the  $\sigma$ 1R to TRPs may favor the open probability of the channel, while CaM will reduce TRP activity by competing and diminishing  $\sigma$ 1R binding. Hence, the resulting activity of the TRP calcium channels may depend on the concentrations of CaM and  $\sigma$ 1R in their cytosolic environment.

The physiological mechanism regulating the NMDAR may be altered by exogenous compounds with antagonist activity at

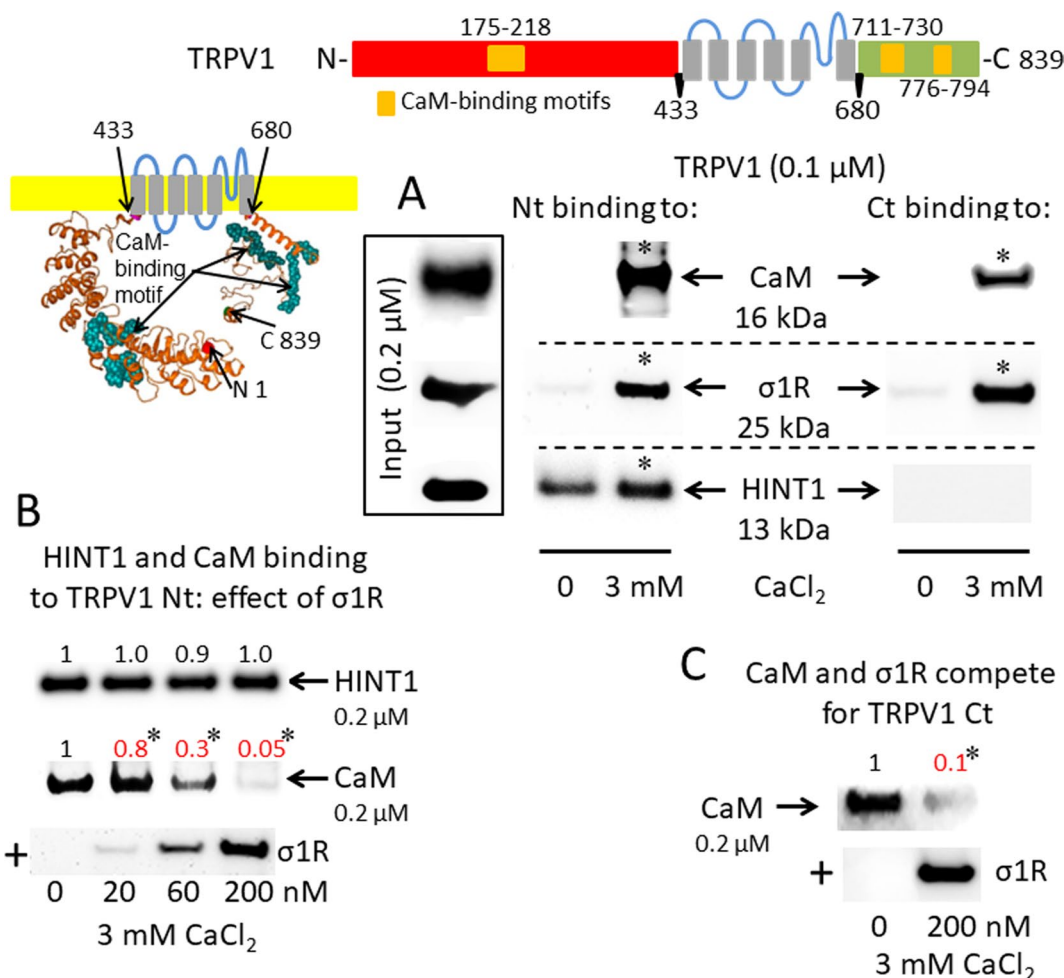


**FIGURE 3 |**  $\sigma$ 1R, HINT1, and CaM binding to the transient receptor potential vanilloid member 1 (TRPV1) calcium channel. **(A)** Interactions between  $\sigma$ 1R, CaM, and HINT1 with the TRPV1. The recombinant TRPV1 N-terminus (aa 1–433) and C-terminus (aa 680–839) (100 nM) were incubated with CaM,  $\sigma$ 1R, and HINT1 (200 nM) in the presence or absence of 3 mM  $\text{CaCl}_2$ . **(B and C)** Competition assays between the  $\sigma$ 1R and CaM or HINT1 for their binding to the N- and C-terminal regions of TRPV1 (details as in **Figure 1**).

the  $\sigma$ 1R, which promote CaM binding to the NR1 C1 subunit by disrupting the  $\sigma$ 1R–NR1 C1 association, thereby inhibiting calcium permeation through the NMDAR. With respect to TRPs, the *in vivo* administration of the  $\sigma$ 1R antagonists BD1063 or progesterone to mice promotes TRPV1 downregulation in DRG sensory neurons (Ortiz-Renteria et al., 2018), suggesting a protective effect of the  $\sigma$ 1R chaperone on TRPV1 integrity. This pharmacological intervention may have disturbed the equilibrium between  $\sigma$ 1R and CaM binding to the TRPV1, thus promoting an anomalous CaM-mediated inhibition of TRP function and the removal of the calcium channel from the neural membrane. The present molecular study showed how CaM,  $\sigma$ 1R and HINT1 bind to cytosolic regions of the selected TRPs; however, the structural organization of the TRP channels raises a series of questions about the manner in which calcium-activated CaM regulates their function. TRPs are homotetramers and, in general, their N- and C-terminal domains contain CaM binding-motifs. Therefore, further studies are needed to elucidate whether

CaM binding to just one site suffices to inhibit the channel or whether the extent of inhibition depends on the number of sites to which CaM binds in the channel, as suggested in a previous study (Rosenbaum et al., 2004). Another relevant issue is whether CaM binding to N-terminal regions collaborates with CaM binding to C-terminal regions, or if it accomplishes a different purpose. Further functional studies are required to address these questions.

The HINT1 and  $\sigma$ 1R proteins are widely distributed in different tissues and are present in most cellular compartments (Hayashi and Su, 2007; Liu et al., 2008). At the neural membrane, HINT1 forms complexes with the cytosolic domains of different GPCRs, including MOR and cannabinoid type 1 (Guang et al., 2004; Sánchez-Blázquez et al., 2014). The  $\sigma$ 1R also interacts with GPCRs and is implicated in the regulation of MOR activity (Sánchez-Blázquez et al., 2012; Rodríguez-Muñoz et al., 2015a). The MOR-associated HINT1 protein binds to the N-terminal domains of the TRPs evaluated in the present study, and this binding moderately increased in the presence of calcium. While

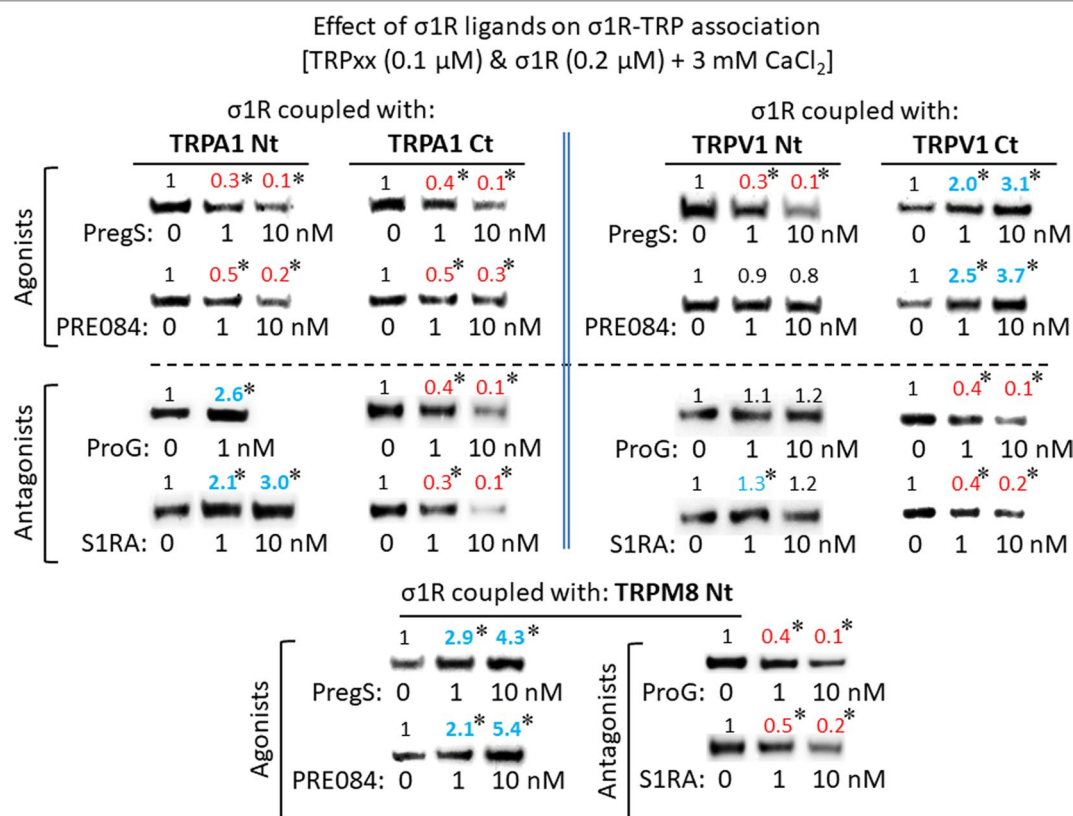


**FIGURE 4 |** The effect of  $\sigma$ 1R ligands on the  $\sigma$ 1R-TRP interactions. Agarose-TRP was incubated with the  $\sigma$ 1R and the agarose-TRP- $\sigma$ 1R complexes were separated from the free  $\sigma$ 1R through three cycles of washing/resuspension. The agarose-TRP- $\sigma$ 1R complexes were then incubated for 30 min with rotation at room temperature (RT) in the presence of increasing concentrations of the  $\sigma$ 1R ligands in a final volume of 300  $\mu$ L (50 mM Tris-HCl [pH 7.5], 3 mM  $\text{CaCl}_2$ , and 0.2% CHAPS). Finally, the  $\sigma$ 1Rs that remained attached to the TRP were resolved by SDS-PAGE and evaluated in immunoblots. Agonists dampened on the association of the  $\sigma$ 1Rs with TRPA1, while antagonist induced different effects on  $\sigma$ 1Rs binding to the TRPA1 N- or C-terminal domains. The  $\sigma$ 1R agonists produced different effects on the TRPV1- $\sigma$ 1R associations, and while the antagonists did not alter these associations at TRPV1 N-terminus, they did diminish these complexes at the TRPV1 C-terminal domain. The association of TRPM8 with the  $\sigma$ 1R was enhanced by agonists and dampened by antagonists. The assays were performed twice, and each point was duplicated. Representative blots are shown. PregS, pregnenolone sulfate; ProG, progesterone. Details as in **Figure 1**.

**TABLE 1 |** Effect of sigma 1 receptor ( $\sigma$ 1R) ligands on the association of  $\sigma$ 1Rs with different signaling proteins.

Ligands	TRPA1 Nt	TRPA1 Ct	TRPV1 Nt	TRPV1 Ct	TRPM8 Nt	NR1 C0-C1	BiP
PregS	↓	↓	↓	↑	↑	↑ (a)	↓ (b)
PRE084	↓	↓	= *	↑	↑	↑ (a)	↓ (b)
ProG	↑	↓	=	↓	↓	↓ (a)	↑ (b)
S1RA	↑	↓	↑	↓	↓	↓ (a)	–

The arrows ↑ and ↓ indicate the enhancement or reduction in  $\sigma$ 1R-target protein associations, while = denotes no change in such associations, \*even though the ligand does not alter the  $\sigma$ 1R-TRP interaction, the disruptive effect of pregnenolone sulfate (PregS) was impaired. References reporting the effects of  $\sigma$ 1R ligands on the  $\sigma$ 1R-NR1 or  $\sigma$ 1R-binding immunoglobulin protein (BiP) interactions: (a) Rodríguez-Muñoz et al., 2015b, *Antioxid. Redox Signal.* 22: 799–818; (b) Hayashi and Su, 2007, *Cell* 131: 596–610.

PregS, pregnenolone sulfate; ProG, progesterone; BiP, binding immunoglobulin protein.

the HINT1-NMDAR interaction is disrupted by  $\sigma$ 1R binding, the HINT1-TRPM8/V1 N-terminal interactions were not affected by  $\sigma$ 1R, which only impaired HINT1 binding to the TRPA1 N-terminal domain. These observations are compatible

with MOR signaling, and probably that of other GPCRs, to influence TRP activity. Because HINT1 proteins interact with signaling proteins in zinc and redox-dependent and independent manners (Ajit et al., 2007; Rodríguez-Muñoz and Garzón, 2013), HINT1-TRP interactions may connect these channels to different signaling pathways in the membrane. These interactions may also influence events in the nucleus, where HINT1 exerts its anti-tumor activity and interacts with transcription factors (Weiske and Huber, 2005; Scholer et al., 2015).

The issue of ligand activity in modulating the binding of  $\sigma$ 1Rs to different proteins is of particular pharmacological interest. In systems other than the regulation of MOR-mediated analgesia,  $\sigma$ 1R pharmacology is complex, with exogenous ligands producing different effects depending on the system under study (Maurice and Su, 2009). Indeed, researchers have not clearly determined whether ligands are agonists or antagonists when they promote certain  $\sigma$ 1R-mediated effects, such as neuroprotection or anti-convulsing effects (Rodríguez-Muñoz et al., 2018; Sánchez-Blázquez et al., 2018). Thus, the modulatory effects of  $\sigma$ 1R ligands on the interactions of this chaperone are dissimilar and, for new  $\sigma$ 1R interactors, unpredictable. As aforementioned,



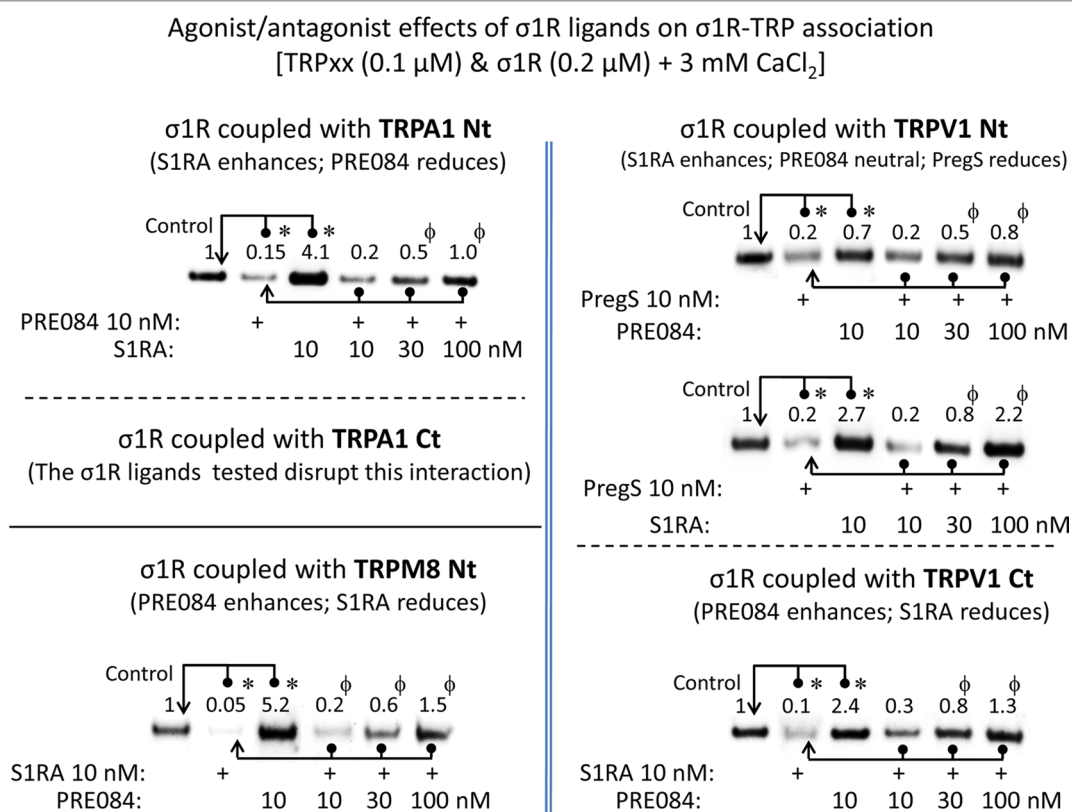


**FIGURE 5 |** The effect of agonism/antagonism of  $\sigma$ 1R ligands on  $\sigma$ 1R-TRP interactions. Agarose TRP- $\sigma$ 1R complexes were incubated in the presence of the competing  $\sigma$ 1R ligands as indicated. The  $\sigma$ 1Rs that remained attached to the TRP were evaluated in immunoblots: \*Significant differences with respect to the control group; \*significant difference with respect to the group receiving only the ligand that diminished the  $\sigma$ 1R-TRP interaction. ANOVA and Dunnett multiple comparisons vs. control group,  $p < 0.05$ . Details as in **Figures 1 and 4**.

this characteristic was initially observed for  $\sigma$ 1R interactions with BiP and NR1 C1 subunits of the NMDAR, where the effects of the ligands tested were completely opposite. The agonists disrupt  $\sigma$ 1R-BiP complexes and antagonists prevent the effect of agonists, but the antagonists disrupt  $\sigma$ 1R-NR1 C1 complexes and agonists oppose the effects of the former ligands. The associations of  $\sigma$ 1Rs with cytosolic regions of TRPA1, TRPM8, and TRPV1 did not escape this complex regulation by  $\sigma$ 1R ligands, and thus the effects of agonists and antagonists on these complexes did not show a common pattern but rather varied, depending on the channel and even the cytosolic region considered. The data from the literature and the present study suggest the existence of at least three main types of interactions of the  $\sigma$ 1R with other proteins. The first type accounts for the negative regulation of MOR analgesia by  $\sigma$ 1Rs, in which the neural glutamate NMDAR plays an essential role (Garzón et al., 2012; Rodríguez-Muñoz et al., 2015b). Antagonists disrupt and agonists promote  $\sigma$ 1R binding to the TRPM8 N-terminus and TRPV1 C-terminus, where  $\sigma$ 1R and CaM compete for binding to the TRP channel. The second classification involves the TRPA1 N-terminal region and probably the TRPV1 N-terminus, and it corresponds to the interaction of the  $\sigma$ 1R with BiP in the ER (Hayashi and Su, 2007). In this situation, agonists disrupt  $\sigma$ 1R binding and antagonists promote or fail to modify it, although they block the effects of

agonists. Again, the  $\sigma$ 1R and CaM compete for binding to the TRP channel. In the third category, agonists and antagonists disrupt  $\sigma$ 1R binding to the TRPA1 C-terminal domain.

Overall, the effects of different ligands on the interactions of this chaperone with its targets are similar to those described for the agonists of most GPCRs, which is actually known as agonist bias. This phenomenon is typical of exogenous ligands, although some reports have described this signaling pathway preference for GPCRs with various endogenous ligands, e.g., the endogenous opioids and the MOR (Thompson et al., 2015). The cytosolic regions of a given 7-TM GPCR bind to different G proteins and certain ligands exhibit a preference to activate the receptor when it is coupled to some but not all the regulated G proteins. We have characterized this situation for clonidine and agonists of the MOR and delta-opioid receptors (Sánchez-Blázquez et al., 1999; Sánchez-Blázquez et al., 2001); the affinity exhibited by opioid agonists, but not antagonists, depends on the class of G protein coupled to the MOR (Garzón et al., 1998). More relevantly, those opioid agonists exhibiting biased activity through discrete combinations of MOR with G proteins bind to the other combinations, but without triggering the signaling pathways. Thus, agonist-biased MOR opioids also display antagonism toward the effects of other biased or unbiased agonists while acting on MOR-G protein combinations on which

the former are inactive (Sánchez-Blázquez and Garzón, 1988; Garzón et al., 1994). Thus, the GPCR field and concrete studies of the MOR have shown that ligands may behave as biased agonists and even antagonists, depending in the class of G protein coupled to the opioid receptor.

The situation described for GPCR and G proteins compares satisfactorily with the findings being documented for the  $\sigma$ 1R in its interactions with signaling proteins. The G proteins that interact with the GPCR determine the agonist/antagonist activity of the ligands, and the different signaling proteins that associate with the  $\sigma$ 1R determine the activity of a given ligand, namely, dissociation or stabilization. Thus, the  $\sigma$ 1R would compare with a GPCR, as the interacting proteins, BiP, NR1 C1, and TRP cytosolic domains, play similar roles to the different classes of G proteins, Gi, Go, Gz, Gq, etc. As observed for the interactions of the MOR with different G proteins (Garzón et al., 1998), the conformation adopted by  $\sigma$ 1R when it binds to the NR1 C1 and BiP must differ, and the conformation when binding to the TRPA1 C-terminus may also be different. The association of the  $\sigma$ 1R with the TRPV1 N-terminus was diminished by pregnenolone sulfate but only mildly by PRE084. In this situation, the latter ligand binds to the  $\sigma$ 1R and diminishes the effects of the neurosteroid. Antagonism was also detected, and the  $\sigma$ 1R ligands that did not influence  $\sigma$ 1R–TRP interactions diminished the effects of the active ligands. Thus, one should not expect any particular  $\sigma$ 1R ligand to exert a similar effect on all TRP channels, as its activity is likely to depend on the channel type and even on the particular cytosolic region analyzed.

TRP channels have been implicated in a wide range of physiological activities. In peripheral nerves, ganglia, and the substantia gelatinosa of the dorsal horn, the activation of TRP channels by different agents contributes to pain perception and even allodynia. The expression of certain TRPs in supraspinal areas, such as those included in this study, suggest that they may participate in other signaling processes that are yet to be defined. The precise role of HINT1 in modulating TRPM8 and TRPV1 channels remains to

be explored, although the proposed connections between TRPV1 and MOR (Ortiz-Renteria et al., 2018) suggest that the  $\sigma$ 1R–HINT1 protein complex functions to connect calcium channels such as the TRPs and NMDAR with this GPCR. Thus,  $\sigma$ 1R ligands exhibit biased activity to regulate subsets of  $\sigma$ 1R interactions with third partner proteins, and this finding may be exploited in the development of site-specific drugs with therapeutic significance.

## AUTHOR CONTRIBUTIONS

JG and PS-B designed the research, wrote the manuscript, and obtained the funding. EC-M and YO performed the experiments and the statistical analysis of data. MM helped to perform the analysis with constructive discussions. All authors approved the final manuscript.

## FUNDING

This work was supported by MICINN Plan Nacional I+D+i [grant number RT 2018-093677-B-100]. EC-M was supported by a Grant from MECID [FPU 15/02356].

## ACKNOWLEDGMENTS

We would like to thank Gabriela de Alba, Veronica Merino, and Maria Jose López for their excellent technical assistance.

## SUPPLEMENTARY MATERIAL

The Supplementary Material for this article can be found online at: <https://www.frontiersin.org/articles/10.3389/fphar.2019.00634/full#supplementary-material>

## REFERENCES

- Ajit, S. K., Ramineni, S., Edris, W., Hunt, R. A., Hum, W. T., Hepler, J. R., et al. (2007). RGSZ1 interacts with protein kinase C interacting protein PKCI-1 and modulates mu opioid receptor signaling. *Cell. Signal.* 19, 723–730. doi: 10.1016/j.cellsig.2006.09.008
- Camprubi-Robles, M., Planells-Cases, R., and Ferrer-Montiel, A. (2009). Differential contribution of SNARE-dependent exocytosis to inflammatory potentiation of TRPV1 in nociceptors. *FASEB J.* 23, 3722–3733. doi: 10.1096/fj.09-134346
- Caterina, M. J., Leffler, A., Malmberg, A. B., Martin, W. J., Trafton, J., Petersen-Zeitz, K. R., et al. (2000). Impaired nociception and pain sensation in mice lacking the capsaicin receptor. *Science* 288, 306–313. doi: 10.1126/science.288.5464.306
- Cobos, E. J., Entrena, J. M., Nieto, F. R., Cendan, C. M., and Del, P. E. (2008). Pharmacology and therapeutic potential of sigma(1) receptor ligands. *Curr. Neuropharmacol.* 6, 344–366. doi: 10.2174/157015908787386113
- Davis, J. B., Gray, J., Gunthorpe, M. J., Hatcher, J. P., Davey, P. T., Overend, P., et al. (2000). Vanilloid receptor-1 is essential for inflammatory thermal hyperalgesia. *Nature* 405, 183–187. doi: 10.1038/35012076
- Diaz, J. L., Zamanillo, D., Corbera, J., Baeyens, J. M., Maldonado, R., Pericas, M. A., et al. (2009). Selective sigma-1 (sigma1) receptor antagonists: emerging target for the treatment of neuropathic pain. *Cent. Nerv. Syst. Agents Med. Chem.* 9, 172–183. doi: 10.2174/1871524910909030172
- Ehlers, M. D., Zhang, S., Bernhardt, J. P., and Haganir, R. L. (1996). Inactivation of NMDA receptors by direct interaction of calmodulin with the NR1 subunit. *Cell* 84, 745–755. doi: 10.1016/S0092-8674(00)81052-1
- Fajardo, O., Meseguer, V., Belmonte, C., and Viana, F. (2008). TRPA1 channels mediate cold temperature sensing in mammalian vagal sensory neurons: pharmacological and genetic evidence. *J. Neurosci.* 28, 7863–7875. doi: 10.1523/jneurosci.1696-08.2008
- Garzón, J., Castro, M., and Sánchez-Blázquez, P. (1998). Influence of Gz and Gi2 transducer proteins in the affinity of opioid agonists to mu receptors. *Eur. J. Neurosci.* 10, 2557–2564. doi: 10.1046/j.1460-9568.1998.t01-1-00267.x
- Garzón, J., Martínez-Peña, Y., and Sánchez-Blázquez, P. (1994). Dissimilar efficacy of opioids to produce mu-mediated analgesia: role of Gx/z and Gi2 transducer proteins. *Life Sci.* 55, L205–L212. doi: 10.1016/0024-3205(94)90048-5
- Garzón, J., Rodríguez-Muñoz, M., and Sánchez-Blázquez, P. (2012). Direct association of Mu-opioid and NMDA glutamate receptors supports their cross-regulation: molecular implications for opioid tolerance. *Curr. Drug Abuse Rev.* 5, 199–226. doi: 10.2174/1874473711205030199
- Guang, W., Wang, H., Su, T., Weinstein, I. B., and Wang, J. B. (2004). Role of mPKCI, a novel mu-opioid receptor interactive protein, in receptor desensitization, phosphorylation, and morphine-induced analgesia. *Mol. Pharmacol.* 66, 1285–1292. doi: 10.1124/mol.66.5
- Hasan, R., Leeson-Payne, A. T., Jaggar, J. H., and Zhang, X. (2017). Calmodulin is responsible for Ca(2+)-dependent regulation of TRPA1 Channels. *Sci. Rep.* 7, 45098–. doi: 10.1038/srep45098

- Hayashi, T. (2015). Sigma-1 receptor: the novel intracellular target of neuropsychotropic drugs. *J. Pharmacol. Sci.* 127, 2–5. doi: 10.1016/j.jpshs.2014.07.001
- Hayashi, T., and Su, T. P. (2007). Sigma-1 receptor chaperones at the ER-mitochondrion interface regulate Ca(2+) signaling and cell survival. *Cell* 131, 596–610. doi: 10.1016/j.cell.2007.08.036
- Huang, J., Zhang, X., and McNaughton, P. A. (2006). Inflammatory pain: the cellular basis of heat hyperalgesia. *Curr. Neuropharmacol.* 4, 197–206. doi: 10.2174/157015906778019554
- Hudson, L. J., Bevan, S., Wotherspoon, G., Gentry, C., Fox, A., and Winter, J. (2001). VR1 protein expression increases in undamaged DRG neurons after partial nerve injury. *Eur. J. Neurosci.* 13, 2105–2114. doi: 10.1046/j.0953-816x.2001.01591.x
- Jordt, S. E., Bautista, D. M., Chuang, H. H., McKemy, D. D., Zygmunt, P. M., Hogestatt, E. D., et al. (2004). Mustard oils and cannabinoids excite sensory nerve fibres through the TRP channel ANKTM1. *Nature* 427, 260–265. doi: 10.1038/nature02282
- Julius, D. (2013). TRP channels and pain. *Annu. Rev. Cell Dev. Biol.* 29, 355–384. doi: 10.1146/annurev-cellbio-101011-155833
- Kaneko, Y., and Szallasi, A. (2014). Transient receptor potential (TRP) channels: a clinical perspective. *Br. J. Pharmacol.* 171, 2474–2507. doi: 10.1111/bph.12414
- Katsura, H., Obata, K., Mizushima, T., Yamanaka, H., Kobayashi, K., Dai, Y., et al. (2006). Antisense knock down of TRPA1, but not TRPM8, alleviates cold hyperalgesia after spinal nerve ligation in rats. *Exp. Neurol.* 200, 112–123. doi: 10.1016/j.expneurol.2006.01.031
- Kim, H. W., Kwon, Y. B., Roh, D. H., Yoon, S. Y., Han, H. J., Kim, K. W., et al. (2006). Intrathecal treatment with sigma1 receptor antagonists reduces formalin-induced phosphorylation of NMDA receptor subunit 1 and the second phase of formalin test in mice. *Br. J. Pharmacol.* 148, 490–498. doi: 10.1038/sj.bjp.0706764
- Kitaichi, K., Chabot, J. G., Moebius, F. F., Flandorfer, A., Glossmann, H., and Quirion, R. (2000). Expression of the purported sigma(1) [sigma(1)] receptor in the mammalian brain and its possible relevance in deficits induced by antagonism of the NMDA receptor complex as revealed using an antisense strategy. *J. Chem. Neuroanat.* 20, 375–387. doi: 10.1016/S0891-0618(00)00106-X
- Lishko, P. V., Procko, E., Jin, X., Phelps, C. B., and Gaudet, R. (2007). The ankyrin repeats of TRPV1 bind multiple ligands and modulate channel sensitivity. *Neuron* 54, 905–918. doi: 10.1016/j.neuron.2007.05.027
- Liu, Q., Puche, A. C., and Wang, J. B. (2008). Distribution and expression of protein kinase C interactive protein (PKC1/HINT1) in mouse central nervous system (CNS). *Neurochem. Res.* 33, 1263–1276. doi: 10.1007/s11064-007-9578-4
- Martin, W. R., Eades, C. G., Thompson, J. A., Huppler, R. E., and Gilbert, P. E. (1976). The effects of morphine- and nalorphine- like drugs in the nondependent and morphine-dependent chronic spinal dog. *J. Pharmacol. Exp. Ther.* 197, 517–532.
- Maurice, T., and Su, T. P. (2009). The pharmacology of sigma-1 receptors. *Pharmacol. Ther.* 124, 195–206. doi: 10.1016/j.pharmthera.2009.07.001
- Mei, J., and Pasternak, G. W. (2002). Sigma1 receptor modulation of opioid analgesia in the mouse. *J. Pharmacol. Exp. Ther.* 300, 1070–1074. doi: 10.1124/jpet.300.3.1070
- Mickle, A. D., Shepherd, A. J., and Mohapatra, D. P. (2015). Sensory TRP channels: the key transducers of nociception and pain. *Prog. Mol. Biol. Transl. Sci.* 131, 73–118. doi: 10.1016/bs.pmbts.2015.01.002
- Numazaki, M., Tominaga, T., Takeuchi, K., Murayama, N., Toyooka, H., and Tominaga, M. (2003). Structural determinant of TRPV1 desensitization interacts with calmodulin. *Proc. Natl. Acad. Sci. U.S.A.* 100, 8002–8006. doi: 10.1073/pnas.1337252100
- Obata, K., Katsura, H., Mizushima, T., Yamanaka, H., Kobayashi, K., Dai, Y., et al. (2005). TRPA1 induced in sensory neurons contributes to cold hyperalgesia after inflammation and nerve injury. *J. Clin. Invest.* 115, 2393–2401. doi: 10.1172/JCI25437
- Ortiz-Renteria, M., Juarez-Contreras, R., Gonzalez-Ramirez, R., Islas, L. D., Sierra-Ramirez, F., Llorente, I., et al. (2018). TRPV1 channels and the progesterone receptor Sig-1R interact to regulate pain. *Proc. Natl. Acad. Sci. U.S.A.* 115, E1657–E1666. doi: 10.1073/pnas.1715972115
- Owsianik, G., D'hoedt, D., Voets, T., and Nilius, B. (2006). Structure-function relationship of the TRP channel superfamily, in *Reviews of Physiology, Biochemistry and Pharmacology*, vol. 156. Ed. S. Amara (Berlin, Heidelberg: Springer), 61–90. doi: 10.1007/s10254-005-0006-0
- Patapoutian, A., Tate, S., and Woolf, C. J. (2009). Transient receptor potential channels: targeting pain at the source. *Nat. Rev. Drug Discov.* 8, 55–68. doi: 10.1038/nrd2757
- Rodríguez-Muñoz, M., and Garzón, J. (2013). Nitric oxide and zinc-mediated protein assemblies involved in mu opioid receptor signaling. *Mol. Neurobiol.* 48, 769–782. doi: 10.1007/s12035-013-8465-z
- Rodríguez-Muñoz, M., Cortés-Montero, E., Pozo-Rodríguez, A., Sánchez-Blázquez, P., and Garzón-Niño, J. (2015a). The ON/OFF switch, sigma1R-HINT1 protein, controls GPCR-NMDA receptor cross-regulation: implications in neurological disorders. *Oncotarget* 6, 35458–35477. doi: 10.18632/oncotarget.6064
- Rodríguez-Muñoz, M., Sánchez-Blázquez, P., Herrero-Labrador, R., Martínez-Murillo, R., Merlos, M., Vela, J. M., et al. (2015b). The sigma1 receptor engages the redox-regulated HINT1 protein to bring opioid analgesia under NMDA receptor negative control. *Antioxid. Redox Signal.* 22, 799–818. doi: 10.1089/ars.2014.5993
- Rodríguez-Muñoz, M., Sánchez-Blázquez, P., and Garzón, J. (2018). Fenfluramine diminishes NMDA receptor-mediated seizures via its mixed activity at serotonin 5HT2A and type 1 sigma receptors. *Oncotarget* 9, 23373–23389. doi: 10.18632/oncotarget.25169
- Roh, D. H., Kim, H. W., Yoon, S. Y., Seo, H. S., Kwon, Y. B., Kim, K. W., et al. (2008). Intrathecal injection of the sigma(1) receptor antagonist BD1047 blocks both mechanical allodynia and increases in spinal NR1 expression during the induction phase of rodent neuropathic pain. *Anesthesiology* 109, 879–889. doi: 10.1097/ALN.0b013e3181895a83
- Romero, L., Zamanillo, D., Nadal, X., Sánchez-Arroyos, R., Rivera-Arconada, I., Dordal, A., et al. (2012). Pharmacological properties of S1RA, a new sigma-1 receptor antagonist that inhibits neuropathic pain and activity-induced spinal sensitization. *Br. J. Pharmacol.* 166, 2289–2306. doi: 10.1111/j.1476-5381.2012.01942.x
- Rosenbaum, T., Gordon-Shaag, A., Munari, M., and Gordon, S. E. (2004). Ca<sup>2+</sup>/calmodulin modulates TRPV1 activation by capsaicin. *J. Gen. Physiol.* 123, 53–62. doi: 10.1085/jgp.200308906
- Sánchez-Blázquez, P., and Garzón, J. (1988). Pertussis toxin differentially reduces the efficacy of opioids to produce supraspinal analgesia in the mouse. *Eur. J. Pharmacol.* 152, 357–361. doi: 10.1016/0014-2999(88)90732-7
- Sánchez-Blázquez, P., Gómez-Serranillos, P., and Garzón, J. (2001). Agonists determine the pattern of G-protein activation in mu-opioid receptor-mediated supraspinal analgesia. *Brain Res. Bull.* 54, 229–235. doi: 10.1016/S0361-9230(00)00448-2
- Sánchez-Blázquez, P., Pozo-Rodríguez, A., Merlos, M., and Garzón, J. (2018). The Sigma-1 receptor antagonist, S1RA, reduces stroke damage, ameliorates post-stroke neurological deficits and suppresses the overexpression of MMP-9. *Mol. Neurobiol.* 55, 4940–4951. doi: 10.1007/s12035-017-0697-x
- Sánchez-Blázquez, P., Rodríguez-Díaz, M., DeAntonio, I., and Garzón, J. (1999). Endomorphin-1 and endomorphin-2 show differences in their activation of mu opioid receptor-regulated G proteins in supraspinal antinociception in mice. *J. Pharmacol. Exp. Ther.* 291, 12–18.
- Sánchez-Blázquez, P., Rodríguez-Muñoz, M., Bailón, C., and Garzón, J. (2012). GPCRs promote the release of zinc ions mediated by nNOS/NO and the redox transducer RGS22 protein. *Antioxid. Redox Signal.* 17, 1163–1177. doi: 10.1089/ars.2012.4517
- Sánchez-Blázquez, P., Rodríguez-Muñoz, M., Herrero-Labrador, R., Burguenio, J., Zamanillo, D., and Garzón, J. (2014). The calcium-sensitive Sigma-1 receptor prevents cannabinoids from provoking glutamate NMDA receptor hypofunction: implications in antinociception and psychotic diseases. *Int. J. Neuropsychopharmacol.* 17, 1943–1955. doi: 10.1017/S1461145714000029
- Sánchez-Fernández, C., Montilla-García, A., Gonzalez-Cano, R., Nieto, F. R., Romero, L., Artacho-Córdón, A., et al. (2014). Modulation of peripheral mu-opioid analgesia by sigma1 receptors. *J. Pharmacol. Exp. Ther.* 348, 32–45. doi: 10.1124/jpet.113.208272
- Sarria, I., Ling, J., Zhu, M. X., and Gu, J. G. (2011). TRPM8 acute desensitization is mediated by calmodulin and requires PIP(2): distinction from tachyphylaxis. *J. Neurophysiol.* 106, 3056–3066. doi: 10.1152/jn.00544.2011
- Scherer, P. C., Zaccor, N. W., Neumann, N. M., Vasavda, C., Barrow, R., Ewald, A. J., et al. (2017). TRPV1 is a physiological regulator of mu-opioid receptors. *Proc. Natl. Acad. Sci. U.S.A.* 114, 13561–13566. doi: 10.1073/pnas.1717005114
- Scholer, J., Ferralli, J., Thiry, S., and Chiquet-Ehrismann, R. (2015). The intracellular domain of teneurin-1 induces the activity of microphthalmia-associated transcription factor (MITF) by binding to transcriptional repressor HINT1. *J. Biol. Chem.* 290, 8154–8165. doi: 10.1074/jbc.M114.615922

- Su, T. P., Hayashi, T., Maurice, T., Buch, S., and Ruoho, A. E. (2010). The sigma-1 receptor chaperone as an inter-organelle signaling modulator. *Trends Pharmacol. Sci.* 31, 557–566. doi: 10.1016/j.tips.2010.08.007
- Su, T. P., London, E. D., and Jaffe, J. H. (1988). Steroid binding at sigma receptors suggests a link between endocrine, nervous, and immune systems. *Science* 240, 219–221. doi: 10.1126/science.2832949
- Thompson, G. L., Lane, J. R., Coudrat, T., Sexton, P. M., Christopoulos, A., and Canals, M. (2015). Biased agonism of endogenous opioid peptides at the mu-opioid receptor. *Mol. Pharmacol.* 88, 335–346. doi: 10.1124/mol.115.098848
- Weiske, J., and Huber, O. (2005). The histidine triad protein Hint1 interacts with Pontin and Reptin and inhibits TCF-beta-catenin-mediated transcription. *J. Cell Sci.* 118, 3117–3129. doi: 10.1242/jcs.02437
- Xing, H., Chen, M., Ling, J., Tan, W., and Gu, J. G. (2007). TRPM8 mechanism of cold allodynia after chronic nerve injury. *J. Neurosci.* 27, 13680–13690. doi: 10.1523/JNEUROSCI.2203-07.2007
- Yap, K. L., Kim, J., Truong, K., Sherman, M., Yuan, T., and Ikura, M. (2000). Calmodulin target database. *J. Struct. Funct. Genomics* 1, 8–14. doi: 10.1023/A:1011320027914
- Conflict of Interest Statement:** MM is employed by Company Esteve Pharmaceuticals.
- The remaining authors declare that the research was conducted in the absence of any commercial or financial relationships that could be construed as a potential conflict of interest.

Copyright © 2019 Cortés-Montero, Sánchez-Blázquez, Onetti, Merlos and Garzón. This is an open-access article distributed under the terms of the Creative Commons Attribution License (CC BY). The use, distribution or reproduction in other forums is permitted, provided the original author(s) and the copyright owner(s) are credited and that the original publication in this journal is cited, in accordance with accepted academic practice. No use, distribution or reproduction is permitted which does not comply with these terms.





# Sigma-1 Receptor Inhibition Reduces Neuropathic Pain Induced by Partial Sciatic Nerve Transection in Mice by Opioid-Dependent and -Independent Mechanisms

Inmaculada Bravo-Caparrós<sup>1,2,3</sup>, Gloria Perazzoli<sup>3,4</sup>, Sandra Yeste<sup>5</sup>, Domagoj Cikes<sup>6</sup>, José Manuel Baeyens<sup>1,2,3</sup>, Enrique José Cobos<sup>1,2,3,7\*</sup> and Francisco Rafael Nieto<sup>1,2,3\*</sup>

## OPEN ACCESS

### Edited by:

Vsevolod V. Gurevich,  
Vanderbilt University,  
United States

### Reviewed by:

Srimal Aminda Samaranayake,  
Vanderbilt University,  
United States  
Xavier Nadal Roura,  
Independent researcher,  
Canada  
Arunachalam Muthuraman,  
AIMST University, Malaysia

### \*Correspondence:

Enrique José Cobos  
ejcobos@ugr.es  
Francisco R. Nieto  
fnieto@ugr.es

### Specialty section:

This article was submitted to  
Experimental Pharmacology and  
Drug Discovery,  
a section of the journal  
Frontiers in Pharmacology

**Received:** 01 February 2019

**Accepted:** 15 May 2019

**Published:** 12 June 2019

### Citation:

Bravo-Caparrós I, Perazzoli G, Yeste S, Cikes D, Baeyens JM, Cobos EJ and Nieto FR (2019) Sigma-1 Receptor Inhibition Reduces Neuropathic Pain Induced by Partial Sciatic Nerve Transection in Mice by Opioid-Dependent and -Independent Mechanisms. *Front. Pharmacol.* 10:613. doi: 10.3389/fphar.2019.00613

<sup>1</sup> Department of Pharmacology, School of Medicine, University of Granada, Granada, Spain, <sup>2</sup> Institute of Neuroscience, Biomedical Research Center, University of Granada, Granada, Spain, <sup>3</sup> Biosanitary Research Institute, University Hospital Complex of Granada, Granada, Spain, <sup>4</sup> Department of Human Anatomy and Embryology, School of Medicine, University of Granada, Granada, Spain, <sup>5</sup> Drug Discovery and Preclinical Development, Esteve, Barcelona, Spain, <sup>6</sup> Institute of Molecular Biotechnology, Vienna, Austria, <sup>7</sup> Teófilo Hernando Institute for Drug Discovery, Madrid, Spain

Sigma-1 ( $\sigma_1$ ) receptor antagonists are promising tools for neuropathic pain treatment, but it is unknown whether  $\sigma_1$  receptor inhibition ameliorates the neuropathic signs induced by nerve transection, in which the pathophysiological mechanisms and response to drug treatment differ from other neuropathic pain models. In addition,  $\sigma_1$  antagonism ameliorates inflammatory pain through modulation of the endogenous opioid system, but it is unknown whether this occurs during neuropathic pain. We investigated the effect of  $\sigma_1$  inhibition on the painful hypersensitivity associated with the spared nerve injury (SNI) model in mice. Wild-type (WT) mice developed prominent cold (acetone test), mechanical (von Frey test), and heat hypersensitivity (Hargreaves test) after SNI.  $\sigma_1$  receptor knockout ( $\sigma_1$ -KO) mice did not develop cold allodynia and showed significantly less mechanical allodynia, although they developed heat hyperalgesia after SNI. The systemic acute administration of the selective  $\sigma_1$  receptor antagonist S1RA attenuated all three types of SNI-induced hypersensitivity in WT mice. These ameliorative effects of S1RA were reversed by the administration of the  $\sigma_1$  agonist PRE-084, and were absent in  $\sigma_1$ -KO mice, indicating the selectivity of S1RA-induced effects. The opioid antagonist naloxone and its peripherally restricted analog naloxone methiodide prevented S1RA-induced effects in mechanical and heat hypersensitivity, but not in cold allodynia, indicating that opioid-dependent and -independent mechanisms are involved in the effects of this  $\sigma_1$  antagonist. The repeated administration of S1RA twice a day during 10 days reduced SNI-induced cold, mechanical, and heat hypersensitivity without inducing analgesic tolerance during treatment. These effects were observed up to 12 h after the last administration, when S1RA was undetectable in plasma or brain, indicating long-lasting pharmacodynamic effects. These data suggest that  $\sigma_1$  antagonism may have therapeutic value for the treatment of neuropathic pain induced by the transection of peripheral nerves.

**Keywords:** neuropathic pain, spared nerve injury, sigma-1 receptors, S1RA, endogenous opioid system, mechanical allodynia, cold allodynia, heat hyperalgesia

## INTRODUCTION

Neuropathic pain is a debilitating chronic pain condition resulting from a lesion or disease of the somatosensory system (Colloca et al., 2017). The prevalence of neuropathic pain in the general population has been estimated in the range of 6.9–10% (van Hecke et al., 2014), and it is expected to rise in the future (Colloca et al., 2017). Despite the enormous efforts devoted to both clinical and preclinical research, neuropathic pain treatment remains an unmet clinical need (Finnerup et al., 2015).

The sigma-1 ( $\sigma_1$ ) receptor is a unique ligand-operated chaperone expressed at high levels in several key pain control areas in both the peripheral and central nervous system, where it interacts with different receptors and ion channels to modulate them (Su et al., 2016; Sánchez-Fernández et al., 2017). The pharmacology of  $\sigma_1$  receptors has been deeply studied, and there are currently selective  $\sigma_1$  agonists (such as PRE-084) and antagonists (such as S1RA), to study  $\sigma_1$  receptor function (Sánchez-Fernández et al., 2017). Substantial evidence points to a prominent role for these receptors in neuropathic pain of diverse etiology (Merlos et al., 2017; Sánchez-Fernández et al., 2017), and shows that pain-like behaviors are attenuated in  $\sigma_1$ -knockout (KO) mice (de la Puente et al., 2009; Nieto et al., 2012) and in wild-type (WT) animals treated with  $\sigma_1$  receptor antagonists (Roh et al., 2008; Nieto et al., 2012; Romero et al., 2012; Gris et al., 2016; Kang et al., 2016). The mechanisms involved in the antineuropathic effects of  $\sigma_1$  inhibition are only partially known and have been well studied in the central nervous system, specifically in the dorsal spinal cord, where these receptors control central sensitization (reviewed in Sánchez-Fernández et al., 2017).

There are differences between the pathophysiological mechanisms and responses to drug treatment for neuropathic pain induced by different types of injury to the peripheral nerves (Aley and Levine, 2002; Baron et al., 2010; Hershman et al., 2014; Finnerup et al., 2015). In particular, different neuroplastic changes (Casals-Díaz et al., 2009) and gene expression profiles (Griffin et al., 2007; Costigan et al., 2010) have been reported after denervation or constriction/ligation of the sciatic nerve. Surgical interventions inevitably results in nerve transection, and as a consequence, significant number of patients experience neuropathic pain (Borsook et al., 2013). However, all studies to date on the role of  $\sigma_1$  receptors in neuropathic pain after mechanical injury to peripheral nerves has focused on models of sciatic nerve constriction/ligation (Roh et al., 2008; de la Puente et al., 2009; Espinosa-Juárez et al., 2017a); thus the role of  $\sigma_1$  receptors in neuropathic pain induced by nerve transection has never been explored. Transection of the tibial and common peroneal branches of the sciatic nerve results in persistent neuropathic pain in rodents, manifested by marked hypersensitivity in the territory of the intact sural branch. Hence, this neuropathic pain model is termed the spared nerve injury (SNI) model (Decosterd and Woolf, 2000).

In view of these antecedents, the first goal of the present study was to test whether the inhibition of  $\sigma_1$  receptors alleviated the painful hypersensitivity associated with SNI-induced neuropathic

pain. This was investigated by comparing SNI-induced neuropathic hypersensitivity in WT and  $\sigma_1$ -KO mice, and by testing the effects, in animals with neuropathy, of the acute and repeated administration of the selective  $\sigma_1$  antagonist S1RA, which is currently under clinical development for the treatment of neuropathic pain (Abadías et al., 2013; Bruna et al., 2018).

Opioid receptors have been described as part of the interactome of  $\sigma_1$  receptors. This is relevant since  $\sigma_1$  receptors physically interact with opioid receptors restraining their functioning (reviewed in Sánchez-Fernández et al., 2017), so that  $\sigma_1$  receptor inhibition enhances analgesia induced by opioid drugs in nociceptive pain at both central (Mei and Pasternak, 2002) and peripheral sites (Sánchez-Fernández et al., 2013; Sánchez-Fernández et al., 2014; Prezzavento et al., 2017), and can increase the antihyperalgesic effects of endogenous opioid peptides (EOPs) produced naturally by immune cells that accumulate at the inflamed site to relieve inflammatory pain (Tejada et al., 2017). During neuropathic pain there is a prominent recruitment of immune cells harboring EOPs at both peripheral and central sites (reviewed in Ref. Tejada et al., 2018). However, whether  $\sigma_1$  receptors modulate endogenous opioid analgesia in neuropathic pain remains completely unknown. Therefore, the second goal of this study was to evaluate the possible contribution of the endogenous opioid system to the antineuropathic effects induced by S1RA in the mouse model of SNI.

## METHODS

### Animals

Most experiments were performed in 8- to 11-week-old female WT CD-1 mice (Charles River, Barcelona, Spain) and  $\sigma_1$ -KO CD-1 mice (Laboratorios Esteve, Barcelona, Spain). Some experiments were performed on male mice from the same strain and genotypes. Taking into account that male mice are much more aggressive to other mice than female animals (Edwards, 1968), and that stress such as that induced by fights with the alpha male can induce opioid analgesia (Miczek et al., 1982), we considered that this behavior of male mice might be a confounder in our experiments in the context on the modulation of endogenous opioid analgesia by  $\sigma_1$  receptors. Therefore, we performed most experiments in female mice. However, we also tested male mice in some key experiments (see the Results section) to explore a possible sexual dimorphism in  $\sigma_1$ -mediated modulation of SNI-induced hypersensitivity. Female animals were tested at random times throughout the estrous cycle. Mice were housed in colony cages with free access to food and water prior to the experiments, and were kept in temperature- and light-controlled rooms ( $22 \pm 2^\circ\text{C}$ , and light–dark cycle of 12 h). The experiments were done during the light phase (from 9:00 a.m. to 3:00 p.m.). Animal care was in accordance with international standards (European Communities Council Directive 2010/63), and the protocol of the study was approved by the Research Ethics Committee of the University of Granada, Spain.

### Spared Nerve Injury

Mice were anesthetized with isoflurane (2%), and SNI surgery was performed as previously described (Bourquin et al., 2006). Briefly, an incision was made in the left thigh skin and was followed by

**Abbreviations:** EOP, endogenous opioid peptide; i.p., intraperitoneal; KO, knockout;  $\sigma_1$ , sigma-1; SNI, spared nerve injury; WT, wild-type.

an incision made directly through the biceps femoris muscle, exposing the sciatic nerve and its three terminal branches (the sural, common peroneal, and tibial nerves). The tibial and common peroneal branches of the sciatic nerve were ligated with a silk suture and transected distally, while the sural nerve was left intact. In sham-operated control mice, the sciatic nerve terminal branches were exposed but neither ligated nor transected. The day of SNI surgery is referred to as day 0. In some mice, SNI surgery induced hypoesthesia/anesthesia in the territory of the paw innervated by the sural nerve, instead of inducing sensory hypersensitivity. This was considered to be a consequence of a failed surgery and the mice were discontinued from further evaluations. These mice accounted for less than 1% of the mice tested.

## Drugs and Drug Administration

### Acute Treatment Protocol

We used two selective  $\sigma_1$  receptor ligands: the  $\sigma_1$  antagonist S1RA (E-52862.HCl; 4-[2-[[5-methyl-1-(2-naphthalenyl)-1H-pyrazol-3-yl]oxy]ethyl] morpholine) (8–128 mg/kg; DC Chemicals, Shanghai, China), and the  $\sigma_1$  agonist PRE-084 (2-[4-morpholinethyl]-1-phenylcyclohexanecarboxylate hydrochloride) (Tocris Cookson Ltd., Bristol, United Kingdom) (Cobos et al., 2008). In addition, we used the following opioid receptor ligands: the opioid agonist morphine hydrochloride (0.5–2 mg/kg; General Directorate of Pharmacy and Drugs, Spanish Ministry of Health), the opioid antagonist naloxone hydrochloride and its peripherally restricted analog naloxone methiodide (Sigma-Aldrich, Madrid, Spain). The doses of S1RA s.c. (subcutaneously) and morphine used to reverse mechanical, heat, and cold hypersensitivities were determined in the experiments shown in the “Results” section. The dose of PRE-084 used in the present study (32 mg/kg, s.c.) was selected based on our previous studies (Entrena et al., 2009; Montilla-García et al., 2018). The doses of naloxone (1 mg/kg, s.c.) and naloxone methiodide (2 mg/kg, s.c.) are those used in our previous studies (Sánchez-Fernández et al., 2014; Tejada et al., 2017). All drugs were dissolved to their final concentrations in sterile physiological saline just before administration, and were administered subcutaneously (s.c.) in the interscapular area in an injection volume of 5 mL/kg. The control animals received the same volume of the drug solvent (saline) s.c. All drugs were administered 7 days after surgery, when pain hypersensitivity was fully developed, and their effects were tested as explained in the Behavioral Assays section. When the effects of the association of two different drugs were evaluated, each injection was performed in a different area of the interscapular zone. In all cases, behavioral evaluations after drug administration were performed by an observer blinded to the treatment.

### Repeated (10 days) Treatment Protocol

Treatment was given twice a day (every 12 h) *via* the intraperitoneal (i.p.) route with S1RA 25 mg/kg or vehicle, since it has been previously described that S1RA was efficacious using this administration protocol in a model of neuropathic pain induced by nerve ligation (Romero et al., 2012). Treatment started in the day of surgery (first injection 30 min before the injury) and was maintained for up to day 9 (i.e., 10 days of treatment). The effects of treatments were evaluated on days 7 (30 min after the administration of S1RA or

saline), 10 (12 h after the last administration of S1RA or saline), 11, and 14 after nerve injury (36 and 108 h after the last administration of S1RA or saline, respectively) in each animal. Behavioral evaluations after repeated drug administration were performed by an observer blinded to the treatment.

## Behavioral Assays

### Time Course Studies

To elucidate the time course of SNI-induced pain hypersensitivity in WT and  $\sigma_1$ -KO mice, the behavioral responses were tested before surgery (baseline value). Then SNI surgery was performed and behavioral tests were carried out 3, 7, 14, and 21 days after SNI in each animal.

To investigate the acute effects of drugs on pain-related behaviors associated with SNI, presurgery baseline responses were evaluated, and then SNI surgery was performed. Seven days after the surgical procedure, when SNI-induced mechanical, heat, and cold hypersensitivities were fully developed, pretreatment measurements were made (time 0) and then the drugs or saline were injected s.c., and the response of the animal to the nociceptive test was measured again 30, 90, and 180 min after the injection.

In all cases, each mouse was evaluated in only one nociceptive test and received drug treatment or saline only once. All behavioral evaluations were recorded by an observer blinded to the genotype and treatment.

### Procedure to Measure Mechanical Allodynia

Mechanical allodynia was assessed with von Frey filaments according to the up–down method (Chaplan et al., 1994), with slight modifications. On each day of evaluation the mice were habituated for 60 min in individual transparent plastic boxes (7 × 7 × 13 cm) placed on a wire mesh platforms. After the acclimation period, filaments were applied to the plantar ipsilateral hind paw in the sural nerve territory, pressed upward to cause a slight bend in the fiber, and left in place for 2–3 s. Calibrated von Frey monofilaments (Stoelting, Wood Dale, IL, USA) with bending forces that ranged from 0.02 to 1.4 g were applied using the up–down paradigm, starting with the 0.6 g filament and allowing 10 s between successive applications. The response to the filament was considered positive if immediate licking/biting, flinching, or rapid withdrawal of the stimulated paw was observed. In each consecutive test, if there was no response to the filament, a stronger stimulus was then selected; if there was a positive response, a weaker one was then used.

### Procedure to Measure Cold Allodynia

Cold allodynia was tested by gently touching the plantar skin of the hind paw with an acetone drop, as previously described (Nieto et al., 2008). On each day of evaluation the mice were housed and habituated for 30 min in individual transparent plastic enclosures (7 × 7 × 13 cm) with a floor made of wire mesh. Acetone was applied three times to the ipsilateral hind paw at intervals of 30 s, and the duration of biting or licking of the hind paw was recorded with a stopwatch and reported as the cumulative time of biting/licking in all three measurements. A cutoff time of 10 s was used in each of the three trials, because animals rarely licked their hind paw for more than 10 s. During

the presurgery baseline evaluation we discarded  $\approx 5\%$  of the mice tested due to an exaggerated atypical response to the acetone ( $>5$  s of cumulative responses to acetone in the three measures).

### Procedure to Measure Heat Hyperalgesia

To measure heat hyperalgesia we used the Hargreaves method (Tejada et al., 2014), with slight modifications as previously described (Hargreaves et al., 1988). Mice were habituated for 2 h in individual plastic chambers ( $9 \times 9 \times 22$  cm) placed on a glass floor maintained at  $30^\circ\text{C}$ . After habituation, a beam of radiant heat was focused to the plantar surface of the ipsilateral hind paw with a plantar test apparatus (IITC, Los Angeles, CA, USA), until the mouse made a withdrawal response. Each mouse was tested three times, and the latencies were averaged for each animal. At least 60 s were allowed between consecutive measurements. A cutoff latency time of 20 s was used in each measurement to avoid lesions to the skin and unnecessary suffering.

### Determination of the Concentration of S1RA in Plasma and Brain Tissue

Animals were treated as described in the Repeated (10 Days) Treatment Protocol section, and the concentration of S1RA in plasma and brain tissue was measured 30 min and 12 h after the last i.p. administration. Briefly, a terminal blood sample was drawn from each mouse by cardiac puncture at the appropriate time after vehicle or drug administration. Blood samples were collected in heparinized tubes and centrifuged at  $2,000 \times g$  for 10 min to obtain plasma. Immediately after blood extraction, whole brains were removed. Plasma samples and brains were stored at  $-80^\circ\text{C}$  until analysis. Each brain was weighted and homogenized in 4 mL Dulbecco's phosphate buffered saline immediately before drug concentrations were determined. Protein was precipitated with acetonitrile, and samples were analyzed by high-performance liquid chromatography-triple quadrupole mass spectrometry (HPLC-MS/MS) according

to a previously described procedure (Romero et al., 2012). The concentration of the compound in plasma or brain was determined by least-squares linear regression with a calibration curve.

### Data Analysis

For behavioral studies, statistical analysis was carried out with two-way repeated-measures analysis of variance (ANOVA). For the study of the S1RA levels determined by HPLC-MS/MS assay, statistical analysis was performed with two-way ANOVA. The Bonferroni *post hoc* test was performed in all cases. The differences between values were considered significant when the *p*-value was below 0.05. All data were analyzed with SigmaPlot 12.0 software (Systat Software Inc., San Jose, CA, USA).

## RESULTS

### Comparison of Spared Nerve Injury-Induced Neuropathic Pain in $\sigma_1$ Receptor Knockout and Wild-Type Mice

We studied the involvement of the  $\sigma_1$  receptor in neuropathic pain after SNI by comparing the response to mechanical, heat, and cold stimuli in WT and  $\sigma_1$ -KO female mice. The baseline responses to the von Frey, Hargreaves, and acetone tests before surgery did not differ significantly between  $\sigma_1$ -KO and WT animals in any group tested (Figure 1A–C). In the sham-operated groups there were no significant postsurgery changes in the responses to any of the three behavioral tests in either  $\sigma_1$ -KO or WT animals (Figure 1A–C). However, after SNI surgery, WT mice developed mechanical allodynia, manifested as a significant reduction in the mechanical threshold, which was detectable as early as day 3 after surgery, was greatest on day 7, and remained observable throughout the 21-day evaluation period.  $\sigma_1$ -KO mice also developed mechanical allodynia; however, it was significantly less

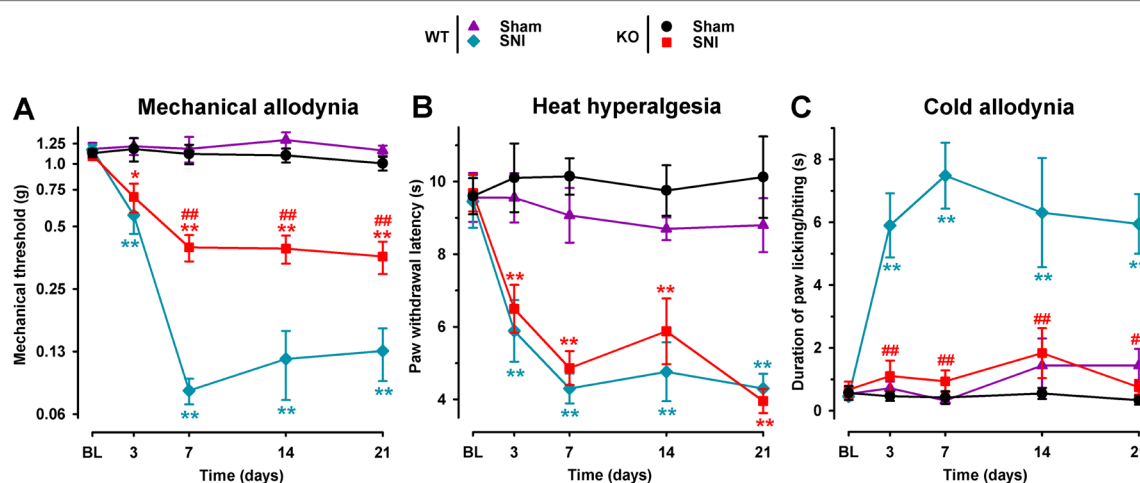


**FIGURE 1 |** Comparison of spared nerve injury (SNI)-induced neuropathic pain behaviors in female wild-type (WT) and  $\sigma_1$  receptor knockout (KO) mice. The von Frey threshold (A), latency to hind paw withdrawal in the Hargreaves test (B), and duration of hind paw licking or biting in the acetone test (C) were recorded 1 day before (baseline, BL) and on days 3, 7, 14, and 21 after surgery in the paw ipsilateral to the surgery. Each point and vertical line represent the mean  $\pm$  SEM of the values obtained in 10–12 animals. Statistically significant differences between the values in the sham and SNI groups on the same day: \**P* < 0.05; \*\**P* < 0.01; and among WT and KO groups: ##*P* < 0.01 (two-way repeated-measures ANOVA followed by Bonferroni test).



pronounced than in WT mice, and the differences between WT and  $\sigma_1$ -KO mice were statistically significant from day 7 to day 21 (**Figure 1A**). Both WT and  $\sigma_1$ -KO mice developed a similar degree of heat hypersensitivity in the Hargreaves test after SNI, with paw withdrawal latencies to heat stimulation significantly lower than those in sham-operated mice of both genotypes and at all time points evaluated after SNI (**Figure 1B**). Wild-type mice with SNI also developed marked cold allodynia, manifested as a significantly longer increase in the duration of paw licking/biting induced by acetone from day 3 throughout the evaluation period in comparison to the control WT sham group (**Figure 1C**). In contrast, SNI surgery had no significant effect on the postsurgery responses in  $\sigma_1$ -KO mice in the acetone test, given that the values in this group were virtually identical to those in the  $\sigma_1$ -KO sham group throughout the evaluation period (**Figure 1C**). These results are summarized in **Table 1**.

We also compared mechanical, heat, and cold hypersensitivities induced by SNI in female and male animals from both genotypes. On day 7 after SNI, sensory hypersensitivity to the three types of stimuli was equivalent in WT female and male mice (**Figure 2**).  $\sigma_1$ -KO mice of both sexes showed an equivalent reduction of mechanical allodynia, while showing the same extent of heat hyperalgesia than WT mice, but no cold hypersensitivity (**Figure 2A–C**, respectively).

In summary, SNI surgery induced mechanical, heat, and cold hypersensitivity in WT mice of both sexes. However, SNI surgery led to a clearly different pattern of neuropathic signs in  $\sigma_1$ -KO mice irrespectively of the sex tested, as these female or male mutant mice developed heat hyperalgesia, but did not develop cold allodynia and showed significantly less mechanical allodynia.

### Effects of the Acute Systemic Administration of the Selective $\sigma_1$ Receptor Antagonist S1RA on Spared Nerve Injury-Induced Mechanical, Cold, and Heat Hypersensitivity

To test the effects of acute pharmacological antagonism by the  $\sigma_1$  receptor on SNI-induced neuropathic pain, the selective  $\sigma_1$  receptor antagonist S1RA was administered s.c. to female WT mice after neuropathy was fully developed (7 days after surgery). The threshold force needed to evoke pain-like responses before treatment with S1RA or saline was significantly lower than in the baseline measurement (**Figure 3A**, time 0), thus showing mechanical allodynia. Saline administration did not significantly modify SNI-induced mechanical allodynia during the 3-h test period (**Figure 3A**). In contrast, the acute administration of S1RA (32–128 mg/kg) attenuated mechanical allodynia in a dose-dependent manner (**Figure 3A**). In mice with SNI, paw withdrawal latencies to radiant heat were significantly shorter, in comparison to their baseline measurements, in all groups of animals before S1RA or saline administration (**Figure 3B**, time 0). Saline administration did not significantly modify SNI-induced heat hyperalgesia, whereas the s.c. administration of S1RA (25–64 mg/kg) dose-dependently inhibited this response (**Figure 3B**). In the acetone test, WT mice 7 days after SNI and

**TABLE 1 |** Summary of the main results obtained in this study on the effect of the acute administration of S1RA to female wild-type mice and the effects seen on of  $\sigma_1$  receptor knockout female mice on the spared nerve injury model of neuropathic pain. The figures that show the results for the different experiments are indicated.

Type of sensory hypersensitivity	Wild-type mice			$\sigma_1$ receptor knockout mice		
	Efficacy*	Potency*	PRE-084	Without any treatment*	S1RA effects	S1RA effects
Mechanical allodynia	++	+	Yes	Partially reduced	Figure 1A	Absent
Heat hyperalgesia	+++	++	Yes	Fully present	Figure 1B	Absent
Cold allodynia	+++	+++	Yes	Absent	Figure 1C	Not tested

\*Experiments where male mice were also tested with similar results to female mice (see Figures 2 and 6).

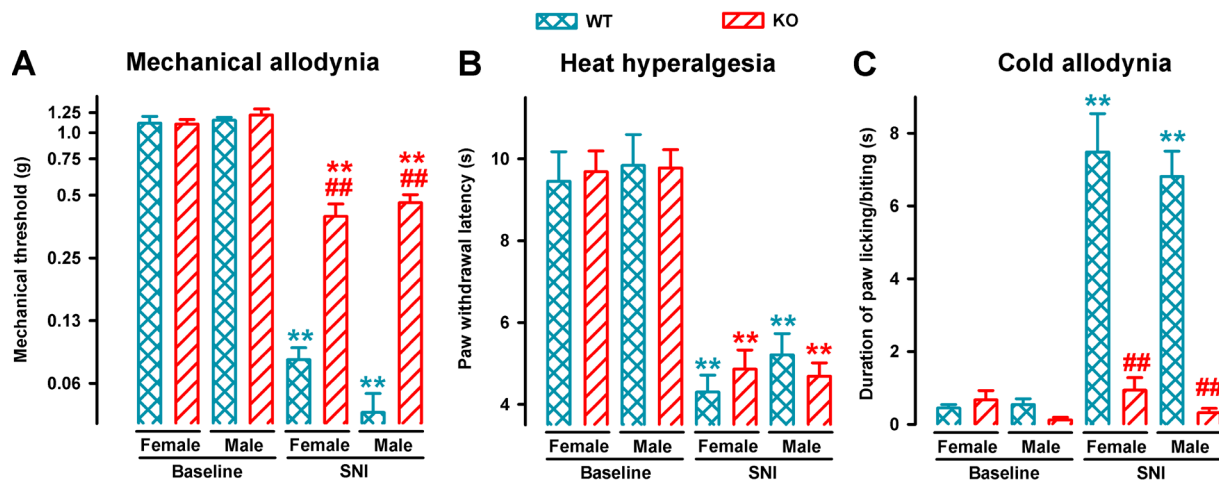


**FIGURE 2** | Comparison of SNI-induced neuropathic pain behaviors in female and male WT and  $\sigma_1$ -KO mice. The von Frey threshold (A), the latency to hind paw withdrawal in the Hargreaves test (B), and duration of hind paw licking or biting in the acetone test (C) were recorded 1 day before (baseline) and 7 days after surgery in the paw ipsilateral to the surgery. Each point and vertical line represent the mean  $\pm$  SEM of the values obtained in 8–12 animals. Statistically significant differences between the values on the presurgery (baseline) day and 7 days after SNI in mice of the same sex: \*\* $P < 0.01$ ; and between WT and KO groups of mice of the same sex: ## $P < 0.01$ . There were no statistical differences between values from mice of different sexes under the same experimental conditions (two-way repeated-measures ANOVA followed by Bonferroni test).

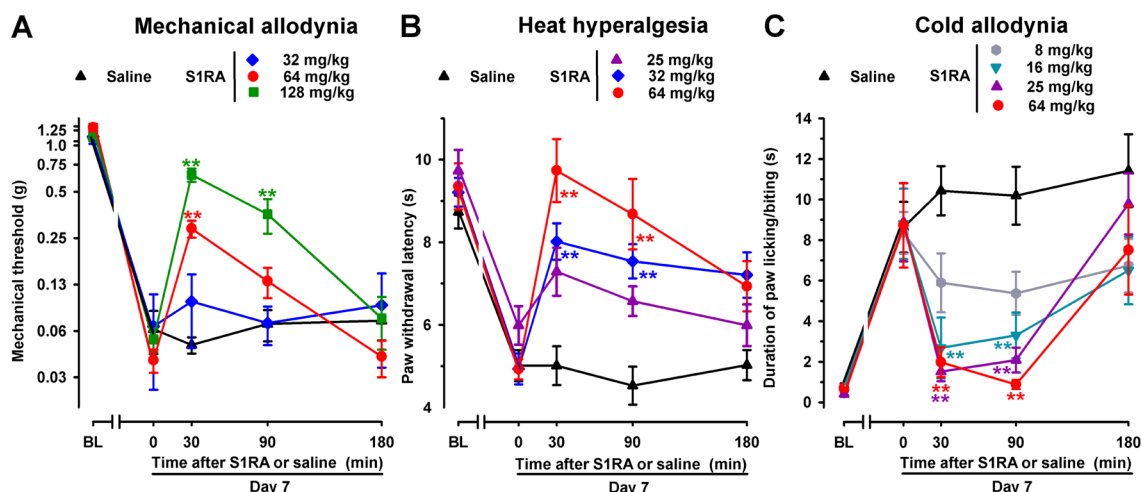


**FIGURE 3** | Time course of the effects of a single subcutaneous (s.c.) injection of S1RA (8–128 mg/kg) or saline on mechanical allodynia (A), heat hyperalgesia (B), and cold allodynia (C), in female WT mice with SNI, 7 days after surgery. The von Frey threshold (A), the latency to hind paw withdrawal in the Hargreaves test (B), and the duration of hind paw licking or biting in the acetone test (C) were recorded 1 day before (baseline, BL) and 7 days (Day 7) after surgery in the paw ipsilateral to the surgery. On day 7, the responses to test stimuli were recorded immediately before (time 0) and at several times (30, 90, and 180 min) after injection of the drug or saline. Each point and vertical line represent the mean  $\pm$  SEM of the values obtained in 8–11 animals. Statistically significant differences between S1RA- and saline-treated groups at the same time after treatment: \*\* $P < 0.01$  (two-way repeated-measures ANOVA followed by Bonferroni test).

before treatment with S1RA or saline (time 0) showed a longer duration of paw licking/biting in response to acetone (Figure 3C, time 0). In these mice, a single s.c. injection of saline did not modify the response to acetone at any of the time points tested (Figure 3C). However, a single s.c. injection of S1RA (8–64 mg/kg) dose-dependently reduced the duration of acetone-induced paw licking/biting from 30 to 90 min after treatment (Figure 3C). Among the three sensory modalities explored in female mice, cold allodynia was the most sensitive outcome to the effects of S1RA, as it was fully reversed by 16 mg/kg of this compound, whereas S1RA 64 mg/kg was needed to fully reverse heat hyperalgesia,

and we had to increase the dose of S1RA up to 128 mg/kg to induce a prominent (although partial) effect on SNI-induced mechanical allodynia (compare Figure 3A–C). These results are summarized in Table 1.

In contrast to the effect of the  $\sigma_1$  receptor antagonist S1RA, the selective  $\sigma_1$  agonist PRE-084 (32 mg/kg, s.c.), when tested 7 days after SNI, did not alter SNI-induced mechanical-, heat-, or cold-hypersensitivity in female WT mice (Figure 4A–C, respectively). However, when PRE-084 (32 mg/kg, s.c.) and S1RA were associated, the antiallodynic and antihyperalgesic effects of this  $\sigma_1$  antagonist were abolished (Figure 4A–C), suggesting

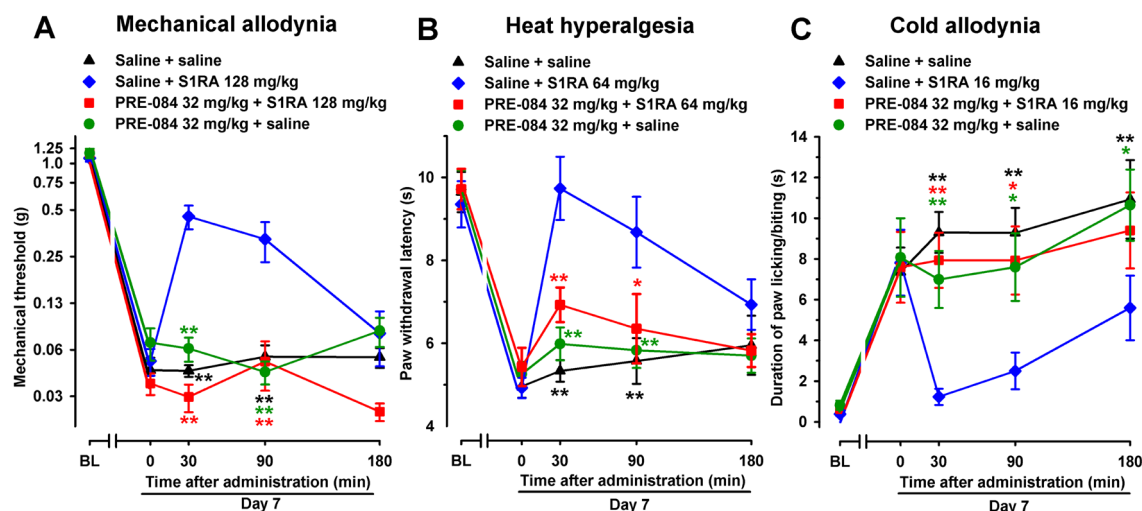


**FIGURE 4 |** The  $\sigma_1$  receptor agonist PRE-084 reversed the effects of the  $\sigma_1$  receptor antagonist S1RA in female WT mice with SNI 7 days after surgery. Mechanical allodynia (A), heat hyperalgesia (B), and cold allodynia (C) were evaluated 1 day before (baseline, BL) and 7 days (day 7) after surgery, in the paw ipsilateral to the surgery. On day 7, the responses to test stimuli were recorded immediately before (time 0) and at several times (30, 90, and 180 min) after injection of the drugs or saline. Each point and vertical line represent the mean  $\pm$  SEM of the values obtained in 8–14 animals. Statistically significant differences in comparison to the saline+S1RA group: \* $P < 0.05$ ; \*\* $P < 0.01$  (two-way repeated-measures ANOVA followed by Bonferroni test).

that the effects of S1RA were mediated by the pharmacological antagonism of  $\sigma_1$  receptors.

To further verify the role  $\sigma_1$  receptors on the effects induced by S1RA in SNI-induced hypersensitivity, we compared its effects in female WT and mice lacking  $\sigma_1$  receptors ( $\sigma_1$ -KO mice). We tested the effects of this drug in  $\sigma_1$ -KO mice only for SNI-induced mechanical allodynia, which was partially developed in these mice, and heat hypersensitivity, which fully developed in  $\sigma_1$ -KO mice; whereas we did not test for the possible effects of S1RA on cold allodynia, since this type of hypersensitivity was absent in  $\sigma_1$ -KO mice (as shown in Figure 1). WT mice given the  $\sigma_1$  antagonist S1RA showed less SNI-induced mechanical allodynia (Figure 5A) and heat hyperalgesia (Figure 5B), but the administration of S1RA to  $\sigma_1$ -KO mice did not induce significant antiallodynic or antihyperalgesic effects in these mutant mice (Figure 5A and B).

Therefore, both the reversion of the effects of S1RA by PRE-084 and the absence of activity of S1RA in mice lacking  $\sigma_1$  receptors suggest that off-target effects did not contribute to the antineuropathic effects of the  $\sigma_1$  antagonist S1RA in this neuropathic pain model.

### Contribution of the Endogenous Opioid System to Antineuropathic Effects of the Systemic Administration of S1RA on Spared Nerve Injury-Induced Neuropathic Pain

In female WT mice, the association of the opioid antagonist naloxone (1 mg/kg, s.c.) with S1RA administered 7 days after SNI surgery completely reversed the ameliorative effects produced by the  $\sigma_1$  antagonist on hypersensitivity to mechanical (Figure 6A) and heat stimuli (Figure 6B). We also tested the effects of the peripherally restricted opioid antagonist naloxone methiodide on the antineuropathic effects of S1RA, and observed that peripheral

opioid antagonism was also able to fully reverse the effects of S1RA on mechanical and heat hypersensitivity (Figure 6A and B). These data suggest that the effects induced by the  $\sigma_1$  antagonist on SNI-induced mechanical and heat hypersensitivity require the participation of the opioid system at the peripheral level. In contrast, naloxone treatment did not alter the effects of S1RA on cold allodynia (Figure 6C), suggesting that opioid-independent effects induced by S1RA were involved in the decrease in this type of hypersensitivity. These results are summarized in Table 1.

We tested these same doses of S1RA in male mice and found equivalent results than those found in female mice: the acute administration of the  $\sigma_1$  receptor antagonist S1RA to male mice partially reversed SNI-induced mechanical allodynia but completely reversed heat and cold hypersensitivity (Figure 6D–F, respectively). Similar to the results shown with female mice, the ameliorative effects of S1RA on mechanical and heat SNI-induced hypersensitivity in male mice were reversed by naloxone methiodide, whereas naloxone did not reverse the effects of S1RA on cold allodynia (Figure 6D–F, respectively).

In order to explore whether the endogenous opioid system influences pain hypersensitivity induced by SNI in female mice, we administered naloxone (1 mg/kg) and naloxone methiodide (2 mg/kg) in the absence of S1RA to WT mice 7 days after SNI. No significant effects were observed with any of the opioid antagonists in any of the three sensory modalities explored (Figure 7A–C).

### Effects of the Systemic Administration of Morphine on Spared Nerve Injury-Induced Cold and Mechanical Allodynia and Heat Hyperalgesia

To test the effects of an opioid drug on SNI-induced sensory hypersensitivity, we evaluated the effects of morphine in this

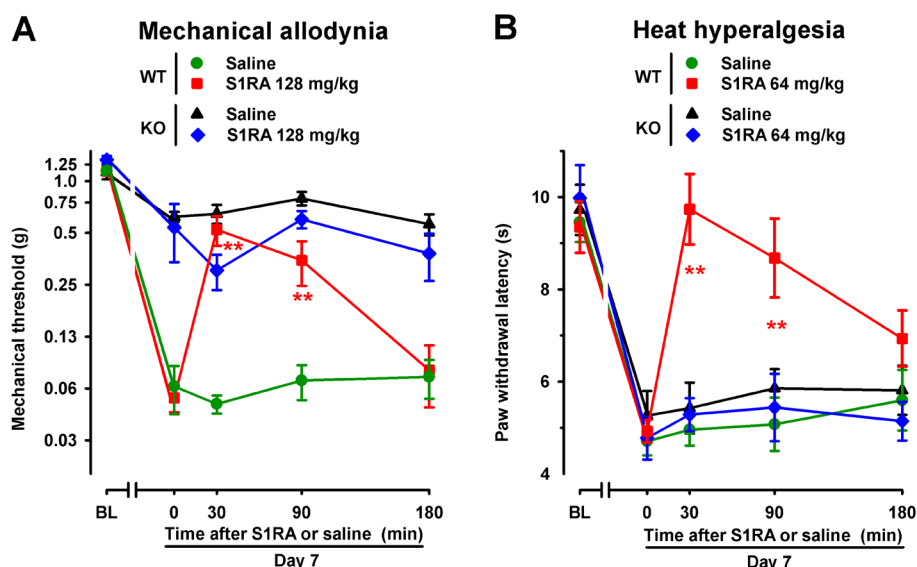


**FIGURE 5 |** Time course of the effects of a single s.c. injection of S1RA (64–128 mg/kg) or saline on mechanical allodynia **(A)** and heat hyperalgesia **(B)** in female WT and  $\sigma_1$ -KO mice with SNI 7 days after surgery. The von Frey threshold **(A)** and latency to hind paw withdrawal in the Hargreaves test **(B)** were evaluated 1 day before (baseline, BL) and 7 days (day 7) after surgery in the paw ipsilateral to the surgery. On day 7 the responses to test stimuli were recorded immediately before (time 0) and at several times (30, 90, and 180 min) after injection of the drug or saline. Each point and vertical line represent the mean  $\pm$  SEM of the values obtained in 8–14 animals. Statistically significant differences between S1RA- and saline-treated groups at the same time after treatment were found in WT mice (\*\* $P < 0.01$ ) but not in  $\sigma_1$ -KO mice (two-way repeated-measures ANOVA followed by Bonferroni test).

neuropathic pain model in female mice. As expected, acute administration of the morphine solvent (saline) had no effect on hypersensitivity following SNI surgery (**Figure 8A–C**). However, the administration of morphine (1 and 2 mg/kg, s.c.) led to significantly less mechanical allodynia associated with SNI, with a more prolonged effect at the highest dose tested (**Figure 8A**). In addition, acute treatment with morphine (0.5 and 1 mg/kg) inhibited, in a dose-dependent manner, both heat hyperalgesia (**Figure 8B**) and cold allodynia (**Figure 8C**) induced by SNI. Whereas a single s.c. injection of morphine (1 mg/kg) completely reversed heat and cold hypersensitivity induced by SNI, the effect of morphine on SNI-induced mechanical allodynia was weaker, leading to only a partial reduction (see **Figure 8A–C**).

To elucidate the possible contribution of peripheral opioid receptors to the antinociceptive effects induced by morphine in SNI mice, we associated morphine administration with the injection of the opioid antagonists naloxone or naloxone methiodide. As expected, naloxone (1 mg/kg s.c.) completely reversed the antinociceptive effect of morphine in all three sensory modalities explored, with values indistinguishable from those in mice treated with the drug solvent (**Figure 9A–C**). However, naloxone methiodide (2 mg/kg) completely reversed the effect of morphine (1 mg/kg) on mechanical allodynia (**Figure 9A**), and markedly reduced its effects on heat hyperalgesia (**Figure 9B**), whereas it did not reverse the effect of morphine on SNI-induced cold allodynia (**Figure 9C**). These data suggest that peripheral opioid receptors contributed to the ameliorative effects induced by morphine only in hypersensitivity to mechanical and heat stimuli induced by SNI, but not in cold allodynia.

## Effect of Repeated Treatment With S1RA on Neuropathic Pain-Related Behaviors

To study the effect of prolonged pharmacological antagonism of the  $\sigma_1$  receptors on the development of SNI-induced neuropathy, we administered to WT female mice two daily injections of S1RA (25 mg/kg, i.p.) or saline, starting 30 min before surgery and continuing up to day 9. Mechanical allodynia (**Figure 10A**), heat hyperalgesia (**Figure 10B**), and cold allodynia (**Figure 10C**) induced by SNI were suppressed by the repeated administration of S1RA when measured on day 7 after surgery, 30 min after its administration.

The antineuropathic effects induced by repeated treatment with S1RA were still significant in all three sensory modalities explored (compared to treatment with the vehicle only) on day 10, 12 h after the last administration of S1RA (**Figure 10A–C**). However, the antineuropathic effects of S1RA disappeared in longer periods after treatment was discontinued: allodynia and hyperalgesia values on days 11 and 14 were indistinguishable from those in the vehicle-treated group (**Figure 10A–C**).

In contrast, acute treatment with S1RA (25 mg/kg, i.p.) had no significant effect on mechanical or heat hypersensitivities (**Figure 11A and B**), but significantly inhibited SNI-induced cold hypersensitivity (**Figure 11C**), in agreement with the previously commented higher sensitivity of S1RA effects on SNI-induced cold allodynia with respect to mechanical and heat hypersensitivity. The effects of this dose of S1RA lasted longer when administered s.c. than i.p. (compare **Figure 3C and 11C**), suggesting a faster drug elimination of the later.

Taking into account that the acute administration of a dose of S1RA which lacks of effect on mechanical and heat hypersensitivity



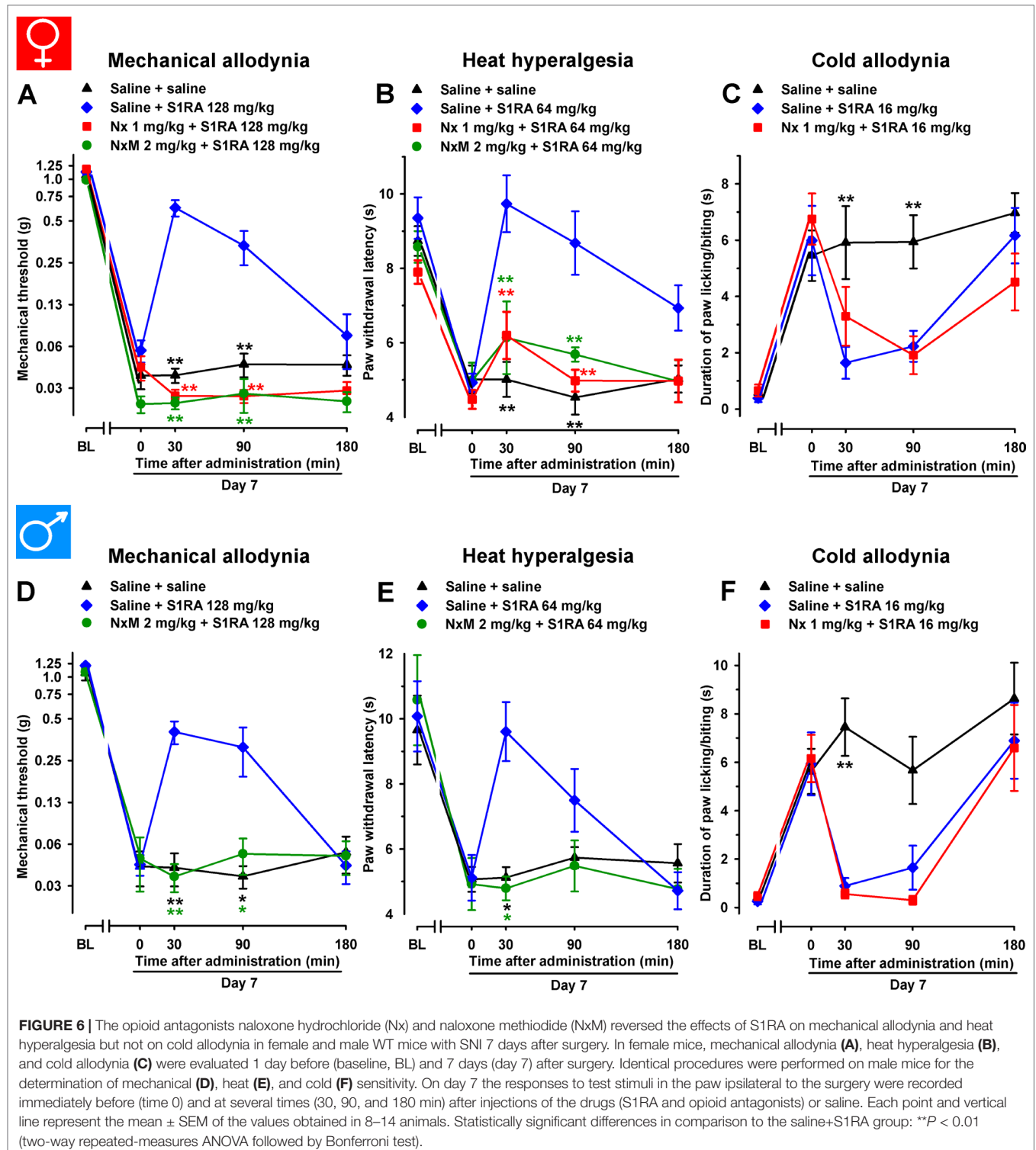


**FIGURE 6 |** The opioid antagonists naloxone hydrochloride (Nx) and naloxone methiodide (NxM) reversed the effects of S1RA on mechanical allodynia and heat hyperalgesia but not on cold allodynia in female and male WT mice with SNI 7 days after surgery. In female mice, mechanical allodynia (A), heat hyperalgesia (B), and cold allodynia (C) were evaluated 1 day before (baseline, BL) and 7 days (day 7) after surgery. Identical procedures were performed on male mice for the determination of mechanical (D), heat (E), and cold (F) sensitivity. On day 7 the responses to test stimuli in the paw ipsilateral to the surgery were recorded immediately before (time 0) and at several times (30, 90, and 180 min) after injections of the drugs (S1RA and opioid antagonists) or saline. Each point and vertical line represent the mean  $\pm$  SEM of the values obtained in 8–14 animals. Statistically significant differences in comparison to the saline+S1RA group:  $^{**}P < 0.01$  (two-way repeated-measures ANOVA followed by Bonferroni test).

and induced only a transient effect on cold allodynia, but the repeated treatment with this same dose of S1RA induced a marked and long-lasting effect on the three outcomes examined, we conclude that repeated treatment with this drug results in an improvement of its effects.

## Concentration of S1RA in Plasma and Brain Tissue After Repeated Administration

To test whether the sustained antinociceptive effects induced by the repeated administration of S1RA 12 h after the discontinuation of drug treatment (i.e., on day 10) was due

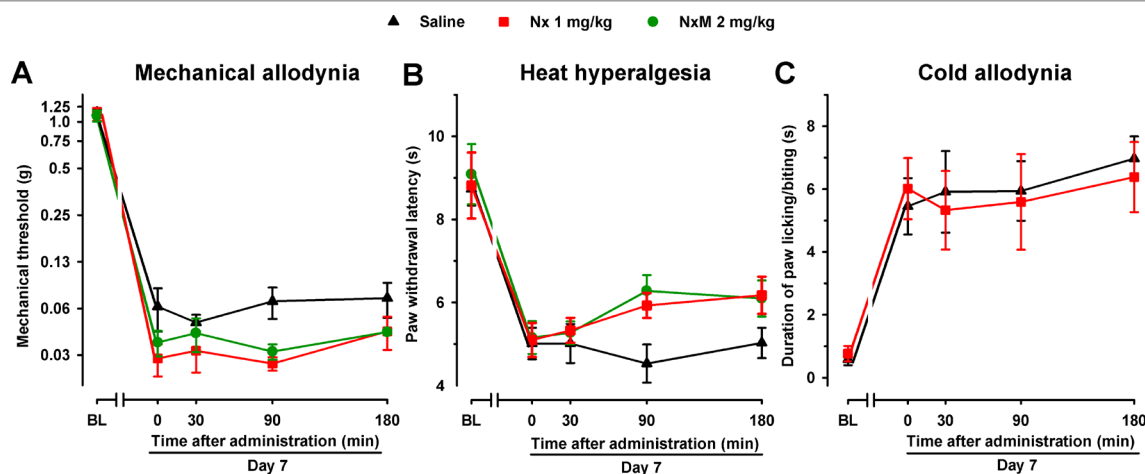


**FIGURE 7 |** The opioid antagonists Nx and NxM had no effect per se in female WT mice with SNI 7 days after surgery. Mechanical allodynia (A), heat hyperalgesia (B), and cold allodynia (C) were evaluated 1 day before (baseline, BL) and 7 days (day 7) after surgery in the paw ipsilateral to the surgery. On day 7 the responses to test stimuli were recorded immediately before (time 0) and at several times (30, 90, and 180 min) after injection of the opioid antagonist or saline. Each point and vertical line represent the mean  $\pm$  SEM of the values obtained in 8–10 animals. Neither of the treatments produced statistically significant differences in comparison to the saline group (two-way repeated-measures ANOVA followed by Bonferroni test).

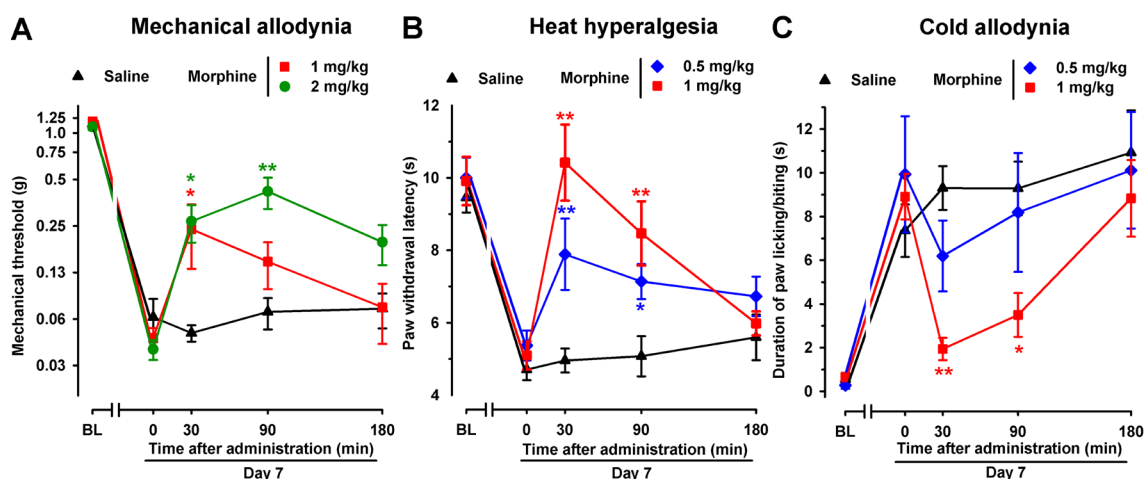


**FIGURE 8 |** Time course of the effects of a single s.c. injection of morphine (0.5–2 mg/kg) or saline on mechanical allodynia (A), heat hyperalgesia (B), and cold allodynia (C) in female WT mice with SNI 7 days after surgery. The von Frey threshold (A), latency to hind paw withdrawal in the Hargreaves test (B), and duration of hind paw licking or biting in the acetone test (C) were recorded 1 day before (baseline, BL) and 7 days (day 7) after surgery in the paw ipsilateral to the surgery. On day 7 the responses to test stimuli were recorded immediately before (time 0) and at several times (30, 90, and 180 min) after injection of the drug or saline. Each point and vertical line represent the mean  $\pm$  SEM of the values obtained in 8–13 animals. Statistically significant differences between morphine- and saline-treated groups at the same time after treatment: \* $P < 0.05$ ; \*\* $P < 0.01$  (two-way repeated-measures ANOVA followed by Bonferroni test).

to the presence of any drug remaining in the organism, the concentrations of S1RA in plasma and brain tissue were measured 30 min and 12 h after the last dose of S1RA. On day 9 of repeated treatment, 30 min after the last administration of S1RA (25 mg/kg, i.p.), we found significant levels of this  $\sigma_1$  antagonist in both plasma and brain, with a much higher concentration in the latter (red bars in **Figure 12A** and **B**). In contrast, 12 h after the last administration, we observed no appreciable levels of this  $\sigma_1$  antagonist in any sample analyzed (**Figure 12A** and **B**).

## DISCUSSION

The main findings of the present study are that: 1) pharmacological antagonism or genetic inactivation of  $\sigma_1$  receptors reduces neuropathic pain induced by peripheral nerve transection (SNI model); 2) the ameliorative effects on SNI-induced hypersensitivity to mechanical and heat stimuli (but not to cold stimuli) produced by  $\sigma_1$  receptor antagonism are mediated by modulation of the endogenous opioid system; and 3) repeated treatment with S1RA induces prolonged ameliorative effects which lasted longer than the presence of the drug in the organism.

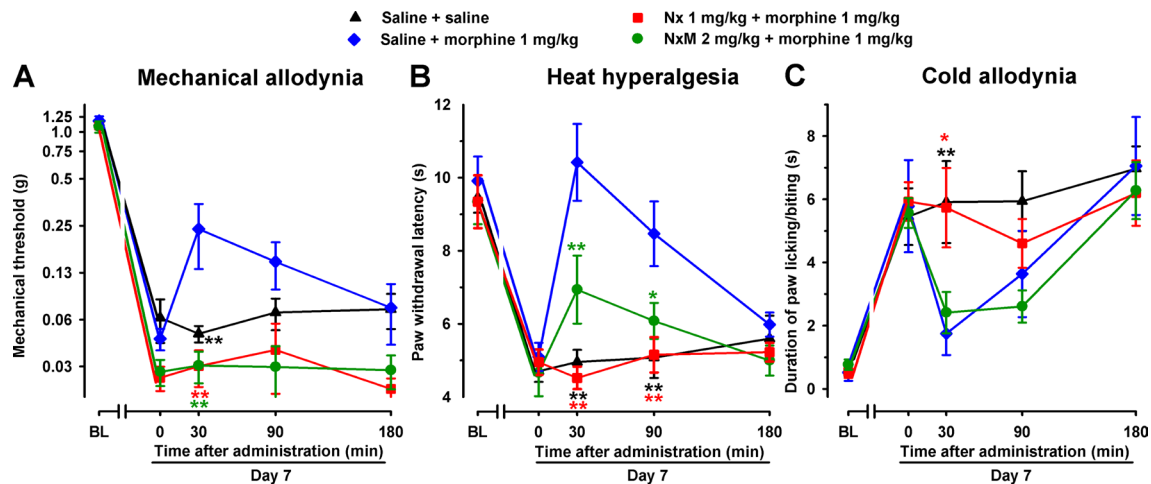


**FIGURE 9 |** Differential ability of Nx and NxM to reverse the effects of morphine on mechanical allodynia, heat hyperalgesia, and cold allodynia in female WT mice with SNI 7 days after surgery. Mechanical allodynia (A), heat hyperalgesia (B), and cold allodynia (C) were evaluated 1 day before (baseline, BL) and 7 days (day 7) after surgery in the paw ipsilateral to the surgery. On day 7 the responses to test stimuli were recorded immediately before (time 0) and at several times (30, 90, and 180 min) after injections of the drugs (morphine and opioid antagonists) or saline. Each point and vertical line represent the mean  $\pm$  SEM of the values obtained in 8–14 animals. Statistically significant differences in comparison to the saline+morphine group: \* $P < 0.05$ ; \*\* $P < 0.01$  (two-way repeated-measures ANOVA followed by Bonferroni test).

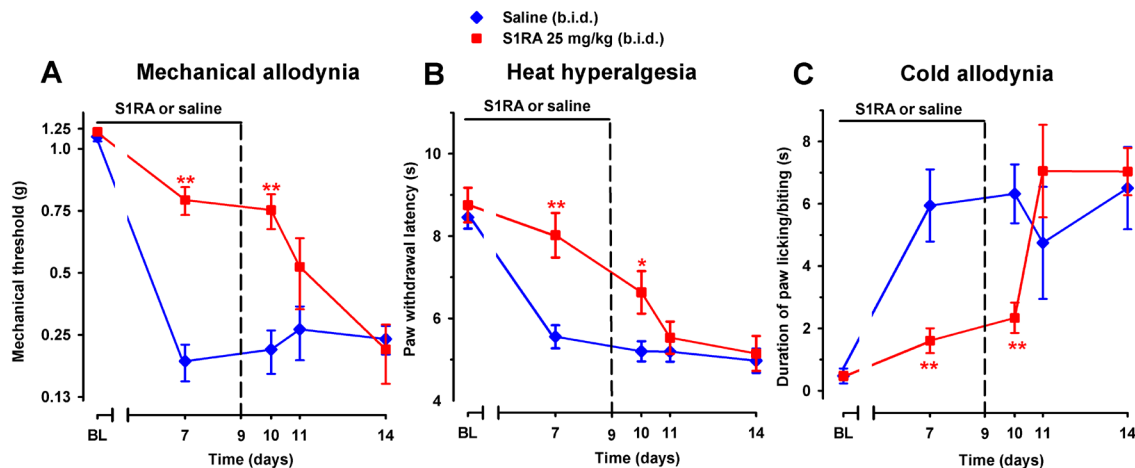


**FIGURE 10 |** Time course of the effect of repeated treatment with S1RA on mechanical allodynia (A), heat hyperalgesia (B), and cold allodynia (C) induced by SNI in female WT mice. The mice were treated twice daily with either saline or S1RA (25 mg/kg, i.p.). The first injection was administered 30 min before SNI surgery. Responses were recorded in each animal before SNI (baseline, BL) and 30 min after the administration of S1RA or saline on day 7 in the paw ipsilateral to the surgery. Treatment was continued until day 9 and the mice were evaluated again on days 10, 11, and 14 postsurgery. The black horizontal line at the top of each figure illustrates the duration of treatment with S1RA or saline. Each point and vertical line represent the mean  $\pm$  SEM of the values obtained in 10–14 animals. Statistically significant differences between S1RA- and saline-treated groups on the same day after treatment: \* $P < 0.05$ ; \*\* $P < 0.01$  (two-way repeated-measures ANOVA followed by Bonferroni test).

Basal sensitivity to mechanical, cold, and heat stimulation in mice lacking  $\sigma_1$  receptors, in the absence of nerve injury, did not differ from that in WT mice. This is in agreement with previous studies (de la Puente et al., 2009; Nieto et al., 2012) and suggests that the basic mechanisms of nociceptive transduction are intact in mice lacking  $\sigma_1$  receptors. We showed that WT mice after SNI surgery developed mechanical, cold, and heat hypersensitivities with time courses similar to those previously reported in mice (Bourquin et al., 2006; Guida et al., 2015; Liu et al., 2015; Cobos et al., 2018).

In addition, the extent of the sensory hypersensitivity was similar between female and male WT mice. In mice lacking  $\sigma_1$  receptors from either sex, however, SNI surgery induced a very different pattern of painful hypersensitivity: these mutant mice did not develop cold allodynia and showed significantly less mechanical allodynia, whereas they developed heat hyperalgesia normally. This is consistent with previous work in other neuropathic pain models, which found that  $\sigma_1$ -KO mice had significantly reduced mechanical and cold allodynia induced by chemotherapy (Nieto et al., 2012) or

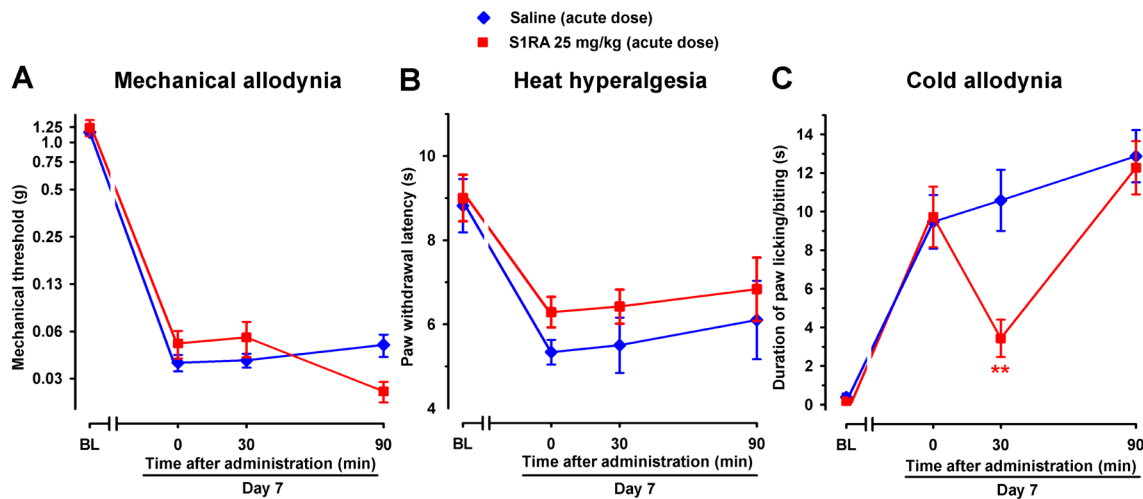


**FIGURE 11** | Time course of the effects of a single i.p. injection of S1RA (25 mg/kg) or saline on mechanical allodynia (A), heat hyperalgesia (B), and cold allodynia (C) in female WT mice with SNI 7 days after surgery. Responses were recorded in each animal before SNI (baseline, BL) and 7 days (day 7) after surgery. On day 7 the responses to test stimuli in the paw ipsilateral to the surgery were recorded immediately before (time 0) and at two times (30 and 90 min) after injection of the drug or saline. Each point and vertical line represent the mean  $\pm$  SEM of the values obtained in six to eight animals. Statistically significant differences between S1RA- and saline-treated groups at the same time after treatment: \*\* $P < 0.01$  (two-way repeated-measures ANOVA followed by Bonferroni test).

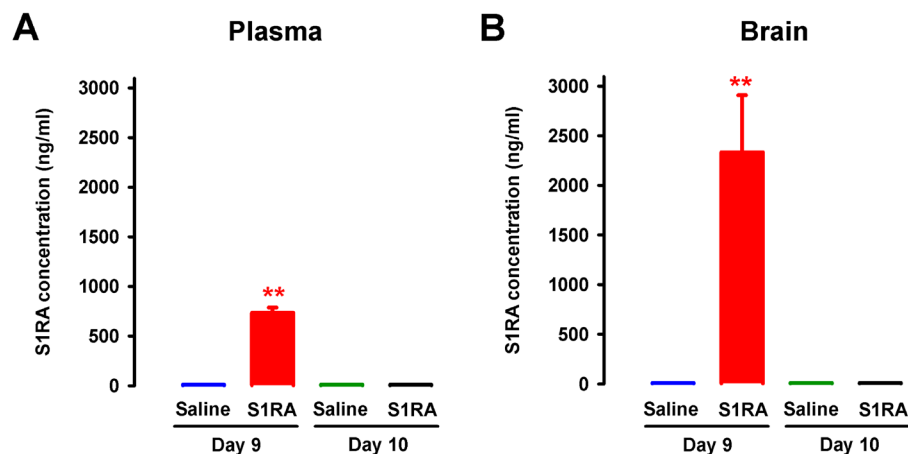


**FIGURE 12** | Concentrations of S1RA in plasma and brain tissue after its repeated administration in female WT. The levels of S1RA were measured by high-performance liquid chromatography–triple quadrupole mass spectrometry (HPLC-MS/MS) in plasma (A) and brain homogenates (B). Mice were treated from day 0 to day 9 twice daily with either saline or S1RA (25 mg/kg, i.p.). Plasma and brain samples were obtained on day 9 (30 min after S1RA or saline administration) and day 10 (12 h after S1RA or saline administration). Each bar and vertical line represent the mean  $\pm$  SEM of the values obtained in five to six animals (A and B). Statistically significant differences between the levels 30 min after S1RA administration and the rest of the experimental groups: \*\* $P < 0.01$  (two-way ANOVA followed by Bonferroni test).

by partial sciatic nerve ligation (de la Puente et al., 2009); the latter study also found that heat hyperalgesia developed normally (de la Puente et al., 2009). However, it was recently reported that  $\sigma_1$ -KO mice showed, in addition to the reduction in mechanical allodynia, a significant attenuation of heat hypersensitivity induced by spinal cord injury (Castany et al., 2018) or diabetic neuropathy (Wang et al., 2018). Taken together, studies with  $\sigma_1$ -KO mice suggest that the role of  $\sigma_1$  receptors during neuropathic pain depends on the sensory modality explored and the type of injury.

The acute pharmacological antagonism of  $\sigma_1$  receptor with S1RA administration, once the painful neuropathy was fully

established in WT mice, significantly (although partially) attenuated mechanical allodynia and fully reversed cold hypersensitivity induced by SNI. In addition, and in contrast to our findings with  $\sigma_1$ -KO mice, acute S1RA administration also abolished SNI-induced heat hyperalgesia in female or male WT mice. Previous studies in other neuropathic pain models reported that the systemic acute administration of  $\sigma_1$  antagonists (including S1RA) reversed not only neuropathic cold and mechanical allodynia (Nieto et al., 2012; Romero et al., 2012; Gris et al., 2016; Espinosa-Juárez et al., 2017b; Paniagua et al., 2017; Castany et al., 2018; Wang et al., 2018) but also heat



hyperalgesia (Díaz et al., 2012; Romero et al., 2012; Paniagua et al., 2017; Castany et al., 2018; Wang et al., 2018), findings which are also in clear agreement with our results. Therefore, there is an apparent divergence between the reduction in heat hyperalgesia in S1RA-treated WT mice, and the normal development of heat hypersensitivity in  $\sigma_1$ -KO mice after SNI. This inconsistency cannot be explained by a nonspecific off-target effect of S1RA, because here we show that the acute ameliorative effects induced by S1RA in all three sensory modalities explored in the present study were abolished by the selective  $\sigma_1$  agonist PRE-084, which did not show any effects “per se,” as previously described in a different neuropathic pain model (Espinosa-Juárez et al., 2017b). In addition, the administration of S1RA to  $\sigma_1$ -KO mice had no effect on SNI-induced mechanical and heat hypersensitivity. Therefore, these results argue in favor of a  $\sigma_1$ -mediated action induced by this drug. In fact, it is known that S1RA has exquisite selectivity for  $\sigma_1$  receptors (Romero et al., 2012). The discrepancy between the effect of genetic and pharmacological inhibition of  $\sigma_1$  receptors on heat hypersensitivity was also found in other studies of neuropathic pain (de la Puente et al., 2009; Romero et al., 2012) and during inflammatory pain (Tejada et al., 2014). In addition, conflicting results between  $\sigma_1$  knockout and pharmacological antagonism have been reported in the modulation of opioid-induced analgesia in nociceptive heat pain (Vidal-Torres et al., 2013). Studies of pain mechanisms that used the genetic and pharmacological inhibition of other receptors have also obtained contradictory results (Petrus et al., 2007; Bonin et al., 2011), which have been attributed to compensatory mechanisms developed by mutant mice. Therefore, this issue appears to be a general concern in experiments with knockout animals. Taking into account these antecedents, we suggest that  $\sigma_1$ -KO mice develop these purported compensatory mechanisms in heat pain pathways but not in other pain pathways in which the knockout replicated the effects of  $\sigma_1$  antagonists.

After peripheral nerve injury, neuroinflammatory processes occur with the recruitment of myriad immune cells at the site of injury (Treutlein et al., 2018) and in the dorsal root ganglia (Kwon et al., 2013), where the somas of peripheral sensory neurons are located. These immune cells release a variety of inflammatory mediators that contribute to neuropathic pain, but they also produce EOPs which have analgesic potential (reviewed in Refs. Ji et al., 2014; Stein, 2016; Tejada et al., 2018). In our experimental conditions, opioid antagonism caused by the administration of naloxone or its peripherally restricted analog naloxone methiodide did not exacerbate pain hypersensitivity in any sensory modality explored, suggesting that the tonic endogenous activity of the opioid system is limited in SNI mice. Importantly, the ameliorative effects induced by S1RA in SNI-induced mechanical and heat hypersensitivity were reversed by both naloxone and naloxone methiodide. These results suggest that  $\sigma_1$  inhibition ameliorates SNI-induced mechanical and heat hypersensitivity through a mechanism dependent on peripherally produced EOPs, whose actions are tonically limited by  $\sigma_1$  receptors. This dependence on the peripheral opioid system of the effects induced by S1RA on mechanical and heat hypersensitivity was seen in both female and male mice, indicating a lack of sexual dimorphism in these effects. It was recently reported that  $\sigma_1$

antagonism produced opioid-dependent antihyperalgesic effects during inflammation by enhancing the action of EOPs released by immune cells that accumulate at the inflamed site (Tejada et al., 2017). Interestingly,  $\sigma_1$  receptors are expressed in the somas of all peripheral sensory neurons (Mavlyutov et al., 2016; Montilla-García et al., 2018), at a much higher density than in central pain-related areas (Sánchez-Fernández et al., 2014). In light of these antecedents, it can be hypothesized that our results for the effects of S1RA on neuropathic mechanical and heat hypersensitivity may also be attributable to the enhancement, by  $\sigma_1$  antagonism, of the peripheral antinociceptive actions of EOPs produced by immune cells. Further research is guaranteed to determine the exact EOP/EOPs involved in the opioid-dependent effects induced by  $\sigma_1$  antagonism during neuropathic pain.

It has been reported that peripheral immune cells do not contribute equally to every modality of sensory hypersensitivity after peripheral nerve injury. In fact, peripheral macrophages and T-cells promote both mechanical allodynia and heat hyperalgesia (Kobayashi et al., 2015; Cobos et al., 2018), whereas their influence in cold allodynia is very limited, which suggest that it is due to neuronal mechanisms rather than to neuroimmune interactions (Cobos et al., 2018). Here we show that the effects of S1RA on cold allodynia in either female or male mice are independent of opioid activation, which is consistent with the known inhibitory effects of S1RA on neuronal sensitization (Romero et al., 2012; Paniagua et al., 2017). In this connection it was previously reported that the effects of  $\sigma_1$  antagonists in other pain models such as capsaicin-induced secondary hypersensitivity (Entrena et al., 2009) or formalin-induced pain (Tejada et al., 2017) were not sensitive to naloxone treatment. Taking into account the wide variety of protein partners (other than opioid receptors) that benefit from the chaperoning actions of  $\sigma_1$  receptors (reviewed in Refs. Su et al., 2016; Sánchez-Fernández et al., 2017), it is not surprising that multiple opioid and nonopioid mechanisms simultaneously participate on the ameliorative effects of  $\sigma_1$  antagonism.

We also found that whereas morphine only partially reversed mechanical allodynia, it was able to fully suppress heat and cold hypersensitivity induced by SNI—effects which resemble those induced by S1RA. The effects of morphine on mechanical and heat hypersensitivity, but not on cold allodynia, were sensitive to the peripheral opioid antagonist naloxone methiodide. These results suggest that peripheral opioid effects are markedly weaker in cold allodynia than in mechanical or heat hypersensitivity, and are consistent with the absence of peripherally mediated opioid effects on the inhibition of cold allodynia induced by S1RA.

We also tested the effects of the repeated administration of S1RA, which was administered preemptively before surgery and subsequently administered twice a day during the next 9 days. Plasma levels of S1RA in mice after repeated treatment with this drug were similar to or lower than the levels of this drug in humans after daily oral S1RA treatment at therapeutic doses (Abadias et al., 2013; Bruna et al., 2018). We found that the sustained administration of S1RA induced prolonged ameliorative effects on the hypersensitivity to mechanical, heat, and cold stimuli, without any evidence of tolerance to the antineuropathic effects during the evaluation period. This may be relevant given that some effects of S1RA, as shown in the

present study, involve the opioid system, and it is well known that sustained opioid treatment induced analgesic tolerance (Morgan and Christie, 2011). Therefore, although we show that the effects of  $\sigma_1$  antagonism are partially mediated by the opioid system, this does not necessarily imply the development of analgesic tolerance.

We evaluated the effects of the repeated administration of S1RA starting before neuropathic pain was established, and found that it had marked effects on mechanical, heat, and cold hypersensitivity. However, when the same dose of S1RA was acutely administered once neuropathic pain was fully established, its effects were limited and observed only in cold allodynia. Therefore, S1RA showed higher efficacy after repeated treatment than after a single treatment. It is unlikely that the greater effects induced by repeated treatment of S1RA were due to drug accumulation, since we previously showed that repeated treatment with the same protocol as in the present study did not result in increased levels of S1RA with time (Romero et al., 2012). In addition, here we show that 12 h after treatment was discontinued, there were no appreciable levels of S1RA in either plasma or brain tissue, indicating the complete elimination of this compound between doses. Interestingly, although no S1RA remained in the organism 12 h after its last administration, drug effects were still significantly evident in all three sensory modalities. Our results are consistent with previous studies in which the repeated administration of  $\sigma_1$  antagonists (including S1RA) consistently induced a long-lasting reduction of the development of mechanical, cold, and heat hypersensitivity in models of neuropathic pain of different etiologies (Nieto et al., 2012; Gris et al., 2016; Paniagua et al., 2017). It is unclear whether these prolonged effects induced by the repeated treatment with S1RA might be due to the production of an active metabolite not detected in our determinations. However, it is known that  $\sigma_1$  receptors can influence gene transcription, which might account for the long-lasting effects observed (Tsai et al., 2015). In fact, repeated treatment with the  $\sigma_1$  agonist PRE-084, which is chemically unrelated to S1RA, had long-lasting proallodynic effects (Entrena et al., 2016). Taken together, these results suggest that the repeated treatment with  $\sigma_1$  ligands

might have sustained pharmacodynamic effects, not restricted to S1RA and its possible active metabolites, although further experiments are needed to clarify this issue. Regardless of the precise mechanism, our data suggest that repeated treatment with S1RA may have potential therapeutic utility in the context of neuropathies induced by nerve transection during surgery, when the precise time of nerve injury can be anticipated and preventive treatment can be given.

In summary, this study demonstrates that  $\sigma_1$  antagonism may be a potentially effective therapeutic tool to inhibit neuropathic pain induced by peripheral nerve transection. In addition, our findings support the notion that  $\sigma_1$  antagonism induces both opioid-dependent and -independent effects during neuropathic pain.

## AUTHOR CONTRIBUTIONS

EJC and FRN designed research; IB-C, GP, SY, DC, and FRN performed research; IB-C, SY, FRN, and JMB analyzed data; IB-C, JMB, EJC, and FRN wrote the paper. All authors read and approved the final version of the manuscript.

## FUNDING

IB-C was supported by an FPU grant from the Spanish Ministry of Education, Culture, and Sports. This study was partially supported by the Spanish Ministry of Economy and Competitiveness (MINECO, grant SAF2016-80540-R), the Junta de Andalucía (grant CTS 109), and funding from Esteve and the European Regional Development Fund (ERDF). This research was done in partial fulfillment of the requirements for the doctoral thesis of IB-C.

## ACKNOWLEDGMENTS

We thank K. Shashok for improving the use of English in the manuscript.

## REFERENCES

- Abadias, M., Escriche, M., Vaqué, A., Sust, M., and Encina, G. (2013). Safety, tolerability and pharmacokinetics of single and multiple doses of a novel sigma-1 receptor antagonist in three randomized phase I studies. *Br. J. Clin. Pharmacol.* 75 (1), 103–117. doi: 10.1111/j.1365-2125.2012.04333.x
- Aley, K. O., and Levine, J. D. (2002). Different peripheral mechanisms mediate enhanced nociception in metabolic/toxic and traumatic painful peripheral neuropathies in the rat. *Neuroscience* 111 (2), 389–97. doi: 10.1016/S0306-4522(02)00009-X
- Baron, R., Binder, A., and Wasner, G. (2010). Neuropathic pain: diagnosis, pathophysiological mechanisms, and treatment. *Lancet Neurol.* 9 (8), 807–819. doi: 10.1016/S1474-4422(10)70143-5
- Bonin, R. P., Labrakakis, C., Eng, D. G., Whissell, P. D., De Koninck, Y., and Orser, B. A. (2011). Pharmacological enhancement of  $\delta$ -subunit-containing GABAA receptors that generate a tonic inhibitory conductance in spinal neurons attenuates acute nociception in mice. *Pain* 152 (6), 1317–1326. doi: 10.1016/j.pain.2011.02.011
- Borsook, D., Kussman, B. D., George, E., Becerra, L. R., and Burke, D. W. (2013). Surgically induced neuropathic pain: understanding the perioperative process. *Ann. Surg.* 257 (3), 403–412. doi: 10.1097/SLA.0b013e3182701a7b
- Bourquin, A. F., Süveges, M., Pertin, M., Gilliard, N., Sardy, S., Davison, A. C., et al. (2006). Assessment and analysis of mechanical allodynia-like behavior induced by spared nerve injury (SNI) in the mouse. *Pain* 122 (1–2), 14. doi: 10.1016/j.pain.2005.10.036
- Bruna, J., Videla, S., Argyriou, A. A., Velasco, R., Villoria, J., Santos, C., et al. (2018). Efficacy of a novel sigma-1 receptor antagonist for oxaliplatin-induced neuropathy: a randomized, double-blind, placebo-controlled phase IIa clinical trial. *Neurotherapeutics* 15 (1), 178–189. doi: 10.1007/s13311-017-0572-5
- Casals-Díaz, L., Vivó, M., and Navarro, X. (2009). Nociceptive responses and spinal plastic changes of afferent C-fibers in three neuropathic pain models induced by sciatic nerve injury in the rat. *Exp. Neurol.* 217 (1), 84–95. doi: 10.1016/j.expneurol.2009.01.014
- Castany, S., Gris, G., Vela, J. M., Verdú, E., and Boadas-Vaello, P. (2018). Critical role of sigma-1 receptors in central neuropathic pain-related behaviours after mild spinal cord injury in mice. *Sci. Rep.* 8 (1), 3873. doi: 10.1038/s41598-018-22217-9

- Chaplan, S. R., Bach, F. W., Pogrel, J. W., and Chung JM, Y. T. (1994). Quantitative assessment of tactile allodynia in the rat paw. *J. Neurosci. Methods* 53 (1), 55–63. doi: 10.1016/0165-0270(94)90144-9
- Cobos, E. J., Entrena, J. M., Nieto, F. R., Cendan, C. M., and Del Pozo, E. (2008). Pharmacology and therapeutic potential of sigma1 receptor ligands. *Curr. Neuropharmacol.* 6 (4), 344–366. doi: 10.2174/157015908787386113
- Cobos, E. J., Nickerson, C. A., Gao, F., Chandran, V., Bravo-Caparrós, I., González-Cano, R., et al. (2018). Mechanistic differences in neuropathic pain modalities revealed by correlating behavior with global expression profiling. *Cell Rep.* 22 (5), 1301–1312. doi: 10.1016/j.celrep.2018.01.006
- Colloca, L., Ludman, T., Bouhassira, D., Baron, R., Dickenson, A. H., Yarnitsky, D., et al. (2017). Neuropathic pain. *Nat. Rev. Dis. Primers* 3, 17002. doi: 10.1038/nrdp.2017.2
- Costigan, M., Belfer, I., Griffin, R. S., Dai, F., Barrett, L. B., Coppola, G., et al. (2010). Multiple chronic pain states are associated with a common amino acid-changing allele in KCNS1. *Brain* 133 (9), 2519–2527. doi: 10.1093/brain/awq195
- Díaz, J. L., Cuberes, R., Berrocal, J., Contijoch, M., Christmann, U., Fernández, A., et al. (2012). Synthesis and biological evaluation of the 1-arylpyrazole class of  $\sigma 1$  receptor antagonists: identification of 4-[2-(5-methyl-1-(naphthalen-2-yl)-1H-pyrazol-3-yl)oxy]ethylmorpholine (SIRA, E-52862). *J. Med. Chem.* 55 (19), 8211–8124. doi: 10.1021/jm3007323
- de la Puente, B., Nadal, X., Portillo-Salido, E., Sánchez-Arroyos, R., Ovalle, S., Palacios, G., et al. (2009). Sigma-1 receptors regulate activity-induced spinal sensitization and neuropathic pain after peripheral nerve injury. *Pain* 145 (3), 294–303. doi: 10.1016/j.pain.2009.05.013
- Decosterd, I., and Woolf, C. J. (2000). Spared nerve injury: an animal model of persistent peripheral neuropathic. *Pain* 87 (2), 149–158. doi: 10.1016/S0304-3959(00)00276-1
- Edwards, D. A. (1968). Mice: fighting by neonatally androgenized females. *Science* 161 (3845), 1027–1028. doi: 10.1126/science.161.3845.1027
- Entrena, J. M., Cobos, E. J., Nieto, F. R., Cendán, C. M., Gris, G., Del Pozo, E., et al. (2009). Sigma-1 receptors are essential for capsaicin-induced mechanical hypersensitivity: studies with selective sigma-1 ligands and sigma-1 knockout mice. *Pain* 143 (3), 252–261. doi: 10.1016/j.pain.2009.03.011
- Entrena, J. M., Sánchez-Fernández, C., Nieto, F. R., González-Cano, R., Yeste, S., Cobos, E. J., et al. (2016). Sigma-1 receptor agonism promotes mechanical allodynia after priming the nociceptive system with capsaicin. *Sci. Rep.* 6, 37835. doi: 10.1038/srep37835
- Espinosa-Juárez, J. V., Jaramillo-Morales, O. A., Navarrete-Vázquez, G., Melo-Hernández, L. A., Déciga-Campos, M., and López-Muñoz, F. J. (2017a). N-(2-morpholin-4-yl-ethyl)-2-(1-naphthyl)acetamide inhibits the chronic constriction injury-generated hyperalgesia via the antagonism of sigma-1 receptors. *Eur. J. Pharmacol.* 812, 1–8. doi: 10.1016/j.ejphar.2017.06.026
- Espinosa-Juárez, J. V., Jaramillo-Morales, O. A., and López-Muñoz, F. J. (2017b). Haloperidol decreases hyperalgesia and allodynia induced by chronic constriction injury. *Basic Clin. Pharmacol. Toxicol.* 121 (6), 471–479. doi: 10.1111/bcpt.12839
- Finnerup, N. B., Attal, N., Haroutounian, S., McNicol, E., Baron, R., Dworkin, R. H., et al. (2015). Pharmacotherapy for neuropathic pain in adults: a systematic review and meta-analysis. *Lancet Neurol.* 14 (2), 162–173. doi: 10.1016/S1474-4422(14)70251-0
- Griffin, R. S., Costigan, M., Brenner, G. J., Ma, C. H., Scholz, J., Moss, A., et al. (2007). Complement induction in spinal cord microglia results in anaphylatoxin C5a-mediated pain hypersensitivity. *J. Neurosci.* 27 (32), 8699–8708. doi: 10.1523/JNEUROSCI.2018-07.2007
- Gris, G., Portillo-Salido, E., Aubel, B., Darbaky, Y., Deseure, K., Vela, J. M., et al. (2016). The selective sigma-1 receptor antagonist E-52862 attenuates neuropathic pain of different aetiology in rats. *Sci. Rep.* 6, 24591. doi: 10.1038/srep24591
- Guida, F., Lattanzi, R., Boccella, S., Maftei, D., Romano, R., Marconi, V., et al. (2015). PC1, a non-peptide PKR1-preferring antagonist, reduces pain behavior and spinal neuronal sensitization in neuropathic mice. *Pharmacol. Res.* 91, 36–46. doi: 10.1016/j.phrs.2014.11.004
- Hargreaves, K., Dubner, R., Brown, F., and Flores C, J. J. (1988). A new and sensitive method for measuring thermal nociception in cutaneous hyperalgesia. *Pain* 32 (1), 77–88. doi: 10.1016/0304-3959(88)90026-7
- Hershman, D. L., Lacchetti, C., and Dworkin, R. H. (2014). Prevention and management of chemotherapy-induced peripheral neuropathy in survivors of adult cancers: American Society of Clinical Oncology clinical practice guideline. *J. Clin. Oncol.* 32 (18), 1941–1967. doi: 10.1200/JOP.2014.001776
- Ji, R. R., Xu, Z. Z., and Gao, Y. J. (2014). Emerging targets in neuroinflammation-driven chronic pain. *Nat. Rev. Drug. Discov.* 13 (7), 533–548. doi: 10.1038/nrd4334
- Kang, D. W., Moon, J. Y., Choi, J. G., Kang, S. Y., Ryu, Y., Park, J. B., et al. (2016). Antinociceptive profile of levo-tetrahydropalmatine in acute and chronic pain mice models: role of spinal sigma-1 receptor. *Sci. Rep.* 6, 37850. doi: 10.1038/srep37850
- Kobayashi, Y., Kiguchi, N., Fukazawa, Y., Saika, F., Maeda, T., and Kishioka, S. (2015). Macrophage-T cell interactions mediate neuropathic pain through the glucocorticoid-induced tumor necrosis factor ligand system. *J. Biol. Chem.* 290 (20), 12603–12613. doi: 10.1074/jbc.M115.636506
- Kwon, M. J., Kim, J., Shin, H., Jeong, S. R., Kang, Y. M., Choi, J. Y., et al. (2013). Contribution of macrophages to enhanced regenerative capacity of dorsal root ganglia sensory neurons by conditioning injury. *J. Neurosci.* 33 (38), 15095–15108. doi: 10.1523/JNEUROSCI.0278-13.2013
- Liu, S., Mi, W. L., Li, Q., Zhang, M. T., Han, P., Hu, S., et al. (2015). Spinal IL-33/ST2 signaling contributes to neuropathic pain via neuronal CaMKII-CREB and astroglial JAK2-STAT3 cascades in mice. *Anesthesiology* 123 (5), 1154–1169. doi: 10.1097/ALN.0000000000000850
- Mavlyutov, T. A., Duellman, T., Kim, H. T., Epstein, M. L., Leese, C., Davletov, B. A., et al. (2016). Sigma-1 receptor expression in the dorsal root ganglion: reexamination using a highly specific antibody. *Neuroscience* 331, 148–157. doi: 10.1016/j.neuroscience.2016.06.030
- Mei, J., and Pasternak, G. W. (2002). Sigma 1 receptor modulation of opioid analgesia in the mouse. *J. Pharmacol. Exp. Ther.* 300 (3), 1070–1074. doi: 10.1124/jpet.300.3.1070
- Merlos, M., Romero, L., Zamanillo, D., Plata-Salamán, C., and Vela, J. M. (2017). Sigma-1 receptor and pain. *Handb. Exp. Pharmacol.* 244, 131–161. doi: 10.1007/164\_2017\_9
- Miczek, K. A., Thompson, M. L., and Shuster, L. (1982). Opioid-like analgesia in defeated mice. *Science* 215 (4539), 1520–1522. doi: 10.1126/science.7199758
- Montilla-García, Á., Perazzoli, G., Tejada, M. Á., González-Cano, R., Sánchez-Fernández, C., Cobos, E. J., et al. (2018). Modality-specific peripheral antinociceptive effects of  $\mu$ -opioid agonists on heat and mechanical stimuli: contribution of sigma-1 receptors. *Neuropharmacology* 135, 328–342. doi: 10.1016/j.neuropharm.2018.03.025
- Morgan, M. M., and Christie, M. J. (2011). Analysis of opioid efficacy, tolerance, addiction and dependence from cell culture to human. *Br. J. Pharmacol.* 164 (4), 1322–1334. doi: 10.1111/j.1476-5381.2011.01335.x
- Nieto, F. R., Entrena, J. M., Cendán, C. M., Del Pozo, E., Vela, J. M., and Baeyens, J. M. (2008). Tetrodotoxin inhibits the development and expression of neuropathic pain induced by paclitaxel in mice. *Pain* 137 (3), 520–531. doi: 10.1016/j.pain.2007.10.012
- Nieto, F. R., Cendán, C. M., Sánchez-Fernández, C., Cobos, E. J., Entrena, J. M., Tejada, M. A., et al. (2012). Role of sigma-1 receptors in paclitaxel-induced neuropathic pain in mice. *J. Pain* 13 (11), 1107–1121. doi: 10.1016/j.jpain.2012.08.006
- Paniagua, N., Girón, R., Goicoechea, C., López-Miranda, V., Vela, J. M., Merlos, M., et al. (2017). Blockade of sigma 1 receptors alleviates sensory signs of diabetic neuropathy in rats. *Eur. J. Pain.* 21 (1), 61–72. doi: 10.1002/ejp.897
- Petrus, M., Peier, A. M., Bandell, M., Hwang, S. W., Huynh, T., Olney, N., et al. (2007). A role of TRPA1 in mechanical hyperalgesia is revealed by pharmacological inhibition. *Mol. Pain.* 17:3, 40. doi: 10.1186/1744-8069-3-40
- Prezavento, O., Arena, E., Sánchez-Fernández, C., Turnaturi, R., Parenti, C., Marrazzo, A., et al. (2017). (+)- and (-)-Phenazocine enantiomers: evaluation of their dual opioid agonist/ $\sigma 1$  antagonist properties and antinociceptive effects. *Eur. J. Med. Chem.* 125, 603–610. doi: 10.1016/j.ejmech.2016.09.077
- Roh, D. H., Kim, H. W., Yoon, S. Y., Seo, H. S., Kwon, Y. B., Kim, K. W., et al. (2008). Intrathecal injection of the sigma1 receptor antagonist BD1047 blocks both mechanical allodynia and increases in spinal NR1 expression during the induction phase of rodent neuropathic pain. *Anesthesiology* 109 (5), 879–889. doi: 10.1097/ALN.0b013e3181895a83
- Romero, L., Zamanillo, D., Nadal, X., Sánchez-Arroyos, R., Rivera-Arconada, I., Dordal, A., et al. (2012). Pharmacological properties of SIRA, a new sigma-1 receptor antagonist that inhibits neuropathic pain and activity-induced spinal sensitization. *Br. J. Pharmacol.* 166 (8), 2289–2306. doi: 10.1111/j.1476-5381.2012.01942.x
- Sánchez-Fernández, C., Nieto, F. R., González-Cano, R., Artacho-Cordón, A., Romero, L., Montilla-García, Á., et al. (2013). Potentiation of morphine-induced mechanical antinociception by  $\sigma 1$  receptor inhibition: role of peripheral  $\sigma 1$  receptors. *Neuropharmacology* 70, 348–358. doi: 10.1016/j.neuropharm.2013.03.002

- Sánchez-Fernández, C., Montilla-García, Á, González-Cano, R., Nieto, F. R., Romero, L., Artacho-Cordón, A., et al. (2014). Modulation of peripheral  $\mu$ -opioid analgesia by  $\sigma_1$  receptors. *J. Pharmacol. Exp. Ther.* 348 (1), 32–45. doi: 10.1124/jpet.113.208272
- Sánchez-Fernández, C., Entrena, J. M., Baeyens, J. M., and Cobos, E. J. (2017). Sigma-1 receptor antagonists: a new class of neuromodulatory analgesics. *Adv. Exp. Med. Biol.* 964, 109–132. doi: 10.1007/978-3-319-50174-1\_9
- Stein, C. (2016). Opioid receptors. *Annu. Rev. Med.* 67, 433–451. doi: 10.1146/annurev-med-062613-093100
- Su, T. P., Su, T. C., Nakamura, Y., and Tsai, S. Y. (2016). The sigma-1 receptor as a pluripotent modulator in living systems. *Trends Pharmacol. Sci.* 37 (4), 262–278. doi: 10.1016/j.tips.2016.01.003
- Tejada, M. A., Montilla-García, A., Sánchez-Fernández, C., Entrena, J. M., Perazzoli, G., Baeyens, J. M., et al. (2014). Sigma-1 receptor inhibition reverses acute inflammatory hyperalgesia in mice: role of peripheral sigma-1 receptors. *Psychopharmacology (Berl)* 231 (19), 3855–3869. doi: 10.1007/s00213-014-3524-3
- Tejada, M. A., Montilla-García, A., Cronin, S. J., Cikes, D., Sánchez-Fernández, C., González-Cano, R., et al. (2017). Sigma-1 receptors control immune-driven peripheral opioid analgesia during inflammation in mice. *Proc. Natl. Acad. Sci. U. S. A.* 114 (31), 8396–8401. doi: 10.1073/pnas.1620068114
- Tejada, M. A., Montilla-García, Á, González-Cano, R., Bravo-Caparrós, I., Ruiz-Cantero, M. C., Nieto, F. R., et al. (2018). Targeting immune-driven opioid analgesia by sigma-1 receptors: opening the door to novel perspectives for the analgesic use of sigma-1 antagonists. *Pharmacol. Res.* 131, 224–230. doi: 10.1016/j.phrs.2018.02.008
- Treutlein, E. M., Kern, K., Weigert, A., Tarighi, N., Schuh, C. D., Nüsing, R. M., et al. (2018). The prostaglandin E2 receptor EP3 controls CC-chemokine ligand 2-mediated neuropathic pain induced by mechanical nerve damage. *J. Biol. Chem.* 293 (25), 9685–9695. doi: 10.1074/jbc.RA118.002492
- Tsai, S. Y., Chuang, J. Y., Tsai, M. S., Wang, X. F., Xi, Z. X., Hung, J. J., et al. (2015). Sigma-1 receptor mediates cocaine-induced transcriptional regulation by recruiting chromatin-remodeling factors at the nuclear envelope. *Proc. Natl. Acad. Sci. U. S. A.* 112 (47), E6562–E6570. doi: 10.1073/pnas.1518894112
- van Hecke, O., Austin, S. K., Khan, R. A., Smith, B. H., and Tórrance, N. (2014). Neuropathic pain in the general population: a systematic review of epidemiological studies. *Pain* 155 (4), 654–662. doi: 10.1016/j.pain.2013.11.013
- Vidal-Torres, A., de la Puente, B., Rocasbalbas, M., Tourino, C., Bura, S. A., Fernández-Pastor, B., et al. (2013). Sigma-1 receptor antagonism as opioid adjuvant strategy: enhancement of opioid antinociception without increasing adverse effects. *Eur. J. Pharmacol.* 711 (1–3), 63–72. doi: 10.1016/j.ejphar.2013.04.018
- Wang, X., Feng, C., Qiao, Y., and Zhao, X. (2018). Sigma 1 receptor mediated HMGB1 expression in spinal cord is involved in the development of diabetic neuropathic pain. *Neurosci. Lett.* 668, 164–168. doi: 10.1016/j.neulet.2018.02.002

**Conflict of Interest Statement:** SY was employed by Esteve.

The remaining authors declare that the research was conducted in the absence of any commercial or financial relationships that could be construed as a potential conflict of interest.

The authors declare that this study received funding from Esteve. This company had no role in study design, data collection and analysis, decision to publish, or preparation of the manuscript.

Copyright © 2019 Bravo-Caparrós, Perazzoli, Yeste, Cikes, Baeyens, Cobos and Nieto. This is an open-access article distributed under the terms of the Creative Commons Attribution License (CC BY). The use, distribution or reproduction in other forums is permitted, provided the original author(s) and the copyright owner(s) are credited and that the original publication in this journal is cited, in accordance with accepted academic practice. No use, distribution or reproduction is permitted which does not comply with these terms.





# *In vitro* and *in vivo* Human Metabolism of (S)-[<sup>18</sup>F]Fluspidine – A Radioligand for Imaging $\sigma_1$ Receptors With Positron Emission Tomography (PET)

## OPEN ACCESS

### Edited by:

Stephen Timothy Safrany,  
Royal College of Surgeons in Ireland -  
Bahrain, Bahrain

### Reviewed by:

Aren Van Waarde,  
University Medical Center Groningen,  
Netherlands  
Robert Henry Mach,  
University of Pennsylvania,  
United States

### \*Correspondence:

Friedrich-Alexander Ludwig  
f.ludwig@hzdr.de

<sup>†</sup>These authors have contributed  
equally to this work

### Specialty section:

This article was submitted to  
Experimental Pharmacology  
and Drug Discovery,  
a section of the journal  
Frontiers in Pharmacology

Received: 28 February 2019

Accepted: 29 April 2019

Published: 13 June 2019

### Citation:

Ludwig F-A, Fischer S, Houska R,  
Hoepping A, Deuther-Conrad W,  
Schepmann D, Patt M, Meyer PM,  
Hesse S, Becker G-A, Zientek FR,  
Steinbach J, Wünsch B, Sabri O and  
Brust P (2019) *In vitro* and *in vivo*  
Human Metabolism  
of (S)-[<sup>18</sup>F]Fluspidine – A Radioligand  
for Imaging  $\sigma_1$  Receptors With  
Positron Emission Tomography (PET).  
Front. Pharmacol. 10:534.  
doi: 10.3389/fphar.2019.00534

Friedrich-Alexander Ludwig<sup>1\*</sup>, Steffen Fischer<sup>1</sup>, Richard Houska<sup>1</sup>, Alexander Hoepping<sup>2</sup>, Winnie Deuther-Conrad<sup>1</sup>, Dirk Schepmann<sup>3</sup>, Marianne Patt<sup>4</sup>, Philipp M. Meyer<sup>4</sup>, Swen Hesse<sup>4,5</sup>, Georg-Alexander Becker<sup>4</sup>, Franziska Ruth Zientek<sup>4,5</sup>, Jörg Steinbach<sup>1</sup>, Bernhard Wünsch<sup>3</sup>, Osama Sabri<sup>4†</sup> and Peter Brust<sup>1†</sup>

<sup>1</sup> Department of Neuroradiopharmaceuticals, Helmholtz-Zentrum Dresden-Rossendorf, Institute of Radiopharmaceutical Cancer Research, Leipzig, Germany, <sup>2</sup> ABX Advanced Biochemical Compounds GmbH, Radeberg, Germany, <sup>3</sup> Department of Pharmaceutical and Medicinal Chemistry, University of Münster, Münster, Germany, <sup>4</sup> Department of Nuclear Medicine, Leipzig University, Leipzig, Germany, <sup>5</sup> Integrated Research and Treatment Center (IFB) Adiposity Diseases, Leipzig University, Leipzig, Germany

(S)-[<sup>18</sup>F]fluspidine ((S)-[<sup>18</sup>F]**1**) has recently been explored for positron emission tomography (PET) imaging of sigma-1 receptors in humans. In the current report, we have used plasma samples of healthy volunteers to investigate the radiometabolites of (S)-[<sup>18</sup>F]**1** and elucidate their structures with LC-MS/MS. For the latter purpose additional *in vitro* studies were conducted by incubation of (S)-[<sup>18</sup>F]**1** and (S)-**1** with human liver microsomes (HLM). *In vitro* metabolites were characterized by interpretation of MS/MS fragmentation patterns from collision-induced dissociation or by use of reference compounds. Thereby, structures of corresponding radio-HPLC-detected radiometabolites, both *in vitro* and *in vivo* (human), could be identified. By incubation with HLM, mainly debenzoylation and hydroxylation occurred, beside further mono- and di-oxygenations. The product hydroxylated at the fluoroethyl side chain was glucuronidated. Plasma samples (10, 20, 30 min p.i., *n* = 5-6), obtained from human subjects receiving 250–300 MBq (S)-[<sup>18</sup>F]**1** showed 97.2, 95.4, and 91.0% of unchanged radioligand, respectively. In urine samples (90 min p.i.) the fraction of unchanged radioligand was only 2.6% and three major radiometabolites were detected. The one with the highest percentage, also found in plasma, matched the glucuronide formed *in vitro*. Only a small amount of debenzoylated metabolite was detected. In conclusion, our metabolic study, in particular the high fractions of unchanged radioligand in plasma, confirms the suitability of (S)-[<sup>18</sup>F]**1** as PET radioligand for sigma-1 receptor imaging.

**Keywords:** sigma-1 receptors, fluspidine, positron emission tomography, radiometabolites, liquid chromatography-mass spectrometry, liver microsomes

## INTRODUCTION

The two enantiomers (S)- and (R)-[<sup>18</sup>F]fluspidine ((S)- and (R)-[<sup>18</sup>F]1'-benzyl-3-(2-fluoroethyl)-3*H*-spiro[2-benzofuran-1,4'-piperidine], (S)-**1** and (R)-**1**, **Figure 1**) are radioligands which have been developed for positron emission tomography (PET) imaging of sigma-1 receptors (S1R) in human (Weber et al., 2017).

S1R are expressed in the central nervous system (CNS) as well as in peripheral tissues (Rousseaux and Greene, 2015). They are located in both the plasma membrane and the mitochondria-associated membrane of the endoplasmic reticulum, where they are involved in different physiological and pathophysiological processes, e.g., regulations of ion channels and neurotransmitter receptors. The role of S1R has been increasingly recognized as they serve as a novel promising target for the therapy of, e.g., cancer (Tesei et al., 2018) or cardiovascular diseases (Stracina and Novakova, 2018) as well as of CNS disorders (Jia et al., 2018; Penke et al., 2018), notably Alzheimer's disease (Maurice and Gogvadze, 2017), Parkinson's disease and depression (Fishback et al., 2010). PET offers the possibility for earlier diagnoses or monitoring of therapeutic processes (Brust et al., 2014b; Honer et al., 2014; Barthel et al., 2015; Song et al., 2018; Jia et al., 2019).

(S)-**1** and (R)-**1** are derived from a structural optimization process for the purpose of PET of spirocyclic piperidines which possess high affinity toward S1R and selectivity over a variety of other receptors (Maier and Wünsch, 2002a,b; Große Mastrup et al., 2009a, 2011; Maisoniai et al., 2011; Holl et al., 2014; Nakane et al., 2018). Attempts to improve the synthesis of (S)-**1**

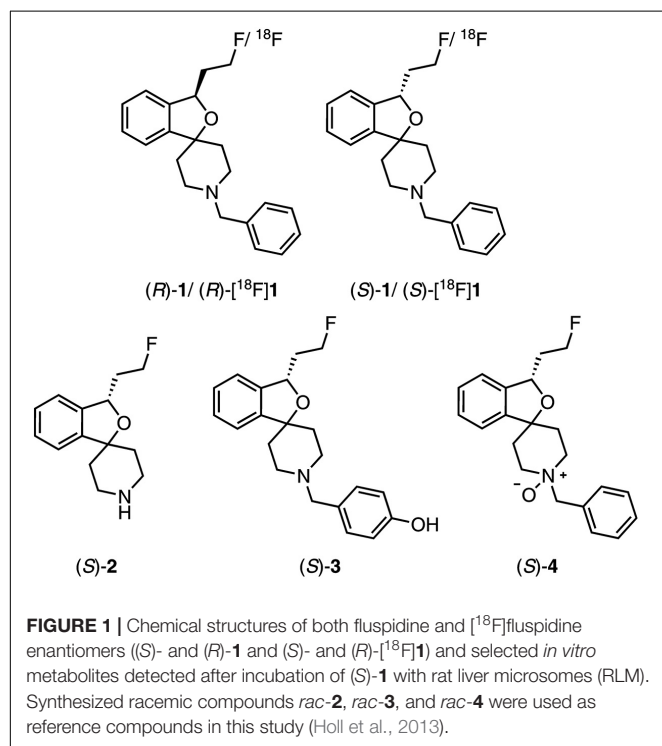
or (R)-**1** (Holl et al., 2013) culminated in a recently published synthesis route, which circumvents chiral HPLC separation by an enantioselective reduction step and additionally forms the basis for further easily accessible structural modifications (Nakane et al., 2018).

Labeling with fluorine-18 has been described for racemic [<sup>18</sup>F]fluspidine (rac-[<sup>18</sup>F]**1**) and its [<sup>18</sup>F]fluoroalkyl homologs (Große Mastrup et al., 2009b; Fischer et al., 2011; Maisoniai et al., 2011, 2012; Maisoniai-Besset et al., 2014) as well as for enantiomerically pure (S)- and (R)-[<sup>18</sup>F]**1**, both made available by automated synthesis procedures suitable for application in human studies (Brust et al., 2014a; Kranz et al., 2016).

As a prerequisite for clinical studies both enantiomeric radioligands have been investigated in animals (mice, pigs, and monkeys) with regard to radiation dosimetry and toxicity (Kranz et al., 2016) and regarding specificity and kinetic modeling (Brust et al., 2014a; Baum et al., 2017). The studies revealed that both (S)-[<sup>18</sup>F]**1** and its *R*-enantiomer appeared to be suitable for S1R imaging in humans. First clinical trials using (S)-[<sup>18</sup>F]**1** to quantify the S1R availability in patients with major depressive disorder and Huntington's disease have been performed (EudraCT Numbers: 2014-005427-27, 2016-001757-41).

The present study reports on accompanying investigations on the metabolic fate of (S)-[<sup>18</sup>F]**1**. Beside determination of the fraction of unchanged radioligand in plasma for providing an arterial input function, which enables reliable analysis of PET data, a characterization of the formed radiometabolites (metabolites bearing a radioactive nuclide) is of interest (Pawelke, 2005). However, the low mass of radioligands in plasma samples, which is related to the use of substances with high molar activities in PET studies, usually prevents a direct structural elucidation. This difficulty can be overcome by means of *in vitro* investigations (Jia and Liu, 2007; Asha and Vidyavathi, 2010) supported by liquid chromatography-mass spectrometry (LC-MS) or -tandem mass spectrometry (LC-MS/MS) (Bier et al., 2006; Amini et al., 2013; Ludwig et al., 2016, 2018) to enable interpretation of radiometabolite profiles obtained by radio-HPLC, e.g., during a clinical study.

In a detailed study the metabolism of racemic fluspidine (rac-**1**) as well as its fluoroalkyl homologs and the corresponding <sup>18</sup>F-radioligands have been investigated covering incubations with rat liver microsomes (RLM) and *in vivo* studies in mice, respectively (Wiese et al., 2016). Similarly, enantiomerically pure (S)-**1** as well as (R)-**1** have been investigated *in vitro* and structural elucidation with LC-MS has been conducted for metabolites formed by incubations with RLM under conditions for oxygenation (Holl et al., 2013). Mainly formed metabolites of (S)-**1** resulted from debenzoylation ((S)-**2**), hydroxylation at the phenyl ring ((S)-**3**), and *N*-oxidation ((S)-**4**) and their structures are provided in **Figure 1**. Further, hydroxylation at the piperidine moiety and at the fluoroethyl side chain was observed, as well as the formation of three di-oxygenated degradation products. For the corresponding radioligand (S)-[<sup>18</sup>F]**1** metabolic stability in piglets has been reported, whereby in plasma 48% of the radioligand remained unchanged at 16 min post injection (Brust et al., 2014a). However,



structures of radiometabolites formed *in vivo* have not been elucidated so far.

In the present study, the metabolism of (S)-[<sup>18</sup>F]**1** was investigated using human liver microsomes (HLM) to structurally characterize *in vitro* metabolites. The *in vitro* metabolite profile was used to identify radiometabolites in human plasma and urine after administration of (S)-[<sup>18</sup>F]**1** thereby providing knowledge about the metabolic pathways of this radioligand in the human body.

## MATERIALS AND METHODS

### Chemicals and Reagents

Acetonitrile (gradient grade) was purchased from VWR International (Darmstadt, Germany). Acetonitrile and water (both for LC-MS) were purchased from Fisher Scientific (Schwerte, Germany). Ammonium acetate (for HPLC) was purchased from Acros Organics (Geel, Belgium). Ammonium acetate (LC-MS), testosterone, 4-nitrophenol, β-nicotinamide adenine dinucleotide 2'-phosphate reduced tetrasodium salt (NADPH), uridine 5'-diphosphoglucuronic acid trisodium salt (UDPGA), alamethicin, MgCl<sub>2</sub>, and β-glucuronidase were purchased from Sigma-Aldrich (Merck KGaA, Darmstadt, Germany). GIBCO human liver microsomes (HLM, pooled donors, 20 mg/mL) were purchased from Life Technologies (Thermo Fisher Scientific, Darmstadt, Germany). Dulbecco's phosphate-buffered saline (PBS) (without Ca<sup>2+</sup>, Mg<sup>2+</sup>) was purchased from Biochrom (Berlin, Germany). (S)-**1**, *rac*-**2**, *rac*-**3**, and *rac*-**4** were synthesized as reported in literature (Holl et al., 2013).

### Radiosynthesis of (S)-[<sup>18</sup>F]**1**

(S)-[<sup>18</sup>F]**1** was synthesized by nucleophilic no-carrier-added (n.c.a.) <sup>18</sup>F-substitution of the tosyl precursor under GMP conditions for human application according to a procedure previously reported (Fischer et al., 2011; Maisonia-Beset et al., 2014; Kranz et al., 2016).

### Incubations With Human Liver Microsomes (HLM)

#### Time- and Concentration-Dependent Metabolic Transformation of (S)-[<sup>18</sup>F]**1**

Incubations had a final volume of 250 μL and were performed in PBS (pH 7.4) as follows (Ludwig et al., 2018), with final concentrations as provided in brackets. Respective amounts of a solution of (S)-**1** of 0.1 mg/mL [ $<1$  μM (referring to estimated molar activity; no addition of carrier), 2, and 20 μM] in acetonitrile were put into test tubes and the solvent was evaporated using the DB-3D TECHNE Sample Concentrator (Biostep, Jahnndorf, Germany) at room temperature under a stream of nitrogen. PBS and HLM (1 mg/mL) and ~5 MBq (S)-[<sup>18</sup>F]**1** (molar activity: 17 GBq/μmol, at the start of incubations) in 100 μL PBS were added, mixed vigorously, and pre-incubated at 37°C for 3 min. Analogously pre-incubated NADPH (2 mM) was added and mixtures were shaken gently at 37°C using

the BioShake iQ (QUANTIFOIL Instruments, Jena, Germany). After 0, 2, 5, 10, 15, 20, 30, 40, 50, and 60 min, samples of 20 μL were taken and added to 80 μL cold acetonitrile (−20°C), followed by vigorous shaking (30 s), cooling on ice (4 min), and centrifugation at 14,000 rpm (10 min). Supernatants (90 μL) were diluted with water (30 μL) and immediately analyzed by radio-HPLC (system II).

### Incubation of (S)-[<sup>18</sup>F]**1** and Non-radioactive References for Identification of *in vitro* Metabolites and Radiometabolites

Incubations with (S)-[<sup>18</sup>F]**1**, (S)-**1**, and *rac*-**2**, *rac*-**3**, and *rac*-**4** as substrate, had a final volume of 250 μL and were performed in PBS (pH 7.4) in duplicate. In the following, the final concentrations are provided in brackets. For incubations of (S)-[<sup>18</sup>F]**1** together with (S)-**1** under conditions for oxidation and glucuronidation, a solution of (S)-**1** of 0.1 mg/mL (2 μM) in acetonitrile was put into test tubes and the solvent was evaporated using the DB-3D TECHNE Sample Concentrator (Biostep) at room temperature under a stream of nitrogen. HLM (1 mg/mL) and alamethicin (50 μg/mL, from methanolic solution) were mixed (Fisher et al., 2000), kept on ice for 15 min and added to the test tubes. PBS, ~5 MBq (S)-[<sup>18</sup>F]**1** in 20 μL PBS, and MgCl<sub>2</sub> (2 mM) were added, mixed vigorously and the mixture was pre-incubated at 37°C for 3 min. After addition of analogously pre-incubated NADPH (2 mM) and UDPGA (5 mM), the incubations were continued by gentle shaking at 37°C for 120 min using the BioShake iQ (QUANTIFOIL Instruments). After termination by adding 1.0 mL of cold acetonitrile (−20°C) and vigorous mixing for 30 s, the mixtures were stored at 4°C for 5 min. After centrifugation at 14,000 rpm (Eppendorf Centrifuge 5424) for 10 min and the concentration of the supernatants at 50°C under a flow of nitrogen (DB-3D TECHNE Sample Concentrator) residual volumes of 40–70 μL each were obtained, which were reconditioned by adding water to provide samples of 100 μL, which were immediately analyzed by radio-HPLC and stored at 4°C until analysis by LC-MS/MS. HLM incubations of *rac*-**2**, *rac*-**3**, and *rac*-**4**, as substrate were performed in similar manner. Incubations without HLM, NADPH, UDPGA, and substrates, respectively, were performed as negative controls and to provide conditions only for oxygenation and not glucuronidation, and vice versa. As positive controls, testosterone (for oxygenation) and 4-nitrophenol (for glucuronidation) were incubated at appropriate concentrations, similarly to the protocol described above. Complete conversions of both were confirmed by RP-HPLC analyses with UV detection.

In order to investigate the cleavage of formed glucuronides (see section “β-Glucuronidase Cleavage of Microsomal-Formed Metabolite **M12**”), microsomal incubation of (S)-**1** was performed in quadruplicate with higher amounts of the substrate and the reagents as follows (final concentrations in brackets): (S)-**1** (200 μM), HLM (2 mg/mL), NADPH (4 mM), MgCl<sub>2</sub> (5 mM), alamethicin (0.1 mg/mL), UDPGA (10 mM). After addition of acetonitrile, resulting mixtures were combined and further processing was proceeded as described above. The obtained sample was separated chromatographically using the

HPLC system I (Section “Radio-HPLC”) with UV monitoring at 210 nm. The constituent eluting at 24.6 min (**M12**) was collected manually and further used for cleavage experiments as described in Section “ $\beta$ -Glucuronidase Cleavage of Microsomal-Formed Metabolite **M12**.”

### $\beta$ -Glucuronidase Cleavage of Microsomal-Formed Metabolite **M12**

To 10  $\mu$ L of a solution of metabolite **M12** (Section “Incubation of (S)-[<sup>18</sup>F]1 and Non-radioactive References for Identification of *in vitro* Metabolites and Radiometabolites”), 32  $\mu$ L acetate buffer (NaOAc/AcOH, 100 mM, pH 4.5–5.0), and 8  $\mu$ L  $\beta$ -glucuronidase from *Helix pomatia* Type H-3 (aqueous solution,  $\geq 90,000$  units/mL, final:  $\geq 14,400$  units/mL) were added. The mixture was shaken gently at 37°C for 2 h, then 50  $\mu$ L of cold acetonitrile (4°C) were added and mixed vigorously. After centrifugation at 14,000 rpm (Eppendorf Centrifuge 5424) for 15 min, 40  $\mu$ L of the supernatant was diluted with 60  $\mu$ L of water and analyzed by LC-MS/MS monitoring the MRM transitions  $m/z$  518.2/342.2 (as for glucuronides of mono-oxygenated metabolites, e.g., **M12**) and 342.2/91.1 (as for mono-oxygenated metabolites, e.g., **M5**).

### Investigation of the Metabolism of (S)-[<sup>18</sup>F]1 in Humans

All investigations were conducted in the framework of an approved and registered clinical study (EudraCT Number: 2014-005427-27).

After injection of 244.6–290.4 MBq (mean: 265.5 MBq) of (S)-[<sup>18</sup>F]1 into 8 healthy controls arterial blood samples ( $\sim 16$  mL) were withdrawn at 10, 20, and 30 min. The samples were collected directly into S-Monovettes® 9 mL K3E (SARSTEDT, Nümbrecht, Germany) and stored on ice. After 90 or 120 min, urine ( $\sim 8$  mL) was collected and stored on ice. Plasma was obtained by centrifugation of blood samples at 7,000 rpm (UNIVERSAL 320 R, Hettich, Germany) for 7 min. Protein precipitation and extraction with acetonitrile was conducted as follows. Method A: 10  $\times$  1.6 mL cold acetonitrile ( $-35^\circ\text{C}$ ) were added to 10  $\times$  400  $\mu$ L plasma, shaken for 3 min, cooled at 4°C for 5 min and centrifuged at 7,000 rpm (Eppendorf Centrifuge 5424) for 5 min. Supernatants were collected and the precipitates were extracted with 1.6 mL acetonitrile each. The combined supernatants were concentrated at 70°C under a flow of nitrogen (Sample Concentrator DB-3D TECHNE) to provide residual volumes of 40–70  $\mu$ L, which were reconditioned by adding water to obtain samples of 100  $\mu$ L, which were immediately analyzed by radio-HPLC (system I). Method B: similar to method A, using 2  $\times$  8 mL cold acetonitrile ( $-35^\circ\text{C}$ ) and 2  $\times$  2 mL plasma. After centrifugation, the precipitates were extracted with 2  $\times$  4 mL acetonitrile.

For monitoring of the efficiency of extraction for (S)-[<sup>18</sup>F]1 and its radiometabolites, the precipitants and aliquots of plasma and supernatants were taken and measured in a calibrated gamma counter (Wallac WIZARD 3, Perkin Elmer, Shelton, CT, United States). The recovery in % was calculated as follows:  $\text{recovery} = \text{activity}_{\text{supernatant}} / (\text{activity}_{\text{supernatant}} + \text{activity}_{\text{precipitate}})$

$\times 100\%$ . Urine samples were analyzed without any pre-treatment.

### Radio-HPLC

System I: Analyses were performed on a JASCO LC-2000 system (JASCO Labor- und Datentechnik, Gross-Umstadt, Germany) including a UV-2070 UV-VIS detector (monitoring at 210 nm) online with a GABI Star radioactivity flow detector (raytest Isotopenmessgeräte, Straubenhardt, Germany) with a NaI detector (2  $\times$  2" pinhole, 16 mm  $\times$  30 mm). Chromatographic separations were achieved using a Multospher 120 RP 18 AQ-5 $\mu$ -column, 250 mm  $\times$  4.6 mm, 5  $\mu$ m, including pre-column, 10 mm  $\times$  4 mm (CS-Chromatographie Service, Langerwehe, Germany). The solvent system consisted of eluent A: water/acetonitrile, 95:5 (v/v), containing NH<sub>4</sub>OAc (20 mM) and eluent B: water/acetonitrile, 20:80 (v/v), containing NH<sub>4</sub>OAc (20 mM). Linear gradient elution (% acetonitrile) at a flow rate of 1.0 mL/min: 0–5 min, 5%; 5–55 min, 5–80%; 55–65 min, 80%; 65–66 min, 80–5%; 66–76 min, 5%.

System II: Analyses of samples from microsomal incubations to determine time and concentration dependency of microsomal transformation were performed on a JASCO X-LC system (JASCO Labor- und Datentechnik) equipped with a UV/Vis detector UV-2070 (monitoring at 210 nm) and a radioactivity flow detector GABI Star (raytest Isotopenmessgeräte, Straubenhardt, Germany) including NaI detector (2  $\times$  2" pinhole, 16 mm  $\times$  30 mm). Chromatographic separations were achieved using a Multospher 120 RP 18 AQ-3 $\mu$ -column, 125 mm  $\times$  3 mm, 3  $\mu$ m, including pre-column, 10 mm  $\times$  3 mm (CS-Chromatographie Service) at a column temperature of 20°C, at a flow rate of 0.7 mL/min and a runtime of 5.0 min. The isocratic solvent system consisted of water/acetonitrile 40:60 (v/v), containing NH<sub>4</sub>OAc (20 mM). Unchanged (S)-[<sup>18</sup>F]1 eluted at a retention time of 4.1 min, whilst formed radiometabolites eluted at 0.6–2.2 min. The percentages of unchanged (S)-[<sup>18</sup>F]1 were calculated from HPLC data as follows:  $\text{Fraction of (S) - [}^{18}\text{F]1 (\%)} = \text{Peak area}_{(\text{S})-[^{18}\text{F]1} / (\text{Peak area}_{(\text{S})-[^{18}\text{F]1} + \text{Peak area}_{\text{radiometabolites}}) \times 100\%$

### LC-MS/MS Analyses

Analyses were performed on an Agilent 1260 Infinity Quaternary LC system (Agilent Technologies, Böblingen, Germany) coupled with a QTRAP 5500 hybrid linear ion-trap triple quadrupole mass spectrometer (AB SCIEX, Concord, ON, Canada). Data were acquired and processed using Analyst software (Version 1.6.1, AB SCIEX) and for further data processing OriginPro 2017G (OriginLab, Northampton, MA, United States) was used. For chromatographic separations a Multospher 120 RP 18 AQ-3 $\mu$ -column, 125 mm  $\times$  3 mm, 3  $\mu$ m, including pre-column, 10 mm  $\times$  3 mm (CS-Chromatographie Service) was used. The solvent system consisted of eluent A: water containing NH<sub>4</sub>OAc (2 mM) and eluent B: water/acetonitrile, 20:80 (v/v), containing NH<sub>4</sub>OAc (2 mM). Linear gradient elution (% acetonitrile) at a flow rate of 0.7 mL/min, at 40°C: 0–10 min, 5–80%; 10–12 min, 80%; 12–16 min, 5%. The mass spectrometer was operated in positive electrospray ionization mode with the following parameters: curtain gas (CUR) 35, collision gas (CAD) medium,



ion spray voltage (IS) 5500, temperature (TEM) 550, ion source gas 1 (GS1) 60, and ion source gas 2 (GS2) 50.

For multiple reaction monitoring (MRM) scan type: appropriate MRM transitions, scan time 40 ms; declustering potential (DP) 110; entrance potential (EP) 10; collision energy (CE) 40; collision cell exit potential (CXP) 10.

For enhanced product ion (EPI) scan type: products of selected *m/z* values, scan rate 10000 Da/s, dynamic fill time, CAD high, and further parameters as used for MRM scans. In EPI chromatograms obtained, a range of background was selected manually and subtracted from ranges of interest to result in EPI spectra as provided in the **Supplementary Material**.

For the MS<sup>3</sup> scan type the excitation energy (AF2) was optimized prior to data acquisition.

## RESULTS AND DISCUSSION

### Investigation of the Metabolism of (S)-[<sup>18</sup>F]1 and (S)-1 *in vitro* Using Human Liver Microsomes (HLM)

#### Time- and Concentration-Dependent Microsomal Transformation

In order to obtain basic information about the metabolic stability *in vitro*, the time course of the degradation of (S)-[<sup>18</sup>F]1 was investigated in presence of different concentrations of (S)-1 [no-carrier-added (n.c.a.), <1 μM] and carrier-added: 2 and 20 μM]. For that purpose, incubations were performed in PBS with HLM and NADPH at 37°C. At defined time points (until 60 min) samples were taken and added to cold acetonitrile to terminate the incubations. After centrifugation, the fractions of remaining (S)-[<sup>18</sup>F]1 were determined by radio-HPLC.

The time course of degradation is illustrated in **Figure 2**. The fraction of (S)-[<sup>18</sup>F]1 represents the fraction of both remaining (S)-[<sup>18</sup>F]1 and (S)-1, with regard to formed (radio)metabolites. After 60 min, only 3% of unchanged (S)-[<sup>18</sup>F]1 (n.c.a.) was detectable, whilst after 30 min incubation 14% of unchanged radioligand was present. Similar percentages were found using

2 μM (S)-1, whereas at a concentration of 20 μM the metabolic degradation was diminished, which can be explained by saturation of the degrading cytochrome P450 enzyme system. 50% of unchanged (S)-[<sup>18</sup>F]1 could be detected (a) after 10 min for both n.c.a. and a concentration of 2 μM and (b) after 17 min for a concentration of 20 μM of added (S)-1. Therefore, for most carrier-added experiments a concentration of 2 μM was chosen.

The metabolic stability of *rac*-1, (S)-1, and (R)-1 have previously been studied *in vitro* using RLM in presence of NADPH. After 30 min, *rac*-1 showed the lowest stability (~13%) among the fluoroalkyl homologs tested (Wiese et al., 2016), whereas 73% of intact (S)-1 was still present after the same incubation time (Holl et al., 2013). Compared with our results from HLM (14%) this might suggest that (S)-1 has higher stability in rats than in human. However, for RLM incubations, beside different incubation conditions, (S)-1 was used at a concentration of 320 μM, which is a substantially higher concentration than the 2 μM used in the present study and might explain the low microsomal degradation in RLM.

#### Structure Elucidation of Metabolites and Radiometabolites

Carrier-added (S)-[<sup>18</sup>F]1, that means the radioligand in presence of (S)-1 (2 μM, unless otherwise stated), was incubated with HLM in PBS at 37°C for 120 min, in presence of NADPH and UDPGA. Both cofactors provide conditions for oxygenation or glucuronidation, respectively, and were used either separately or combined. After termination of the experiment by adding cold acetonitrile, the mixtures were centrifuged and the supernatants investigated by LC-MS/MS, as well as radio-HPLC. The compounds *rac*-2, *rac*-3, and *rac*-4 were incubated identically and the prepared samples were analyzed by LC-MS/MS.

#### Detection and structure elucidation of *in vitro* metabolites of (S)-1 by LC-MS/MS

Prior to LC-MS/MS measurements the parameters for MRM scan mode were optimized using (S)-1 (exact mass: 325.18). In preparation for detailed structural characterization, EPI and MS<sup>3</sup> measurements were performed for (S)-1 as well as for *rac*-2, *rac*-3, and *rac*-4 and fragmentation patterns were interpreted. As shown in **Figure 3A**, most relevant for (S)-1 was the formation of the tropylium cation [*m/z* 91.1, (C<sub>7</sub>H<sub>7</sub>)<sup>+</sup>]. Consequently, this fragment as well as its derived ions [e.g., *m/z* 107.1, (C<sub>7</sub>H<sub>7</sub>+O)<sup>+</sup>] were used for most of the MRM scans to detect metabolites. Further observed fragment ions observed in EPI or MS<sup>3</sup> spectra (**Figure 3B**) were interpreted as shown in **Figure 3C**.

For selective detection of metabolites, MRM transitions, which covered products of, e.g., debenzoylation, defluorination, single, and multiple oxygenations as well as single and multiple glucuronidation of (S)-1 or its intermediate metabolites, were monitored. After incubation of (S)-1 with HLM in presence of NADPH a series of metabolites (M1–M10) could be detected (**Figure 4** and **Table 1**).

First, defluorination of (S)-1 was not observed. As also reported for RLM (Holl et al., 2013), (S)-1 underwent debenzoylation and metabolite **M1** could be detected

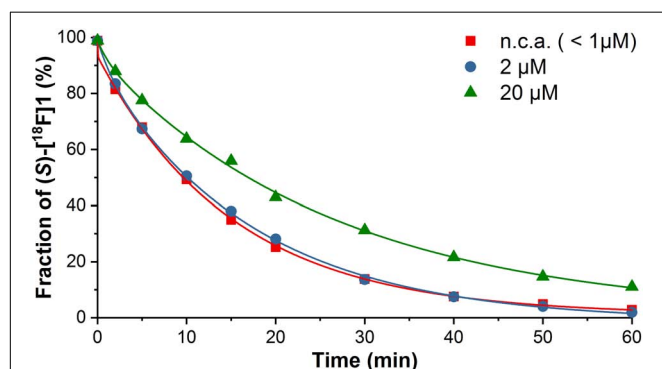


**FIGURE 2 |** Microsomal metabolic transformation of (S)-[<sup>18</sup>F]1 at different concentrations of carrier ((S)-1) by HLM and NADPH in PBS at 37°C (Section “Time- and Concentration-Dependent Metabolic Transformation of (S)-[<sup>18</sup>F]1”) determined by radio-HPLC (system II in Section “Radio-HPLC”).

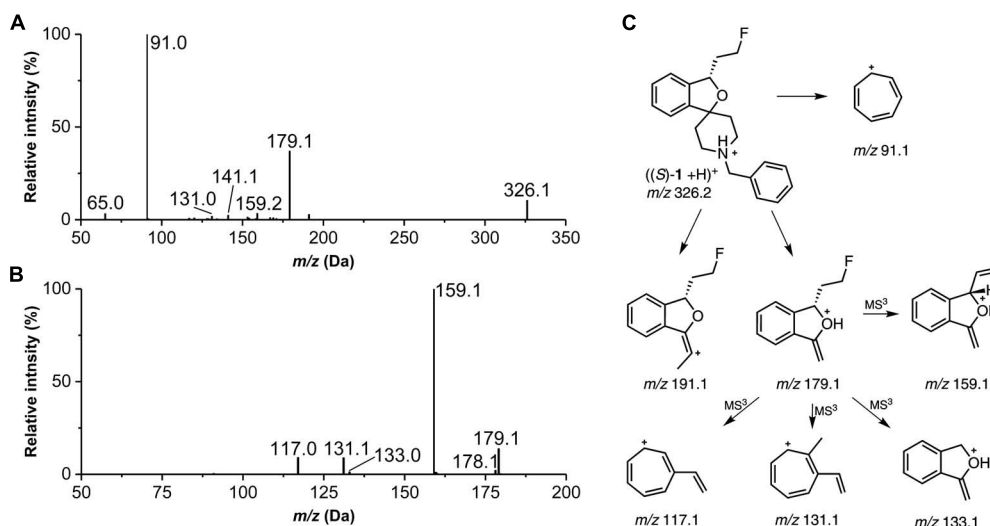


**FIGURE 3 |** MS/MS data of (S)-1 (exact mass: 325.18). **(A)** enhanced product ion (EPI) spectrum, precursor ion at  $m/z$  326.2 (CE 40). **(B)** MS3 spectrum of  $m/z$  326.2/179.1 (AF2 0.125). **(C)** Proposed fragmentation pathway for (S)-1 (in some of the structures of fragment ions positive charges were placed at specific atoms for illustrative purposes).

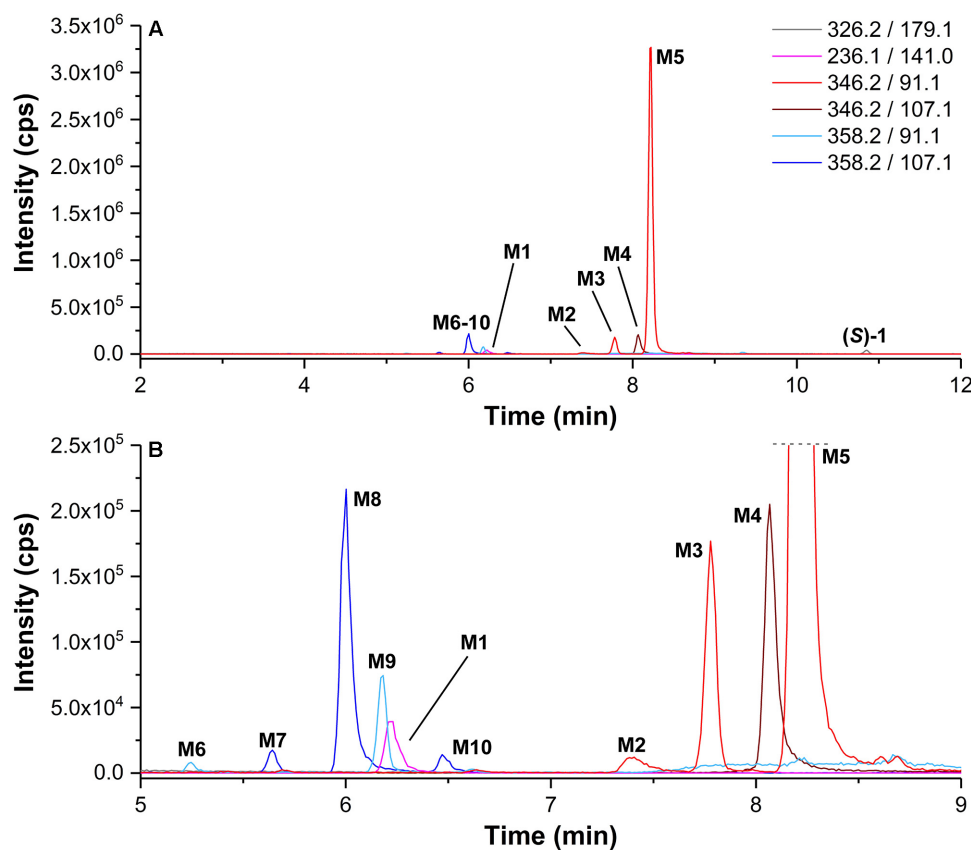


**FIGURE 4 |** **(A)** Multiple reaction monitoring (MRM) chromatograms (Section “LC-MS/MS Analyses”) recorded after incubation of (S)-1 (2  $\mu$ M) with HLM in presence of NADPH in PBS at 37°C for 120 min (Section “Incubation of (S)-[<sup>18</sup>F]1 and Non-radioactive References for Identification of *in vitro* Metabolites and Radiometabolites”). **(B)** enlarged detail of **A**. MRM transitions as provided in the legend. Data are summarized in **Table 1**.

**TABLE 1** | LC-MS/MS data of metabolites (Section “LC-MS/MS Analyses”) detected after incubation of (S)-**1** with HLM (NADPH, UDPGA).

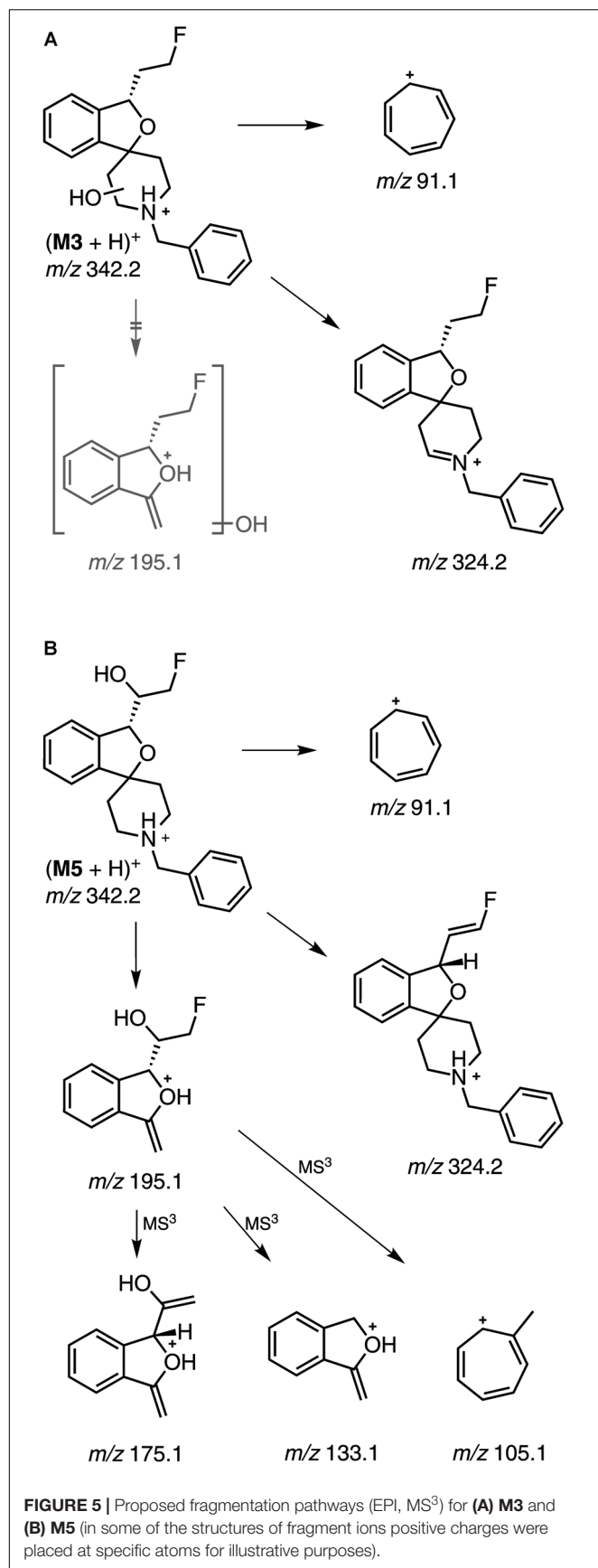
Metabolite	t <sub>R</sub> (min) <sup>a</sup>	MRM transition	EPI fragmentation <sup>b</sup> (% intensity in brackets)	Metabolic pathway
M1	6.24	236.1/141.0	141.1 (100), 128.0 (64), 154.1 (53), 153.1 (50), 115.1 (29), 129.1 (25), 143.1 (22), 165.0 (10), 117.1 (5), 127.1 (5), 152.0 (5), 155.2 (5), 142.1 (5)	debenzylation
M2	7.38	342.2/91.1	— <sup>c</sup>	N-oxidation
M3	7.79	342.2/91.1	91.0 (100), 342.2 (26), 187.1 (7), 185.2 (6), 175.1 (6), 120.1 (6), 205.1 (5), 324.2 (5), 232.1 (4), 167.1 (4), 250.1 (3), 131.1 (3)	hydroxylation (at piperidine)
M4	8.07	342.2/107.1	107.0 (100), 236.1 (18), 218.2 (6), 189.1 (4), 169.1 (2), 91.0 (2), 179.1 (2), 107.6 (1), 143.0 (1), 342.1 (1)	hydroxylation (at 4-phenyl)
M5	8.22	342.2/91.1	342.2 (100), 195.1 (22), 91.0 (17), 207.1 (2), 205.2 (1), 134.1 (0.9), 250.1 (0.7), 120.0 (0.7), 324.2 (0.4)	hydroxylation (at fluoroethyl)
M6	5.24	358.2/91.1	— <sup>c</sup>	di-oxygenation
M7	5.64	358.2/107.1	107.0 (100), 84.0 (91), 139.1 (44), 167.1 (22), 219.2 (11), 122.0 (10), 141.0 (8), 152.2 (8), 134.0 (7), 185.0 (5), 124.1 (5), 112.1 (5), 78.9 (5), 76.9 (4), 129.1 (4)	di-oxygenation (1x OH at phenyl)
M8 <sup>d</sup>	6.01	358.2/107.1	107.0 (100), 252.1 (81), 205.1 (22), 358.1 (11), 185.1 (6), 234.1 (6), 257.0 (4), 139.1 (4), 83.9 (3), 195.1 (3), 159.1 (3)	di-oxygenation (1x OH at 4-phenyl)
M9 <sup>d</sup>	6.18	358.2/91.1	91.0 (100), 83.9 (74), 358.2 (35), 147.1 (32), 139.0 (31), 191.1 (20), 149.1 (17), 203.1 (14), 183.1 (12), 256.9 (11), 122.0 (8), 120.0 (8), 155.0 (7), 124.1 (5), 184.9 (5), 141.1 (5), 152.2 (5), 212.2 (5)	di-oxygenation
M10	6.47	358.2/107.1	— <sup>c</sup>	di-oxygenation (1x OH at phenyl)
M11	3.72	252.1/141.0	— <sup>c</sup>	debenzylation + oxygenation
M12	3.53	518.2/342.2	342.1 (100), 195.1 (10), 518.1 (8), 207.1 (2), 120.1 (1), 91.0 (0.5)	hydroxylation (at fluoroethyl) + glucuronidation
M13, M18, M19, M21 <sup>e</sup>	3.00, 4.04, 4.19, 4.45	518.2/342.2	— <sup>c</sup>	oxygenation + glucuronidation
M14, M15, M16, M17, M20 <sup>e</sup>	3.22, 3.35, 3.85, 3.98, 4.36	534.2/358.2	— <sup>c</sup>	di-oxygenation + glucuronidation
(S)- <b>1</b>	10.85	326.2/179.2	91.0 (100), 179.1 (37), 326.1 (10), 159.2 (3), 65.0 (3), 191.1 (3), 141.1 (2), 131.0 (2), 153.1 (1), 167.1 (1), 169.0 (1), 120.1 (1), 154.1 (1), 117.0 (1)	parent

<sup>a</sup>Retention time; <sup>b</sup>collision energy (CE) 40, except for **M5** and **M8** (CE 30), further parameters for data acquisition described in Section “LC-MS/MS Analyses”; <sup>c</sup>not recorded due to low intensity; <sup>d</sup>EPI spectra were recorded after LC separations at 15°C instead of 40°C to achieve complete separation of **M8** and **M9**; <sup>e</sup>data have been summarized for reasons of space.

by monitoring the MRM transition  $m/z$  236.1 ( $M-CHC_6H_5 + H$ )<sup>+</sup>/141.0. Both the retention time ( $t_R = 6.24$  min) and the fragmentation pattern obtained by EPI scans matched that of *rac*-**2**. EPI spectra for **M1** and other metabolites are provided in the **Supplementary Material**.

The metabolites **M2–M5** were formed by single oxygenation of (S)-**1**. Two of them, **M2** and **M4**, could be characterized by comparison with synthesized references. The retention time of **M2** ( $t_R = 7.38$  min) matched that of the *N*-oxide *rac*-**4** and the fragmentation pattern for  $m/z$  342.2 ( $M+O+H$ )<sup>+</sup> appeared similar. However, **M2** was most likely not a product of CYP-mediated oxidation, since it was detected also in NADPH-free incubations with comparable low intensity. **M4** ( $t_R = 8.07$  min) was identified as an hydroxylation product of (S)-**1**, bearing the hydroxyl function at the phenyl ring of the benzyl substituent, proven by an MRM transition of  $m/z$  342.2 ( $M+O+H$ )<sup>+</sup>/107.1 ( $C_7H_7+O$ )<sup>+</sup>. Both the retention time and the fragmentation pattern were highly similar to that of *rac*-**3**, which indicates that **M4** was hydroxylated at the *para* position of the phenyl ring. In contrast, **M3** could be detected by recording an MRM transition of  $m/z$  342.2 ( $M+O+H$ )<sup>+</sup>/91.1 ( $C_7H_7$ )<sup>+</sup>. In this case,

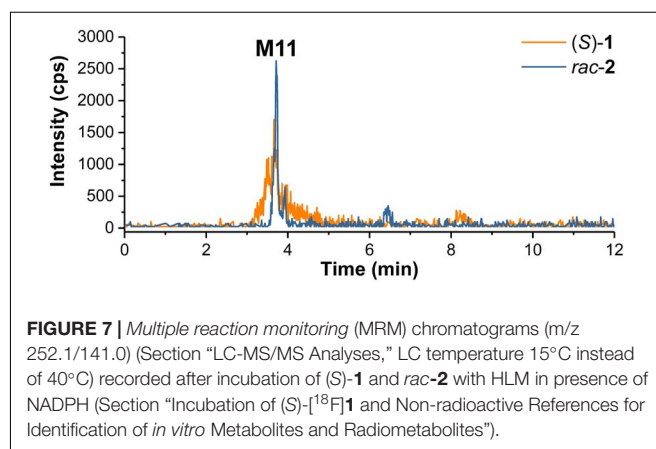
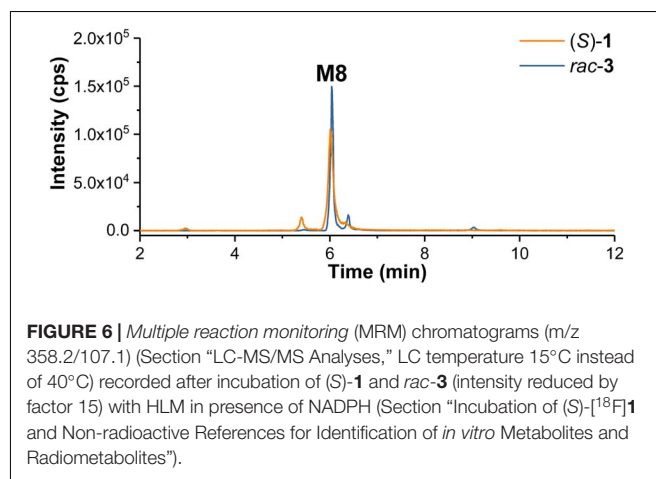
a hydroxylation at the benzyl group could be excluded, due to the occurrence of the tropylium cation [ $(C_7H_7)^+$ ] as for (S)-**1**. In the EPI spectrum, the fragment ion  $m/z$  324.2 resulted from a loss of water ( $m/z -18$ ) as one can expect as a result of a hydroxylation at the piperidine moiety. This interpretation was underpinned by the absence of a corresponding oxygenated methylene-dihydroisobenzofuranium fragment ion ( $m/z$  195.1) (**Figure 5A**). In contrast, for **M5** the fragment ion of  $m/z$  195.1 provided evidence for a hydroxylation at the fluoroethyl-dihydroisobenzofuran moiety of the molecule (**Figure 5B**). Subsequent fragmentation in MS<sup>3</sup> experiments further revealed a hydroxylation at the fluoroethyl side chain, as also substantiated by detected elimination of water ( $m/z -18$ ). Beside MS<sup>3</sup> data, in particular the fragment ion  $m/z$  175.1, suggests that hydroxylation took place at the carbon atom next to the chiral center of the molecule, as it has been discussed in literature (Holl et al., 2013). As reported, after incubation with RLM, a hydroxylation at the fluoroethyl side chain was observed only when (S)-**1** but not (R)-**1** was incubated, which indicated that a reaction at the carbon atom closer to the chiral center appears to be more likely.



As shown in **Figure 4**, also products from di-oxygenations (**M6–M10**) were found. Since they were detected by one of the MRM transitions either  $m/z$  358.2 ( $M+2O+H$ )<sup>+</sup>/91.1 ( $C_7H_7$ )<sup>+</sup> or  $m/z$  358.2 ( $M+2O+H$ )<sup>+</sup>/107.1 ( $C_7H_7+O$ )<sup>+</sup>, they could be divided in those with absent (**M6**, **M9**) and those with a single hydroxyl function (**M7**, **M8**, **M10**) at the phenyl ring. HLM incubation of the *para*-hydroxy-phenyl derivative *rac*-3 [instead of (*S*)-1] resulted in the formation of a di-oxygenated metabolite that matched **M8** with regard to its retention time (**Figure 6**). The EPI spectrum of **M8** showed a loss of water ( $m/z$  –18) which provided an indication of a hydroxyl function either at the piperidine moiety or the fluoroethyl chain (**Figure 10**).

The possible metabolism by debenzoylation and hydroxylation was studied in detail, since it has been reported for incubation with RLM (Holl et al., 2013). For that purpose, *rac*-2 instead of (*S*)-1 was incubated with HLM in presence of NADPH. By recording the MRM transition  $m/z$  252.1/141.0 the minor metabolite **M11** ( $t_R$  = 3.72 min) was detected after incubation of both (*S*)-1 and *rac*-2 (**Figure 7**). However, due to very low signal intensities no further characterization was possible.

The *in vitro* metabolites of (*S*)-1 detected in the current study after incubation with HLM correspond, to a large extent, to those reported from RLM incubations (Holl et al., 2013). Debenzoylation





(M1) and mono-oxygenations (M2–M5) were observed for both cases, even though in different proportions. Further, 5 and 3 di-oxygenated products were detectable after incubation with HLM and RLM, respectively, which might be a result of different MS detectors and methods used in both studies. However, a twofold hydroxylation at the phenyl moiety reported for RLM was not found for HLM.

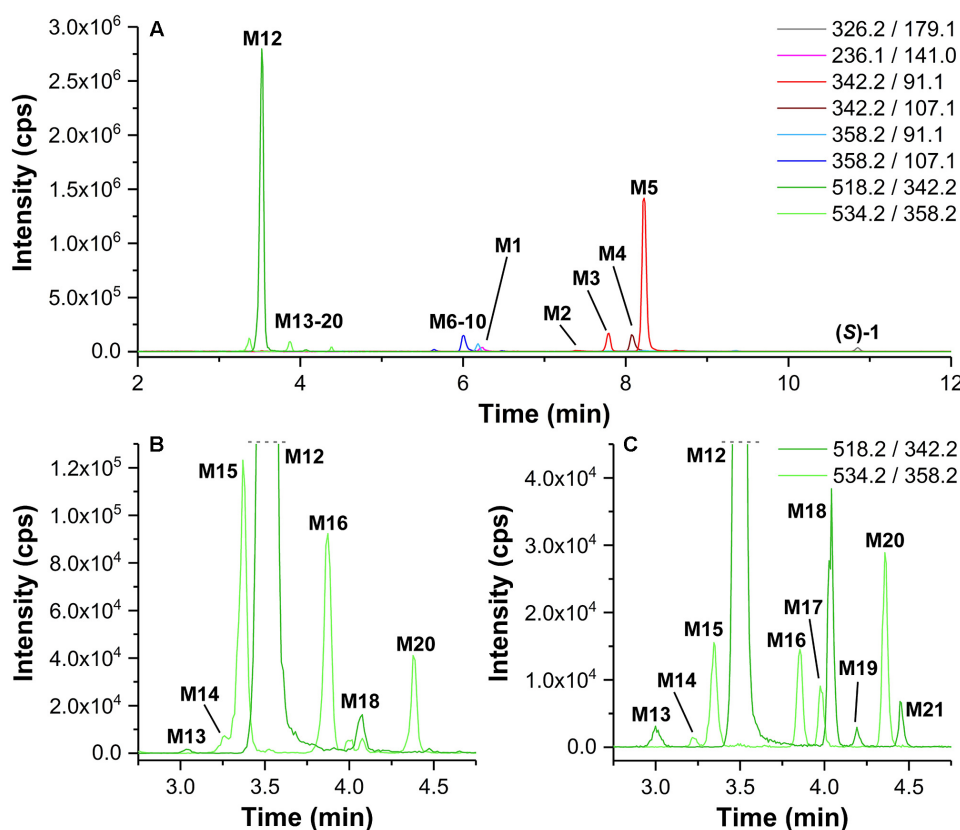
Samples from incubations of (S)-1 with HLM were investigated regarding the formation of conjugates with glucuronic acid by monitoring MRM transitions corresponding to a neutral loss of  $m/z$  176.0 ( $C_6H_8O_6$ ) as characteristic for glucuronides in positive-ion mode (Levsen et al., 2005). Only after incubation in presence of both cofactors NADPH and UDPGA glucuronide formation of (S)-1 was observed. Thus, not (S)-1 but its intermediate metabolites, previously formed by oxygenations, were glucuronidated. As shown in **Figure 8A**, one main glucuronide (M12,  $t_R = 3.53$  min), formed after mono-oxygenation was detected by monitoring the MRM transition  $518.2$  ( $M+O+C_6H_8O_6+H$ )<sup>+</sup>/ $342.1$  ( $M+O+H$ )<sup>+</sup>. In addition, glucuronide conjugates of previously formed di-oxygenation products were detected, but with low signal intensities (**Figures 8A,B**). After incubation with (S)-1 at a concentration of 200  $\mu$ M instead of 2  $\mu$ M (**Figure 8C**)

5 mono-oxygenated glucuronides (M12, M13, M18, M20, M21) and 5 di-oxygenated glucuronides (M14–M17, M20) were found.

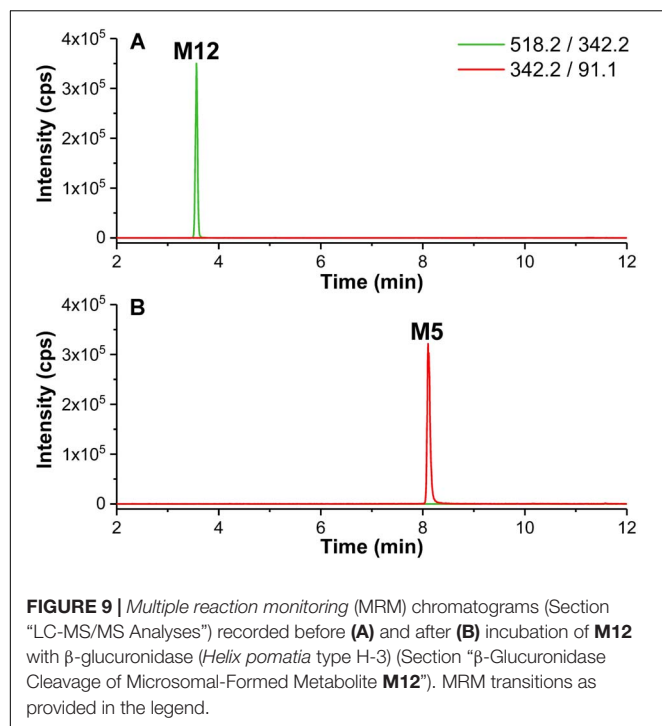
For the main glucuronide M12, collision-induced fragment ions at  $m/z$  342.1, 324.1 and in particular  $m/z$  195.1 correspond to those found for the hydroxyl-fluoroethyl metabolite M5, which provides a clear indication that it serves as an intermediate for subsequent glucuronidation. For further validation, the glucuronide cleavage was studied for M12. In brief, a solution of M12, obtained from HLM incubations and subsequent HPLC separation, was stirred at 37°C with  $\beta$ -glucuronidase (*Helix pomatia* type H-3) in acetate buffer (Yilmazer et al., 2001; Xu et al., 2002) and samples were inspected by measuring appropriate MRM transitions. During incubation with  $\beta$ -glucuronidase M12 was cleaved completely whereas M5 was the only product observed (**Figure 9**), also proven by comparison with LC-MS/MS data from HLM incubation.

#### Identification of *in vitro* radiometabolites of (S)-[<sup>18</sup>F]1

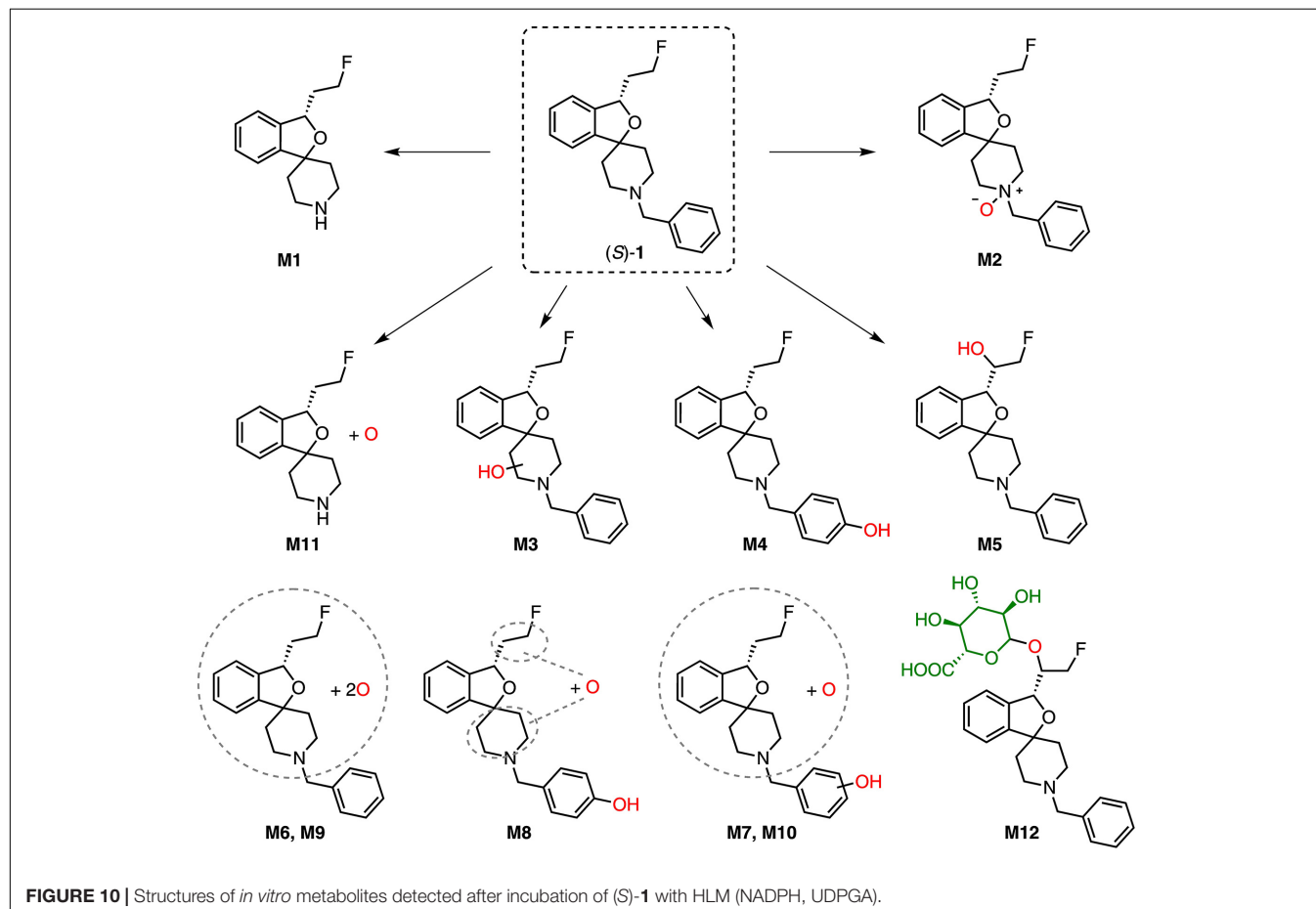
After HLM incubation in presence of NADPH a series of radiometabolites was detected by HPLC with a radioactivity flow detector (**Figure 11**). Incubations with both NADPH and UDPGA resulted in further products, due to glucuronide conjugation. Generally, patterns of radiometabolites resulting



**FIGURE 8 | (A)** Multiple reaction monitoring (MRM) chromatograms (Section “LC-MS/MS Analyses”) recorded after incubation of (S)-1 (2  $\mu$ M) with HLM in presence of NADPH and UDPGA in PBS at 37°C for 120 min (Section “Incubation of (S)-[<sup>18</sup>F]1 and Non-radioactive References for Identification of *in vitro* Metabolites and Radiometabolites”). **(B)** enlarged detail of **A**, showing MRM chromatograms for glucuronide conjugates of mono- and di-oxygenated metabolites. **(C)** detail according to **B**, but after incubation of (S)-1 at 200  $\mu$ M. MRM transitions as provided in the legends. Data are summarized in **Table 1**.



from (S)-[<sup>18</sup>F]1 largely matched those of metabolites of (S)-1 in LC-MS/MS (MRM) chromatograms. First assignments were done by comparative measurements using *rac*-2, *rac*-3, *rac*-4 with UV monitoring at 210 nm. Thus, [<sup>18</sup>F]M1, [<sup>18</sup>F]M2, and [<sup>18</sup>F]M4 could be characterized as products of debenzoylation, *N*-oxidation, and hydroxylation at the *para* position of the phenyl ring, due to their co-elution with the corresponding non-radioactive references (Figure 11). It is interesting to note that the *N*-oxide [<sup>18</sup>F]M2 eluted later than [<sup>18</sup>F]M3–[<sup>18</sup>F]M5, which is in contrast to the elution order observed in LC-MS/MS. However, by comparison with data from LC-MS/MS, [<sup>18</sup>F]M3 and [<sup>18</sup>F]M5 could clearly be identified as products of mono-hydroxylation at the piperidine moiety and the fluoroethyl side chain, respectively. The same applies to the UDPGA-dependently formed radiometabolite [<sup>18</sup>F]M12, which was deduced as formed by a hydroxylation at the fluoroethyl side chain of (S)-[<sup>18</sup>F]1 and subsequent glucuronidation, as demonstrated for the mainly formed non-radioactive glucuronic acid conjugate M12 (Section “Detection and structure elucidation of *in vitro* metabolites of (S)-1 by LC-MS/MS”). Further, minor <sup>18</sup>F-bearing glucuronides were detected ([<sup>18</sup>F]Md) but could only tentatively be assigned to glucuronides formed after previous mono- or di-oxygenation, as numerous of such corresponding non-radioactive products were found by LC-MS/MS (Figure 8).



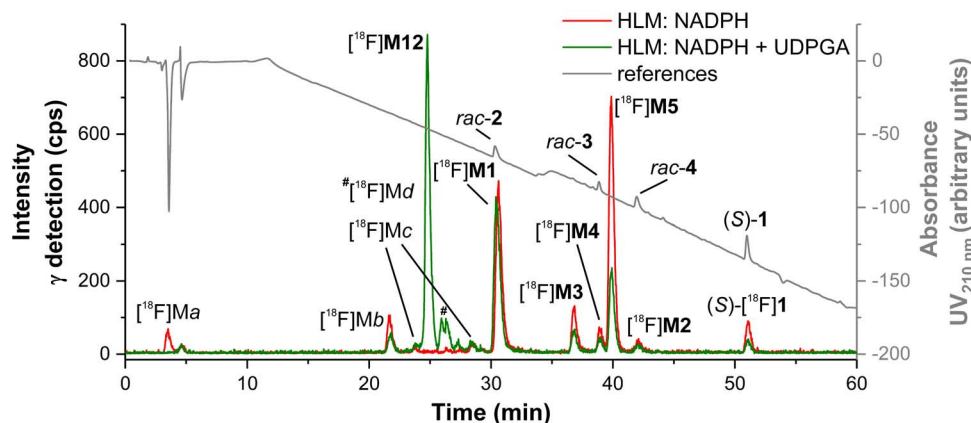
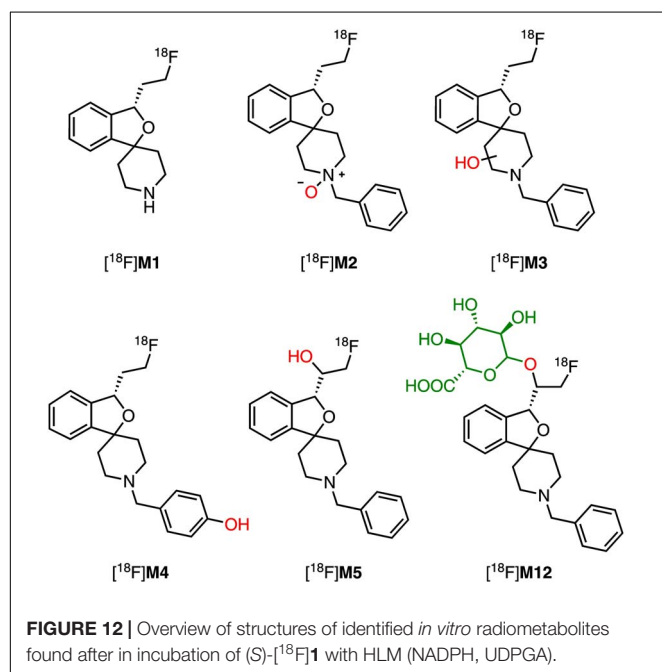


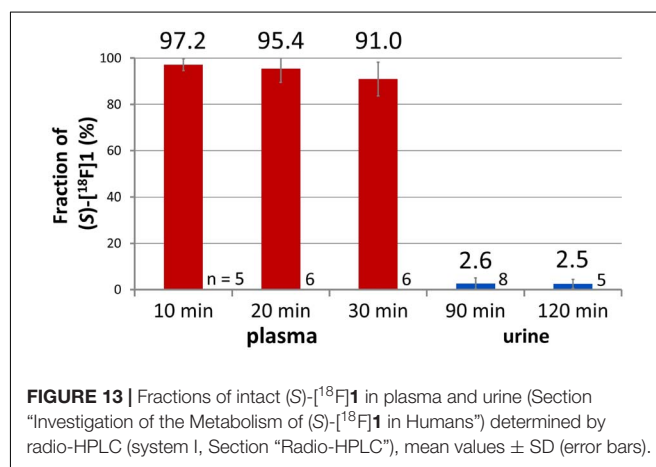
**FIGURE 11** | Radio-HPLC chromatograms (system I, Section “Radio-HPLC”) recorded after incubation of (S)-[<sup>18</sup>F]1 (carrier-added, (S)-1, 2 μM) with HLM (NADPH and UDPGA as stated in the legend) (Section “Incubation of (S)-[<sup>18</sup>F]1 and Non-radioactive References for Identification of *in vitro* Metabolites and Radiometabolites”) combined with an UV-HPLC chromatogram (210 nm) of a mixture of references.



The molecular identity of further radiometabolites ([<sup>18</sup>F]Ma-[<sup>18</sup>F]Mc) could not be elucidated. Thus, to interpret [<sup>18</sup>F]Mb as a product of debenzoylation and additional oxygenation or [<sup>18</sup>F]Mc as multiple oxygenation products remains speculative, although those transformations were demonstrated for (S)-1 (Section “Detection and structure elucidation of *in vitro* metabolites of (S)-1 by LC-MS/MS”). Structures of identified *in vitro* radiometabolites of (S)-[<sup>18</sup>F]1 are summarized in **Figure 12**.

## Investigation of the Metabolism of (S)-[<sup>18</sup>F]1 in Human

After administration of 244.6–290.4 MBq (mean: 265.5 MBq) (S)-[<sup>18</sup>F]1 to eight healthy controls, plasma and urine samples



were taken at 10, 20, and 30 min post injection and measured by radio-HPLC as described for the *in vitro* investigations in Section “Identification of *in vitro* radiometabolites of (S)-[<sup>18</sup>F]1.” Plasma samples were prepared by adding cold acetonitrile followed by centrifugation and evaporation of the supernatant. Two different procedures (method A and B), using different volumes of plasma and solvent, including a second extraction step of the formed residue, were established. For both methods, the recovery of activity was in the range of 92–97%.

Urine samples, taken after 90 or 120 min post injection were measured by radio-HPLC without further preparation.

## Metabolic Stability in Humans

Samples of plasma showed a high fraction of intact (S)-[<sup>18</sup>F]1 (**Figure 13**). At 10, 20, and 30 min post injection (S)-[<sup>18</sup>F]1 still represented 97.2 ± 2.6% (mean ± SD), 95.4 ± 5.9%, and 91.0 ± 7.3% of the total plasma activity. In urine, at 90 and 120 min post injection, (S)-[<sup>18</sup>F]1 represented

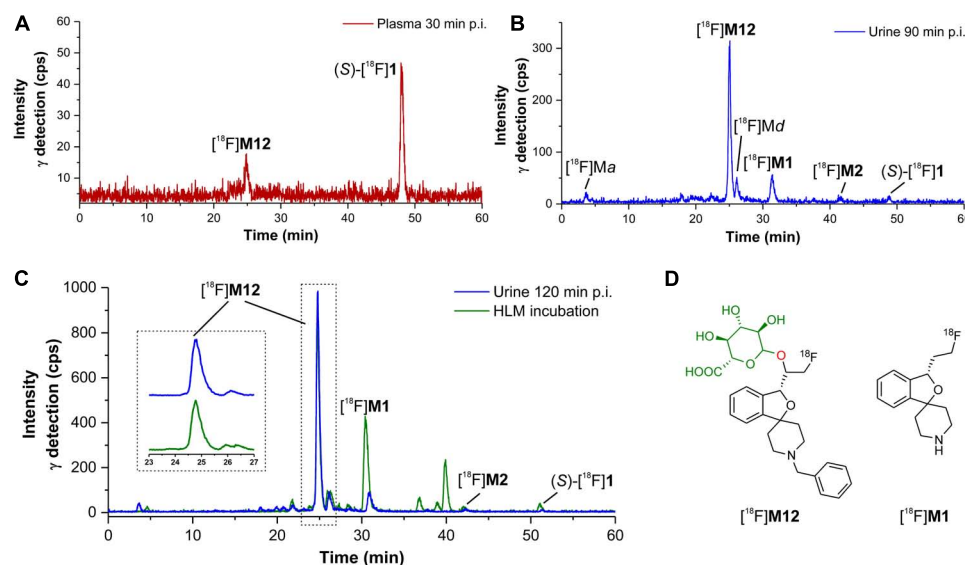


**FIGURE 14 |** Identification of radiometabolites of (S)-[<sup>18</sup>F]1 formed in humans (Sections “Investigation of the Metabolism of (S)-[<sup>18</sup>F]1 in Humans” and “Incubation of (S)-[<sup>18</sup>F]1 and Non-radioactive References for Identification of *in vitro* Metabolites and Radiometabolites”). **(A)** radio-HPLC chromatogram from plasma (30 min post injection). **(B)** radio-HPLC chromatogram from urine (90 min post injection). **(C)** comparison of radio-HPLC chromatograms from urine (120 min post injection) and HLM incubation (NADPH, UDPGA), including enlarged section. **(D)** structures of identified main radiometabolites formed in humans ([<sup>18</sup>F]M12: plasma and urine, [<sup>18</sup>F]M1: urine). All chromatograms were recorded using radio-HPLC system I (Section “Radio-HPLC”).

0.0–7.9% of the total activity due to the high fraction of excreted radiometabolites.

Metabolism rates have been reported for *rac*-[<sup>18</sup>F]1 or (S)-[<sup>18</sup>F]1 in mice, pigs, and monkeys. In mouse plasma the fraction of unchanged *rac*-[<sup>18</sup>F]1 was  $89 \pm 3\%$  at 30 min post injection (Wiese et al., 2016). For (S)-[<sup>18</sup>F]1 it was shown that in plasma of piglets 37% of the radioligand remained unchanged at 30 min post injection (Brust et al., 2014a). In rhesus monkeys (S)-[<sup>18</sup>F]1 still represented 50% of the total activity in plasma at the same time point (Baum et al., 2017), which is less than found for *rac*-[<sup>18</sup>F]1 in mice (89%). Surprisingly, the estimated value for (S)-[<sup>18</sup>F]1 in human plasma (91.0% at 30 min post injection) is in considerable accordance with published *in vivo* data from mice.

The obtained *in vitro* data (Section “Time- and Concentration-Dependent Microsomal Transformation”) could not predict the levels of (S)-[<sup>18</sup>F]1 in human plasma, due to further metabolic pathways beside CYP-mediated degradation, in particular conjugation with glucuronic acid (Section “Characterization of Radiometabolites Formed in Humans”) and resulting excretion.

### Characterization of Radiometabolites Formed in Humans

In **Figure 14** representative radio-HPLC chromatograms from plasma (A) and urine (B) samples are shown, obtained after administration of (S)-[<sup>18</sup>F]1. For characterization of radiometabolites the chromatograms from urine and HLM incubations (Section “Detection and structure elucidation of *in vitro* metabolites of (S)-1 by LC-MS/MS”) were compared (**Figure 14C**). Several previously characterized *in vitro*

radiometabolites are also formed *in vivo* in human. The main radiometabolite detected in urine and plasma was identified as the glucuronide conjugate [<sup>18</sup>F]M12, which was formed after hydroxylation at the fluoroethyl side chain (**Figure 14D**). In plasma [<sup>18</sup>F]M12 was the only radiometabolite detected and increased over time. As found after incubations with HLM, debenzoylation and to a very low extent also *N*-oxidation was observed resulting in [<sup>18</sup>F]M1 and [<sup>18</sup>F]M2, respectively. Further *in vivo* radiometabolites could not be identified with certainty, although found *in vitro*. For example, the fast eluting [<sup>18</sup>F]Ma most likely refers to [<sup>18</sup>F]fluoride, whereas [<sup>18</sup>F]Md might result from further glucuronide conjugates as discussed in Section “Identification of *in vitro* radiometabolites of (S)-[<sup>18</sup>F]1.”

Deduced from the retention behaviors in the radio-HPLC, no radiometabolite appeared to have a higher lipophilicity than (S)-[<sup>18</sup>F]1. Taking into account that in mouse brain 98% of *rac*-[<sup>18</sup>F]1 remained unchanged at 60 min post injection (Wiese et al., 2016), the absence of radiometabolites in human brain is highly likely as well.

### CONCLUSION

As demonstrated, radiometabolites of (S)-[<sup>18</sup>F]1 formed *in vivo* in humans could be characterized by means of *in vitro* investigations and LC-MS/MS. For that purpose HLM were used in presence of NADPH and UDPGA to generate metabolites of (S)-1 as well as the corresponding radiometabolites of (S)-[<sup>18</sup>F]1, which revealed to be relevant *in vivo*. Investigations by LC-MS/MS and comparison with obtained radio-HPLC data



showed that debenzoylation, hydroxylation at the fluoroethyl side chain, and a subsequent glucuronidation were predominant for metabolic degradation *in vitro*. Further, minor oxygenated metabolites were detected and characterized. Defluorination, which is a critical aspect of a radioligand and leads to non-specific accumulation of radioactivity in bone tissue resulting from <sup>18</sup>F-fluoride, was not observed. In human plasma unchanged (S)-[<sup>18</sup>F]**1** represented 91% of the total activity at 30 min post injection. Based on results obtained *in vitro*, formed radiometabolites could be characterized. Thus, hydroxylation at the fluoroethyl side chain of (S)-[<sup>18</sup>F]**1** and subsequent conjugation with glucuronic acid ([<sup>18</sup>F]**M12**) occurred as the main metabolic pathway in humans. Besides, debenzoylation of the molecule was observed ([<sup>18</sup>F]**M1**). Our metabolic study, in particular the high fractions of unchanged radioligand in plasma, confirms the suitability of (S)-[<sup>18</sup>F]fluspidine ((S)-[<sup>18</sup>F]**1**) as PET radioligand for sigma-1 receptor imaging.

## DATA AVAILABILITY

The raw data supporting the conclusions of this manuscript will be made available by the authors, without undue reservation, to any qualified researcher.

## ETHICS STATEMENT

The use of (S)-[<sup>18</sup>F]fluspidine ((S)-[<sup>18</sup>F]**1**) for human application was authorized by the competent authorities in Germany, the Federal Institute for Drugs and Medical Devices (Bundesamt für Arzneimittel und Medizinprodukte, BfArM) and the Federal Office for Radiation Protection (Bundesamt für Strahlenschutz, BfS) as well as by the local ethics committee. The study was conducted in accordance

with the Declaration of Helsinki. Informed consent was obtained from all healthy volunteers (age ≥ 18). All investigations were conducted in the framework of an approved and registered clinical study EudraCT-Nr.: 2014-005427-27.

## AUTHOR CONTRIBUTIONS

F-AL, SF, AH, WD-C, DS, MP, JS, BW, and PB conceived and designed the experiments. F-AL, SF, RH, MP, and FZ conducted the experiments. F-AL, SF, RH, and MP analyzed the data. F-AL, SF, RH, AH, DS, MP, PMM, SH, G-AB, FZ, JS, BW, OS, and PB wrote or contributed to the writing of the manuscript.

## FUNDING

The studies were financially supported by the German Research Foundation (Deutsche Forschungsgemeinschaft, DFG). DFG-GZ: 233201168, SA 669/11-1, WU 176/13-1 and STE 601/11-1.

## ACKNOWLEDGMENTS

We thank Dr. René Smits (ABX GmbH, Radeberg, Germany) for his support and scientific advice. We further thank Ms. Tina Spalholz for the conduction of microsomal incubations.

## SUPPLEMENTARY MATERIAL

The Supplementary Material for this article can be found online at: <https://www.frontiersin.org/articles/10.3389/fphar.2019.00534/full#supplementary-material>

## REFERENCES

- Amini, N., Nakao, R., Schou, M., and Halldin, C. (2013). Identification of PET radiometabolites by cytochrome P450, UHPLC/Q-ToF-MS and fast radio-LC: applied to the PET radioligands [<sup>11</sup>C]flumazenil, [<sup>18</sup>F]FE-PE2I, and [<sup>11</sup>C]PBR28. *Anal. Bioanal. Chem.* 405, 1303–1310. doi: 10.1007/s00216-012-6541-2
- Asha, S., and Vidyavathi, M. (2010). Role of human liver microsomes in *in vitro* metabolism of drugs—a review. *Appl. Biochem. Biotechnol.* 160, 1699–1722. doi: 10.1007/s12010-009-8689-6
- Barthel, H., Seibyl, J., and Sabri, O. (2015). The role of positron emission tomography imaging in understanding Alzheimer's disease. *Expert Rev. Neurother.* 15, 395–406. doi: 10.1586/14737175.2015.1023296
- Baum, E., Cai, Z., Bois, F., Holden, D., Lin, S.-F., Lara-Jaime, T., et al. (2017). PET imaging evaluation of four  $\sigma_1$  radiotracers in nonhuman primates. *J. Nucl. Med.* 58, 982–988. doi: 10.2967/jnumed.116.188052
- Bier, D., Holschbach, M. H., Wutz, W., Olsson, R. A., and Coenen, H. H. (2006). Metabolism of the A1 adenosine receptor positron emission tomography ligand [<sup>18</sup>F]8-cyclopentyl-3-(3-fluoropropyl)-1-propylxanthine ([<sup>18</sup>F]CPFPX) in rodents and humans. *Drug Metab. Disp.* 34, 570–576. doi: 10.1124/dmd.105.006411
- Brust, P., Deuther-Conrad, W., Becker, G., Patt, M., Donat, C. K., Stittsworth, S., et al. (2014a). Distinctive *in vivo* kinetics of the new  $\sigma_1$  receptor ligands (R)-(+)- and (S)-(–)-<sup>18</sup>F-fluspidine in porcine brain. *J. Nucl. Med.* 55, 1730–1736. doi: 10.2967/jnumed.114.137562
- Brust, P., van den Hoff, J., and Steinbach, J. (2014b). Development of <sup>18</sup>F-labeled radiotracers for neuroreceptor imaging with positron emission tomography. *Neurosci. Bull.* 30, 777–811. doi: 10.1007/s12264-014-1460-6
- Fischer, S., Wiese, C., Große Maestrup, E., Hiller, A., Deuther-Conrad, W., Scheunemann, M., et al. (2011). Molecular imaging of  $\sigma$  receptors: synthesis and evaluation of the potent  $\sigma_1$  selective radioligand [<sup>18</sup>F]fluspidine. *Eur. J. Nucl. Med. Mol. Imaging* 38, 540–551. doi: 10.1007/s00259-010-1658-z
- Fishback, J. A., Robson, M. J., Xu, Y.-T., and Matsumoto, R. R. (2010). Sigma receptors: potential targets for a new class of antidepressant drug. *Pharmacol. Ther.* 127, 271–282. doi: 10.1016/j.pharmthera.2010.04.003
- Fisher, M. B., Campanale, K., Ackermann, B. L., Vandenbranden, M., and Wrighton, S. A. (2000). *In vitro* glucuronidation using human liver microsomes and the pore-forming peptide alamethicin. *Drug Metab. Disp.* 28, 560–566.
- Große Maestrup, E., Wiese, C., Schepmann, D., Hiller, A., Fischer, S., Scheunemann, M., et al. (2009a). Synthesis of spirocyclic  $\sigma_1$  receptor ligands as potential PET radiotracers, structure-affinity relationships and *in vitro* metabolic stability. *Bioorg. Med. Chem.* 17, 3630–3641. doi: 10.1016/j.bmc.2009.03.060

- Große Mastrup, E., Fischer, S., Wiese, C., Schepmann, D., Hiller, A., Deuther-Conrad, W., et al. (2009b). Evaluation of spirocyclic 3-(3-Fluoropropyl)-2-benzofurans as  $\sigma_1$  receptor ligands for neuroimaging with positron emission tomography. *J. Med. Chem.* 52, 6062–6072. doi: 10.1021/jm900909e
- Große Mastrup, E., Wiese, C., Schepmann, D., Brust, P., and Wünsch, B. (2011). Synthesis, pharmacological activity and structure affinity relationships of spirocyclic  $\sigma_1$  receptor ligands with a (2-fluoroethyl) residue in 3-position. *Bioorg. Med. Chem.* 19, 393–405. doi: 10.1016/j.bmc.2010.11.013
- Holl, K., Falck, E., Köhler, J., Schepmann, D., Humpf, H.-U., Brust, P., et al. (2013). Synthesis, characterization, and metabolism studies of fluspidine enantiomers. *ChemMedChem* 8, 2047–2056. doi: 10.1002/cmdc.201300322
- Holl, K., Schepmann, D., Daniliuc, C. G., and Wünsch, B. (2014). Sharpless asymmetric dihydroxylation as the key step in the enantioselective synthesis of spirocyclic  $\sigma_1$  receptor ligands. *Tetrahedron: Asymmetry* 25, 268–277. doi: 10.1016/j.tetasy.2013.12.009
- Honer, M., Gobbi, L., Martarello, L., and Comley, R. A. (2014). Radioligand development for molecular imaging of the central nervous system with positron emission tomography. *Drug Discov. Today* 19, 1936–1944. doi: 10.1016/j.drudis.2014.08.012
- Jia, H., Zhang, Y., and Huang, Y. (2019). Imaging sigma receptors in the brain: new opportunities for diagnosis of Alzheimer's disease and therapeutic development. *Neurosci. Lett.* 691, 3–10. doi: 10.1016/j.neulet.2018.07.033
- Jia, J., Cheng, J., Wang, C., and Zhen, X. (2018). Sigma-1 receptor-modulated neuroinflammation in neurological diseases. *Front. Cell. Neurosci.* 12:314. doi: 10.3389/fncel.2018.00314
- Jia, L., and Liu, X. (2007). The conduct of drug metabolism studies considered good practice (II): in vitro experiments. *Curr. Drug Metab.* 8, 822–829. doi: 10.2174/138920007782798207
- Kranz, M., Sattler, B., Wüst, N., Deuther-Conrad, W., Patt, M., Meyer, P., et al. (2016). Evaluation of the enantiomer specific biokinetics and radiation doses of [<sup>18</sup>F]fluspidine—a new tracer in clinical translation for imaging of  $\sigma_1$  receptors. *Molecules* 21:1164. doi: 10.3390/molecules21091164
- Levsen, K., Schiebel, H.-M., Behnke, B., Dötzer, R., Dreher, W., Elend, M., et al. (2005). Structure elucidation of phase II metabolites by tandem mass spectrometry: an overview. *J. Chromatogr. A* 1067, 55–72. doi: 10.1016/j.chroma.2004.08.165
- Ludwig, F.-A., Fischer, S., Smits, R., Deuther-Conrad, W., Hoepping, A., Tiepolt, S., et al. (2018). Exploring the metabolism of (+)-[<sup>18</sup>F]Flubatine in vitro and in vivo: LC-MS/MS aided identification of radiometabolites in a clinical PET study. *Molecules* 23:E464. doi: 10.3390/molecules23020464
- Ludwig, F.-A., Smits, R., Fischer, S., Donat, C. K., Hoepping, A., Brust, P., et al. (2016). LC-MS supported studies on the in vitro metabolism of both enantiomers of flubatine and the in vivo metabolism of (+)-[<sup>18</sup>F]Flubatine—A positron emission tomography radioligand for imaging  $\alpha 4\beta 2$  nicotinic acetylcholine receptors. *Molecules* 21:1200. doi: 10.3390/molecules21091200
- Maier, C. A., and Wünsch, B. (2002a). Novel spiroperidines as highly potent and subtype selective  $\sigma$ -receptor ligands. Part 1. *J. Med. Chem.* 45, 438–448. doi: 10.1021/jm010992z
- Maier, C. A., and Wünsch, B. (2002b). Novel  $\sigma$  receptor ligands. Part 2. SAR of spiro[2]benzopyran-1,4'-piperidines and spiro[2]benzofuran-1,4'-piperidines with carbon substituents in position 3. *J. Med. Chem.* 45, 4923–4930. doi: 10.1021/jm020889p
- Maisonial, A., Große Mastrup, E., Fischer, S., Hiller, A., Scheunemann, M., Wiese, C., et al. (2011). A [<sup>18</sup>F]-labeled fluorobutyl-substituted spirocyclic piperidine derivative as a selective radioligand for PET imaging of  $\Sigma_{\text{M}}$  receptors. *ChemMedChem* 6, 1401–1410. doi: 10.1002/cmdc.201100108
- Maisonial, A., Große Mastrup, E., Wiese, C., Hiller, A., Schepmann, D., Fischer, S., et al. (2012). Synthesis, radiofluorination and pharmacological evaluation of a fluoromethyl spirocyclic PET tracer for central  $\sigma_1$  receptors and comparison with fluoroalkyl homologs. *Bioorg. Med. Chem.* 20, 257–269. doi: 10.1016/j.bmc.2011.11.002
- Maisonial-Beset, A., Funke, U., Wenzel, B., Fischer, S., Holl, K., Wünsch, B., et al. (2014). Automation of the radiosynthesis and purification procedures for [<sup>18</sup>F]Fluspidine preparation, a new radiotracer for clinical investigations in PET imaging of  $\sigma_1$  receptors in brain. *Appl. Rad. Isot.* 84, 1–7. doi: 10.1016/j.apradiso.2013.10.015
- Maurice, T., and Gogvadze, N. (2017). Role of sigma1 receptors in learning and memory and Alzheimer's disease-type dementia. *Adv. Exp. Med. Biol.* 964, 213–233. doi: 10.1007/978-3-319-50174-1\_15
- Nakane, S., Yoshinaka, S., Iwase, S., Shuto, Y., Bunse, P., Wünsch, B., et al. (2018). Synthesis of fluspidine via asymmetric NaBH<sub>4</sub> reduction of silicon enolates of  $\beta$ -keto esters. *Tetrahedron* 74, 5069–5084. doi: 10.1016/j.tet.2018.04.005
- Pawelke, B. (2005). Metabolite analysis in positron emission tomography studies: examples from food sciences. *Amino Acids* 29, 377–388. doi: 10.1007/s00726-005-0202-0
- Penke, B., Fulop, L., Szucs, M., and Frecska, E. (2018). The role of sigma-1 receptor, an intracellular chaperone in neurodegenerative diseases. *Curr. Neuropharmacol.* 16, 97–116. doi: 10.2174/1570159X15666170529104323
- Rousseaux, C. G., and Greene, S. F. (2015). Sigma receptors [ $\sigma$ R]: biology in normal and diseased states. *J. Recept. Sig. Transduct. Res.* 36, 327–388. doi: 10.3109/10799893.2015.1015737
- Song, T., Han, X., Du, L., Che, J., Liu, J., Shi, S., et al. (2018). The role of neuroimaging in the diagnosis and treatment of depressive disorder: a recent review. *Curr. Pharm. Des.* 24, 2515–2523. doi: 10.2174/1381612824666180727111142
- Stracina, T., and Novakova, M. (2018). Cardiac sigma receptors - an update. *Physiol. Res.* 67, S561–S576.
- Tesei, A., Cortesi, M., Zamagni, A., Arienti, C., Pignatta, S., Zanoni, M., et al. (2018). Sigma receptors as endoplasmic reticulum stress “gatekeepers” and their modulators as emerging new weapons in the fight against cancer. *Front. Pharmacol.* 9:711. doi: 10.3389/fphar.2018.00711
- Weber, F., Brust, P., Laurini, E., Priel, S., and Wünsch, B. (2017). Fluorinated PET tracers for molecular imaging of  $\sigma_1$  receptors in the central nervous system. *Adv. Exp. Med. Biol.* 964, 31–48. doi: 10.1007/978-3-319-50174-1\_4
- Wiese, C., Große Mastrup, E., Galla, F., Schepmann, D., Hiller, A., Fischer, S., et al. (2016). Comparison of in silico, electrochemical, in vitro and in vivo metabolism of a homologous series of (Radio)fluorinated  $\sigma_1$  receptor ligands designed for positron emission tomography. *ChemMedChem* 11, 2445–2458. doi: 10.1002/cmdc.201600366
- Xu, X., Ziegler, R. G., Waterhouse, D. J., Saavedra, J. E., and Keefer, L. K. (2002). Stable isotope dilution high-performance liquid chromatography-electrospray ionization mass spectrometry method for endogenous 2- and 4-hydroxysterones in human urine. *J. Chromatogr. B* 780, 315–330. doi: 10.1016/S1570-0232(02)00539-1
- Yilmazer, M., Stevens, J. F., and Buhler, D. R. (2001). In vitro glucuronidation of xanthohumol, a flavonoid in hop and beer, by Rat and human liver microsomes. *FEBS Lett.* 491, 252–256. doi: 10.1016/S0014-5793(01)02210-4

**Conflict of Interest Statement:** AH is employed by company ABX advanced biochemical compounds GmbH.

The remaining authors declare that the research was conducted in the absence of any commercial or financial relationships that could be construed as a potential conflict of interest.

Copyright © 2019 Ludwig, Fischer, Houska, Hoepping, Deuther-Conrad, Schepmann, Patt, Meyer, Hesse, Becker, Zientek, Steinbach, Wünsch, Sabri and Brust. This is an open-access article distributed under the terms of the Creative Commons Attribution License (CC BY). The use, distribution or reproduction in other forums is permitted, provided the original author(s) and the copyright owner(s) are credited and that the original publication in this journal is cited, in accordance with accepted academic practice. No use, distribution or reproduction is permitted which does not comply with these terms.



# Role of Sigma Receptors in Alcohol Addiction

Sema G. Quadir, Pietro Cottone and Valentina Sabino\*

Laboratory of Addictive Disorders, Departments of Pharmacology and Psychiatry, Boston University School of Medicine, Boston, MA, United States

## OPEN ACCESS

### Edited by:

Ebru Aydar,  
University College London,  
United Kingdom

### Reviewed by:

Elena Martín-García,  
Universidad Pompeu Fabra,  
Spain  
Carlo Cifani,  
University of Camerino, Italy  
Sheketha R. Hauser,  
Indiana University Bloomington,  
United States

### \*Correspondence:

Valentina Sabino  
vsabino@bu.edu

### Specialty section:

This article was submitted to  
Experimental Pharmacology  
and Drug Discovery,  
a section of the journal  
Frontiers in Pharmacology

Received: 08 February 2019

Accepted: 27 May 2019

Published: 14 June 2019

### Citation:

Quadir SG, Cottone P and Sabino V  
(2019) Role of Sigma Receptors  
in Alcohol Addiction.  
Front. Pharmacol. 10:687.  
doi: 10.3389/fphar.2019.00687

Pharmacological treatments for alcohol use disorder (AUD) are few in number and often ineffective, despite the significant research carried out so far to better comprehend the neurochemical underpinnings of the disease. Hence, research has been directed towards the discovery of novel therapeutic targets for the treatment of AUD. In the last decade, the sigma receptor system has been proposed as a potential mediator of alcohol reward and reinforcement. Preclinical studies have shown that the motivational effects of alcohol and excessive ethanol consumption involve the recruitment of the sigma receptor system. Furthermore, sigma receptor antagonism has been shown to be sufficient to inhibit many behaviors related to AUDs. This paper will review the most current evidence in support of this receptor system as a potential target for the development of pharmacological agents for the treatment of alcohol addiction.

**Keywords:** alcoholism, drinking, dependence, ethanol, consumption

## INTRODUCTION

Alcohol is the most ubiquitously consumed mind-altering substance in the world, and it is considered responsible for 25% of the mortality in people aged 20–30. The lifetime prevalence of alcohol use disorder (AUD) in the United States is estimated to be 29.1% (Hasin et al., 2007; Grant et al., 2015).

AUD is a multifactorial complex disorder with multiple genes and environmental factors interacting to produce the phenotype of addiction (Koob and Le Moal, 2005). **Table 1** illustrates the 11 diagnostic criteria of AUD according to the most recent edition of the *Diagnostic and Statistical Manual of Mental Disorders, Fifth Edition* (DSM-V) (American Psychiatric Association, 2013). Notably, while tolerance and withdrawal were already among the criteria in previous editions, this edition includes craving for the first time, likely to convey the importance of behavioral over pharmacological components.

The negative impact of alcohol on health makes the discovery of novel potential therapeutic targets for AUD the subject of extensive research. One of these has been identified in Sigma receptors (Sig-Rs). Two subtypes of Sig-Rs have been identified, sigma-1 receptor (Sig-1R) and sigma-2 receptor (Sig-2R); this review will focus exclusively on the available evidence concerning Sig-1R. Indeed, since Sig-2R was only cloned in 2017 (Alon et al., 2017), very few selective ligands have been available and, therefore, most evidence in the context of alcohol and other addictions has been obtained using either non-selective Sig-1R/Sig-2R or Sig-1R selective ligands. Specifically, we will summarize research showing that manipulations of Sig-1R impact ethanol-induced changes in locomotor function, acquisition and expression of conditioned place preference (CPP), alcohol consumption and seeking behavior, and reinstatement of alcohol-seeking behavior, as well as deficits in cognitive function induced by alcohol.

**TABLE 1 |** Alcohol use disorder (AUD) diagnostic criteria.

Category	Criteria	Description
Impaired control	C1	Drinking more than intended
	C2	Unable to cut down or stop drinking
	C3	Spending a lot of time drinking or recovering from drinking
	C4	Wanting a drink so badly you can't think of anything else (craving)
Social impairment	C5	Drinking interferes with home, family, job, or school
	C6	Drinking even though it causes trouble with friends or family
	C7	Giving up on important activities to drink instead
Risky use	C8	Drinking and getting into situations that increase chances of getting hurt
	C9	Continuing to drink despite becoming anxious, depressed, or experiencing memory blackout
Pharmacological indicators	C10	Needing to drink more to feel the same effect (tolerance)
	C11	Experiencing withdrawal symptoms such as restlessness, nausea, seizures, and hallucinations

The 11 criteria used to characterize AUD can be divided into four categories—impaired control, social impairment, risky use, and pharmacological indicators. Severity of AUD is defined by the number of symptoms present (2–3: mild, 4–5: moderate, 6 or more: severe) (American Psychiatric Association, 2013).

## Sigma Receptors

Two subtypes of Sig-Rs have been described: Sig-1R and Sig-2R. While both are sensitive to haloperidol and 1,3-di(2-tolyl) guanidine, Sig-1Rs are more sensitive to benzomorphans such as (+)-SKF-10,047, dextromethorphan, and carbetapentane (Bouchard and Quirion, 1997). In addition, the two receptor subtypes differ in size, with Sig-1R having a larger molecular weight (Alon et al., 2017). Proposed endogenous ligands include N,N-dimethyltryptamine and neurosteroids (Fontanilla et al., 2009); interestingly, psychostimulants, such as cocaine, lidocaine, and methamphetamine, have all been shown to bind Sig-1R, although with rather weak affinity (Sharkey et al., 1988; Nguyen et al., 2005).

### Sig-1R Structure and Localization

Sig-1R is a 25–29 kDa protein encoded by the *SIGMAR1* gene (Prasad et al., 1998). In 2016, Schmidt and colleagues solved the crystal structure of human Sig-1R and found it to be a trimer, with each protomer containing one transmembrane domain (Schmidt et al., 2016). The gene that encodes the human Sig-1R is found on band p13 of chromosome 9 and is ~7 kbp long, coding four exons (encoding a 25.3 kDa protein) and three introns (Aydar et al., 2002; Matsumoto et al., 2003). Although Sig-1R shows no homology with any other known mammalian proteins, Sig-1R shares 30% identity and 67% similarity with a yeast sterol isomerase, consistent with the observation that sterol-producing tissues have high levels of Sig-1R mRNA (Balasuriya et al., 2012).

Sig-1Rs are found both intracellularly and on the plasma membrane (Aydar et al., 2002). Specifically, they have been shown to be extensively associated with cholesterol-enriched loci on the endoplasmic reticulum, as well as on the

mitochondrion-associated endoplasmic reticulum membrane (Alonso et al., 2000; Hayashi and Su, 2001; Hayashi and Su, 2003). Upon activation, the receptors move laterally toward the periphery of the cell (Hayashi and Su, 2003). Sig-1Rs have been shown to be in cell bodies and on dendrites, but not on axon terminals or fibers table (Alonso et al., 2000).

### Receptor signaling

Sig-1R has been shown to associate with a variety of proteins such as ankyrin B, heat shock protein 70, phospholipase C, and thus protein kinase C (PKC), protein kinase A, and glucose-related protein/immunoglobulin heavy-chain-binding protein, among others (Morin-Surun et al., 1999; Hayashi and Su, 2001; Matsumoto et al., 2003; Hayashi and Su, 2007; Kim et al., 2008). In addition, Sig-1Rs modulate voltage-gated ion channels, such as the N-type  $\text{Ca}^{2+}$  channel, Nav1.5, Kv1.2, Kv1.3, Kv1.4, and Kv1.5 (Aydar et al., 2002; Balasuriya et al., 2012; Kinoshita et al., 2012; Kourrich et al., 2013; Liu et al., 2017; Zhang et al., 2017). While Sig-1Rs are not G-protein coupled, they physically associate with certain G-protein coupled receptors, such as mu opioid and dopamine D1 and D2 receptors, modulating their activity (Kim et al., 2010; Navarro et al., 2010; Navarro et al., 2013). Additional studies determined that Sig-1R also modulates dopamine transporters (Hong et al., 2017).

Sig-1R activation has been shown to potentiate N-methyl-D-aspartate receptor (NMDAR)-induced  $\text{Ca}^{2+}$  influx, mainly through the facilitation of PKC-mediated phosphorylation of the GluN1 subunit (Roh et al., 2011). Sig-1R activation has also been linked to increased GluN2a, GluN2b, and postsynaptic density protein 95 expression, as well as to NMDAR subunit redistribution and increased NMDAR trafficking to the synapse (Pabba et al., 2014). In addition, Sig-1R activation potentiates the release of several neurotransmitters, such as acetylcholine, dopamine, and brain-derived neurotrophic factor (Ault and Werling, 1997; Matsuno et al., 1997; Fujimoto et al., 2012), all of which are perturbed in AUD (Moykkynen and Korpi, 2012; Engel and Jerlhag, 2014; Wu et al., 2014). This indicates Sig-1R as a critically important target for the study of AUD.

### Sigma Receptors and Locomotor Effects of Alcohol

At low doses, alcohol stimulates locomotor activity (Risinger and Oakes, 1996). This activation, which is thought to occur through the stimulation of the mesolimbic system, is hypothesized to be an index of its abuse liability (Phillips and Shen, 1996).

The role of Sig-1R in alcohol-induced locomotion has been studied in mice. Although Sig-1R agonists and antagonists *per se* fail to influence locomotor activity, Maurice and colleagues demonstrated that Sig-1R blockade *via* the selective antagonist N-[2-(3,4-dichlorophenyl)ethyl]-N-methyl-2-(dimethylamino) ethylamine (BD-1047) inhibits the increase in locomotor activity induced by 1 g/kg of ethanol, in a dose-dependent manner (Maurice et al., 2003). However, treatment with the Sig-1R selective agonist 2-(4-morpholine) ethyl 1-phenylcyclohexanecarboxylate (PRE-084) fails to influence alcohol-induced locomotion (Maurice, 2003). This could be indicative of



Sig-1R antagonists decreasing the response of the mesolimbic dopamine system. Interestingly, Sig-1R agonists have been shown to increase cocaine and methamphetamine-induced locomotor activity, while antagonists have been shown to decrease this response (Takahashi et al., 2000; Liu and Matsumoto, 2008). The reason why Sig-1R agonists increase cocaine and methamphetamine-induced locomotor activity but fail to influence alcohol-induced locomotor activity is unclear, and it may be related to the specific mechanisms of action of psychostimulants.

Despite the fact that ethanol-induced locomotion stimulation is easily observed in Swiss mice, C57BL/6J mice are not as sensitive to the stimulatory effects of ethanol (Becker and Hale, 1989; Maurice et al., 2003; Valenza et al., 2016). To unmask the sedative effects of alcohol in C57BL/6J mice, ethanol is often co-administered with the benzodiazepine partial inverse agonist RO15-4513 (Becker and Hale, 1989). Valenza and colleagues (2016) employed this technique to examine the stimulatory effects in C57BL/6J lacking the *SIGMAR1* gene, which encodes the Sig-1R. Sig-1R KO mice were found to be less sensitive to the locomotor stimulating effects of 1.5 g/kg alcohol when compared to WT (Valenza et al., 2016). As the stimulant effects of alcohol are thought to be related to its motivational and rewarding properties (Phillips and Shen, 1996), the reduced sensitivity of Sig-1R KO mice to the stimulant effects of alcohol may reflect a reduced sensitivity to its motivational effects, which may, in turn, be responsible for their increased alcohol intake (i.e., higher amounts of alcohol required to feel euphoric effects) (Valenza et al., 2016).

At high doses, alcohol acts as a central nervous system depressant. A single study investigated the effects of Sig-1R ligands on ethanol-induced sedation and found that Sig-1R KO do not differ from WT in either loss of righting reflex or sleep duration, suggesting that Sig-1R is not involved in the sedative effects of ethanol (Valenza et al., 2016). These studies corroborate the notion that Sig-1Rs are involved in the stimulatory, but not the sedating, effects of ethanol.

## Sigma Receptors and the Rewarding Properties of Alcohol

One of the most common tests to examine the rewarding properties of substances in animals is the place conditioning paradigm. The systemic administration of the selective Sig-1R agonist PRE-084 prior to ethanol enhances ethanol-induced CPP (Maurice et al., 2003). Studies using intracerebroventricular administration of the same agonist also showed a facilitation of the acquisition of ethanol-induced CPP (Bhutada et al., 2012). Moreover, pretreatment with the Sig-1R antagonist BD-1047, administered during conditioning, blocks the acquisition of ethanol-induced CPP (Maurice et al., 2003), while its intracerebroventricular administration has been shown to reduce both acquisition and expression (Bhutada et al., 2012). Lastly, neither Sig-1R agonists nor antagonists affect place preference when administered alone (Romieu et al., 2000; Maurice et al., 2003). Altogether, these studies show that Sig-Rs bidirectionally modulate the rewarding properties of alcohol.

## Sigma Receptors and Alcohol Drinking

Evidence from both human and animal studies strongly implicates Sig-1Rs involvement in alcohol drinking. In relation to preclinical studies, these have all been performed in rodents and they can be divided into two types: passive home cage alcohol drinking studies and active operant alcohol self-administration studies.

### Home Cage Alcohol Drinking

Many home cage drinking studies have been performed in The Scripps Research Institute (TSRI) Sardinian alcohol-preferring rats (Scr:sP), a line that descends directly from Sardinian alcohol preferring rats, which were selectively bred to drink high amounts of alcohol (Colombo et al., 2006; Sabino et al., 2013). Ethanol-naïve Scr:sP rats have elevated Sig-1R levels in the NAcc when compared to ethanol-naïve outbred Wistar rats (Blasio et al., 2015). After 4 weeks of voluntary ethanol consumption, Sig-1R levels in the NAcc of Scr:sP rats returned back to baseline, suggesting that this could be a mechanism for the reduced motivation to drink after chronic drinking (Blasio et al., 2015). Interestingly, the changes in protein level only occurred in the NAcc and not in the central nucleus of the amygdala, perhaps implicating the mesolimbic dopaminergic system (Blasio et al., 2015). This is consistent with previous studies demonstrating the modulation of dopaminergic neurotransmission by Sig-1Rs (Ault and Werling, 1999; Navarro et al., 2010; Navarro et al., 2013). In line with these findings, the selective Sig-1R antagonists NE-100 and BD-1063 both reduce ethanol home cage drinking in Scr:sP rats, without affecting total fluid intake or food intake (Sabino et al., 2009b; Blasio et al., 2015). NE-100 also fails to affect food intake or sucrose preference, suggesting that the effects of the drug are selective for alcohol (Sabino et al., 2009b). However, in that study, rats developed tolerance to NE-100 treatment within 1 week, similar to opioid receptor antagonist treatments (Overstreet et al., 1999; Sabino et al., 2009b).

Sig-1R KO mice exhibit increased alcohol preference and drink more alcohol compared to WT mice (Sabino et al., 2009b; Valenza et al., 2016). The effect observed is specific for alcohol, as genotypes did not differ in their intake or preference for either the bitter tasting quinine or the sweet tasting saccharin, ruling out altered taste perception (Valenza et al., 2016). The data obtained in Sig-1R KO may appear counterintuitive and in contrast with the general hypothesis that Sig-1R hyperactivity contributes to excessive ethanol intake. However, it is possible that developmental compensatory changes in expression of other genes may occur in Sig-1R KO mice, e.g., an up-regulation of Sig-2Rs, which may explain some of the observed effects.

### Operant Alcohol Self-Administration

A method used to assess the reinforcing properties of alcohol is the use of operant conditioning, where rodents must lever press in order to obtain alcohol. Sig-R activation *via* daily systemic treatment of the Sig-1R/Sig-2R agonist 1,3-di-(2-tolyl)guanidine (DTG) is able to induce binge-like drinking (defined as blood

alcohol concentration >80 mg/dl) in Scr:sP rats under a fixed ratio 1 ratio of reinforcement, effect blocked by the selective Sig-1R antagonist BD-1063 (Sabino et al., 2011). Consistent with a bidirectional modulation of alcohol self-administration, treatment with the selective Sig-1R antagonist BD-1063 decreases ethanol responding in Scr:sP rats in a dose-dependent manner (Sabino et al., 2009a).

Another schedule of reinforcement widely used in psychopharmacological research on alcohol is the progressive ratio schedule of reinforcement, which allows studying subjects' motivation to obtain the reinforcer (Hodos, 1961). Daily systemic treatment of DTG increases, whereas acute BD-1063 administration decreases, the breakpoint for alcohol in Scr:sP rats, thus demonstrating the bi-directional role of Sig-1R also in modulating the motivational properties of ethanol (Sabino et al., 2009a; Sabino et al., 2011).

Additional studies examined the role of Sig-1R in alcohol dependence in Wistar rats. Dependence was induced *via* chronic intermittent ethanol (CIE) vapor exposure, and this method has been shown to result in high blood alcohol levels (150–200 mg%), compulsive drinking, elevated anxiety, and increased ethanol intake during withdrawal (for review, see Vendruscolo and Roberts, 2014). Pretreatment with the selective Sig-1R antagonist BD-1063 reduces ethanol self-administration in dependent, but not in non-dependent, outbred Wistar rats, without affecting water or saccharin intake, suggesting that Sig-1Rs modulate both genetic and environmental excessive drinking (Sabino et al., 2009a). In addition, compared to ethanol naïve Wistar rats, ethanol-dependent Wistar rats during acute withdrawal and ethanol naïve Scr:sP rats had significantly less Sig-1R mRNA in the NAcc, indicating that repeated cycles of intoxication followed by withdrawal mirror the phenotype observed in Scr:sP rats (Sabino et al., 2009a).

Lastly, repeated DTG administration in Scr:sP rats results in an increase in  $\mu$ - and  $\delta$ -opioid receptor gene expression in the ventral tegmental area (VTA) (Sabino et al., 2011), indicating that Sig-R activation may lead to disinhibition of the mesolimbic dopaminergic VTA-NAcc pathway, resulting in increased dopamine release and increased reward sensitivity.

## Sigma Receptors and Relapse-Like Behaviors

Relapse after abstinence remains one of the most problematic barriers to treating AUDs. Cravings, or tenacious urges, to drink alcohol or engage in alcohol-seeking behaviors often occur during periods of abstinence and result in relapse (Martin-Fardon and Weiss, 2013). In rodents, this may be modeled by exposing animals to alcohol, then forcing them to abstain for a period of time, and lastly presenting alcohol again. Under these conditions, vehicle-treated abstinent Scr:sP rats dramatically increase their ethanol intake upon renewed presentation of alcohol, and blocking Sig-1R with the selective Sig-1R antagonist NE-100 blocks this ethanol deprivation effect (Sabino et al., 2009b). This study thus paves the way for more research into the role of Sig-1R in behaviors related to alcohol-seeking and relapse.

Another procedure is the priming-induced alcohol-seeking method, which mimics the human condition known as “one drink, one drunk,” initially described by Jellinek and later validated by Hodgson and colleagues (Jellinek, 1952; Hodgson et al., 1979). In the context of reinstatement of ethanol-induced CPP, the administration of the selective Sig-1R agonist PRE-084 intracerebroventricularly was shown to be sufficient to induce reinstatement (Bhutada et al., 2012). Furthermore, pretreatment with the Sig-1R antagonist BD-1047 dose-dependently blocks both ethanol-induced and PRE-084-induced reinstatement, thus confirming that Sig-1R activation is required for priming-induced reinstatement (Bhutada et al., 2012).

Another important factor for relapse is the powerful effect that drug-paired cues exert on behavior. Selectively antagonizing Sig-1R with BD-1047 blocks reinstatement induced by ethanol- or palatable food-associated cues (Martin-Fardon et al., 2012), thus indicating that this modulation is not specific to drug reward as it also applies to seeking behavior for highly palatable food. In a seeking-taking chained second-order schedule of reinforcement, in which an alcohol-associated incentive stimulus maintains alcohol-seeking behavior (Everitt, 2014), the Sig-1R selective antagonist BD-1063 dose-dependently reduces alcohol-seeking behavior (Blasio et al., 2015), suggesting a role for Sig-1R in incentive motivational mechanisms controlling ethanol-seeking and intake. Together, these studies provide insight into the critical role of the Sig-1R system in relapse-related behaviors.

## Sigma Receptors and Cognitive Impairment During Alcohol Withdrawal

Withdrawal after chronic alcohol consumption has been linked to deficits in cognitive function in human subjects (Sabia et al., 2011). While the Sig-R system has been highly implicated in cognitive function (Matsuno et al., 1997), only few studies have examined the putative role of Sig-R system in chronic alcohol-induced cognitive impairment.

Using the novel object recognition task, Meunier and colleagues (2006) assessed cognitive function during protracted withdrawal in mice that had undergone chronic alcohol consumption (4 months). Alcohol withdrawn mice showed increased anxiety-like behaviors, elevated locomotion, and impaired object recognition; systemic administration of either the Sig-1R selective antagonist BD-1047 or the selective agonist igmesine is able to restore the habituation response (defined as decreased interactions with previously presented objects), but only the latter corrected reactions to spatial change and novelty (Meunier et al., 2006). These mice also show upregulated hippocampal Sig-1R expression, which normalized after repeated administration of either Sig-1R ligand (Meunier et al., 2006), indicating that Sig-1R levels may be responsible for the cognitive deficits seen in alcohol withdrawal.

Although the object recognition task provides direct evidence for the role of Sig-1R in cognition, other studies have used slice electrophysiology to examine the role of Sig-1Rs in hippocampal long-term potentiation (LTP). Initial studies that investigated the effect of CIE *via* vapor on LTP development

in stimulatory CA1 synapses found juvenile rats in withdrawal from CIE vapors and increased NMDAR independence compared to their non-CIE vapor-treated counterparts (Sabeti and Gruol, 2008). Furthermore, this increase in NMDAR independence in LTP is blocked by administration of the Sig-1R antagonist BD-1047, thus providing evidence for the role of the Sig-1R.

Subsequent studies found that early adolescent CIE vapor rats in withdrawal show depressed LTP excitability after high amplitude stimulus compared to controls (Sabeti, 2011). The decreases in action potential spike amplitude and excitatory postsynaptic potentiation in these subjects are reverted back to normal values by the Sig-1R antagonist BD-1047, suggesting that alcohol withdrawal may activate Sig-1Rs and therefore dampen the excitatory inputs during LTP (Sabeti, 2011). A recent study found that the decreased levels of neuron-specific nuclear protein/Fox-03 caused by CIE application to hippocampal explants can be reversed by treatment with the Sig-1R antagonist BD-1047 (Reynolds et al., 2016).

Together, these results indicate a strong role for Sig-1Rs in alcohol withdrawal-related neuroadaptations and symptomatology.

## Limitations

The studies reviewed in this manuscript have all focused on preclinical work performed in rodents. However, it is important

to note that many of the studies involve animals consuming high amounts of alcohol and, therefore, caution should be exerted before extrapolating the results to humans. A single human study has so far shown a possible role for Sig-1R in AUD, specifically that a Japanese population of alcoholic subjects display three polymorphisms in the 5' untranslated region of the gene coding Sig-1Rs (*SIGMAR1*) that are highly associated with alcoholism (Miyatake et al., 2004). Additional human studies are indeed warranted to confirm that the rodent studies mentioned in this review have a translational value.

It is also important to note that all of the studies described in this review were performed in male animals. Since some neurobiological mechanisms of AUD are sexually dimorphic and alcohol use does differ between men and women (Erol and Karpyak, 2015), further studies hold potential for providing essential information regarding this gap.

## Concluding Remarks

The Sig-R system is proving to be a promising pharmacological target for AUD treatment. In various animal models, Sig-1R antagonists reduce alcohol consumption, motivation to drink, and alcohol-seeking behavior, demonstrating a critical role for Sig-1Rs in these behaviors (see Table 2). Since current Food and Drug Administration (FDA)-approved medications for AUD, i.e., disulfiram, naltrexone, and acamprosate, have been shown to have limited efficacy, Sig-1R targeting drugs could represent

**TABLE 2 |** Summary of the pharmacological findings included in this review.

Behavior	Drug type	Results	Citation
Locomotor	Antagonist (BD-1047)	Inhibited ethanol-induced (1 g/kg) locomotor activity	(Maurice et al., 2003)
	Agonist (PRE-084)	No effect on ethanol-induced (0.5 g/kg) locomotor activity	(Maurice et al., 2003)
	Genetic KO	Inhibited ethanol-induced (1.5 g/kg) locomotor activity	(Valenza et al., 2016)
	Genetic KO	No differences in sedative effects of alcohol	(Valenza et al., 2016)
Rewarding properties	Agonist (PRE-084)	Enhanced CPP	(Bhutada et al., 2012; Maurice et al., 2003)
Home cage drinking	Antagonist (BD-1047)	Diminished CPP	(Bhutada et al., 2012)
	Antagonist (NE-100)	Reduced ethanol intake	(Sabino et al., 2009b)
	Antagonist (BD-1063)	Reduced ethanol intake	(Blasio et al., 2015)
	Genetic KO	Increased ethanol intake and preference	(Valenza et al., 2016)
Operant self-administration	Agonist (DTG)	Induce binge-like drinking	(Sabino et al., 2011)
	Antagonist (BD-1063)	Reduced ethanol intake	(Sabino et al., 2009a)
Motivation to drink	Agonist (DTG)	Increased breakpoint	(Sabino et al., 2011)
	Antagonist (BD-1063)	Decreased breakpoint	(Sabino et al., 2009a)
Alcohol deprivation effect	Antagonist (NE-100)	Inhibited alcohol deprivation effect	(Sabino et al., 2009b)
Reinstatement of CPP	Agonist (PRE-084)	Induced CPP	(Bhutada et al., 2012)
	Antagonist (BD-1047)	Inhibited ethanol and PRE-084-induced reinstatement	(Bhutada et al., 2012)
Reinstatement of operant behavior	Antagonist (BD-1047)	Inhibited reinstatement of both food and alcohol cue-induced reinstatement	(Martin-Fardon et al., 2012)
Seeking-taking chained schedule of reinforcement	Antagonist (BD-1063)	Reduced alcohol-seeking	(Blasio et al., 2015)
Cognitive impairment during alcohol withdrawal	Agonist (igmesine)	Restored cognitive responses in withdrawn mice	(Meunier et al., 2006)
	Antagonist (BD-1047)	Restored cognitive responses in withdrawn mice	(Meunier et al., 2006)
LTP	Antagonist (BD-1047)	Blocks increase in NMDAR-independent LTP seen in withdrawn rats	(Sabeti and Gruol, 2008)
	Antagonist (BD-1047)	Blocks action potential spike amplitude and excitatory post-synaptic potentiation in withdrawn rats	(Sabeti, 2011)

This table summarizes the major findings presented.

BD-1047, N-[2-(3,4-dichlorophenyl)ethyl]-N-methyl-2-(dimethylamino)ethylamine; PRE-084, 2-(4-morpholine) ethyl 1-phenylcyclohexane-1-carboxylate; KO, sigma-1 knockout; NMDAR, N-methyl-D-aspartate receptor; LTP, long-term potentiation; BD-1063, 1-[2-(3,4-dichlorophenyl)ethyl]-4-methylpiperazine; NE-100, 4-methoxy-3-(2-phenylethoxy)-N,N-dipropylbenzeneethanamine; CPP, conditioned place preference; DTG, 1,3-Di-o-tolylguanidine.



a promising therapeutic option. Yet, the precise routes of action through which the Sig-1R system impacts alcohol's effects are unknown, and therefore, additional studies to unveil these mechanisms and the relationship between Sig-1R and alcohol will be vital to comprehending AUD from a neurobiological standpoint and developing novel and more efficacious pharmacological therapeutics.

## AUTHOR CONTRIBUTIONS

All authors made substantial contributions to conception and design of this review. SQ drafted the manuscript. VS and PC

substantially and critically revised it for intellectual content. All authors gave final approval for its submission.

## FUNDING

This work was supported by the National Institutes on Alcohol Abuse and Alcoholism [grant numbers AA024439 (VS), AA025038 (VS), and AA026051 (PC)] and the Burroughs Wellcome Fund (SQ) through the Transformative Training Program in Addiction Sciences. Its contents are solely the responsibility of the authors and do not necessarily represent the official views of the National Institutes of Health.

## REFERENCES

- Alon, A., Schmidt, H. R., Wood, M. D., Sahn, J. J., Martin, S. F., and Kruse, A. C. (2017). Identification of the gene that codes for the sigma2 receptor. *Proc. Natl. Acad. Sci. U.S.A.* 114, 7160–7165. doi: 10.1073/pnas.1705154114
- Alonso, G., Phan, V., Guillemain, I., Saunier, M., Legrand, A., Anoa, M., et al. (2000). Immunocytochemical localization of the sigma(1) receptor in the adult rat central nervous system. *Neuroscience* 97, 155–170. doi: 10.1016/S0306-4522(00)00014-2
- American Psychiatric Association (2013). *Alcohol use disorder*. Washington, DC: American Psychiatric Association
- Ault, D. T., and Werling, L. L. (1997). Differential modulation of NMDA-stimulated [3H]dopamine release from rat striatum by neuropeptide Y and sigma receptor ligands. *Brain Res.* 760, 210–217. doi: 10.1016/S0006-8993(97)00283-7
- Ault, D. T., and Werling, L. L. (1999). Phencyclidine and dizocilpine modulate dopamine release from rat nucleus accumbens via sigma receptors. *Eur. J. Pharmacol.* 386, 145–153. doi: 10.1016/S0014-2999(99)00769-4
- Aydar, E., Palmer, C. P., Klyachko, V. A., and Jackson, M. B. (2002). The sigma receptor as a ligand-regulated auxiliary potassium channel subunit. *Neuron* 34, 399–410. doi: 10.1016/S0896-6273(02)00677-3
- Balasuriya, D., Stewart, A. P., Crottes, D., Borgese, F., Soriani, O., and Edwardson, J. M. (2012). The sigma-1 receptor binds to the Nav1.5 voltage-gated Na<sup>+</sup> channel with 4-fold symmetry. *J. Biol. Chem.* 287, 37021–37029. doi: 10.1074/jbc.M112.382077
- Becker, H. C., and Hale, R. L. (1989). Ethanol-induced locomotor stimulation in C57BL/6 mice following RO15-4513 administration. *Psychopharmacology* 99, 333–336. doi: 10.1007/BF00445553
- Bhutada, P. S., Mundhada, Y. R., Ghodki, Y. R., Chaware, P., Dixit, P. V., Jain, K. S., et al. (2012). Influence of sigma-1 receptor modulators on ethanol-induced conditioned place preference in the extinction-reinstatement model. *Behav. Pharmacol.* 23, 25–33. doi: 10.1097/FBP.0b013e32834eafe6
- Blasio, A., Valenza, M., Iyer, M. R., Rice, K. C., Steardo, L., Hayashi, T., et al. (2015). Sigma-1 receptor mediates acquisition of alcohol drinking and seeking behavior in alcohol-preferring rats. *Behav. Brain Res.* 287, 315–322. doi: 10.1016/j.bbr.2015.03.065
- Bouchard, P., and Quirion, R. (1997). [3H]1,3-di(2-tolyl)guanidine and [3H](+) pentazocine binding sites in the rat brain: autoradiographic visualization of the putative sigma1 and sigma2 receptor subtypes. *Neuroscience* 76, 467–477. doi: 10.1016/S0306-4522(96)00221-7
- Colombo, G., Lobina, C., Carai, M. A., and Gessa, G. L. (2006). Phenotypic characterization of genetically selected Sardinian alcohol-preferring (sP) and -non-preferring (sNP) rats. *Addict. Biol.* 11, 324–338. doi: 10.1111/j.1369-1600.2006.00031.x
- Engel, J. A., and Jerlhag, E. (2014). Alcohol: mechanisms along the mesolimbic dopamine system. *Prog. Brain Res.* 211, 201–233. doi: 10.1016/B978-0-444-63425-2.00009-X
- Erol, A., and Karpayak, V. M. (2015). Sex and gender-related differences in alcohol use and its consequences: contemporary knowledge and future research considerations. *Drug Alcohol Depend.* 156, 1–13. doi: 10.1016/j.drugalcdep.2015.08.023
- Everitt, B. J. (2014). Neural and psychological mechanisms underlying compulsive drug seeking habits and drug memories—indications for novel treatments of addiction. *Eur. J. Neurosci.* 40 (1), 2163–2182. doi: 10.1111/ejn.12644
- Fontanilla, D., Johannessen, M., Hajipour, A. R., Cozzi, N. V., Jackson, M. B., and Ruoho, A. E. (2009). The hallucinogen N,N-dimethyltryptamine (DMT) is an endogenous sigma-1 receptor regulator. *Science* 323, 934–937. doi: 10.1126/science.1166127
- Fujimoto, M., Hayashi, T., Urfer, R., Mita, S., and Su, T. P. (2012). Sigma-1 receptor chaperones regulate the secretion of brain-derived neurotrophic factor. *Synapse* 66, 630–639. doi: 10.1002/syn.21549
- Grant, B. F., Goldstein, R. B., Saha, T. D., Chou, S. P., Jung, J., Zhang, H., et al. (2015). Epidemiology of DSM-5 alcohol use disorder: results from the the National Epidemiologic Survey on Alcohol and Related Conditions III. *JAMA Psychiatry* 72, 757–766. doi: 10.1001/jamapsychiatry.2015.0584
- Hasin, D. S., Stinson, F. S., Ogburn, E., and Grant, B. F. (2007). Prevalence, correlates, disability, and comorbidity of DSM-IV alcohol abuse and dependence in the United States: results from the National Epidemiologic Survey on Alcohol and Related Conditions. *Arch. Gen. Psychiatry* 64, 830–842. doi: 10.1001/archpsyc.64.7.830
- Hayashi, T., and Su, T. P. (2001). Regulating ankyrin dynamics: roles of sigma-1 receptors. *Proc. Natl. Acad. Sci. U.S.A.* 98, 491–496. doi: 10.1073/pnas.98.2.491
- Hayashi, T., and Su, T. P. (2003). Intracellular dynamics of sigma-1 receptors (sigma(1) binding sites) in NG108-15 cells. *J. Pharmacol. Exp. Ther.* 306, 726–733. doi: 10.1124/jpet.103.051292
- Hayashi, T., and Su, T. P. (2007). Sigma-1 receptor chaperones at the ER-mitochondrion interface regulate Ca(2+) signaling and cell survival. *Cell* 131, 596–610. doi: 10.1016/j.cell.2007.08.036
- Hodgson, R., Rankin, H., and Stockwell, T. (1979). Alcohol dependence and the priming effect. *Behav. Res. Ther.* 17, 379–387. doi: 10.1016/0005-7967(79)90009-3
- Hodos, W. (1961). Progressive ratio as a measure of reward strength. *Science* 134, 943–944. doi: 10.1126/science.134.3483.943
- Hong, W. C., Yano, H., Hiranita, T., Chin, F. T., McCurdy, C. R., Su, T. P., et al. (2017). The sigma-1 receptor modulates dopamine transporter conformation and cocaine binding and may thereby potentiate cocaine self-administration in rats. *J. Biol. Chem.* 292, 11250–11261. doi: 10.1074/jbc.M116.774075
- Jellinek, E. M. (1952). Phases of alcohol addiction. *Q. J. Stud. Alcohol* 13, 673–684. doi: 10.15288/QJSA.1952.13.673
- Kim, F. J., Kovalyshyn, I., Burgman, M., Neilan, C., Chien, C. C., and Pasternak, G. W. (2010). Sigma 1 receptor modulation of G-protein-coupled receptor signaling: potentiation of opioid transduction independent from receptor binding. *Mol. Pharmacol.* 77, 695–703. doi: 10.1124/mol.109.057083
- Kim, H. W., Roh, D. H., Yoon, S. Y., Seo, H. S., Kwon, Y. B., Han, H. J., et al. (2008). Activation of the spinal sigma-1 receptor enhances NMDA-induced pain via PKC- and PKA-dependent phosphorylation of the NR1 subunit in mice. *Br. J. Pharmacol.* 154, 1125–1134. doi: 10.1038/bjp.2008.159
- Kinoshita, M., Matsuoka, Y., Suzuki, T., Mirrelees, J., and Yang, J. (2012). Sigma-1 receptor alters the kinetics of Kv1.3 voltage gated potassium channels but not the sensitivity to receptor ligands. *Brain Res.* 1452, 1–9. doi: 10.1016/j.brainres.2012.02.070
- Koob, G. F., and Le Moal, M., (2005). *Neurobiology of Addiction*. New York, NY: Academic Press.
- Kourrich, S., Hayashi, T., Chuang, J. Y., Tsai, S. Y., Su, T. P., and Bonci, A. (2013). Dynamic interaction between sigma-1 receptor and Kv1.2 shapes neuronal and behavioral responses to cocaine. *Cell* 152, 236–247. doi: 10.1016/j.cell.2012.12.004



- Liu, X., Fu, Y., Yang, H., Mavlyutov, T., Li, J., McCurdy, C. R., et al. (2017). Potential independent action of sigma receptor ligands through inhibition of the Kv2.1 channel. *Oncotarget* 8, 59345–59358. doi: 10.18632/oncotarget.19581
- Liu, Y., and Matsumoto, R. R. (2008). Alterations in fos-related antigen 2 and sigma1 receptor gene and protein expression are associated with the development of cocaine-induced behavioral sensitization: time course and regional distribution studies. *J. Pharmacol. Exp. Ther.* 327, 187–195. doi: 10.1124/jpet.108.141051
- Martin-Fardon, R., Strong, E. M., and Weiss, F. (2012). Effect of sigma(1) receptor antagonism on ethanol and natural reward seeking. *Neuroreport* 23, 809–813. doi: 10.1097/WNR.0b013e32835717c8
- Martin-Fardon, R., and Weiss, F. (2013). Modeling relapse in animals. *Curr. Top Behav. Neurosci.* 13, 403–432. doi: 10.1007/978-3-642-28720-6\_202
- Matsumoto, R. R., Liu, Y., Lerner, M., Howard, E. W., and Brackett, D. J. (2003). Sigma receptors: potential medications development target for anti-cocaine agents. *Eur. J. Pharmacol.* 469, 1–12. doi: 10.1016/S0014-2999(03)01723-0
- Matsumoto, K., Senda, T., Kobayashi, T., Okamoto, K., Nakata, K., and Mita, S. (1997). SA4503, a novel cognitive enhancer, with sigma 1 receptor agonistic properties. *Behav. Brain Res.* 83, 221–224. doi: 10.1016/S0166-4328(97)86074-3
- Maurice, D. H. (2003). Does sildenafil indirectly inhibit phosphodiesterase 3 in vascular smooth muscle? *Hypertension* 41, e2. doi: 10.1161/01.HYP.0000054979.81019.0A
- Maurice, T., Casalino, M., Lacroix, M., and Romieu, P. (2003). Involvement of the sigma 1 receptor in the motivational effects of ethanol in mice. *Pharmacol. Biochem. Behav.* 74, 869–876. doi: 10.1016/S0091-3057(03)00002-9
- Meunier, J., Demeilliers, B., Celerier, A., and Maurice, T. (2006). Compensatory effect by sigma1 (sigma1) receptor stimulation during alcohol withdrawal in mice performing an object recognition task. *Behav. Brain Res.* 166, 166–176. doi: 10.1016/j.bbr.2005.07.019
- Miyatake, R., Furukawa, A., Matsushita, S., Higuchi, S., and Suwaki, H. (2004). Functional polymorphisms in the sigma1 receptor gene associated with alcoholism. *Biol. Psychiatry* 55, 85–90. doi: 10.1016/j.biopsych.2003.07.008
- Morin-Surun, M. P., Collin, T., Denavit-Saubie, M., Baulieu, E. E., and Monnet, F. P. (1999). Intracellular sigma1 receptor modulates phospholipase C and protein kinase C activities in the brainstem. *Proc. Natl. Acad. Sci. U.S.A.* 96, 8196–8199. doi: 10.1073/pnas.96.14.8196
- Moykkyinen, T., and Korpi, E. R. (2012). Acute effects of ethanol on glutamate receptors. *Basic Clin. Pharmacol. Toxicol.* 111, 4–13. doi: 10.1111/j.1742-7843.2012.00879.x
- Navarro, G., Moreno, E., Aymerich, M., Marcellino, D., McCormick, P. J., Mallol, J., et al. (2010). Direct involvement of sigma-1 receptors in the dopamine D1 receptor-mediated effects of cocaine. *Proc. Natl. Acad. Sci. U.S.A.* 107, 18676–18681. doi: 10.1073/pnas.1008911107
- Navarro, G., Moreno, E., Bonaventura, J., Brugarolas, M., Farre, D., Aguinaga, D., et al. (2013). Cocaine inhibits dopamine D2 receptor signaling via sigma-1-D2 receptor heteromers. *PLoS One* 8, e61245. doi: 10.1371/journal.pone.0061245
- Nguyen, E. C., McCracken, K. A., Liu, Y., Pouw, B., and Matsumoto, R. R. (2005). Involvement of sigma (sigma) receptors in the acute actions of methamphetamine: receptor binding and behavioral studies. *Neuropharmacology* 49, 638–645. doi: 10.1016/j.neuropharm.2005.04.016
- Overstreet, D. H., Kampov-Polevoy, A. B., Rezvani, A. H., Braun, C., Bartus, R. T., and Crews, F. T. (1999). Suppression of alcohol intake by chronic naloxone treatment in P rats: tolerance development and elevation of opiate receptor binding. *Alcohol. Clin. Exp. Res.* 23, 1761–1771. doi: 10.1097/0000374-199911000-00008
- Pabba, M., Wong, A. Y., Ahlskog, N., Hristova, E., Biscaro, D., Nassrallah, W., et al. (2014). NMDA receptors are upregulated and trafficked to the plasma membrane after sigma-1 receptor activation in the rat hippocampus. *J. Neurosci.* 34, 11325–11338. doi: 10.1523/JNEUROSCI.0458-14.2014
- Phillips, T. J., and Shen, E. H. (1996). Neurochemical bases of locomotion and ethanol stimulant effects. *Int. Rev. Neurobiol.* 39, 243–282. doi: 10.1016/S0074-7742(08)60669-8
- Prasad, P. D., Li, H. W., Fei, Y. J., Ganapathy, M. E., Fujita, T., Plumley, L. H., et al. (1998). Exon-intron structure, analysis of promoter region, and chromosomal localization of the human type 1 sigma receptor gene. *J. Neurochem.* 70, 443–451. doi: 10.1046/j.1471-4159.1998.70020443.x
- Reynolds, A. R., Saunders, M. A., and Prendergast, M. A. (2016). Ethanol stimulates endoplasmic reticulum inositol triphosphate and sigma receptors to promote withdrawal-associated loss of neuron-specific nuclear protein/Fox-3. *Alcohol. Clin. Exp. Res.* 40, 1454–1461. doi: 10.1111/acer.13097
- Risinger, F. O., and Oakes, R. A. (1996). Dose- and conditioning trial-dependent ethanol-induced conditioned place preference in Swiss-Webster mice. *Pharmacol. Biochem. Behav.* 55, 117–123. doi: 10.1016/0091-3057(96)00069-X
- Roh, D. H., Choi, S. R., Yoon, S. Y., Kang, S. Y., Moon, J. Y., Kwon, S. G., et al. (2011). Spinal neuronal NOS activation mediates sigma-1 receptor-induced mechanical and thermal hypersensitivity in mice: involvement of PKC-dependent GluN1 phosphorylation. *Br. J. Pharmacol.* 163, 1707–1720. doi: 10.1111/j.1476-5381.2011.01316.x
- Romieu, P., Martin-Fardon, R., and Maurice, T. (2000). Involvement of the sigma1 receptor in the cocaine-induced conditioned place preference. *Neuroreport* 11, 2885–2888. doi: 10.1097/00001756-200009110-00011
- Sabeti, J. (2011). Ethanol exposure in early adolescence inhibits intrinsic neuronal plasticity via sigma-1 receptor activation in hippocampal CA1 neurons. *Alcohol. Clin. Exp. Res.* 35, 885–904. doi: 10.1111/j.1530-0277.2010.01419.x
- Sabeti, J., and Gruol, D. L. (2008). Emergence of NMDAR-independent long-term potentiation at hippocampal CA1 synapses following early adolescent exposure to chronic intermittent ethanol: role for sigma-receptors. *Hippocampus* 18, 148–168. doi: 10.1002/hipo.20379
- Sabia, S., Gueguen, A., Berr, C., Berkman, L., Ankri, J., Goldberg, M., et al. (2011). High alcohol consumption in middle-aged adults is associated with poorer cognitive performance only in the low socio-economic group. Results from the GAZEL cohort study. *Addiction* 106, 93–101. doi: 10.1111/j.1360-0443.2010.03106.x
- Sabino, V., Cottone, P., Blasio, A., Iyer, M. R., Steardo, L., Rice, K. C., et al. (2011). Activation of sigma-receptors induces binge-like drinking in Sardinian alcohol-preferring rats. *Neuropsychopharmacology* 36, 1207–1218. doi: 10.1038/npp.2011.5
- Sabino, V., Cottone, P., Zhao, Y., Iyer, M. R., Steardo, L., Jr., Steardo, L., et al. (2009a). The sigma-receptor antagonist BD-1063 decreases ethanol intake and reinforcement in animal models of excessive drinking. *Neuropsychopharmacology* 34, 1482–1493. doi: 10.1038/npp.2008.192
- Sabino, V., Cottone, P., Zhao, Y., Steardo, L., Koob, G. F., and Zorrilla, E. P. (2009b). Selective reduction of alcohol drinking in Sardinian alcohol-preferring rats by a sigma-1 receptor antagonist. *Psychopharmacology* 205, 327–335. doi: 10.1007/s00213-009-1548-x
- Sabino, V., Narayan, A. R., Zeric, T., Steardo, L., and Cottone, P. (2013). mTOR activation is required for the anti-alcohol effect of ketamine, but not memantine, in alcohol-preferring rats. *Behav. Brain Res.* 247, 9–16. doi: 10.1016/j.bbr.2013.02.030
- Schmidt, H. R., Zheng, S., Gurpinar, E., Koehl, A., Manglik, A., and Kruse, A. C. (2016). Crystal structure of the human sigma1 receptor. *Nature* 532, 527–530. doi: 10.1038/nature17391
- Sharkey, J., Glen, K. A., Wolfe, S., and Kuhar, M. J. (1988). Cocaine binding at sigma receptors. *Eur. J. Pharmacol.* 149, 171–174. doi: 10.1016/0014-2999(88)90058-1
- Takahashi, S., Miwa, T., and Horikomi, K. (2000). Involvement of sigma 1 receptors in methamphetamine-induced behavioral sensitization in rats. *Neurosci. Lett.* 289, 21–24. doi: 10.1016/S0304-3940(00)01258-1
- Valenza, M., DiLeo, A., Steardo, L., Cottone, P., and Sabino, V. (2016). Ethanol-related behaviors in mice lacking the sigma-1 receptor. *Behav. Brain Res.* 297, 196–203. doi: 10.1016/j.bbr.2015.10.013
- Vendruscolo, L. F., and Roberts, A. J. (2014). Operant alcohol self-administration in dependent rats: focus on the vapor model. *Alcohol* 48, 277–286. doi: 10.1016/j.alcohol.2013.08.006
- Wu, J., Gao, M., and Taylor, D. H. (2014). Neuronal nicotinic acetylcholine receptors are important targets for alcohol reward and dependence. *Acta Pharmacol. Sin.* 35, 311–315. doi: 10.1038/aps.2013.181
- Zhang, K., Zhao, Z., Lan, L., Wei, X., Wang, L., Liu, X., et al. (2017). Sigma-1 receptor plays a negative modulation on N-type calcium channel. *Front. Pharmacol.* 8, 302. doi: 10.3389/fphar.2017.00302

**Conflict of Interest Statement:** The authors declare that the research was conducted in the absence of any commercial or financial relationships that could be construed as a potential conflict of interest.

Copyright © 2019 Quadir, Cottone and Sabino. This is an open-access article distributed under the terms of the Creative Commons Attribution License (CC BY). The use, distribution or reproduction in other forums is permitted, provided the original author(s) and the copyright owner(s) are credited and that the original publication in this journal is cited, in accordance with accepted academic practice. No use, distribution or reproduction is permitted which does not comply with these terms.



# Characterization of Sigma 1 Receptor Antagonist CM-304 and Its Analog, AZ-66: Novel Therapeutics Against Allodynia and Induced Pain

Thomas J. Cirino<sup>1</sup>, Shainnel O. Eans<sup>1</sup>, Jessica M. Medina<sup>1</sup>, Lisa L. Wilson<sup>1</sup>, Marco Mottinelli<sup>2</sup>, Sebastiano Intagliata<sup>2</sup>, Christopher R. McCurdy<sup>2</sup> and Jay P. McLaughlin<sup>1\*</sup>

<sup>1</sup> Department of Pharmacodynamics, University of Florida, Gainesville, FL, United States, <sup>2</sup> Department of Medicinal Chemistry, University of Florida, Gainesville, FL, United States

## OPEN ACCESS

### Edited by:

Ebru Aydar,  
University College London,  
United Kingdom

### Reviewed by:

Francisco Javier López-Muñoz,  
Centro de Investigación y de Estudios  
Avanzados (CINVESTAV), Mexico  
Halina Machelska,  
Charité Medical University of Berlin,  
Germany  
Enrique Portillo-Salido,  
Esteve Pharmaceuticals, Spain

### \*Correspondence:

Jay P. McLaughlin  
jmclaughlin@cop.ufl.edu

### Specialty section:

This article was submitted to  
Experimental Pharmacology  
and Drug Discovery,  
a section of the journal  
Frontiers in Pharmacology

**Received:** 28 February 2019

**Accepted:** 24 May 2019

**Published:** 14 June 2019

### Citation:

Cirino TJ, Eans SO, Medina JM,  
Wilson LL, Mottinelli M, Intagliata S,  
McCurdy CR and McLaughlin JP  
(2019) Characterization of Sigma 1  
Receptor Antagonist CM-304 and Its  
Analog, AZ-66: Novel Therapeutics  
Against Allodynia and Induced Pain.  
Front. Pharmacol. 10:678.  
doi: 10.3389/fphar.2019.00678

Sigma-1 receptors (S1R) and sigma-2 receptors (S2R) may modulate nociception without the liabilities of opioids, offering a promising therapeutic target to treat pain. The purpose of this study was to investigate the *in vivo* analgesic and anti-allodynic activity of two novel sigma receptor antagonists, the S1R-selective CM-304 and its analog the non-selective S1R/S2R antagonist AZ-66. Inhibition of thermal, induced chemical or inflammatory pain, as well as the allodynia resulting from chronic nerve constriction injury (CCI) and cisplatin exposure as models of neuropathic pain were assessed in male mice. Both sigma receptor antagonists dose-dependently (10–45 mg/kg, i.p.) reduced allodynia in the CCI and cisplatin neuropathic pain models, equivalent at the higher dose to the effect of the control analgesic gabapentin (50 mg/kg, i.p.), although AZ-66 demonstrated a much longer duration of action. Both CM-304 and AZ-66 produced antinociception in the writhing test [0.48 (0.09–1.82) and 2.31 (1.02–4.81) mg/kg, i.p., respectively] equivalent to morphine [1.75 (0.31–7.55) mg/kg, i.p.]. Likewise, pretreatment (i.p.) with either sigma-receptor antagonist dose-dependently produced antinociception in the formalin paw assay of inflammatory pain. However, CM-304 [17.5 (12.7–25.2) mg/kg, i.p.] and AZ-66 [11.6 (8.29–15.6) mg/kg, i.p.] were less efficacious than morphine [3.87 (2.85–5.18) mg/kg, i.p.] in the 55°C warm-water tail-withdrawal assay. While AZ-66 exhibited modest sedative effects in a rotarod assay and conditioned place aversion, CM-304 did not produce significant effects in the place conditioning assay. Overall, these results demonstrate the S1R selective antagonist CM-304 produces antinociception and anti-allodynia with fewer liabilities than established therapeutics, supporting the use of S1R antagonists as potential treatments for chronic pain.

**Keywords:** Sigma, allodynia, analgesia, chronic pain, sedation, addiction

## INTRODUCTION

Chronic pain is the number one cause of adult disability in the United States. According to the National Institutes of Health, an estimated 20 million individuals suffer from some form of peripheral neuropathy (NINDS, 2018). Current existing primary treatments for managing chronic pain include anticonvulsants (i.e., gabapentin, pregabalin), followed by secondary treatments including tricyclic

antidepressants (e.g., amitriptyline, desipramine) and mu opioid receptor (MOR)-selective agonists (e.g., morphine), but the liabilities of these treatments greatly offset their therapeutic benefits (Yaksh and Wallace, 2011). These agents all cause drowsiness and impair locomotor ability, posing a significant risk when operating machinery and increasing the risk of falling, which in the elderly has been linked to increased mortality risk (Calandre et al., 2016; Mangram et al., 2016). More concerning is the potential for MOR agonists to demonstrate tolerance as well as opioid-induced hyperalgesia (DeLeo et al., 2004), and produce constipation, respiratory depression, substance abuse and addiction (Rosenblum et al., 2008). Overall, there remains a clear need for new, safer non-opioid options to treat chronic pain.

Sigma receptor antagonists are emerging as potential therapeutics and adjuvants to treat nerve injury, neuroinflammation, and the modulation of nociception (Vidal-Torres et al., 2013; Davis, 2015). Although once thought to be a member of the opioid family (Martin et al., 1976) or a binding site on N-Methyl-D-aspartate (NMDA) receptors (Wong et al., 1988), subsequent cloning of the sigma-1 (S1R; Hanner et al., 1996) and sigma-2 receptors (S2R; Alon et al., 2017) is leading to a more defined role of this system in biological systems. In particular, S1R are thought to play an active modulatory role in pain signaling, both centrally and peripherally (Kim et al., 2008; Roh et al., 2011). Sigma-1 receptors (S1Rs) are intracellular chaperone proteins (Walker et al., 1990) that modulate both central sensitization of pain (Gris et al., 2016) as well as oxidative stress (Pal et al., 2012). S1Rs were reported to be upregulated at the site of partial sciatic nerve ligation (Shen et al., 2017b), and pharmacological antagonism with the early selective sigma receptor antagonist E52862 reduced neuropathic nociception and spinal sensitization (de la Puente et al., 2009; Romero et al., 2012), and has been found effective in treating neurogenic pain (Wunsch, 2012). Notably, existing commonly used antagonists have limited specificity between the sigma receptors (BD1067) and sometimes significant affinity for other targets (notably Haloperidol; Matsumoto and Pouw, 2000; Matsumoto et al., 2001). However, the recent translational validation of E52862 as an efficacious treatment for oxaliplatin-induced neuropathy in a phase II clinical trial (Bruna et al., 2018)

has reinvigorated interest in the development of newer, selective sigma receptor antagonists.

The recent characterization of CM-304 (**Figure 1**) found it to be a selective S1R antagonist, with >100-fold selectivity over S2R, and >10,000-fold selectivity over 59 other targets, including opioid and 5-HT receptors (James et al., 2012; James et al., 2014). The autoradiographic labeling of FTC146, the radiolabeled analog of CM-304, was abolished in S1R knock out mice, further demonstrating the S1R selectivity of this antagonist (Shen et al., 2015). While readily penetrating the CNS, CM-304 possesses a short *in vivo* half-life (115 min) and modest clearance (Cl = 33 ml/min/kg) (Avery et al., 2017). Seeking to improve the pharmacokinetics of this selective S1R antagonist, the analog AZ-66 was developed and shown to be a longer-lasting antagonist that possesses high affinity for both the S1R and S2R (Seminario et al., 2012; Jamalapuram et al., 2013; Avery et al., 2017; **Figure 1**).

We hypothesized that the S1R selective antagonist CM-304 and non-selective S1R/S2R antagonist AZ-66 would produce significant anti-allodynic and antinociceptive effects in mouse models of chronic, induced pain with fewer liabilities of use as displayed by established analgesic agents. Activity of the two antagonists was examined in mouse assays of thermal (tail-flick), chemical (acetic acid), and induced inflammatory pain (formalin), as well as the chronic nerve constriction injury (CCI) and cisplatin-induced neuropathy (CISN) models of neuropathic pain and allodynia. Furthermore, C57BL/6J mice administered CM-304 and AZ-66 were examined for respiratory, locomotor, and sedative effects using the Comprehensive Lab Animal Monitoring System (CLAMS) and rotarod assay, and possible rewarding or aversive effects with the conditioned place preference (CPP) assay.

## METHODS

### Subjects

Adult male C57BL/6J (The Jackson Laboratory, Bar Harbor, ME, USA) and CD-1 (Charles River Laboratories, Wilmington, MA, USA) mice were housed five to a cage, and tested at 8–12 weeks

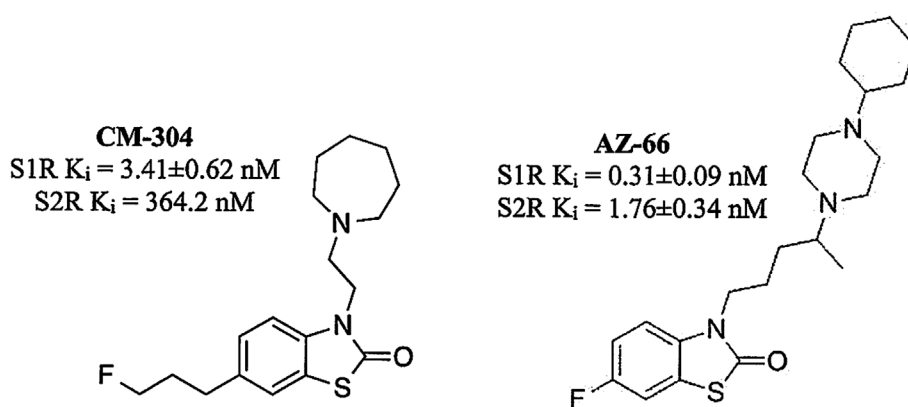


**FIGURE 1** | Structures of **CM-304** and **AZ-66**.

of age. C57BL/6J mice are established subjects in antinociceptive (Mogil et al., 1996; Wilson et al., 2003) respiratory and locomotor (Reilly et al., 2010) and place-conditioning assays (Brabant et al., 2005; Orsini et al., 2005). Analgesic effects were further confirmed in CD-1 mice, a strain also well validated for antinociceptive (Mogil et al., 2005) and thermal and mechanical anti-allodynic testing (LaCroix-Fralish et al., 2005; Feehan et al., 2017). Animal studies are reported in compliance with the ARRIVE guidelines (Kilkenny et al., 2010; McGrath and Lilley, 2015). Final sample sizes (i.e., a fixed number of animals for a particular test) were not predetermined by a statistical method, and animals were assigned to groups randomly. Drug treatment experiments were conducted in a blinded fashion. No animals were excluded from statistical analysis.

Mice were housed in a temperature and humidity controlled room at the University of Florida (Gainesville, Florida, USA) vivarium on a 12:12-h light/dark cycle with free access to food and water except during experimental sessions. All procedures were preapproved and conducted in accordance with the Institutional Animal Care and Use Committee at the University of Florida as specified by the 2011 NIH *Guide for the Care and Use of Laboratory Animals*. Upon the completion of testing, all mice were euthanized by inhalation of carbon dioxide, followed by cervical dislocation as a secondary measure, as recommended by the American Veterinary Medical Association.

## Materials, Drug Preparation, and Administration

The sigma receptor antagonists CM-304 and AZ-66 were synthesized and isolated as hydrochloride salts as described previously (McCurdy et al., 2014). All drugs and chemicals otherwise used were purchased from Sigma-Aldrich (St. Louis, MO, USA). For experiments, sterile isotonic saline (0.9%) was used to dissolve drugs to desired concentrations for testing (morphine, U50,488, E52862, AZ-66, and CM-304, 0.3–4.5 mg/ml). Gabapentin was dissolved in 5% Dimethyl sulfoxide (DMSO)/isotonic saline to 5.0 mg/ml concentration. All drugs were administered intraperitoneally (i.p.) in a volume of 250 µl per 25 g body weight.

## Behavioral Assays

### Chronic Constriction Injury

Chronic constriction injuries (CCIs) were made to isoflurane (2.5%) anesthetized CD-1 mice (Hoot et al., 2010). This manipulation induces hyperalgesia and mechanical allodynia within 7 days, modeling neuropathic pain (Bennett and Xie, 1988; Pitcher et al., 1999; Cheng et al., 2002; Xu et al., 2004). Briefly, mice were anesthetized and an incision made along the surface of the biceps femoris (Hoot et al., 2010). Blunt forceps were inserted into the muscle belly to split the muscle and expose the right sciatic nerve. The tips of the forceps were passed under the sciatic nerve to pass two 5–0 chromic gut sutures (Ethicon, Cornelia, GA) under the nerve, 1 mm apart. The sutures were tied loosely around the nerve and knotted twice to prevent slippage, and skin was closed with 2–3 ligatures of 6–0 nylon. Mice were allowed to recover for 7 days prior to the initiation

of testing. Mice so injured were confirmed hypersensitive to tactile stimulation with a series of von Frey hairs prior to testing, typically removing the ipsilateral paw from contact with just ~20% of the baseline force required. Animals in neuropathic pain are hypersensitive to tactile stimulation (allodynia), and respond to lower pressure. Allodynic mice were then administered (i.p.) either vehicle (5% DMSO), morphine (10 mg/kg, i.p.), E52862 (30 mg/kg, i.p.), gabapentin (50 mg/kg, i.p.), CM-304 or AZ-66 (10–45 mg/kg, i.p., each). Every 20 min for 80 min, the threshold for tactile allodynia was measured using a series of calibrated von Frey filaments possessing a bending force from 0.4 to 6 g until the threshold that induced paw withdrawal was found as a measure of nocifension (Bennett and Xie, 1988; Pitcher et al., 1999; Cheng et al., 2002; Xu et al., 2004). The filaments were applied by ascending strength, and threshold was defined as two withdrawals per trial of the same filament strength. Responsiveness to von Frey fibers is indicative of mechanical allodynia as uninjured mice do not respond with paw withdrawal at these strengths. Data are expressed as percent of baseline paw withdrawal thresholds following stimulation of the ipsilateral hind paw with von Frey filaments. This was utilized to account for innate variability between mice. % antiallodynia =  $100 \times ([\text{mean paw withdrawal force } \{g\} \text{ in control group} - \text{paw withdrawal force } \{g\} \text{ of each mouse}] / \text{mean paw withdrawal force } [g] \text{ in control group})$ .

### Cisplatin-Induced Neuropathy Assay

The effectiveness of the sigma-receptor antagonists or control compounds against a chemically induced neuropathy, produced by treatment with cisplatin (2.3 mg/kg, i.p.) on alternating days with lactated Ringer's solution on intervening days over a 9-day period, was determined (Zhou et al., 2016). Drug efficacy screening was conducted on day 10 to minimize the potential effect that repeated testing may have on endpoints. Anti-allodynic effects against mechanical allodynia were determined with measurements using a series of calibrated von Frey monofilaments, as described above in the CCI assay.

### Acetic Acid Stretching Assay

Antinociceptive efficacy against visceral, chemical pain using the acetic acid stretching assay was assessed with C57BL/6J mice as described previously (Bidlack et al., 2002; Eans et al., 2015). Twenty-five minutes after receiving a single dose of test drug, an i.p. injection of 0.9% acetic acid (0.25 ml per 25 g body wt.) was administered to each mouse. After 5 min, the number of stretches displayed by each mouse was counted for an additional 15 min. Antinociception for each tested mouse was calculated by comparing the test group to a control group in which mice were treated with the appropriate vehicle (i.p.) using the formula:

$$\% \text{ antinociception} = ([\{\text{average stretches in the vehicle group}\} - \{\text{number of stretches in each test mouse}\}] / [\text{average stretches in vehicle group}]) \times 100.$$

### Formalin Assay

Additional testing of antinociceptive potency against inflammatory pain was performed using the formalin assay in C57BL/6J mice



as previously described (Cheng et al., 2002). Following a 30-min pretreatment of a single dose of vehicle control or test drug (i.p.), an intraplantar (i.pl.) injection of 5% formalin (2.5 µg in 15 µl) was administered into the right hind paw. Paw-licking duration was recorded in 5-min intervals for 60 min following injection. The last 55 min was used to determine response to an inflammatory stimulus. Data were analyzed as area under the curve (AUC) representing summed time mice spent licking their inflamed hind paw.

### Tail-Withdrawal Assay

The 55°C warm-water tail-withdrawal assay was conducted in C57BL/6J mice as a measure of acute thermal antinociception as described previously (Reilly et al., 2010). Briefly, each mouse was tested for baseline tail-withdrawal latency prior to drug administration. Following drug administration (i.p.), the latency for each mouse to withdraw the tail was measured every 10 min until latency returned to the baseline value. A maximum response time of 15 s was utilized to prevent tissue damage. If the mouse failed to display a tail-withdrawal response within 15 s, the tail was removed from the water and the animal was assigned a maximal antinociceptive score of 100%. Data are reported as percent antinociception, calculated by the equation: % antinociception =  $100 \times ([\text{test latency} - \text{baseline latency}] / [15 - \text{baseline latency}])$ . This was utilized to account for innate variability between mice.

### CLAMS Measurement of Respiration Rate and Spontaneous Locomotor Testing

Respiration rates and spontaneous ambulation rates were monitored using the automated, computer-controlled Comprehensive Lab Animal Monitoring System (CLAMS) (Columbus Instruments, Columbus, OH) as described previously (Reilly et al., 2010). Freely moving mice were habituated in closed, sealed individual apparatus cages (23.5 cm × 11.5 cm × 13 cm) for 60 min before testing. To start testing, mice were administered (i.p.) drug or vehicle and 5 min later confined to the CLAMS testing cages for 120 min. Using a pressure transducer built into the sealed CLAMS cage, the respiration rate (breaths/min) of each occupant mouse was measured. Infrared beams located in the floor measured locomotion as ambulations, from the number of sequential breaks of adjacent beams. Data are expressed as percent of vehicle control response.

### Rotarod Assay to Assess Motor Coordination

Possible sedative effects of vehicle, morphine, U50,488, CM-304 or AZ-66 were assessed by rotarod performance, as described previously (Eans et al., 2015). Following seven habituation trials (the last utilized as a baseline measure of rotarod performance), mice were administered (i.p.) test agent: vehicle (5% DMSO/95% saline; 12 mice), morphine or U50,488 (10 mg/kg, i.p. each, eight mice each), or CM-304 or AZ-66 (45 mg/kg, i.p. each; 10 mice each) and assessed after 10 min in accelerated speed trials (180 s max latency at 0–20 rpm) over a 60-min period, measuring time to fall (in seconds). To normalize for each mouse's individual performance, data are expressed as the average of the percent change from baseline performance for each mouse. Decreased latencies to fall in the rotarod test indicate impaired motor performance.

### Conditioned Place Preference

An automated, balanced three-compartment place conditioning apparatus (San Diego Instruments, San Diego, CA) and 2-day counterbalanced conditioning design was used (similar to Eans et al., 2013). Prior to place conditioning, mice were allowed free access to all three chambers of the apparatus for 30 min to determine initial outer chamber preference. Time spent in each chamber was recorded. Prior to place conditioning, the 98 animals tested did not demonstrate significant differences in their time spent exploring the left ( $552.8 \pm 12.5$  s) versus right ( $590.8 \pm 12.9$  s) compartments ( $P = 0.09$ ; Student's *t*-test). Each day mice were administered assay vehicle (0.9% saline, i.p.) and consistently confined in a randomly assigned outer compartment (i.e., half of each group in the right chamber, half in the left chamber). Four hours later, C57BL/6J mice were administered compound and confined to the opposite compartment for 40 min of place conditioning in the appropriate outer compartment. All place conditioning was repeated for a second day, and final place preference was determined 24 h later. Data are plotted as the difference in time spent in the eventual conditioning-drug paired and vehicle-paired compartments. By convention, a positive value reflects a conditioned preference and a negative value conditioned aversion for the drug-paired side. Results compared the pre-conditioning responses and post-conditioning responses between sets.

### Control Testing

To validate assay function, comparison control experiments for each assay (either negative controls with vehicle, or positive controls with agents such as morphine or gabapentin) were performed in small cohorts alongside testing of novel compounds throughout the study.

### Statistical Analysis

The data and statistical analysis comply with the recommendations on experimental design and analysis in pharmacology (Curtis et al., 2015). All data are presented as mean ± SEM, with a significance set at  $P < 0.05$ , denoted by the asterisk (\*). All data were statistically evaluated with Prism 7.0 software (GraphPad Software, La Jolla, California, USA). All statistical analysis were examined for normality and equal variance using GraphPad. All data demonstrated normality and equal variance, justifying parametric analysis. Dose response lines were analyzed by linear or nonlinear regression modeling and ED<sub>50</sub> values (dose yielding 50% effect) along with 95% confidence limits using each individual data points. CLAMS data are reported as the % of matching vehicle control responses. The rotarod data are expressed as the % change from baseline performance, a standard normalization that compensates for each individual animal's baseline response. CPP data are reported as the difference in time spent in the drug- and vehicle-paired compartments between pre-conditioning and post-conditioning responses. Significant differences in behavioral data were analyzed by ANOVA (one-way or two-way repeated measures), with significant results further analyzed with Dunnett's, Sidak, or Tukey's Honestly significant difference (HSD) *post hoc* tests as appropriate for significant pairwise comparisons within and between groups.

## RESULTS

### Sigma Receptor Antagonists Dose-Dependently Alleviate Multiple Modalities of Induced Nociception

We first completed the characterization of a set of established control analgesics in the mouse CCI assay of neuropathic pain. Following administration through the intraperitoneal (i.p.) route and using von Frey filaments to measure mechanical allodynia, the mu-opioid receptor agonist, morphine (10 mg/kg), the sigma-receptor antagonist E52862 (30 mg/kg), and the established treatment for neuropathic pain, gabapentin (50 mg/kg, given 60 min prior to testing), all significantly attenuated the reduced paw withdrawal threshold caused by CCI (factor *treatment*:  $F_{(3,151)} = 4.01$ ,  $p = 0.009$  and factor *time*:  $F_{(3,151)} = 31.7$ ,  $p < 0.0001$ ; two-way ANOVA and Tukey's multiple comparison *post hoc* test; **Figure 2**). These results were consistent with established observations 1) that gabapentin produces antiallodynia useful in the treatment of neuropathic pain, 2) that sigma receptor antagonists as represented by E52862 may also produce antiallodynia, and 3) that morphine, while somewhat efficacious, is less effective than gabapentin ( $p < 0.05$ , 20 and 40 min time points).

Following i.p. administration, both CM-304 and AZ-66 demonstrated anti-allodynic effects in the CCI assay. CM-304 (**Figure 3A**) produced significant relief of CCI-induced allodynia in a dose- and time-dependent manner (factor *treatment*:  $F_{(4,171)} = 26.11$ ,  $p < 0.0001$  and factor *time*:  $F_{(3,171)} = 6.71$ ,  $p = 0.0003$ ; two-way ANOVA and Tukey's *post hoc* test). These effects were short-lasting (less than 60 min) even at the highest dose, consistent with the known rapid metabolism of

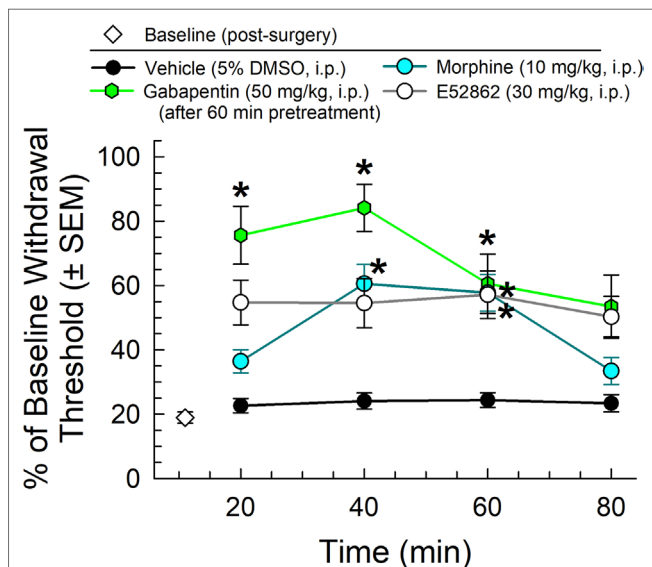


**FIGURE 2 |** Dose- and time-dependent antiallodynic activity of morphine (blue circles), gabapentin (green hexagons), or the sigma-receptor antagonist E52862 after i.p. administration in the mouse chronic constriction injury (CCI) assay. \* = significantly greater than vehicle effect (black circles) at matching time points,  $p < 0.05$ ; two-way ANOVA w/Tukey's *post hoc* test.  $N = 10$ –12 mice/point.

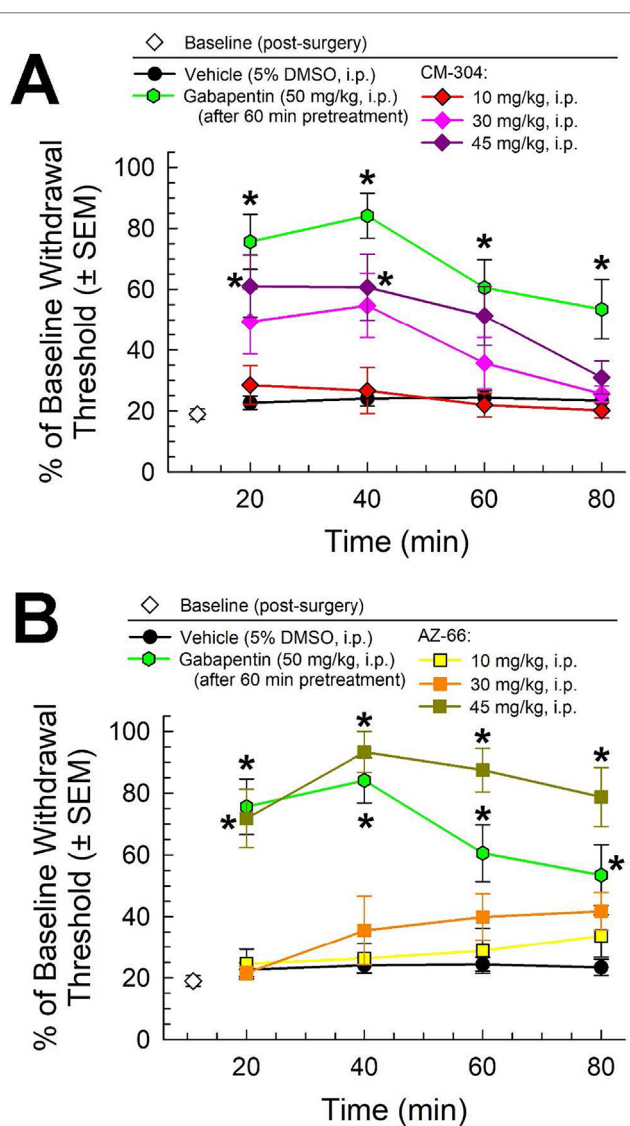


**FIGURE 3 |** Dose- and time-dependent antiallodynic activity of (A) CM-304 (diamonds) and (B) AZ-66 (squares) in the mouse chronic constriction injury (CCI) assay. Gabapentin (green hexagons, 60-min pretreatment) is included as a positive control; vehicle (5% DMSO; black circles) is included as a negative control. \* = significantly greater than vehicle effect,  $p < 0.05$ ; two-way ANOVA w/Tukey's *post hoc* test.  $N = 8$ –10 mice treated with a single dose of sigma receptor antagonist and 11 mice for gabapentin.

this ligand. In contrast, the antiallodynic efficacy of AZ-66 (**Figure 3B**) was significant only at the higher dose tested (45 mg/kg; factor *treatment*:  $F_{(4,171)} = 51.4$ ,  $p < 0.0001$ ), but it was also significantly elevated above the effects of gabapentin for an extended period ( $p = 0.04$ ; 60 min time point, Student's *t*-test). The completion of this testing confirms the anti-allodynic activity of both S1R and mixed affinity S1R/S2R antagonists against neuropathic pain.

Similarly, morphine (10 mg/kg) and gabapentin (50 mg/kg, given 60 min prior to testing) all significantly attenuated the reduced paw withdrawal threshold caused by chronic exposure to

CISN (factor *treatment*:  $F_{(2,80)} = 75.3$ ,  $p < 0.001$ ; two-way ANOVA and Tukey's multiple comparison *post hoc* test; **Figure 4**). The sigma receptor antagonists demonstrated modest anti-allodynic effects in the CISN assay, with significant dose-dependent effects upon treatment with higher doses (45 mg/kg) of either CM-304 (factor *treatment*:  $F_{(2,100)} = 14.48$ ,  $p < 0.0001$ ; **Figure 4A**) or AZ-66 (factor *treatment*:  $F_{(2,96)} = 10.58$ ,  $p < 0.0001$ ; **Figure 4B**).

We further evaluated the sigma receptor antagonists CM-304 and AZ-66 in the mouse acetic acid writhing test and formalin assay to evaluate visceral and inflammatory pain, respectively. On the basis of the activity in the neuropathic pain assays, we administered

AZ-66 and CM-304 through the intraperitoneal route and examined antinociceptive efficacy *in vivo* in mouse models of visceral, chemical pain (the acetic-acid writhing assay; **Figure 5**). The sigma-receptor antagonists produced dose-dependent antinociception in the writhing assay, with  $ED_{50}$  values (and 95% confidence intervals) of 0.48 (0.09–1.82) mg/kg, i.p. (CM-304) and 2.31 (1.02–4.81) mg/kg, i.p. (AZ-66). These effects are comparable to the analgesia of the established opioid agonists morphine [1.75 (0.27–1.15) mg/kg, i.p.] and U50,488 [2.13 (0.04–49.8) mg/kg, i.p.] (**Figure 5**).

Likewise, testing of the sigma-receptor antagonists in the mouse formalin assay showed significant dose-dependent analgesic efficacy against inflammatory pain, with both CM-304 and AZ-66 equally reducing the amount of time that animals spent licking the inflamed paw in a dose-dependent manner as compared to vehicle-treated mice ( $F_{(3,33)} = 4.93$ ,  $p = 0.006$  and  $F_{(3,34)} = 5.51$ ;  $p = 0.003$ , respectively; one-way ANOVA w/ Dunnett's *post hoc* test; **Figure 6**).

We next evaluated the antinociceptive abilities of CM-304 and AZ-66 against a thermal nociceptive stimulus in the mouse 55°C warm-water tail-withdrawal assay. The MOR agonist morphine and KOR agonist U50,488 produced dose-dependent antinociception with  $ED_{50}$  and 95% C.I. values of 3.87 (2.85–5.18) and 8.11 (6.19–9.94) mg/kg, i.p., respectively (**Figure 7**). In contrast, AZ-66 exhibited antinociception with an  $ED_{50}$  value of 11.6 (8.29–15.6) mg/kg, i.p., while the selective S1R antagonist CM-304 produced antinociception with an  $ED_{50}$  value of 17.5 (12.7–25.2) mg/kg, i.p., significantly less efficacious than morphine ( $F_{(2,145)} = 17.3$ ;  $p < 0.0001$ ; nonlinear regression modeling).

## Evaluation of CM-304 and AZ-66 *In Vivo* for Potential Clinical Liabilities

Following administration through the intraperitoneal route, the mu-opioid receptor agonist, morphine (10 and 30 mg/kg),

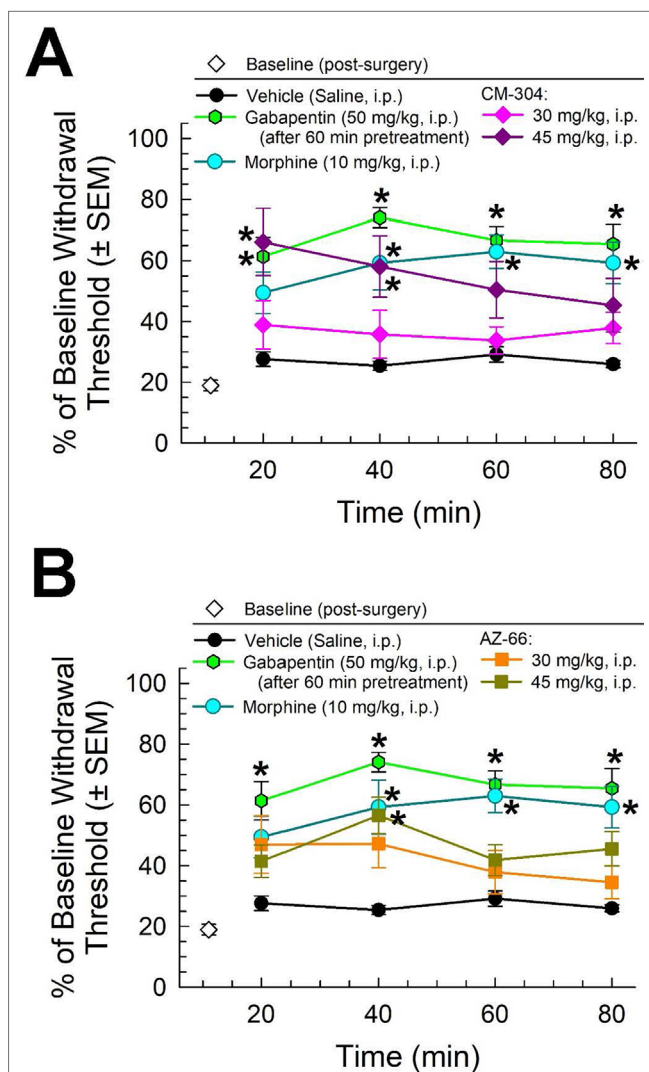


**FIGURE 4 |** Dose- and time-dependent antiallodynic activity of (A) CM-304 (diamonds) and (B) AZ-66 (squares) in the mouse chemotherapy-induced neuropathy (CISN) assay. Morphine (blue circles) and gabapentin (green hexagons, 60-min pretreatment) are included as positive controls; vehicle (saline; black circles) is included as a negative control. \* = significantly greater than vehicle effect,  $p < 0.05$ ; two-way ANOVA w/Tukey's *post hoc* test.  $N = 9$ –10 mice treated with a single dose of sigma receptor antagonists, six mice treated with morphine, nine mice treated with gabapentin, and eight mice treated with saline alone.

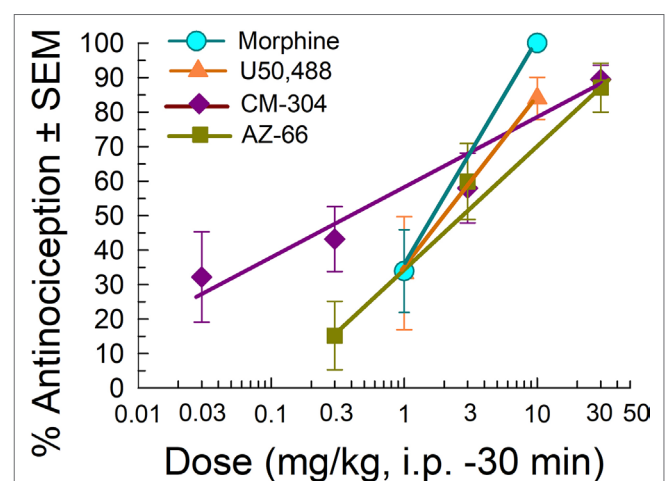


**FIGURE 5 |** Dose-dependent antinociception of sigma-receptor antagonists CM-304 and AZ-66 following i.p. administration in the mouse acetic-acid writhing assay. Opioid agonists morphine and U50,488 are shown as positive controls. All points represent average response  $\pm$  SEM at peak effect, 30 min after admin in 8–14 mice.



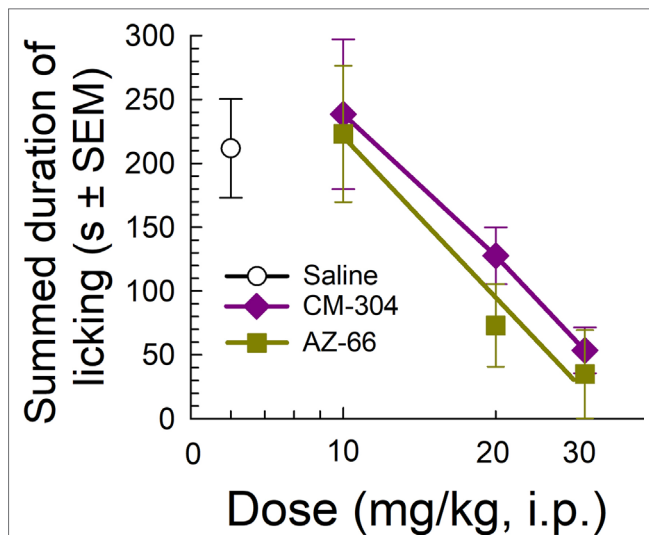


**FIGURE 6 |** Dose-dependent antinociception of sigma-receptor antagonists CM-304 and AZ-66 following i.p. administration in the mouse formalin assay. Control mice treated with saline (0.9%, i.p.;  $n = 8$ ). All points represent average response ± SEM administered to 8–10 mice.

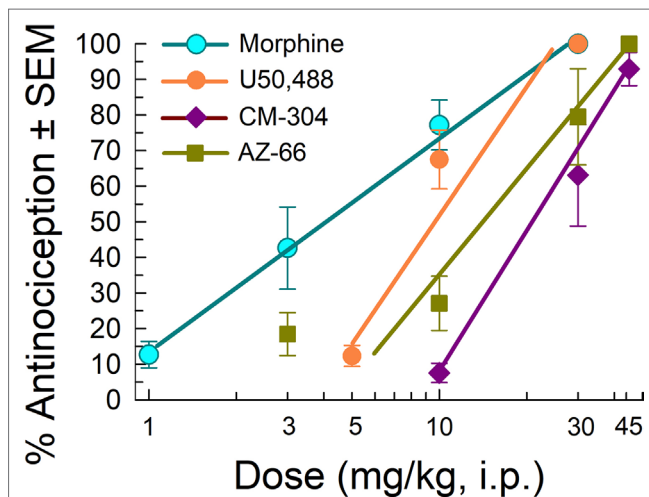


**FIGURE 7 |** Testing efficacy against acute thermal nociception in the 55°C warm-water tail-withdrawal test. Opioid agonists morphine and U50,488 are shown as positive controls. Morphine and U50,488 points represent average response ± SEM at peak effect, 30 min after admin in eight or 16 mice. All points with CM-304 and AZ-66 represent average response ± SEM at peak effect, 20 min after admin in eight mice/dose tested.

and the kappa-opioid-receptor agonist U50,488 [10 mg/kg; and 30 mg/kg not shown]) showed different results on respiration rate in the CLAMS. Compared to vehicle, morphine significantly reduced respiration rate (factor *treatment* × *time*:  $F_{(20,420)} = 2.05$ ,  $p = 0.005$ ; two-way ANOVA and Dunnett's multiple comparison *post hoc* test; **Figure 8A**). In contrast, U50,488 did not significantly reduce respiration at any time point (and, in fact, showed a trend toward increased respiration). Likewise, significant differences

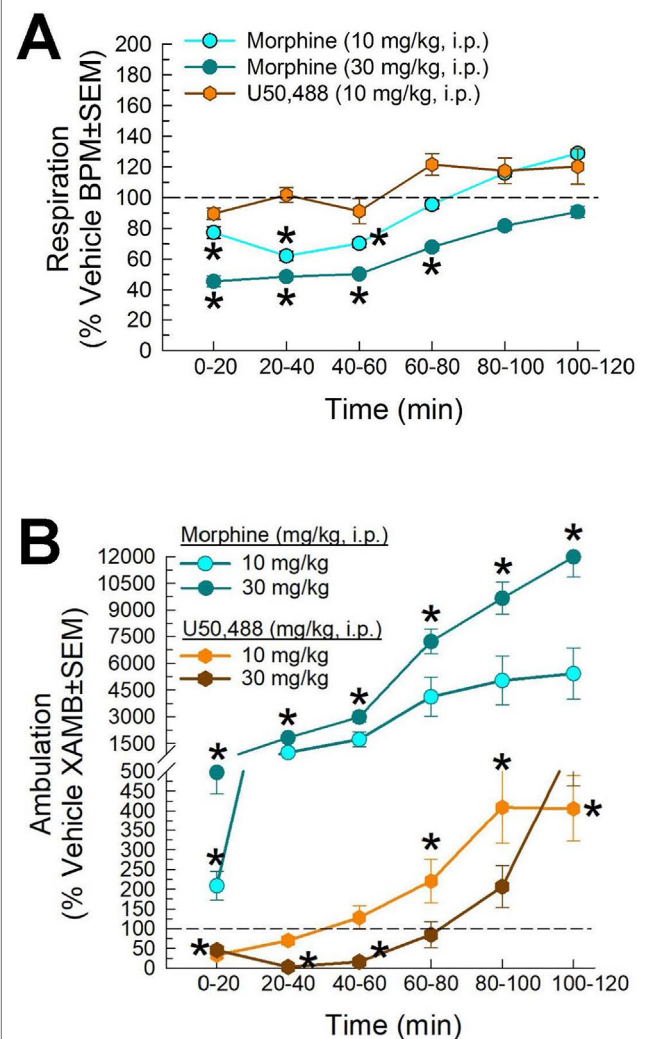
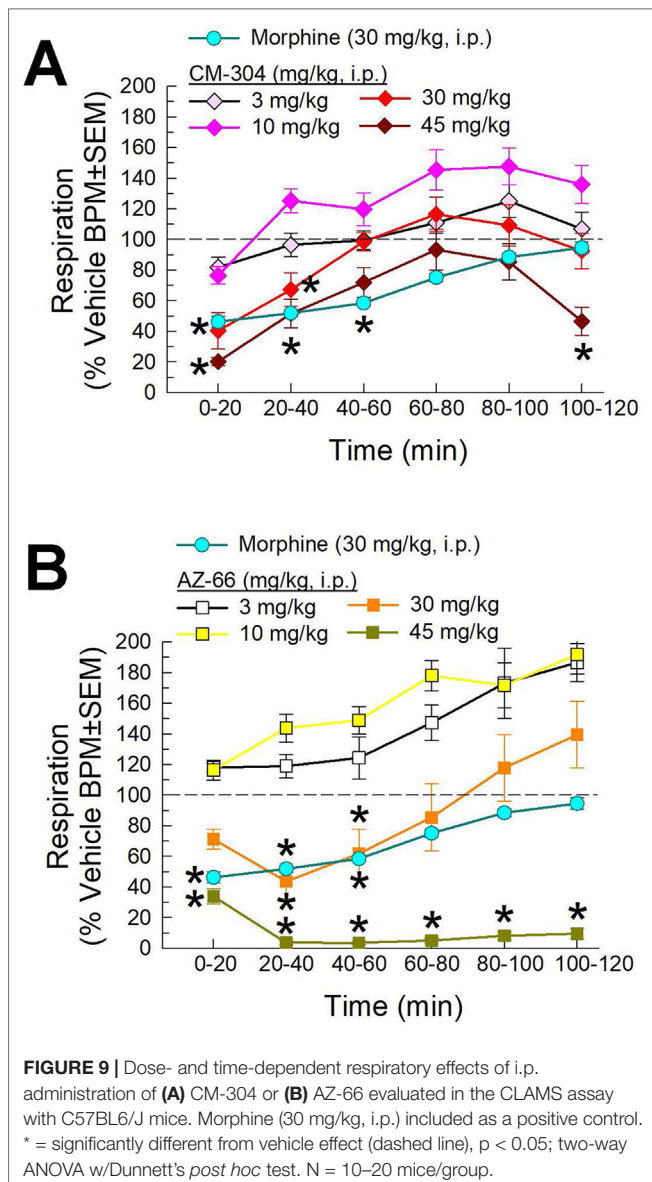


**FIGURE 8 |** Dose- and time-dependent (A) respiratory depression and (B) spontaneous locomotor effects of morphine (cyan circles) or U50,488 (orange hexagons) evaluated in the CLAMS assay with C57BL6/J mice. \* = significantly greater than vehicle effect (dashed line),  $p < 0.05$ ; two-way ANOVA w/Dunnett's *post hoc* test.  $N = 16$ –20 mice/group.

of drug-induced locomotion were observed (factor *treatment* × *time*:  $F_{(20,429)} = 36.4$ ,  $p < 0.0001$ ; two-way ANOVA and Dunnett's *post hoc* test), with morphine producing dose-dependent increased locomotor activity, while U50,488 suppressed spontaneous locomotion (**Figure 8B**). Overall, these results were consistent with established observations that mu-opioid agonists suppress respiration while producing psychostimulatory effects, key liabilities in clinical use.

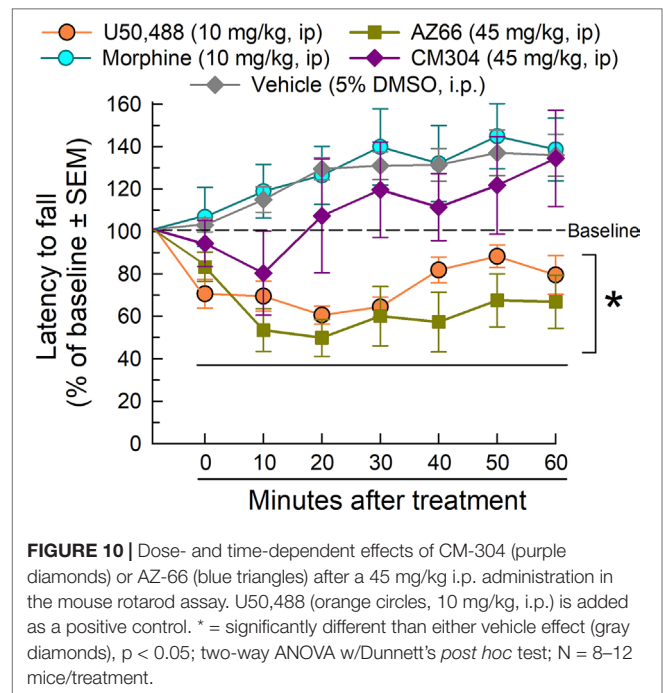
We then completed the characterization of the respiratory effects of the lead compounds CM-304 and AZ-66. Following i.p. administration, both compounds demonstrated dose-dependent reductions in respiration in this assay. CM-304 (**Figure 9A**) and AZ-66 (**Figure 9B**) produced significant dose- and time-dependent respiratory depression (*treatment* × *time*:  $F_{(25,504)} = 2.31$ ,  $p = 0.0004$  and  $F_{(25,450)} = 2.81$ ,  $p < 0.0001$ , respectively;





two-way ANOVA and Dunnett's multiple comparison *post hoc* test). Notably, these effects were more pronounced with AZ-66, with significant respiratory depression extending 2 h after administration of the 45 mg/kg, i.p. dose (Figure 9B).

The rotarod assay is a measure of coordinated locomotor activity and sedation, measuring evoked locomotion that eliminates the potential complication of natural sleep during testing. AZ-66 and CM-304 were evaluated at the 45 mg/kg, i.p. dose that reduced respiration, yet proved to be effective in the neuropathic pain assays. In rotarod testing (Figure 10), morphine was without effect, but U50,488 significantly impaired locomotion as compared to vehicle (factor *treatment*:  $F_{(4,301)} = 36.5$ ,  $p < 0.0001$  and factor *time*:  $F_{(6,301)} = 2.44$ ,  $p = 0.03$ ; two-way ANOVA and Dunnett's *post hoc* test). Whereas AZ-66 significantly impaired evoked locomotion over time, CM-304 did not significantly impair locomotion at any time tested.



Confirming these findings, similar results were observed on ambulations measured in the CLAMS assay, presented as % vehicle effect. CM-304 was found to significantly (if modestly) increase ambulations in the second hour of testing (factor *treatment*:  $F_{(4,354)} = 10.2$ ,  $p < 0.0001$ ; two-way ANOVA and Dunnett's *post hoc* test; Supplemental Figure 1A). Notably, although CM-304 did initially reduce raw ambulations in a dose-dependent manner (factor *treatment* × *time*:  $F_{(20,345)} = 5.72$ ,  $p < 0.0001$ ; two-way ANOVA and Dunnett's *post hoc* test at 0–20 min; Supplemental Figure 2B), this effect was not significant when normalized to the response of vehicle-treated mice ( $p = 0.54$ , 0.77 and 0.99 for the 45 mg/kg, i.p. dose response across time points in the first hour; Dunnett's *post hoc* test). Otherwise, consistent with the rotarod results, AZ-66 consistently produced a significant dose-dependent general reduction in ambulatory activity (factor *treatment*:  $F_{(4,432)} = 5.28$ ,  $p = 0.0004$  and factor *time*:  $F_{(5,432)} = 10.6$ ,  $p < 0.0001$ ; two-way ANOVA and Dunnett's *post hoc* test; Supplemental Figure 1B).

## Evaluation of CM-304 and AZ-66 With the Mouse Conditioned Place Preference Assay

Mice were place conditioned for 40 min each of 2 days with morphine, the KOR-selective agonist U50,488, or the sigma-receptor antagonists CM-304 or AZ-66, using i.p. doses producing significant and consistent anti-allodynic effects (45 mg/kg). While morphine produced significant conditioned-place preference (CPP) and U50,488 produced conditioned-place aversion (CPA) (factor: *treatment* × *conditioning*:  $F_{(3,194)} = 8.79$ ;  $P < 0.001$ ; two-way ANOVA and Sidak's multiple comparisons *post hoc* test), the S1R antagonist CM-304 produced place-conditioning responses

similar to preconditioning responses ( $p = 0.99$ ; **Figure 11**). In contrast, AZ-66 produced significant condition place aversion ( $p = 0.006$ ; **Figure 11**).

## DISCUSSION

Recent endeavors have demonstrated that the radiolabeled version of CM-304, [ $^{18}\text{F}$ ]-FTC-146, accumulates in the brain and periphery, is well tolerated, absorbed at acceptable doses in humans, and is able to accurately locate the site of nerve injury in rats (Hjornevik et al., 2017; Shen et al., 2017a; Shen et al., 2017b). As a viable PET agent, an early phase I clinical trial is investigating [ $^{18}\text{F}$ ]-FTC-146 distribution in patients suffering from complex regional pain syndrome (CRPS) and sciatica to determine how S1R expression is altered in chronic pain states in humans (ClinicalTrials.gov, 2016). While previous work examining AZ-66 and/or CM-304 have demonstrated their ability to prevent stimulant-induced neurotoxicity (Seminario et al., 2012) and S1R agonist self-administration (Katz et al., 2016), their role as anti-nociceptive/allodynic agents have been evaluated for the first time here. The current data provide evidence that sigma receptor antagonists CM-304 and AZ-66 produced antinociceptive and anti-allodynic effects observed in behavioral assays of various modalities of inducible pain, while remaining less effective in a model of thermal reflexive pain. Although the non-selective S1R/S2R antagonist AZ-66 produced equivalent anti-allodynic, but longer-lasting effects in CCI compared to CM-304, it also produced mild locomotor impairment and

conditioned place aversion (CPA). In contrast, the S1R selective antagonist CM-304 produced anti-allodynic effects without significant locomotor impairment or CPA. Further development of sigma receptor antagonists, in particular CM-304, may prove useful in providing relief to individuals suffering from poorly managed pain disorders like chronic pain.

CCI of the sciatic nerve and CISN are two commonly used rodent models of neuropathic pain, arising from sciatica and chemotherapeutic-associated pain respectively. An established “gold standard” for treating neuropathic pain, gabapentin, showed anti-allodynic efficacy at a dose (50 mg/kg i.p.) consistent with previous CCI and CISN studies (Ahn et al., 2009; Kinsey et al., 2009; Long et al., 2009; Ahmad et al., 2017), after a 1-h pretreatment to avoid confounding sedative effects. The present sigma receptor antagonists CM-304 and AZ-66 were as efficacious as the single dose of gabapentin in both models after immediate treatment with a dose of 45 mg/kg, i.p. Furthermore, we confirmed that the commercially available sigma-receptor antagonist E52862 is also efficacious in CCI at a similar dose (30 mg/kg). These data are consistent with the results of a recent phase II clinical study demonstrating E52862 efficacy in treating oxaliplatin-associated neuropathy in humans (Bruna et al., 2018). CCI and CISN both produce neuropathy but are thought to differ somewhat in underlying etiology associated with the development of allodynia. CCI is a focal injury of the sciatic nerve, and has been shown to upregulate sigma-1 receptor expression in the spinal cord, enhance central sensitization, and activate microglia in both the spinal cord and supraspinally throughout the brain (Roh et al., 2008; Barcelon et al., 2019). In comparison, the pathology of CISN may be more complex, with changes of morphology and molecular physiology of peripheral sensory nerves further associated with a neuronal inflammatory response that may impact both the peripheral and central nervous system in ways not yet fully understood to promote allodynia (Starobova and Vetter, 2017). Collectively, this underscores the limits of the current tests to ascertain where CM-304 or AZ-66 may be acting to prevent allodynia. For instance, the dorsal root ganglion (DRG), but not dorsal horn of spinal cord, has been implicated in the development of CISN-associated allodynia, but unlike CCI, CISN is not thought to activate spinal microglia (Zheng et al., 2011; Lessans et al., 2019), and the impact of chemotherapy on S1R expression in either the dorsal horn or DRG has yet to be elucidated. Future detailed investigations using S1R-CRE mice to evaluate the role of spinal, supraspinal, and peripheral sigma receptors in neuropathic pain might clarify this matter. Meanwhile, the current data support earlier reports demonstrating the therapeutic sensitivity of chemotherapy-induced neuropathy to S1R antagonism (Aley and Levine, 2002; Gris et al., 2016).

While CM-304 and AZ-66 demonstrated less efficacy in the 55°C warm-water tail withdrawal assay than morphine, this is consistent with previous literature (Vidal-Torres et al., 2013). Both sigma receptor antagonists were effective in treating inflammation-induced paw licking, supporting a broad therapeutic spectrum for the sigma receptor antagonists across the distinct etiologies contributing to neuropathic and inflammatory pain (Xu and Yaksh, 2011). The antinociception attributed to

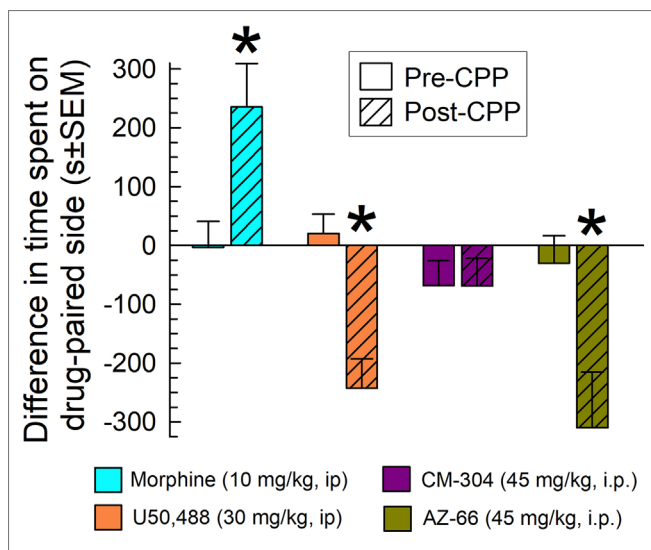


**FIGURE 11** | CM-304 (45 mg/kg/d, i.p.;  $N = 34$ ) did not demonstrate place-conditioning preference (as did morphine,  $N = 17$ ) or aversion, whereas AZ-66 (45 mg/kg/d, i.p.,  $N = 19$ ) demonstrated CPA similar to U50,488 ( $N = 28$ ) in the mouse conditioned place preference assay. \* = post-conditioning response (striped bars) significantly different from matching pre-CPP response (matching open bars),  $p < 0.05$ ; two-way ANOVA w/Sidak's *post hoc* test.

early sigma receptor antagonists was often found to be mediated by off-target effects such as opioid (Martin et al., 1976) or NMDA receptors (Wong et al., 1988). While affinity for other receptor targets associated with antinociception was not examined here, and thus directly discounted, it is notable that modern radiolabeled receptor competition binding assays have reported CM-304 to have both high affinity and selectivity for the S1R over 59 other receptor targets such as serotonin receptors (James et al., 2012; James et al., 2014), while AZ-66 had high affinity for both S1R and S2R (Seminario et al., 2012), suggesting a role for these respective receptors in the current results. From what is known of nociception and sigma receptors, it is most feasible that CM-304 and AZ-66 exerted anti-allodynic and antinociceptive effects through antagonism of sigma-receptors. Inflammation and neuropathy exhibit similar increases in glutamatergic signaling and gliosis in the dorsal horn, immune cell invasion, and elevations of TNF- $\alpha$  in the DRG thought to sensitize nociceptive signaling. However, neuropathy but not inflammation is associated with an increase in voltage-dependent calcium channel subunit  $\alpha$ -2/ $\delta$ -1 in the DRG, a proposed site of action for gabapentinoids (Patel and Dickenson, 2016). Consistent with our current results, the administration of E52862 has been reported to reduce inflammatory allodynic responses induced by carrageenan and complete Freund's adjuvant without altering carrageenan-induced paw edema, confirming that sigma antagonists modulate nociception without resolving the underlying pathology (Gris et al., 2014). Given that previous studies have indicated a higher density of sigma receptors in the DRG compared to the dorsal horn or supraspinal brain regions mediating nociception (specifically, the periaqueductal gray and basolateral amygdala), these results may suggest the dorsal root ganglia is a target of particular interest for sigma receptor involvement in the various and diverse modalities of pain (Sánchez-Fernández et al., 2014). Future anatomical and behavioral studies are expected to elucidate this concept.

Gabapentinoids like gabapentin have been reported to produce undesirable side effects including motor incoordination and respiratory depression that may lead to noncompliance or discontinuation, supporting the preclinical screening of novel therapeutics for these and other liabilities (Kaufman and Struck, 2011; Yaksh and Wallace, 2011; Evoy et al., 2017). Utilizing the CLAMS, both spontaneous locomotion and respiration were measured. Morphine, the prototypical MOR agonist, produced hyper-locomotion and decreases in respiration rate, while U50,488, a KOR-selective agonist, produced transient hypo-locomotion without altering respiration. CM-304 and AZ-66 significantly reduced respiration in a dose-dependent manner, although at a sub-therapeutic dose (10 mg/kg, i.p.) both compounds produced respiratory hyperventilation. It is not readily evident how CM-304 and AZ-66 induced respiratory depression, although the effects were more pronounced with AZ-66. To the best of our knowledge, this is the first time any sigma receptor antagonist has been evaluated for potential respiratory effects, a concern motivated by the current epidemic of opioid abuse. It is conceivable that sigma antagonists prevent S1R and/or S2R promotion of respiration. S1R RNA is heavily expressed in the medulla and less so in the hypothalamus (Lein et al., 2007). Both brain regions mediate

arousal and sedation, suggesting possible modulation by sigma receptors in these behaviors. However, unlike the well-documented respiratory depression directly mediated by activation of mu opioid receptors in the brain's respiratory network (Dahan et al., 2001), detailed investigation of sigma receptor mediation of breathing rate with plethysmography matched with electrophysiology of respiratory centers remains to be done. Alternatively, the sigma-receptor antagonists might indirectly affect respiration by decreasing locomotor activity. AZ-66 demonstrated disruption of coordinated locomotion in the rotarod assay, similar to U50,488, an agent known to produce motor incoordination and sedation (Zhang et al., 2015; Dunn et al., 2018). However, CM-304 was without significant inhibitory effects on locomotion, and in any case, the potential sedative effects of sigma-receptor antagonists are also not well understood. Further work is required to assess the effects of the sigma receptors (both sigma-1 and sigma-2) on respiration and locomotor activity, evaluating hypnotic vs. sedative effects. Future mapping studies of the distribution of S2Rs in brain and additional testing with new compounds showing selective antagonism for S2Rs may offer new insights into the role of sigma receptors in respiration, arousal, and sedation.

Substance abuse and addiction are additional concerns for the use of analgesics, given the epidemic of misused prescription opioids (Seth et al., 2018). To assess potential rewarding or aversive effects of CM-304 or AZ-66, we utilized the condition place preference/aversion assay (CPP/CPA). At supra-therapeutic dosing (45 mg/kg/day), CM-304 produced neither CPP or aversion, while AZ-66 unexpectedly produced conditioned place aversion similar to U50,488. The mechanism underlying the aversive effects of AZ-66 is not known. Kappa opioid receptor agonists produce dysphoria in humans (Pfeiffer et al., 1986) and conditioned place aversion in animals (Chefer et al., 2013), but AZ-66 does not demonstrate affinity for opioid receptors (Seminario et al., 2012). It is conceivable that the present results suggest that S2R antagonists may produce aversion. Notably, previous work has demonstrated that neither CM-304 nor AZ-66 altered the reinstating effect of a priming dose of cocaine in rats demonstrating extinction after being trained to self-administer this psychostimulant (Katz et al., 2016). However, both sigma-receptor antagonists were able to block self-administration of the S1R agonists (+)-pentazocine or PRE-084 (Katz et al., 2016). Notably, these tests only examined reinstatement effects under extinction conditions, and with much lower individual doses (albeit through the same route) than tested here, but they highlight the burgeoning literature suggesting a modulating role for sigma receptors in reward and substance abuse. With the recent isolation of the S2R gene and anticipated transgenic animals, investigations into the specific contributions of S1R and S2R to reward or aversive states are expected to contribute new insights to this question. In the meantime, ongoing studies will evaluate whether selective S2R antagonists mimic AZ-66 conditioned place aversion, as well as the action of these compounds in self-administration assays.

While attributed to antagonist effects at S1R and S2R, the exact mechanisms underlying the anti-allodynic and antinociceptive efficacy of CM-304 and AZ-66 in various



inducible modalities of pain warrant further study. Previous studies have suggested a role for other signaling and receptor targets. For instance, sigma receptor antagonism was found to enhance norepinephrine levels while reducing formalin-induced glutamate release in the spinal cord, as well as attenuate wind up responses in spinal cords sensitized to repetitive nociceptive stimulation (Romero et al., 2012; Vidal-Torres et al., 2014). The latter effect on central sensitization may be a critical component in treating chronic pain for novel therapeutics. Activation of spinal S1Rs has also been reported to enhance NMDA receptor induced pain *via* a PKC/PKA-dependent phosphorylation of NR1 subunit on the NMDA receptor in male ICR mice. Interestingly, sigma agonists only potentiated pain when the NMDA system was activated by nociception (Kim et al., 2008; Yoon et al., 2010). Inhibitors of phospholipase C (PLC), PKC, and  $\text{Ca}^{2+}$ -ATPase attenuated the S1R mediated pain facilitation, implicating the involvement of these secondary pathways in sigma receptor activation and nociceptive signaling (Roh et al., 2008). Agonist induced hypersensitivity and increased phosphorylation of the NR1 subunit were also blocked by NOS inhibitors, reversing sigma agonist-induced increased nNOS activity. This effect was blocked when protein phosphatase calcineurin was applied, but not soluble guanylyl cyclase (sGC; Roh et al., 2011). In sum, these signaling mechanisms combine to increase levels of intracellular calcium and activity of the phospholipase C-IP<sub>3</sub> signaling cascades, potentially promoting nociception when sigma receptors are recruited by noxious stimuli to the plasma membrane of nociceptive components (Ueda et al., 2001). While direct examination of these nociceptive mechanisms was beyond the scope of this initial characterization study, we anticipate the present selective sigma receptor antagonists will facilitate future studies to better evaluate these factors free of off-target or subtype-receptor interactions.

Patients who suffer from neuropathic pain tend to require escalating treatment and report less effective pain relief (Torrance et al., 2007). Given the increasing side effects of clinically used opioids with increased dosage to compensate for limited efficacy, they are now considered second-line treatment for neuropathic pain. Calcium channel  $\alpha 2\text{-}\delta$  ligands such as gabapentin are now considered a first-line treatment (O'Connor and Dworkin, 2009). However, these compounds also demonstrate adverse effects. Gabapentin is known to produce sedation, dizziness, and more importantly peripheral edema in patients, with renal insufficiency a major precaution when prescribing. Gabapentin given to elderly patients was also observed to cause or exacerbate cognitive or gait impairment (Calandre et al., 2016; Mangram et al., 2016). Several weeks may also be required to determine the effective dose, and evidence suggests that gabapentin is ineffective when treating chemotherapy induced neuropathic pain, indicating a need for alternative therapies (Wong et al., 2005; O'Connor and Dworkin, 2009). As suggested by the current data, S1R-selective antagonists such as CM-304 may provide analgesia and anti-allodynia with fewer liabilities of use. Supporting this concept, it is notable that the radioligand analog of CM-304, FTC-146 (James et al., 2012; James et al., 2014), has been successful and well tolerated in phase I clinical trials to image S1Rs upregulated

at the site of neuropathic injury with good safety indications (Shen et al., 2017a; Shen et al., 2017b). Taken together, these data suggest highly selective, metabolically stable S1R antagonists hold promise as novel non-opioid therapeutics for chronic pain management in complex patients.

Beyond the direct anti-allodynic effects of the sigma receptor antagonists, it is feasible they have value as adjuvants for pain management. The S1R antagonist E52862 was shown to potentiate morphine induced antinociception while also producing antinociception in morphine-tolerant mice (Vidal-Torres et al., 2013). Enhancement of morphine analgesia did not coincide with enhancement of other opioid effects, such as physical dependence, inhibition of GI transit, or mydriasis (Vidal-Torres et al., 2013). It is conceivable that adjuvant use of S1R antagonists co-administered with lower doses of opioids may produce adequate pain management without the adverse effects associated with elevated doses of opioids. The effects of CM-304 and AZ-66 on opioid-mediated analgesia and side effects such as antinociceptive tolerance were not evaluated in the present study, but warrant future study.

## CONCLUSION

The current findings support the development of sigma receptor antagonists as emerging novel therapeutics for the treatment of multiple modalities of pain.

## DATA AVAILABILITY STATEMENT

The datasets generated for this study are available on request to the corresponding author.

## ETHICS STATEMENT

This study was carried out in accordance with the recommendations of the 2011 NIH Guide for the Care and Use of Laboratory Animals and ARRIVE guidelines overseen by the Institutional Animal Care and Use Committee at the University of Florida. The protocols (#201609530 and 201710031) were approved by the Institutional Animal Care and Use Committee at the University of Florida.

## AUTHOR CONTRIBUTIONS

CM and JPM participated in research design. TC, SE, JMM, and LW conducted the experiments. MM and SI contributed new reagents or analytic tools. TC, LW, and JPM performed data analysis. TC, LW, CM, and JPM wrote and contributed to the writing of the manuscript.

## ACKNOWLEDGMENTS

This research was supported by the Office of the Assistant Secretary of Defense for Health Affairs through the Peer Reviewed Medical



Research Program under Award No. W81XWH-17-1-0558 to CRM and JPM. Opinions, interpretations, conclusions and recommendations are those of the authors and are not necessarily endorsed by the Department of Defense. Additional technical support provided by Dr. Kristen Hymel is appreciated.

## REFERENCES

- Ahmad, N., Subhan, F., Islam, N. U., Shahid, M., Rahman, F. U., and Sewell, R. D. E. (2017). Gabapentin and its salicylaldehyde derivative alleviate allodynia and hypoalgesia in a cisplatin-induced neuropathic pain model. *Eur. J. Pharmacol.* 814, 302–312. doi: 10.1016/j.ejphar.2017.08.040
- Ahn, K., Johnson, D. S., Mileni, M., Beidler, D., Long, J. Z., McKinney, M. K., et al. (2009). Discovery and characterization of a highly selective FAAH inhibitor that reduces inflammatory pain. *Chem. Biol.* 16, 411–420. doi: 10.1016/j.chembiol.2009.02.013
- Aley, K. O., and Levine, J. D. (2002). Different peripheral mechanisms mediate enhanced nociception in metabolic/toxic and traumatic painful peripheral neuropathies in the rat. *Neuroscience* 111, 389–397. doi: 10.1016/S0306-4522(02)00009-X
- Alon, A., Schmidt, H. R., Wood, M. D., Sahn, J. J., Martin, S. F., and Kruse, A. C. (2017). Identification of the gene that codes for the  $\sigma_2$  receptor. *Proc. Natl. Acad. Sci.* 114 (27), 7160–7165. doi: 10.1073/pnas.1705154114
- Avery, B. A., Vuppala, P. K., Jamalapuram, S., Sharma, A., Mesangeau, C., Chin, F. T., et al. (2017). Quantification of highly selective sigma-1 receptor antagonist CM304 using liquid chromatography tandem mass spectrometry and its application to a pre-clinical pharmacokinetic study. *Drug Test. Anal.* 9 (8), 1236–1242. doi: 10.1002/dta.2156
- Barcelon, E. E., Cho, W. H., Jun, S. B., and Lee, S. J. (2019). Brain microglial activation in chronic pain-associated affective disorder. *Front. Neurosci.* 13, 213. doi: 10.3389/fnins.2019.00213
- Bidlack, J. M., Cohen, D. J., McLaughlin, J. P., Lou, R., Ye, Y., and Wentland, M. P. (2002). 8-Carboxamidocyclazocine: a long-acting, novel benzomorphan. *J. Pharmacol. Exp. Ther.* 302 (1), 374–380. doi: 10.1124/jpet.302.1.374
- Bennett, G. J., and Xie, Y. K. (1988). A peripheral mononeuropathy in rat that produces disorders of pain sensation like those seen in man. *Pain* 33 (1), 87–107. doi: 10.1016/0304-3959(88)90209-6
- Brabant, C., Quertemont, E., and Tirelli, E. (2005). Influence of the dose and the number of drug-context pairings on the magnitude and the long-lasting retention of cocaine-induced conditioned place preference in C57BL/6J mice. *Psychopharmacology* 180 (1), 33–40. doi: 10.1007/s00213-004-2138-6
- Bruna, J., Videla, S., Argyriou, A. A., Velasco, R., Villoria, J., Santos, C., et al. (2018). Efficacy of a novel sigma-1 receptor antagonist for oxaliplatin-induced neuropathy: a randomized, double-blind, placebo-controlled phase IIa clinical trial. *Neurotherapeutics* 15, 178–189. doi: 10.1007/s13311-017-0572-5
- Calandre, E. P., Rico-Villademoros, F., and Slim, M. (2016). Alpha. *Expert Rev. Neurother.* 16, 1263–1277. doi: 10.1080/14737175.2016.1202764
- Chefer, V. I., Bäckman, C. M., Gigante, E. D., and Shippenberg, T. S. (2013). Kappa opioid receptors on dopaminergic neurons are necessary for kappa-mediated place aversion. *Neuropsychopharmacology* 38 (13), 2623–2631. doi: 10.1038/npp.2013.171
- Cheng, H. Y. M., Pitcher, G. M., Laviolette, S. R., Whishaw, I. Q., Tong, K. I., Kockeritz, L. K., et al. (2002). DREAM is a critical transcriptional repressor for pain modulation. *Cell* 108 (1), 31–43. doi: 10.1016/S0092-8674(01)00629-8
- ClinicalTrials.gov. National Library of Medicine (U.S.) [18F]FTC-146 PET/MRI in Healthy Volunteers and in CRPS and Sciatica. Identifier NCT02753101. (2016). Retrieved April 27, 2019 from: <https://clinicaltrials.gov/ct2/show/study/NCT02753101>.
- Curtis, M. J., Bond, R. A., Spina, D., Ahluwalia, A., Alexander, S. P., Gienbycz, M. A., et al. (2015). Editorial. *Br. J. Pharmacol.* 172, 3461–3471. doi: 10.1111/bph.12856
- Dahan, A., Sarton, E., Teppema, L., Olivier, C., Nieuwenhuijs, D., Matthes, H. W., et al. (2001). Anesthetic potency and influence of morphine and sevoflurane on respiration in  $\mu$ -opioid receptor knockout mice. *Anesthesiology* 94, 824–832. doi: 10.1097/0000542-200105000-00021
- Davis, M. P. (2015). Sigma-1 receptors and animal studies centered on pain and analgesia. *Expert Opin. Drug Discov.* 10 (8), 885–900. doi: 10.1517/17460441.2015.1051961
- de la Puente, B., Nadal, X., Portillo-Salido, E., Sánchez-Arroyos, R., Ovalle, S., Palacios, G., et al. (2009). Sigma-1 receptors regulate activity-induced spinal sensitization and neuropathic pain after peripheral nerve injury. *Pain* 145 (3), 294–303. doi: 10.1016/j.pain.2009.05.013
- DeLeo, J. A., Tanga, F. Y., and Tawfik, V. L. (2004). Neuroimmune activation and neuroinflammation in chronic pain and opioid tolerance/hyperalgesia. *Neuroscientist* 10 (1), 40–52. doi: 10.1177/1073858403259950
- Dunn, A. D., Reed, B., Guariglia, C., Dunn, A. M., Hillman, J. M., and Kreek, M. J. (2018). Structurally related kappa opioid receptor agonists with substantial differential signaling bias: neuroendocrine and behavioral effects in C57BL/6 mice. *Int. J. Neuropsychopharmacol.* 21, 847–857. doi: 10.1093/ijnp/ppy034
- Eans, S. O., Ganno, M. L., Reilly, K. J., Patkar, K. A., Senadheera, S. N., Aldrich, J. V., et al. (2013). The macrocyclic tetrapeptide [D-Trp] CJ-15,208 produces short-acting  $\kappa$  opioid receptor antagonism in the CNS after oral administration. *Br. J. Pharmacol.* 169 (2), 426–436. doi: 10.1111/bph.12132
- Eans, S. O., Ganno, M. L., Mizrahi, E., Houghten, R. A., Dooley, C. T., McLaughlin, J. P., et al. (2015). Parallel synthesis of hexahydroimidazodiazepines heterocyclic peptidomimetics and their in vitro and in vivo activities at  $\mu$  (MOR),  $\delta$  (DOR), and  $\kappa$  (KOR) opioid receptors. *J. Med. Chem.* 58 (12), 4905–4917. doi: 10.1021/jm501637c
- Evoy, K. E., Morrison, M. D., and Saklad, S. R. (2017). Abuse and misuse of pregabalin and Gabapentin. *Drugs* 77, 403–426. doi: 10.1007/s40265-017-0700-x
- Feehan, A. K., Morgenweck, J., Zhang, X., Amgott-Kwan, A. T., and Zadina, J. E. (2017). Novel endomorphin analogs are more potent and longer-lasting analgesics in neuropathic, inflammatory, postoperative and visceral pain relative to morphine. *J. Pain* 18, 1526–1541. doi: 10.1016/j.jpain.2017.08.007
- Gris, G., Merlos, M., Vela, J. M., Zamanillo, D., and Portillo-Salido, E. (2014). SIRA, a selective sigma-1 receptor antagonist, inhibits inflammatory pain in the carrageenan and complete Freund's adjuvant models in mice. *Behav. Pharmacol.* 25, 226–235. doi: 10.1097/FBP.0000000000000038
- Gris, G., Portillo-Salido, E., Aubel, B., Darbaky, Y., Deseure, K., Vela, J. M., et al. (2016). The selective sigma-1 receptor antagonist E-52862 attenuates neuropathic pain of different aetiology in rats. *Sci Rep.* 6, 24591. doi: 10.1038/srep24591
- Hanner, M., Moebius, F. F., Flandorfer, A., Knaus, H. G., Striessnig, J., Kempner, E., et al. (1996). Purification, molecular cloning, and expression of the mammalian sigma1-binding site. *Proc. Natl. Acad. Sci.* 93 (15), 8072–8077. doi: 10.1073/pnas.93.15.8072
- Hjornevik, T., Cipriano, P. W., Shen, B., Park, J. H., Gulaka, P., Holley, D., et al. (2017). Biodistribution and radiation dosimetry of (18)F-FTC-146 in humans. *J. Nucl. Med.* 58, 2004–2009. doi: 10.2967/jnumed.117.192641
- Hoot, M. R., Sim-Selley, L. J., Poklis, J. L., Abdullah, R. A., Scoggins, K. L., Selley, D. E., et al. (2010). Chronic constriction injury reduces cannabinoid receptor 1 activity in the rostral anterior cingulate cortex of mice. *Brain Res.* 1339, 18–25. doi: 10.1016/j.brainres.2010.03.105
- Jamalapuram, S., Vuppala, P. K., Abdelazeem, A. H., McCurdy, C. R., and Avery, B. A. (2013). Ultra-performance liquid chromatography tandem mass spectrometry method for the determination of AZ66, a sigma receptor ligand, in rat plasma and its application to in vivo pharmacokinetics. *Biomed. Chromatogr.* 27, 1034–1040. doi: 10.1002/bmc.2901
- James, M. L., Shen, B., Nielsen, C. H., Behera, D., Buckmaster, C. L., Mesangeau, C., et al. (2014). Evaluation of  $\sigma$ -1 receptor radioligand 18F-FTC-146 in rats and squirrel monkeys using PET. *J. Nucl. Med.* 55 (1), 147–153. doi: 10.2967/jnumed.113.120261
- James, M. L., Shen, B., Zavaleta, C. L., Nielsen, C. H., Mesangeau, C., Vuppala, P. K., et al. (2012). New positron emission tomography (PET) radioligand for

## SUPPLEMENTARY MATERIAL

The Supplementary Material for this article can be found online at: <https://www.frontiersin.org/articles/10.3389/fphar.2019.00678/full#supplementary-material>

- imaging  $\sigma$ -1 receptors in living subjects. *J. Med. Chem.* 55 (19), 8272–8282. doi: 10.1021/jm300371c
- Katz, J. L., Hiranita, T., Kopajtic, T. A., Rice, K. C., Mesangeau, C., Narayanan, S., et al. (2016). Blockade of cocaine or  $\sigma$  receptor agonist self administration by subtype-selective  $\sigma$  receptor antagonists. *J. Pharmacol. Exp. Ther.* 358 (1), 109–124. doi: 10.1124/jpet.116.232728
- Kaufman, K. R., and Struck, P. J. (2011). Gabapentin-induced sexual dysfunction. *Epilepsy Behav.* 21, 324–326. doi: 10.1016/j.yebeh.2011.04.058
- Kilkenny, C., Browne, W. J., Cuthill, I. C., Emerson, M., and Altman, D. G. (2010). Improving bioscience research reporting: the ARRIVE guidelines for reporting animal research. *PLoS Biol.* 8 (6), e1000412. doi: 10.1371/journal.pbio.1000412
- Kim, H. W., Roh, D. H., Yoon, S. Y., Seo, H. S., Kwon, Y. B., Han, H. J., et al. (2008). Activation of the spinal sigma-1 receptor enhances NMDA-induced pain via PKC- and PKA-dependent phosphorylation of the NR1 subunit in mice. *Br. J. Pharmacol.* 154, 1125–1134. doi: 10.1038/bjp.2008.159
- Kinsey, S. G., Long, J. Z., O'Neal, S. T., Abdullah, R. A., Poklis, J. L., Boger, D. L., et al. (2009). Blockade of endocannabinoid-degrading enzymes attenuates neuropathic pain. *J. Pharmacol. Exp. Ther.* 330, 902–910. doi: 10.1124/jpet.109.155465
- LaCroix-Fralish, M. L., Rutkowski, M. D., Weinstein, J. N., Mogil, J. S., and DeLeo, J. A. (2005). The magnitude of mechanical allodynia in a rodent model of lumbar radiculopathy is dependent on strain and sex. *Spine (Phila Pa 1976)* 30, 1821–1827. doi: 10.1097/01.brs.0000174122.63291.38
- Lein, E. S., Hawrylycz, M. J., Ao, N., Ayres, M., Bensinger, A., Bernard, A., et al. (2007). Genome-wide atlas of gene expression in the adult mouse brain. *Nature* 445, 168–176. doi: 10.1038/nature05453
- Lessans, S., Lassiter, C. B., Carozzi, V., Heindel, P., Semperboni, S., Oggioni, N., et al. (2019). Global transcriptomic profile of dorsal root ganglion and physiological correlates of cisplatin-induced peripheral neuropathy. *Nurs. Res.* 68, 145–155. doi: 10.1097/NNR.0000000000000338
- Long, J. Z., Nomura, D. K., Vann, R. E., Walentiny, D. M., Booker, L., Jin, X., et al. (2009). Dual blockade of FAAH and MAGL identifies behavioral processes regulated by endocannabinoid crosstalk in vivo. *Proc. Natl. Acad. Sci. U.S.A.* 106, 20270–20275. doi: 10.1073/pnas.0909411106
- Mangram, A., Dzandu, J., Harootunian, G., Zhou, N., Sohn, J., Corneille, M., et al. (2016). Why elderly patients with ground level falls die within 30 days and beyond? *J. Gerontol. Geriatr. Res.* 5, 289. doi: 10.4172/2167-7182.1000289
- Martin, W., Eades, C. G., Thompson, J., Huppler, R. E., and Gilbert, P. E. (1976). The effects of morphine and nalorphine-like drugs in the nondependent and morphine-dependent chronic spinal dog. *J. Pharmacol. Exp. Ther.* 197 (3), 517–532. <http://jpet.aspetjournals.org/content/197/3/517.long>
- Matsumoto, R. R., and Pouw, B. (2000). Correlation between neuroleptic binding to  $\sigma$ 1 and  $\sigma$ 2 receptors and acute dystonic reactions. *Eur. J. Pharmacol.* 401, 155–160. doi: 10.1016/S0014-2999(00)00430-1
- Matsumoto, R. R., McCracken, K. A., Pouw, B., Miller, J., Bowen, W. D., Williams, W., et al. (2001). N-alkyl substituted analogs of the  $\sigma$  receptor ligand BD1008 and traditional  $\sigma$  receptor ligands affect cocaine-induced convulsions and lethality in mice. *Eur. J. Pharmacol.* 411, 261–273. doi: 10.1016/S0014-2999(00)00917-1
- McCurdy, C. R., Mesangeau, C., Narayanan, S., Matsumoto, R. R., and Poupaert, J. H. (2014). U.S. Patent No. 8,809,381. Washington, DC: U.S. Patent and Trademark Office.
- McGrath, J. C., and Lilley, E. (2015). Implementing guidelines on reporting research using animals (ARRIVE etc.): new requirements for publication in BJP. *Br. J. Pharmacol.* 172 (13), 3189–3193. doi: 10.1111/bph.12955
- Mogil, J. S., Kest, B., Sadowski, B., and Belknap, J. K. (1996). Differential genetic mediation of sensitivity to morphine in genetic models of opiate antinociception: influence of nociceptive assay. *J. Pharmacol. Exp. Ther.* 276 (2), 532–544. <http://jpet.aspetjournals.org/content/276/2/532.long>
- Mogil, J. S., Smith, S. B., O'Reilly, M. K., and Plourde, G. (2005). Influence of nociception and stress-induced antinociception on genetic variation in isoflurane potency among mouse strains. *Anesthesiology* 103, 751–758. doi: 10.1097/00000542-200510000-00013
- National Institute on Neurological Diseases and Stroke. Peripheral neuropathy fact sheet. <https://www.ninds.nih.gov/Disorders/Patient-Caregiver-Education/Fact-Sheets/Peripheral-Neuropathy-Fact-Sheet> (May 14, 2019).
- O'Connor, A. B., and Dworkin, R. H. (2009). Treatment of neuropathic pain: an overview of recent guidelines. *Am. J. Med.* 122, S22–32. doi: 10.1016/j.amjmed.2009.04.007
- Orsini, C., Bonito-Oliva, A., Conversi, D., and Cabib, S. (2005). Susceptibility to conditioned place preference induced by addictive drugs in mice of the C57BL/6 and DBA/2 inbred strains. *Psychopharmacology (Berl)* 181, 327–336. doi: 10.1007/s00213-005-2259-6
- Pal, A., Fontanilla, D., Gopalakrishnan, A., Chae, Y. K., Markley, J. L., and Ruoho, A. E. (2012). The sigma-1 receptor protects against cellular oxidative stress and activates antioxidant response elements. *Eur. J. Pharmacol.* 682, 12–20. doi: 10.1016/j.ejphar.2012.01.030
- Patel, R., and Dickenson, A. H. (2016). Mechanisms of the gabapentinoids and  $\alpha$ 2  $\delta$ -1 calcium channel subunit in neuropathic pain. *Pharmacol. Res. Perspect.* 4 (2), e00205. doi: 10.1002/prp2.205
- Pfeiffer, A., Brantl, V., Herz, A., and Emrich, H. M. (1986). Psychotomimesis mediated by kappa opiate receptors. *Science* 233, 774–776. doi: 10.1126/science.3016896
- Pitcher, G. M., Ritchie, J., and Henry, J. L. (1999). Nerve constriction in the rat: model of neuropathic, surgical and central pain. *Pain* 83, 37–46. doi: 10.1016/S0304-3959(99)00085-8
- Reilly, K. J., Giulianotti, M., Dooley, C. T., Nefzi, A., McLaughlin, J. P., and Houghten, R. A. (2010). Identification of two novel, potent, low-liability antinociceptive compounds from the direct in vivo screening of a large mixture-based combinatorial library. *AAPS J.* 12, 318–329. doi: 10.1208/s12248-010-9191-3
- Roh, D. H., Choi, S. R., Yoon, S. Y., Kang, S. Y., Moon, J. Y., Kwon, S. G., et al. (2011). Spinal neuronal NOS activation mediates sigma-1 receptor-induced mechanical and thermal hypersensitivity in mice: involvement of PKC-dependent GluN1 phosphorylation. *Br. J. Pharmacol.* 163, 1707–1720. doi: 10.1111/j.1476-5381.2011.01316.x
- Roh, D. H., Kim, H. W., Yoon, S. Y., Seo, H. S., Kwon, Y. B., Kim, K. W., et al. (2008). Intrathecal injection of the sigma(1) receptor antagonist BD1047 blocks both mechanical allodynia and increases in spinal NR1 expression during the induction phase of rodent neuropathic pain. *Anesthesiology* 109, 879–889. doi: 10.1097/ALN.0b013e3181895a83
- Romero, L., Zamanillo, D., Nadal, X., Sánchez-Arroyos, R., Rivera-Arconada, I., Dordal, A., et al. (2012). Pharmacological properties of S1RA, a new sigma-1 receptor antagonist that inhibits neuropathic pain and activity-induced spinal sensitization. *Br. J. Pharmacol.* 166, 2289–2306. doi: 10.1111/j.1476-5381.2012.01942.x
- Rosenblum, A., Marsch, L. A., Joseph, H., and Portenoy, R. K. (2008). Opioids and the treatment of chronic pain: controversies, current status, and future directions. *Exp. Clin. Psychopharmacol.* 16, 405–416. doi: 10.1037/a0013628
- Sánchez-Fernández, C., Montilla-García, Á., González-Cano, R., Nieto, F. R., Romero, L., Artacho-Cordón, A., et al. (2014). Modulation of peripheral  $\mu$ -opioid analgesia by  $\sigma$ 1 receptors. *J. Pharmacol. Exp. Ther.* 348, 32–45. doi: 10.1124/jpet.113.208272
- Seminario, M. J., Robson, M. J., Abdelazeem, A. H., Mesangeau, C., Jamalapuram, S., Avery, B. A., et al. (2012). Synthesis and pharmacological characterization of a novel sigma receptor ligand with improved metabolic stability and antagonistic effects against methamphetamine. *AAPS J.* 14 (1), 43–51. doi: 10.1208/s12248-011-9311-8
- Seth, P., Rudd, R. A., Noonan, R. K., and Haegerich, T. M. (2018). Quantifying the epidemic of prescription opioid overdose deaths. *Am. J. Public Health* 108, 500–502. doi: 10.2105/AJPH.2017.304265
- Shen, B., James, M. L., Andrews, L., Lau, C., Chen, S., Palmer, M., et al. (2015). Further validation to support clinical translation of [(18)F]FTC-146 for imaging sigma-1 receptors. *EJNMMI Res.* 5 (1), 49. doi: 10.1186/s13550-015-0122-2
- Shen, B., Park, J. H., Hjernevik, T., Cipriano, P. W., Yoon, D., Gulaka, P. K., et al. (2017a). Radiosynthesis and first-in-human PET/MRI evaluation with clinical-grade [(18)F]FTC-146. *Mol. Imaging Biol.* 19 (5), 779–786. doi: 10.1007/s11307-017-1064-z
- Shen, B., Behera, D., James, M. L., Reyes, S. T., Andrews, L., Cipriano, P. W., et al. (2017b). Visualizing nerve injury in a neuropathic pain model with [(18)F] FTC-146 PET/MRI. *Theranostics* 7 (11), 2794. doi: 10.7150/thno.19378
- Starobova, H., and Vetter, I. (2017). Pathophysiology of chemotherapy-induced peripheral neuropathy. *Front. Mol. Neurosci.* 10, 174. doi: 10.3389/fnmol.2017.00174
- Torrance, N., Smith, B. H., Watson, M. C., and Bennett, M. I. (2007). Medication and treatment use in primary care patients with chronic pain of predominantly neuropathic origin. *Fam. Pract.* 24, 481–485. doi: 10.1093/fampra/cmm042

- Ueda, H., Inoue, M., Yoshida, A., Mizuno, K., Yamamoto, H., Maruo, J., et al. (2001). Metabotropic neurosteroid/sigma-receptor involved in stimulation of nociceptor endings of mice. *J. Pharmacol. Exp. Ther.* 298, 703–710. <http://jpet.aspetjournals.org/content/298/2/703.long>
- Vidal-Torres, A., de la Puente, B., Rocasalbas, M., Touriño, C., Bura, S. A., Fernández-Pastor, B., et al. (2013). Sigma-1 receptor antagonism as opioid adjuvant strategy: enhancement of opioid antinociception without increasing adverse effects. *Eur. J. Pharmacol.* 711, 63–72. doi: 10.1016/j.ejphar.2013.04.018
- Vidal-Torres, A., Fernández-Pastor, B., Carceller, A., Vela, J. M., Merlos, M., and Zamanillo, D. (2014). Effects of the selective sigma-1 receptor antagonist S1RA on formalin-induced pain behavior and neurotransmitter release in the spinal cord in rats. *J. Neurochem.* 129, 484–494. doi: 10.1111/jnc.12648
- Walker, J. M., Bowen, W. D., Walker, F. O., Matsumoto, R. R., De Costa, B., and Rice, K. C. (1990). Sigma receptors: biology and function. *Pharmacol. Rev.* 42, 355–402. <http://pharmrev.aspetjournals.org/content/42/4/355.long>
- Wilson, S. G., Smith, S. B., Chesler, E. J., Melton, K. A., Haas, J. J., Mitton, B., et al. (2003). The heritability of antinociception: common pharmacogenetic mediation of five neurochemically distinct analgesics. *J. Pharmacol. Exp. Ther.* 304, 547–559. doi: 10.1124/jpet.102.041889
- Wong, E. H., Knight, A. R., and Woodruff, G. N. (1988). [3H] MK-801 labels a site on the N-methyl-D-aspartate receptor channel complex in rat brain membranes. *J. Neurochem.* 50 (1), 274–281. doi: 10.1111/j.1471-4159.1988.tb13260.x
- Wong, G., Michalak, J., Sloan, J., Mailliard, J., Nikcevich, D., Novotny, P., et al. (2005). “A phase III double blinded, placebo controlled, randomized trial of gabapentin in patients with chemotherapy-induced peripheral neuropathy: a North Central Cancer Treatment Group study,” in *ASCO Annual Meeting Proceedings: Journal of Clinical Oncology*. 2005 May 13–17; Orlando, Florida: American Society of Clinical Oncology. doi: 10.1200/jco.2005.23.16\_suppl.8001
- Wunsch, B. (2012). The sigma(1) receptor antagonist S1RA is a promising candidate for the treatment of neurogenic pain. *J. Med. Chem.* 55, 8209–8210. doi: 10.1021/jm3011993
- Xu, M., Petraschka, M., McLaughlin, J. P., Westenbroek, R. E., Caron, M. G., Lefkowitz, R. J., et al. (2004). Neuropathic pain activates the endogenous kappa opioid system in mouse spinal cord and induces opioid receptor tolerance. *J. Neurosci.* 24, 4576–4584. doi: 10.1523/JNEUROSCI.5552-03.2004
- Xu, Q., and Yaksh, T. L. (2011). A brief comparison of the pathophysiology of inflammatory versus neuropathic pain. *Curr. Opin. Anaesthesiol.* 24 (4), 400–407. doi: 10.1097/ACO.0b013e32834871df
- Yaksh, T. L., and Wallace, M. S. (2011). “Opioids, analgesia, and pain management,” in *Goodman and Gilman's the Pharmacological Basis of Therapeutics* (New York: McGraw-Hill Medical), 481–526.
- Yoon, S. Y., Roh, D. H., Seo, H. S., Kang, S. Y., Moon, J. Y., Song, S., et al. (2010). An increase in spinal dehydroepiandrosterone sulfate (DHEAS) enhances NMDA-induced pain via phosphorylation of the NR1 subunit in mice: involvement of the sigma-1 receptor. *Neuropharmacology* 59, 460–467. doi: 10.1016/j.neuropharm.2010.06.007
- Zhang, L. S., Wang, J., Chen, J. C., Tao, Y. M., Wang, Y. H., Xu, X. J., et al. (2015). Novel  $\kappa$ -opioid receptor agonist MB-1C-OH produces potent analgesia with less depression and sedation. *Acta Pharmacol. Sin.* 36 (5), 565–571. doi: 10.1038/aps.2014.145
- Zheng, F. Y., Xiao, W. H., and Bennett, G. J. (2011). The response of spinal microglia to chemotherapy-evoked painful peripheral neuropathies is distinct from that evoked by traumatic nerve injuries. *Neuroscience* 176, 447–454. doi: 10.1016/j.neuroscience.2010.12.052
- Zhou, W., Kavelaars, A., and Heijnen, C. J. (2016). Metformin prevents Cisplatin-induced cognitive impairment and brain damage in mice. *PLoS One* 11, e0151890. doi: 10.1371/journal.pone.0151890

**Conflict of Interest Statement:** The authors declare that the research was conducted in the absence of any commercial or financial relationships that could be construed as a potential conflict of interest.

Copyright © 2019 Cirino, Eans, Medina, Wilson, Mottinelli, Intagliata, McCurdy and McLaughlin. This is an open-access article distributed under the terms of the Creative Commons Attribution License (CC BY). The use, distribution or reproduction in other forums is permitted, provided the original author(s) and the copyright owner(s) are credited and that the original publication in this journal is cited, in accordance with accepted academic practice. No use, distribution or reproduction is permitted which does not comply with these terms.



# Small-Molecule Modulators of Sigma1 and Sigma2/TMEM97 in the Context of Cancer: Foundational Concepts and Emerging Themes

Halley M. Oyer, Christina M. Sanders and Felix J. Kim\*

Department of Cancer Biology, Sidney Kimmel Cancer Center at Thomas Jefferson University, Philadelphia, PA, United States

## OPEN ACCESS

### Edited by:

Tangui Maurice,  
INSERM U1198 Mécanismes  
Moléculaires dans les Démences  
Neurodégénératives, France

### Reviewed by:

Arnold Eino Ruoho,  
University of Wisconsin School of  
Medicine and Public Health,  
United States  
Daniela Rossi,  
University of Pavia, Italy

### \*Correspondence:

Felix J. Kim  
felix.kim@jefferson.edu

### Specialty section:

This article was submitted to  
Experimental Pharmacology  
and Drug Discovery,  
a section of the journal  
Frontiers in Pharmacology

**Received:** 10 May 2019

**Accepted:** 04 September 2019

**Published:** 21 October 2019

### Citation:

Oyer HM, Sanders CM and Kim FJ  
(2019) Small-Molecule Modulators  
of Sigma1 and Sigma2/TMEM97 in  
the Context of Cancer: Foundational  
Concepts and Emerging Themes.  
Front. Pharmacol. 10:1141.  
doi: 10.3389/fphar.2019.01141

There are two known subtypes of the so-called sigma receptors, Sigma1 and Sigma2. Sigma1 (encoded by the *SIGMAR1* gene and also known as Sigma-1 receptor, S1R) is a unique pharmacologically regulated integral membrane chaperone or scaffolding protein that allosterically modulates the activity of its associated proteins. Sigma2, recently identified as transmembrane protein 97 (TMEM97), is an integral membrane protein implicated in cellular cholesterol homeostasis. A number of publications over the past two decades have suggested a role for both sigma proteins in tumor biology. Although there is currently no clinically used anti-cancer drug that targets Sigma1 or Sigma2/TMEM97, a growing body of evidence supports the potential of small-molecule compounds with affinity for these proteins, putative sigma ligands, as therapeutic agents to treat cancer. In preclinical models, these compounds have been reported to inhibit cancer cell proliferation, survival, adhesion, and migration; furthermore, they have been demonstrated to suppress tumor growth, to alleviate cancer-associated pain, and to exert immunomodulatory properties. Here, we will address the known knowns and the known unknowns of Sigma1 and Sigma2/TMEM97 ligand actions in the context of cancer. This review will highlight key discoveries and published evidence in support of a role for sigma proteins in cancer and will discuss several fundamental questions regarding the physiological roles of sigma proteins in cancer and sigma ligand mechanism of action.

**Keywords:** Sigma1, Sigma2/TMEM97, cancer, pharmacology, autophagy, proteostasis, metabolism

## DISCOVERY, REDISCOVERY, AND IDENTIFICATION OF SIGMA1 AND SIGMA2/TMEM97 RECEPTORS

The notion of sigma receptors began with the discovery of the Sigma1-binding site in 1976 (Martin et al., 1976). In this study, three distinct classes of opioid receptors, mu, kappa, and sigma were proposed based upon behavioral studies with morphine, ketocyclazocine, and SKF10047. The opioid receptor antagonist naltrexone antagonized all of these compounds, which led to the identification of sigma as an opioid receptor (Martin et al., 1976). However, in the original study, the stereoisomer of SKF10047 used was not described. Subsequent studies used (+)-SKF10047 to define the putative sigma receptor as clearly not opioid (Su, 1982). Since then, a large number of chemically diverse compounds that have affinity for sigma receptors have been reported (reviewed in Cobos EJ et al., 2008; Maurice and Su, 2009; Narayanan et al., 2011; Weber and Wunsch, 2017). Based primarily on



ligand-binding studies with this growing number of compounds, the putative sigma receptors were subdivided into two subtypes, Sigma1 and Sigma2 (Hellewell and Bowen, 1990).

Sigma1 (*SIGMAR1*; also known as Sigma1-receptor and several other names (Kim, 2017) has been more extensively characterized than Sigma2. The cloning of Sigma1 revealed that it was unlike any traditional receptor (Hanner et al., 1996). Indeed, Sigma1 shares no significant homology with any other protein encoded in the human genome (Hanner et al., 1996; Schmidt et al., 2016). Full-length human Sigma1 is an approximately 26 kilodalton (kDa) protein that comprises 223 amino acids. According to the recently published crystal structure, Sigma1 has a single integral membrane domain with a short ER luminal amino-terminal peptide and most of the carboxy-terminal region of the protein extending into the cytoplasm (Hanner et al., 1996; Schmidt et al., 2016). Emerging evidence suggests that Sigma1 is a novel, pharmacologically responsive, oligomeric, and integral membrane chaperone or scaffolding protein (Hayashi and Su, 2007; Crottes et al., 2011; Crottes et al., 2016; Thomas et al., 2017) that is enriched in the secretory pathway, particularly the endoplasmic reticulum (ER) of most cancer cells (reviewed in Kim and Maher, 2017). In the context of tumor biology, Sigma1 appears to be a component of the cancer cell support machinery (Kim and Maher, 2017). Sigma1 has been proposed to function as oligomeric structures including dimers, trimers, tetramers, and higher order oligomers (Gromek et al., 2014; Schmidt et al., 2016). Changes in oligomeric structures may correspond with differential response to Sigma1 ligands (Gromek et al., 2014; Mishra et al., 2015; Schmidt et al., 2018; Yano et al., 2018). Although the label “receptor” persists, it is now clear that Sigma1 does not fit the traditional definition of receptor. Sigma1 itself has no known intrinsic signaling or enzymatic activity, rather it allosterically modulates the intracellular signaling and activities of its associated proteins (reviewed in Maurice and Su, 2009; Kim and Maher, 2017; Pasternak, 2017).

Sigma2 had long remained a pharmacologically defined entity (Bowen, 2000; Zeng et al., 2017; Abate et al., 2018). Recently, the Sigma2 receptor was identified as an integral membrane protein called transmembrane protein 97 (TMEM97, also known as MAC30) (Alon et al., 2017; Kim and Pasternak, 2017), a member of the insulin-like growth factor-binding protein family (Murphy et al., 1993; Schmit and Michiels, 2018). TMEM97 has been implicated in cholesterol metabolism (Wilcox et al., 2007; Sanchez-Pulido and Ponting, 2014; Ebrahimi-Fakhari et al., 2016; Riad et al., 2018) and has been shown specifically to influence cellular cholesterol trafficking by binding to Niemann–Pick disease, type C1 (NPC1) protein (Bartz et al., 2009; Ebrahimi-Fakhari et al., 2016). TMEM97 also has been implicated in several types of cancer (Schmit and Michiels, 2018). The pharmacologically defined Sigma2-binding site has been implicated in myriad diseases and disorders, including cancer and neurodegenerative diseases (Wheeler et al., 2000; Crawford and Bowen, 2002; Crawford et al., 2002; Narayanan et al., 2011; Guo and Zhen, 2015; Abate et al., 2018). However, the molecular basis of these associations remains unclear. Validation of Sigma2/TMEM97 as the pharmacological target of Sigma2 ligands should enable molecular characterization of this sigma-binding

site and open the door to more studies exploring the mechanism of action of putative sigma receptor ligands.

## SIGMA1 AND SIGMA2/TMEM97 EXPRESSION IN CANCER

Over the past two decades, a number of publications have suggested a potential role for Sigma1 (Kim and Maher, 2017) and Sigma2/TMEM97 (Abate et al., 2018; Schmit and Michiels, 2018) in tumor biology. Until recently, for Sigma1, this association was largely based on two lines of evidence: (Martin et al., 1976) elevated expression of *SIGMAR1* transcripts and Sigma1 protein, primarily in cancer cell lines and some tumors (Kim and Maher, 2017) and (Su, 1982) antiproliferative and apoptosis inducing effects of some small-molecule inhibitors (putative antagonists) of Sigma1 on cancer cell lines (reviewed extensively in (Kim and Maher, 2017) and briefly outlined in **Table 1**). The physiological significance of elevated Sigma1 in tumors remains poorly understood, and how *SIGMAR1* gene expression is regulated in cancer remains unclear. However, Sigma1 RNAi knockdown and some small-molecule inhibitors of Sigma1 inhibit cancer cell growth, proliferation, mobility, and survival and suppress xenografted tumor growth, suggesting that functional Sigma1 is required for tumorigenesis and tumor progression (Spruce et al., 2004; Sun et al., 2014; Kim and Maher, 2017; Thomas et al., 2017). Conversely, in some studies, increased Sigma1 protein levels through overexpression of recombinant Sigma1 and enhancing Sigma1 with small-molecule activators (putative agonists) have been reported to promote cell growth, proliferation, mobility, and cell survival (Zhu et al., 2003; Spruce et al., 2004; Maurice and Su, 2009; Sun et al., 2014; Thomas et al., 2017; Maher et al., 2018).

As it had remained a pharmacologically defined entity until recently, the elevated expression and levels of Sigma2 have been extrapolated from radioligand binding of cancer cell lines (Bowen, 2000; Wheeler et al., 2000; Zeng et al., 2017). Through pharmacological studies, Sigma2 also has been proposed as a potential drug target in cancer (Wheeler et al., 2000; Crawford and Bowen, 2002; Crawford et al., 2002), and radiotracers with affinity for Sigma2 have been developed as tumor imaging agents (Zeng et al., 2017). The recent identification of Sigma2 as TMEM97 now provides a molecular entity to elucidate the mechanism of action of historical Sigma2 ligands. However, it also raises questions regarding Sigma2 pharmacology in the context of cancer.

There are relatively few publications specifically regarding TMEM97 in cancer. Nevertheless, TMEM97 is reported to be upregulated in cancer cell lines and tumors including esophageal, gastric, colorectal, breast, ovarian surface epithelium (suggesting a role in ovarian cancer), oral squamous, and non-small cell lung cancer (NSCLC) (reviewed in Kayed et al., 2004; Wilcox et al., 2007; Schmit and Michiels, 2018). The pharmacologically defined Sigma2-binding site is reported to be enriched in a broad range of cancer cell lines and solid tumors, including breast and pancreatic (Wheeler et al., 2000; Choi et al., 2001; Hou et al., 2006; Zeng et al., 2007) cancers. However, the reported levels of TMEM97 are not always consistent with those of the pharmacologically defined Sigma2-binding site. For example, Sigma2 binding is

elevated in pancreas cancer cell lines, and several published studies demonstrate the potential for Sigma2 ligands as pancreatic cancer therapeutic (Kashiwagi et al., 2007) and imaging agents (Zeng et al., 2017). However, in at least one published study, pancreatic and renal cancers are reported to express low levels of TMEM97 (Kayed et al., 2004). TMEM97 mRNA transcript levels were reported to be highly variable in commonly used pancreatic cancer cell lines with generally low levels of protein (Kayed et al., 2004; Schmit and Michiels, 2018). Elevated TMEM97 expression has been associated with poor clinical outcomes and tumor progression in gastric, colorectal (Moparthi et al., 2007), breast and ovarian (Xiao et al., 2013; Yang et al., 2013), squamous cell lung cancer (SQCLC) (Ding et al., 2016), and non-small cell lung cancer (NSCLC) (Han et al., 2013; Ding et al., 2017). Interestingly, in the latter, high TMEM97 levels correlated with poor patient survival and resistance to platinum-based chemotherapy treatment (Chen et al., 2016; Ding et al., 2017). TMEM97 has been implicated in cancer drug resistance in several reports (Abate et al., 2018).

Furthermore, TMEM97 appears to play the role of tumor suppressor or promotes tumor growth, depending upon the cancer type. TMEM97 has been proposed as a potential tumor suppressor in pancreas (Kayed et al., 2004) and prostate cancer (Ramalho-Carvalho et al., 2018). In contrast, TMEM97 contributes to xenografted tumor growth using glioma and gastric cancer cell line models (Xu et al., 2014; Qiu et al., 2015). In these studies, TMEM97 knockdown in commonly used glioma (U373, U87) and gastric cancer (AGS, BGC-823) cell lines resulted in decreased cell proliferation, migration, and invasion in *in vitro* assays (Xu et al., 2014; Qiu et al., 2015). In contrast to these knockdown studies, Zeng et al. recently published that knockdown and knockout of TMEM97 did not suppress the proliferation or viability of HeLa cells (Zeng et al., 2019). Furthermore, this study proposed that TMEM97 does not mediate Sigma2 ligand-induced cytotoxicity of HeLa cells (Zeng et al., 2019). This study raises important questions regarding our current knowledge of Sigma2 pharmacology in the context of cancer. Considering the apparent context-dependent actions of Sigma2/TMEM97, it will be of interest to further evaluate this approach in a broader range of cancer cell lines.

The recent identification of the Sigma2-binding site as TMEM97 presents an opportunity to merge two fields: for the TMEM97 field to benefit from the decades of medicinal chemistry that has produced a plethora of small-molecule compounds with affinity for Sigma2, and equally, for the Sigma2 field to elucidate the pharmacological mechanism of action of these compounds. It will be interesting to follow the evolution of this subfield over the next several years.

## PUTATIVE AGONISTS AND ANTAGONISTS OF SIGMA1 AND SIGMA2/TMEM97

As it was originally identified as a receptor, small molecules with affinity for Sigma1 and 2, so-called sigma receptor ligands, have been classified as putative agonists and antagonists. These classifications may be inaccurate, as Sigma1 is not a bona fide receptor. Sigma1 has been associated with myriad signaling and transduction systems largely through studies with these ligands (Kruse, 2016; Sabino

and Cottone, 2016; Katz et al., 2017; Kim, 2017; Kim and Maher, 2017; Kourrich, 2017; Kruse, 2017; Laurini et al., 2017; Maurice and Gogvadze, 2017; Merlos et al., 2017; Pasternak, 2017; Weber and Wunsch, 2017; Zeng et al., 2017). However, Sigma1 has no known intrinsic activity, and a preponderance of evidence suggests that it exerts its actions through allosteric modulation of other proteins and signaling systems (Hayashi and Su, 2007; Maurice and Su, 2009; Kim and Maher, 2017; Pasternak, 2017). Thus, Sigma1 ligands may function as allosteric modulators of protein-protein interactions (PPIs) (Thompson et al., 2012; Cesa et al., 2015; Kim and Maher, 2017; Pricer et al., 2017). In the absence of identified intrinsic activity of the protein itself, the concept of Sigma1 “agonism” and “antagonism” is atypical, such that antagonist actions mimic phenotypes observed in genetic knockdown or knockout animal models (reviewed in Maurice and Su, 2009; Kim and Maher, 2017; Merlos et al., 2017). The term modulator may more accurately define compounds with affinity for Sigma1 (Su et al., 2010; Kim and Maher, 2017). Recently, the oligomeric state of Sigma1 was proposed to be differentially modulated by Sigma1 agonists and antagonists (Gromek et al., 2014; Yano et al., 2018). This was supported by molecular dynamics studies based on the published Sigma1 crystal structure (Schmidt et al., 2018; Yano et al., 2018).

As we have recently published a more comprehensive review of the literature and perspective on Sigma1 biology and Sigma1 pharmacology in the context of cancer elsewhere (Kim and Maher, 2017), in the present review article, we will focus on and expand our discussion of Sigma1 and Sigma2/TMEM97 ligands and their actions in cancer-relevant physiological processes, including cancer cell proliferation, growth, motility, migration, survival, and death (by apoptotic and non-apoptotic mechanisms), as well as protein homeostasis, lipid metabolism, and immune modulation. We also discuss the safety of sigma modulators as well as potential therapeutic benefits in cancer and cancer treatment-associated comorbidities.

Although endogenous ligands for Sigma1 and Sigma2/TMEM97 have not been clearly established, sigma receptor ligands were initially defined as agonists and antagonists based on rodent behavior assays (discussed in Cobos EJ et al., 2008; Maurice and Su, 2009; Katz et al., 2017; Kim, 2017; Kim and Maher, 2017; Kruse, 2017; Maurice and Gogvadze, 2017; Merlos et al., 2017; Pasternak, 2017; Weber and Wunsch, 2017), wherein synthetic Sigma1 agonists generally promoted the actions of other drugs, such as neurosteroids, cocaine, and amphetamines. Conversely, Sigma1 antagonists either produced no behavioral changes (Matsumoto et al., 2001; Maurice and Gogvadze, 2017) or attenuated stimulant triggered behaviors (Maurice et al., 1998; McCracken et al., 1999). For example, the neurosteroid pregnenolone and dehydroepiandrosterone, both of which have affinity for Sigma1, were neuroprotective and thus classified as Sigma1 agonists, whereas progesterone blocked their neuroprotective effects and thus was classified as a Sigma1 antagonist (Maurice et al., 1998). These studies are reviewed and discussed in detail elsewhere (Cobos EJ et al., 2008; Maurice and Su, 2009; Katz et al., 2017; Kim, 2017; Kim and Maher, 2017; Kruse, 2017; Maurice and Gogvadze, 2017; Merlos et al., 2017; Pasternak, 2017; Weber and Wunsch, 2017).

Inhibitions of cancer cell proliferation and cell viability have been considered measures of Sigma1 inhibition (putative antagonism), and this is largely consistent with the effects of Sigma1 ablation/knockdown on cancer cells (reviewed in 15). However, as we discuss below, the distinction between putative agonists and antagonists does not strictly apply.

There remains no established biochemical or molecular mechanism of action to clearly define Sigma1 agonist/activator and antagonist/inhibitor activity. However, recently, oligomerization has been proposed as a readout of differential Sigma1 agonist/activator *versus* antagonist/inhibitor activity (Gromek et al., 2014; Yano et al., 2018). This is consistent with a role for Sigma1 as an allosteric modulator of protein–protein interactions and associated protein signaling.

The definition of Sigma2/TMEM97 agonist and antagonist remains unclear. Zeng et al. have proposed that Sigma2 selective compounds with cancer cell cytotoxic effects on cancer cells should be classified as agonists. This is based on the cytotoxicity of siramesine, which the authors cite as a commonly accepted Sigma2 agonist (Zeng et al., 2014). Using this approach, the authors have categorized Sigma2 ligands as agonists, partial agonists, and antagonists (Zeng et al., 2014). However, these do not provide molecular basis for pharmacological mechanism of action of Sigma2 ligands.

## ACTIONS OF PUTATIVE ACTIVATORS/AGONISTS AND INHIBITORS/ANTAGONISTS OF SIGMA1 AND SIGMA2/TMEM97 IN STANDARD PRECLINICAL MODELS OF CANCER

Much of our knowledge regarding Sigma1 and Sigma2/TMEM97 in tumor biology is derived from studies with synthetic compounds. Several prototypic Sigma1 and Sigma2/TMEM97 compounds are reported to influence cancer cell survival, proliferation, growth, adhesion, motility, and protein homeostasis pathways, thereby suggesting a potentially broad range of therapeutic opportunities for targeting these proteins (reviewed in Kim and Maher, 2017). Several key prototypic compounds are highlighted in **Table 1**.

### Antiproliferative and Proapoptotic Actions of Sigma1 Inhibitors/Antagonists

In preclinical laboratory models of cancer, Sigma1 inhibition or putative antagonism is generally associated with inhibition of cancer cell proliferation and viability. Interestingly, Sigma1 putative antagonists/inhibitors as originally defined by behavioral endpoints have generally correlated with inhibition of cancer cell proliferation and in some cases induction of apoptosis (Colabufo et al., 2004; Spruce et al., 2004). Importantly, this is consistent with the general proliferation, growth, and survival inhibiting effects of Sigma1 RNAi knockdown (reviewed in Kim and Maher, 2017). A detailed and extensive review and discussion of the antiproliferative and proapoptotic actions of sigma modulators is provided elsewhere (Kim and Maher, 2017).

Importantly, the *in vivo* anti-tumor efficacy of several prototypic Sigma1 antagonists/inhibitors has been reported, highlighting their drug-like properties and potential for drug development. Furthermore, most of these studies report efficacious tumor growth inhibition with minimal toxicity in mouse models (reviewed in Kim and Maher, 2017).

### Proliferative and Prosurvival Actions of Sigma1 Activators/Agonists

In most *in vitro* cancer biology studies, Sigma1 agonists/activators have been used to observe pharmacological competition to confirm Sigma1 selective actions. Typically, Sigma1 agonists/activators appear to have no effect on cell proliferation and tumor growth (Kim and Maher, 2017). The common prototypic agonists used to this end include (+)-pentazocine, (+)-SKF10047, PRE-084, 4-(N-benzylpiperidin-4-yl)-4-iodobenzamide (4-IBP), and SA4503. In some cases, these putative agonists/activators are reported to promote cancer cell proliferation and tumor growth (reviewed in 15). However, some publications report the contrary that some of these same compounds inhibit cell proliferation and trigger cell cycle arrest (Megalizzi et al., 2007; Megalizzi et al., 2009). It is difficult to reconcile these discrepancies. However, the notion of agonist/activator and antagonist/inhibitor classifications may be inaccurate, and what these classifications mean in the context of cancer cell biology remains unclear.

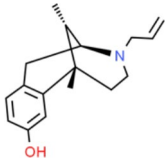
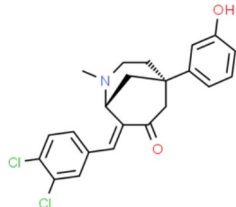
### Cytotoxic actions of Sigma2/TMEM97 Agonists/Activators

Interestingly, Zeng et al. reported that neither Sigma2/TMEM97 nor PGRMC1 (which was originally identified as the Sigma2-binding site Xu et al., 2011; Abate et al., 2015; Zeng et al., 2016; Pati et al., 2017b)-mediated Sigma2 ligand-induced cytotoxicity (Zeng et al., 2019). Based on this surprising discovery, the authors propose a closer evaluation of the mechanisms underlying Sigma2 ligand-induced cytotoxicity (Zeng et al., 2019). Thus, the anti-cancer mechanism of action of putative Sigma2 selective compounds remains unclear.

### Combined Sigma1 Inhibitors/Antagonists and Sigma2/TMEM97 Agonist/Activators

Most putative sigma receptor ligands have affinity for both Sigma1 and Sigma2/TMEM97, albeit with differences in subtype-binding affinity (reviewed in 15 and **Table 1**). It has been proposed that the antiproliferative and proapoptotic activities of these compounds may involve a combination of Sigma1 antagonism/inhibition and Sigma2 agonism (Zeng et al., 2014). However, when this concept was proposed, Sigma2 was still a pharmacologically defined entity as the identity of Sigma2 has been controversial (Abate et al., 2015; Pati et al., 2017b). Furthermore, the definition of Sigma2 agonism is unclear. The recent identification of TMEM97 as Sigma2 (Alon et al., 2017) should accelerate the elucidation of the pharmacological mechanism of action of putative Sigma2 ligands. Furthermore, more data are needed to clarify the roles of TMEM97 alone and in relation to Sigma1 in cancer pharmacology (Schmit and Michiels, 2018).

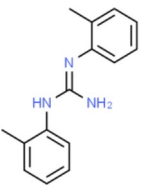
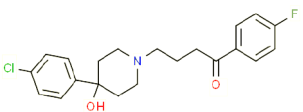
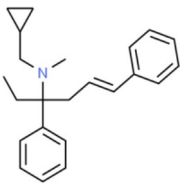
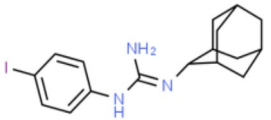
**TABLE 1 |** Prototypical small-molecule Sigma1 and Sigma2/TMEM97 modulators/ligands.

Compound	Binding affinity (Sigma1 and 2) and references	Putative action	Assays used	Summary of results	References
(+)-Pentazocine 	<ul style="list-style-type: none"> <li>• Sigma1 (<math>K_i</math>): 3.9–23.3 nM (Hellewell et al., 1994; John et al., 1999; Colabufo et al., 2004; Azzariti et al., 2006)</li> <li>• Sigma2 (<math>K_i</math>): 1,542–6,611 nM (Hellewell et al., 1994; Vilner and Bowen, 2000; Choi et al., 2001; Ishiwata et al., 2006)</li> </ul>	Agonist (Sigma1)	MTT, MTS, apoptosis assays, light microscopy of cell morphology changes	In most functional studies, it did not impact cell viability or proliferation, and it has been used to block the anticancer actions (cytotoxicity and/or proliferation arrest) of Sigma1 inhibitors/antagonists such as IPAG and rimcazole. In some cases, (+)-pentazocine reported to result in cell detachment and rounding of cells and inhibition of cell proliferation. ( $^3H$ ) (+)-pentazocine is a commonly used radioligand used to quantify and define Sigma1-binding sites.	(Brent and Pang, 1995; Colabufo et al., 2004; Spruce et al., 2004; Rybczynska et al., 2008; Korpis et al., 2014)
(+)-SKF10047 	<ul style="list-style-type: none"> <li>• Sigma1 (<math>K_i</math>): 54–597 nM (Hellewell et al., 1994; Vilner et al., 1995a; Ryan-Moro et al., 1996; Vilner and Bowen, 2000)</li> <li>• Sigma2 (<math>K_i</math>): 11,170–39,740 nM (Hellewell et al., 1994; Vilner and Bowen, 2000)</li> </ul>	Agonist (Sigma1)	MTT, MTS, or apoptosis assays, light microscopy of cell morphology changes	(+)-SKF10047 has been used to block the anticancer actions (cytotoxicity and/or proliferation arrest) of Sigma1 inhibitors/antagonists such as IPAG and rimcazole. Demonstrated immune modulatory effects by altering cytokine production as well as cytokine-induced signaling in tumor cells. In some cases, (+)-SKF10047 has been reported to result in cell detachment, rounding of cells, and inhibition of proliferation.	(Brent and Pang, 1995; Zhu et al., 2003; Spruce et al., 2004; Do et al., 2013)
BD1047 	<ul style="list-style-type: none"> <li>• Sigma1 <math>K_i</math>: 0.6–5.3 nM (Matsumoto et al., 1995; Vilner et al., 1995a; Vilner et al., 1995b; Cobos et al., 2005; Entrena et al., 2009)</li> <li>• Sigma2 <math>K_i</math>: 47 nM (Matsumoto et al., 1995)</li> </ul>	Antagonist (Sigma1)	MTS, apoptosis assays, light microscopy of cell morphology changes, <i>in vivo</i> tumor model	Minimal anticancer activity, despite putative antagonist status (defined in behavioral assays). Induced altered cell morphology, but did not cause cancer death. Blocked antiproliferative and cytotoxic actions of Sigma2/TMEM97 ligands. Blocked PRE-084-induced tumor growth in immune competent mouse tumor implantation model.	(Vilner et al., 1995a; Moody et al., 2000; Zhu et al., 2003; Spruce et al., 2004; Kim and Maher, 2017)
CB-184 	<ul style="list-style-type: none"> <li>• Sigma1 <math>K_i</math>: 7,436 nM (Bowen et al., 1995)</li> <li>• Sigma2 <math>K_i</math>: 13 nM (Bowen et al., 1995)</li> </ul>	Agonist (Sigma2/TMEM97)	MTT, LDH release, apoptosis assays	Cytotoxic effect in cancer cell line cultures as single agent. Potentiated cytotoxic chemotherapeutic agents actinomycin D and doxorubicin. Reported to trigger p53- and caspase- independent apoptosis.	(Bowen et al., 1995; Crawford and Bowen, 2002; Crawford et al., 2002)

(Continued)

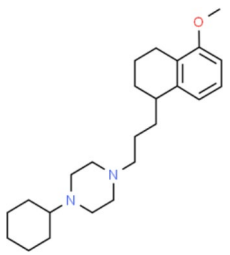
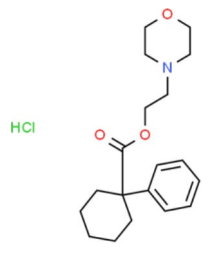
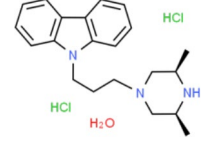
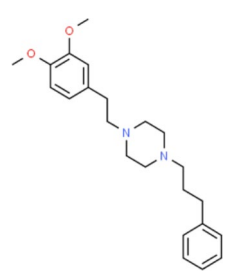


TABLE 1 | Continued

Compound	Binding affinity (Sigma1 and 2) and references	Putative action	Assays used	Summary of results	References
DTG 	<ul style="list-style-type: none"> <li>• Sigma1 <math>K_i</math>: 45–203 nM (Hellewell et al., 1994; Vilner et al., 1995a; Vilner and Bowen, 2000; Marrazzo et al., 2011b; Zampieri et al., 2016)</li> <li>• Sigma2 (<math>K_i</math>): 13–58 nM (Hellewell et al., 1994; Vilner and Bowen, 2000; Marrazzo et al., 2011b; Zampieri et al., 2016)</li> </ul>	Agonist (Sigma1 and Sigma2/ TMEM97)	MTT, LDH release, apoptosis assays	Blocked voltage-activated K <sup>+</sup> currents and induced p27 <sup>Kip1</sup> levels, inhibition of cell proliferation in some studies by proposed G1 cell cycle arrest. Blocked haloperidol-induced cytotoxicity.	(Brent and Pang, 1995; Moody et al., 2000; Colabufo et al., 2004; Renaudo et al., 2004; Kim and Maher, 2017)
Haloperidol 	<ul style="list-style-type: none"> <li>• Sigma1 (<math>K_i</math>): 1–40 nM (Vilner and Bowen, 1993; Hellewell et al., 1994; Vilner et al., 1995a; Vilner and Bowen, 2000; Choi et al., 2001; Holl et al., 2009a; Holl et al., 2009b; Holl et al., 2009c; Marrazzo et al., 2011a; Marrazzo et al., 2011b; Weber et al., 2014)</li> <li>• Sigma2 (<math>K_i</math>): 12–221 nM (Hellewell et al., 1994; Vilner and Bowen, 2000; Choi et al., 2001; Holl et al., 2009a; Holl et al., 2009b; Holl et al., 2009c; Marrazzo et al., 2011a; Marrazzo et al., 2011b; Weber et al., 2014)</li> </ul>	Antagonist (Sigma1)	MTT, MTS, trypan blue exclusion, apoptosis assays, micrographs of cell morphology changes, colony formation, soft agar assay	Antiproliferative and proapoptotic actions in range of cancer cell lines. Reported to induce unfolded protein response and autophagy. Anticancer actions of haloperidol have been proposed to be both Sigma1- and Sigma2-mediated.	(Brent and Pang, 1995; Vilner et al., 1995a; Moody et al., 2000; Colabufo et al., 2004; Spruce et al., 2004; Wang et al., 2004; Nordenberg et al., 2005; Rybczynska et al., 2008; Megalizzi et al., 2009; Sunnam et al., 2010; Pal et al., 2011; Kim et al., 2012; Schrock et al., 2013; Korpis et al., 2014; Kim and Maher, 2017)
Igmesine 	<ul style="list-style-type: none"> <li>• Sigma1 (<math>IC_{50}</math>): 39 nM (Roman et al., 1990)</li> </ul>	Agonist (Sigma1)	Trypan blue exclusion, apoptosis assays, cell cycle assays	Inhibited cell proliferation of some cell lines. Blocked voltage-activated K <sup>+</sup> currents and induced p27 <sup>Kip1</sup> levels, suggesting G1 arrest. Was not cytotoxic and did not induce caspase-mediated apoptosis.	(Renaudo et al., 2004; Renaudo et al., 2007; Gueguinou et al., 2017; Kim and Maher, 2017)
IPAG 	<ul style="list-style-type: none"> <li>• Sigma1 (<math>K_d</math>): 3 nM (Wilson et al., 1991; Schrock et al., 2013)</li> <li>• Sigma1 low-affinity site (<math>K_i</math>): 500–8,000 nM (Brimson et al., 2011)</li> </ul>	Antagonist (Sigma1)	Trypan blue exclusion, MTT, MTS, CellTiter-Glo, apoptosis assays, cell cycle, soft agar, colony formation assays, <i>in vivo</i> imaging	Selective and potent anticancer activities in range of cancer cell lines, with reported antiproliferative and proapoptotic actions. Induces unfolded protein response and autophagy. Mimics RNAi-mediated knockdown of Sigma1. Triggers lysosomal and proteasomal degradation of cancer promoting signaling proteins including PD-L1, ErbB receptors, and androgen receptor. Multiple high and low-affinity Sigma1-binding sites with distinct activities in intact cancer cells identified. Radiolabeled IPAG tracer used as selective <i>in vivo</i> tumor imaging agent.	(Spruce et al., 2004; Megalizzi et al., 2009; Brimson et al., 2011; Kim et al., 2012; Schrock et al., 2013; Kim and Maher, 2017; Thomas et al., 2017; Maher et al., 2018; Gangangari et al., 2019)

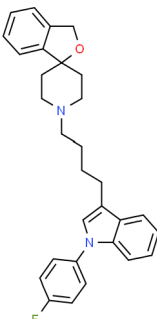
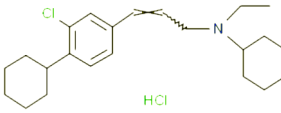
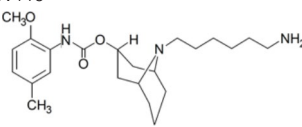
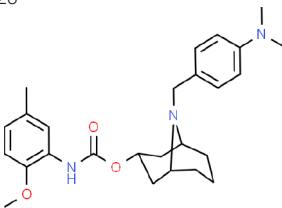
(Continued)

TABLE 1 | Continued

Compound	Binding affinity (Sigma1 and 2) and references	Putative action	Assays used	Summary of results	References
PB28 	<ul style="list-style-type: none"> <li>• Sigma1 (K): 10 nM (Azzariti et al., 2006)</li> <li>• Sigma2 (K): 0.28 nM (Azzariti et al., 2006)</li> </ul>	Agonist (Sigma2/TMEM97)	MTT, CellTiter-Glo, apoptosis assays, <i>in vivo</i> tumor xenografts	Cytotoxic agent that induces ceramide-dependent/caspase-independent apoptosis in part by triggering the production of mitochondrial superoxide radicals. PB28 also reduced P-gp expression on cancer cell lines. Potentiates doxorubicin. Inhibited tumor growth <i>in vivo</i> .	(Colabufo et al., 2004; Azzariti et al., 2006; Hornick et al., 2010; Hornick et al., 2012a; Hornick et al., 2012b; Niso et al., 2013a; Korpis et al., 2014; Pati et al., 2017a; Kim and Maher, 2017)
PRE-084 	<ul style="list-style-type: none"> <li>• Sigma1 (K): 53 nM (Garces-Ramirez et al., 2011)</li> <li>• Sigma2 (K): 32,100 nM (Garces-Ramirez et al., 2011)</li> </ul>	Agonist (Sigma1)	Trypan blue exclusion, flow cytometry, tumor allografts	Promoted tumor growth in immune competent mouse tumor allograft model by an IL-10-dependent mechanism. No clear evidence of effects on cancer cell proliferation in cell autonomous culture <i>in vitro</i> or in xenografts.	(Zhu et al., 2003; Kim et al., 2012; Kim and Maher, 2017)
Rimcazole 	<ul style="list-style-type: none"> <li>• Sigma1 (K): 406–1,165 nM (Tanaka et al., 1995; Vilner et al., 1995a)</li> <li>• Sigma2 (K): 571–852 nM (Schepmann et al., 2011)</li> </ul>	Antagonist (Sigma1)	Trypan blue exclusion, MTT, MTS, CellTiter-Glo, apoptosis assays, cell cycle assays, soft agar colony formation assays, <i>in vivo</i> tumor xenografts	Decreased viability, inhibition of cell proliferation, induction of apoptosis. Inhibition of colony formation in 2D colony formation and 3D soft agar assays. HIF1 $\alpha$ induction by rimcazole contributes to its anticancer effects. Inhibited tumor growth and cancer cell proliferation in xenograft studies.	(Brent and Pang, 1995; Spruce et al., 2004; Achison et al., 2007; Rybczynska et al., 2008; Rybczynska et al., 2013; Happy et al., 2015; Kim and Maher, 2017)
SA4503 	<ul style="list-style-type: none"> <li>• Sigma1 (K): 4.6 nM (Lever et al., 2006)</li> <li>• Sigma2 (K): 63.1 nM (Lever et al., 2006)</li> </ul>	Agonist (Sigma1)	Trypan blue exclusion, confocal microscopy, <i>in vivo</i> tumor imaging	Blocks IPAG-induced autophagic degradation of PD-L1 in cancer cells. Promotes PD-L1 cell surface expression on cancer cells. ( <sup>11</sup> C)SA4503 development as a tumor imaging agent.	(Ramakrishnan et al., 2013; Kim and Maher, 2017; Maher et al., 2018)

(Continued)

TABLE 1 | Continued

Compound	Binding affinity (Sigma1 and 2) and references	Putative action	Assays used	Summary of results	References
Siramesine 	<ul style="list-style-type: none"> <li>• Sigma1 (K): 10 nM (Niso et al., 2013a)</li> <li>• Sigma2 (K): 13 nM (Niso et al., 2013a)</li> </ul>	Agonist (Sigma2/TMEM97)	MTT, MTS, LDH release, apoptosis assays, <i>in vivo</i> tumor xenograft studies	Lysosomotropic detergent that triggers lysosomal membrane permeabilization and leakage, increased reactive oxygen species, and apoptotic cell death of cancer cells. MEFs transformed with Src or Ras oncogenes sensitized to siramesine-induced cytotoxicity. Inhibited tumor growth in xenograft studies.	(Ostenfeld et al., 2005; Ostenfeld et al., 2008; Hornick et al., 2010; Zeng et al., 2012; Niso et al., 2013b; Zeng et al., 2014; Kim and Maher, 2017)
SR31747A 	<ul style="list-style-type: none"> <li>• Sigma1 (K): 3 nM (Laggner et al., 2005)</li> </ul>	Antagonist (Sigma1)	MTT, MTS assays, <i>in vivo</i> tumor xenografts	Immune modulatory and antiproliferative activities. Inhibited proliferation of range of cancer cell lines. Potentiated tumor growth inhibition of flutamide and tamoxifen in xenograft studies.	(Berthois et al., 2003; Ferrini et al., 2003; Casellas et al., 2004; Kim and Maher, 2017)
SV119 	<ul style="list-style-type: none"> <li>• Sigma1 (K): 1,418 nM (Vangveravong et al., 2006)</li> <li>• Sigma2 (K): 5–8 nM (Vangveravong et al., 2006; Hornick et al., 2010)</li> </ul>	Agonist (Sigma2/TMEM97)	MTS, CellTiter-Glo, LDH release, cell cycle assays, apoptosis assays, colony formation, <i>in vivo</i> tumor xenografts	Inhibited cancer cell proliferation <i>in vitro</i> . Less potent than siramesine. Induced autophagy. SV119 alone induced apoptosis and potentiated cytotoxic and antitumor effects of gemcitabine and paclitaxel <i>in vitro</i> and in xenografted tumors <i>in vivo</i> .	(Kashiwagi et al., 2007; Kashiwagi et al., 2009; Hornick et al., 2010; Spitzer et al., 2012; Zeng et al., 2012; McDonald et al., 2017)
WC-26 	<ul style="list-style-type: none"> <li>• Sigma1 (K): 1,436 nM 138</li> <li>• Sigma2 (K): 2.58 nM 138</li> </ul>	Agonist (Sigma2/TMEM97)	MTS, MTT, LDH release assay, apoptosis assays, colony formation assay	Inhibited cancer cell proliferation and triggered apoptosis <i>in vitro</i> . Induced autophagy. Potentiated doxorubicin-induced cytotoxicity.	(Kashiwagi et al., 2007; Chu et al., 2009; Zeng et al., 2012; McDonald et al., 2017)

## CELLULAR PATHWAYS, PROCESSES, AND SIGNALING SYSTEMS ENGAGED BY MODULATION OF SIGMA1 AND SIGMA2/TMEM97

Much of the sigma ligand-related cancer literature includes endpoint readouts of cell proliferation and cell death. A growing body of literature reports the cellular pathways and processes engaged by modulation of Sigma1 and what we now know to be Sigma2/TMEM97. The cellular and molecular mechanisms underlying these effects remain poorly understood. However, several themes are emerging, implicating Sigma1 in the modulation of protein and lipid homeostasis, autophagy, and ion channel regulation (Kim and Maher, 2017).

### Regulators of Protein and Lipid Homeostasis

Cancer cells are associated with aberrant growth and metabolism, resulting in increased demand for protein production, corresponding membrane biogenesis, and *de novo* synthesized fatty acids as an energy source. This renders tumors particularly dependent on factors that maintain homeostasis of protein and lipid metabolism (Ma and Hendershot, 2004a; Ma and Hendershot, 2004b; Denoyelle et al., 2006; Jones and Thompson, 2009; Luo et al., 2009; Sonenberg and Hinnebusch, 2009). Emerging data suggest that Sigma1 is a multifunctional chaperone or scaffolding protein involved in maintaining ER protein homeostasis and supporting the increased demand for secretory pathway protein synthesis associated with tumor growth (Kim and Maher, 2017). Pharmacological modulation of Sigma1 in cancer cells has been shown to alter the protein synthesis, post-translational modification, trafficking, and degradation of cancer promoting proteins (Hayashi and Su, 2007; Crottes et al., 2011; Kim et al., 2012; Schrock et al., 2013; Crottes et al., 2016; Thomas et al., 2017). In this respect, Sigma1 ligands are reminiscent of proteostasis regulators (Powers et al., 2009).

Proliferation is associated with regulation of growth, which involves the increase in biomass essential for successful cell doubling (Luo et al., 2009). Sigma1 modulators can be used to control biomass of cancer cells *via* regulation of protein translation (Kim et al., 2012) and protein degradation *via* ubiquitin proteasome system (UPS)-mediated and autophagosomal degradation mechanisms (Schrock et al., 2013; Thomas et al., 2017; Maher et al., 2018). Sigma1 modulators have also been shown to impact cellular pathways driving cell growth, such as PI3K/Akt/mTOR (Spruce et al., 2004; Kim et al., 2012; Zeng et al., 2012). Sigma1 inhibition did this in a PTEN-independent manner (Kim et al., 2012; Schrock et al., 2013; Kim and Maher, 2017; Thomas et al., 2017).

### Unfolded Protein Response (UPR) and Autophagy

Sigma1 antagonists/inhibitors have been shown to trigger the unfolded protein response (UPR) in cancer cells. Schrock et al. evaluated a panel of structurally diverse compounds with affinity for Sigma1 and found that a subset of prototypic Sigma1 antagonists/inhibitors-induced UPR and autophagy in a range of

cancer cell lines in a dose- and time-responsive manner (Schrock et al., 2013). Of note, these effects were reversible upon washout of the compound, as demonstrated with IPAG, a selective high-affinity Sigma1 antagonist/inhibitor (Kim et al., 2012; Schrock et al., 2013; Thomas et al., 2017). If the basis of Sigma1 ligand action is modulation of PPI, then the reversal of these actions following compound removal suggests that these Sigma1 antagonist/inhibitor-mediated effects require high occupancy of Sigma1 and that disruption of Sigma1 PPIs requires continuous target engagement. Consistent with this notion, Schrock et al. demonstrated that IPAG induced apoptosis, but only after extended treatment, suggesting that an apoptosis trigger occurs when a certain threshold is surpassed (Schrock et al., 2013). These studies suggest that Sigma1 modulators may be useful as pharmacological regulators of cancer cell protein homeostasis (Kim et al., 2012; Schrock et al., 2013; Thomas et al., 2017).

### Cholesterol/Lipid Binding

There are preliminary but intriguing data regarding a potential role for sigma proteins in lipid metabolism. As discussed above, cancer cells are particularly dependent on factors that maintain lipid homeostasis (Ma and Hendershot, 2004a; Ma and Hendershot, 2004b; Denoyelle et al., 2006; Jones and Thompson, 2009; Luo et al., 2009; Sonenberg and Hinnebusch, 2009) due to rapid growth and corresponding abnormal metabolism. Although a role for Sigma1 in lipid metabolism has not been established, a few studies have implicated a physiological role for Sigma1 and Sigma2/TMEM97 in cholesterol dynamics.

Sigma1 has been hypothesized to contain two cholesterol-binding domains (CBD) adjacent to the Sigma1 ligand-binding site (Palmer et al., 2007; Schmidt et al., 2016). Sigma1 has been proposed to contribute to remodeling of cholesterol rich lipid rafts, and in one report, Sigma1 binding to cholesterol was inhibited by (+)-SKF10047 (Palmer et al., 2007). Thus, disruption of Sigma1 may alter the cholesterol content of the surrounding lipid bilayer, and the subsequent remodeling of lipid rafts would disrupt the signaling complexes dependent on these stabilizing and organizing platforms (Simons and Toomre, 2000; Aydar et al., 2002; Aydar et al., 2004; Jacobson et al., 2007; Palmer et al., 2007; Balasuriya et al., 2014).

Choline was recently proposed as an endogenous Sigma1 agonist/activator (Brailoiu et al., 2019). Interestingly, choline is a lipid precursor associated with aggressive prostate cancer (Richman et al., 2012; Zadra et al., 2013; Pavlova and Thompson, 2016). Clinically, choline intake has been associated with an increased risk of lethal prostate cancer (Richman et al., 2012). Altogether, these data provide evidence of a role for Sigma1 in cancer cell lipid metabolism. This is an interesting and emerging area of research that remains poorly understood.

Expression of Sigma2/TMEM97, along with several cholesterol biosynthesis genes, was reported to be induced by progesterone in ovarian surface epithelial (OSE) cells, the cell type from which ovarian cancer often derives. In this context, upregulation of TMEM97 in OSE cells by progesterone was proposed to protect against the development of ovarian cancer (Wilcox et al., 2007).

Recently, Sigma2/TMEM97 was shown to interact with low-density lipoprotein (LDL) receptor and to be involved in LDL



uptake (Riad et al., 2018). This is consistent with the published role of TMEM97 in cholesterol homeostasis (see above).

## Cell Motility, Migration, and Adhesion

Sigma1 RNAi knockdown and treatment with (+)-SKF10047, a putative agonist/activator, have been shown to disrupt cancer cell motility, migration, and adhesion *in vitro* by regulating cell surface expression of  $\beta$ -integrin (Aydar et al., 2006; Palmer et al., 2007). The correlation between Sigma1 knockdown and (+)-SKF10047 treatment is surprising and is inconsistent with the definition of (+)-SKF10047 as an agonist/activator. Treatment of cancer cells *in vitro* with (+)-SKF10047 decreased Sigma1- $\beta$ -integrin association in lipid raft fractions and resulted in Sigma1 dissociation from lipid rafts (Palmer et al., 2007). Others have reported that 4-IBP and haloperidol inhibited cell migration and motility of multiple cancer cell lines including human glioblastoma (U373-MG), melanoma (C32), NSCLC (A549), and prostate cancer (PC3) (Megalizzi et al., 2007; Rybczynska et al., 2008; Megalizzi et al., 2009). These *in vitro* data have been used as evidence to suggest that Sigma1 plays a role in metastasis (Aydar et al., 2006; Palmer et al., 2007; Aydar et al., 2016). However, whether Sigma1 and its pharmacological modulators impact metastasis in *in vivo* models remains unclear. No studies to establish the role of Sigma1 in metastasis *in vivo* have been reported.

## Allosteric Regulation of Oncogenic Driver Proteins and Signaling Axes

The protein homeostasis regulating properties of Sigma1 ligands may be exploited to modulate oncogenic protein signaling. The actions of Sigma1 modulators are largely defined by their associated signaling systems. Emerging data support the notion that Sigma1 is an allosteric modulator/regulator of signaling proteins and signaling axes. Sigma1 ligands can selectively regulate the stability, trafficking, and signaling of oncogenic driver proteins (Kim and Maher, 2017; Thomas et al., 2017; Maher et al., 2018).

Recently, Sigma1 was found to regulate aberrant androgen receptor (AR) activity and stability in prostate cancer cells (Thomas et al., 2017). The objectives of this study were to better understand the interaction of Sigma1 with an oncogenic protein, in this case AR, and to determine the potential therapeutic value of targeting Sigma1 in this context (Thomas et al., 2017). Sigma1 physically associated with AR, and pharmacological inhibition of Sigma1 blocked AR nuclear translocation and suppressed its transcriptional activity in response to androgen (5 $\alpha$ -dihydrotestosterone [5 $\alpha$ -DHT]). It also triggered the proteasomal degradation of AR and constitutively active AR splice variants (ARVs). Sigma1 also interacts with ErbB receptors, and the prototypic Sigma1 antagonist/inhibitor dose-responsively suppressed ErbB-2 and -3 receptor protein levels (Thomas et al., 2017).

## Ion channels in cancer

Several studies have shown Sigma1 ligand modulation of ion channel activity in cancer cell lines (Renaudo et al., 2004; Renaudo et al., 2007; Wu and Bowen, 2008; Crottes et al., 2011; Balasuriya et al., 2014; Crottes et al., 2016; Gueguinou et al., 2017). This has been

reviewed extensively elsewhere (Crottes et al., 2013; Kim and Maher, 2017). Interestingly, Sigma1 putative agonist/activators were used in many of these studies to support the notion that Sigma1 modulation of ion channel activities can suppress cancer cell proliferation, adhesion, motility, and migration (Renaudo et al., 2004; Renaudo et al., 2007; Wu and Bowen, 2008; Crottes et al., 2011; Balasuriya et al., 2014; Crottes et al., 2016; Gueguinou et al., 2017; ). Very recently, choline was proposed as an endogenous Sigma1 agonist/activator based on its ability to bind Sigma1 and mimic other putative Sigma1 agonists by potentiating Ca<sup>2+</sup> signals evoked by inositol triphosphate receptors (IP<sub>3</sub>Rs) (Brailoiu et al., 2019).

## IMMUNE MODULATION

A growing body of evidence demonstrates that inhibition of Sigma1 can suppress growth, decrease proliferation, and induce apoptosis in multiple cancer cell lines through regulation of cell-intrinsic signaling in cancer cells (Kim and Maher, 2017). However, the impact of targeting Sigma1 may extend beyond regulation of cell-intrinsic signaling proteins and pathways. Several publications describe the immunomodulatory properties of Sigma1 ligands (Bourrie et al., 1995; Carayon et al., 1995; Derocq et al., 1995; Bourrie et al., 1996; Carayon et al., 1996; Bourrie et al., 2002; Zhu et al., 2003; Bourrie et al., 2004; Gardner et al., 2004). Sigma1 agonists/activators PRE-084 and (+)-SKF10047 stimulate production of immunosuppressive cytokines that block the host antitumor immune response in the tumor microenvironment (reviewed in Kim and Maher, 2017). In at least one reported study, PRE-084 and (+)-SKF10047 induced the extracellular secretion of IL-10, TGF- $\beta$ , and PGE<sub>2</sub>, while decreasing IFN- $\gamma$  at the tumor site (Zhu et al., 2003). The increase in TGF- $\beta$  production or secretion was observed only in tumor-bearing mice and was absent in normal, non-tumor bearing mice (Zhu et al., 2003). PRE-084 has been shown to promote tumor growth in a syngeneic lung cancer (L1C2 murine alveolar cell carcinoma) model in part by inducing IL-10 at the tumor site (Zhu et al., 2003). Co-treatment with PRE-084 and BD1047 (putative Sigma1 antagonist or inhibitor) blocked the tumor growth promoting effects of PRE-084, showing that this effect is Sigma1-mediated. An anti-IL-10 antibody (JES-2A5) blocked the tumor growth promoting effect of PRE-084, showing that tumor growth is at least partially dependent on IL-10. The immunomodulatory or tumor growth effects of BD1047 alone were not evaluated in this study (Zhu et al., 2003). Thus, these studies did not determine whether putative Sigma1 antagonists/inhibitors can mediate antitumor immune responses.

Recently, it was discovered that the stability, trafficking, and activity of programmed death-ligand 1 (PD-L1, alternately named B7-H1, CD274) could be differentially modulated by SA4503 (Sigma1 agonist/activator) and IPAG (Sigma1 antagonist/inhibitor) (Maher et al., 2018). Sigma1 inhibition by IPAG caused the autolysosomal degradation of PD-L1 in PC3 (hormone-insensitive prostate cancer) and MDA-MB-231 (triple-negative breast cancer) cell lines and reduced the levels of functional PD-L1 on the surface of the cells (Maher et al., 2018). Knockdown of Sigma1 by shRNA also reduced PD-L1 levels, showing consistency with the effects of the Sigma1 antagonist/inhibitor IPAG. When the Sigma1 agonist/

activator SA4503 was applied alone, the surface levels of PD-L1 increased. When SA4503 was applied with IPAG, the IPAG-mediated decrease of PD-L1 levels was blocked, displaying Sigma1 selective activity (Maher et al., 2018). Induction of PD-L1 by interferon gamma was also blocked by IPAG (Maher et al., 2018). This report demonstrates that PD-L1 production and activity can be regulated by Sigma1 modulation either directly through cell-intrinsic mechanisms or indirectly by immune response-induced cytokine-mediated feedback loops. Thus, Sigma1 ligands may regulate the tumor immune microenvironment. These lines of evidence warrant studies to determine antitumor immunity activity induced by Sigma1 modulation.

## SAFETY OF SIGMA MODULATION

We previously reviewed clinical and preclinical evidences demonstrating that the on-target actions of Sigma1 modulators do not induce adverse effects (Kim and Maher, 2017). Since then, clinical evidence in support of the safety of Sigma2 modulation/inhibition has been reported (Grundman et al., 2019). The safety and efficacy of Sigma1 modulation are also being evaluated in human clinical trials of S1RA (Sigma1 selective antagonist/inhibitor, also known as E-52862). Proof of concept for the safety and efficacy of Sigma1 modulation has been reviewed extensively elsewhere (Abadias et al., 2013; Kim and Maher, 2017; Merlos et al., 2017; Bruna et al., 2018; Grundman et al., 2019).

## CANCER-ASSOCIATED PAIN

The role of Sigma1 in pain has been studied for decades (reviewed in Pasternak, 2017). However, there are relatively few published studies focused on the utility of sigma receptor ligands in cancer-associated pain. Although a role for sigma receptors in cancer pain remains poorly understood, emerging evidence suggests that Sigma1 selective drugs such as S1RA/E-52862, which is in clinical trials to assess its ability to produce non-opioid analgesia (see above), may be effective agents in this space. Recently, an exploratory randomized, double-blind, placebo-controlled phase II clinical trial generated preliminary proof of concept that treatment with S1RA could mitigate oxaliplatin-induced peripheral neuropathy in patients with colorectal cancer receiving FOLFOX treatment (Bruna et al., 2018). In this hypothesis generating study, intermittent treatment with the Sigma1 antagonist/inhibitor was associated with reduced acute oxaliplatin-induced peripheral neuropathy and allowed patients to be exposed to higher doses of oxaliplatin. Furthermore, the Sigma1 antagonist/inhibitor showed an acceptable safety profile (Bruna et al., 2018). The authors explain that this study, although exciting, must be confirmed broadly to be certain of the protective effects against acute and severe cumulative neuropathy. These studies raise an important question regarding the multiple properties of Sigma1 antagonists/inhibitors. Can a small-molecule Sigma1 antagonist/inhibitor that shows antineoplastic capabilities also be used to manage cancer-associated pain? To

date, no clinically used compounds exhibiting these Sigma1 pharmacology properties have been reported.

## CONCLUSIONS AND PERSPECTIVES

Over the past several decades, the story of sigma receptors has undergone many twists and turns, and this is reflected in the broad and complex literature. The field is rapidly evolving, and some of the anchor pieces of the sigma receptor puzzle (Kim, 2017; Kim and Maher, 2017) are starting to emerge. It is now evident that Sigma1 is not a traditional receptor or signaling protein. In the context of cancer, Sigma1 appears to function as a scaffold or chaperone, a component of the cancer cell support machinery. Sigma2 has long remained a pharmacologically defined entity and was recently identified as Sigma2/TMEM97 (Alon et al., 2017); however, important questions remain regarding inconsistencies between the traditional Sigma2 radioligand-binding site and TMEM97 (addressed above).

From a pharmacological perspective, Sigma1 appears to be an allosteric modulator of multiple signaling systems. The increasing number of Sigma1 interacting proteins implicates this protein in a variety of pathophysiological roles. Yet, published *SIGMAR1* KO mice are viable without overt phenotype, at least under routine animal husbandry conditions. Several tumor xenograft studies report absence of measurable adverse effects at efficacious doses (Kim and Maher, 2017). Clinically, a recent phase I trial with a putative Sigma1 inhibitor/antagonist demonstrated proof of concept that such drugs can be safe (see above). A recent phase I trial of a putative Sigma2/TMEM97 targeting compound too was reported to be well tolerated (Grundman et al., 2019). Altogether, sigma drugs appear to elicit distinct actions at Sigma1 and Sigma2/TMEM97 in physiological compared to pathophysiological contexts. These distinct responses may reflect the tissue and disease context-dependent composition of Sigma1-associated multiprotein complexes. An important question is whether Sigma1 and Sigma2/TMEM97 protein complexes change composition, localization, protein-protein interaction dynamics, and dependencies with disease.

An essential missing piece of the sigma puzzle is a clear definition of drug molecular mechanisms of action that translate into downstream physiological response and tumor promoting as well as inhibiting actions of Sigma1 modulation. Recent reports demonstrate Sigma1 compounds can trigger differential changes in Sigma1 oligomerization status corresponding to putative inhibition/antagonism and activation/agonism (Gromek et al., 2014; Yano et al., 2018), and these changes may be responses to corresponding differential conformational shifts based on putative antagonist and agonist status (Kim and Pasternak, 2018; Schmidt et al., 2018). These molecular mechanism studies also show that ligand binding of Sigma1 is a complex, multistep process (Kim and Pasternak, 2018; Schmidt et al., 2018). These initial studies will require further validation and expansion. Breakthroughs in understanding the role of sigma proteins in cancer and the value of sigma targeting agents in cancer and establishing meaningful structure-activity relationships for drug discovery and development will require more systematic and in-depth analyses of intracellular signaling cascades and pathways that connect compound molecular mechanism of

action to physiological response. In this respect, the field of sigma proteins in the context of cancer is still relatively under explored and in its early stages. There is a significant need to evaluate different, more sophisticated *in vitro* and *in vivo* experimental cancer models to accurately measure physiological impact and correlation to anti-tumor response.

Targeting Sigma1 and Sigma2/TMEM97 to treat cancer would be highly novel approaches. The multifunctionality and apparent disease-dependent actions of these drug targets offer new therapeutic opportunities. The challenge will be to understand how to modulate them in a physiological and pathophysiological context-dependent manner.

## REFERENCES

- Abadias, M., Escriche, M., Vaque, A., Sust, M., and Encina, G. (2013). Safety, tolerability and pharmacokinetics of single and multiple doses of a novel sigma-1 receptor antagonist in three randomized phase I studies. *Br. J. Clin. Pharmacol.* 75, 103–117. doi: 10.1111/j.1365-2125.2012.04333.x
- Abate, C., Niso, M., Infantino, V., Menga, A., and Berardi, F. (2015). Elements in support of the 'non-identity' of the PGRMC1 protein with the sigma2 receptor. *Eur. J. Pharmacol.* 758, 16–23. doi: 10.1016/j.ejphar.2015.03.067
- Abate, C., Niso, M., and Berardi, F. (2018). Sigma-2 receptor: past, present and perspectives on multiple therapeutic exploitations. *Future Med. Chem.* 10, 1997–2018. doi: 10.4155/fmc-2018-0072
- Achison, M., Boylan, M. T., Hupp, T. R., and Spruce, B. A. (2007). HIF-1alpha contributes to tumour-selective killing by the sigma receptor antagonist rimcazole. *Oncogene* 26, 1137–1146. doi: 10.1038/sj.onc.1209890
- Alon, A., H. R. Schmidt, M. D. Wood, J. J. Sahn, S. F. Martin and A. C. Kruse. (2017). Identification of the gene that codes for the sigma2 receptor. *Proc. Natl. Acad. Sci. U. S. A.* 114 (27), 7160–7165. doi: 10.1073/pnas.1705154114
- Aydar, E., Palmer, C. P., Klyachko, V. A., and Jackson, M. B. (2002). The sigma receptor as a ligand-regulated auxiliary potassium channel subunit. *Neuron* 34, 399–410. doi: 10.1016/S0896-6273(02)00677-3
- Aydar, E., Palmer, C. P., and Djamgoz, M. B. (2004). Sigma receptors and cancer: possible involvement of ion channels. *Cancer Res.* 64, 5029–5035. doi: 10.1158/0008-5472.CAN-03-2329
- Aydar, E., Onganer, P., Perrett, R., Djamgoz, M. B., and Palmer, C. P. (2006). The expression and functional characterization of sigma (sigma) 1 receptors in breast cancer cell lines. *Cancer Lett.* 242, 245–257. doi: 10.1016/j.canlet.2005.11.011
- Aydar, E., Stratton, D., Fraser, S. P., Djamgoz, M. B., and Palmer, C. (2016). Sigma-1 receptors modulate neonatal Nav1.5 ion channels in breast cancer cell lines. *Eur. Biophys. J.* 45 (7), 671–683. doi: 10.1007/s00249-016-1135-0
- Azzariti, A., Colabufo, N. A., Berardi, F., Porcelli, L., Niso, M., Simone, G. M., et al. (2006). Cyclohexylpiperazine derivative PB28, a sigma2 agonist and Sigma1 antagonist receptor, inhibits cell growth, modulates P-glycoprotein, and synergizes with anthracyclines in breast cancer. *Mol. Cancer Ther.* 5 (7), 1807–1816. doi: 10.1158/1535-7163.Mct-05-0402
- Balasuriya, D., D'Sa, L., Talker, R., Dupuis, E., Maurin, F., Martin, P., et al. (2014). A direct interaction between the sigma-1 receptor and the hERG voltage-gated K<sup>+</sup> channel revealed by atomic force microscopy and homogeneous time-resolved fluorescence (HTRF(R)). *J. Biol. Chem.* 289 (46), 32353–32363. doi: 10.1074/jbc.M114.603506
- Bartz, F., Kern, L., Erz, D., Zhu, M., Gilbert, D., Meinhof, T., et al. (2009). Identification of cholesterol-regulating genes by targeted RNAi screening. *Cell Metab.* 10 (1), 63–75. doi: 10.1016/j.cmet.2009.05.009
- Berthois, Y., Bourrie, B., Galieue, S., Vidal, H., Carayon, P., Martin, P. M., et al. (2003). SR31747A is a sigma receptor ligand exhibiting antitumoural activity both *in vitro* and *in vivo*. *Br. J. Cancer* 88 (3), 438–446. doi: 10.1038/sj.bjc.6600709
- Bourrie, B., Bouaboula, M., Benoit, J. M., Derocq, J. M., Esclangon, M., Le Fur, G., et al. (1995). Enhancement of endotoxin-induced interleukin-10 production by SR 31747A, a sigma ligand. *Eur. J. Immunol.* 25 (10), 2882–2887. doi: 10.1002/eji.1830251026
- Bourrie, B., Benoit, J. M., Derocq, J. M., Esclangon, M., Thomas, C., Le Fur, G., et al. (1996). A sigma ligand, SR 31747A, potentially modulates Staphylococcal enterotoxin B-induced cytokine production in mice. *Immunology* 88 (3), 389–93. doi: 10.1046/j.1365-2567.1996.d01-657.x
- Bourrie, B., et al. (2002). SSR125329A, a high affinity sigma receptor ligand with potent anti-inflammatory properties. *Eur. J. Pharmacol.* 456, 123–131. doi: 10.1016/S0014-2999(02)02646-8
- Bourrie, B., Bribe, E., Derocq, J. M., Vidal, H., and Casellas, P. (2004). Sigma receptor ligands: applications in inflammation and oncology. *Curr. Opin. Invest. Drugs* 5, 1158–1163.
- Bowen, W. D. (2000). Sigma receptors: recent advances and new clinical potentials. *Pharm. Acta Helv.* 74, 211–218. doi: 10.1016/S0031-6865(99)00034-5
- Bowen, W. D., Bertha, C. M., Vilner, B. J., and Rice, K. C. (1995). CB-64D and CB-184: ligands with high sigma 2 receptor affinity and subtype selectivity. *Eur. J. Pharmacol.* 278, 257–260. doi: 10.1016/0014-2999(95)00176-L
- Brailoiu, E., Chakraborty, S., Brailoiu, G. C., Zhao, P., Barr, J. L., Ilies, M. A., et al. (2019). Choline Is an Intracellular Messenger Linking Extracellular Stimuli to IP3-Evoked Ca(2+) Signals through Sigma-1 Receptors. *Cell Rep.* 26 (2), 330–337. doi: 10.1016/j.celrep.2018.12.051
- Brent, P. J., and Pang, G. T. (1995). Sigma binding site ligands inhibit cell proliferation in mammary and colon carcinoma cell lines and melanoma cells in culture. *Eur. J. Pharmacol.* 278, 151–160. doi: 10.1016/0014-2999(95)00115-2
- Brimson, J. M., Brown, C. A., and Safrany, S. T. (2011). Antagonists show GTP-sensitive high-affinity binding to the sigma-1 receptor. *Br. J. Pharmacol.* 164, 772–780. doi: 10.1111/j.1476-5381.2011.01417.x
- Bruna, J., Videla, S., Argyriou, A. A., Velasco, R., Villoria, J., Santos, C., et al. (2018). Efficacy of a novel sigma-1 receptor Antagonist for oxaliplatin-induced neuropathy: a randomized, double-blind, placebo-controlled phase IIa clinical trial. *Neurotherapeutics* 15 (1), 178–189. doi: 10.1007/s13311-017-0572-5
- Carayon, P., et al. (1995). The sigma ligand SR 31747 prevents the development of acute graft-versus-host disease in mice by blocking IFN-gamma and GM-CSF mRNA expression. *Int. J. Immunopharmacol.* 17, 753–761. doi: 10.1016/0192-0561(95)00066-B
- Carayon, P., Petitpretre, G., Bourrie, B., Le Fur, G., and Casellas, P. (1996). *In vivo* effects of a new immunosuppressive sigma ligand, SR 31747, on mouse thymus. *Immunopharmacol. Immunotoxicol.* 18, 179–191. doi: 10.3109/08923979609052731
- Casellas, P., et al. (2004). SR31747A: a peripheral sigma ligand with potent antitumor activities. *Anticancer Drugs* 15, 113–118. doi: 10.1097/00001813-200402000-00003
- Cesa, L. C., Mapp, A. K., and Gestwicki, J. E. (2015). Direct and propagated effects of small molecules on protein-protein interaction networks. *Front. Bioeng. Biotechnol.* 3, 119. doi: 10.3389/fbioe.2015.00119
- Chen, R., et al. (2016). Overexpression of MAC30 is resistant to platinum-based chemotherapy in patients with non-small cell lung cancer. *Technol. Cancer Res. Treat.* 15, 815–820. doi: 10.1177/1533034615605208
- Choi, S. R., et al. (2001). Development of a Tc-99m labeled sigma-2 receptor-specific ligand as a potential breast tumor imaging agent. *Nucl. Med. Biol.* 28, 657–666. doi: 10.1016/S0969-8051(01)00234-7
- Chu, W., et al. (2009). New N-substituted 9-azabicyclo[3.3.1]nonan-3alpha-yl phenylcarbamate analogs as sigma2 receptor ligands: synthesis, *in vitro*

## AUTHOR CONTRIBUTIONS

HO, CS, and FK contributed to the writing and editing of the manuscript.

## ACKNOWLEDGMENTS

F.J. Kim was supported by an American Cancer Society Institutional Research Grant at Thomas Jefferson University, Sidney Kimmel Cancer Center Pilot Study Award, Thomas Jefferson University start-up funds, and Sidney Kimmel Cancer Center Support Grant 5P30CA056036-17.



- characterization, and evaluation as PET imaging and chemosensitization agents. *Bioorg. Med. Chem.* 17, 1222–1231. doi: 10.1016/j.bmc.2008.12.025
- Cobos EJ, E. J., Nieto, F. R., Cendán, C. M., and Del Pozo, E. (2008). Pharmacology and therapeutic potential of Sigma1 receptor ligands. *Curr. Neuropharmacol.* 6, 344–366. doi: 10.2174/157015908787386113
- Cobos, E. J., Baeyens, J. M., and Del Pozo, E. (2005). Phenytoin differentially modulates the affinity of agonist and antagonist ligands for sigma 1 receptors of guinea pig brain. *Synapse* 55, 192–195. doi: 10.1002/syn.20103
- Colabufio, N. A., et al. (2004). Antiproliferative and cytotoxic effects of some sigma2 agonists and Sigma1 antagonists in tumour cell lines. *Naunyn Schmiedeberg's Arch. Pharmacol.* 370, 106–113. doi: 10.1007/s00210-004-0961-2
- Crawford, K. W., and Bowen, W. D. (2002). Sigma-2 receptor agonists activate a novel apoptotic pathway and potentiate antineoplastic drugs in breast tumor cell lines. *Cancer Res.* 62, 313–322.
- Crawford, K. W., Coop, A., and Bowen, W. D. (2002). Sigma(2) Receptors regulate changes in sphingolipid levels in breast tumor cells. *Eur. J. Pharmacol.* 443, 207–209. doi: 10.1016/S0014-2999(02)01581-9
- Crottes, D., et al. (2011). Sig1R protein regulates hERG channel expression through a post-translational mechanism in leukemic cells. *J. Biol. Chem.* 286, 27947–27958. doi: 10.1074/jbc.M111.226738
- Crottes, D., Guizouarn, H., Martin, P., Borgese, F., and Soriani, O. (2013). The sigma-1 receptor: a regulator of cancer cell electrical plasticity? *Front. Physiol.* 4, 175. doi: 10.3389/fphys.2013.00175
- Crottes, D., et al. (2016). SIGMAR1 regulates membrane electrical activity in response to extracellular matrix stimulation to drive cancer cell invasiveness. *Cancer Res.* 76, 607–618. doi: 10.1158/0008-5472.CAN-15-1465
- Denoyelle, C., et al. (2006). Anti-oncogenic role of the endoplasmic reticulum differentially activated by mutations in the MAPK pathway. *Nat. Cell Biol.* 8, 1053–1063. doi: 10.1038/ncb1471
- Derocq, J. M., Bourrie, B., Segui, M., Le Fur, G., and Casellas, P. (1995). *In vivo* inhibition of endotoxin-induced pro-inflammatory cytokines production by the sigma ligand SR 31747. *J. Pharmacol. Exp. Ther.* 272, 224–230.
- Ding, H., et al. (2016). Prognostic value of MAC30 expression in human pure squamous cell carcinomas of the lung. *Asian Pac. J. Cancer Prev.* 17, 2705–2710. doi: 10.7314/APJCP.2016.17.5.2705
- Ding, H., et al. (2017). The prognostic effect of mac30 expression on patients with non-small cell lung cancer receiving adjuvant chemotherapy. *Technol. Cancer Res. Treat.* 16, 645–653. doi: 10.1177/1533034616670443
- Do, W., et al. (2013). Sigma 1 receptor plays a prominent role in IL-24-induced cancer-specific apoptosis. *Biochem. Biophys. Res. Commun.* 439, 215–220. doi: 10.1016/j.bbrc.2013.08.057
- Ebrahimi-Fakhari, D., et al. (2016). Reduction of TMEM97 increases NPC1 protein levels and restores cholesterol trafficking in niemann-pick type C1 disease cells. *Hum. Mol. Genet.* 25, 3588–3599. doi: 10.1093/hmg/ddw204
- Entrena, J. M., et al. (2009). Sigma-1 receptors are essential for capsaicin-induced mechanical hypersensitivity: studies with selective sigma-1 ligands and sigma-1 knockout mice. *Pain* 143, 252–261. doi: 10.1016/j.pain.2009.03.011
- Ferrini, J. B., et al. (2003). Transcriptomic classification of antitumor agents: application to the analysis of the antitumoral effect of SR31747A. *Gene Expr.* 11, 125–139. doi: 10.3727/000000003108749026
- Gangangari, K. K., Varadi, A., Majumdar, S., Larson, S. M., Pasternak S. M., and Pillarsetty, N. K. (2019). Imaging sigma-1 receptor (S1R) expression using iodine-124-labeled 1-(4-Iodophenyl)-3-(2-adamantyl)guanidine ([124I] IPAG). *Mol. Imaging Biol.* doi: 10.1007/s11307-019-01369-8
- Garces-Ramirez, L., et al. (2011). Sigma receptor agonists: receptor binding and effects on mesolimbic dopamine neurotransmission assessed by microdialysis. *Biol. Psychiatry* 69, 208–217. doi: 10.1016/j.biopsych.2010.07.026
- Gardner, B., et al. (2004). Cocaine modulates cytokine and enhances tumor growth through sigma receptors. *J. Neuroimmunol.* 147, 95–98. doi: 10.1016/j.jneuroim.2003.10.020
- Gromek, K. A., et al. (2014). The oligomeric states of the purified sigma-1 receptor are stabilized by ligands. *J. Biol. Chem.* 289, 20333–20344. doi: 10.1074/jbc.M113.537993
- Grundman, M., et al. (2019). A phase 1 clinical trial of the sigma-2 receptor complex allosteric antagonist CT1812, a novel therapeutic candidate for alzheimer's disease. *Alzheimer's Dement.* 5, 20–26. doi: 10.1016/j.trci.2018.11.001
- Gueguinou, M., Crottes, D., Chantome, A., Rapetti-Mauss, R., Potier-Cartereau, M., Clarysse, L., et al. (2017). The SigmaR1 chaperone drives breast and colorectal cancer cell migration by tuning SK3-dependent Ca2+ homeostasis. *Oncogene* 36 (25), 3640–3647. doi: 10.1038/onc.2016.501
- Guo, L., and Zhen, X. (2015). Sigma-2 receptor ligands: neurobiological effects. *Curr. Med. Chem.* 22, 989–1003. doi: 10.2174/0929867322666150114163607
- Han, K. Y., et al. (2013). Overexpression of MAC30 is associated with poor clinical outcome in human non-small-cell lung cancer. *Tumour Biol.* 34, 821–825. doi: 10.1007/s13277-012-0612-z
- Hanner, M., et al. (1996). Purification, molecular cloning, and expression of the mammalian Sigma1-binding site. *Proc. Natl. Acad. Sci. U. S. A.* 93, 8072–8077. doi: 10.1073/pnas.93.15.8072
- Happy, M., et al. (2015). Sigma 1 Receptor antagonist potentiates the anti-cancer effect of p53 by regulating ER stress, ROS production, bax levels, and caspase-3 activation. *Biochem. Biophys. Res. Commun.* 456, 683–688. doi: 10.1016/j.bbrc.2014.12.029
- Hayashi, T., and Su, T. P. (2007). Sigma-1 receptor chaperones at the ER-mitochondrion interface regulate Ca(2+) signaling and cell survival. *Cell* 131, 596–610. doi: 10.1016/j.cell.2007.08.036
- Hellewell, S. B., and Bowen, W. D. (1990). A sigma-like binding site in rat pheochromocytoma (PC12) cells: decreased affinity for (+)-benzomorphans and lower molecular weight suggest a different sigma receptor form from that of guinea pig brain. *Brain Res.* 527, 244–253. doi: 10.1016/0006-8993(90)91143-5
- Hellewell, S. B., et al. (1994). Rat liver and kidney contain high densities of sigma 1 and sigma 2 receptors: characterization by ligand binding and photoaffinity labeling. *Eur. J. Pharmacol.* 268, 9–18. doi: 10.1016/0922-4106(94)90115-5
- Holl, R., et al. (2009a). Dancing of the second aromatic residue around the 6,8-diazabicyclo[3.2.2]nonane framework: influence on sigma receptor affinity and cytotoxicity. *J. Med. Chem.* 52, 2126–2137. doi: 10.1021/jm801522j
- Holl, R., Schepmann, D., Bednarski, P. J., Grunert, R., and Wunsch, B. (2009b). Relationships between the structure of 6-substituted 6,8-diazabicyclo[3.2.2]nonan-2-ones and their sigma receptor affinity and cytotoxic activity. *Bioorg. Med. Chem.* 17, 1445–1455. doi: 10.1016/j.bmc.2009.01.012
- Holl, R., Schepmann, D., Grunert, R., Bednarski, P. J., and Wunsch, B. (2009c). Relationships between the structure of 6-allyl-6,8-diazabicyclo[3.2.2]nonane derivatives and their sigma receptor affinity and cytotoxic activity. *Bioorg. Med. Chem.* 17, 777–793. doi: 10.1016/j.bmc.2008.11.043
- Hornick, J. R., et al. (2010). The novel sigma-2 receptor ligand SW43 stabilizes pancreas cancer progression in combination with gemcitabine. *Mol. Cancer* 9, 298. doi: 10.1186/1476-4598-9-298
- Hornick, J. R., et al. (2012a). Lysosomal membrane permeabilization is an early event in sigma-2 receptor ligand mediated cell death in pancreatic cancer. *J. Exp. Clin. Cancer Res.* 31, 41. doi: 10.1186/1756-9966-31-41
- Hornick, J. R., Spitzer, D., Goedegebuure, P., Mach, R. H., and Hawkins, W. G. (2012b). Therapeutic targeting of pancreatic cancer utilizing sigma-2 ligands. *Surgery* 152, S152–S156. doi: 10.1016/j.surg.2012.05.014
- Hou, C., Tu, Z., Mach, R., Kung, H. F., and Kung, M. P. (2006). Characterization of a novel iodinated sigma-2 receptor ligand as a cell proliferation marker. *Nucl. Med. Biol.* 33, 203–209. doi: 10.1016/j.nucmedbio.2005.10.001
- Ishiwata, K., et al. (2006). Evaluation of (+)-p-[11C]methylvesamicol for mapping Sigma1 receptors: a comparison with [11C]SA4503. *Nucl. Med. Biol.* 33, 543–548. doi: 10.1016/j.nucmedbio.2006.01.008
- Jacobson, K., Mouritsen, O. G., and Anderson, R. G. (2007). Lipid rafts: at a crossroad between cell biology and physics. *Nat. Cell Biol.* 9, 7–14. doi: 10.1038/ncb0107-7
- John, C. S., Vilner, B. J., Geyer, B. C., Moody, T., and Bowen, W. D. (1999). Targeting sigma receptor-binding benzamides as *in vivo* diagnostic and therapeutic agents for human prostate tumors. *Cancer Res.* 59, 4578–4583.
- Jones, R. G., and Thompson, C. B. (2009). Tumor suppressors and cell metabolism: a recipe for cancer growth. *Genes Dev.* 23, 537–548. doi: 10.1101/gad.1756509
- Kashiwagi, H., et al. (2007). Selective sigma-2 ligands preferentially bind to pancreatic adenocarcinomas: applications in diagnostic imaging and therapy. *Mol. Cancer* 6, 48. doi: 10.1186/1476-4598-6-48
- Kashiwagi, H., et al. (2009). Sigma-2 receptor ligands potentiate conventional chemotherapies and improve survival in models of pancreatic adenocarcinoma. *J. Transl. Med.* 7, 24. doi: 10.1186/1479-5876-7-24



- Katz, J. L., Hiranita, T., Hong, W. C., Job, M. O., and McCurdy, C. R. (2017). "A role for sigma receptors in stimulant self-administration and addiction," in *Handbook of experimental pharmacology*. Switzerland AG: Springer Nature. doi: 10.1007/164\_2016\_94
- Kayed, H., et al. (2004). Expression analysis of MAC30 in human pancreatic cancer and tumors of the gastrointestinal tract. *Histol. Histopathol.* 19, 1021–1031. doi: 10.14670/hh-19.1021
- Kim, F. J. (2017). "Introduction to sigma proteins: evolution of the concept of sigma receptors," in *Handbook of experimental pharmacology*. Switzerland AG: Springer Nature. 244, 1–11. doi: 10.1007/164\_2017\_41
- Kim, F. J., and Maher, C. M. (2017). "Sigma1 pharmacology in the context of cancer," in *Handbook of experimental pharmacology*. Switzerland AG: Springer Nature. doi: 10.1007/164\_2017\_38
- Kim, F. J., and Pasternak, G. W. (2017). Cloning the sigma2 receptor: wandering 40 years to find an identity. *Proc. Natl. Acad. Sci. U. S. A.* Springer Nature, Switzerland AG 114, 6888–6890. doi: 10.1073/pnas.1708155114
- Kim, F. J., and Pasternak, G. W. (2018). Sigma1 receptor ligand binding: an open-and-shut case. *Nat. Struct. Mol. Biol.* 25, 992–993. doi: 10.1038/s41594-018-0146-1
- Kim, F. J., Schrock, J. M., Spino, C. M., Marino, J. C., and Pasternak, G. W. (2012). Inhibition of tumor cell growth by Sigma1 ligand mediated translational repression. *Biochem. Biophys. Res. Commun.* 426, 177–182. doi: 10.1016/j.bbrc.2012.08.052
- Korpi, K., Weber, F., Wunsch, B., and Bednarski, P. J. (2014). Cytotoxic activities of hydroxyethyl piperazine-based sigma receptor ligands on cancer cells alone and in combination with melphalan, PB28 and haloperidol. *Pharmazie* 69, 917–922.
- Kourrich, S. (2017). "Sigma-1 receptor and neuronal excitability," in *Handbook of experimental pharmacology*. Switzerland AG: Springer Nature. doi: 10.1007/164\_2017\_8
- Kruse, A. (2016). "Structural insights into Sigma1 function," in *Handbook of experimental pharmacology*. Switzerland AG: Springer Nature. doi: 10.1007/164\_2016\_95
- Kruse, A. (2017). "Structural insights into Sigma1 function," in *Handbook of experimental pharmacology*. Switzerland AG: Springer Nature. 244, 13–25. doi: 10.1007/164\_2016\_95
- Laguerre, C., et al. (2005). Discovery of high-affinity ligands of Sigma1 receptor, ERG2, and emopamil binding protein by pharmacophore modeling and virtual screening. *J. Med. Chem.* 48, 4754–4764. doi: 10.1021/jm049073
- Laurini, E., Marson, D., Fermeiglia, M., and Pridl, S. (2017). "3D Homology model of Sigma1 receptor," in *Handbook of experimental pharmacology*. Switzerland AG: Springer Nature. doi: 10.1007/164\_2017\_35
- Lever, J. R., Gustafson, J. L., Xu, R., Allmon, R. L., and Lever, S. Z. (2006). Sigma1 and sigma2 receptor binding affinity and selectivity of SA4503 and fluoroethyl SA4503. *Synapse* 59, 350–358. doi: 10.1002/syn.20253
- Luo, J., Solimini, N. L., and Elledge, S. J. (2009). Principles of cancer therapy: oncogene and non-oncogene addiction. *Cell* 136, 823–837. doi: 10.1016/j.cell.2009.02.024
- Ma, Y., and Hendershot, L. M. (2004a). ER chaperone functions during normal and stress conditions. *J. Chem. Neuroanat.* 28, 51–65. doi: 10.1016/j.jchemneu.2003.08.007
- Ma, Y., and Hendershot, L. M. (2004b). The role of the unfolded protein response in tumour development: friend or foe? *Nat. Rev. Cancer* 4, 966–977. doi: 10.1038/nrc1505
- Maher, C. M., et al. (2018). Small-molecule Sigma1 modulator induces autophagic degradation of PD-L1. *Mol. Cancer Res.* 16, 243–255. doi: 10.1158/1541-7786.MCR-17-0166
- Marrazzo, A., et al. (2011a). Antiproliferative activity of phenylbutyrate ester of haloperidol metabolite II [(+/-)-MRJF4] in prostate cancer cells. *Eur. J. Med. Chem.* 46, 433–438. doi: 10.1016/j.ejmech.2010.10.012
- Marrazzo, A., et al. (2011b). Novel potent and selective  $\sigma$  ligands: evaluation of their agonist and antagonist properties. *J. Med. Chem.* 54, 3669–3673. doi: 10.1021/jm200144j
- Martin, W. R., Eades, C. G., Thompson, J. A., Huppler, R. E., and Gilbert, P. E. (1976). The effects of morphine- and nalorphine-like drugs in the nondependent and morphine-dependent chronic spinal dog. *J. Pharmacol. Exp. Ther.* 197, 517–532.
- Matsumoto, R. R., et al. (1995). Characterization of two novel sigma receptor ligands: antidystonic effects in rats suggest sigma receptor antagonism. *Eur. J. Pharmacol.* 280, 301–310. doi: 10.1016/0014-2999(95)00208-3
- Matsumoto, R. R., et al. (2001). N-alkyl substituted analogs of the sigma receptor ligand BD1008 and traditional sigma receptor ligands affect cocaine-induced convulsions and lethality in mice. *Eur. J. Pharmacol.* 411, 261–273. doi: 10.1016/S0014-2999(00)00917-1
- Maurice, T., and Gogvadze, N. (2017). "Sigma-1 (Sigma1) receptor in memory and neurodegenerative diseases," in *Handbook of experimental pharmacology*. Switzerland AG: Springer Nature. doi: 10.1007/164\_2017\_15
- Maurice, T., and Su, T. P. (2009). The pharmacology of sigma-1 receptors. *Pharmacol. Ther.* 124, 195–206. doi: 10.1016/j.pharmthera.2009.07.001
- Maurice, T., Su, T. P., and Privat, A. (1998). Sigma1 (sigma 1) receptor agonists and neurosteroids attenuate B25-35-amyloid peptide-induced amnesia in mice through a common mechanism. *Neuroscience* 83, 413–428. doi: 10.1016/S0306-4522(97)00405-3
- McCracken, K. A., Bowen, W. D., de Costa, B. R., and Matsumoto, R. R. (1999). Two novel sigma receptor ligands, BD1047 and LR172, attenuate cocaine-induced toxicity and locomotor activity. *Eur. J. Pharmacol.* 370, 225–232. doi: 10.1016/S0014-2999(99)00113-2
- McDonald, E. S., et al. (2017). Sigma-2 ligands and PARP inhibitors synergistically trigger cell death in breast cancer cells. *Biochem. Biophys. Res. Commun.* 486, 788–795. doi: 10.1016/j.bbrc.2017.03.122
- Megalizzi, V., et al. (2007). 4-IBP, a Sigma1 receptor agonist, decreases the migration of human cancer cells, including glioblastoma cells, *in vitro* and sensitizes them *in vitro* and *in vivo* to cytotoxic insults of proapoptotic and proautophagic drugs. *Neoplasia* 9, 358–369. doi: 10.1593/neo.07130
- Megalizzi, V., et al. (2009). Screening of anti-glioma effects induced by sigma-1 receptor ligands: potential new use for old anti-psychiatric medicines. *Eur. J. Cancer* 45, 2893–2905. doi: 10.1016/j.ejca.2009.07.011
- Merlos, M., Romero, L., Zamanillo, D., Plata-Salaman, C., and Vela, J. M. (2017). "Sigma-1 receptor and pain," in *Handbook of experimental pharmacology*. Switzerland AG: Springer Nature. doi: 10.1007/164\_2017\_9
- Mishra, A. K., et al. (2015). The sigma-1 receptors are present in monomeric and oligomeric forms in living cells in the presence and absence of ligands. *Biochem. J.* 466, 263–271. doi: 10.1042/BJ20141321
- Moody, T. W., Leyton, J., and John, C. (2000). Sigma ligands inhibit the growth of small cell lung cancer cells. *Life Sci.* 66, 1979–1986. doi: 10.1016/S0024-3205(00)00523-3
- Moparthi, S. B., et al. (2007). Expression of MAC30 protein is related to survival and biological variables in primary and metastatic colorectal cancers. *Int. J. Oncol.* 30, 91–95. doi: 10.3892/ijo.30.1.91
- Murphy, M., Pykett, M. J., Harnish, P., Zang, K. D., and George, D. L. (1993). Identification and characterization of genes differentially expressed in meningiomas. *Cell Growth Differ.* 4, 715–722.
- Narayanan, S., Bhat, R., Mesangeau, C., Poupaert, J. H., and McCurdy, C. R. (2011). Early development of sigma-receptor ligands. *Future Med. Chem.* 3, 79–94. doi: 10.4155/fmc.10.279
- Niso, M., Abate, C., Ferorelli, S., Cassano, G., Gasparre, G., Perrone, R., et al. (2013a). Investigation of sigma receptors agonist/antagonist activity through N-(6-methoxytetralin-1-yl)- and N-(6-methoxynaphthalen-1-yl)alkyl derivatives of polymethylpiperidines. *Bioorg. Med. Chem.* 21, 1865–1869. doi: 10.1016/j.bmc.2013.01.034
- Niso, M., Abate, C., Contino, M., Ferorelli, S., Azzariti, A., Perrone, R., et al. (2013b). Sigma-2 receptor agonists as possible antitumor agents in resistant tumors: hints for collateral sensitivity. *ChemMedChem* 8, 2026–2035. doi: 10.1002/cmdc.201300291
- Nordenberg, J., et al. (2005). Anti-proliferative activity of haloperidol in B16 mouse and human SK-MEL-28 melanoma cell lines. *Int. J. Oncol.* 27, 1097–1103. doi: 10.3892/ijo.27.4.1097
- Ostenfeld, M. S., et al. (2005). Effective tumor cell death by sigma-2 receptor ligand siramesine involves lysosomal leakage and oxidative stress. *Cancer Res.* 65, 8975–8983. doi: 10.1158/0008-5472.CAN-05-0269
- Ostenfeld, M. S., et al. (2008). Anti-cancer agent siramesine is a lysosomotropic detergent that induces cytoprotective autophagosome accumulation. *Autophagy* 4, 487–499. doi: 10.4161/auto.5774
- Pal, K., et al. (2011). Structure-activity study to develop cationic lipid-conjugated haloperidol derivatives as a new class of anticancer therapeutics. *J. Med. Chem.* 54, 2378–2390. doi: 10.1021/jm101530j
- Palmer, C. P., Mahen, R., Schnell, E., Djamgoz, M. B., and Aydar, E. (2007). Sigma-1 receptors bind cholesterol and remodel lipid rafts in breast cancer cell lines. *Cancer Res.* 67, 11166–11175. doi: 10.1158/0008-5472.CAN-07-1771

- Pasternak, G. W. (2017). "Allosteric modulation of opioid G-protein coupled receptors by Sigma1 receptors," in *Handbook of experimental pharmacology*. Switzerland AG: Springer Nature. doi: 10.1007/164\_2017\_34
- Pati, M. L., et al. (2017a). Sigma-2 receptor agonist derivatives of 1-cyclohexyl-4-[3-(5-methoxy-1,2,3,4-tetrahydronaphthalen-1-yl)propyl]piperazine (PB28) induce cell death via mitochondrial superoxide production and caspase activation in pancreatic cancer. *BMC Cancer* 17, 51. doi: 10.1186/s12885-016-3040-4
- Pati, M. L., et al. (2017b). Sigma-2 receptor and progesterone receptor membrane component 1 (PGRMC1) are two different proteins: proofs by fluorescent labeling and binding of sigma-2 receptor ligands to PGRMC1. *Pharmacol. Res.* 117, 67–74. doi: 10.1016/j.phrs.2016.12.023
- Pavlova, N. N., and Thompson, C. B. (2016). The emerging hallmarks of cancer metabolism. *Cell Metab.* 23, 27–47. doi: 10.1016/j.cmet.2015.12.006
- Powers, E. T., Morimoto, R. I., Dillin, A., Kelly, J. W., and Balch, W. E. (2009). Biological and chemical approaches to diseases of proteostasis deficiency. *Annu. Rev. Biochem.* 78, 959–991. doi: 10.1146/annurev.biochem.052308.114844
- Pricer, R., Gestwicki, J. E., and Mapp, A. K. (2017). From fuzzy to function: the new frontier of protein-protein interactions. *Acc. Chem. Res.* 50, 584–589. doi: 10.1021/acs.accounts.6b00565
- Qiu, G., et al. (2015). RNA interference against TMEM97 inhibits cell proliferation, migration, and invasion in glioma cells. *Tumour Biol.* 36, 8231–8238. doi: 10.1007/s13277-015-3552-6
- Ramakrishnan, N. K., et al. (2013). Small-animal PET with a sigma-ligand, 11C-SA4503, detects spontaneous pituitary tumors in aged rats. *J. Nucl. Med.* 54, 1377–1383. doi: 10.2967/jnumed.112.115931
- Ramallo-Carvalho, J., et al. (2018). A multiplatform approach identifies miR-152-3p as a common epigenetically regulated onco-suppressor in prostate cancer targeting TMEM97. *Clin. Epigenetics* 10, 40. doi: 10.1186/s13148-018-0475-2
- Renaudo, A., et al. (2004). Inhibition of tumor cell proliferation by sigma ligands is associated with K<sup>+</sup> channel inhibition and p27kip1 accumulation. *J. Pharmacol. Exp. Ther.* 311, 1105–1114. doi: 10.1124/jpet.104.072413
- Renaudo, A., L'Hoste, S., Guizouarn, H., Borgese, F., and Soriani, O. (2007). Cancer cell cycle modulated by a functional coupling between sigma-1 receptors and Cl<sup>-</sup> channels. *J. Biol. Chem.* 282, 2259–2267. doi: 10.1074/jbc.M607915200
- Riad, A., et al. (2018). Sigma-2 receptor/TMEM97 and PGRMC-1 increase the rate of internalization of LDL by LDL receptor through the formation of a ternary complex. *Sci. Rep.* 8, 16845. doi: 10.1038/s41598-018-35430-3
- Richman, E. L., et al. (2012). Choline intake and risk of lethal prostate cancer: incidence and survival. *Am. J. Clin. Nutr.* 96, 855–863. doi: 10.3945/ajcn.112.039784
- Roman, F. J., Pascaud, X., Martin, B., Vauche, D., and Junien, J. L. (1990). JO 1784, a potent and selective ligand for rat and mouse brain sigma-sites. *J. Pharm. Pharmacol.* 42, 439–440. doi: 10.1111/j.2042-7158.1990.tb06588.x
- Ryan-Moro, J., Chien, C. C., Standifer, K. M., and Pasternak, G. W. (1996). Sigma binding in a human neuroblastoma cell line. *Neurochem. Res.* 21, 1309–1314. doi: 10.1007/BF02532372
- Rybczynska, A. A., Dierckx, R. A., Ishiwata, K., Elsinga, P. H., and van Waarde, A. (2008). Cytotoxicity of sigma-receptor ligands is associated with major changes of cellular metabolism and complete occupancy of the sigma-2 subpopulation. *J. Nucl. Med.* 49, 2049–2056. doi: 10.2967/jnumed.108.053876
- Rybczynska, A. A., et al. (2013). In vivo responses of human A375M melanoma to a sigma ligand: 18F-FDG PET imaging. *J. Nucl. Med.* 54, 1613–1620. doi: 10.2967/jnumed.113.122655
- Sabino, V., and Cottone, P. (2016). "Sigma receptors and alcohol use disorders," in *Handbook of experimental pharmacology*. Switzerland AG: Springer Nature. doi: 10.1007/164\_2016\_97
- Sanchez-Pulido, L., and Ponting, C. P. (2014). TM6SF2 and MAC30, new enzyme homologs in sterol metabolism and common metabolic disease. *Front. Genet.* 5, 439. doi: 10.3389/fgene.2014.00439
- Schepmann, D., Lehmkuhl, K., Brune, S., and Wunsch, B. (2011). Expression of sigma receptors of human urinary bladder tumor cells (RT-4 cells) and development of a competitive receptor binding assay for the determination of ligand affinity to human sigma(2) receptors. *J. Pharm. Biomed. Anal.* 55, 1136–1141. doi: 10.1016/j.jpba.2011.03.044
- Schmidt, H. R., Zheng, S., Gurpinar, E., Koehl, A., Manglik, A., and Krus, A. C. (2016). Crystal structure of the human sigma receptor. *Nature* 532 (532), 527–530. doi: 10.1038/nature17391
- Schmidt, H. R., Betz, R. M., Dror, R. O., and Kruse, A. C. (2018). Structural basis for Sigma1 receptor ligand recognition. *Nat. Struct. Mol. Biol.* 25, 981–987. doi: 10.1038/s41594-018-0137-2
- Schmit, K., and Michiels, C. (2018). TMEM proteins in cancer: a review. *Front. Pharmacol.* 9, 1345. doi: 10.3389/fphar.2018.01345
- Schrock, J. M., et al. (2013). Sequential cytoprotective responses to Sigma1 ligand-induced endoplasmic reticulum stress. *Mol. Pharmacol.* 84, 751–762. doi: 10.1124/mol.113.087809
- Simons, K., and Toomre, D. (2000). Lipid rafts and signal transduction. *Nat. Rev. Mol. Cell Biol.* 1, 31–39. doi: 10.1038/35036052
- Sonenberg, N., and Hinnebusch, A. G. (2009). Regulation of translation initiation in eukaryotes: mechanisms and biological targets. *Cell* 136, 731–745. doi: 10.1016/j.cell.2009.01.042
- Spitzer, D., et al. (2012). Use of multifunctional sigma-2 receptor ligand conjugates to trigger cancer-selective cell death signaling. *Cancer Res.* 72, 201–209. doi: 10.1158/0008-5472.CAN-11-1354
- Spruce, B. A., et al. (2004). Small molecule antagonists of the sigma-1 receptor cause selective release of the death program in tumor and self-reliant cells and inhibit tumor growth in vitro and in vivo. *Cancer Res.* 64, 4875–4886. doi: 10.1158/0008-5472.CAN-03-3180
- Su, T. P. (1982). Evidence for sigma opioid receptor: binding of [3H]SKF-10047 to etorphine-inaccessible sites in guinea-pig brain. *J. Pharmacol. Exp. Ther.* 223, 284–290.
- Su, T. P., Hayashi, T., Maurice, T., Buch, S., and Ruoho, A. E. (2010). The sigma-1 receptor chaperone as an inter-organelle signaling modulator. *Trends Pharmacol. Sci.* 31, 557–566. doi: 10.1016/j.tips.2010.08.007
- Sun, B., Kawahara, M., Ehata, S., and Nagamune, T. (2014). AAG8 promotes carcinogenesis by activating STAT3. *Cell Signal.* 26, 1863–1869. doi: 10.1016/j.cellsig.2014.04.001
- Sunnam, S. K., et al. (2010). Synthesis and biological evaluation of conformationally restricted sigma(1) receptor ligands with 7,9-diazabicyclo[4.2.2]decane scaffold. *Org. Biomol. Chem.* 8, 5525–5540. doi: 10.1039/c0ob00402b
- Tanaka, M., Shirasaki, T., Kaku, S., Muramatsu, M., and Otomo, S. (1995). Characteristics of binding of [3H]NE-100, a novel sigma-receptor ligand, to guinea-pig brain membranes. *Naunyn Schmiedeberg's Arch. Pharmacol.* 351, 244–251. doi: 10.1007/BF00233243
- Thomas, J. D., Longen, C. G., Oyer, H. M., Chen, N., Maher, C. M., Salvino, J. M., et al. (2017). Sigma1 targeting to suppress aberrant androgen receptor signaling in prostate cancer. *Cancer Res.* 77 (9), 2439–2452. doi: 10.1158/0008-5472.CAN-16-1055
- Thompson, A. D., Dugan, A., Gestwicki, J. E., and Mapp, A. K. (2012). Fine-tuning multiprotein complexes using small molecules. *ACS Chem. Biol.* 7, 1311–1320. doi: 10.1021/cb300255p
- Vangveravong, S., Xu, J., Zeng, C., and Mach, R. H. (2006). Synthesis of N-substituted 9-azabicyclo[3.3.1]nonan-3-yl carbamate analogs as sigma2 receptor ligands. *Bioorg. Med. Chem.* 14, 6988–6997. doi: 10.1016/j.bmc.2006.06.028
- Vilner, B. J., and Bowen, W. D. (1993). Sigma receptor-active neuroleptics are cytotoxic to C6 glioma cells in culture. *Eur. J. Pharmacol.* 244, 199–201. doi: 10.1016/0922-4106(93)90029-9
- Vilner, B. J., and Bowen, W. D. (2000). Modulation of cellular calcium by sigma-2 receptors: release from intracellular stores in human SK-N-SH neuroblastoma cells. *J. Pharmacol. Exp. Ther.* 292, 900–911.
- Vilner, B. J., de Costa, B. R., and Bowen, W. D. (1995a). Cytotoxic effects of sigma ligands: sigma receptor-mediated alterations in cellular morphology and viability. *J. Neurosci.* 15, 117–134. doi: 10.1523/JNEUROSCI.15-01-00117.1995
- Vilner, B. J., John, C. S., and Bowen, W. D. (1995b). Sigma-1 and sigma-2 receptors are expressed in a wide variety of human and rodent tumor cell lines. *Cancer Res.* 55, 408–413.
- Wang, B., et al. (2004). Expression of sigma 1 receptor in human breast cancer. *Breast Cancer Res. Treat.* 87, 205–214. doi: 10.1007/s10549-004-6590-0
- Weber, E., and Wunsch, B. (2017). Medicinal chemistry of Sigma1 receptor ligands: pharmacophore models, synthesis, structure affinity relationships, and pharmacological applications. *Handb. Exp. Pharmacol.* 244, 51–79. doi: 10.1007/164\_2017\_33

- Weber, F., et al. (2014). Synthesis, pharmacological evaluation, and Sigma1 receptor interaction analysis of hydroxyethyl substituted piperazines. *J. Med. Chem.* 57, 2884–2894. doi: 10.1021/jm401707t
- Wheeler, K. T., et al. (2000). Sigma-2 receptors as a biomarker of proliferation in solid tumours. *Br. J. Cancer* 82, 1223–1232. doi: 10.1054/bjoc.1999.1067
- Wilcox, C. B., et al. (2007). Coordinate up-regulation of TMEM97 and cholesterol biosynthesis genes in normal ovarian surface epithelial cells treated with progesterone: implications for pathogenesis of ovarian cancer. *BMC Cancer* 7, 223. doi: 10.1186/1471-2407-7-223
- Wilson, A. A., et al. (1991). Radiosynthesis of sigma receptor ligands for positron emission tomography: 11C- and 18F-labeled guanidines. *J. Med. Chem.* 34, 1867–1870. doi: 10.1021/jm00110a017
- Wu, Z., and Bowen, W. D. (2008). Role of sigma-1 receptor C-terminal segment in inositol 1,4,5-trisphosphate receptor activation: constitutive enhancement of calcium signaling in MCF-7 tumor cells. *J. Biol. Chem.* 283, 28198–28215. doi: 10.1074/jbc.M802099200
- Xiao, M., et al. (2013). Expression of MAC30 protein is related to survival and clinicopathological variables in breast cancer. *J. Surg. Oncol.* 107, 456–462. doi: 10.1002/jso.23269
- Xu, J., et al. (2011). Identification of the PGRMC1 protein complex as the putative sigma-2 receptor binding site. *Nat. Commun.* 2, 380. doi: 10.1038/ncomms1386
- Xu, X. Y., et al. (2014). Down-regulated MAC30 expression inhibits proliferation and mobility of human gastric cancer cells. *Cell. Physiol. Biochem.* 33, 1359–1368. doi: 10.1159/000358703
- Yang, S., et al. (2013). Elevated expression of MAC30 predicts lymph node metastasis and unfavorable prognosis in patients with epithelial ovarian cancer. *Med. Oncol.* 30, 324. doi: 10.1007/s12032-012-0324-7
- Yano, H., et al. (2018). Pharmacological profiling of sigma 1 receptor ligands by novel receptor homomer assays. *Neuropharmacology* 133, 264–275. doi: 10.1016/j.neuropharm.2018.01.042
- Zadra, G., Photopoulos, C., and Loda, M. (2013). The fat side of prostate cancer. *Biochim. Biophys. Acta* 1831, 1518–1532. doi: 10.1016/j.bbailip.2013.03.010
- Zampieri, D., et al. (2016). Computer-assisted design, synthesis, binding and cytotoxicity assessments of new 1-(4-(aryl(methyl)amino)butyl)-heterocyclic sigma 1 ligands. *Eur. J. Med. Chem.* 121, 712–726. doi: 10.1016/j.ejmech.2016.06.001
- Zeng, C., et al. (2007). Subcellular localization of sigma-2 receptors in breast cancer cells using two-photon and confocal microscopy. *Cancer Res.* 67, 6708–6716. doi: 10.1158/0008-5472.CAN-06-3803
- Zeng, C., et al. (2012). Sigma-2 ligands induce tumour cell death by multiple signalling pathways. *Br. J. Cancer* 106, 693–701. doi: 10.1038/bjc.2011.602
- Zeng, C., et al. (2014). Functional assays to define agonists and antagonists of the sigma-2 receptor. *Anal. Biochem.* 448, 68–74. doi: 10.1016/j.ab.2013.12.008
- Zeng, C., Garg, N., and Mach, R. H. (2016). The PGRMC1 protein level correlates with the binding activity of a sigma-2 fluorescent probe (SW120) in rat brain cells. *Mol. Imaging Biol.* 18, 172–179. doi: 10.1007/s11307-015-0891-z
- Zeng, C., McDonald, E. S., and Mach, R. H. (2017). “Molecular probes for imaging the sigma-2 receptor: *in vitro* and *in vivo* imaging studies,” in *Handbook of experimental pharmacology*. Switzerland AG: Springer Nature. doi: 10.1007/164\_2016\_96
- Zeng, C., et al. (2019). TMEM97 and PGRMC1 do not mediate sigma-2 ligand-induced cell death. *Cell Death Discov.* 5, 58. doi: 10.1038/s41420-019-0141-2
- Zhu, L. X., et al. (2003). IL-10 mediates Sigma1 receptor-dependent suppression of antitumor immunity. *J. Immunol.* 170, 3585–3591. doi: 10.4049/jimmunol.170.7.3585

**Conflict of Interest:** The authors declare that the research was conducted in the absence of any commercial or financial relationships that could be construed as a potential conflict of interest.

Copyright © 2019 Oyer, Sanders and Kim. This is an open-access article distributed under the terms of the Creative Commons Attribution License (CC BY). The use, distribution or reproduction in other forums is permitted, provided the original author(s) and the copyright owner(s) are credited and that the original publication in this journal is cited, in accordance with accepted academic practice. No use, distribution or reproduction is permitted which does not comply with these terms.



# Hazards of Using *Masking Protocols* When Performing Ligand Binding Assays: Lessons From the Sigma-1 and Sigma-2 Receptors

Haider Abbas<sup>1,2†</sup>, Preeti Borde<sup>3</sup>, Gary B. Willars<sup>4</sup>, David R. Ferry<sup>5</sup>  
and Stephen T. Safrany<sup>3\*</sup>

<sup>1</sup> School of Pharmacy, University of Wolverhampton, Wolverhampton, United Kingdom, <sup>2</sup> Oncology Department, New Cross Hospital, Wolverhampton, United Kingdom, <sup>3</sup> School of Medicine, RCSI-Bahrain, Adliya, Bahrain, <sup>4</sup> Department of Molecular and Cell Biology, University of Leicester, Leicester, United Kingdom, <sup>5</sup> Gastrointestinal Oncology Strategy, Eli Lilly, Indianapolis, IN, United States

## OPEN ACCESS

### Edited by:

Herve Boutin,  
University of Manchester,  
United Kingdom

### Reviewed by:

Matthew J. Robson,  
University of Cincinnati, United States  
Enrique José Cobos,  
University of Granada, Spain

### \*Correspondence:

Stephen T. Safrany  
ssafrany@rcsi-mub.com

### †Present address:

Haider Abbas,  
Oncology Department, University  
Hospital Birmingham NHS Foundation  
Trust, Birmingham,  
United Kingdom

### Specialty section:

This article was submitted to  
Experimental Pharmacology  
and Drug Discovery,  
a section of the journal  
Frontiers in Pharmacology

**Received:** 06 May 2019

**Accepted:** 02 March 2020

**Published:** 13 March 2020

### Citation:

Abbas H, Borde P, Willars GB,  
Ferry DR and Safrany ST (2020)  
Hazards of Using Masking Protocols  
When Performing Ligand Binding  
Assays: Lessons From the Sigma-1  
and Sigma-2 Receptors.  
Front. Pharmacol. 11:309.  
doi: 10.3389/fphar.2020.00309

Sigma-1 and sigma-2 receptors are emerging therapeutic targets. Although the molecular identity of the sigma-2 receptor has recently been determined, receptor quantitation has used, and continues to use, the sigma-1 selective agents (+) pentazocine or dextralorphan to *mask* the sigma-1 receptor in radioligand binding assays. Here, we have assessed the suitability of currently established saturation and competition binding isotherm assays that are used to quantify parameters of the sigma-2 receptor. We show that whilst the sigma-1 receptor mask (+) pentazocine has low affinity for the sigma-2 receptor ( $K_i$  406 nM), it can effectively compete at this site with [<sup>3</sup>H] di-O-tolyl guanidine (DTG) at the concentrations frequently used to mask the sigma-1 receptor (100 nM and 1  $\mu$ M). This competition influences the apparent affinity of DTG and other ligands tested in this system. A more troublesome issue is that DTG can displace (+) pentazocine from the sigma-1 receptor, rendering it partly *unmasked*. Indeed, commonly used concentrations of (+) pentazocine, 100 nM and 1  $\mu$ M, allowed 37 and 11% respectively of sigma-1 receptors to be bound by DTG (300 nM), which could result in an overestimation of sigma-2 receptor numbers in assays where sigma-1 receptors are also present. Similarly, modelled data for 1  $\mu$ M dextralorphan show that only 71–86% of sigma-1 receptors would be masked in the presence of 300 nM DTG. Therefore, the use of dextralorphan as a masking agent would also lead to the overestimation of sigma-2 receptors in systems where sigma-1 receptors are present. These data highlight the dangers of using masking agents in radioligand binding studies and we strongly recommend that currently used masking protocols are not used in the study of sigma-2 receptors. In order to overcome these problems, we recommend the use of a cell line apparently devoid of sigma-1 receptors [e.g., MCF7 (ATCC HTB-22)] in the absence of any masking agent when determining the affinity of agents for the sigma-2 receptor. In addition, assessing the relative levels of sigma-1 and sigma-2 receptors can be achieved using [<sup>3</sup>H] DTG saturation binding followed by two-site analysis of (+) pentazocine competition binding with [<sup>3</sup>H] DTG.

**Keywords:** dextralorphan, di-O-tolyl guanidine, equilibrium binding, masking, (+) pentazocine, sigma-1 sigma-2, TMEM97



## INTRODUCTION

Sigma receptors were initially described as novel opioid receptors (Martin et al., 1976) but were later found to be a distinct class of receptors consisting of two subtypes: sigma-1 and sigma-2. The sigma-1 receptor has been identified and cloned for some time (Hanner et al., 1996; Kekuda et al., 1996; Mei and Pasternak, 2001; Abate et al., 2010), with the crystal structure of the trimer being recently reported (Schmidt et al., 2016). The molecular identity of the sigma-2 binding site has only very recently been determined as TMEM97, an endoplasmic reticulum-resident transmembrane protein that regulates the sterol transporter NPC1 (Alon et al., 2017). It has been reported that both subtypes of the sigma receptor, but in particular sigma-2, are overexpressed in rapidly dividing normal cells and in tumour cell lines derived from various tissues (Vilner et al., 1995) highlighting a role in cell growth and proliferation with a potential link to cancer.

Sigma-1 receptors have been well-studied and several functions have been described including: modulation and synthesis of dopamine and acetylcholine (Booth and Baldessarini, 1991; Patrick et al., 1993); modulation of N-methyl-D-aspartate (NMDA)-stimulated neurotransmitter release (Gonzalez-Alvarez and Werling, 1995; Monnet et al., 1996); modulation of opioid analgesia (King et al., 1997); and neuroprotective and anti-amnesic activity (Maurice and Lockhart, 1997; Brimson et al., 2018). Sigma-1 receptor antagonists show promise in the treatment (Spruce et al., 2004) and diagnosis (van Waarde et al., 2015) of several cancers. Sigma-2 receptors are mainly involved in the regulation of cell proliferation and viability, with agonists driving changes in cell morphology and a reduction in cell division, leading ultimately to apoptosis (Bowen, 2000).

The current focus on the sigma-2 receptor is underpinned by the observation that its presence not only correlates with the proliferation of tumours but also that it plays an important role in cell survival. *In vitro* studies have shown that sigma-2 ligands can induce apoptosis and hence inhibit tumour growth. As such, it has been proposed that the sigma-2 receptor could be used as both a diagnostic and therapeutic target (van Waarde et al., 2015). Indeed, trials are underway in these areas to determine the potential of the sigma-2 receptor and its ligands in oncology. For example, early trials using radiolabelled sigma-2 ligands in PET imaging have shown success in imaging certain tumours. Furthermore, *in vitro* studies using pancreatic and ovarian cancer cell lines have shown significant increases in the pharmacological effects of chemotherapeutics when used in combination with sigma-2 ligands. Sigma-2 ligands conjugated with anti-cancer drugs are also under development to ensure targeted drug delivery in order to minimise the toxicities associated with chemotherapy (Zeng et al., 2017).

Sigma-1 receptors are usually quantified by radioligand binding assays using the selective ligand (+) pentazocine that binds to the sigma-1 receptor with relatively high affinity. Binding of (+) pentazocine to other proteins appears poor, leading to rapid dissociation from low-affinity sites and little contribution of background or non-specific binding to overall

binding. Although described as an agonist, (+) pentazocine binds with a Hill slope of unity which is not affected by the inclusion of GTP or suramin. In contrast, antagonists bind with low Hill slopes. The addition of GTP or suramin causes loss of the high-affinity state of the sigma-1 receptor for the antagonist and leads to a Hill slope of unity being achieved (Brimson et al., 2011).

Problems arise, however, when radioligand binding assays are performed to study the sigma-2 receptor. In this article, we show that this can overestimate the number of sigma-2 receptors present in a system where sigma-1 receptors are also present. This may also explain why sigma-2 receptors are described as ubiquitous (Stracina and Novakova, 2018).

The standard protocol used for identifying and quantifying the sigma-2 receptor relies on the radioligand [<sup>3</sup>H] di-*O*-tolyl guanidine (DTG). DTG is a pan-sigma ligand, binding both receptors with equal affinity. As most binding assays have been performed in tissues or cell lines containing sigma-1 receptors, it has become standard to determine sigma-2 binding in the presence of either (+) pentazocine or dextralorpham to mask sigma-1 binding sites (Vilner et al., 1995; Chu et al., 2015; Chu and Ruoho, 2015). However, this protocol, whilst fully integrated into the sigma receptor researcher's toolkit, is seriously flawed. Here, we explain the reasons and consequences of relying on a masking protocol and offer alternatives.

## MATERIALS AND METHODS

### General Materials

Tissue culture media, antibiotics, trypsin, and serum were purchased from Invitrogen (Paisley, UK) or Sigma-Aldrich (Ireland). [<sup>3</sup>H] (+) pentazocine ((1*S*,9*S*,13*S*)-1,13-dimethyl-10-(3-methylbut-2-en-1-yl)-10-azatricyclo[deca-2,4,6-trien-4-ol]) and [5-<sup>3</sup>H(N)]-1,3-di-*O*-tolylguanidine (DTG) were purchased from PerkinElmer (Beaconsfield, UK). Other reagents were purchased from Sigma-Aldrich (Poole, UK). Before use, drugs were dissolved in an appropriate vehicle and diluted in assay buffer. The pH of each solution was adjusted to 7.4.

### Tissue Culture and Membrane Preparation

MDA-MB-468 (ATCC HTB-132) and MCF7 (ATCC HTB-22) breast cancer cell lines were obtained from LGC Promotech, UK. MDA-MB-468 cells were maintained in DMEM, high glucose (41965-062) supplemented with 10% foetal calf serum. MCF7 cells were maintained in MEM (M2279) supplemented with 2 mM L-glutamine and 10% foetal calf serum. Cells were cultured at 37°C in a humidified incubator with 5% CO<sub>2</sub>. To prepare membranes for binding studies, cells were suspended in sigma binding buffer [SBB: 50 mM Tris-HCl; pH 8.0, (Vilner et al., 1995)], sonicated (1 min), and then centrifuged (22,000g, 20 min, 4°C). The supernatant was discarded and the pellet suspended in SBB.

### Saturation Binding

#### Sigma-1 Receptor Binding

Assays (total volume 100 µl) were performed using 0–300 nM [<sup>3</sup>H] (+) pentazocine at room temperature for 2 h in SBB as previously described (Vilner et al., 1995). Non-specific binding was determined using 1 mM reduced haloperidol

(Schetz et al., 2007). The concentration of reduced haloperidol to determine non-specific binding was higher than in previous studies, as assays described below used higher concentrations of radioligand than used in standard radioligand binding assays. Assays were terminated by addition of ice-cold tris-buffered saline (TBS: 154 mM NaCl, 10 mM Tris, pH 7.4) and filtration through glass fibre filters (GF/B, Sigma-Aldrich, Poole, UK) using a cell harvester. Tubes and filter discs were washed (2 x 3 ml) with ice-cold TBS, and the filter discs dried under vacuum. Scintillation counting was carried out in ProSafe FC+ cocktail (Meridian Biotechnologies Ltd, Tadworth, UK) after overnight incubation.

### Sigma-2 Receptor Binding

Assays (total volume 100  $\mu$ l) were performed at room temperature for 4 h with 1–300 nM [ $^3$ H] DTG in SBB. Non-specific binding was determined using 1 mM reduced haloperidol. To investigate the effects of (+) pentazocine, [ $^3$ H] DTG saturation curves were performed in the absence or presence of (+) pentazocine [100 nM (Chu and Ruoho, 2015) or 1  $\mu$ M (Shiba et al., 2005; Xu et al., 2005)]. Assays were terminated by addition of ice-cold TBS and filtration through glass fibre filters (GF/C, Sigma-Aldrich, Poole, UK) using a cell harvester. Tubes and filter discs were washed with ice-cold TBS (2 x 3 ml) and the filter discs dried under vacuum. Scintillation counting was carried out in ProSafe FC+ cocktail after overnight incubation.

### Competition Binding Assays

Competition binding assays (total volume 100  $\mu$ l) were performed using a final assay concentration of 50 nM, 100 nM, or 1  $\mu$ M [ $^3$ H] (+) pentazocine with increasing concentrations of DTG (10 nM–1 mM). Alternatively, 10–30 nM [ $^3$ H] DTG was employed in the presence of increasing concentrations of (+) pentazocine (10 nM–1 mM). The assay was then allowed to equilibrate at room temperature for 4 h. After equilibration, the membranes were harvested by rapid filtration through GF/B ([ $^3$ H] (+) pentazocine) or GF/C ([ $^3$ H] DTG) glass fibre filters. Tubes and filter discs were washed with ice-cold TBS (2 x 3 ml), and the filter discs dried under vacuum. Non-specific binding was determined using 1 mM reduced haloperidol. Under these conditions less than 10% of either the [ $^3$ H] (+) pentazocine or [ $^3$ H] DTG was bound.

All data were calculated and presented using GraphPad Prism v7.02.

### Modelling of Dextrallorphan Binding

Whilst (+) pentazocine is the masking drug used by most researchers, several publications have used dextrallorphan as an alternative. We were unable to obtain dextrallorphan for these studies and have therefore modelled binding experiments using published data. Methods for and results from the modelling can be found in **Supplementary Material**.

## RESULTS

Saturation binding of [ $^3$ H] (+) pentazocine to membranes prepared from MCF7 and MDA-MB-468 cells was performed.

MDA-MB-468 cell membranes showed binding with  $K_d$  22 nM ( $pK_d = 7.65 \pm 0.13$ ) and  $B_{max}$  of  $1,730 \pm 330$  fmol/mg protein (**Figure 1**). There was no specific binding of [ $^3$ H] (+) pentazocine to MCF7 cell membranes detected (data not shown). Saturation binding curves were also performed using the pan-sigma ligand [ $^3$ H] DTG, which bound to MCF7 cells with  $K_d$  12 nM ( $pK_d = 7.92 \pm 0.03$ ,  $n = 3$ ) and MDA-MD-468 cell membranes with  $K_d$  13 nM ( $pK_d 7.88 \pm 0.01$ ,  $n = 3$ ). The  $B_{max}$  values were  $2,050 \pm 100$  and  $850 \pm 200$  fmol/mg protein for MCF7 and MDA-MB-468 cells respectively (**Figure 2**).

**Figure 3** shows that (+) pentazocine readily competed with the pan-sigma ligand [ $^3$ H] DTG for the sigma-2 receptor. Our assays were performed using membranes prepared from MCF7 cells, which show no specific binding of [ $^3$ H] (+) pentazocine in radioligand binding assays [**Figure 1** and (Vilner et al., 1995)], and so express very few, if any, sigma-1 receptors. Competition assays were performed using low concentrations (10–30 nM) of [ $^3$ H] DTG. An  $IC_{50}$  of 620 nM was determined, resulting in a  $K_i$  of 406 nM ( $pK_i = 6.39 \pm 0.07$ ,  $n = 4$ ) calculated using the Cheng-Prusoff correction. These results show that whilst the interaction between sigma-2 receptors and (+) pentazocine cannot be shown directly using [ $^3$ H] (+) pentazocine, there is a clear, measurable interaction.

We next sought to determine whether the inclusion of (+) pentazocine would affect the saturation curve of [ $^3$ H] DTG, performing the assay in accordance with frequently used protocols (Chu and Ruoho, 2015). Assays were performed using [ $^3$ H] DTG (1–300 nM) in the absence and presence of (+) pentazocine (100 nM or 1  $\mu$ M) with membranes prepared from MCF7 cells, which, as highlighted above, show no specific binding of [ $^3$ H] (+) pentazocine at the concentrations used in radioligand binding assays. A rectangular hyperbolic curve was obtained in all three conditions (**Figure 4**). Using GraphPad Prism to plot the saturation curves allowed comparisons of  $K_d$ ,

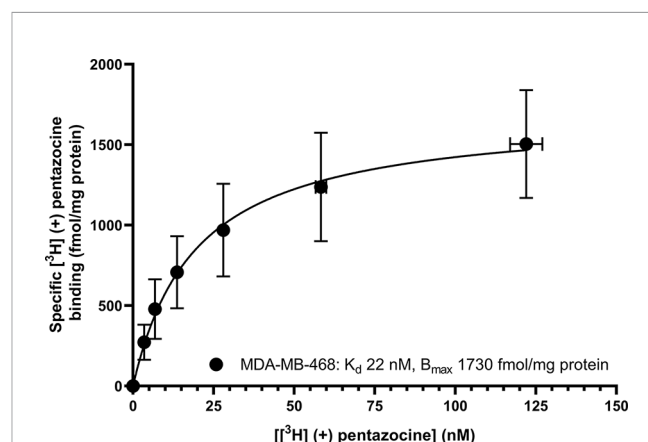
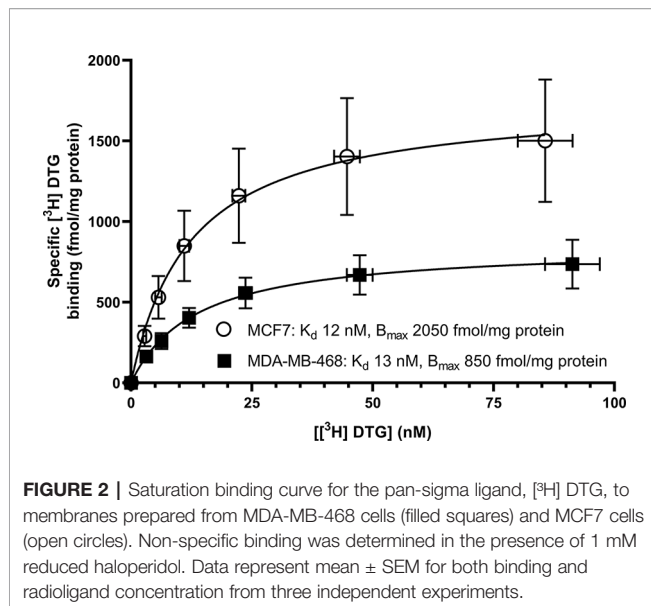
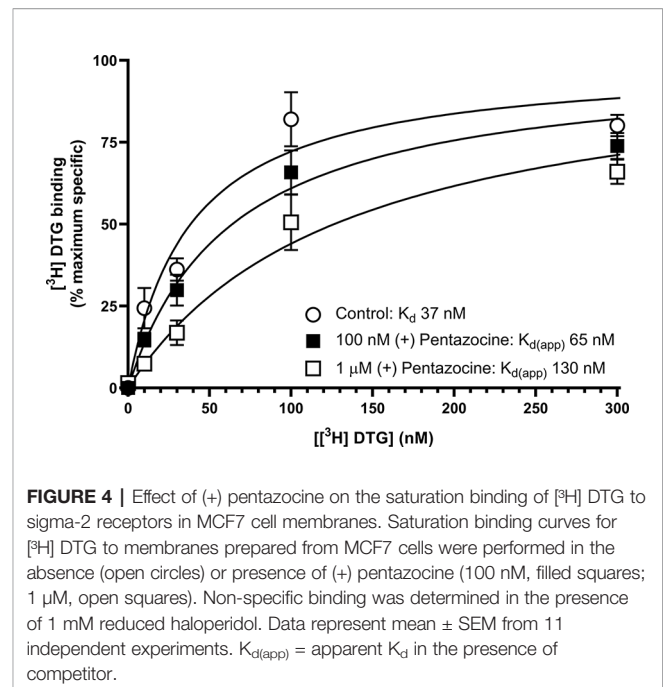


**FIGURE 1 |** Saturation binding curve for [ $^3$ H] (+) pentazocine to membranes prepared from MDA-MB-468 cells. Non-specific binding was determined in the presence of 1 mM reduced haloperidol. Data represent mean  $\pm$  SEM for both binding and radioligand concentration from three independent experiments. No specific binding was observed using [ $^3$ H] (+) pentazocine and membranes prepared from MCF7 cells.

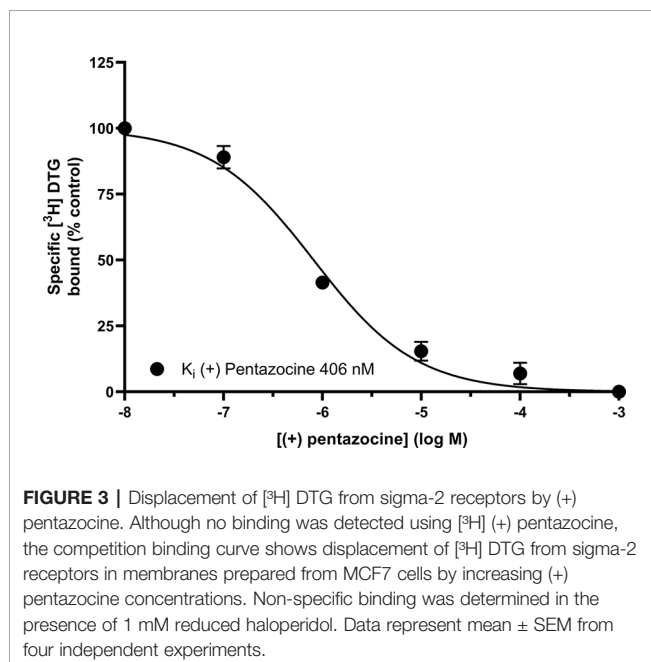


apparent  $K_d$  and  $B_{\max}$  values. We have deliberately not presented results in the form of Scatchard plots, as such linear transformations are not considered suitable for statistical analysis or determination of  $K_d$  or  $B_{\max}$  values (Rodbard et al., 1980; GraphPad, 2020). These experiments were performed using a different batch of  $[^3\text{H}]$  DTG to that used in the saturation binding experiments described above, and a modest difference in  $K_d$  for DTG was observed between this experiment (37 nM,  $pK_d = 7.43 \pm 0.10$ , mean  $\pm$  SEM,  $n = 11$ ) and the saturation analysis shown in **Figure 2** (12 nM). The highest concentration of DTG used (300 nM) bound 88% of the available receptors based on the rectangular hyperbolic fit observed in **Figure 2**. As expected, the inclusion of 100 nM (+) pentazocine



did not affect  $B_{\max}$  calculations. The apparent  $K_d$  was moderately increased to 65 nM ( $pK_d = 7.19 \pm 0.09$ , mean  $\pm$  SEM,  $n = 11$ ) with DTG (300 nM) binding 82% of the available receptors. Inclusion of the higher concentration of (+) pentazocine (1  $\mu\text{M}$ ) again did not affect the calculated  $B_{\max}$ . However, the apparent  $K_d$  was shifted even higher: 130 nM ( $pK_d = 6.89 \pm 0.09$ , mean  $\pm$  SEM,  $n = 11$ ) and DTG (300 nM) binding 71% of the receptors available. These data show that the frequently used protocol for establishing  $K_d$  and  $B_{\max}$  for sigma-2 receptors would give a raised  $K_d$  value for DTG, whilst recognising all sigma-2 receptors in the system.

We also investigated whether  $[^3\text{H}]$  DTG could compete with the *masking agent* (+) pentazocine and bind to sigma-1 receptors. In order to observe loss of (+) pentazocine binding to these sites, experiments were performed in membranes prepared from MDA-MB-468 cells. Incubations of  $[^3\text{H}]$  (+) pentazocine (100 nM and 1  $\mu\text{M}$ ) were performed with the inclusion of increasing concentrations of DTG. Radioligand binding assays are rarely performed with the concentrations of radioligand used here. Preparations of  $[^3\text{H}]$  (+) pentazocine were mixed with unlabelled (+) pentazocine to obtain stocks suitable for these binding studies. The binding of 100 nM  $[^3\text{H}]$  (+) pentazocine was reduced by increasing concentrations of DTG with an  $\text{IC}_{50}$  of 760 nM ( $p\text{IC}_{50} = 6.1 \pm 0.2$ , mean  $\pm$  SEM,  $n = 8$ ). When considering data using 1  $\mu\text{M}$   $[^3\text{H}]$  (+) pentazocine, DTG was, as expected, less effective, with an  $\text{IC}_{50}$  of 2.2  $\mu\text{M}$  ( $p\text{IC}_{50} = 5.7 \pm 0.4$ , mean  $\pm$  SEM,  $n = 6$ ) (**Figure 5**). Using the Cheng-Prusoff correction,  $K_i$  values of 137 and 47 nM for DTG can be calculated at 100 nM and 1  $\mu\text{M}$   $[^3\text{H}]$  (+) pentazocine respectively. Interpolation of the curves allows calculation of the amount of  $[^3\text{H}]$  (+) pentazocine displaced from the sigma-1 sites at different concentrations of DTG (**Table 1**). Data show that 37% of 100 nM  $[^3\text{H}]$  (+) pentazocine and 17% of 1  $\mu\text{M}$   $[^3\text{H}]$  (+) pentazocine was



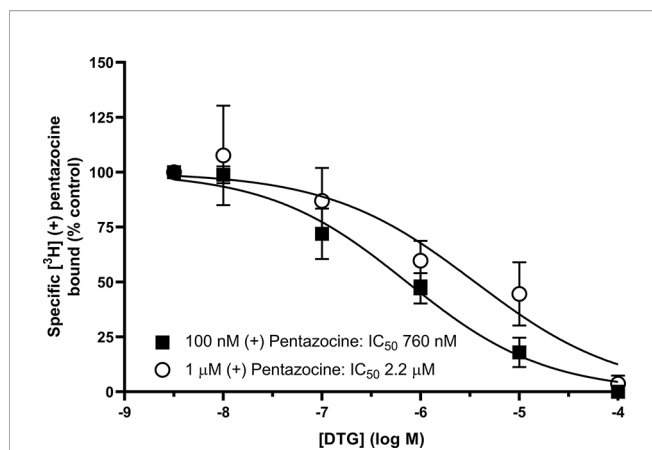


**FIGURE 5 |** Displacement of [ $^3\text{H}$ ] (+) pentazocine from sigma-1 receptors by DTG. Competition binding curve showing the displacement of either 100 nM (filled squares) or 1  $\mu\text{M}$  (open circles) [ $^3\text{H}$ ] (+) pentazocine from sigma-1 receptors in membranes prepared from MDA-MB-468 cells by increasing DTG concentrations. Non-specific binding was determined in the presence of 1 mM reduced haloperidol. Data represent mean  $\pm$  SEM from 8 (100 nM [ $^3\text{H}$ ] (+) pentazocine) or 6 (1  $\mu\text{M}$  [ $^3\text{H}$ ] (+) pentazocine) independent experiments.

displaced by 300 nM DTG. These data show that under conditions frequently used, up to 37% of sigma-1 receptors present would contribute to the DTG signal and inflate the  $B_{\text{max}}$  value. In extreme circumstances, this could account for all the binding observed.

We offer one possible remedy to the current problem of assessing levels of sigma-1 and sigma-2 receptors in cells and tissues in the absence of commercially available sigma-2 receptor-selective radioligands: **Figure 6** shows competition binding between a fixed concentration of [ $^3\text{H}$ ] DTG and a range of concentrations of unlabelled (+) pentazocine in MDA-MB-468 and MCF7 cell membranes. A monophasic competition curve is observed in MCF7 cell membranes. This indicates a single, low affinity site ( $\text{IC}_{50}$  3.3  $\mu\text{M}$ ) is present. In contrast, MDA-MB-468 cells show the existence of sites with high- and low-affinity for (+) pentazocine. Two-site analysis (GraphPad Prism) identifies that 36% of these sites had high affinity ( $\text{IC}_{50}$  21 nM), indicating these are sigma-1 receptors, with the remaining 64% with a low affinity ( $\text{IC}_{50}$  1.3  $\mu\text{M}$ ), representing sigma-2 receptors.

We note that not all groups use (+) pentazocine to mask sigma-1 receptors. Indeed, several publications have used

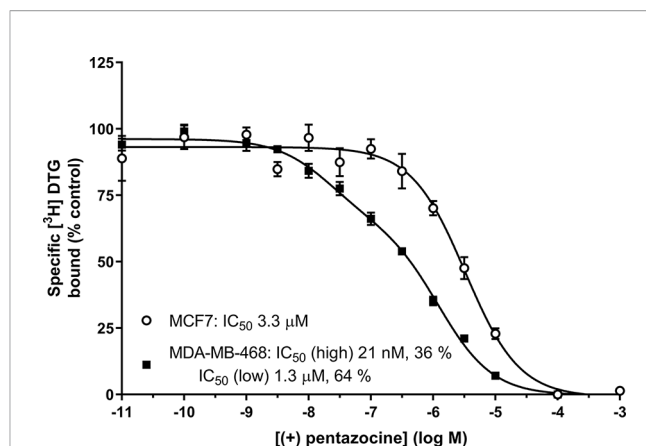


**FIGURE 6 |** Displacement of [ $^3\text{H}$ ] DTG from sigma receptors by (+) pentazocine. Competition binding curve showing the displacement of [ $^3\text{H}$ ] DTG from membranes prepared from MDA-MB-468 cells (filled squares) and MCF7 cells (open circles) by increasing (+) pentazocine concentrations. Non-specific binding was determined in the presence of 1 mM reduced haloperidol. Data represent mean  $\pm$  SEM from 5 (MDA-MB-468) and 4 (MCF7) independent experiments. Curve fitting was achieved comparing a one- and two-site fit (GraphPad Prism).

dextrallorphan. Unfortunately, we have not been able to obtain this ligand but have used modelling to determine whether this may provide a better sigma-1 receptor mask than (+) pentazocine. Results presented in **Supplementary Material** suggest that 1  $\mu\text{M}$  dextrallorphan would bind 2.2–6.3% of the sigma-2 receptors. The addition of 300 nM DTG would displace 88% of this binding. However, DTG would also displace dextrallorphan from the sigma-1 receptor, rendering only 71.5–86.1% of sigma-1 receptors masked (see **Supplementary Material**).

From the above data, it is clear that none of the masking protocols widely accepted should be used. Addition of DTG will compete with the binding of (+) pentazocine and dextrallorphan to both sigma-1 and sigma-2 sites.

## DISCUSSION AND CONCLUSIONS

The results presented here are in keeping with previously published data on all of the agents used. Our affinity of 22 nM for (+) pentazocine at the sigma-1 receptor is both internally and externally consistent. We have previously shown affinities of 7.7 nM (Spruce et al., 2004) and 17 nM (Brimson et al., 2011) (obtained from MDA-MB-468 membranes and permeabilised cells, respectively). A selection of data from other studies with a variety of tissues and conditions gives overlapping results: guinea pig liver microsomes (0.8 nM) (Hanner et al., 1996); mouse lung membranes (1.4 nM) (Lever et al., 2015); guinea pig brain membranes (1.6 nM obtained by means of homologous competition) (Xu et al., 2015); mouse brain homogenates (5.1 nM) (Langa et al., 2003); bovine adrenal medullar membranes (18 nM) (Paul et al., 1993); and rat cerebral membranes (19.9 nM) (Shiba et al., 2005). It is recognised that

**TABLE 1 |** Displacement of [ $^3\text{H}$ ] (+) pentazocine from sigma-1 receptors by increasing concentrations of DTG.

[ $^3\text{H}$ ] (+) pentazocine]	[DTG] 3 nM	[DTG] 10 nM	[DTG] 30 nM	[DTG] 100 nM	[DTG] 300 nM
100 nM	2.5 $\pm$ 0.9	4.7 $\pm$ 1.6	8.6 $\pm$ 2.6	26.3 $\pm$ 9.9	37 $\pm$ 11
1 $\mu\text{M}$	2.9 $\pm$ 2.5	4.8 $\pm$ 3.9	7.6 $\pm$ 5.9	11.6 $\pm$ 8.2	17 $\pm$ 11

Data represent [ $^3\text{H}$ ] (+) pentazocine displaced by increasing concentrations of DTG (as % of binding in the absence of DTG). Data (mean  $\pm$  SEM) are interpolated from individual competition curves,  $n = 8$  (100 nM (+) pentazocine) and  $n = 6$  (1  $\mu\text{M}$  (+) pentazocine). Values are derived using the data presented in **Figure 5**.



differences in the sigma-1 receptor sequences from different species may contribute to some variation in affinity. Only one of the above studies (Hanner et al., 1996) used recombinant protein with a known sequence. In the present study, [ $^3\text{H}$ ] DTG gave a  $B_{\text{max}}$  of  $2,050 \pm 100$  fmol/mg protein of sigma receptors in MCF7 cells. In the absence of any measureable specific [ $^3\text{H}$ ] (+) pentazocine binding, we consider these to be sigma-2 receptors. This is in agreement with previously published data of 2,071 fmol/mg protein (Vilner et al., 1995) in these cells. It is, of course, possible that low levels of sigma-1 receptors are expressed in these MCF7 cells obtained from ATCC. Indeed, Western blotting and immunocytochemical analysis of MCF7 cells obtained from ECACC (Radif et al., 2018) demonstrated the presence of sigma-1 receptors but to our knowledge, no direct comparison of MCF7 cells from these different sources has been made.

The inclusion of (+) pentazocine in binding assays using MCF7 cells caused a rightward shift in the  $K_d$  of [ $^3\text{H}$ ] DTG binding, but had no effect on  $B_{\text{max}}$  calculations. This is unsurprising as (+) pentazocine and [ $^3\text{H}$ ] DTG are competing at the sigma-2 receptors. However, the percentage of sigma-2 receptors bound by DTG at 300 nM DTG falls from 88% (no (+) pentazocine) to 71% in the presence of 1  $\mu\text{M}$  (+) pentazocine, based on interpolation of values shown in **Figure 4**. Our  $K_d$  values of DTG for the sigma-2 receptor, 12–37 nM, are difficult to compare with previous data, as most reported data have been made in the presence of 100 nM–1  $\mu\text{M}$  (+) pentazocine or 1  $\mu\text{M}$  dextrallorphan. Examples include: 22.3 nM (Shiba et al., 2005); 25 nM (Vilner et al., 1995); 30.7 nM (Xu et al., 2005); 39.9 nM (Lever et al., 2006); and 74.8–91.1 nM (Chu et al., 2015). In this respect, our data are in keeping with, and highly comparable to, previous data. As such, our conclusions should be considered relevant to all using these reagents.

The affinity of (+) pentazocine for the sigma-2 receptor has been reported in a number of published studies. However, data in the present study, along with consideration of the methods used in many of the previous studies suggest that a re-evaluation might be appropriate. For example: a  $K_d$  of 56 nM was reported for (+) pentazocine at the sigma-2 receptor in guinea pig brain homogenates ('in the presence of an excess of non-radiolabelled (+) pentazocine for selective masking of sigma-1 receptors') (Sunnam et al., 2011); 327 nM in rat liver homogenate (in the presence of 100 nM (+) pentazocine to mask sigma-1 receptors) (Zampieri et al., 2009); 728 nM in guinea pig brain membranes (in the presence of 200 nM (+) pentazocine) (Lever et al., 2006); 1,440 nM in rat brain homogenates (in the presence of 1  $\mu\text{M}$  (+) pentazocine) (Xu et al., 2005); and 2680 nM in rat cerebral membranes (in the presence of 1  $\mu\text{M}$  (+) pentazocine) (Shiba et al., 2005). Values reported in the absence of a masking concentration of (+) pentazocine include: 1.7–3.3  $\mu\text{M}$  (reported in C6 and NG115-08 cells in the absence of masking agent; these cells were reported as having a very low density of high-affinity (+) pentazocine binding sites) and 2.1–9.4  $\mu\text{M}$  (in the presence of 1  $\mu\text{M}$  dextrallorphan) (Vilner et al., 1995). Thus, although the affinity of (+) pentazocine has been widely reported, the effects of this relatively low-affinity binding have been underestimated.

Our experimental data show the apparent  $K_d$  of [ $^3\text{H}$ ] DTG binding to the sigma-2 receptor increases with increasing (+) pentazocine concentration. Equally, the calculation of  $K_i$  values for novel compounds acting at sigma-2 receptors would be complicated, as DTG, (+) pentazocine and the test compound will be competing at the same site. There may be additional complications if compounds also bind to the sigma-1 receptor with high affinity. If this results in substantial ligand depletion, estimates of affinity at the sigma-2 receptor would be compromised. We would suggest that ideally, determination of binding parameters for the sigma-2 receptor would be best performed using [ $^3\text{H}$ ] DTG and cell preparations devoid of sigma-1 receptors, thereby avoiding the need for a masking agent. This could include, for example, MCF7 cell membranes, although caution should be applied as we have found some of these to contain sigma-1 receptors (Spruce et al., 2004; Radif et al., 2018).

The consequences of the low affinity binding of (+) pentazocine to sigma-2 receptors are likely to be minimal when reporting  $B_{\text{max}}$  values for these receptors in membrane preparations. However, the ability of DTG to compete with (+) pentazocine for sigma-1 receptors is a major concern when (+) pentazocine is being used as a mask for sigma-1 receptors. To date, we are unaware of any cell or tissue reported as lacking sigma-2 receptors but we suggest that determination of sigma-2 sites should be revisited. Data presented here bring into question the previously accepted method of calculating sigma-2 receptor levels in cell lines using [ $^3\text{H}$ ] DTG in the presence of either (+) pentazocine or dextrallorphan to mask sigma-1 receptors. Indeed, our data clearly highlight that the number of sigma-2 receptors will have been overestimated using such methodology, as it is likely that, if present, sigma-1 receptors will also have bound [ $^3\text{H}$ ] DTG.

In terms of any underlying biology, there is little rationale for comparisons between sigma-1 and sigma-2 receptors as, after all, they are very different proteins with very different roles. Despite this, a reliable protocol for determination of sigma-2 sites in the presence of sigma-1 receptors is required. Thus, we propose that alternative methodology is employed to quantitate sigma-2 receptor levels, specifically where masking agents are excluded. The use of (+) pentazocine for the quantitation of sigma-1 receptors is greatly entrenched in our research methodologies. Unless a direct comparison of sigma-1 and sigma-2 receptor levels is required, an ideal way would be to use sigma-2 receptor selective tools (Zeng et al., 2017). However, until these agents are commercially available, we suggest that an alternative would be to use [ $^3\text{H}$ ] DTG to obtain levels of total sigma binding sites (i.e., sigma-1 plus sigma-2 receptors) accompanied by competition binding with (+) pentazocine or another agent selective for one particular receptor. Subsequent two-site analyses would then allow determination of the relative amounts of each target. Such methodology has been used previously: in a rarely cited paper (Kovacs and Larson, 1995) it was shown that [ $^3\text{H}$ ] DTG can be used to label all sigma sites. Using sigma-1-selective agents a biphasic competition curve was demonstrated, equivalent to

sigma-1 and sigma-2 sites. Computer assisted data analysis (e.g. GraphPad Prism, as used here) is sufficiently developed to determine the presence of even a relatively small proportion of a second (affinity) binding site.

Although the methodology described above may provide an alternative strategy for determination of sigma-1 and sigma-2 receptors, this approach has generated inconsistencies. Kovacs and Larson (1995) showed that in spinal cord, [ $^3\text{H}$ ] DTG alone bound 150% of the sites labelled by [ $^3\text{H}$ ] (+) pentazocine, suggesting there were twice as many sigma-1 receptors as sigma-2 receptors. However, when the competition experiments were performed, these suggested the reverse, as (+) pentazocine only displaced 30% of the [ $^3\text{H}$ ] DTG with high affinity (Kovacs and Larson, 1995). Similarly, [ $^3\text{H}$ ] DTG bound to fewer sites than [ $^3\text{H}$ ] (+) pentazocine in several regions of the brain (Walker et al., 1990). Our results with MDA-MB-468 cells also show this discrepancy: **Figure 1** shows that MDA-MB-468 cells had a  $B_{\text{max}}$  of 1730 fmol/mg protein for [ $^3\text{H}$ ] (+) pentazocine and only 850 fmol/mg protein for the pan-sigma ligand [ $^3\text{H}$ ] DTG. **Figure 5** then shows that 36% of these [ $^3\text{H}$ ] DTG binding sites were sigma-1 receptors. Whether such discrepancies arise as a consequence of, for example, the given values of radioligand specific activity, breakdown of the radioligand, tritium exchange between the ligand, and other constituents (including water) or the presence of labelled precursor molecules (Lazareno and Birdsall, 2000) remains to be established. Until that point, this protocol would benefit from further consideration before it is widely accepted.

In addition to the issues described above, two recent publications highlight the possibility that [ $^3\text{H}$ ] DTG binds to something other than sigma-2 receptors. Thus, knock-out of the recently identified sigma-2 binding site, TMEM97, in HeLa cells showed residual binding sites for [ $^3\text{H}$ ] DTG (Riad et al., 2018; Zeng et al., 2019). These sites had an apparent  $K_d$  for DTG of 300–400 nM, with assays performed in the presence of 1  $\mu\text{M}$  (+) pentazocine (to *mask* the sigma-1 receptor). Utilising a derivation of the Michaelis-Menten equation for a competitive antagonist ( $K_{d(\text{app})} = K_d \cdot (1 + [I]/K_i)$ , where  $K_{d(\text{app})}$  is the apparent  $K_d$  of the radioligand in the presence of a competitor at fixed concentration) and the values given in this paper (DTG  $K_d = 12$  nM, (+) pentazocine  $K_i$  (sigma-1 receptor) = 22 nM, [(+) pentazocine] = 1  $\mu\text{M}$ ), the calculated  $K_{d(\text{app})}$  for DTG is 557 nM, which is well within experimental error for suggesting that this residual binding site may be the sigma-1 receptor, despite the suggestion that this is unlikely (Riad et al., 2018). It is noteworthy that RHM-4, a selective sigma-2 receptor ligand [ $K_i$  8.2 nM and 12,900 nM for sigma-2 and sigma-1 receptors, respectively (Hou et al., 2006; Zeng et al., 2019)] was unable to detect this residual binding when used as the radioligand. In this way, [ $^{125}\text{I}$ ] RHM-4 binding the sigma-2 receptor reflects the beauty of [ $^3\text{H}$ ] (+) pentazocine when studying the sigma-1 receptor. [ $^{125}\text{I}$ ] RHM-4 binds the sigma-2 receptor with sufficient dwell time to monitor the interaction readily. Rapid dissociation from the alternative binding sites with low affinity (in this case, sigma-1 receptors) means they do not contribute to any directly observable radioactive signal.

The more recent molecular identification of the sigma-2 receptor (Alon et al., 2017) has allowed the generation of cell

lines lacking either sigma-1 receptors (Mavlyutov et al., 2017) or sigma-2 receptors (Riad et al., 2018). Such cell lines may well prove to be useful in dissecting out the cellular roles of the individual receptor types and contribute to the development of more selective ligands for pharmacological and therapeutic use. Furthermore, despite limitations of the models, the availability of knockout mice, such as that for the sigma 1 receptor (Langa et al., 2003), will undoubtedly contribute to a full understanding of the pathophysiological roles of these receptors. Such developments will certainly add to the available tools and methodologies. However, the present importance of identifying and quantifying sigma receptors (particularly sigma-2 receptors), potentially for tumour imaging and as a molecular target in cancer (see Introduction), highlight that robust methodology must be in place. We hope that the work presented here will sound a note of caution with current methodologies and highlight the need for further consideration and development.

## AUTHOR'S NOTE

**Figures 1 and 6, and Supplementary Figures 1, 2, 3 and 4** appear in preliminary form in the PhD thesis by HA (Expression of sigma receptors in human cancer cell lines and effects of novel sigma-2 ligands on their proliferation, University of Wolverhampton, 2018).

## DATA AVAILABILITY STATEMENT

The datasets generated for this study are available on request to the corresponding author.

## AUTHOR CONTRIBUTIONS

HA, PB, GW and SS were involved in performing the experiments described. HA, DF and SS contributed to the modelling. All authors were involved in drafting and preparation of this manuscript.

## FUNDING

We would like to thank Dudley Group of Hospitals NHS Trust, New Cross Hospital NHS Trust and RCSI-Bahrain for the financial support.

## SUPPLEMENTARY MATERIAL

The Supplementary Material for this article can be found online at: <https://www.frontiersin.org/articles/10.3389/fphar.2020.00309/full#supplementary-material>

## REFERENCES

- Abate, C., Elenewski, J., Niso, M., Berardi, F., Colabufo, N. A., Azzariti, A., et al. (2010). Interaction of the sigma(2) receptor ligand PB28 with the human nucleosome: computational and experimental probes of interaction with the H2A/H2B dimer. *ChemMedChem* 5 (2), 268–273. doi: 10.1002/cmdc.200900402
- Alon, A., Schmidt, H. R., Wood, M. D., Sahn, J. J., Martin, S. F., and Kruse, A. C. (2017). Identification of the gene that codes for the sigma2 receptor. *Proc. Natl. Acad. Sci. U. S. A.* 114 (27), 7160–7165. doi: 10.1073/pnas.1705154114
- Booth, R. G., and Baldessarini, R. J. (1991). (+)-6,7-benzomorphan sigma ligands stimulate dopamine synthesis in rat corpus striatum tissue. *Brain Res.* 557 (1–2), 349–352. doi: 10.1016/0006-8993(91)90159-S
- Bowen, W. D. (2000). Sigma receptors: recent advances and new clinical potentials. *Pharm. Acta Helv.* 74 (2–3), 211–218. doi: 10.1016/S0165-7208(00)80020-3
- Brimson, J. M., Brown, C. A., and Safrany, S. T. (2011). Antagonists show GTP-sensitive high-affinity binding to the sigma-1 receptor. *Br. J. Pharmacol.* 164 (2b), 772–780. doi: 10.1111/j.1476-5381.2011.01417.x
- Brimson, J. M., Safrany, S. T., Qassam, H., and Tencomnao, T. (2018). Dipentylammonium binds to the sigma-1 receptor and protects against glutamate toxicity, attenuates dopamine toxicity and potentiates neurite outgrowth in various cultured cell lines. *Neurotox. Res.* 34 (2), 263–272. doi: 10.1007/s12640-018-9883-5
- Chu, U. B., and Ruoho, A. E. (2015). Sigma receptor binding assays. *Curr. Protoc. Pharmacol.* 71, 1 34 31–31 34 21. doi: 10.1002/0471141755.ph0134s71
- Chu, U. B., Mavlyutov, T. A., Chu, M. L., Yang, H., Schulman, A., Mesangeau, C., et al. (2015). The Sigma-2 Receptor and Progesterone Receptor Membrane Component 1 are different binding sites derived from independent genes. *EBioMedicine* 2 (11), 1806–1813. doi: 10.1016/j.ebiom.2015.10.017
- Gonzalez-Alvear, G. M., and Werling, L. L. (1995). Sigma receptor regulation of norepinephrine release from rat hippocampal slices. *Brain Res.* 673 (1), 61–69. doi: 10.1016/0006-8993(94)01394-W
- GraphPad (2020). *Advice: Avoid Scatchard, Lineweaver-Burke and similar transforms*. [Online]. Available: [https://www.graphpad.com/guides/prism/8/curve-fitting/avoidscatchard\\_lineweaver\\_burkeandsimilartransforms.htm?q=scatchard](https://www.graphpad.com/guides/prism/8/curve-fitting/avoidscatchard_lineweaver_burkeandsimilartransforms.htm?q=scatchard) [Accessed 23 January 2020].
- Hanner, M., Moebius, F. F., Flandorfer, A., Knaus, H. G., Striessnig, J., Kempner, E., et al. (1996). Purification, molecular cloning, and expression of the mammalian sigma1-binding site. *Proc. Natl. Acad. Sci. U. S. A.* 93 (15), 8072–8077. doi: 10.1073/pnas.93.15.8072
- Hou, C., Tu, Z., Mach, R., Kung, H. F., and Kung, M. P. (2006). Characterization of a novel iodinated sigma-2 receptor ligand as a cell proliferation marker. *Nucl. Med. Biol.* 33 (2), 203–209. doi: 10.1016/j.nucmedbio.2005.10.001
- Kekuda, R., Prasad, P. D., Fei, Y. J., Leibach, F. H., and Ganapathy, V. (1996). Cloning and functional expression of the human type 1 sigma receptor (hSigmaR1). *Biochem. Biophys. Res. Commun.* 229 (2), 553–558. doi: 10.1006/bbrc.1996.1842
- King, M., Pan, Y. X., Mei, J., Chang, A., Xu, J., and Pasternak, G. W. (1997). Enhanced kappa-opioid receptor-mediated analgesia by antisense targeting the sigma1 receptor. *Eur. J. Pharmacol.* 331 (1), R5–R6. doi: 10.1016/S0014-2999(97)01064-9
- Kovacs, K. J., and Larson, A. A. (1995). Discrepancies in characterization of sigma sites in the mouse central nervous system. *Eur. J. Pharmacol.* 285 (2), 127–134. doi: 10.1016/0014-2999(95)00383-v
- Langa, F., Codony, X., Tovar, V., Lavado, A., Gimenez, E., Cozar, P., et al. (2003). Generation and phenotypic analysis of sigma receptor type I (sigma 1) knockout mice. *Eur. J. Neurosci.* 18 (8), 2188–2196. doi: 10.1046/j.1460-9568.2003.02950.x
- Lazareno, S., and Birdsall, N. J. (2000). Effects of contamination on radioligand binding parameters. *Trends Pharmacol. Sci.* 21 (2), 57–60. doi: 10.1016/S0165-6147(99)01412-1
- Lever, J. R., Gustafson, J. L., Xu, R., Allmon, R. L., and Lever, S. Z. (2006). Sigma1 and sigma2 receptor binding affinity and selectivity of SA4503 and fluoroethyl SA4503. *Synapse* 59 (6), 350–358. doi: 10.1002/syn.20253
- Lever, J. R., Litton, T. P., and Fergason-Cantrell, E. A. (2015). Characterization of pulmonary sigma receptors by radioligand binding. *Eur. J. Pharmacol.* 762, 118–126. doi: 10.1016/j.ejphar.2015.05.026
- Martin, W. R., Eades, C. G., Thompson, J. A., Huppler, R. E., and Gilbert, P. E. (1976). The effects of morphine- and nalorphine- like drugs in the nondependent and morphine-dependent chronic spinal dog. *J. Pharmacol. Exp. Ther.* 197 (3), 517–532.
- Maurice, T., and Lockhart, B. P. (1997). Neuroprotective and anti-amnesic potentials of sigma (sigma) receptor ligands. *Prog. Neuropsychopharmacol. Biol. Psychiatry* 21 (1), 69–102. doi: 10.1016/S0278-5846(96)00160-1
- Mavlyutov, T. A., Yang, H., Epstein, M. L., Ruoho, A. E., Yang, J., and Guo, L. W. (2017). APEX2-enhanced electron microscopy distinguishes sigma-1 receptor localization in the nucleoplasmic reticulum. *Oncotarget* 8 (31), 51317–51330. doi: 10.18632/oncotarget.17906
- Mei, J., and Pasternak, G. W. (2001). Molecular cloning and pharmacological characterization of the rat sigma1 receptor. *Biochem. Pharmacol.* 62 (3), 349–355. doi: 10.1016/S0006-2952(01)00666-9
- Monnet, F. P., de Costa, B. R., and Bowen, W. D. (1996). Differentiation of sigma ligand-activated receptor subtypes that modulate NMDA-evoked [3H]-noradrenaline release in rat hippocampal slices. *Br. J. Pharmacol.* 119 (1), 65–72. doi: 10.1111/j.1476-5381.1996.tb15678.x
- Patrick, S. L., Walker, J. M., Perkel, J. M., Lockwood, M., and Patrick, R. L. (1993). Increases in rat striatal extracellular dopamine and vacuous chewing produced by two sigma receptor ligands. *Eur. J. Pharmacol.* 231 (2), 243–249. doi: 10.1016/0014-2999(93)90456-R
- Paul, I. A., Basile, A. S., Rojas, E., Youdim, M. B. H., Decosta, B., Skolnick, P., et al. (1993). Sigma-Receptors Modulate Nicotinic Receptor Function in Adrenal Chromaffin Cells. *FASEB J.* 7 (12), 1171–1178. doi: 10.1096/fasebj.7.12.8375616
- Radif, Y., Ndiaye, H., Kalantzi, V., Jacobs, R., Hall, A., Minogue, S., et al. (2018). The endogenous subcellular localisations of the long chain fatty acid-activating enzymes ACSL3 and ACSL4 in sarcoma and breast cancer cells. *Mol. Cell. Biochem.* 448 (1–2), 275–286. doi: 10.1007/s11010-018-3332-x
- Riad, A., Zeng, C., Weng, C. C., Winters, H., Xu, K., Makvandi, M., et al. (2018). Sigma-2 receptor/TMEM97 and PGRMC-1 increase the rate of internalization of LDL by LDL receptor through the formation of a ternary complex. *Sci. Rep.* 8 (1), 16845. doi: 10.1038/s41598-018-35430-3
- Rodbard, D., Munson, P. J., and Thakur, A. K. (1980). Quantitative characterization of hormone receptors. *Cancer* 46 (12), 2907–2918. doi: 10.1002/1097-0142(19801215)46:12<2907::Aid-Cncr2820461433>3.0.Co;2-6
- Schetz, J. A., Perez, E., Liu, R., Chen, S. W., Lee, I., and Simpkins, J. W. (2007). A prototypical Sigma-1 receptor antagonist protects against brain ischemia. *Brain Res.* 1181, 1–9. doi: 10.1016/j.brainres.2007.08.068
- Schmidt, H. R., Zheng, S., Gurpinar, E., Koehl, A., Manglik, A., and Kruse, A. C. (2016). Crystal structure of the human sigma1 receptor. *Nature* 532 (7600), 527–530. doi: 10.1038/nature17391
- Shiba, K., Ogawa, K., and Mori, H. (2005). In vitro characterization of radioiodinated (+)-2-[4-(4-iodophenyl) piperidino]cyclohexanol [(+)-pIV] as a sigma-1 receptor ligand. *Bioorg. Med. Chem.* 13 (4), 1095–1099. doi: 10.1016/j.bmc.2004.11.029
- Spruce, B. A., Campbell, L. A., McTavish, N., Cooper, M. A., Appleyard, M. V., O'Neill, M., et al. (2004). Small molecule antagonists of the sigma-1 receptor cause selective release of the death program in tumor and self-reliant cells and inhibit tumor growth in vitro and in vivo. *Cancer Res.* 64 (14), 4875–4886. doi: 10.1158/0008-5472.CAN-03-3180
- Stracina, T., and Novakova, M. (2018). Cardiac Sigma Receptors - An Update. *Physiol. Res.* 67, S561–S576. doi: 10.33549/physiolres.934052
- Sunnam, S. K., Rack, E., Schepmann, D., and Wunsch, B. (2011). Synthesis of 7,9-diazabicyclo[4.2.2]decane as conformationally restricted kappa receptor agonists: Fine tuning of the dihedral angle of the ethylenediamine pharmacophore. *Eur. J. Med. Chem.* 46 (6), 1972–1982. doi: 10.1016/j.ejmech.2011.01.064
- van Waarde, A., Ryzcynska, A. A., Ramakrishnan, N. K., Ishiwata, K., Elsinga, P. H., and Dierckx, R. A. (2015). Potential applications for sigma receptor ligands in cancer diagnosis and therapy. *Biochim. Biophys. Acta* 1848 (10 Pt B), 2703–2714. doi: 10.1016/j.bbamem.2014.08.022

- Vilner, B. J., John, C. S., and Bowen, W. D. (1995). Sigma-1 and sigma-2 receptors are expressed in a wide variety of human and rodent tumor cell lines. *Cancer Res.* 55 (2), 408–413.
- Walker, J. M., Bowen, W. D., Walker, F. O., Matsumoto, R. R., De Costa, B., and Rice, K. C. (1990). Sigma receptors: biology and function. *Pharmacol. Rev.* 42 (4), 355–402.
- Xu, J., Tu, Z., Jones, L. A., Vangveravong, S., Wheeler, K. T., and Mach, R. H. (2005). [3H]N-[4-(3,4-dihydro-6,7-dimethoxyisoquinolin-2(1H)-yl)butyl]-2-methoxy-5-methyl benzamide: a novel sigma-2 receptor probe. *Eur. J. Pharmacol.* 525 (1-3), 8–17. doi: 10.1016/j.ejphar.2005.09.063
- Xu, R., Lord, S. A., Peterson, R. M., Fergason-Cantrell, E. A., Lever, J. R., and Lever, S. Z. (2015). Ether modifications to 1-[2-(3,4-dimethoxyphenyl)ethyl]-4-(3-phenylpropyl)piperazine (SA4503): effects on binding affinity and selectivity for sigma receptors and monoamine transporters. *Bioorg. Med. Chem.* 23 (1), 222–230. doi: 10.1016/j.bmc.2014.11.007
- Zampieri, D., Mamolo, M. G., Laurini, E., Florio, C., Zanette, C., Fermeglia, M., et al. (2009). Synthesis, biological evaluation, and three-dimensional in silico pharmacophore model for sigma(1) receptor ligands based on a series of substituted benzo[d]oxazol-2(3H)-one derivatives. *J. Med. Chem.* 52 (17), 5380–5393. doi: 10.1021/jm900366z
- Zeng, C., McDonald, E. S., and Mach, R. H. (2017). Molecular probes for imaging the sigma-2 receptor: in vitro and in vivo imaging studies. *Handb. Exp. Pharmacol.* 244, 309–330. doi: 10.1007/164\_2016\_96
- Zeng, C., Weng, C. C., Schneider, M. E.Jr., Puentes, L., Riad, A., Xu, K., et al. (2019). TMEM97 and PGRMC1 do not mediate sigma-2 ligand-induced cell death. *Cell Death Discov.* 5, 58. doi: 10.1038/s41420-019-0141-2

**Conflict of Interest:** Author DF is employed by Eli Lilly.

The remaining authors declare that the research was conducted in the absence of any commercial or financial relationships that could be construed as a potential conflict of interest.

Copyright © 2020 Abbas, Borde, Willars, Ferry and Safrany. This is an open-access article distributed under the terms of the Creative Commons Attribution License (CC BY). The use, distribution or reproduction in other forums is permitted, provided the original author(s) and the copyright owner(s) are credited and that the original publication in this journal is cited, in accordance with accepted academic practice. No use, distribution or reproduction is permitted which does not comply with these terms.



# Advantages of publishing in Frontiers



## OPEN ACCESS

Articles are free to read  
for greatest visibility  
and readership



## FAST PUBLICATION

Around 90 days  
from submission  
to decision



## HIGH QUALITY PEER-REVIEW

Rigorous, collaborative,  
and constructive  
peer-review



## TRANSPARENT PEER-REVIEW

Editors and reviewers  
acknowledged by name  
on published articles

## Frontiers

Avenue du Tribunal-Fédéral 34  
1005 Lausanne | Switzerland

**Visit us:** [www.frontiersin.org](http://www.frontiersin.org)

**Contact us:** [info@frontiersin.org](mailto:info@frontiersin.org) | +41 21 510 17 00



## REPRODUCIBILITY OF RESEARCH

Support open data  
and methods to enhance  
research reproducibility



## DIGITAL PUBLISHING

Articles designed  
for optimal readership  
across devices



## FOLLOW US

@frontiersin



## IMPACT METRICS

Advanced article metrics  
track visibility across  
digital media



## EXTENSIVE PROMOTION

Marketing  
and promotion  
of impactful research



## LOOP RESEARCH NETWORK

Our network  
increases your  
article's readership